Prediction of Transitional Boundary Layer Properties for CFD Software in Engineering Flows

Allan Thomson

A thesis submitted in partial fulfilment of the
requirements of the University of Abertay Dundee
for the degree of Doctor of Philosophy

February 1997

I certify that this thesis is a true and accurate version of the thesis approved by the examiners.

Signed [redacted] Date 27th March 1997

(Director of Studies)

Acknowledgements

I am extremely grateful to Dr. C. J. Fraser for his guidance and support on both the professional and personal level throughout my doctoral programme.

My sincere thanks to 'ma belle amie' Gisele for her continual encouragement and the interesting and diverse discussions on the more abstract side of post graduate study.

The financial support of the University of Abertay Dundee is gratefully acknowledged.

CONTENTS

Abstract

Two linear combination models for the transition zone in two-dimensional incompressible boundary layers have been programmed into the commercially available computational fluid dynamics software suite of programs, PHOENICS as a sink of momentum. It has been shown that it was possible to use a laminar velocity profile to predict laminar, transitional and turbulent boundary layer parameters.

Method one, attributable to Fraser, Higazy and Milne (1994), was tested against a variety of flows including zero and constant adverse and favourable pressure gradients, and also the varying pressure gradient Rolls Royce T3C flows. The method gives good prediction of skin friction and transition length when the start of transition was in zero and favourable pressure gradient flows, but the transition length was always under predicted when the start of transition was in adverse pressure gradient.

Method two, attributable to Solomon, Walker and Gostelow (1995) was tested in flows where the start of transition was in adverse pressure gradient. This method will probably give an improved prediction of transition length, but the results were highly sensitive to the properties of the flow at the start of transition.

It has been shown that in order to predict the start of transition using the Abu-Ghannam and Shaw (1980) correlation, a meaningful average of free stream turbulence intensity in the flow was required. It was found that a reasonable estimate could be found by integrating the free stream intensity value from the inlet and taking the average.

A new method was developed to overcome the limitations of the Abu-Ghannam and Shaw correlation, and is based on the turbulent energy equation. The method

used integrated averages of properties across the boundary layer starting from the leading edge and marching downstream. The boundary layer model was coupled to the free stream by a correlation which was found, using the Rolls Royce T3A, T3A-, T3B and T3C data, to be a function of free stream turbulence intensity, dissipation length scale and pressure gradient parameter. The method was found to give good prediction of the start of transition, and hence skin friction in the favourable pressure gradient flows. Unfortunately there was not enough data to extend this correlation to adverse pressure gradients.

Nomenclature

A	area (m^2)
a	ratio of the major Reynolds stress to the turbulent kinetic energy (= $-u'w'$ / k)
AK	log - law constant used in PHOENICS (= 0.435)
B	turbulent wall - law intercept constant
C	coefficient in source term
c	ratio of local velocity to upstream velocity
C_{1E}, C_{2E}, C_{3E}	constants in k - ε model 1.44, 1.92, 1.0
C_f	local skin friction coefficient = $2\tau_w/\rho W^2$
$C_\mu C_D$	constant in k - ε turbulence model (= 0.09)
E	roughness parameter
G_b	volumetric production rate of kinetic energy by gravitational forces (m^2/s^3)
g	gravitational vector (m/s^2)
H	shape parameter = δ^*/θ
H_s	shape parameter = δ/θ
H_l	shape parameter = $(\delta - \delta^*)/\theta$
k	kinetic energy (m^2/s^2)
l_ε	dissipation length scale (m)
ℓ_m	turbulent length scale (m)
m	pressure gradient parameter = $(\theta^2/\nu)(dW/dz)$
N	non-dimensional spot formation parameter

n	spot generation rate (m^{-1} s^{-1})
N_o	non-dimensional spot formation parameter for zero pressure gradient flows
NX, NY, NZ	number of computational cells in x, y, z directions respectively
P_k	volumetric production rate of kinetic energy by shear forces (m^2/s^3)
Pr	Prandtl number
q	turbulence intensity (%)
R_θ	momentum thickness Reynolds number = $W\theta/\nu$
$R_{\theta f}$	ficticious momentum thickness Reynolds number upstream of which infinitesimal distrubances are damped out.
R_λ	transition length Reynolds number = $W\lambda/\nu$
S	shear parameter
S	source term *Chapter 2*
s	PHOENICS friction factor (= $\frac{\tau}{\rho U^2}$)
s_z	secondary source term
T	a geometric multiplier
t	time (s)
U	main flow velocity *Chapter 2* (m/s)
u	velocity vector (m/s)
u', v', w'	root mean square values of the fluctuating velocity components
V	value in source term
W	main flow velocity (m/s)
x	transverse co-ordinate; stream wise co-ordinate *Chapter 2* (m)
Y	normal distance of first grid point from wall *Chapter 2* (m)

Y^+	dimensionless wall distance (= $Y\upsilon^*/\nu$)
z	stream wise co-ordinate (m)
z_s	location of the start of transition (m)

Greek Symbols

α	angle between locus of successive spot positions
β	Clauser parameter = $-\lambda_t^2 H\theta/W(dW/dz)$
δ^*	boundary layer displacement thickness (m)
δ	boundary layer thickness (m)
ε	dissipation term in turbulence model (m^2/s^3)
γ	turbulence intermittency close to the wall
ϕ	variable in question
Γ	diffusive exchange coefficient for ϕ
κ	Kármán constant = 0.41
Π	Coles wake parameter
λ	Stream wise distance between the 25 and 75 percent turbulence intermittency locations (m)
λ_p	Pohlhaussen parameter (= $\delta^2/\nu.dW/dz$)
λ_t	$(2/Cf)^{0.5}$
μ	dynamic viscosity (Ns/m^2)
μ_t	turbulent viscosity (Ns/m^2)
ν	kinematic viscosity (m^2/s)
θ	momentum thickness (m)
ρ	fluid density (kg/m^3)

σ	spot propagation parameter (dimensionless)
σ_ε	empirical constant in ε equation (= 1.314)
σ_k	empirical constant in kinetic energy equation (= 1.0)
τ	shear stress (N/m^2)
υ^*	resultant friction velocity (m/s)

Subcripts

bc	boundary condition
c	in cell value
i, j	co-ordinate direction
L	laminar
N	nearest wall
r	resultant, parallel to the wall at the first grid node
s	start of transition
T	turbulent condition
t	transitional
w	wall condition

1. Introduction

The use of computational fluid dynamics (CFD) to predict internal and external flows has risen dramatically in the past decade because the need to predict complex flow properties has become increasingly paramount as the quest for higher efficiency from components is sought. Commercial CFD software can perform complex flow simulations for either laminar or turbulent flow. Most engineering flows are either laminar or turbulent, therefore these commercial codes are ideally suited for the purpose. There are however, flows which in some regions, are neither fully laminar nor fully turbulent. The flow in this region is in a state of transition between the two. One such region of flow is that on the external surfaces of a gas turbine blade.

Flow over solid bodies can generally be split into two regimes: inviscid and viscous. The inviscid region is usually remote from the surface and frictional effects are negligible, whilst in the viscous region the frictional effects are dominant and are generated within a thin film close to the surface called a boundary layer. The prediction of boundary layer parameters is extremely important as they have direct relevance to the aerodynamic and heat transfer characteristics of the body shape.

A boundary layer growing from the leading edge of a plate will generally start off as a laminar flow, undergo a transition process, where the flow is both laminar and turbulent, and continue to grow into a fully developed turbulent boundary layer. Fully developed laminar and turbulent boundary layers are quite well understood and their properties can be predicted quite accurately by a number of

methods e.g. integral methods, finite difference solutions. However the transition process is still not well understood.

1.1 Transition Models

Narasimha (1985) classified the calculation methods for transitional flows into four groups and a brief description is given below:

1.1.1 Linear Combination

This method was initially conceived by Emmons (1951) in his classical work on turbulent spots. He proposed that the transition region could be represented by the switching of laminar and turbulent velocity profiles in an intermittently turbulent flow. Linear combination methods make use of empirical correlations to predict onset of transition and transition length. According to Gostelow et. al (1994) one of the limitations of the linear combination methods is that the laminar flow component can separate under moderate adverse pressure gradients and this can cause computational difficulties. The problem is exacerbated when Thwaites' (1949) method is used to predict the laminar boundary layer component in adverse pressure gradient and computational errors can be as large as ± 15% close to separation.

1.1.2 Algebraic Models

The algebraic stress model is an economical way of accounting for the anisotropy of the Reynolds stresses without having to solve Reynolds stress transport equations. Rodi (1980) proposed that if the convective and diffusive terms are modelled or removed then the Reynolds stress equations are reduced to a set of algebraic equations. They have no capability for predicting the transition process

and therefore require a similar amount of empiricism as the linear combination method. The effect of intermittency is modelled by allowing the effective viscosity to increase from laminar to turbulent values in a prescribed manner in the transition zone by some other procedure.

1.1.3 Differential Models

Gostelow, Hong, Walker and Dey (1994) reported that Savill (1992,1993) had recently reviewed the predictive capability of one or two equation turbulence models for the by-pass mode of transition under moderately high free-stream turbulence levels. Savill concluded that the k - ε level of closure was the minimum level required to achieve any generality in predictions and reported that most of the k - ε models failed to predict transition onset to any accuracy. The best methods used appropriate low Reynolds number damping factors to be able to reasonably predict transition onset, but the predicted transition length was far too short. To overcome this problem, further damping factors were introduced but this can adversely effect the prediction of skin friction.

1.1.4 Higher Order Models

Reynolds stress transport models are able to capture more of the physics of bypass transition but suffer the same problems of computational expense and inapplicability at low free-stream turbulence levels. Direct numerical simulation has given valuable insights into the physics of transition, but is generally too costly for engineering type flow situations.

The prediction of the transitional boundary layer is not usually a problem as most engineering type flows are either laminar or fully turbulent. There are, however,

flow situations where the transition region is of prime importance, e.g. turbomachine blades, Formula 1 racing cars, etc.

In the past five years computing power has increased at a tremendous rate, and it is now possible to solve complex fluid flow problems on a desktop, or even a laptop computer, with programs that were previously only available for a work station or mainframe. These commercial computational fluid dynamic (CFD) codes e.g. FLUENT, PHOENICS, STAR CD have chosen not to incorporate the simple linear combination transition type modelling in favour of low Reynolds number extensions to the well known k - ε turbulence models and large eddy simulations. These models require thousands of computational cells in the boundary layer, hence the computational cost is large and it is also more difficult to achieve convergence.

1.2 Scope of the Thesis

The methods described by Fraser, Higazy and Milne (1994) and Solomon Walker and Gostelow (1995) have been programmed into the commercially available computational fluid dynamics software suite PHOENICS. Extensive testing has shown the inadequacy of the present correlations, e.g. Abu-Ghannam and Shaw (1980), Mayle (1991), for the prediction of the start of transition. To try to alleviate this problem a new method has been devised to predict the start of transition, based on the Rolls Royce, ERCOFTAC flows T3A, T3A-, T3B and T3C. using the turbulent energy equations.

2. Computational Fluid Dynamics

Computational fluid dynamics is the art of replacing the governing partial differential equations of fluid flow with numbers and advancing these numbers in space and/or time to obtain a numerical description of the field of interest.

2.1 PHOENICS CFD Software

PHOENICS is an acronym for: Parabolic, Hyperbolic or Elliptic Numerical Integration Code Series. It is a general-purpose CFD software package and can be used for simulating single and multi-phase flow, heat/mass transfer and chemical reaction phenomena. It consists of an input file (Q1), pre-processor (SATELLITE), solver (EARTH) and graphical output (PHOTON or AUTOPLOT) (Figure 2.1).

Although PHOENICS is capable of solving many complex fluid flow problems, it is possible for the user to insert their own FORTRAN coding into a GROUND subroutine. Thus it is possible to supplement a tried, tested and proven code with specialist programming or modify the existing features.

2.2 The Mathematical Basis of PHOENICS

Variables may be thought of as being dependent: the subject of a conservation equation, or auxiliary constant, or derived from an algebraic expression. In each case they can be further divided into either scalar (e.g. pressure, temperature) or vector (velocities, u, v, w) quantities. The distinction between vectors and scalars is important, because they are stored at different locations in space. Scalars are stored at centre points of six-sided cells and represent the value typical of the whole cell; vectors are stored at the centre point of the six cell faces, Figure 2.2.

PHOENICS employs a structured, cartesian or body fitted co-ordinate (bfc) grid. The conservation equation solved by PHOENICS for single phase flow can be written as:

$$\frac{\partial(\rho\phi)}{\partial t} + \nabla \bullet (\rho\phi \mathbf{u}) - \nabla \bullet (\Gamma \nabla\phi) = S\phi \qquad (2.1)$$

The above conservation equation cannot be solved numerically in differential form. Hence PHOENICS solves a finite-volume formulation of the equation. The finite volume equations are obtained by integrating the differential equation over the cell volume and interpolation assumptions are required to obtain scalar values at cell centres and vector quantities at cell faces. After integration the finite volume equations (equation 2.1) take the form at the point P (refer to Figure 2.2):

$$a_P \cdot \phi_P = \sum_{i=N,S,E,W,H,L,Time} a_i \phi_i + \text{source terms} \qquad (2.1a)$$

where: $$a_P = \sum_{i=N,S,E,W,H,L,Time} a_i \qquad (2.1b)$$

The a's take the form:

$$\text{Area} \times \rho \times \text{velocity} + \frac{\text{Area} \times \Gamma}{\text{cell centre to face distance}} + \frac{\rho \times \text{volume}}{\text{time step}}$$

convection term	diffusion term	transient term

Boundary conditions can be input to PHOENICS as linearised sources for cells adjacent to boundaries. They appear on the right hand side of equation 2.1 for a variable ϕ, i.e.

$$\frac{\partial(\rho\phi)}{\partial t} + \nabla \bullet (\rho\phi \mathbf{u}) - \nabla \bullet (\Gamma \nabla\phi) = S\phi + S_{bc1} + S_{bc2} + \ldots + S_{bcn} \qquad (2.2)$$

linear. Boundary conditions are represented in PHOENICS as linearised sources for cells adjacent to walls i.e.

$$S_{bc} = TC(V-\phi) \qquad (2.3)$$

Where T is the TYPE, a geometric multiplier, C is the coefficient and V is the value. As a consequence of the integration procedure, the source is required per cell, which has units ϕ kg/s. The TYPE is used to convert the source *from* any given set of units.

2.3 Data Input to PHOENICS

PHOENICS Input Language (PIL) allows commands input to the pre-processor to become immediately effective.

The specification of boundary conditions requires two kinds of information:

(a) Where and when the boundary is

(b) The values of T, C and V

Where, when and T are defined in a PATCH command i.e.

PATCH(name, type, IXF, IXL, IYF, IYL, IZF, IZL, ITF, ITL)

Where: name is a unique patch name

type is T

IXF, IXL are the first and last IX in the patch, and similar for y, z and time.

The remainder of (b) is specified in a COVAL command i.e.

COVAL(name, variable, coefficient, value)

Where: name is the patch name to which the command refers

variable is a solved-for variable

coefficient is C

value is V

2.4 Boundary Layer Properties in PHOENICS

2.4.1 Laminar Wall Functions

Laminar wall functions do not exist, as the harmonic mean option in the solution procedure does all that is required (i.e. relates to how the diffusion coefficients, or viscosities, are averaged in order to provide the values used in the finite domain equations). Skin friction however must be calculated by the user in the subroutine GROUND.FOR.

2.4.2 Turbulence Modelling

The k - ε turbulence model proposed by Harlow and Nakayama in 1968 is by far the most widely-used two-equation eddy-viscosity turbulence model, mainly because that ε was long believed to require no extra terms near walls. The popularity of the model, and its wide use and testing, has thrown light on both its capabilities and its short comings, which are well-documented in the literature. PHOENICS provides the standard high-Reynolds-number form of the k - ε model, as presented by Launder and Spalding (1974), with inclusion of allowance for buoyancy effects.

For high turbulent Reynolds numbers, the standard form of the k - ε model may be summarised as follows, with i, j denoting the chosen co-ordinate direction:

$$\frac{\partial(\rho k)}{\partial t}+\frac{\partial}{\partial x_i}\left[\rho k U_i-\frac{\rho \nu_T}{\sigma_k}\frac{\partial k}{\partial x_i}\right]=\rho\left(P_k+G_b-\varepsilon\right) \qquad (2.4)$$

$$\frac{\partial(\rho\varepsilon)}{\partial t}+\frac{\partial}{\partial x_i}\left[\rho\varepsilon U_i-\frac{\rho\nu_T}{\sigma_\varepsilon}\frac{\partial\varepsilon}{\partial x_i}\right]=\rho\frac{k}{\varepsilon}\left(C_{1E}P_k+C_{3E}G_b-C_{2E}\varepsilon\right) \tag{2.5}$$

where:

$$\nu_T=C_\mu C_D\frac{k^2}{\varepsilon} \tag{2.6}$$

$$P_k=\nu_T\left(\frac{\partial U_i}{\partial x_j}+\frac{\partial U_j}{\partial x_i}\right)\frac{\partial U_i}{\partial x_j} \tag{2.7}$$

$$G_b=-\nu_t g_i\frac{\frac{\partial\rho}{\partial x_i}}{\rho Pr_T} \tag{2.8}$$

2.4.3 Turbulent Wall Functions

PHOENICS already has built in turbulent wall functions which bridge the viscous sub-layer by employing empirical formulae, to provide near wall boundary conditions for the mean flow and turbulent transport equation. These formulae connect the wall conditions to the dependent variables at the near-wall grid node, thus eliminating the need to continue the computational grid right down to the wall. It also avoids the need to account for viscous effects in the turbulence model.

There are two main types of wall functions provided in PHOENICS, namely:

(1) equilibrium log - wall functions

(2) non - equilibrium log - wall functions

2.4.3.1 Equilibrium log - wall functions

The following wall functions are those appropriate to a near-wall layer in local equilibrium and if U denotes the velocity in the major flow direction then:

$$\frac{U_r}{\upsilon^*} = \frac{\ln(E\,Y^+)}{\kappa} \tag{2.9}$$

$$k = \frac{\upsilon^{*2}}{\sqrt{C_\mu C_D}} \tag{2.10}$$

$$\varepsilon = \frac{C_\mu C_D^{3/4}\, k^{3/2}}{\kappa\, Y} \tag{2.11}$$

Equation (2.9) is the well known law of the wall and strictly speaking should only be applied to a point whose Y^+ is in the range $30 < Y^+ < 130$. The boundary condition for kinetic energy assumes that the turbulence is in local equilibrium and consequently, this set of wall functions is not really suitable under separated conditions, as turbulent energy diffusion towards the wall is significant, leading to appreciable departures from local equilibrium. The wall function defined by equation (2.9) is implemented in the momentum equations by the way of source terms which take the form:

$$S_{momentum} = \rho\, s\, abs(U_r)\,(U_w - U_c) \tag{2.12}$$

The friction factor is determined from:

$$s = \max < s_{turbulent}, s_{laminar} > \tag{2.13}$$

where: $$s_{laminar} = \nu/(U_r\, Y) \tag{2.14}$$

$$s_{turbulent} = \left(\frac{k}{\ln\left(E\left(U_r\, Y / \nu \right) \sqrt{s_{turbulent}} \right)^2} \right) \tag{2.15}$$

2.4.3.2 Non - equilibrium log - wall functions

A generalisation to equation (2.9) was proposed by Launder and Spalding (1974), which takes the form:

$$\frac{U_r \sqrt{k}}{\upsilon^{*2}} = \frac{\ln\left(\frac{E\, C_\mu C_D^{1/4} \sqrt{k}\, Y}{\nu}\right)}{AK\, C_\mu C_D^{1/4}} \tag{2.16}$$

Equation (2.16) is implemented into the momentum equations via equations (2.12) to (2.14), except that $s_{turbulent}$ is now given by:

$$s_{turbulent} = \frac{AK\sqrt{k}\, C_\mu C_D^{1/4}}{U_r \ln\left(\frac{E\, C_\mu C_D^{1/4} \sqrt{k}\, Y}{\nu}\right)} \tag{2.17}$$

The value of the kinetic energy at the near-wall point is calculated from its own transport equation with the diffusion of energy to the wall being set equal to zero. This transport equation contains the production rate, the dissipation rate, and the average rates of these two terms for the near-wall cell are determined by making an analytical integration over the control volume and assuming that the shear stress and kinetic energy are constant across the near-wall cell. The mean value of turbulence energy production over the near wall cell is represented as:

$$k_{production} = \frac{\upsilon^{*2} U_r}{2Y} \tag{2.18}$$

The cell-averaged dissipation rate, appearing in the sink term for the kinetic energy equation is fixed to the following expression:

$$\varepsilon = \frac{C_\mu C_D^{3/4}\, k^{3/2} \ln\left(\frac{E\, C_\mu C_D^{1/4} \sqrt{k}\, Y}{\nu}\right)}{(2\, AK\, Y)} \tag{2.19}$$

Under conditions of local equilibrium, $k_{production}/\varepsilon$ must equal unity, and this may be verified by dividing equation (2.18) by equation (2.19), using equation (2.17), and noting that $s_{turbulent} = \frac{\upsilon^{*2}}{U_r^2}$ and $\upsilon^{*2} = k\sqrt{C_\mu C_D}$.

However, in the formula for the near-wall viscosity, the dissipation rate is calculated using the values at the nodal point given by equation (2.11) above.

2.4.4 Low Reynolds Number Turbulence Modelling

An alternative to wall functions is to use a fine-grid analysis in which computations are extended through the viscosity-affected sub-layer close enough to the wall to allow laminar-flow boundary conditions to be applied. The low-Reynolds-number extension of Lam and Bremhorst (1981) may be applied to the standard k - ε model. It employs a transport equation for the total dissipation rate, with the advantage that the model requires no additional source terms. However, a disadvantage of the model is that one of the damping functions requires the calculation of the local distance to the nearest wall denoted by Y_N.

The Lam - Bremhorst low-Reynolds-number k - ε model differs from the standard high-Reynolds-number model in that the empirical coefficients $C_\mu C_D$, C_{1E} and C_{2E} are multiplied respectively by the functions:

$$F_\mu = \left[1 - \exp\left(-0.0165\,Re_N\right)\right]^2 \left(1 + \frac{20.5}{Re_T}\right) \tag{2.20}$$

$$F_1 = 1 + \left(\frac{0.05}{F_\mu}\right)^3 \tag{2.21}$$

$$F_2 = 1 - \exp\left[-\left(Re_T\right)^2\right] \tag{2.22}$$

where:

$$Re_N = \frac{Y_N \sqrt{k}}{\nu} \quad \text{and} \quad Re_T = \frac{k^2}{\varepsilon \nu}$$

For high-turbulence Reynolds numbers, Re_N or Re_T, the functions F_μ, F_1 and F_2 multiplying the three constants tend to unity. The boundary conditions $k = 0$ and $d(\varepsilon)/dy = 0$ are applied at the wall.

2.5 Inadequacy of k - ε Turbulence Model in Transitional Flows

A trial was carried out using the standard k - ε model with equilibrium wall functions to predict skin friction in transitional, adverse and favourable pressure gradient flows using the Abu - Ghannam and Shaw (1980) data. The predictions were not good even though Y^+ was within the recommended limits ($30 \leq Y^+ \leq 130$) for the favourable pressure gradient case and slightly outside the upper limit (maximum $Y^+ \approx 170$) for the adverse pressure gradient flow, Figures 2.3 - 2.6. The low Reynolds number turbulence model was another alternative and probably would have given better results, but due to the size of the computational grid (40 - 60 computational cells across the boundary layer), limited computer resources and a slow convergence rate, no attempt was made to predict the boundary layer properties using this model.

2.6 Boundary Layer Transition Modelling

A two-dimensional transitional boundary layer model was developed and programmed into PHOENICS through the GROUND subroutine to operate in two different ways:

(1) Based on a free stream velocity distribution obtained from a solved laminar frictionless flow field used to predict transitional boundary layer parameters.

(2) Assuming the boundary layer is a sink of momentum.

Both models use the integral methods of Thwaites (1949) and White (1991) for laminar and turbulent boundary layers respectively. The transition model was the linear combination of the laminar and turbulent boundary layers based on an intermittency distribution of Dhawan and Narisimha (1958). The models have been coded into PHOENICS and work on the z - x plane, with z as the major flow direction. No account was taken of surface roughness because this was a secondary effect.

Model (1) takes the velocity parallel to the surface in the IX + 1 cell and calculates the boundary layer parameters . This method was very fast and will provide a reasonable estimate as to whether a transitional analysis is required. The method does not work well when the radius of curvature of the surface is comparable to the boundary layer thickness. The method takes no account of displacement thickness, therefore the velocity profile will be underestimated, leading to an overestimate of skin friction

Model (2) considered the boundary layer as a sink of momentum thus:

$$\tau_w = -\frac{C_f}{2}\rho W^2 \tag{2.23}$$

Where C_f was calculated in the subroutine GROUND. This was input to PHOENICS, as a retarding force.

$$\tau_w.\text{area} = \rho\frac{C_f}{2}\text{area}.W_c^*(0.0 - W_c) \tag{2.24}$$

Compare with the form $S = TC(V-\phi)$ with $S = \tau_w$.area, T = area, $C = C_f/2.\rho.W_c^*$ and V = 0.0. Note: W_c^* is the current in-cell value of velocity. In a converged solution $W_c = W_c^*$

Equation (2.24) can be attached to a wall in PHOENICS with the following two lines of PIL, for example:

PATCH(WALLW,WEST,1,1,1,1,2,98,1,1)

COVAL(WALLW,W1,GRND,0.0)

This corresponds to a boundary condition on the a WEST wall (IX = 1, IY = 1) and stretching along the z slabs 2 to 98. Note that the coefficient is set equal to GRND. This allows the coefficient, C to be calculated by user defined coding in the subroutine GROUND.FOR.

2.7 Convergence Criteria

The residuals (imbalances in the finite volume equations) are the criteria used in PHOENICS to monitor the convergence of the solution. According to Madhav (1996), for a steady state flow, they are defined at the point P as:

$$\text{error at P} = \sum_{i=N,S,E,W,H,L} a_i(\phi_i - \phi_P) + \text{source terms} \qquad (2.25)$$

This definition of error is extended to the whole field for elliptic cases and if:

$$\frac{\sum_{\text{cells}} |\text{error at P}|}{\text{RESREF}(\phi)} < 1.0 \qquad (2.26)$$

solution for that variable stops. When this criteria is met for all the variables the solution is deemed to be converged.

The value of RESREF is based on the net sum of fluxes for a variable, which can be calculated internally by PHOENICS and takes the value:

$$\text{RESREF}(\phi) = \text{RESFAC} \times \text{TOTFLO}(\phi)/(\text{NX.NY.NZ}) \qquad (2.27)$$

TOTFLO(ϕ) has the following terms for all variables except pressure:

sources $$\sum_{\text{cells sources}} \sum C(V - \phi_P)$$

convection $$\sum_{\text{cells cell}} \sum \left(\max\left[0, (\dot{m}\phi_i)\right]\right)$$

diffusion $$\sum_{\text{cells cell}} \sum \left(\max\left[0, \left(\frac{\Gamma}{\Delta} A(\phi_i - \phi_P)\right)\right]\right)$$

In the convention used above the subscript ***cell*** denotes summation in all directions of the computational cell, whilst the subscript ***cells*** denotes summation of all the computational cells in the domain. The subscript ***sources*** denotes the summation of all the sources in a computational cell. $\dot{m}$ is the mass flow rate and Δ in the diffusion term denotes the cell face to cell centre distance.

For pressure TOTFLO(p1) is:

$$\sum_{\text{cells cell}} \sum \max[0, \dot{m}]$$

The supplementary variable RESFAC acted as a tolerance in equation (2.27). Its default value was 0.01, which meant that the solution had convergence when the errors were 1% of the reference fluxes. On all first runs of computational simulations attempted in this thesis, the variable RESFAC was reset to 0.005, after a converged solution was achieved for RESFAC = 0.01, and the calculations restarted from the previous solution and ran to convergence or at least another 100 iterations which ever came first. In all cases there was no appreciable difference in the predicted properties.

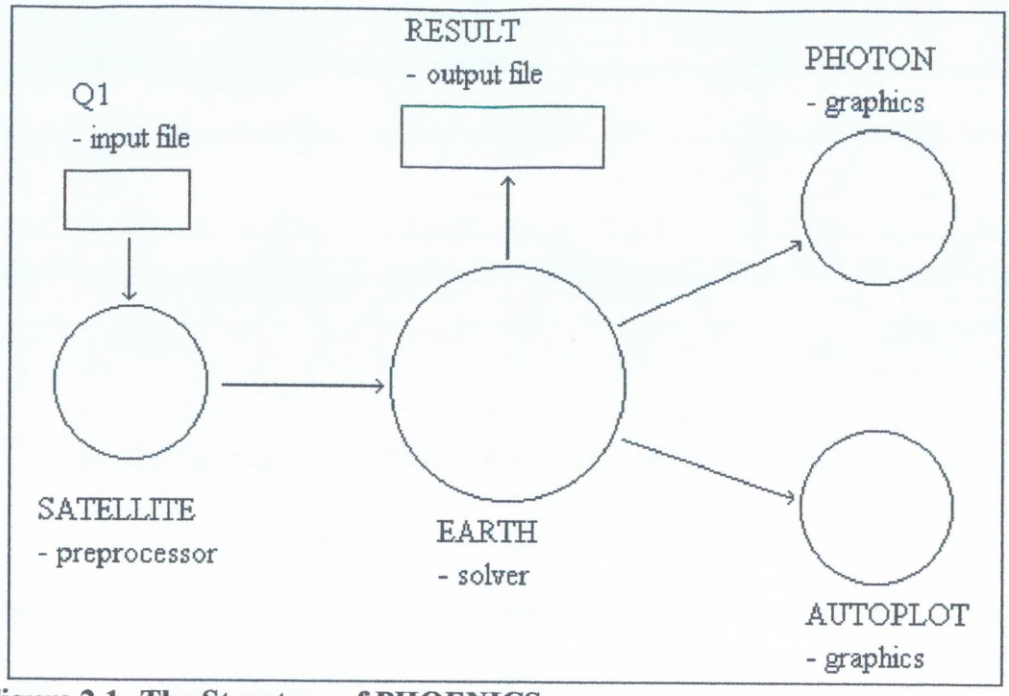

Figure 2.1: The Structure of PHOENICS

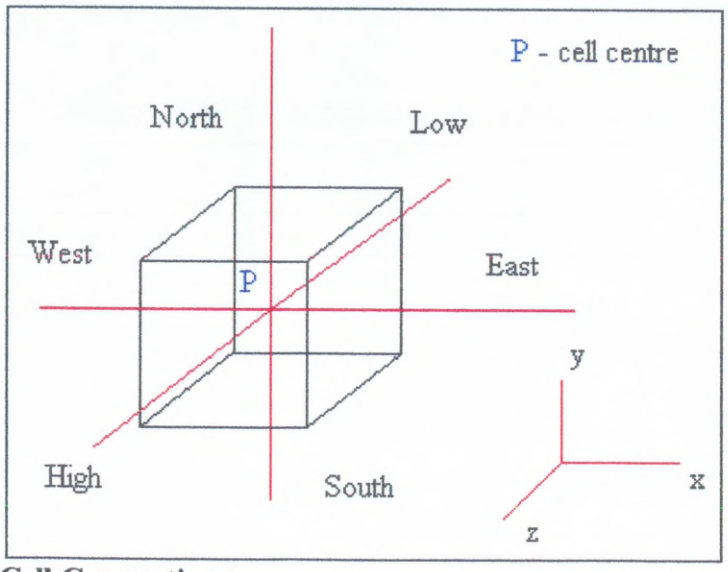

Figure 2.2: Cell Convention

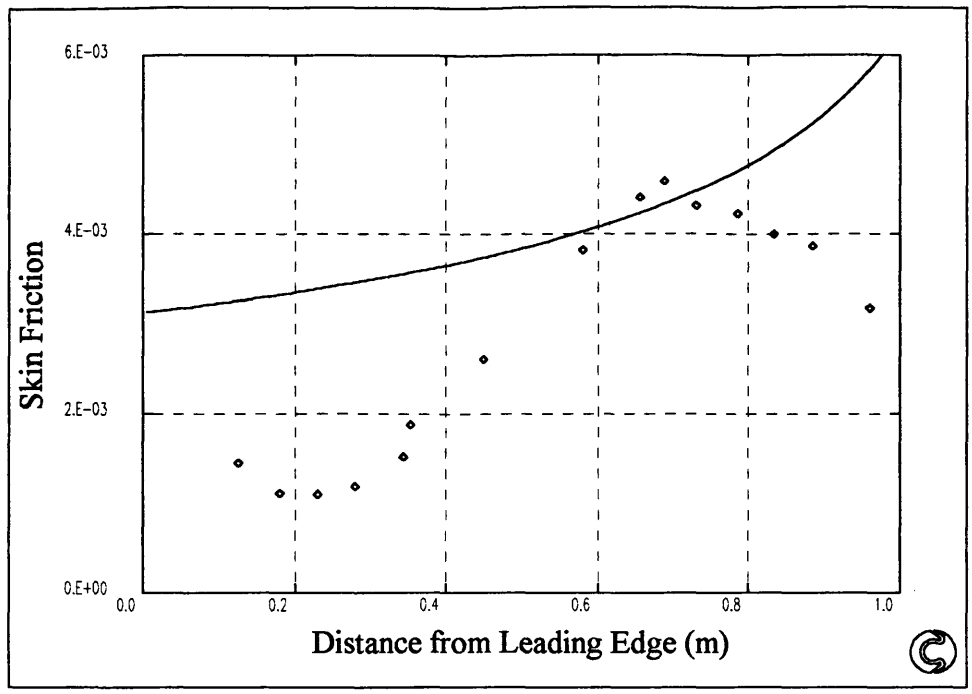

Figure 2.3: Abu-Ghannam & Shaw Adverse dp

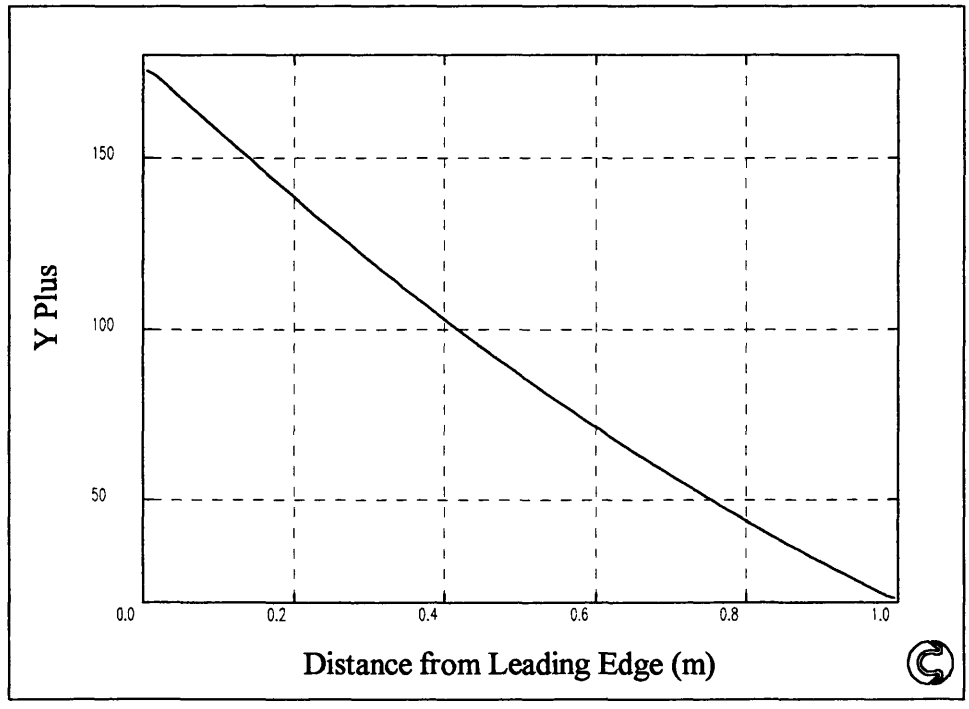

Figure 2.4: Abu-Ghannam & Shaw Adverse dp

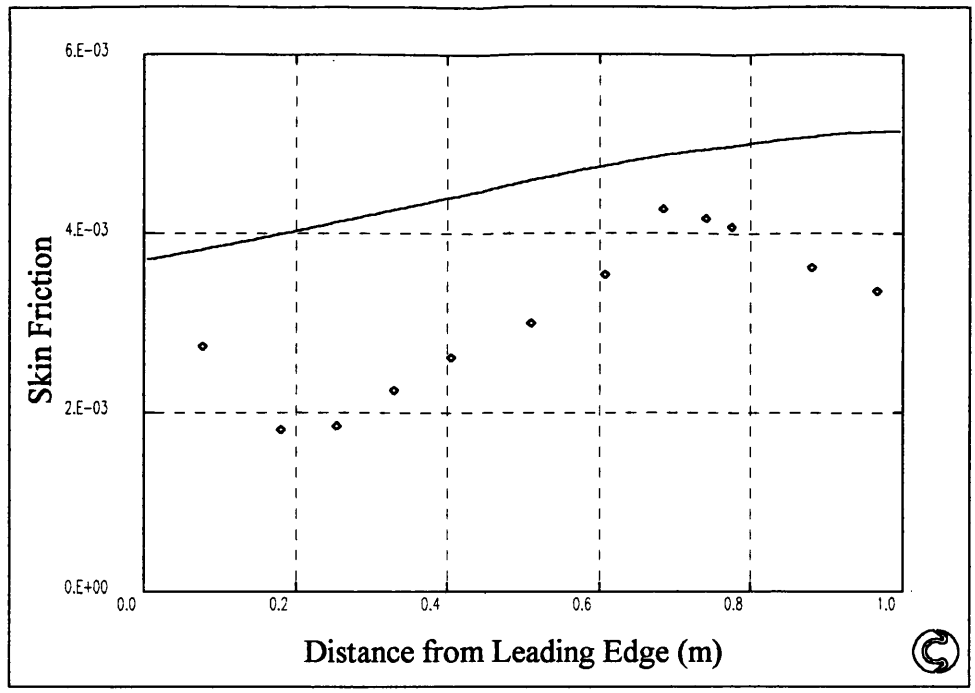

Figure 2.5: Abu-Ghannam & Shaw Favourable dp

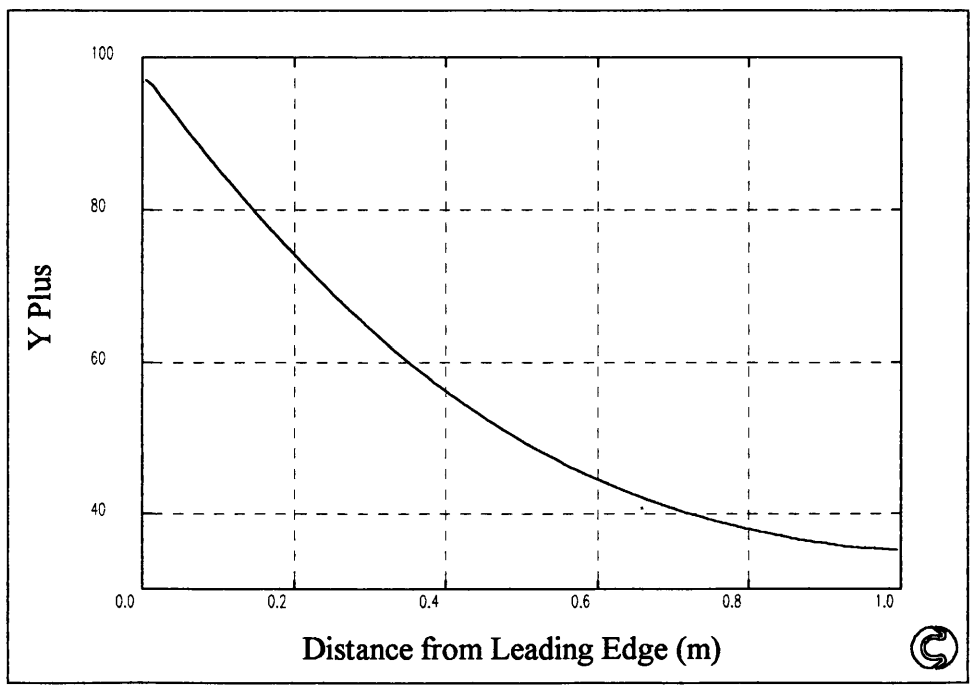

Figure 2.6: Abu-Ghannam & Shaw Favourable dp

3. Boundary Layer Modelling

3.1 Introduction

Today with the ever increasing power of desktop, or even laptop, computers fluid dynamic problems have become relatively easy to solve using readily available computational fluid dynamic packages e.g. STAR-CD, PHOENICS, FLUENT. These codes can solve laminar or turbulent flow fields. Since the majority of engineering type flows are turbulent, a great emphasis has been placed on turbulence modelling, and a number of turbulence models have been incorporated into these codes ranging from the simple and computationally efficient zero equation constant viscosity model to the complex, computationally expensive low Reynolds number models as already discussed in Chapter 1. In this thesis boundary layer parameters were predicted using integral methods, based on the freestream velocity profile.

3.2 Laminar Boundary Layers

The method that was used to predict the laminar boundary layer properties is attributable to Holstein and Bohlen (1940) which was modified and improved by Thwaites (1949). This method was later extended by Dey and Narasimha (1990).

3.2.1 The Correlation Method of Thwaites

Thwaites showed that the momentum thickness of all types of laminar boundary layers could be predicted accurately (±3 %), by:

$$\theta = \left(\frac{0.45\nu}{W^6} \int_0^z W^5 dz \right)^{0.5} \tag{3.1}$$

Thwaites defined the parameter, m as:

$$m = \frac{\theta^2}{\nu}\frac{dW}{dz} \tag{3.2}$$

Holstein and Bohlen (1940) suggest that a shear-factor and shape-factor correlation can be written in terms of a single parameter, m

$$S(m) = \frac{\tau_w \theta}{\mu W} \tag{3.3}$$

$$H(m) = \frac{\delta^*}{\theta} \tag{3.4}$$

A simple and accurate curve fit was proposed by Thwaites' (1949) for the shear function S(m), viz.

$$S(m) \approx (m + 0.09)^{0.62} \tag{3.5}$$

White (1991) proposed the following polynomial curve fit for H(m):

$$H(m) \approx 2.0 + 4.14z - 83.5z^2 + 854z^3 - 3337z^4 + 4576z^5 \tag{3.6}$$

where $z = (0.25 - m)$

White (1991) states that the accuracy of Thwaites method is about ± 5% for favourable or mild adverse pressure gradients, but may be as much as ± 15% near the separation point. It can however be regarded as one of the better available one-parameter methods. The major limitation of Thwaites method is that the range of values for the pressure gradient parameter, m, must be less than 0.25. It was found, for the flows considered here, that the simple rectangular integration method was sufficient to give accurate results when integrating equation (3.1).

3.2.2 An Extension to Thwaites' Method

Dey and Narasimha (1990) proposed an extension to Thwaites method to allow the pressure gradient parameter m to reach values as high as 0.4. They went on to

$$-0.082 \leq m \leq 0.4$$

An improved approximation to θ in highly favourable pressure gradients may be obtained by using the expression:

$$\theta^2 = \left(\frac{0.45\nu}{W^6}\right)\left\{\int_0^z W^5\,dz + 0.9\int_0^z\left[(W'^2/W^7)\left(\int_0^z W^5\,dz\right)^2\right]dz\right\} \qquad (3.7)$$

The proposed variation of boundary layer thickness/momentum thickness, H_δ with m can be approximated by the following expressions:

$$H_\delta \approx 7.85 + 2.8(1 - \exp(-750m^3)), \qquad 0 \leq m \leq 0.4 \qquad (3.8)$$

$$H_\delta \approx 7.85 + 10.5m + 232.14m^2, \qquad -0.082 \leq m \leq 0.0 \qquad (3.9)$$

The proposed variation of shape factor, H with pressure gradient parameter, m can be approximated by the following expressions:

$$H^{-1} \approx 0.385 + 0.37m + 0.073m^{1/2}, \qquad 0.0 \leq m \leq 0.4 \qquad (3.10)$$

$$H^{-1} \approx 0.385 + 0.44m - 13.26m^2, \qquad -0.082 \leq m \leq 0.0 \qquad (3.11)$$

The skin friction coefficient can be approximated by:

$$HW\theta C_f/2\nu \approx 0.57 + 0.51mH^2, \qquad -0.082 \leq m \leq 0.4 \qquad (3.12)$$

3.3 Turbulent Boundary Layer

The method that was used to predict the turbulent boundary layer properties is attributable to White (1991). The method uses the von Kármán (1911) momentum relation, combined with a suitable correlation between the wake parameters Π and β.

The momentum integral relation is:

$$\frac{d\theta}{dz} + (2+H)\frac{\theta}{W}\frac{dW}{dz} = \frac{C_f}{2} \qquad (3.13)$$

By re-arranging the integral parameters of Coles (1968), wall-wake law:

$$\lambda_t = a(\Pi)\frac{H-1}{H} \qquad \text{where} \quad a(\Pi) = \frac{2+3.179\Pi+1.5\Pi^2}{\kappa(1+\Pi)} \tag{3.14}$$

$$Re_\theta = \frac{1+\Pi}{\kappa H}\exp(\kappa\lambda_t - \kappa B - 2\Pi) \tag{3.15}$$

where $\lambda_t^2 = 2/C_f$: $\kappa = 0.41$: $B = 5.5$

White showed that elimination of Π from (3.14) and (3.15) yields a unique relation between C_f, H and R_θ, and the result of which can be curve fit by the following relation:-

$$C_f = \frac{0.3\exp(-1.33H)}{(\log_{10} Re_\theta)^{1.74+0.31H}} \tag{3.16}$$

A simple way to close the von Kármán - type integral method is an approximate correlation between Coles' (1968) wake parameter and the Clauser (1954) parameter β.

$$\beta = -\lambda_t^2 H\frac{\theta}{W}\frac{dW}{dz} \tag{3.17}$$

Das (1987) proposed the following polynomial correlation:

$$\beta \approx -0.4 + 0.76\Pi + 0.42\Pi^2 \tag{3.18}$$

There are now enough equations to close the method. Using initial values for skin friction coefficient and momentum thickness it is possible to predict using an iterative procedure, the shear stress coefficient, the displacement and momentum thicknesses. The bisection method was chosen as the iterative procedure as an upper and lower limit could be specified for shape factor, thus eliminating instabilities when the shape factor was outside the range $1.0 \leq H \leq 3.5$, and the Euler method was used to integrate equation (3.13). The method, like all integral techniques, requires that the free stream velocity distribution be prescribed.

According to White, this method makes adequate predictions for both favourable and adverse pressure gradients, but no comparisons were given. In order to validate the method, predictions were made of skin friction, momentum thickness and shape factor and compared against data compiled by Coles and Hirst (1968) for favourable (ID 1300), zero (ID 1400) and adverse (ID 1100) pressure gradient flows. The predictions can be described as reasonably good in all pressure gradient flows (Figures 3.1 - 3.9).

Head (1958) defined a new shape factor:

$$H_1 = \frac{(\delta - \delta_1)}{\theta} \tag{3.19}$$

who then showed that H_1 was related to the standard shape factor H. The relationship was later curve-fit by the following formulae:

$$H_1 \approx \begin{cases} 3.3 + 0.8234(H - 1.1)^{-1.287} & \text{for } H \leq 1.6 \\ 3.3 + 1.5501(H - 0.6778)^{-3.064} & \text{for } H \geq 1.6 \end{cases} \tag{3.20}$$

Thus it was now possible to determine the turbulent boundary layer thickness.

3.4 Transition to Turbulence

The linearised stability theory predicts the demise of laminar flow at some finite Reynolds number, it does not predict the onset of turbulence. After the initial breakdown of laminar flow through the amplification of infinitesimal disturbances, the initial instability will grow as a two-dimensional Tollmein-Schlicting wave, travelling in the main flow direction if the flow is incompressible. However, three-dimensionality soon appears as the Tollmein-Schlichting waves begin to rapidly show spanwise and vertical variations. These variations continue to grow and the longitudinal vortices begin a cascading breakdown into smaller units, until the relevant frequencies and wave numbers are approaching randomness. In this

diffusely fluctuating state, intense local changes occur at random times and locations in the flow near the wall. A turbulent spot is thus 'born' and continues to grow, spread and finally coalesce with other spots to form a completely turbulent flow field.

3.4.1 Prediction of Transition Onset

The start of transition does not coincide with the beginning of laminar instability. It can be defined as the region at which the laminar boundary layer parameters begin to deviate from their typical laminar parameters. This point is influenced by: free stream turbulence, pressure gradient, Mach number, surface curvature and Reynolds number.

3.4.1.1 Semi-Empirical Approach

Smith and Gamberoni (1956) and Van Ingen (1956) derived (simultaneously and independently) the e^n method, which proposes that the total amplification ratio of initial disturbances, as computed by linear stability theory at the observed position of transition, was roughly equal for all cases investigated ($A_{recrit} \approx e^9$). e^n methods are time consuming and are only applicable for low free stream turbulence levels ($q < 0.2\%$).

Experimental data shows that for laminar boundary layers developing below a turbulent free stream, the fluctuating velocities within the layer increase in amplitude until some critical value is reached, which initiates transition. Johnson (1994) derived a parameter to predict the development of the velocity fluctuations and proposes the start of transition can be adequately predicted by:

$$Re_{\theta s} = 0.96\left(1+\frac{\lambda_p}{12}\right)\frac{\theta}{\delta}\left(6\times10^{-8}q+6\times10^{-2}\left(q/100\right)^4\right)^{-1/2} \tag{3.21}$$

for $-0.01 \le m \le 0.01$ and $0.2\% \le q \le 5\%$, where λ_p is the Pohlhausen parameter. This model does not take into account the flow history and the relevant value of turbulence intensity to use would be the local value.

3.4.1.2 Empirical Approach

Empirical methods are based on the assumption that the start of transition can be determined, usually as a function of some free stream parameters e.g. turbulence intensity, pressure gradient. Still popular is the Abu-Ghannam and Shaw (1980) correlation which states that the start of transition is a function of free stream turbulence intensity, pressure gradient and flow history. The location of the start of transition was based on the position where a rapid increase in surface velocity was measured by a hot wire anemometer. The start of transition can be alternatively defined as the location where the turbulence intermittency first attains a non-zero value, say 1%.

$$R_{\theta s} = \left[163+\exp\left[g(m)\left[1-\frac{q}{6.91}\right]\right]\right] \tag{3.22}$$

More recent correlations include Mayle (1991) who suggests that for the start of transition, when $q \ge 3\%$, the momentum thickness Reynolds number need only exceed:

$$Re_{\theta s} = 400q^{-5/8} \tag{3.23}$$

A result similar to this was previously obtained by Hourmouziadis (1989) who gave values of the coefficient and exponent as 460 and -0.65 respectively.

3.5 Transition Model

An appropriate transition model should be easy to use, computationally inexpensive and likely to provide accurate results for all transitional flow situations.

The linear combination transition region model combines estimates of turbulent flow field quantities and laminar flow field quantities. The proportion of each quantity is weighted by the intermittency distribution. This kind of transition model can be traced to Emmons (1951) and his classic work on turbulent spots.

3.5.1 Start of Transition

A correlation which has been used extensively in both zero and non-zero pressure gradient flows is attributable to Abu-Ghannam and Shaw (1980). A comparative study was carried out by Fraser, Higazy and Milne (1994) which appeared to indicate that the momentum thickness Reynolds number at the position where turbulence intermittency first attained a non-zero value was about 85 per cent of the value given by equation (3.22):

$$R_{\theta s} = 0.85\left[163 + \exp\left[g(m)\left[1 - \frac{q}{6.91}\right]\right]\right] \tag{3.24}$$

Where:

$$g(m) = 6.91 + 2.48m - 12.27m^2 \qquad \text{for } (m > 0) \tag{3.25}$$

$$g(m) = 6.91 + 12.75m + 63.64m^2 \qquad \text{for } (m < 0) \tag{3.26}$$

3.5.2 Length of Transition

According to Narasimha (1985) the most appropriate non-dimensional turbulent spot formation parameter N is:-:

$$N = \frac{n\sigma\theta_s^3}{\nu} \tag{3.27}$$

This was shown to give a transition length correlation based on the momentum thickness at the start of transition:

$$R_\lambda = \left(0.411\frac{R_{\theta s}^3}{N}\right)^{0.5} \tag{3.28}$$

Fraser, Higazy and Milne (1994) proposed the following functions for N for zero, adverse and favourable pressure gradient flows:

$$N_o \times 10^3 = \frac{47.23}{(10 - \exp(1.7 - q/2))^2} \tag{3.29}$$

$$N = N_o \exp[m(1 - 55m^2)(2.6q + 3.6q^{0.5} - 86)] \tag{3.30}$$

$$N = N_o\left[\exp(-10m^{0.5}) + 300m^4\right] \tag{3.31}$$

They propose an alternative method to calculate transition length. It was assumed that the calculated transition length does not solely depend on the parameters at the start of transition, but is averaged over the flow distance where the turbulence intermittency $0 < \gamma < 0.25$:

$$\lambda_{av} = \left(\frac{1}{z_s}\right)\int_{z_\gamma=0}^{z_\gamma=0.25} \lambda\, dz_s \tag{3.32}$$

Gostelow, Blunden and Walker (1994) proposed an alternative correlation for zero and adverse pressure gradients:

$$N = 0.86 \times 10^{-3} \exp\left(2.134m_s \ln(q_s) - 59.23m_s - 0.564\ln(q_s)\right) \tag{3.33}$$

3.5.3 Intermittency Distribution

Narasimha (1957) showed that when the transition zone model of Emmons (1951), was modified by the concentrated breakdown hypothesis, the resulting function gave a good description of the experimental streamwise intermittency distributions viz.:

$$\gamma = \begin{cases} 1 - \exp\left[-(z - z_s)\ n\sigma / W\right] & (z \geq z_s) \\ 0 & (z < z_s) \end{cases} \tag{3.34}$$

Defining transition length in terms of $\lambda = z|_{\gamma = 0.75} - z|_{\gamma = 0.25}$ leads to Narasimha's universal intermittency distribution:

$$\gamma = 1 - \exp\left(\frac{-0.411(z - z_s)^2}{\lambda^2}\right) \tag{3.35}$$

Gostelow, Melwani and Walker (1995) showed through experiments that the spot spreading angle α and the propagation parameter σ varies significantly with pressure gradient parameter m ($m < 0$). This unexpectedly large variation clearly invalidates the assumption, e.g. Chen and Thyson (1971) and Mayle (1991), that spot propagation characteristics should not vary significantly with pressure gradient through the transition region. The following tentative correlations for the variation of α and σ with m were made by Solomon Walker and Gostelow (1995) from the data assembled by Gostelow, Melwani and Walker (1995):

$$\alpha = 4 + \left(22.14 / \left(0.79 + 2.72\exp\left(47.63 m_s\right)\right)\right) \tag{3.36}$$

$$\sigma = 0.03 + \left(0.37 / \left(0.48 + 3.0\exp\left(52.9 m_s\right)\right)\right) \tag{3.37}$$

According to Solomon, Walker and Gostelow (1995) correlations (3.36) and (3.37) should allow for the influence of free-stream turbulence, and pressure

gradient. However, at present, only pressure gradient is represented since the available data for turbulence level variation are too sparse.

Solomon, Walker and Gostelow (1995) propose a new intermittency distribution whose basic features are as follows:

(a) the concentrated hypothesis of Narasimha is retained;

(b) the spot inception rate is assumed to depend only on the local conditions at transition onset;

(c) the spreading rate of turbulent spots is allowed to vary continuously through the transition zone in response to changes in local pressure gradient parameter m.

Incorporating the new assumptions into the original Chen - Thyson (1971) formulation leads to the following intermittency distribution:

$$\gamma = 1 - \exp\left[-n\int_{z_s}^{z}\frac{\sigma W^{-1}}{\tan(\alpha)}dz\int_{z_s}^{z}\tan(\alpha)dz\right] \tag{3.38}$$

The value of the spot inception rate, n, is inferred from equation. (3.33) and equation (3.31) by using the local value of m at transition onset z_t. The values of α and σ are obtained from equation. (3.36) and equation. (3.37) using the local value of pressure gradient parameter from the laminar component of the linear combination integral computation. This implies that the spot propagation parameters respond instantaneously to changes in pressure gradient, although some lag must be expected in practice.

The basis of a linear combination prediction method is centred on the assumption that the transitional mean velocity can be represented as the intermittency

weighted average of the separate laminar and turbulent boundary layers. The origin of the turbulent boundary layer starting at $z = z_s$.i.e.

$$w_t = (1-\gamma)w_L + \gamma w_T \tag{3.39}$$

The displacement thickness and skin friction can be expressed in a similar manner:

$$\delta_t^* = (1-\gamma)\delta^*_L + \gamma\delta^*_T \tag{3.40}$$

$$C_{f_t} = (1-\gamma)C_{fL} + \gamma C_{fT} \tag{3.41}$$

Evaluation of the momentum thickness, equation (3.42), requires both the laminar and turbulent velocity profiles in the transition region to be fully specified.

$$\theta_t = \gamma(1-\gamma)\int_0^{\delta}\left[w_L(1-w_T) + w_T(1-w_L)\right]dz + (1-\gamma)^2\theta_L + \gamma^2\theta_T \tag{3.42}$$

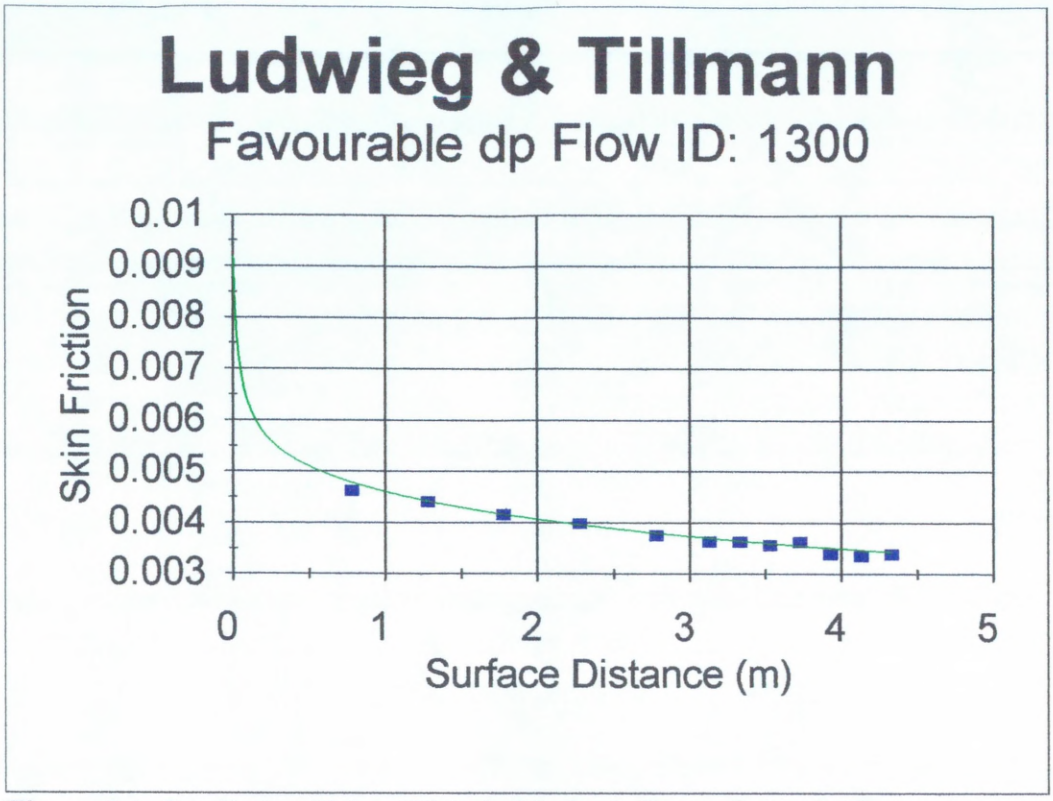

Figure 3.1: Prediction Using White's Method. Data: Coles & Hirst

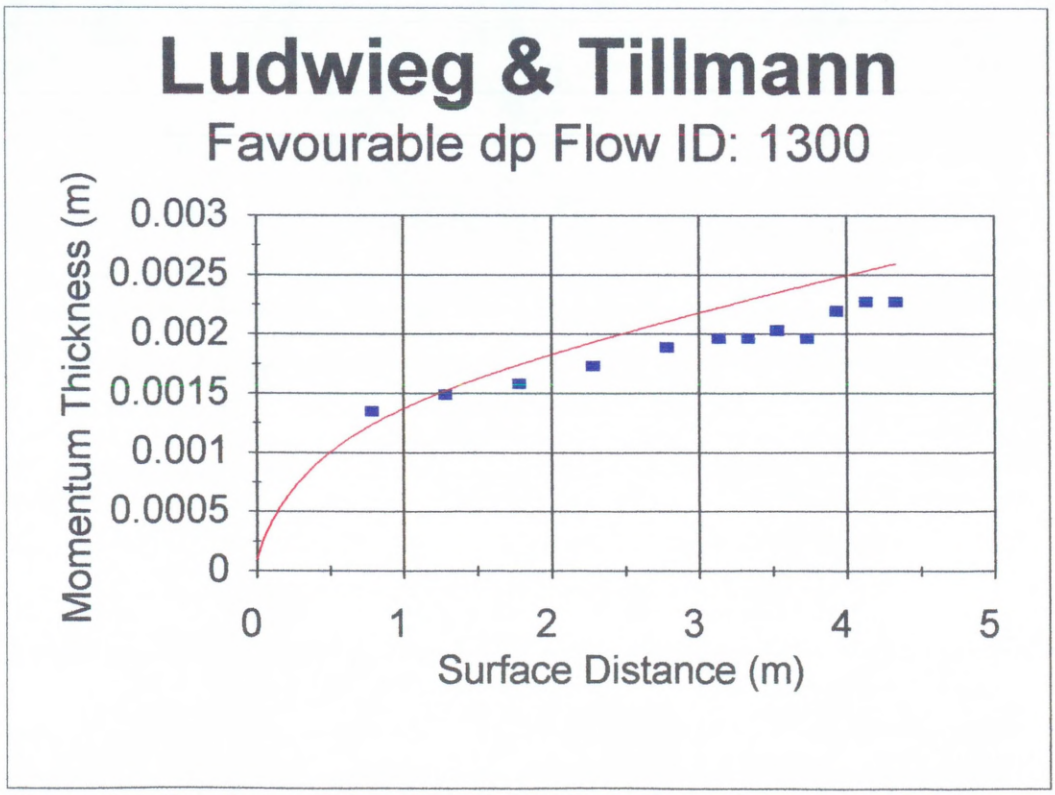

Figure 3.2: Prediction Using White's Method. Data: Coles & Hirst

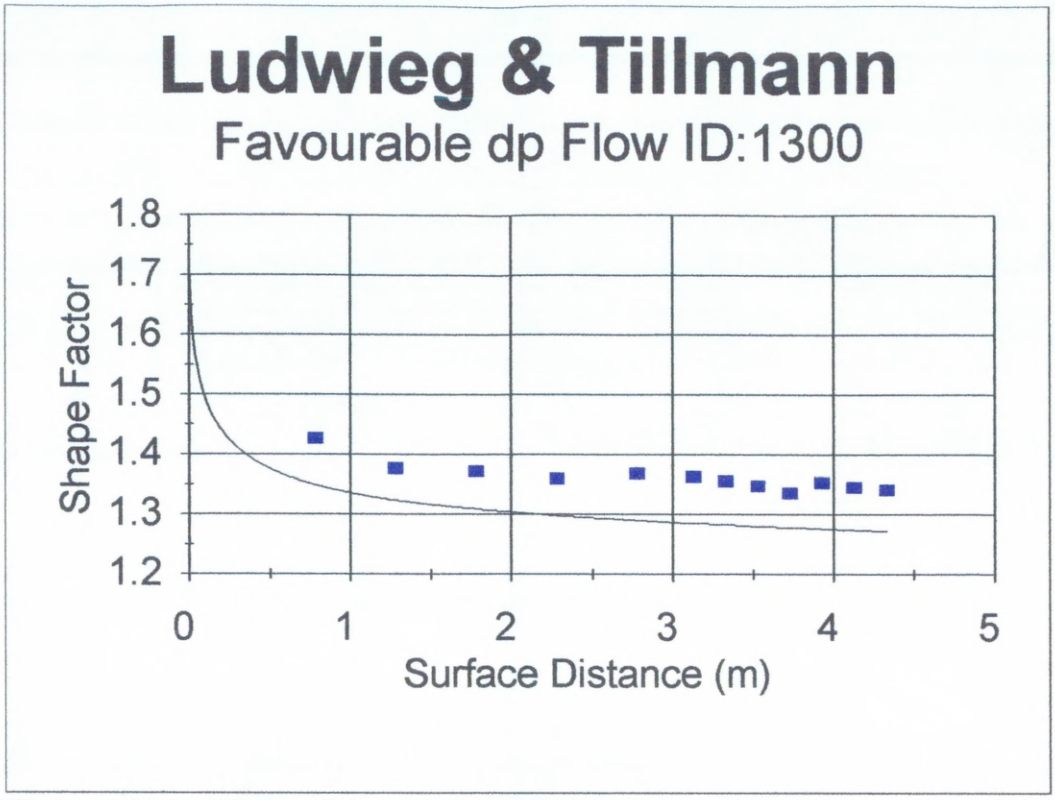

Figure 3.3: Prediction Using White's Method. Data: Coles & Hirst

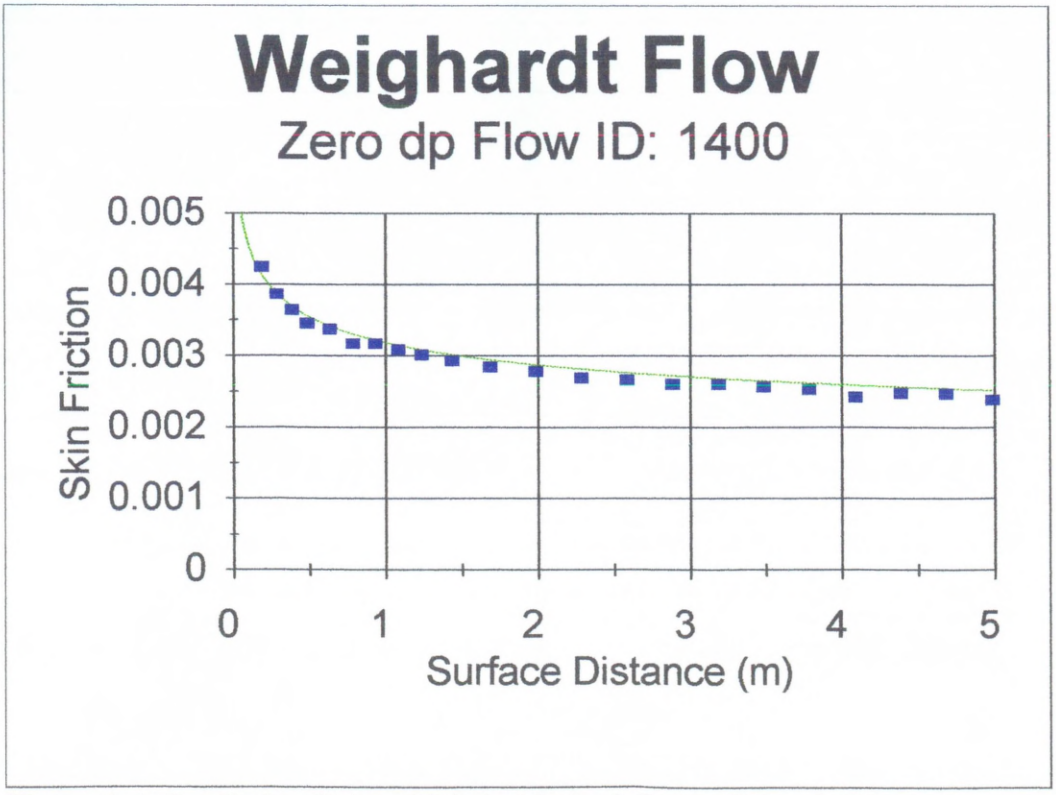

Figure 3.4: Prediction Using White's Method. Data: Coles & Hirst

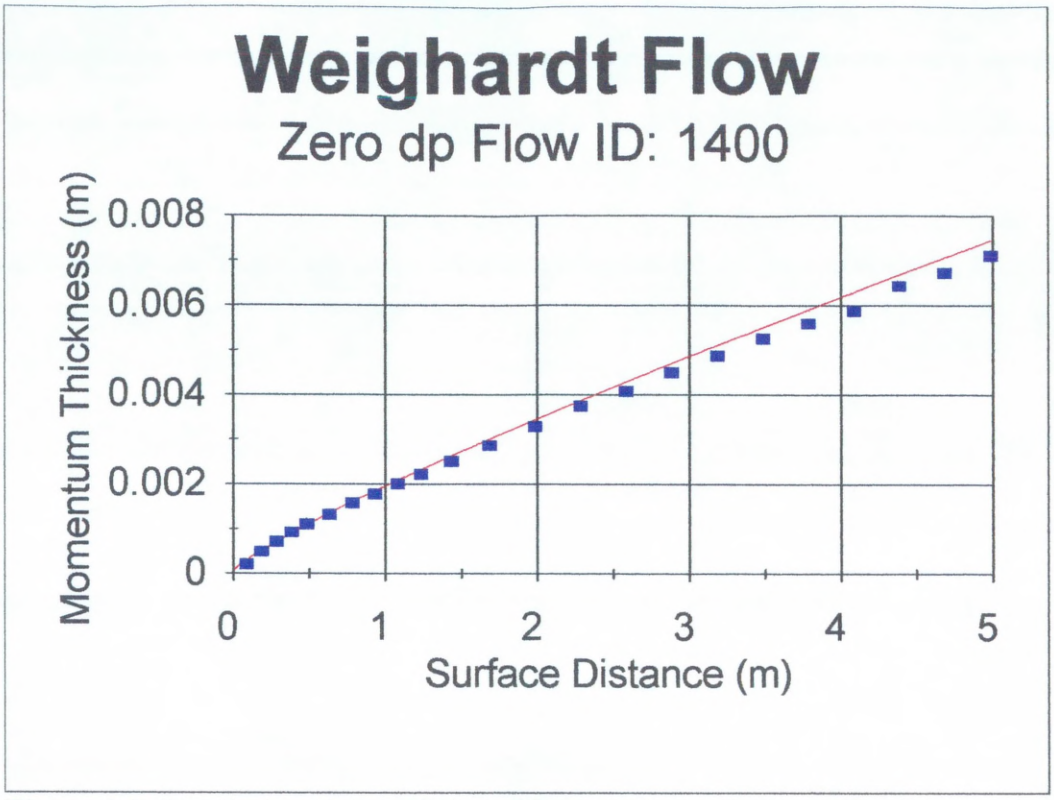

Figure 3.5: Prediction Using White's Method. Data: Coles & Hirst

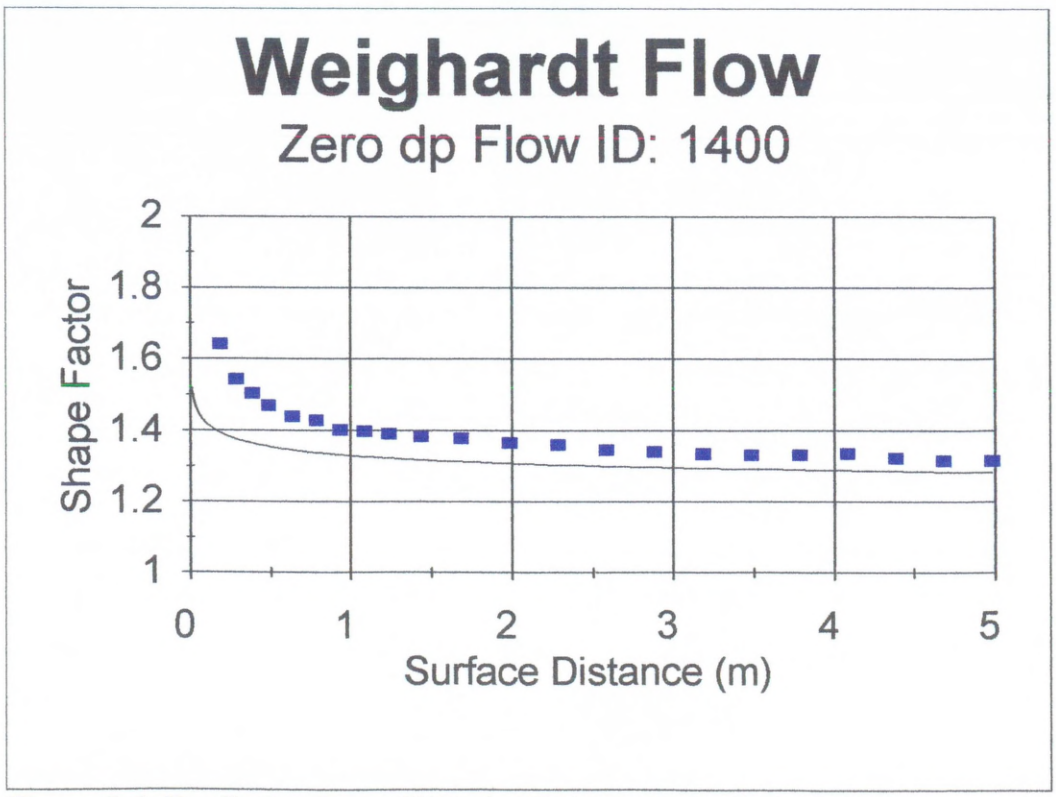

Figure 3.6: Prediction Using White's Method. Data: Coles & Hirst

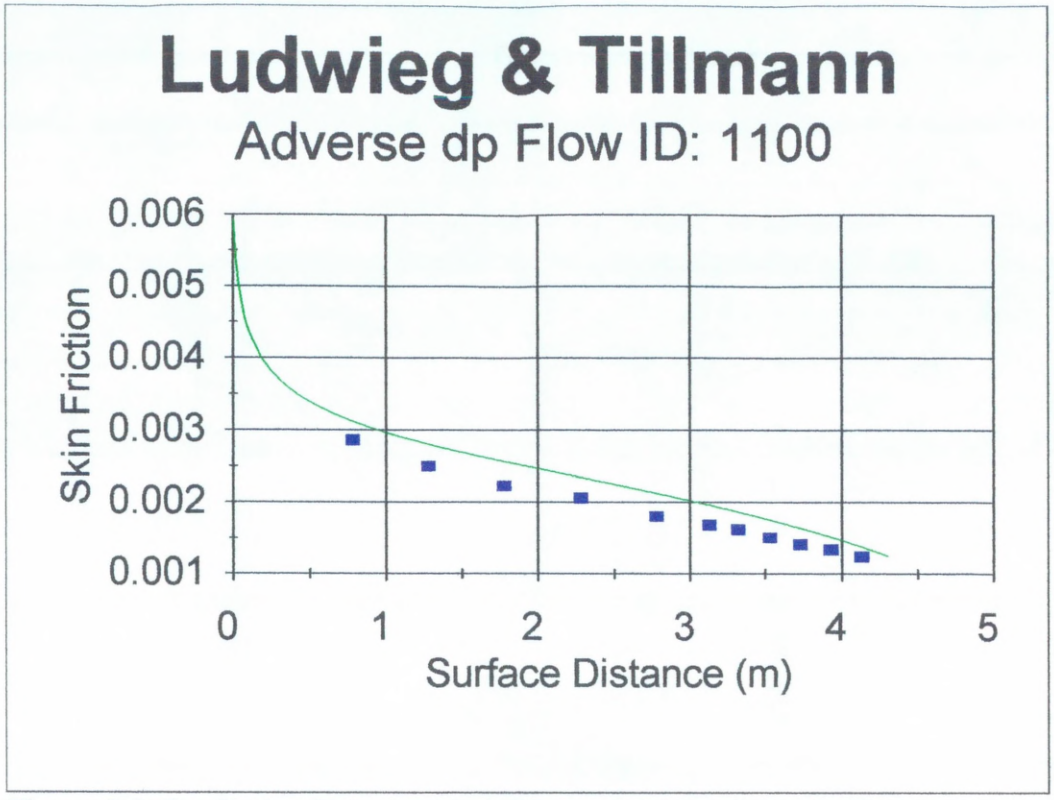

Figure 3.7: Prediction Using White's Method. Data: Coles & Hirst

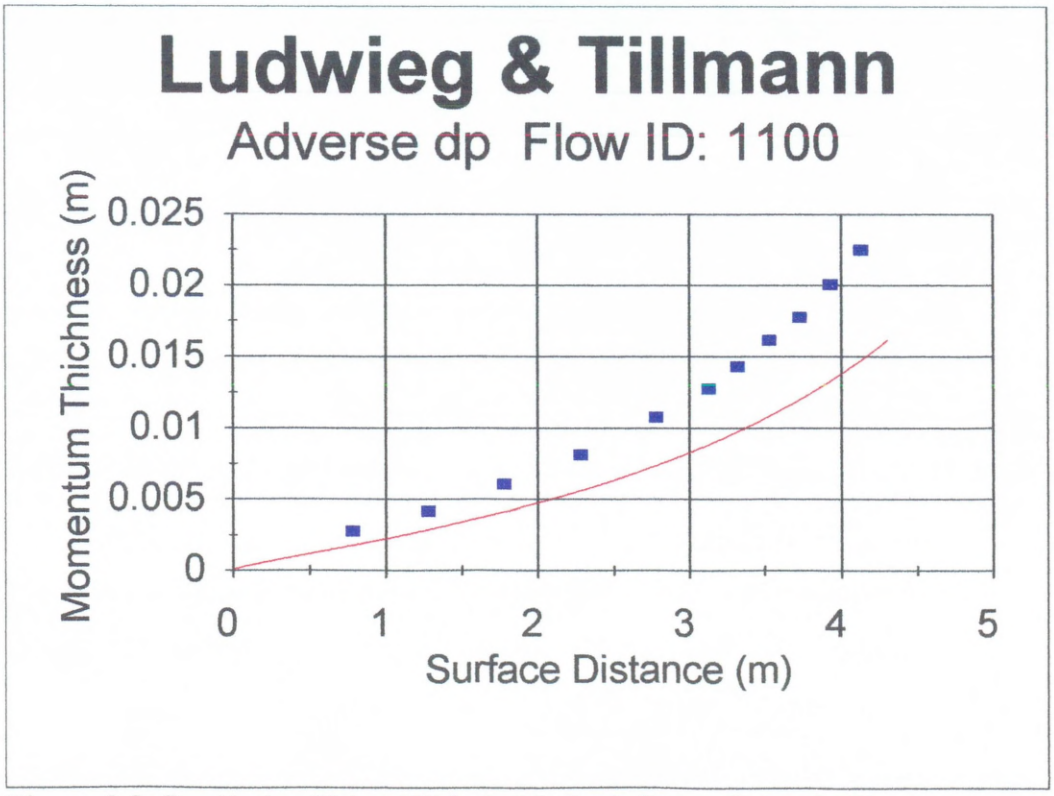

Figure 3.8: Prediction Using White's Method. Data: Coles & Hirst

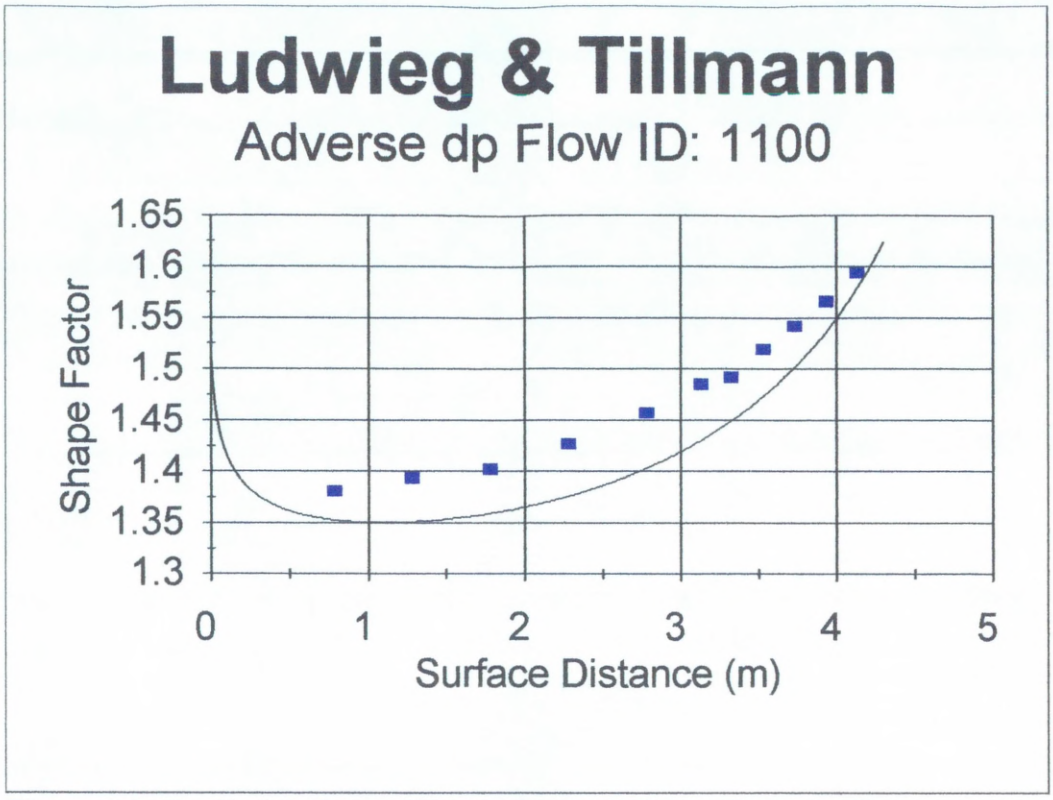

Figure 3.9: Prediction Using White's Method. Data: Coles & Hirst

4. Model Testing

4.1 Quick Basic Program

Before any boundary layer modelling was attempted in PHOENICS a program was written in Microsoft Quick Basic, see Appendix A, (TRANSIT7.BAS) to provide a basis for comparison with the PHOENICS coding. The boundary layer transitional model recommended by Fraser, Higazy and Milne (1994) was programmed and later, for adverse pressure gradient flows, the intermittency distribution was changed to that of Solomon, Walker and Gostelow (1995) (TRANSIT8.BAS). All that was required to be input to the program was a free stream velocity distribution. The model was run, and the predictions of skin friction and intermittency were compared with Abu-Ghannam and Shaw (1980) adverse, favourable and zero pressure gradient flow data. Figures 4.1 - 4.8 show that skin friction and transition length are predicted quite well in adverse, favourable and zero pressure gradient flows, but the start of transition was always predicted early. Figures 4.9 and 4.10 show a slight increase in the length of transition.

Blair and Werle (1981) published plots of transitional Stanton number for flows over a heated flat plate, with an unheated length of 0.043 m at the leading edge in favourable pressure gradient flows. This data was available in digitised form Singer (1991). The program TRANSIT7.BAS was used to predict the skin friction in these cases and the Stanton number for laminar and turbulent flow suggested by Blair was:

$$St\,Pr_L^{2/3} = 0.453\,Re_z^{-1/2}\left[1-\left(\xi/z\right)^{3/4}\right]^{-1/3} \tag{4.1}$$

where ξ was the unheated length.

$$St = \frac{C_f/2}{Pr_T(C_f/2)^{1/2} + (Pr_T - P_s)} \tag{4.2}$$

where: $$P_s = \frac{8.23}{Pr_T}\left[\left(\frac{Pr_L}{Pr_T}\right)^{3/4} - 1\right]\left[1 + 0.28\exp\left(-0.007\frac{Pr_L}{Pr_T}\right)\right]$$

and $Pr_L = 0.71$ and $Pr_T = 0.9$

Correlations (4.1) and (4.2) were found to give good prediction of Stanton number in flow 1 and flow 2 (Figures 4.11, 4.12) but not in flow 3, 5 and 6. It was found that a reasonable prediction of the laminar Stanton number could be achieved if correlation (4.3), which assumes that the whole plate was heated was used (Figures 4.13, 4.14, 4.15).

$$St = 0.332\,Pr_L^{-2/3}\,Re_z^{-1/2} \tag{4.3}$$

Similarly using the Taylor-Prandtl modification to the Reynolds analogy in flow 5 and flow 6 (Figure 4.12, 4.13) gave a reasonable prediction of the turbulent Stanton number.

$$\frac{C_f}{2} = St\left[1 + 5\sqrt{\frac{C_f}{2}}(Pr_T - 1)\right] \tag{4.4}$$

A better prediction of turbulent Stanton number in flow 3 (Figure 4.11) was achieved if the von-Kármán-Boelter-Martinelli extension was used in conjunction with the Reynolds analogy:

$$\frac{C_f}{2} = St\left[1+5\sqrt{\frac{C_f}{2}}(Pr-1)+\ln\left(\frac{5}{6}Pr+\frac{1}{6}\right)\right] \tag{4.5}$$

The start of transition is quite well predicted in zero pressure gradient flows 1, 2 and 3. In the mildly accelerating flow 5, the start of transition is predicted early. In the strong favourable pressure gradient flow 6 the start of transition is predicted very early.

It was decided to discontinue using the Blair and Werle (1981) data, as good or bad predictions of Stanton number could be made depending on the correlation used.

4.2 Transition Model in PHOENICS

The transition model was chosen to operate in the z - x plane in PHOENICS, with z as the major flow direction, because this was the only way that cyclic boundaries can be used in PHOENICS. This was an essential feature if the transition model was to be used to predict boundary layer properties in flows over gas turbine blading. This involved a slight error in the predictions of skin friction, displacement thickness and intermittency. This was due to the fact that these properties were treated as scalars and were hence stored at cell centres. However the prediction method uses the downstream velocity at the cell face, to calculate boundary layer properties. The transition model attributable to Fraser, Higazy and Milne (1994), for both favourable and adverse pressure gradient flows, was written in FORTRAN 77 and programmed into GROUP 19 SECTION 6 of the PHOENICS user accessible subroutine GROUND.FOR and operated on a solved frictionless laminar flow field i.e. a post processing model.

In order to validate the model within PHOENICS, skin friction and intermittency predictions would be made using the Abu-Ghannam and Shaw (1980) data and the TRANSIT7.BAS predictions.

It was clear that when compared with Figures 4.1 and 4.2, the prediction of skin friction and intermittency using the free stream velocity distribution predicted by PHOENICS (Figure 4.16 and 4.17) showed that there was no difference between the TRANSIT7.BAS and PHOENICS output using a solved laminar frictionless flow field. However this method assumes that the boundary layer displacement thickness will have no effect on the free stream velocity profile predicted by a non-frictional analysis.

PHOENICS has the ability to take into account a boundary layer in the flow field by assuming that it acted as a sink of momentum attached to a wall. All that was required to be done was to calculated the skin friction from the free stream velocity profile (either laminar, turbulent or transitional) depending on axial position. This was converted by PHOENICS to a shear stress and hence a retarding force at the wall. The model took the free stream velocity to be in the second computational cell from the wall in the transverse direction. The cell next to the wall contained a velocity, which represents the average flow in the boundary layer.

Two transition models were coded into GROUP 13, SECTION 1 (Appendix B) of the user accessible subroutine GROUND.FOR: the method suggested by Fraser, Higazy and Milne (1994) for both favourable and adverse pressure gradients, and the method described by Solomon, Walker and Gostelow (1995) for adverse pressure gradient.

The predictions of skin friction and intermittency from the momentum sink models and the solved laminar frictionless flow field were compared in Figures 4.18 and 4.19 for the Abu-Ghannam and Shaw (1980) adverse pressure gradient flow and Figures 4.20 and 4.21 for favourable pressure gradient. It was clear that there was practically no difference in the prediction of skin friction or intermittency using the Fraser, Higazy and Milne (1994) method in the post processing model or the momentum sink model, in both favourable and adverse pressure gradient. In the adverse pressure gradient case Solomon, Walker and Gostelow (1995), predicted skin friction and intermittency better as with the Microsoft Quick Basic model TRANSIT8.BAS.

However, at this stage it was unclear where the turbulence intensity quoted in the Abu-Ghannam and Shaw (1980) flows was actually referred to. The Fraser, Higazy and Milne (1994) method required the turbulence intensity at inlet to the domain, whist the Solomon, Walker and Gostelow (1995) model required the turbulence intensity at the start of transition. In both the above models the quoted turbulence intensity in the data was used. The quoted value was later discovered to be at a point somewhere between the inlet and the start of transition.

The author felt that, although in these simple constant pressure gradient cases there was practically no difference in the predictions using the post processing or the momentum sink models, this would not be the case in more complex flows with varying pressure gradients. For this reason the post processing model was not used for any more predictions.

Probably one of the most complete sets of transition data available was the variable pressure gradient, hot-wire anemometry experimental data from Rolls-

Royce Advanced Research Laboratory test cases T3C1-T3C5. These test cases gave detailed measurements of boundary layer parameters on a flat plate for a pressure gradient similar to that over a gas turbine blade. The wind tunnel working section is shown in Figure 4.22. These test cases were modelled in PHOENICS and the above momentum sink transitional models were used to predict boundary layer parameters.

4.3 T3C Test Cases in PHOENICS

A two-dimensional body fitted co-ordinate (bfc) computational grid comprising of 6 x 1 x 114 (x, y, z) cells was constructed (Figure 4.23). The inlet (in PHOENICS notation this corresponds to LOW) boundary was fixed mass flow, the outlet (HIGH) was fixed pressure, the flat plate (WEST) and contoured wall (EAST). The walls were both assumed to be adiabatic. According to Coupland (1995) the inlet turbulence intensity was measured at a point about 200 mm upstream of the leading edge of the flat plate and the plate had a slight incidence of about half a degree. In the computational model the flat plate was adjusted (case T3C2) until the velocity profile was a reasonable fit to the data in laminar frictionless flow. This angle was found to be 0.1° and was used for all the other test cases. In all the following T3C test case figures, the zero on the z axis correspond to the leading edge of the flat plate.

4.3.1 Transition Model Due to Fraser, Higazy and Milne

Test cases T3C1 - T3C5 were run using the method described by Fraser, Higazy and Milne (1994). The turbulence intensity used in the correlations was that at the inlet (T3C1 - 6.6 %, T3C2 - T3C5 - 3 %). This intensity was also assumed to

apply to the Abu-Ghannam and Shaw correlation for the start of transition. Figures 4.24 - 4.43 show plots of velocity profile, skin friction, displacement thickness and intermittency.

Test cases T3C1, Figures 4.24 - 4.27, and T3C5, Figures 4.40 - 4.43 show that, according to skin friction data, transition starts in a favourable pressure gradient. In both cases the predictions of the velocity profile and displacement thickness were quite good. According to the prediction of skin friction, the start of transition is predicted late in case T3C1 and early in case T3C5. Transition length is overpredicted in both cases.

Test cases T3C2 - T3C4, Figures 4.28 - 4.39 show that the start of transition, according to skin friction data occurs in adverse pressure gradient. The prediction of free stream velocity profile and displacement thickness is generally quite good when the flow is not close to separation. According to the skin friction predictions the start of transition is always predicted early and the transition length was always too long.

4.3.2 Transition Model Due to Solomon, Walker and Gostelow

Test cases T3C2 - T3C4 (the start of transition was assumed to be in adverse pressure gradient) were run using the method described by Solomon, Walker and Gostelow (1995) and predictions of velocity profile, skin friction, displacement thickness and intermittency are shown in Figures 4.48 to 4.59. The turbulence intensity used in their correlations was that at the start of transition. Test cases T3C1 (Figures 4.44 - 4.47) and T3C5 (Figures 4.60 -4.63), assumed that the start of transition was in favourable pressure gradient. These test cases were run using the method described previously by Fraser, Higazy and Milne (1994). The

Abu-Ghannam and Shaw correlation was used to predict the start of transition. In both methods, the turbulence intensity used in the correlation was that at the start of transition. The actual turbulence intensity value used was taken from the test data at the measuring station before the minimum skin friction.

It has been shown that in all cases considered here that the start of transition has been moved markedly downstream by changing the value of the turbulence intensity in the correlation for the start of transition. No useful comparison of the length of transition was made because of the vastly differing positions of the start of transition.

It was quite clear from the analysis of the T3C flows that if the value of turbulence intensity used in the Abu-Ghannam and Shaw (1980) correlation is not the value at the inlet to the domain nor the value at the start of transition. It must be based on some average value between the inlet and the start of transition. Using the value of turbulence intensity at the start of transition, which was always considerably less than the value at inlet, had the effect of moving the start of transition downstream in all T3C test cases.

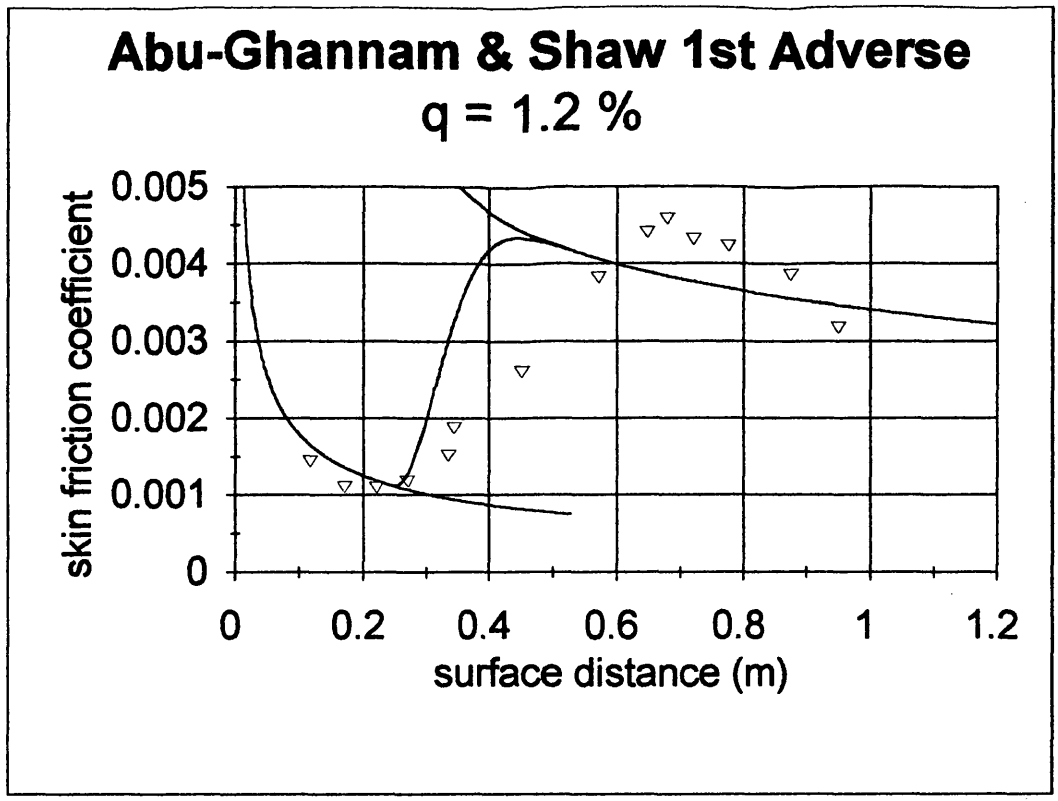

Figure 4.1: Prediction of Skin Friction Using TRANSIT7.BAS

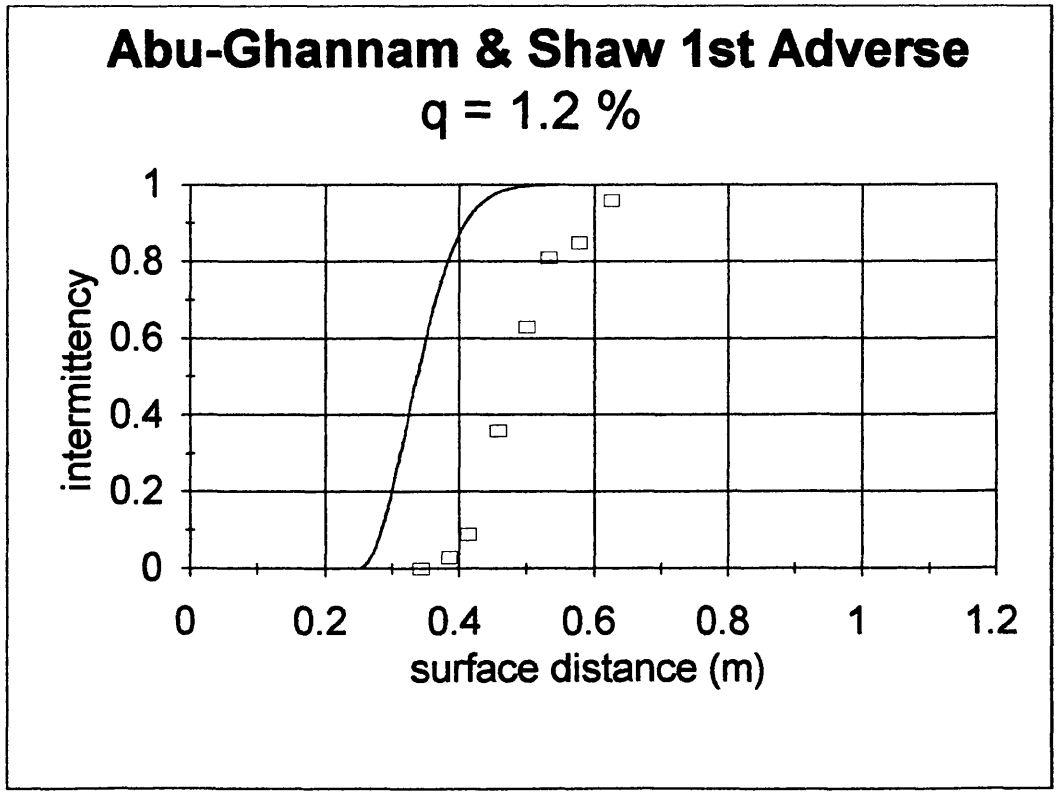

Figure 4.2: Prediction of Intermittency Using TRANSIT7.BAS

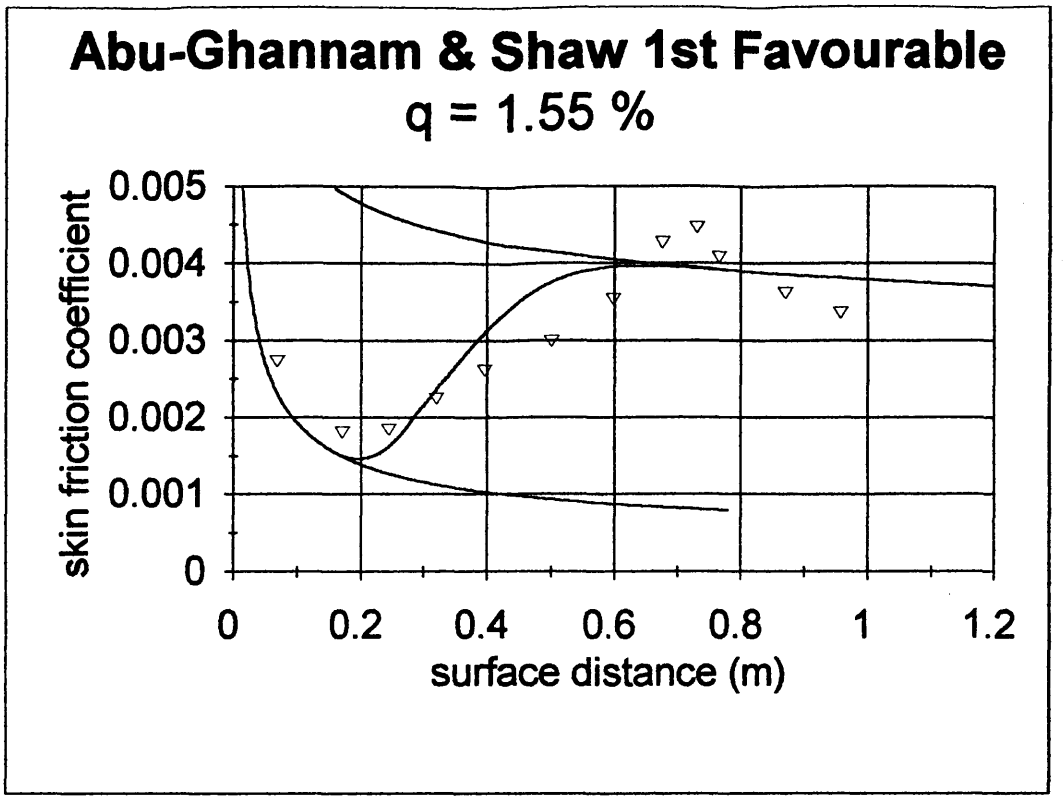

Figure 4.3: Prediction of Skin Friction Using TRANSIT7.BAS

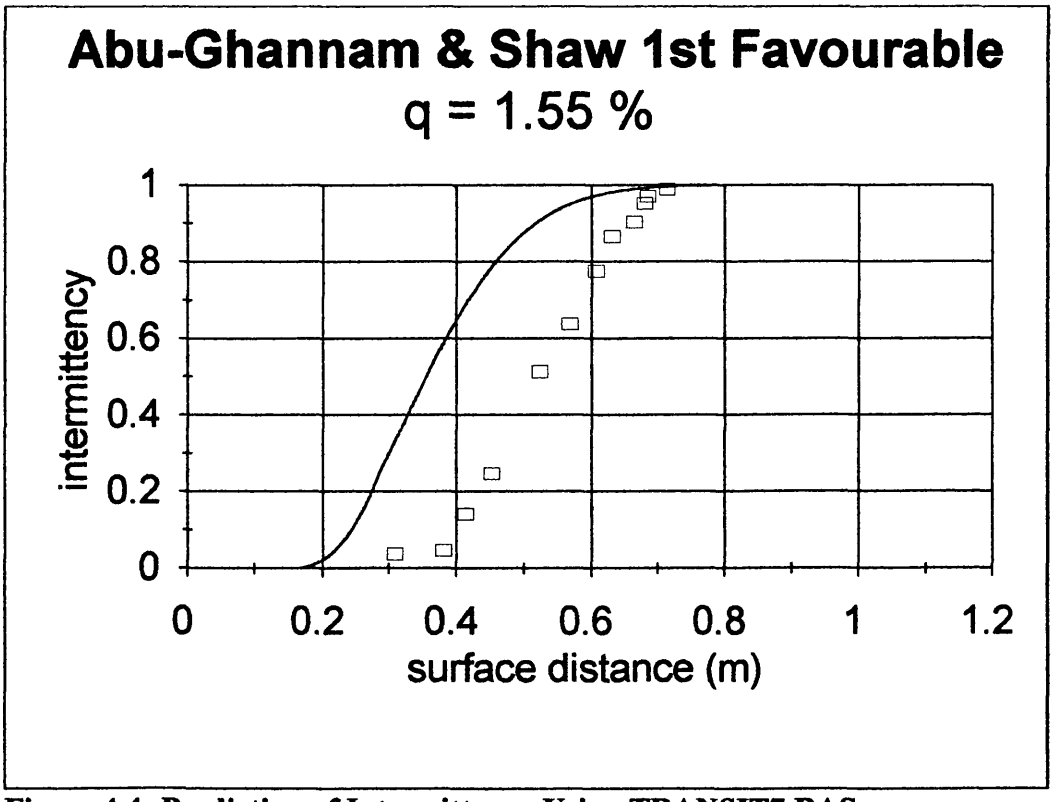

Figure 4.4: Prediction of Intermittency Using TRANSIT7.BAS

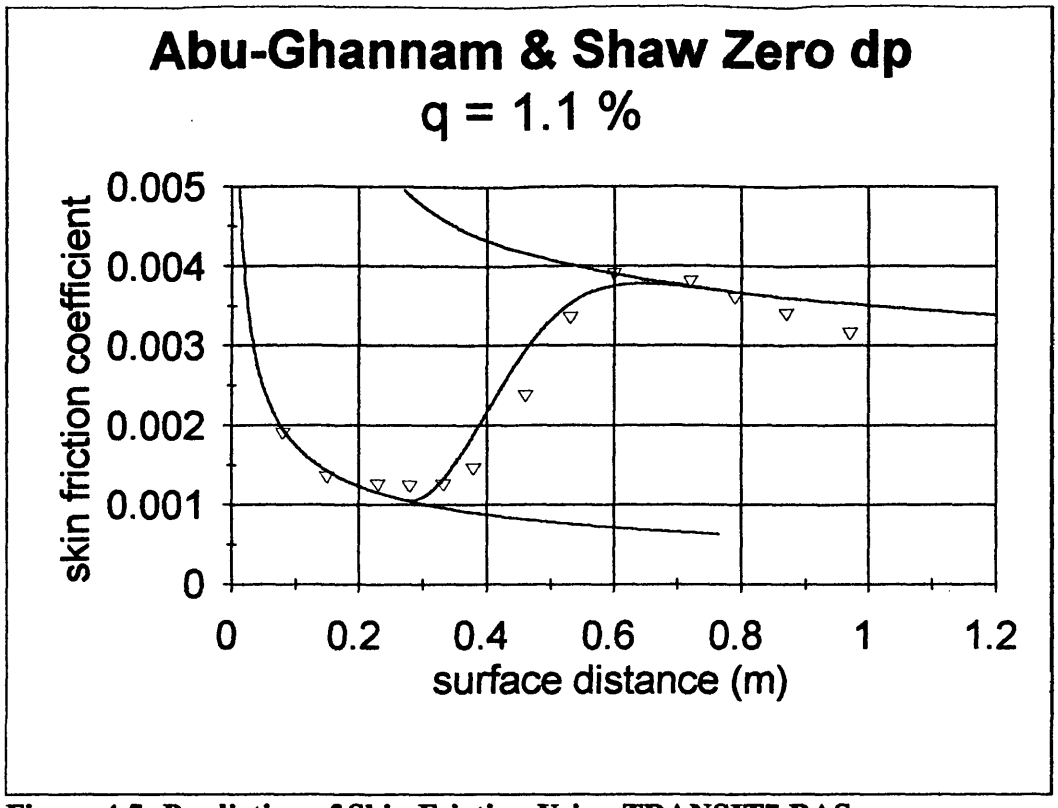

Figure 4.5: Prediction of Skin Friction Using TRANSIT7.BAS

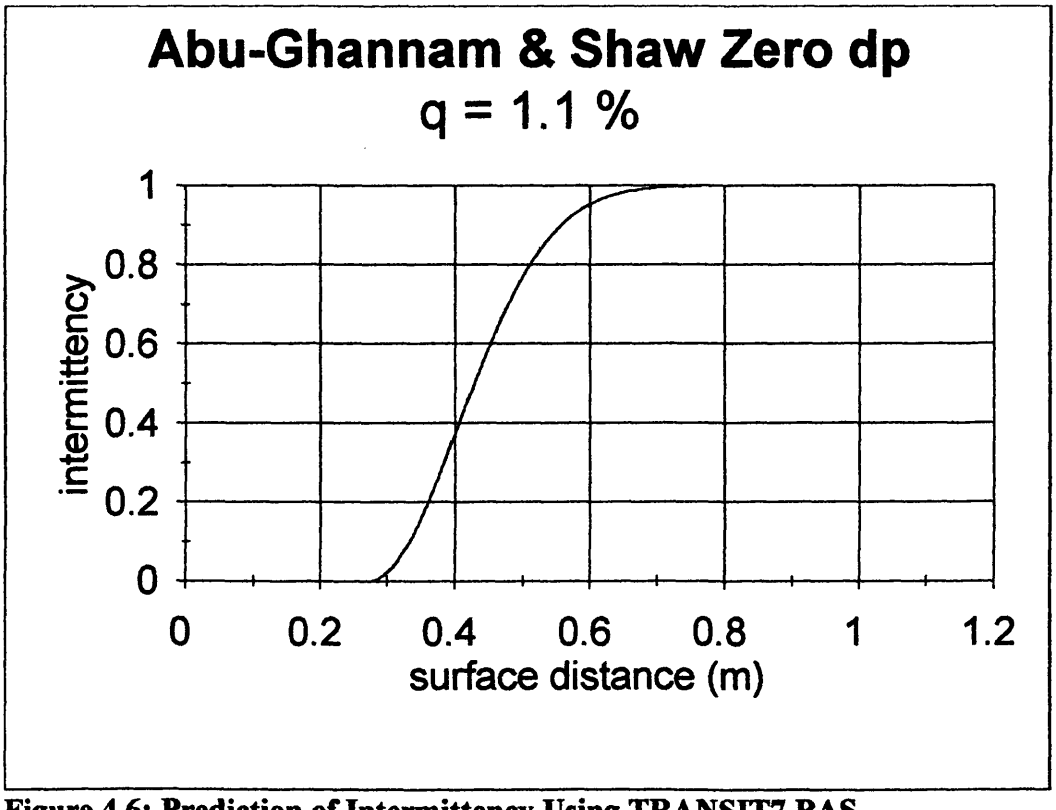

Figure 4.6: Prediction of Intermittency Using TRANSIT7.BAS

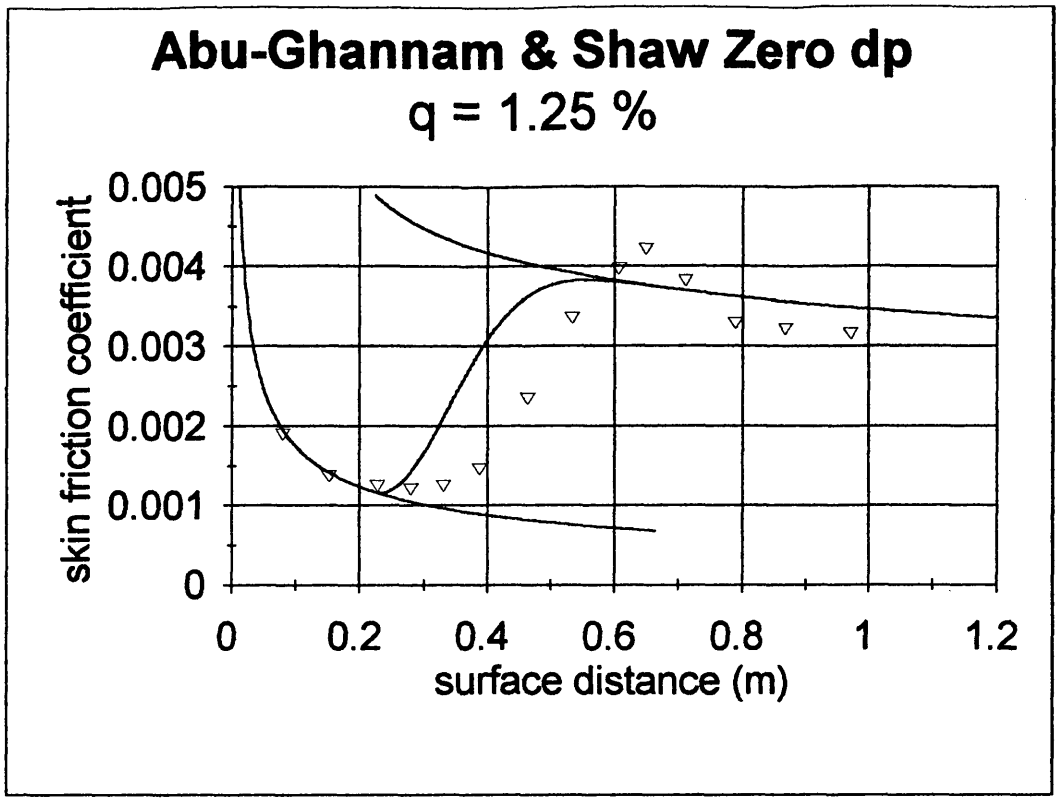

Figure 4.7: Prediction of Skin Friction Using TRANSIT7.BAS

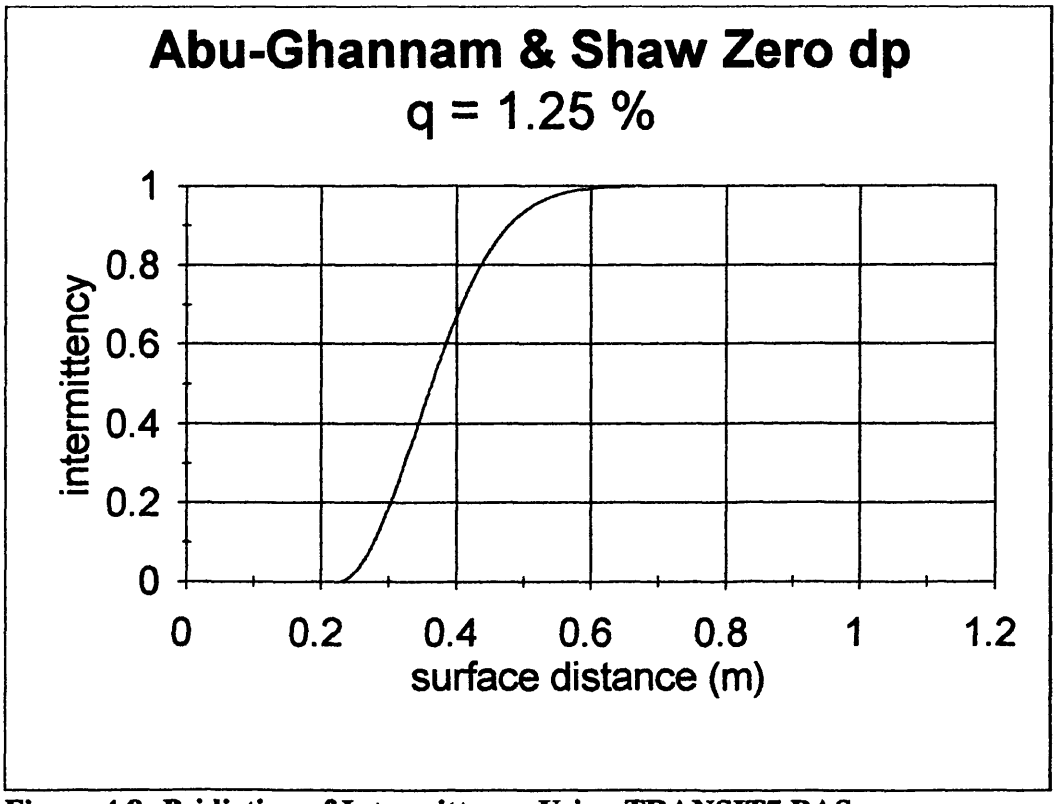

Figure 4.8: Pridiction of Intermittency Using TRANSIT7.BAS

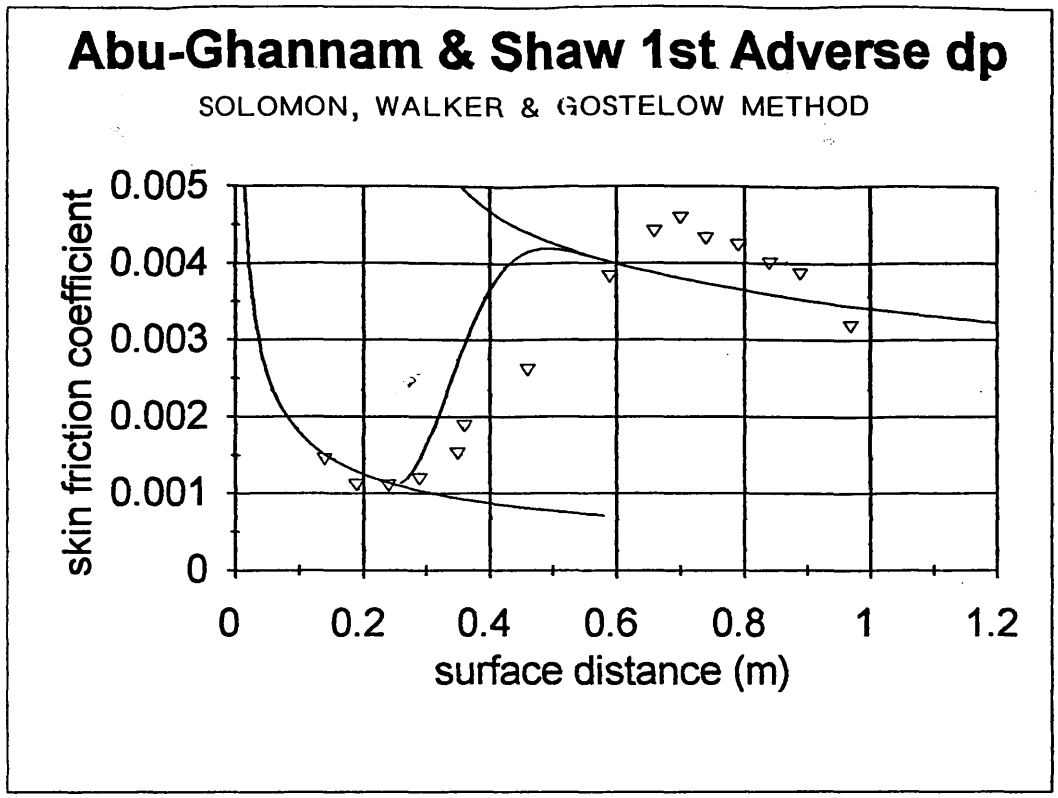

Figure 4.9: Prediction of Skin Friction Using TRANSIT8.BAS

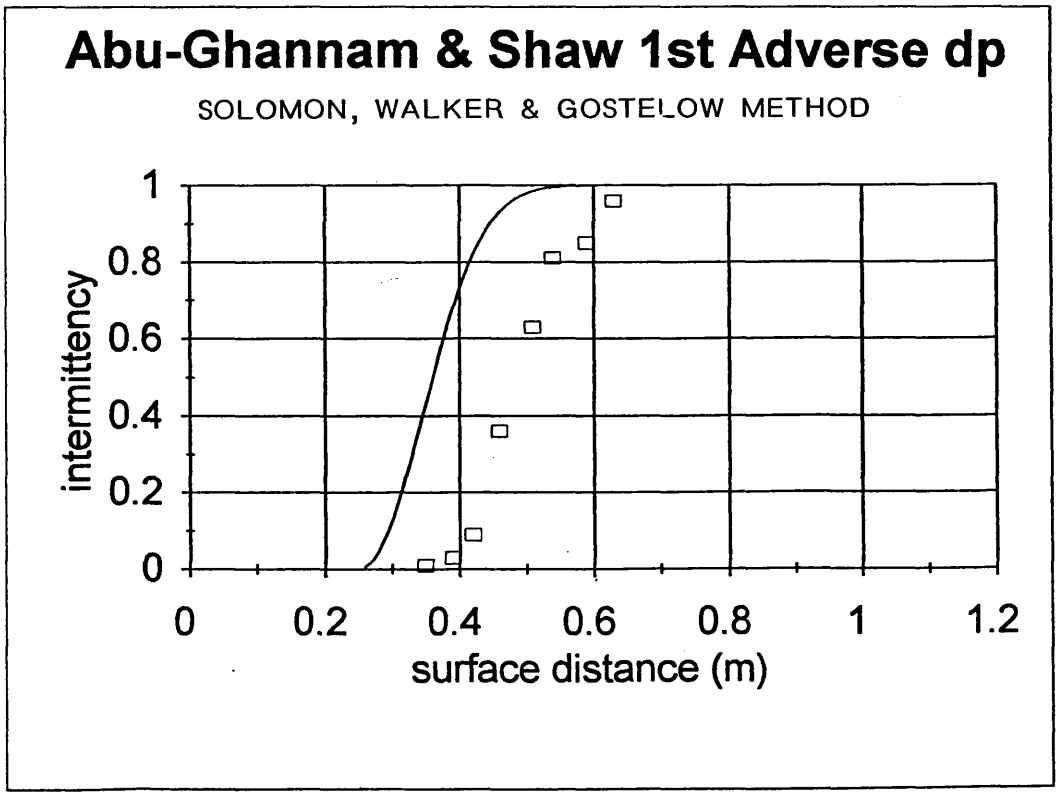

Figure 4.10: Prediction of Intermittency Using TRANSIT8.BAS

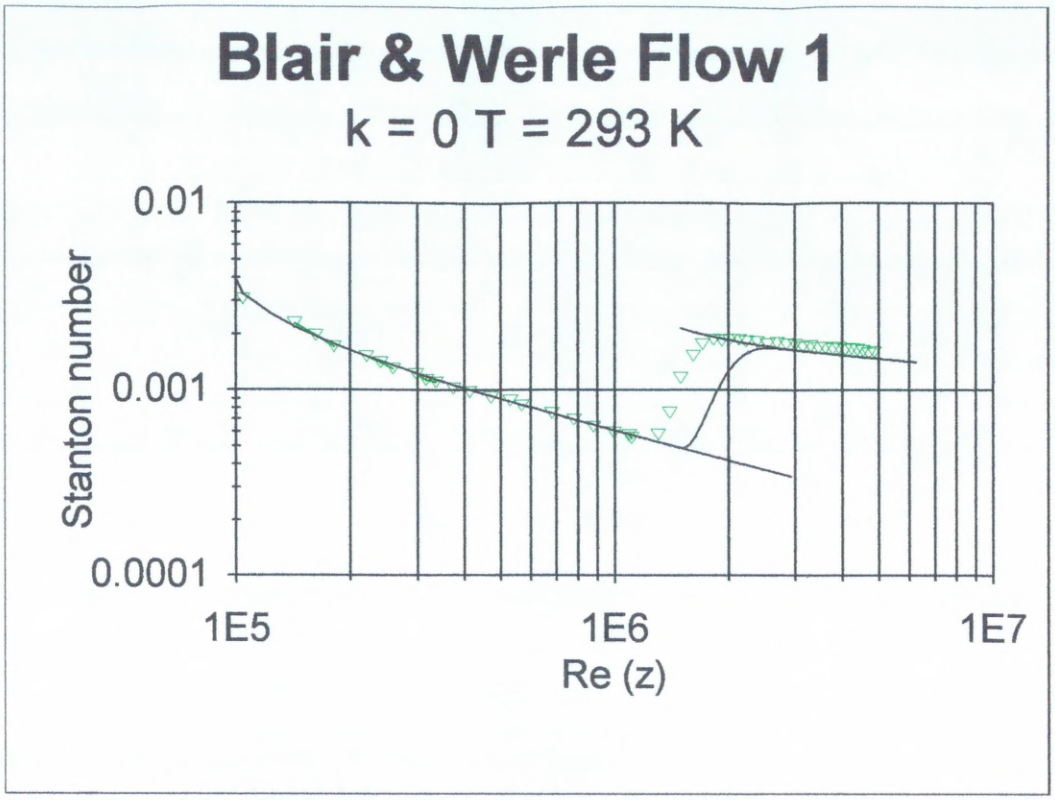

Figure 4.11: Transition Model, Fraser, Higazy and Milne (1994)

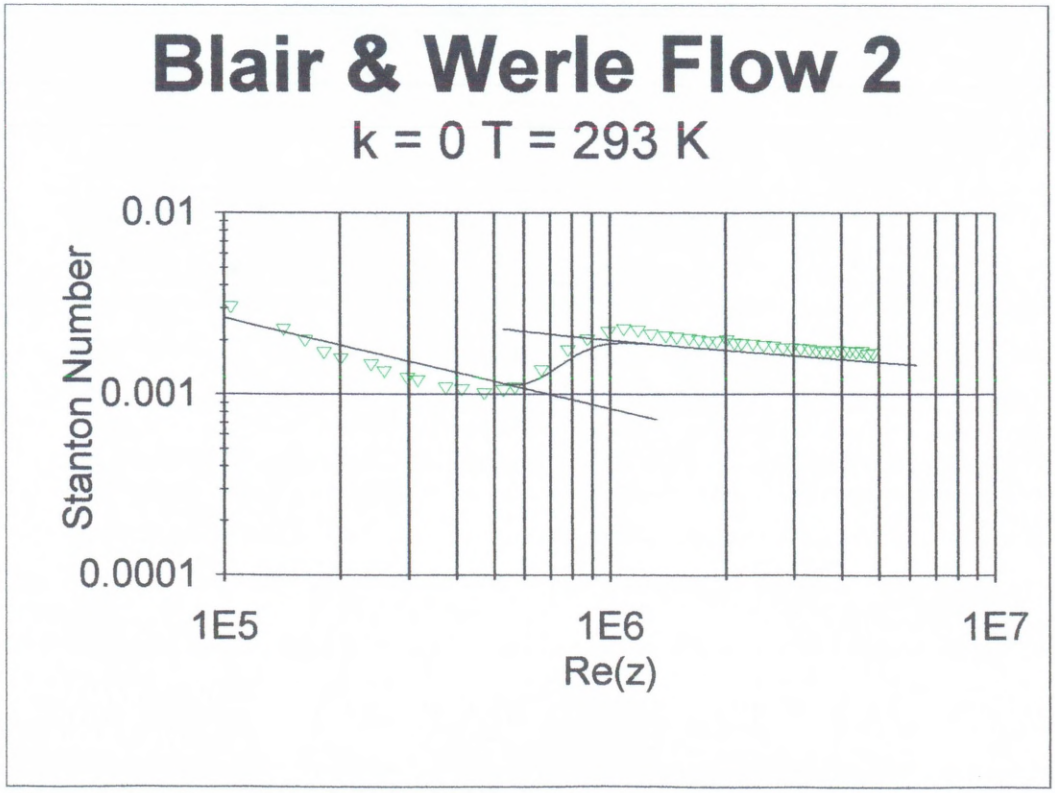

Figure 4.12: Transition Model, Fraser, Higazy and Milne (1994)

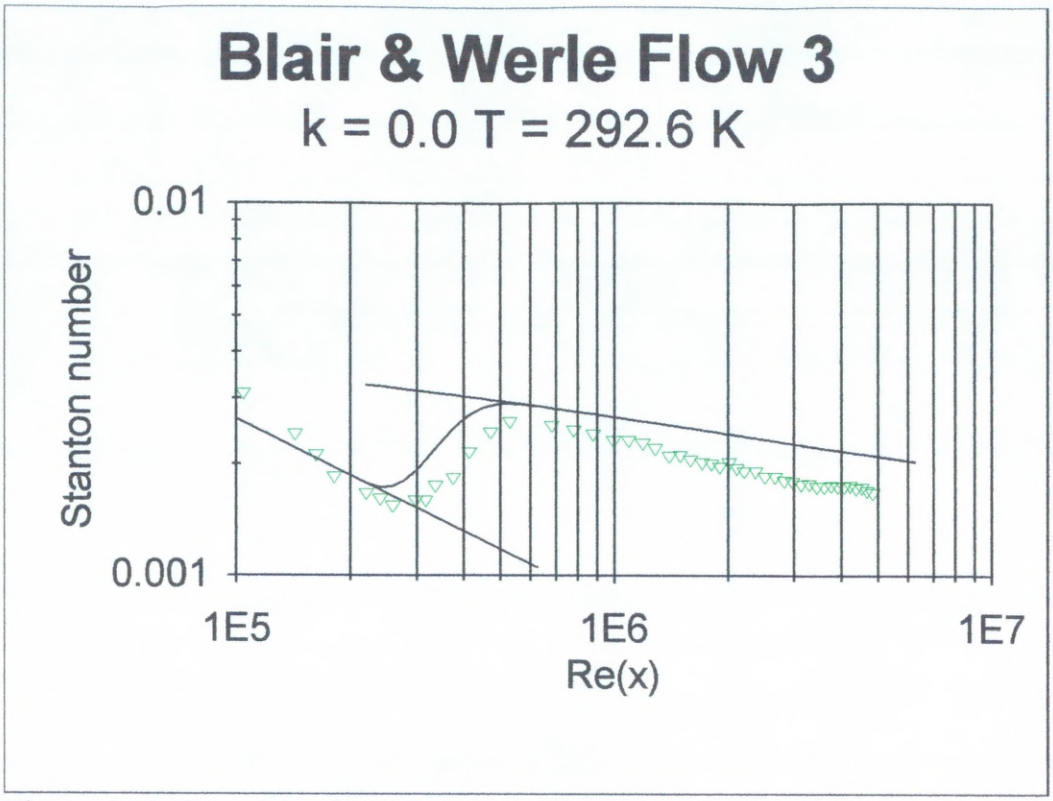

Figure 4.13: Transition Model, Fraser, Higazy and Milne (1994)

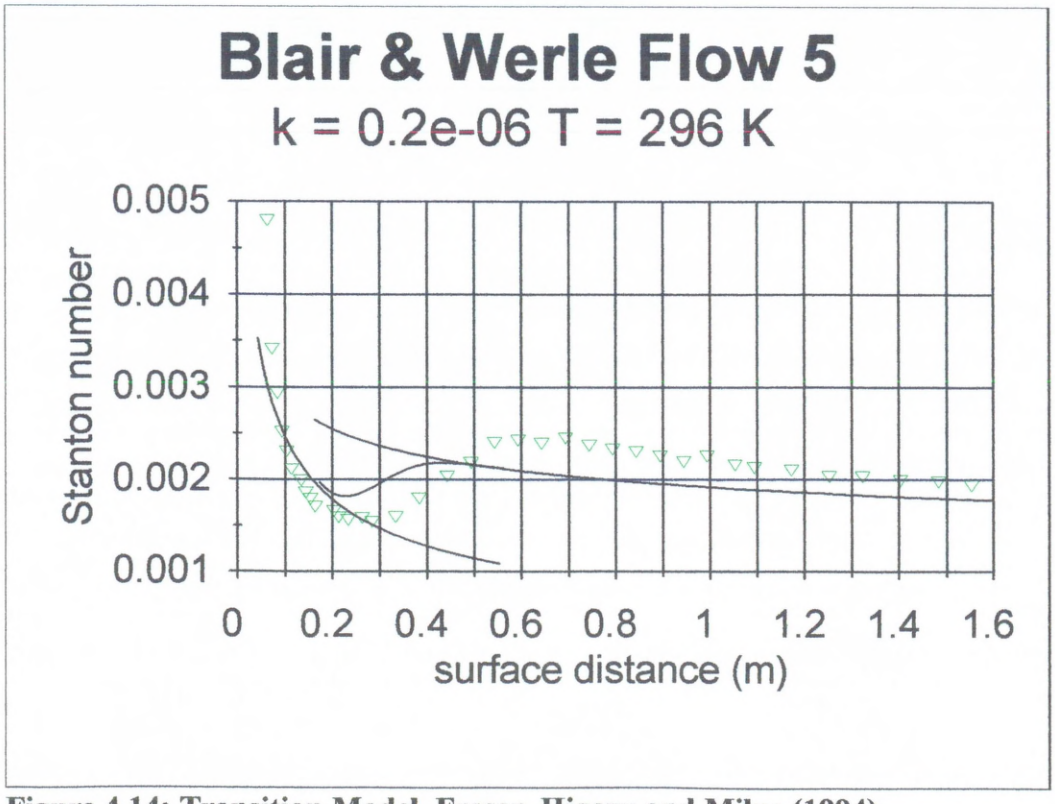

Figure 4.14: Transition Model, Fraser, Higazy and Milne (1994)

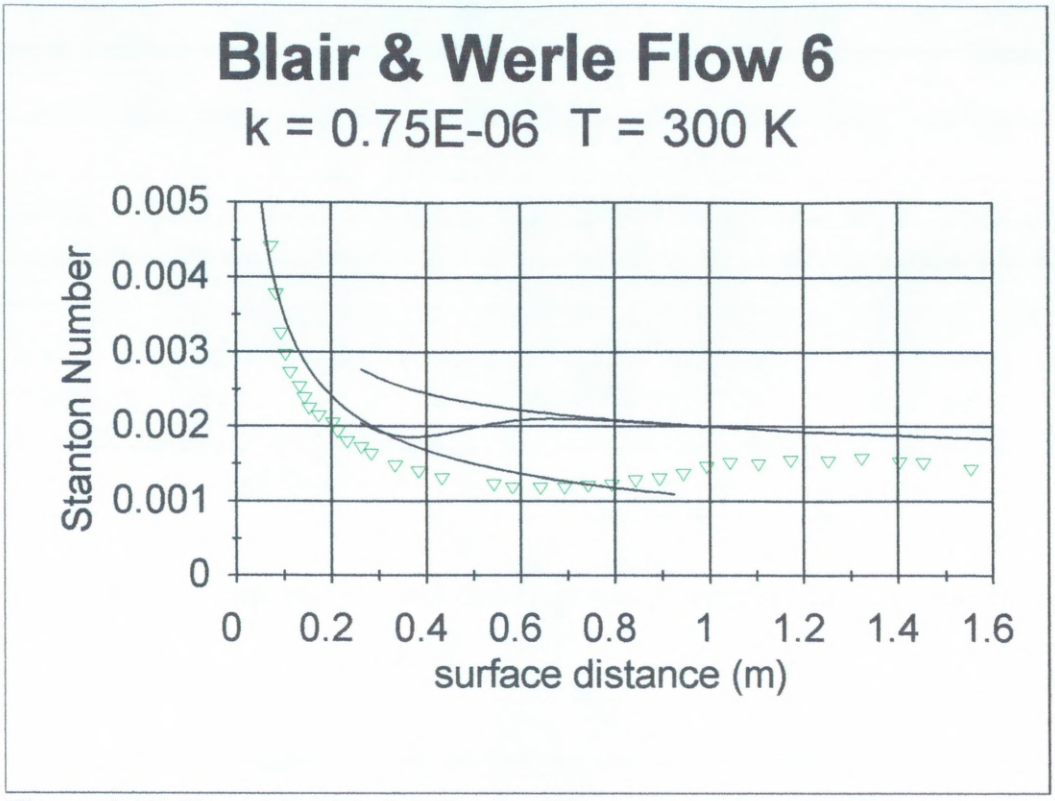

Figure 4.15: Transition Model, Fraser, Higazy and Milne (1994)

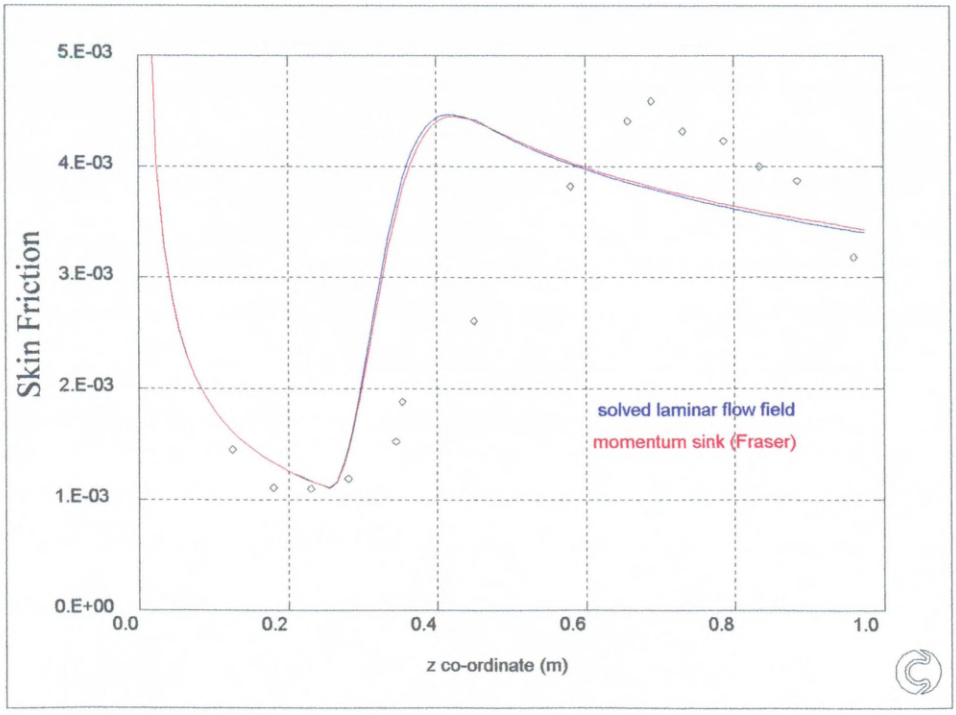

Figure 4.16: Comparison of Solved Flow Field and Momentum Sink

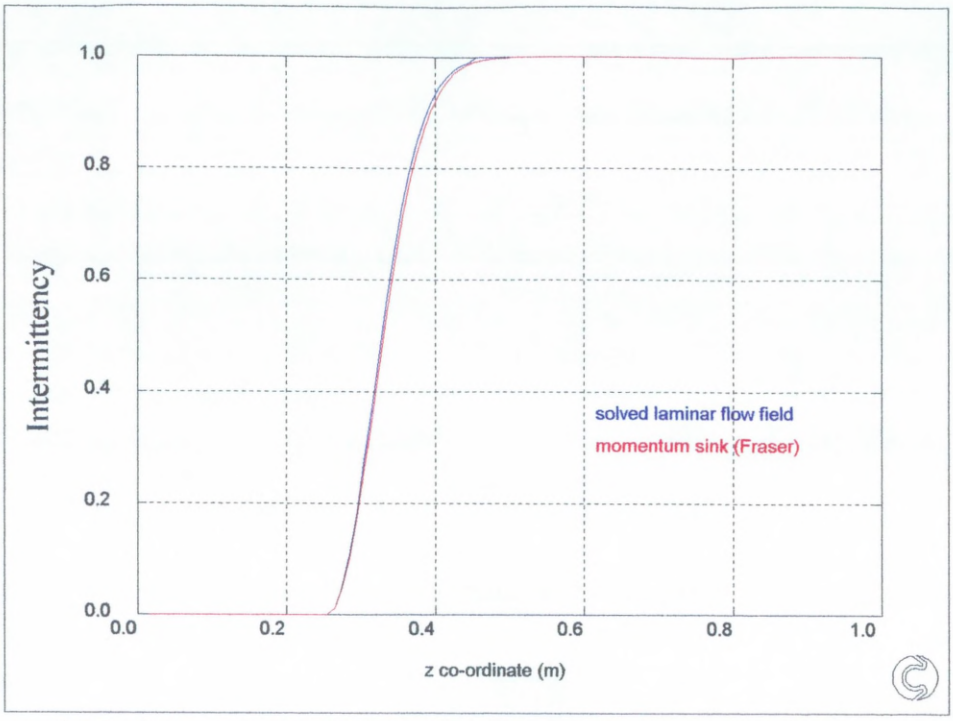

Figure 4.17: Comparison of Methods: Adverse Pressure Gradient

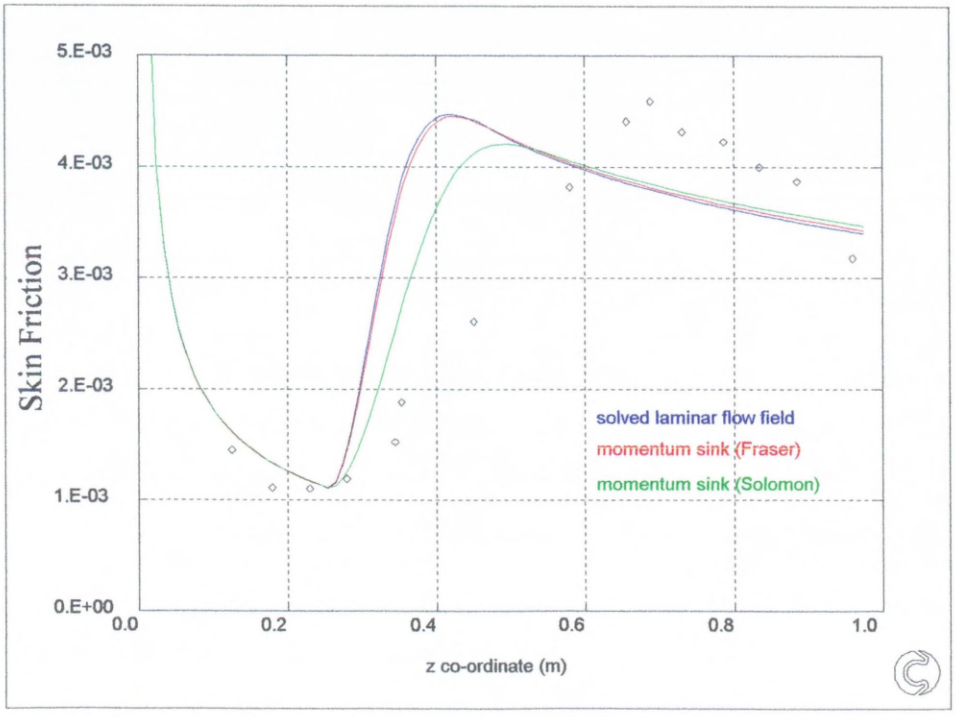

Figure 4.18: Comparison of Methods: Adverse Pressure Gradient

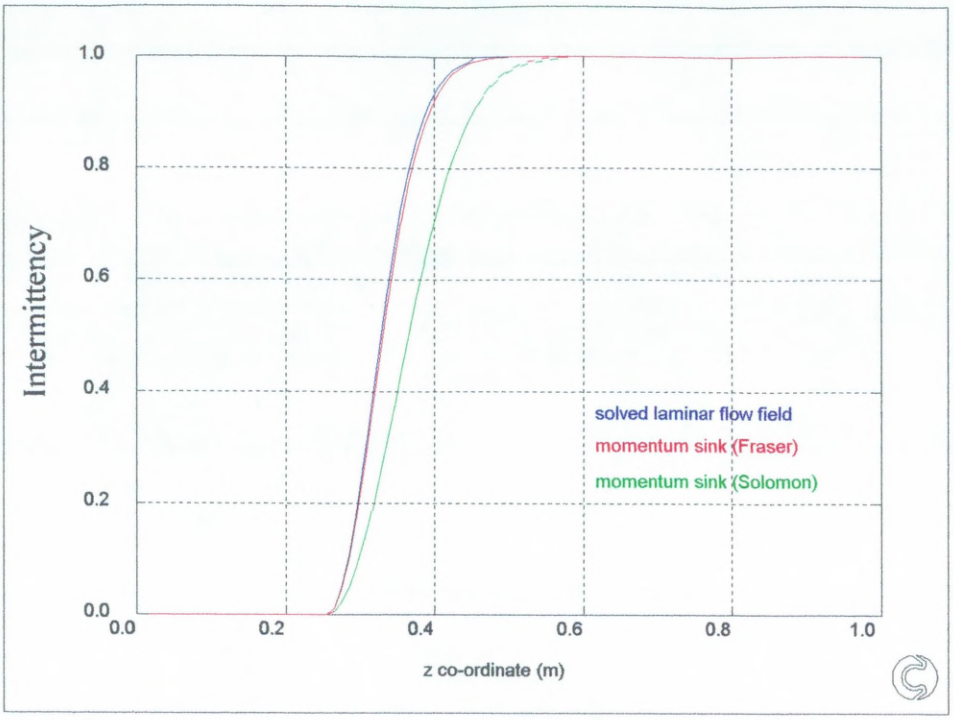

Figure 4.19:Comparison of Methods: Adverse Pressure Gradient

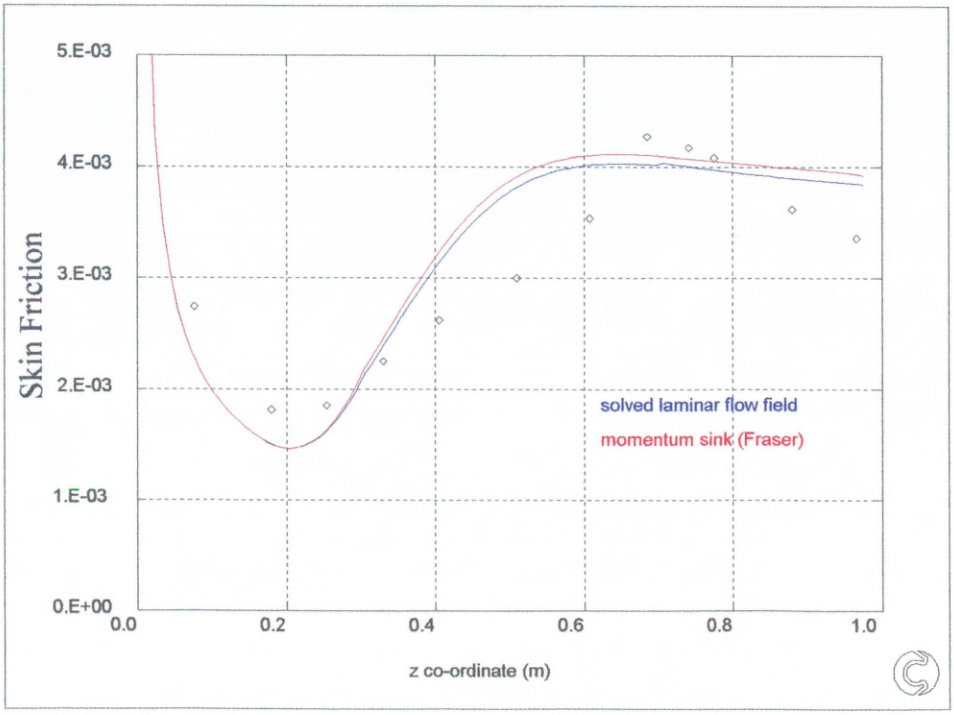

Figure 4.20: Comparison of Methods: Favourable Pressure Gradient

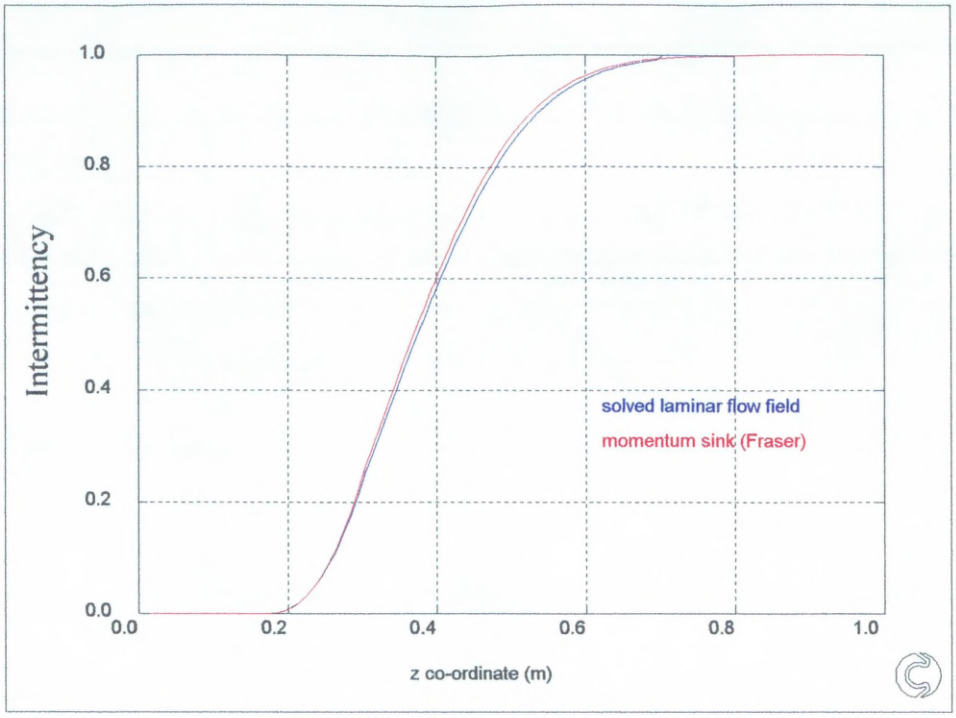

Figure 4.21: Comparison of Methods: Favourable Pressure Gradient

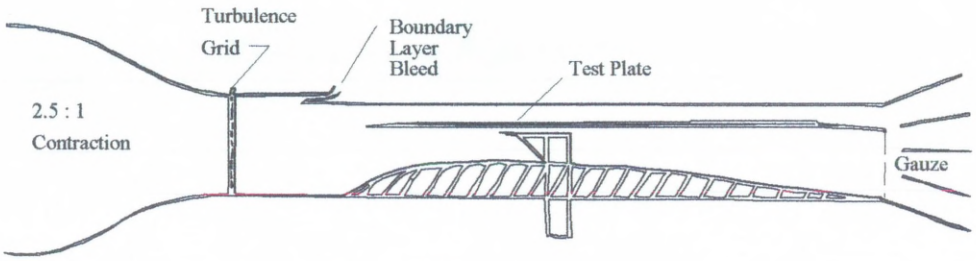

Figure 4.22: A.R.L. Wind Tunnel Working Section

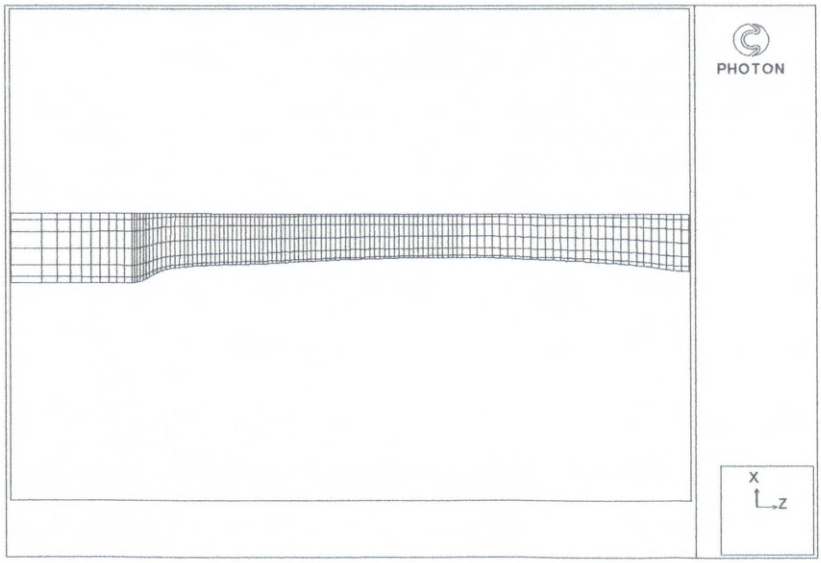

Figure 4.23: Computational Grid

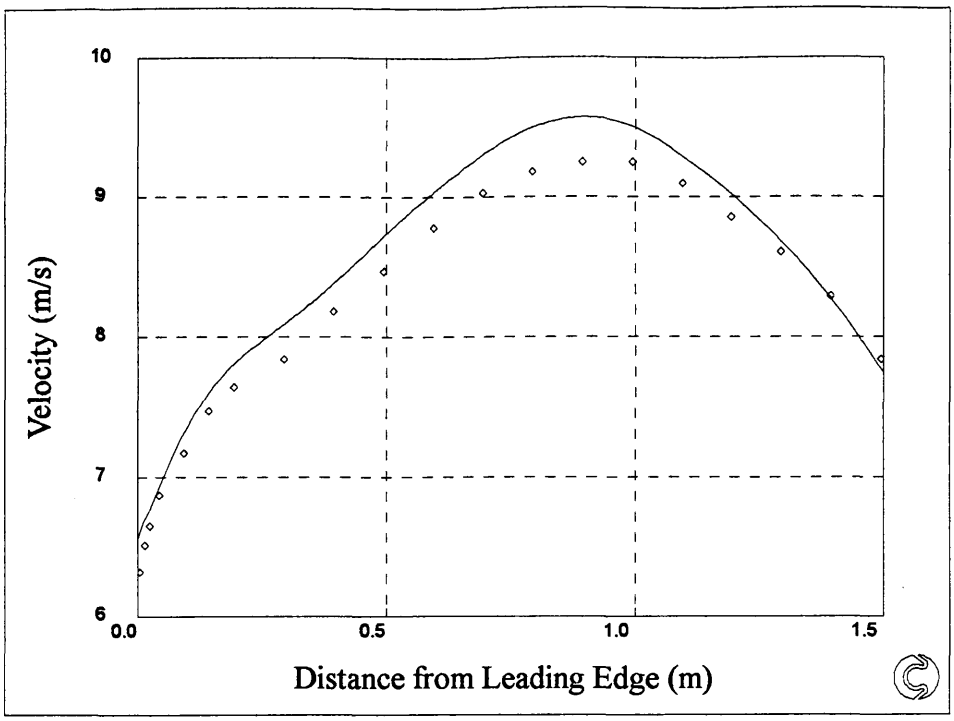

Figure 4.24: T3C1 Velocity Profile Turbulence intensity at Inlet

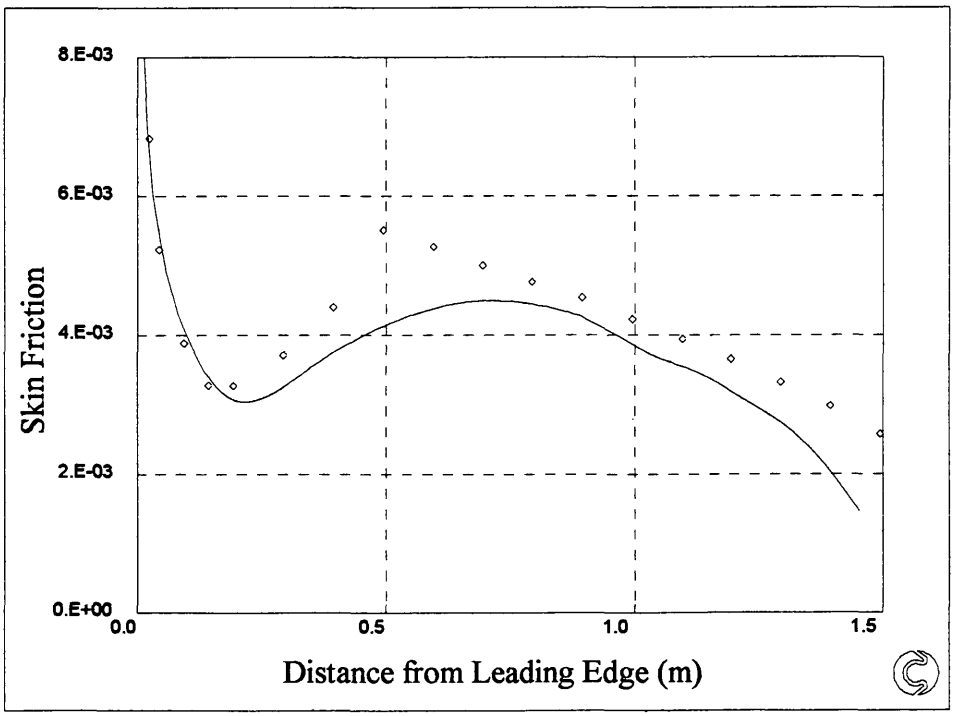

Figure 4.25: T3C1 Skin Friction Turbulence Intensity at Inlet

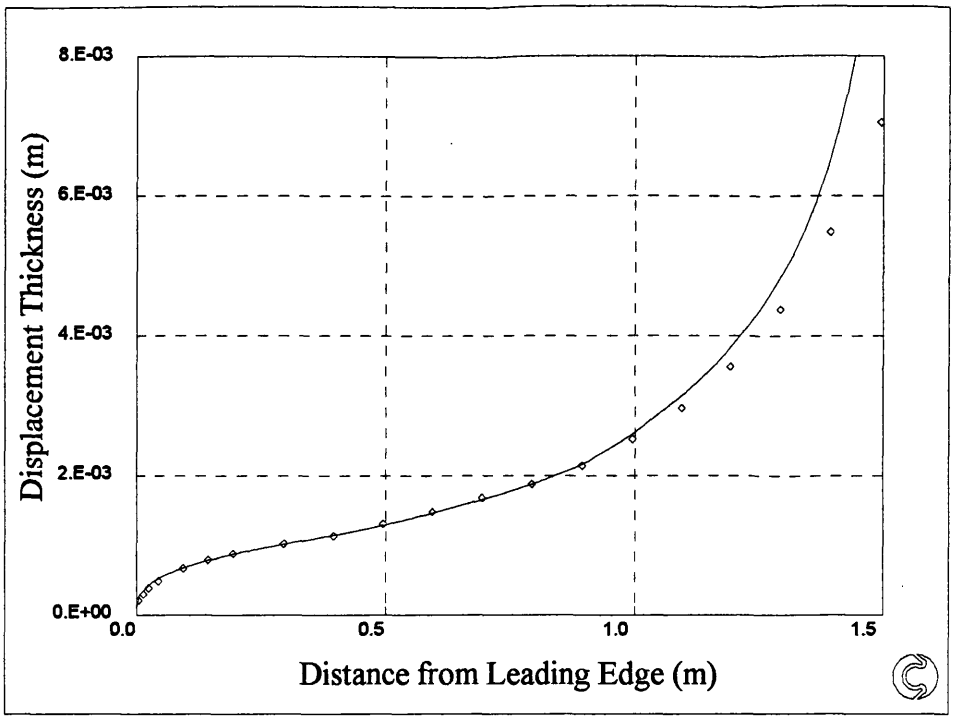

Figure 4.26: T3C1 Displacement Thickness Turbulence Intensity at Inlet

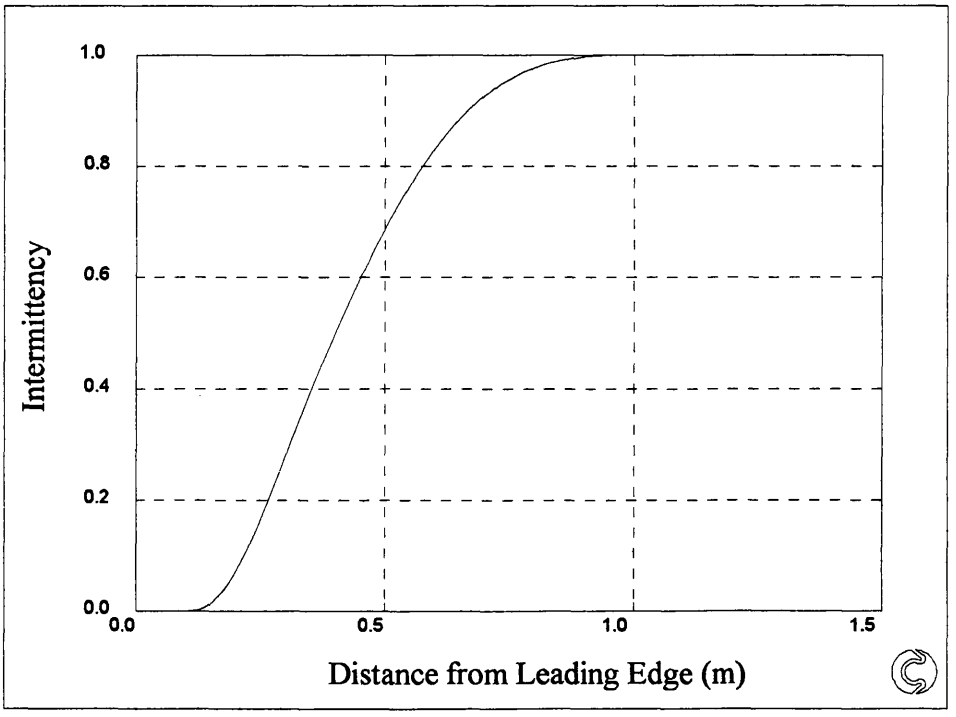

Figure 4.27: T3C1 Intermittency Turbulence Intensity at Inlet

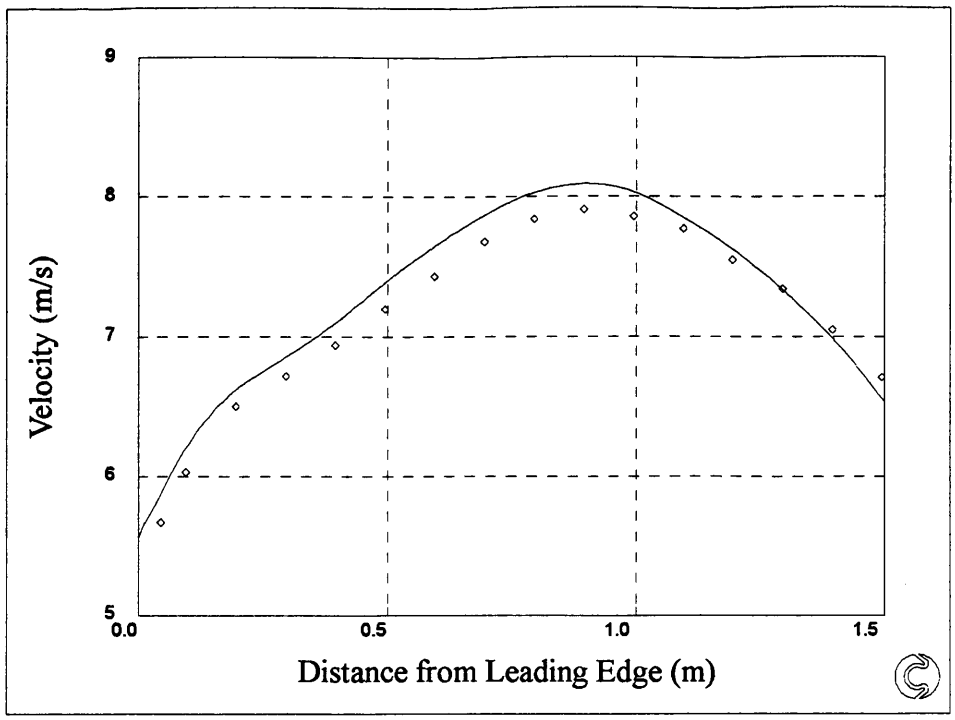

Figure 4.28: T3C2 Velocity Profile Turbulence Intensity at Inlet

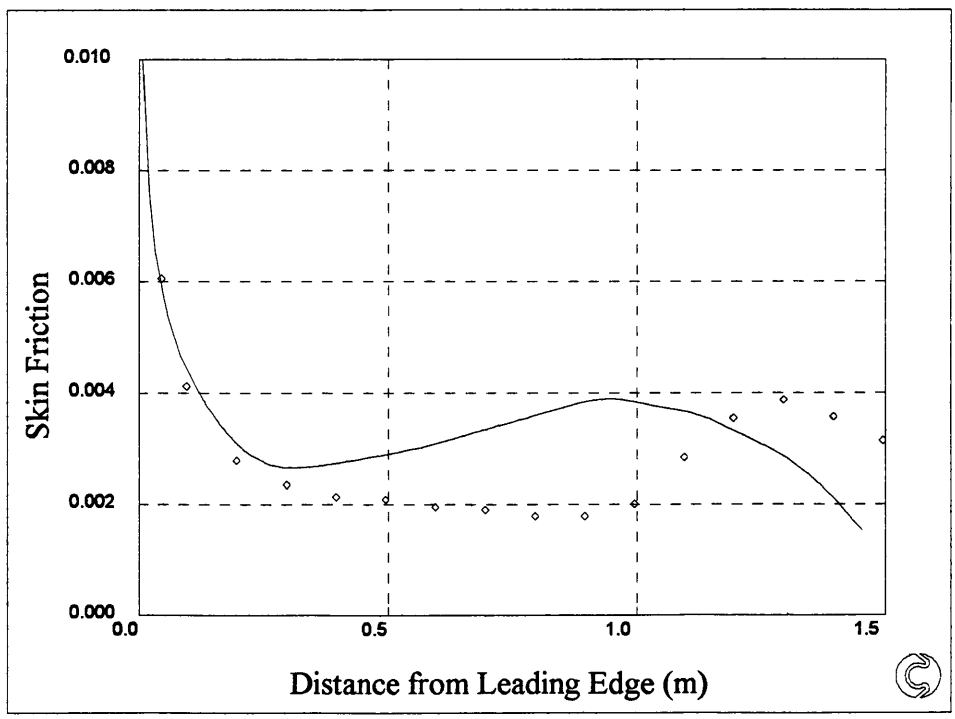

Figure 4.29: T3C2 Skin Friction Turbulence Intensity at Inlet

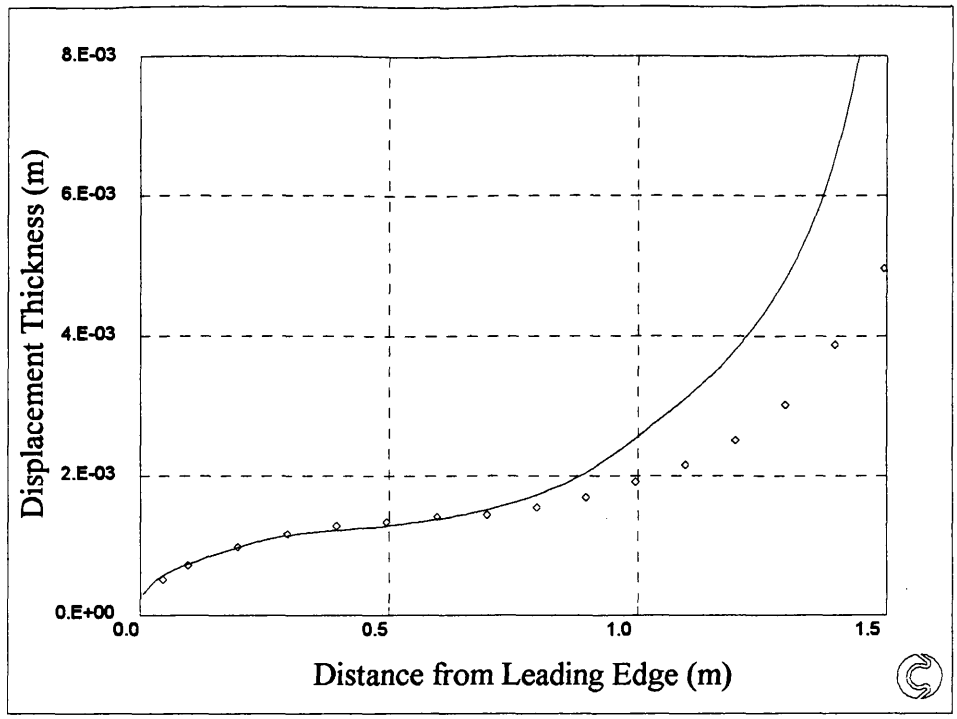

Figure 4.30: T3C2 Displacement Thickness Turbulence Intensity at Inlet

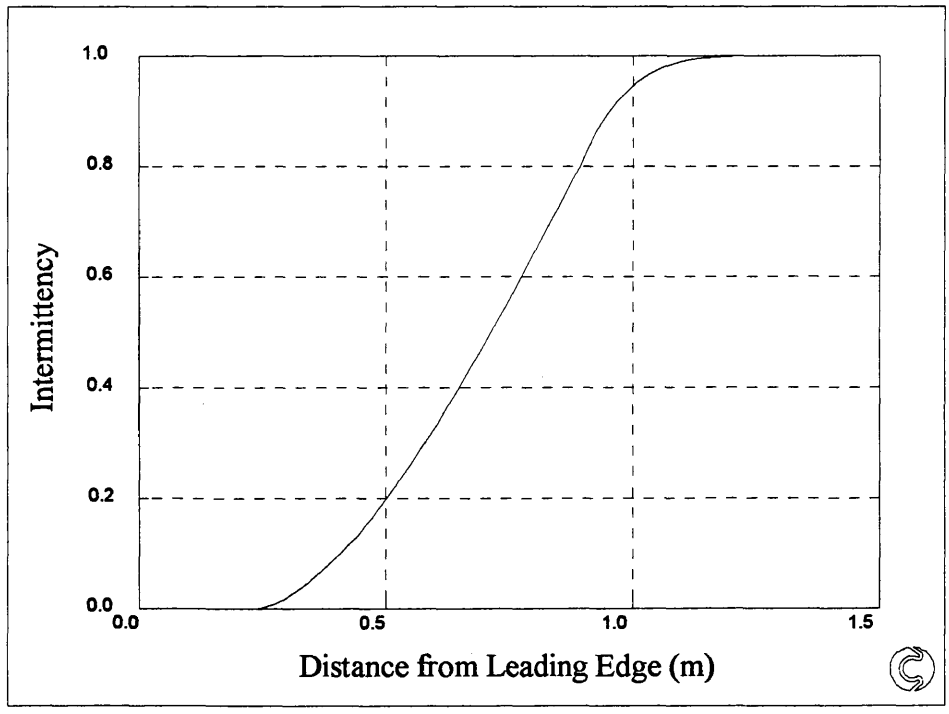

Figure 4.31: T3C2 Intermittency Turbulence Intensity at Inlet

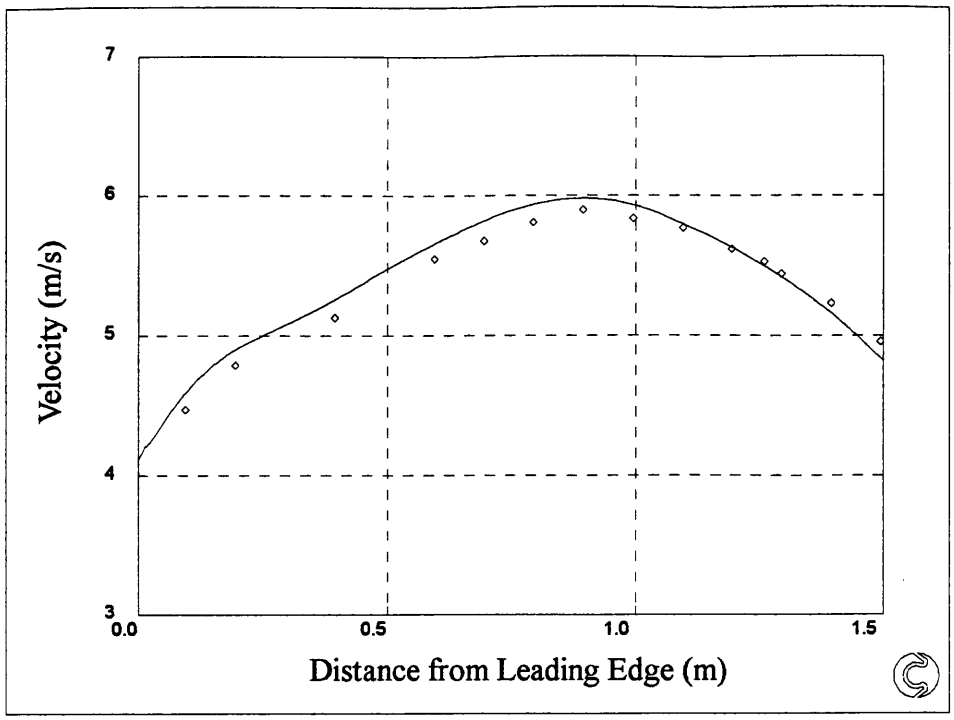

Figure 4.32: T3C3 Velocity Profile Turbulence Intensity at Inlet

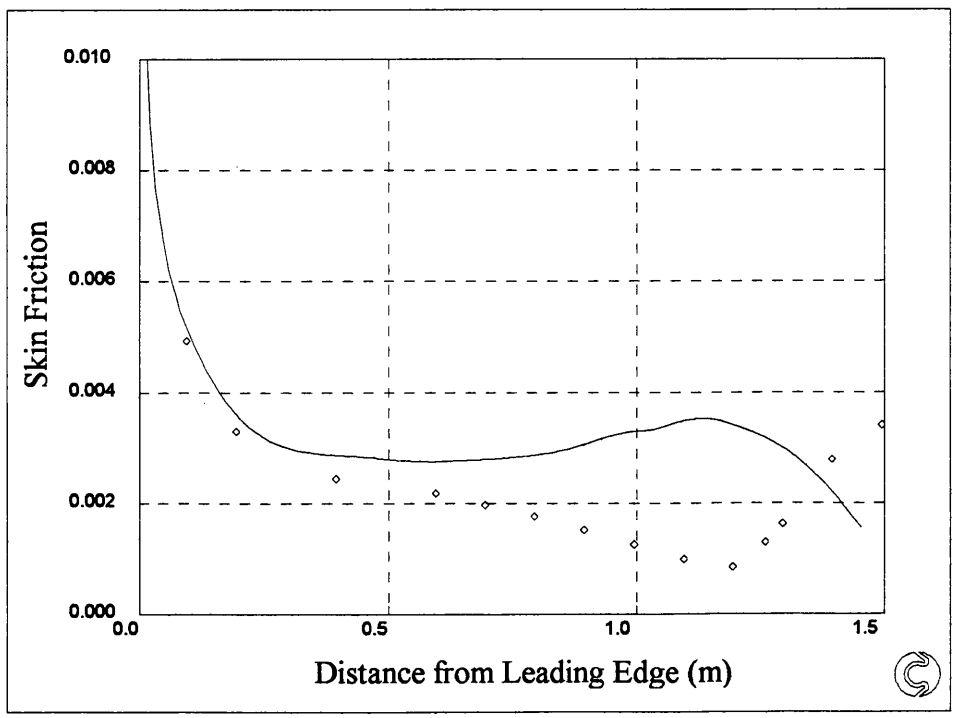

Figure 4.33: T3C3 Skin Friction Turbulence Intensity at Inlet

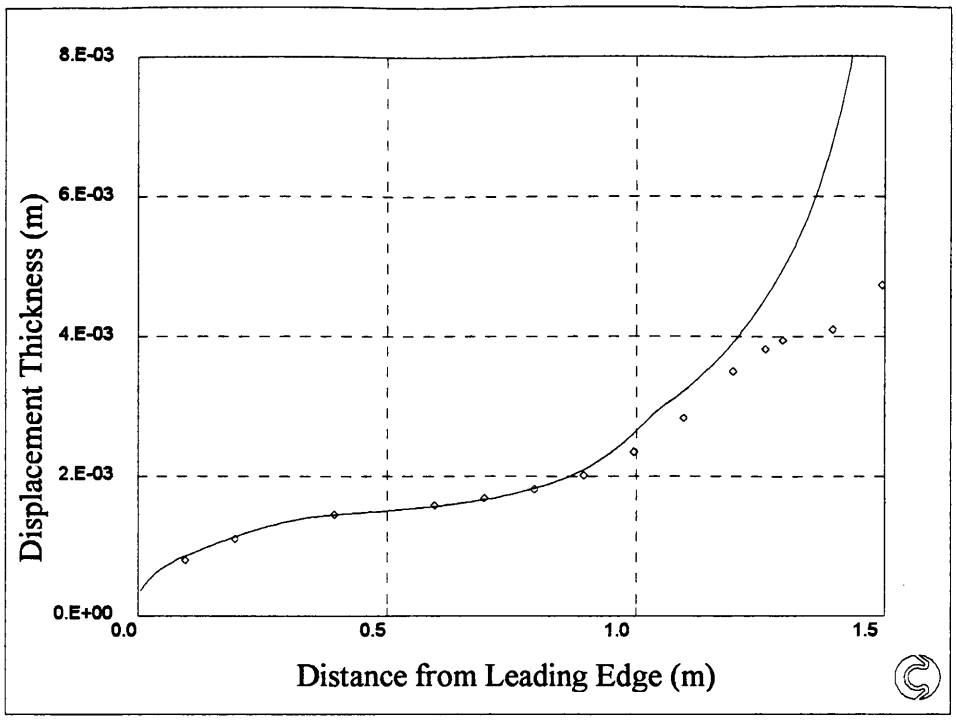

Figure 4.34: T3C3 Displacement Thickness Turbulence Intensity at Inlet

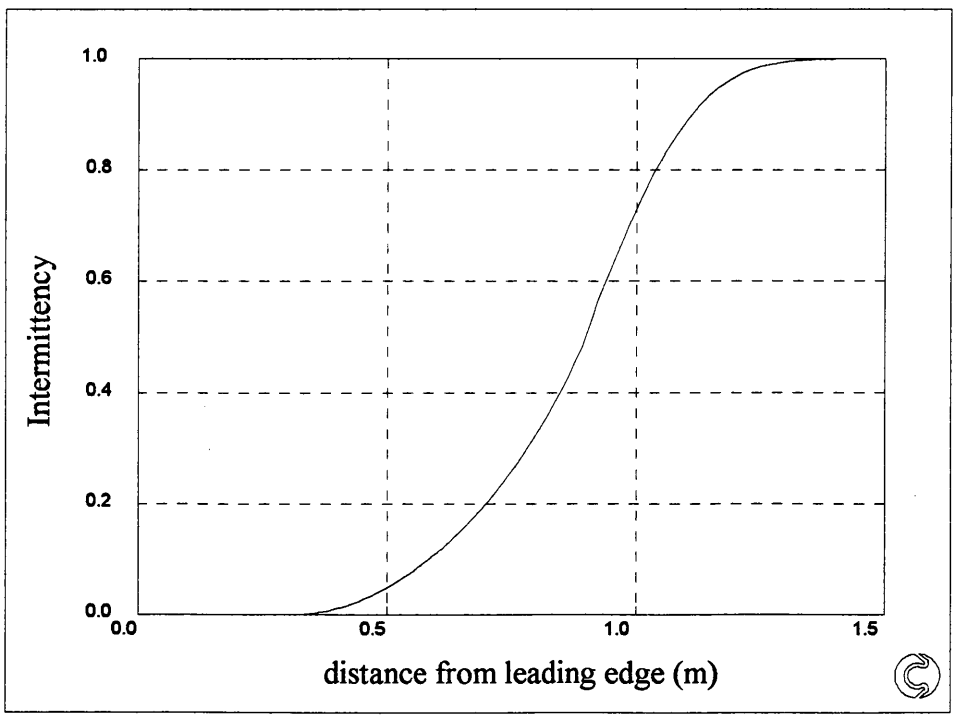

Figure 4.35: T3C3 Intermittency Turbulence Intensity at Inlet

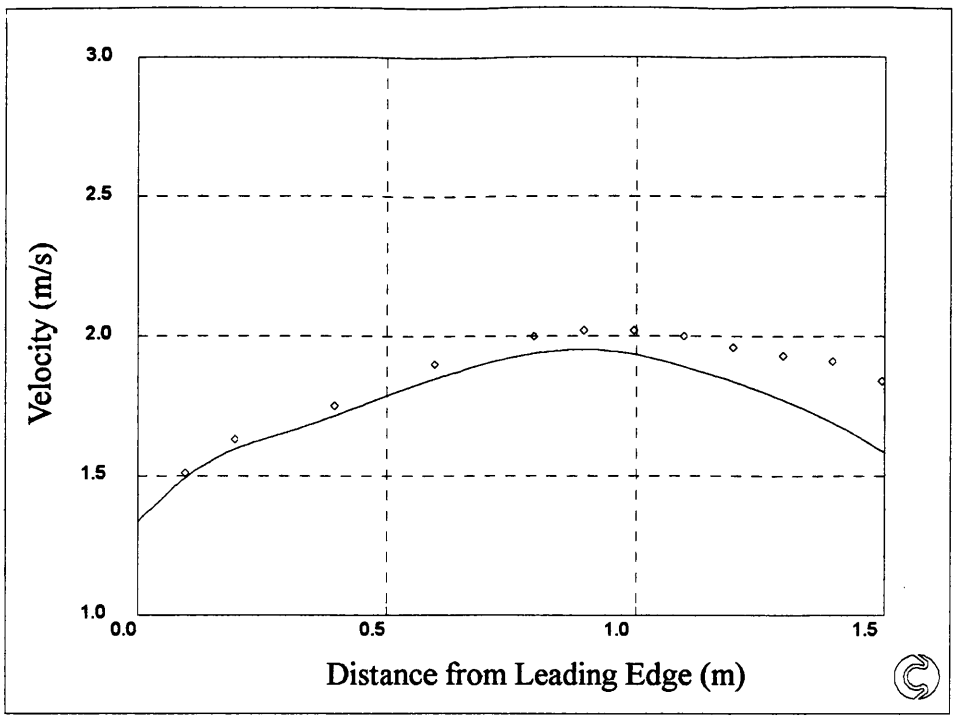

Figure 4.36: T3C4 Velocity Profile Turbulence Intensity at Inlet

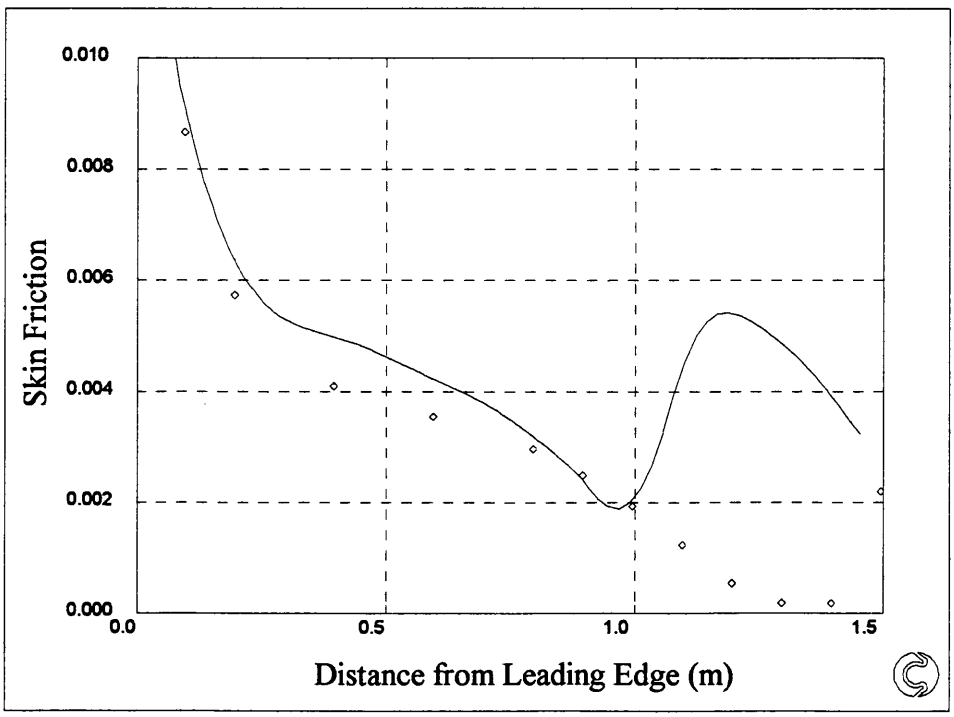

Figure 4.37: T3C4 Skin Friction Turbulence Intensity at Inlet

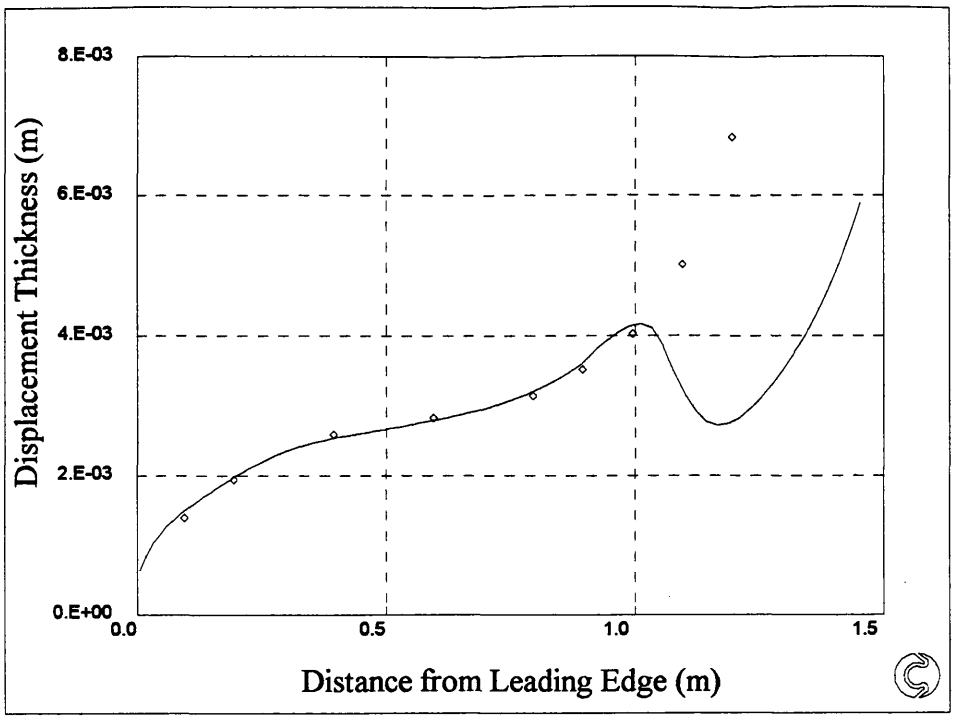

Figure 4.38: T3C4 Displacement Thickness Turbulence Intensity at Inlet

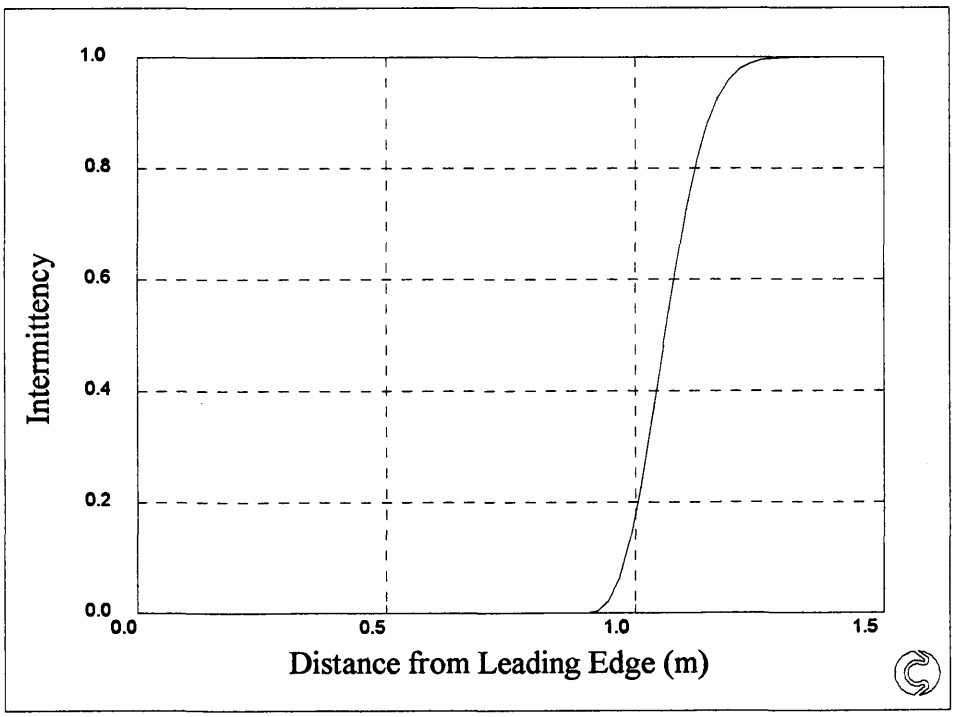

Figure 4.39: T3C4 Intermittency Turbulence Intensity at Inlet

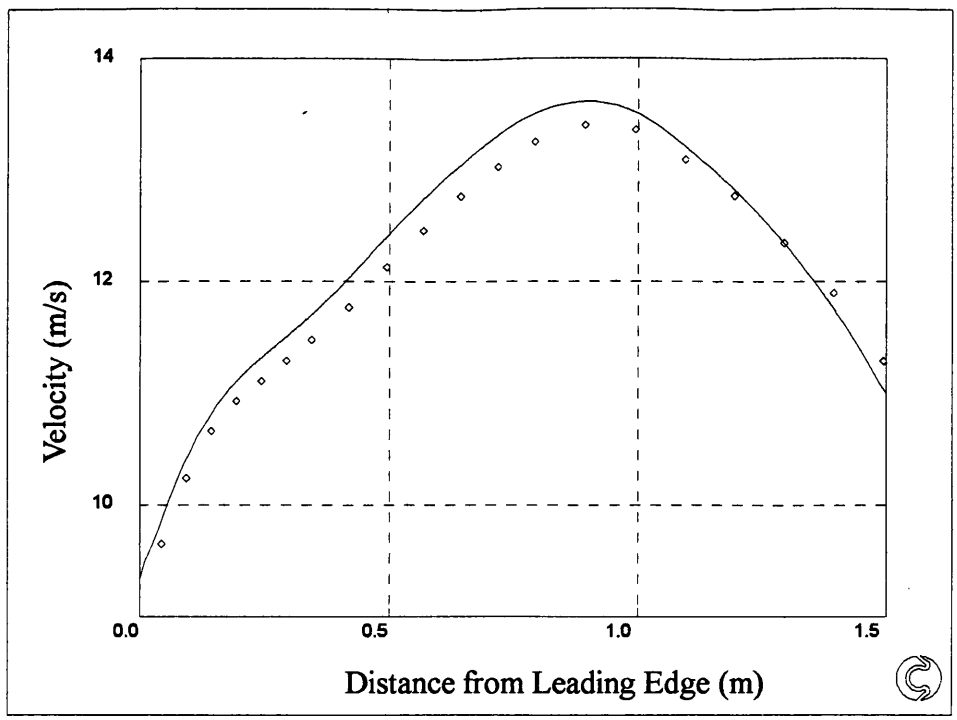

Figure 4.40: T3C5 Velocity Profile Turbulence Intensity at Inlet

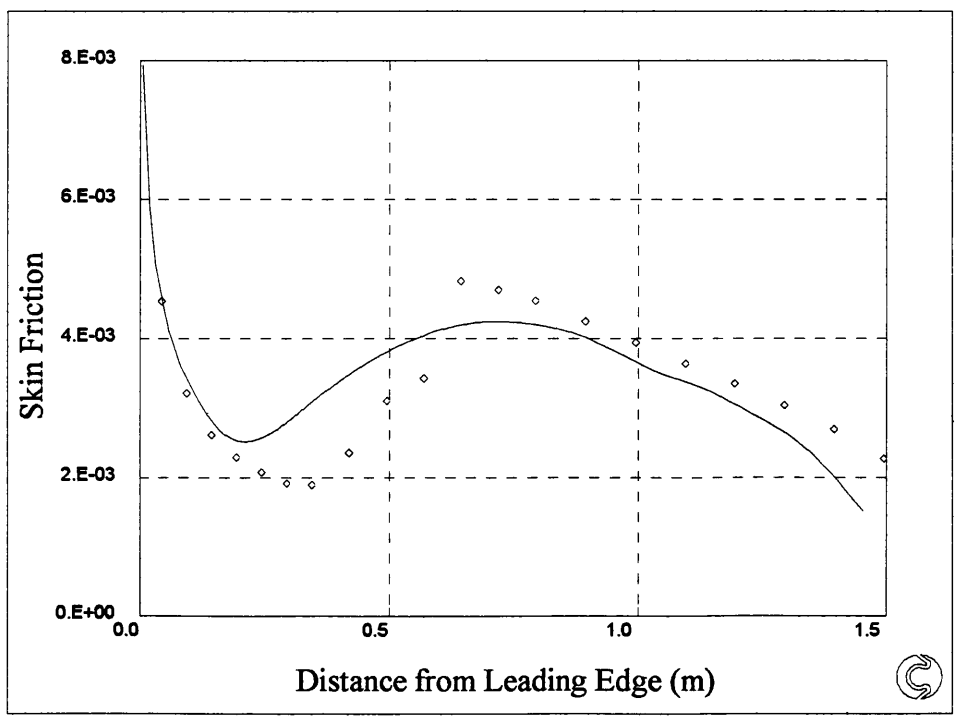

Figure 4.41: T3C5 Skin Friction Turbulence Intensity at Inlet

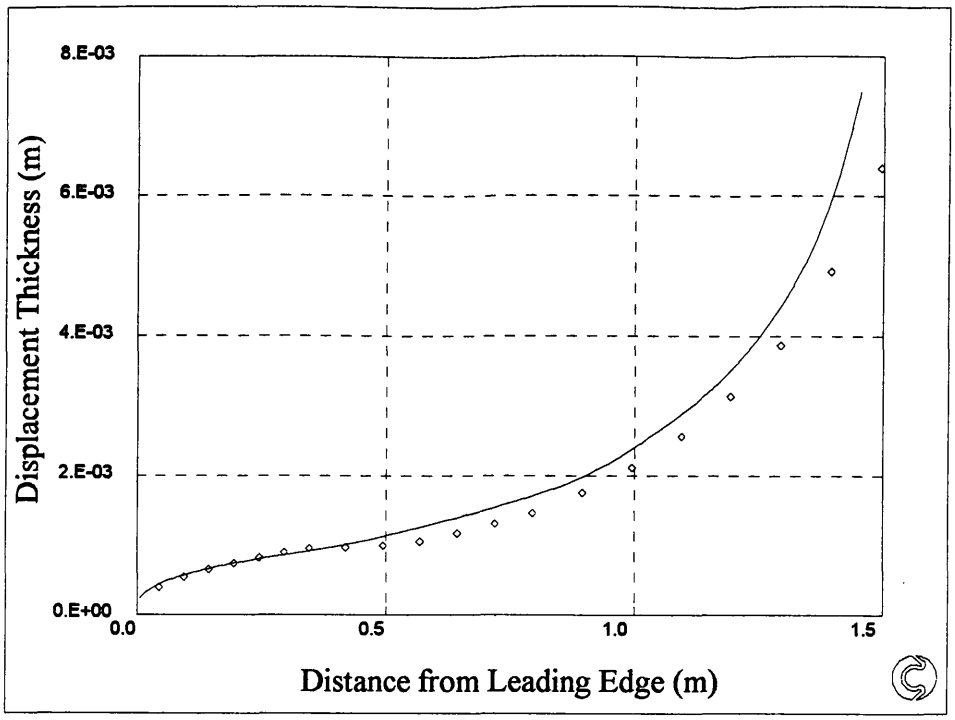

Figure 4.42: T3C5 Displacement Thickness Turbulence Intensity at Inlet

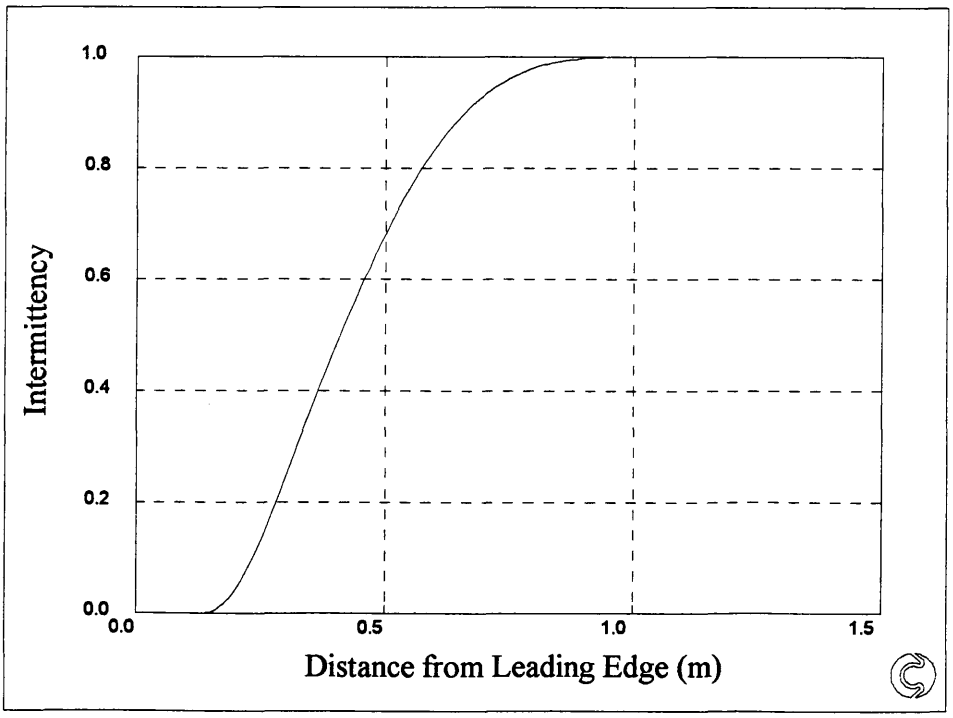

Figure 4.43: T3C5 Intermittency Turbulence Intensity at Inlet

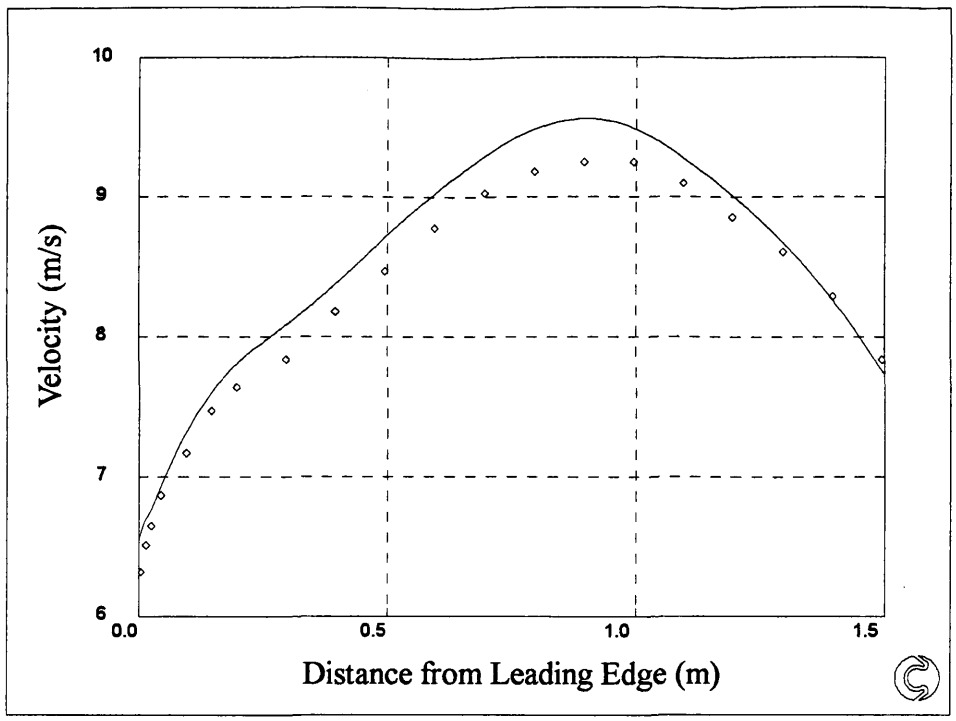

Figure 4.44: T3C1 Velocity Profile Turbulence Intensity at Start of Transition

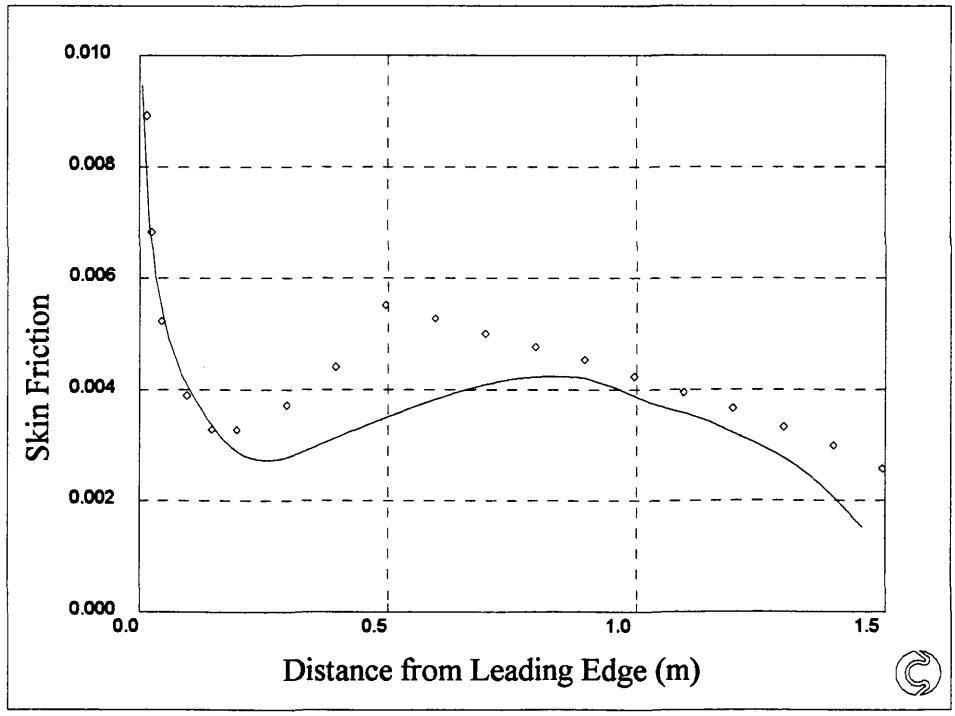

Figure 4.45: Skin Friction Turbulence Intensity at Start of Transition

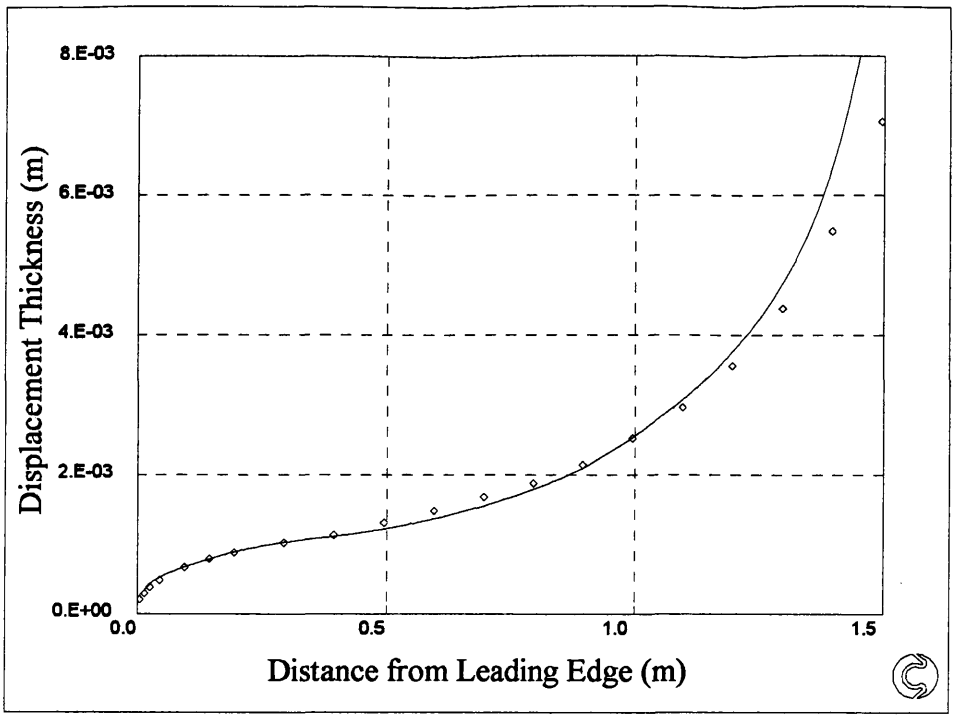

Figure 4.46: T3C1 Displacement Thickness Turbulence Intensity at Start of Transition

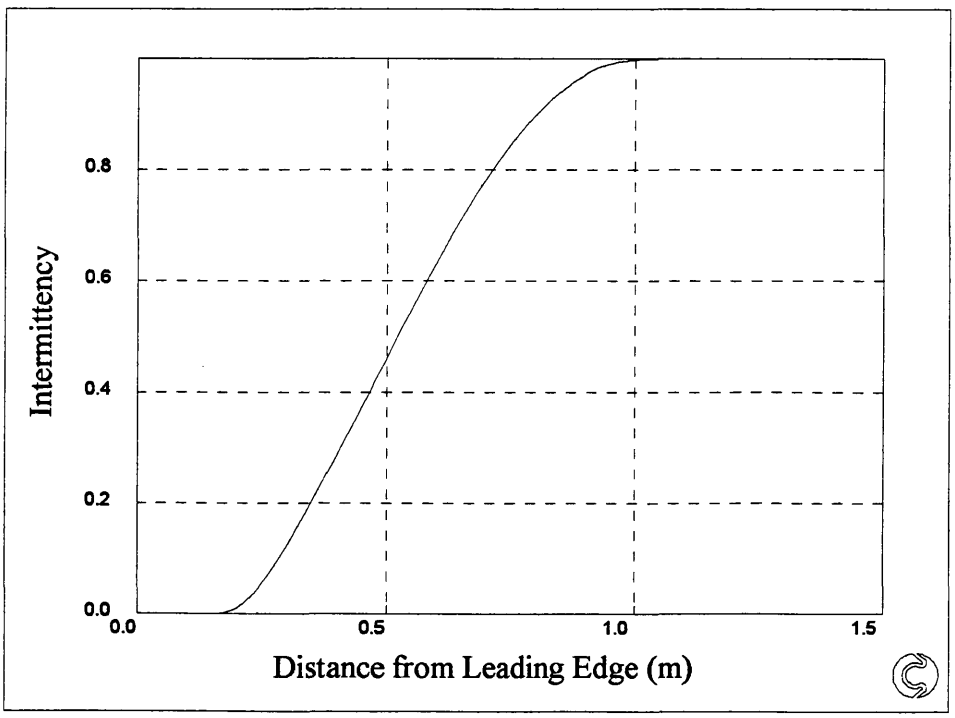

Figure 4.47: T3C1 Intermittency Turbulence Intensity at Start of Transition

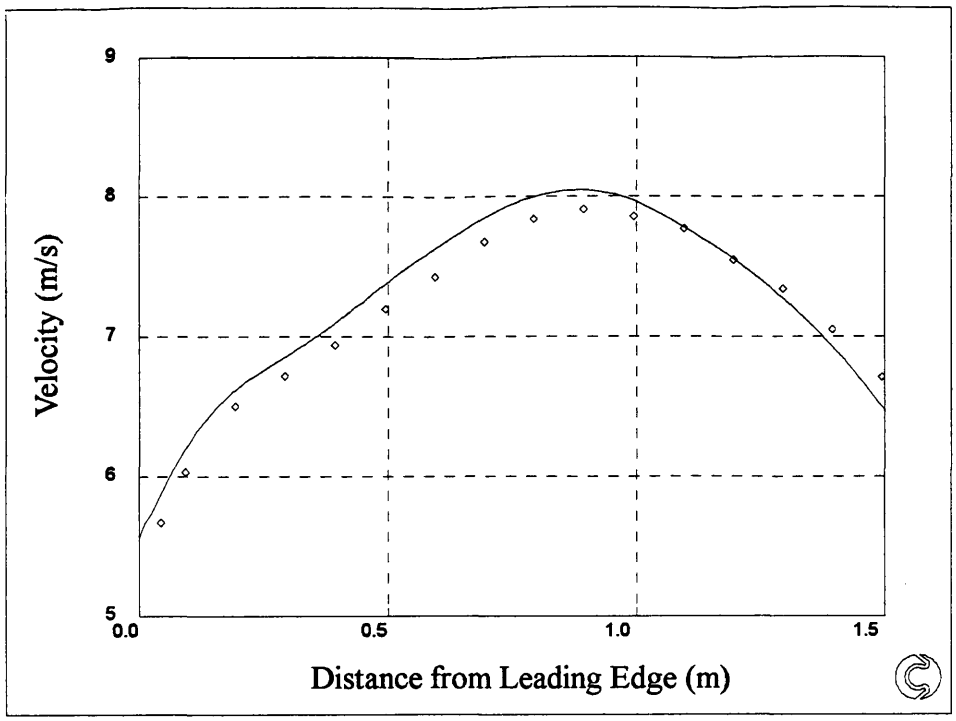

Figure 4.48: T3C2 Velocity Profile Turbulence Intensity at Start of Transition

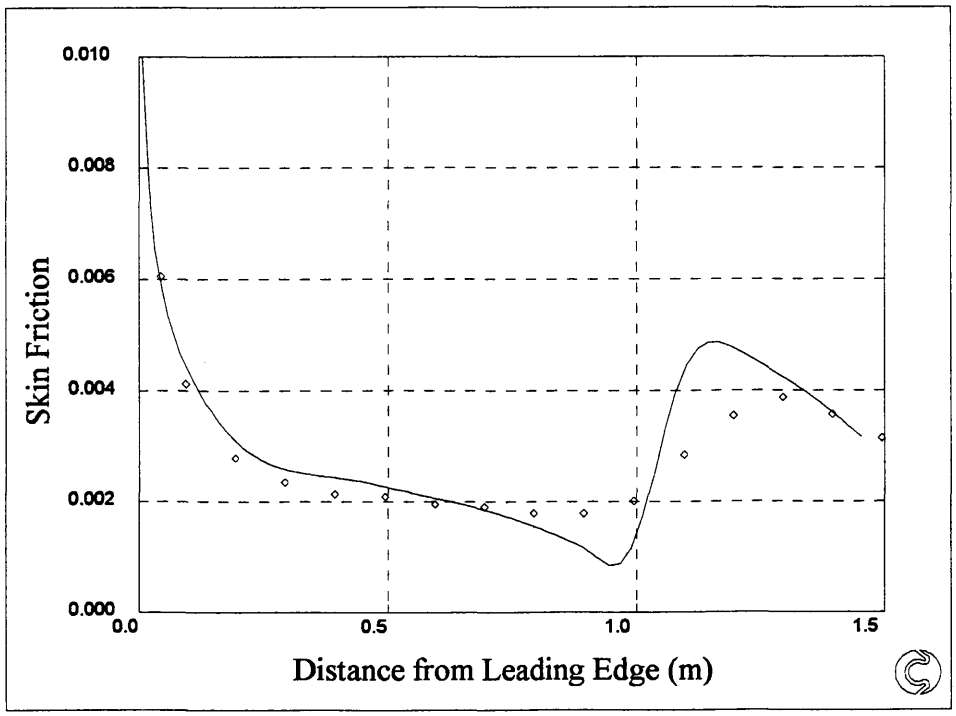

Figure 4.49: T3C2 Skin Friction Turbulence Intensity at Start of Transition

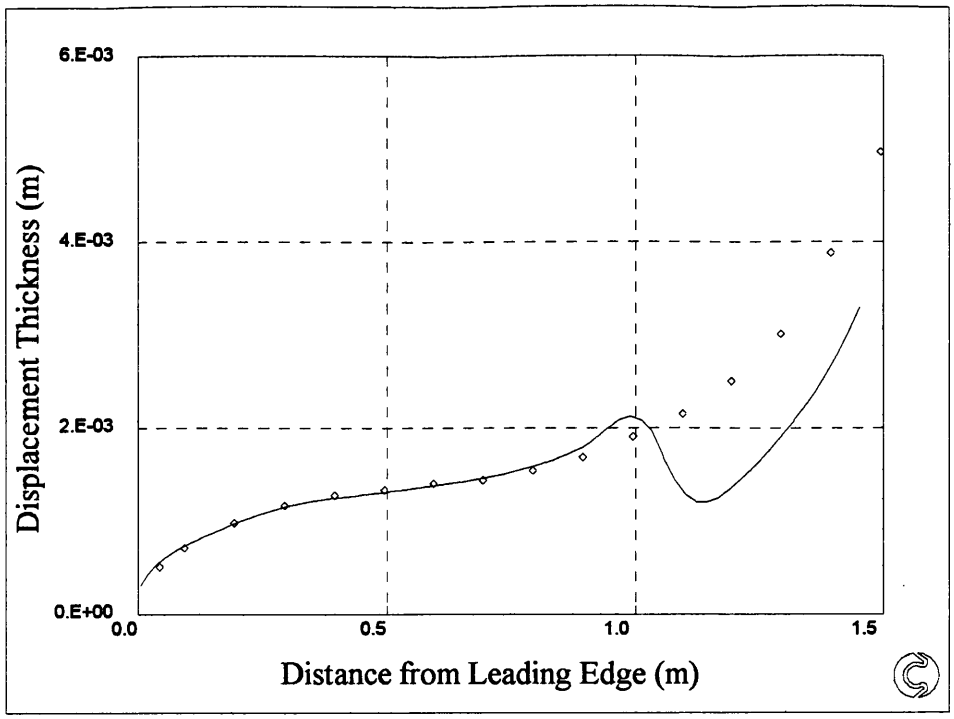

Figure 4.50: T3C2 Displacement Thickness Turbulence Intensity at Start of Transition

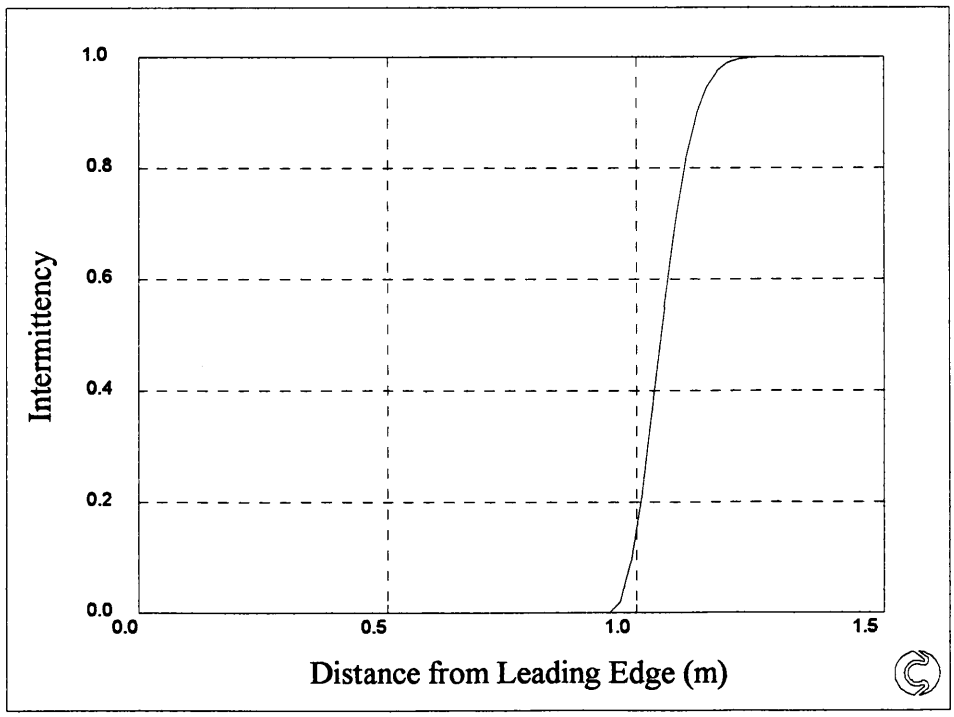

Figure 4.51: T3C2 Intermittency Turbulence Intensity at Start of Transition

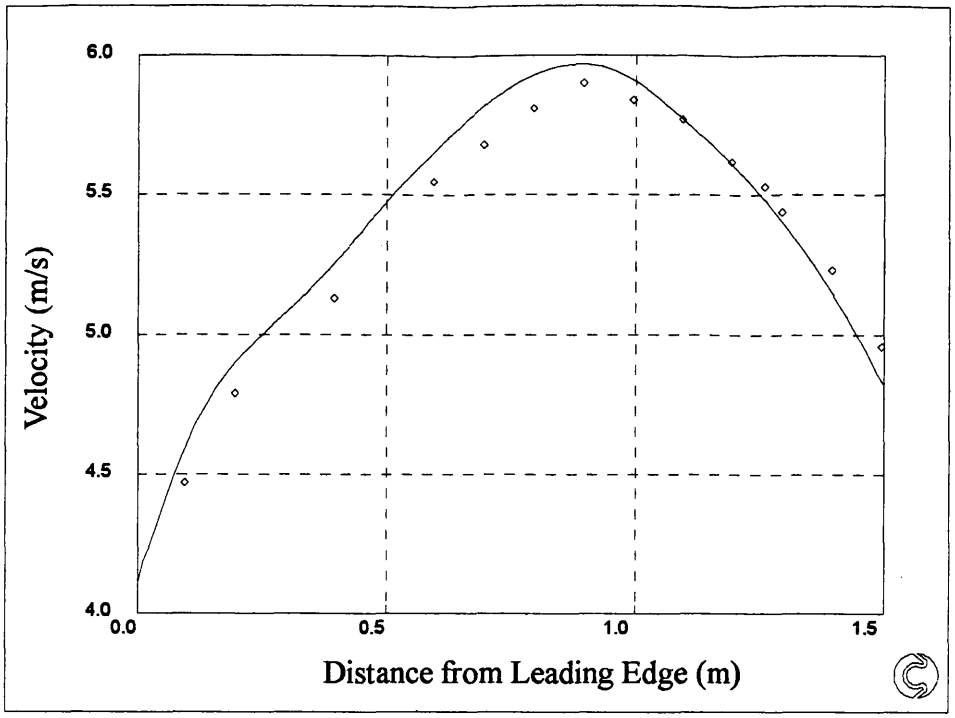

Figure 4.52: T3C3 Velocity Profile Turbulence Intensity at Start of Transition

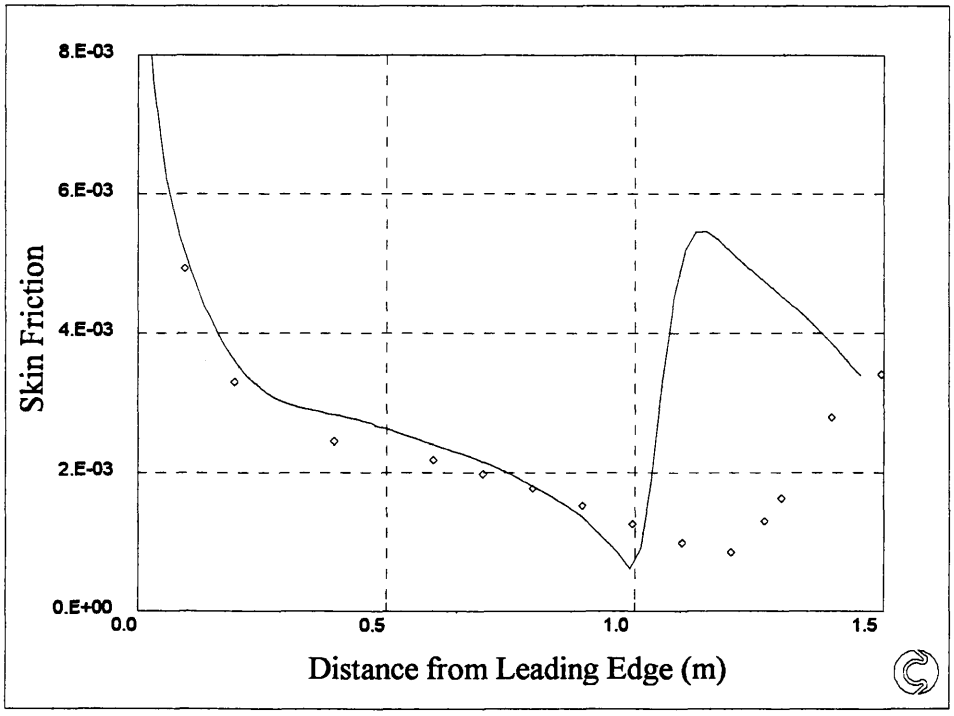

Figure 4.53: T3C3 Skin Friction Turbulence Intensity at Start of Transition

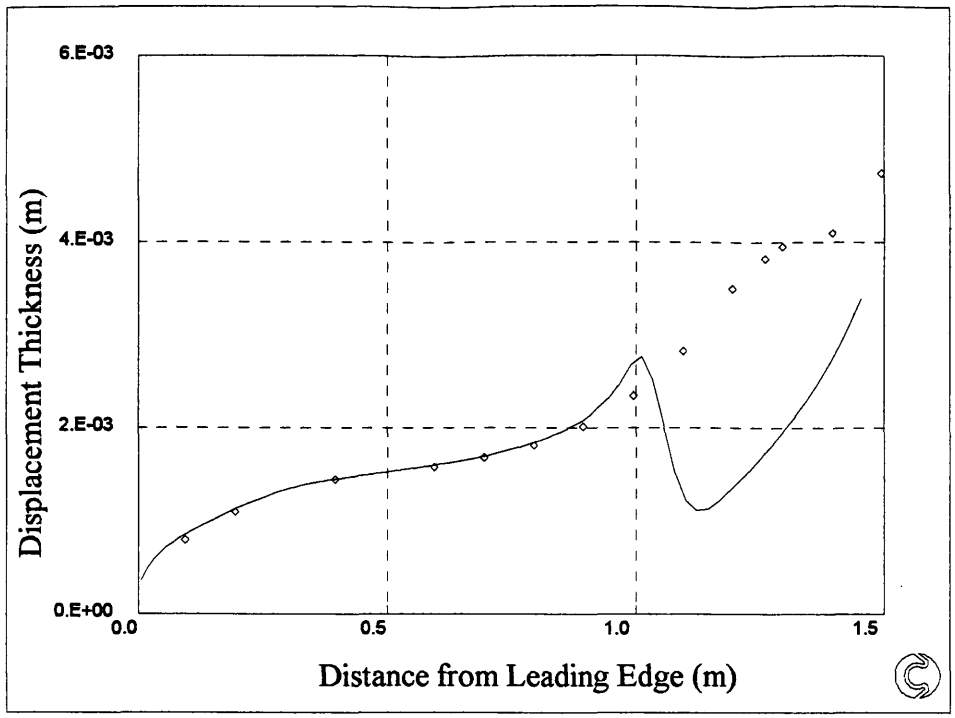

Figure 4.54: T3C3 Displacement Thickness Turbulence Intensity at Start of Transition

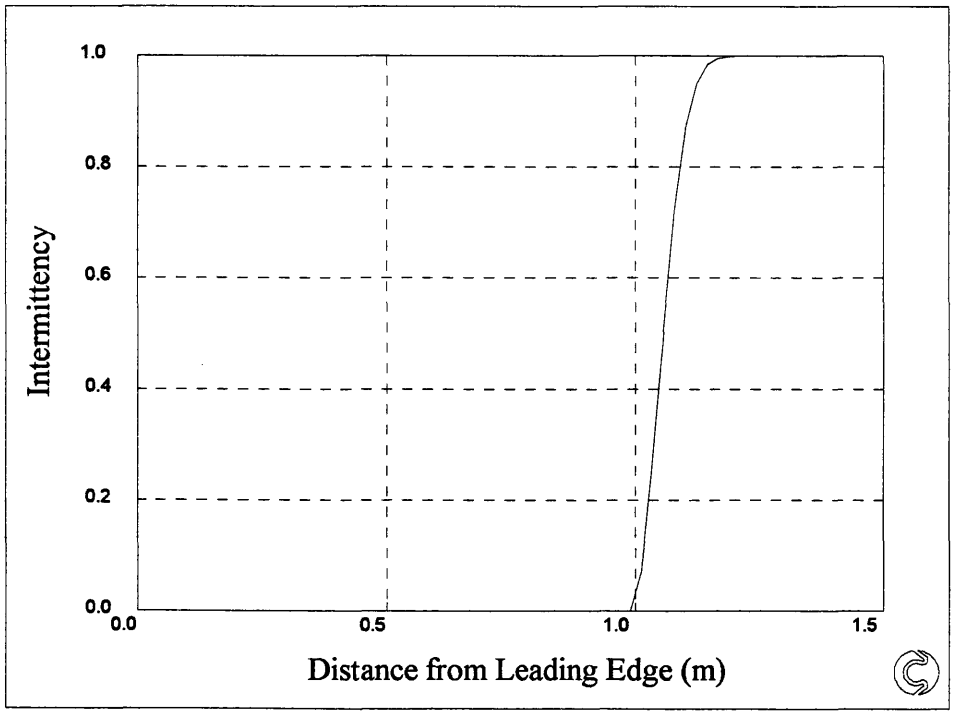

Figure 4.55: T3C3 Intermittency Turbulence Intensity at Start of Transition

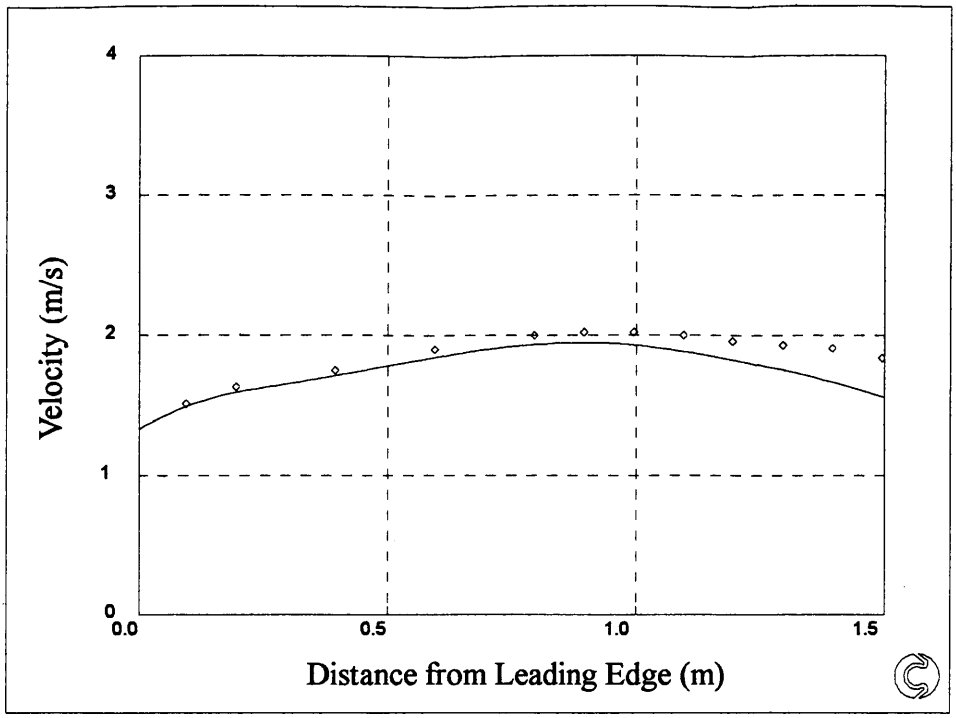

Figure 4.56: T3C4 Velocity Profile Turbulence Intensity at Start of Transition

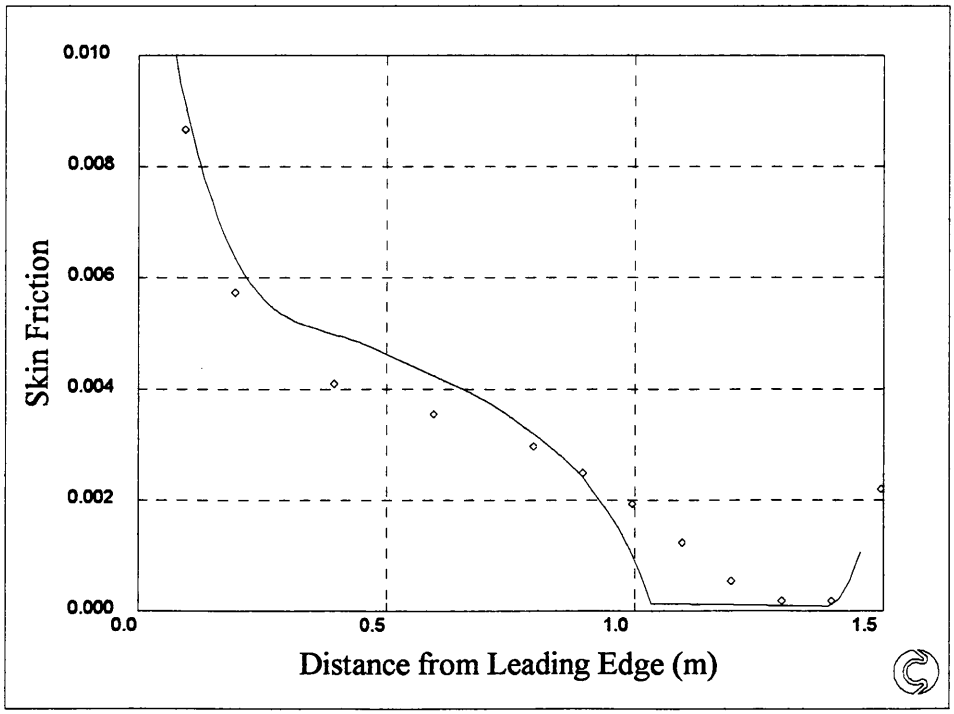

Figure 4.57: T3C4 Skin Friction Turbulence Intensity at Start of Transition

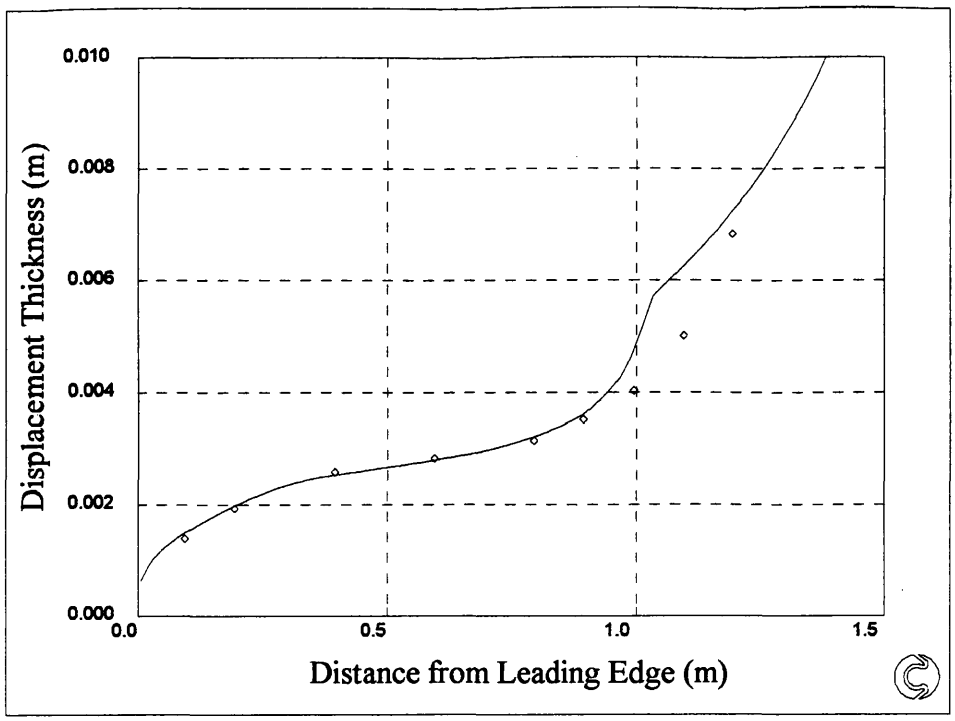

Figure 4.58: T3C4 Displacement Thickness Turbulence Intensity at Start of Transition

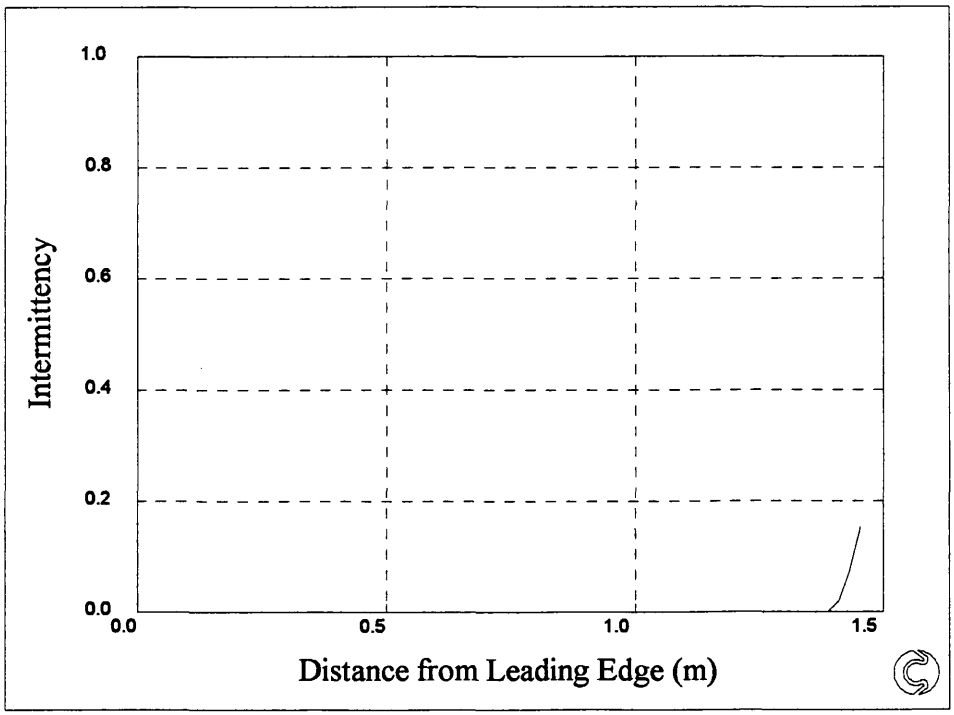

Figure 4.59: T3C4 Intermittency Turbulence Intensity at Start of Transition

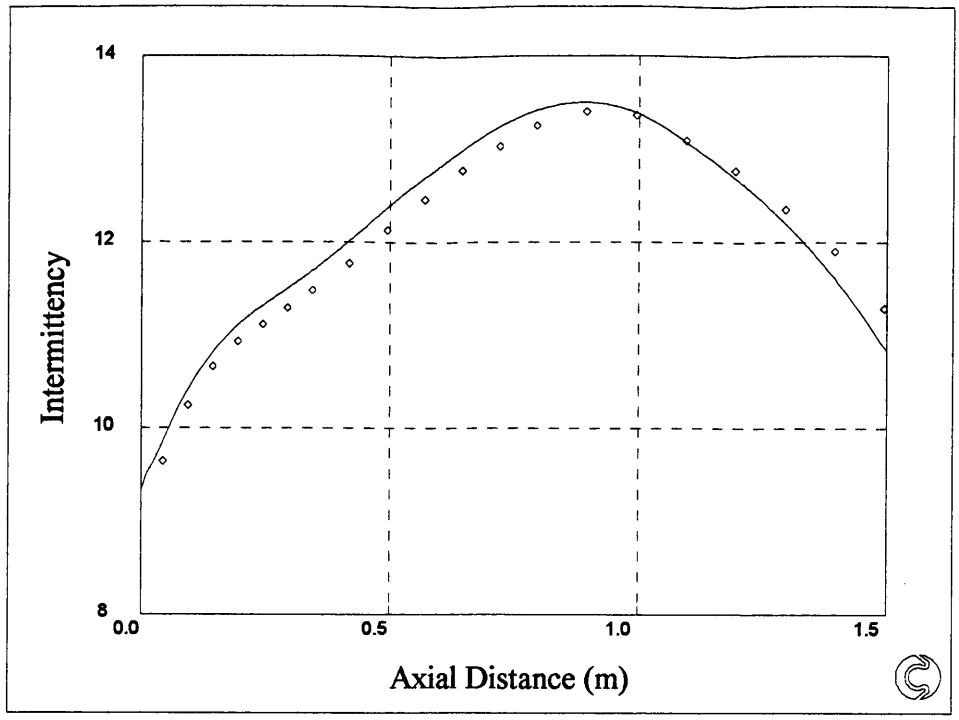

Figure 4.60: T3C5 Velocity Profile Turbulence Intensity at Start of Transition

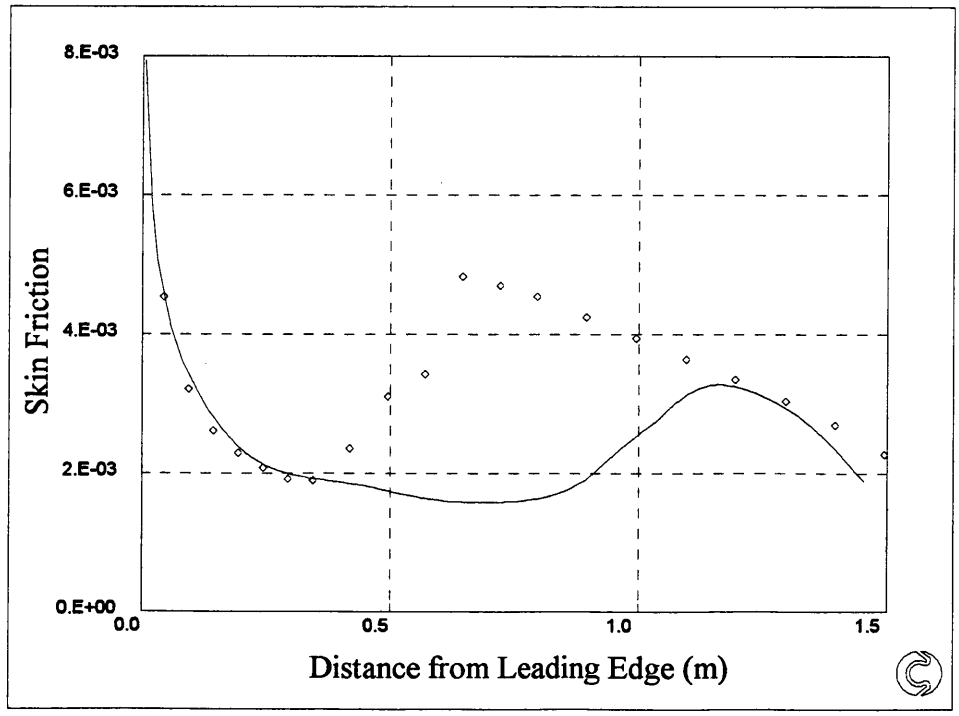

Figure 4.61: T3C5 Skin Friction Turbulence Intensity at Start of Transition

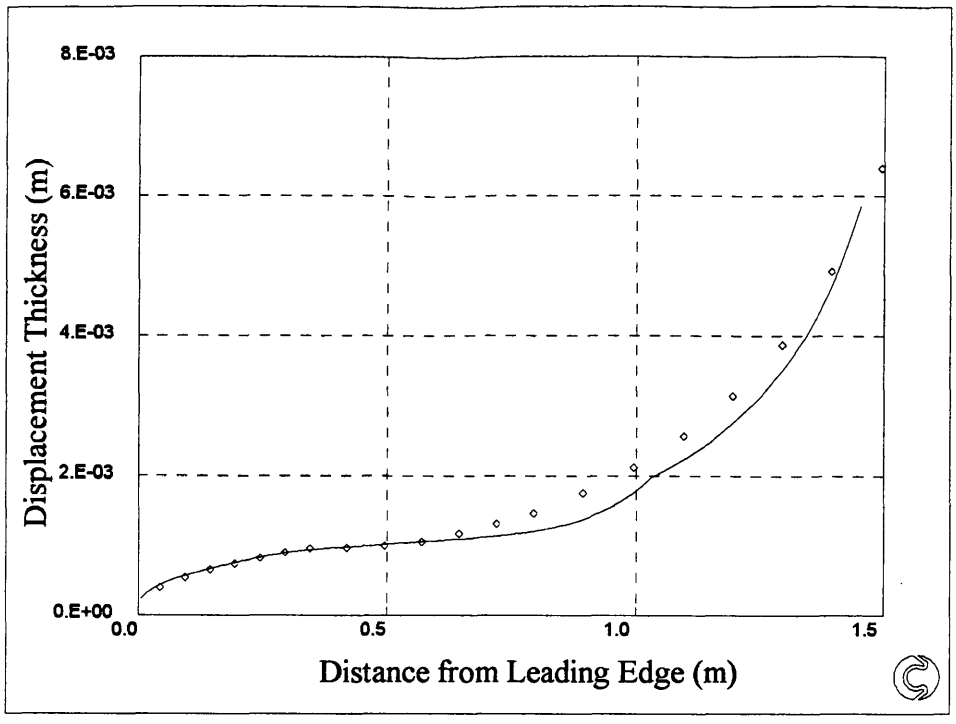

Figure 4.62: T3C5 Displacement Thickness Turbulence Intensity at Start of Transition

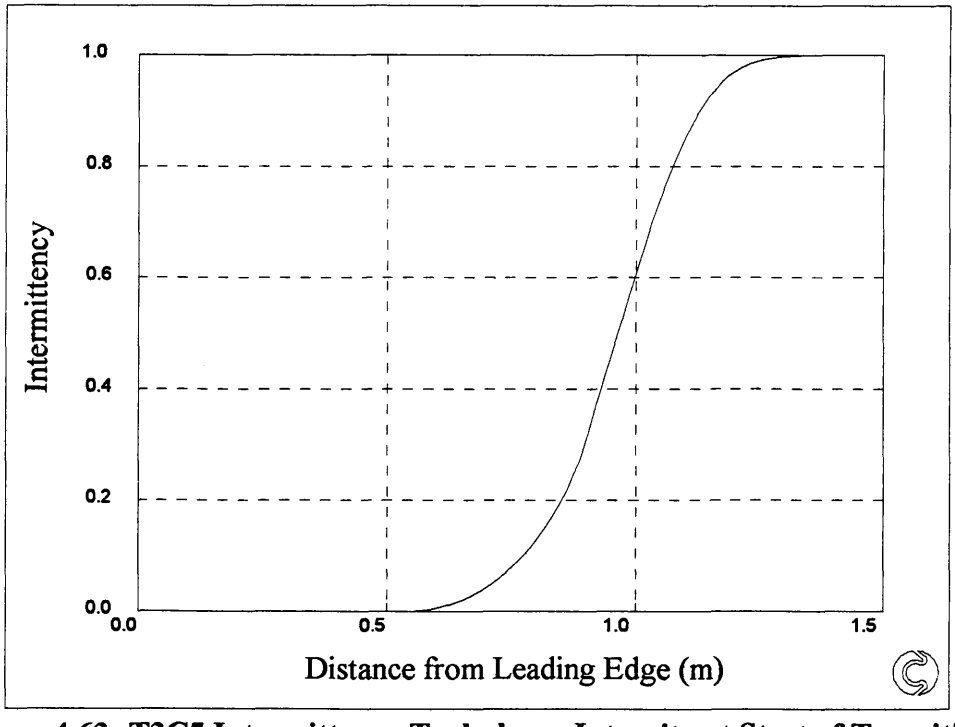

Figure 4.63: T3C5 Intermittency Turbulence Intensity at Start of Transition

5. Turbulence Modelling

5.1 Dunham's Correlation

It was clear from the previous chapter that to give consistently good prediction of the start of transition, it was not possible to use the value of turbulence intensity at either the inlet or start of transition as a representative value in the correlation attributable to Abu - Ghannam and Shaw (1980) or Mayle (1991). Further research into the original report, Abu - Ghannam and Shaw (1980) revealed that the value of the turbulence intensity used in their correlation was measured somewhere between the inlet and the start of transition. Dunham (1972) suggested that the turbulence intensity relevant to the start of transition was some mean turbulence level which characterises the flow throughout the history of the boundary layer. He took this value to be:

$$q = \frac{q_{inlet} + q_{start}}{2} \tag{5.1}$$

The value of turbulence intensity found by using equation (5.1) was used in the Abu - Ghannam and Shaw correlation to predict the start of transition, and the Fraser, Higazy and Milne (1994) method for the transitional properties in the Rolls Royce T3C flows.

Figures 5.1 to 5.20 show predictions of velocity profile, skin friction, displacement thickness and intermittency for flows T3C1 - T3C5. The prediction of velocity profile and displacement thickness is quite good, except for flow T3C4 and probably due to a separation being predicted in that flow. According to the skin friction predictions, the start of transition is predicted late in flow T3C1 and early in flows T3C2, T3C3, T3C4 and T3C5. In general this type of turbulence

intensity averaging gives better predictions than using either the turbulence intensity at inlet to the domain or at the start of transition.

It was thought that the predictions may improve if a better form of averaging the turbulence intensity was devised.

5.2 Batchelor's Method

Although it has been previously shown in the preceding chapters that it is possible to predict turbulent boundary layer properties in transitional flows using a laminar flow field, there was still a requirement to predict the free stream turbulence intensity throughout the flow field. It was possible to do this using the industry standard k - ε turbulence model already built into PHOENICS, but this approach would increase the solution time. Since a rapid solution is the purpose of integral boundary layer methods, this option was rejected.

Batchelor (1953) analysed the change in turbulence level in a uniform stream passing through a distortion, giving exact relations for the case of a symmetrical area change, viz.:

$$\frac{q}{q_\infty} = \left[\frac{1}{2c}\left(1+\frac{F}{c^3}\right)\right]^{0.5} \tag{5.2}$$

where: $$F = \frac{\tan^{-1}\sqrt{c^{-3}-1}}{\sqrt{c^{-3}-1}} \qquad \text{when } c < 1 \tag{5.2a}$$

or $$F = \frac{\log_e\left[c^{3/2}\left(1+\sqrt{1-c^{-3}}\right)\right]}{\sqrt{1-c^{-3}}} \qquad \text{when } c > 1 \tag{5.2b}$$

If equation (5.2) was applied to the stream tube adjacent to the surface of a turbomachine blade and the flow area of that stream-tube changes in the ratio c from upstream to any station on the blade surface (c > 1 being an acceleration of

the flow and c < 1 a diffusion), then using q_∞ to denote the upstream level and q the local value at the station. For incompressible flow c is the ratio of local surface velocity to upstream velocity ($c = w/w_\infty$). Taking c = 0.2 and 5 as the extreme limits of interest, the corresponding range for q/q_∞ was 6.64 to 0.32.

The area change through a cascade of blades is not symmetrical but can be regarded as two-dimensional. Batchelor and Proudman (1954), examined over the limited range ($0.5 < c < 2$), and comparison showed little difference between q/q_∞ and the symmetrical case to be of any practical importance.

The above procedure was coded into PHOENICS applied to test cases T3C1 - T3C5. Prediction of turbulence intensity was poor, Figures 5.21 - 5.25. The error was greater than 125% at some points.

5.3 Prandtl's Mixing Length Model

One of the most simple turbulence models which is widely used by the aerospace industry, Versteeg and Malalasekera (1995) was Prandtl's mixing length model. It was used for two - dimensional turbulent flows when the only significant pressure gradient is in the direction normal to the main flow direction and the only significant Reynolds stress is:

$$\tau_{zx} = \tau_{xz} = -\rho\overline{w'u'} \tag{5.3}$$

For flows in the z - x plane the turbulent Reynolds stress is described by:

$$\tau_{zx} = \tau_{xz} = -\rho\overline{W}'\overline{u}' = \rho\ell_m^2\left|\frac{\partial W}{\partial x}\right|\frac{\partial W}{\partial x} \tag{5.4}$$

where: ℓ_m is the turbulent length scale

Turbulence is a function of the flow and if turbulence changes then one must account for this within the mixing length model by varying ℓ_m. This can be

achieved by means of simple algebraic formulae e.g. Launder and Spalding (1972). A major disadvantage with this model is that in the free stream $\partial W/\partial x$ will be zero, therefore it is not suitable for the purposes required here.

5.4 Two-Equation Models of Turbulence

This limitation described above can be overcome by the use of a two-equation model of turbulence, where both the kinetic energy, k and length scale, ℓ_m were derived from transport equations. Launder and Spalding (1972) define the variable $Z = k^m \ell_m^n$ with m and n being constants. They subsequently derived the following equations for Z and k from the Navier - Stokes equations:

$$\rho\frac{DZ}{Dt} = \frac{\partial}{\partial x}\left(\frac{\mu_t}{\sigma_z}\frac{\partial Z}{\partial x}\right) + Z\left[C_1\frac{\mu_t}{k}\left(\frac{\partial W}{\partial x}\right)^2 - C_2\frac{\rho^2 k}{\mu_t}\right] + s_z \qquad (5.4)$$

$$\rho\frac{Dk}{Dt} = \frac{\partial}{\partial x}\left(\frac{\mu_t}{\sigma_k}\frac{\partial k}{\partial x}\right) + k\left[\frac{\mu_t}{k}\left(\frac{\partial W}{\partial x}\right)^2 - C_D\frac{\rho^2 k}{\mu_t}\right] \qquad (5.5)$$

where: C_1, C_2, C_z are constants in many flows

and s_z are secondary source terms

Spalding (1969) defined an equation, (W equation) for Z in which m = 1, n = -2. Other workers have proposed different equations for Z.

In the type of flows under consideration here, it was presumed that in the free stream there will be no production of turbulence and axial diffusion was presumed negligible compared to axial convection. This was similar to the decay of turbulence behind a fine wire mesh. In this process, the variables were presumed to be only functions of stream wise co-ordinate z; the partial differential equations (5.4) and (5.5) reduce to a pair of ordinary differential equations for k and Z.

$$\rho W \frac{dk}{dz} = -C_D \frac{\rho^2 k^2}{\mu_t} \tag{5.6}$$

$$\rho W \frac{dZ}{dz} = -C_2 \frac{\rho^2 k Z}{\mu_t} \tag{5.7}$$

Launder and Spalding (1972) recommend using the values of 0.09 and 0.17 for C_2 and C_D respectively. Malin (1995) suggests using the k - ε turbulence model to predict the decay of homogeneous free stream turbulence behind a grid. As with Launder and Spalding (1972), axial diffusion of turbulence was presumed negligible compared to axial convection, and turbulent production was zero, the k - ε equations reduce to:

$$W \frac{dk}{dz} = -\varepsilon \tag{5.8}$$

$$W \frac{d\varepsilon}{dz} = C_{2\varepsilon} \frac{\varepsilon^2}{k} \tag{5.9}$$

where $\varepsilon = \dfrac{k^{3/2}}{\ell}$

Substituting equation (5.8) into equation (5.9) and integrating gives:

$$k = \left[k_o - \frac{(1 - C_{2\varepsilon})\varepsilon_o}{k_o^{C_{2\varepsilon}}} \int_{z_0}^{z} \frac{dz}{W} \right]^{\frac{1}{(1-C_{2\varepsilon})}} \tag{5.10}$$

Where: k_o turbulent kinetic energy at inlet

ε_o dissipation at inlet

This method has already been programmed for zero pressure gradient flows in PHOENICS and was available as library case 230. The CFD solution gives an excellent representation of the analytical solution of the decay of free stream kinetic energy in a zero pressure gradient flow behind a wire grid over a flat plate,

see Figure 5.26.

Using a characteristic length of 2 mm for test cases T3C2 - T3C5 (q_{inlet}= 3 %) gave a good prediction of free stream turbulence intensity, and a characteristic length of 4 mm gave a good prediction for case T3C1 (q_{inlet}= 6.6%). The choice of length scale was approximately 10% of grid spacing of the upstream turbulence grid used in the ARL wind tunnel.

Malin's turbulence model, and the choice of length scale at inlet were validated by running test cases T3C1 - T3C5 using Dunham's correlation and the Fraser, Higazy and Milne (1994) method for transitional boundary layer properties. The turbulence intensities used would be calculated by PHOENICS. Plots of velocity profile, skin friction, displacement thickness, intermittency and free stream turbulence intensity are shown in Figures 5.27 - 5.51. There is no significant difference in the predicted properties using the turbulence intensity calculated by Malin's method or that of the data, when using Dunham's (1972) correlation.

The transition method attributable to Solomon, Walker and Gostelow (1995) was used in conjunction with Malin's turbulence model to predict boundary layer properties Figures 5.52 - 5.66. The predictions were almost identical to that of Fraser, Higazy and Milne (1994).

5.5 Integrated Average

Dunham's (1972) method for evaluating turbulence intensity attempts to take into account the history of the flow. It was thought that a more meaningful evaluation of the history of the flow would provide a better average of the turbulence intensity and hence a better prediction of the start of transition using the Abu-Ghannam and Shaw (1980) correlation. With the z direction as the major

flow, the average turbulence intensity from the inlet was calculated from:

$$\bar{q} = \frac{1}{z}\int_{o}^{z} q \, dz \qquad (5.11)$$

Equation 5.11 was programmed into PHOENICS and test cases T3C1 - T3C5 were run again, using the transitional method described by Fraser, Higazy and Milne (1994). Boundary layer properties are shown in Figures 5.67 - 5.91. Using the minimum value of skin friction as the criteria to predict the start of transition, it has been shown that a better, more consistent prediction of the start of transition has been achieved, Figures 5.68, 5.73, 5.78, 5.83, 5.88. The start of transition is predicted late in flow T3C1 and early in all the other T3C flows. If low turbulence intensity at the start of transition was described as less than about 1.5% and high turbulence intensity was described as greater than about 3%, then this agree with the findings of Gostelow et al (1994). They report that the Abu-Ghannam and Shaw correlation at high turbulence levels predicts the start of transition too late, but agree that at low turbulence levels transition is predicted too early.

For completeness, the method described by Solomon, Walker and Gostelow (1995) was used to predict transitional boundary layer properties in flows T3C2, T3C3 and T3C4. using the turbulence intensity integrated average to predict the start of transition, Figures 5.92 - 5.106. It has been shown that the predicted properties are identical to that of Fraser, Higazy and Milne (1994).

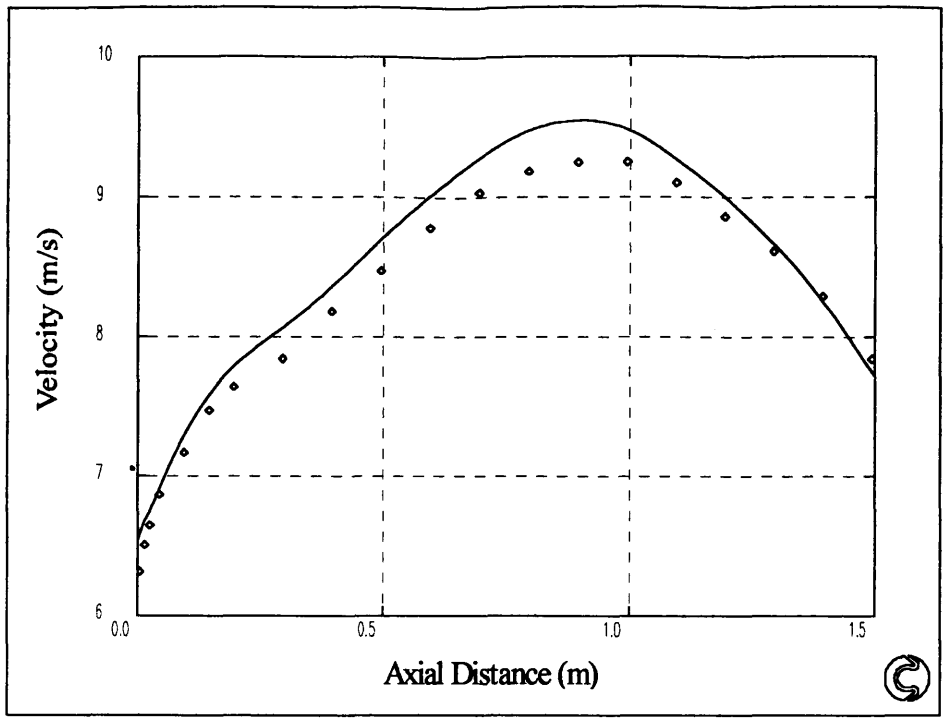

Figure 5.1: T3C1 Fraser/Dunham

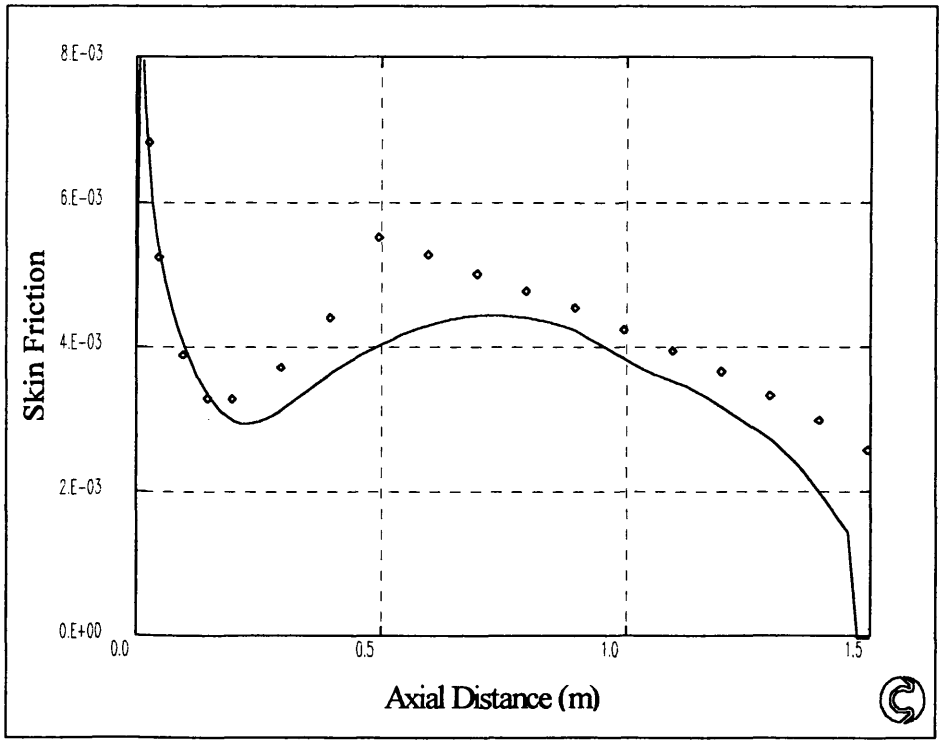

Figure 5.2: T3C1 Fraser/Dunham

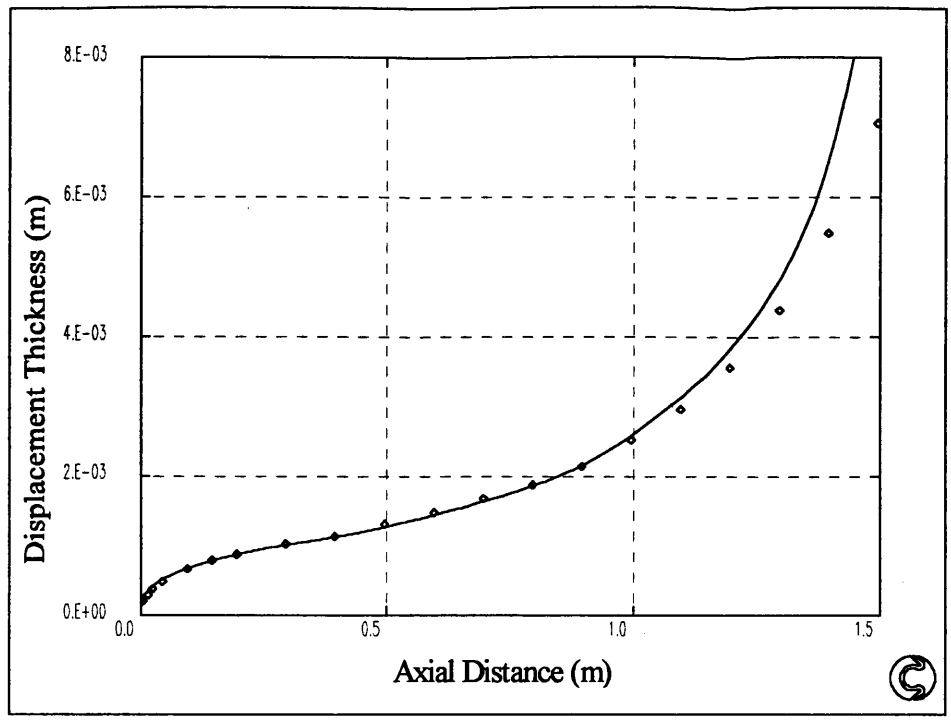

Figure 5.3: T3C1 Fraser/Dunham

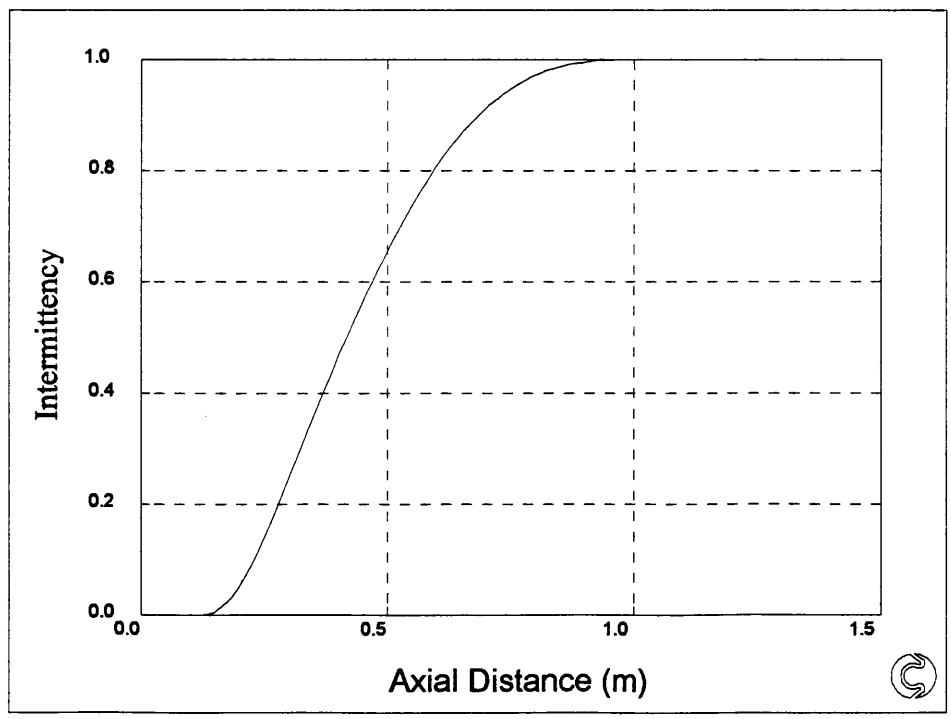

Figure 5.4: T3C1 Fraser/Dunham

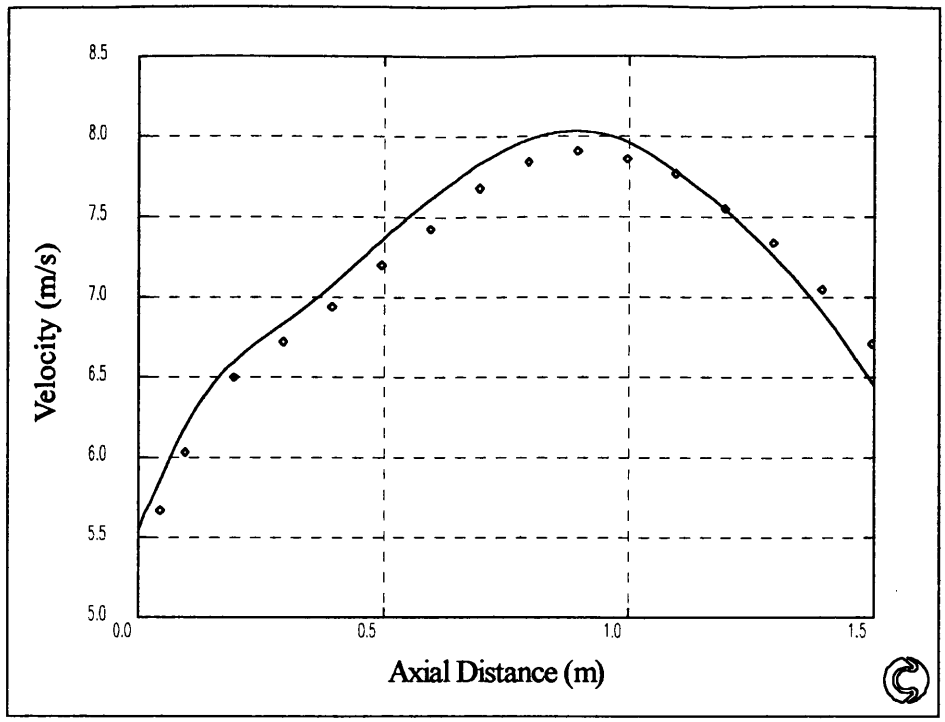

Figure 5.5: T3C2 Fraser/Dunham

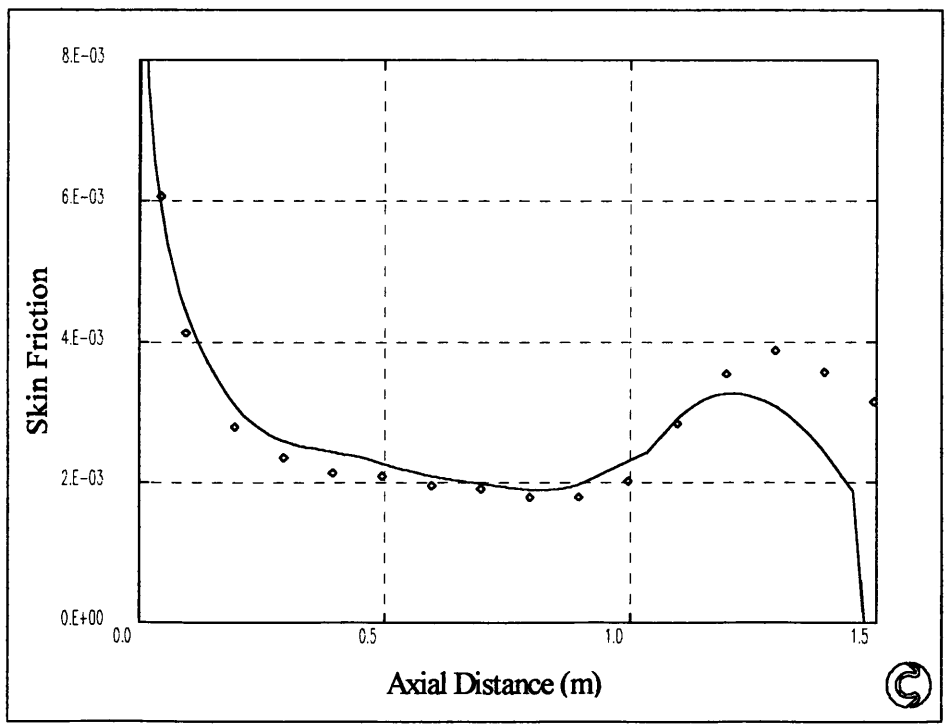

Figure 5.6: T3C2 Fraser/Dunham

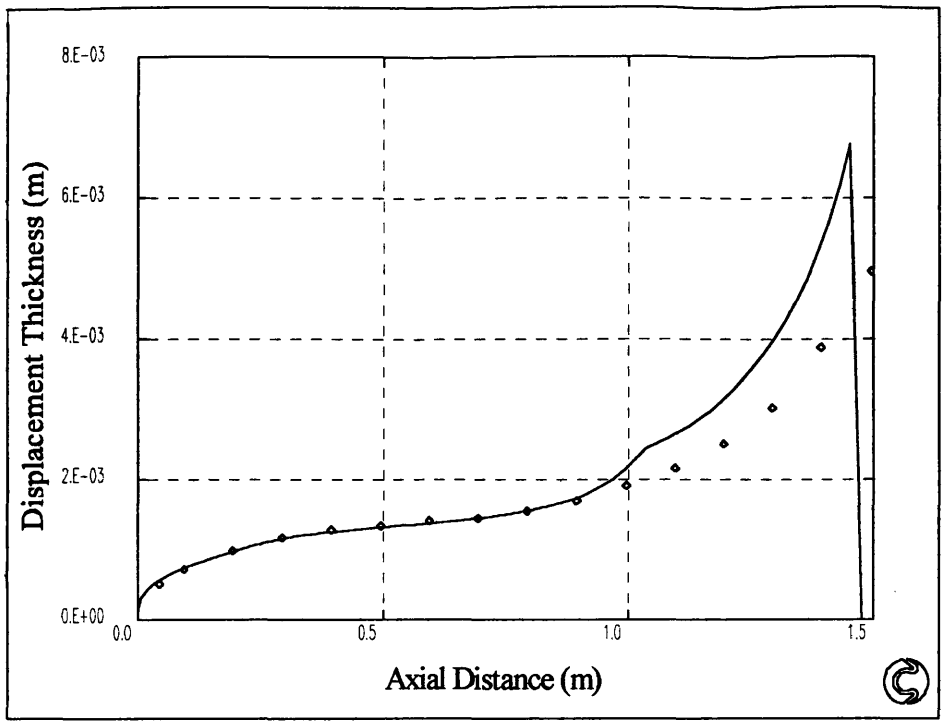

Figure 5.7: T3C2 Fraser/Dunham

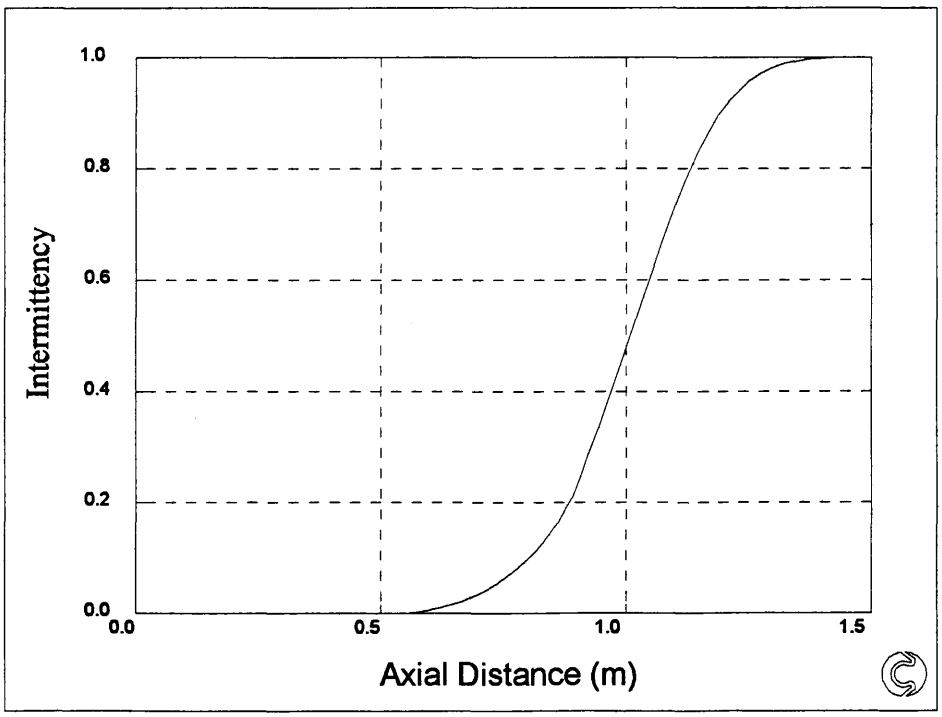

Figure 5.8: T3C2 Fraser/Dunham

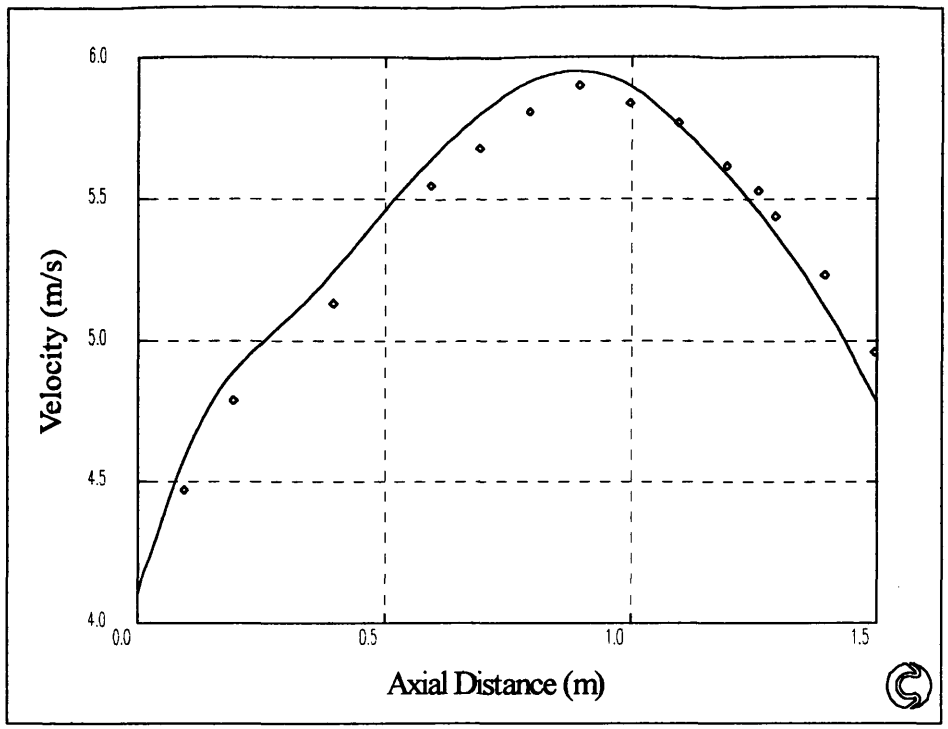

Figure 5.9: T3C3 Fraser/Dunham

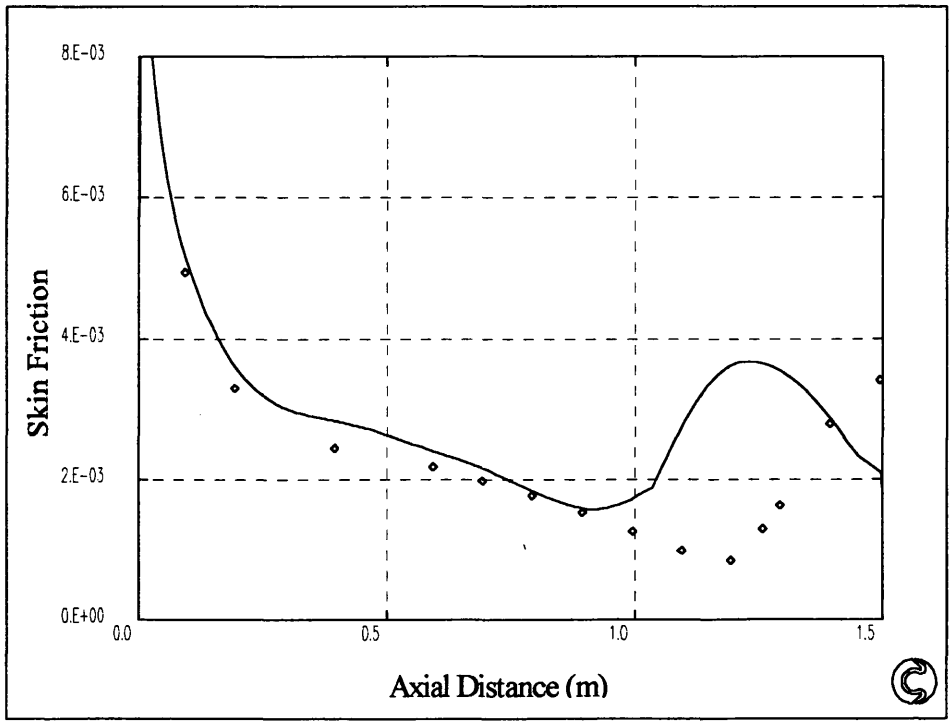

Figure 5.10: T3C3 Fraser/Dunham

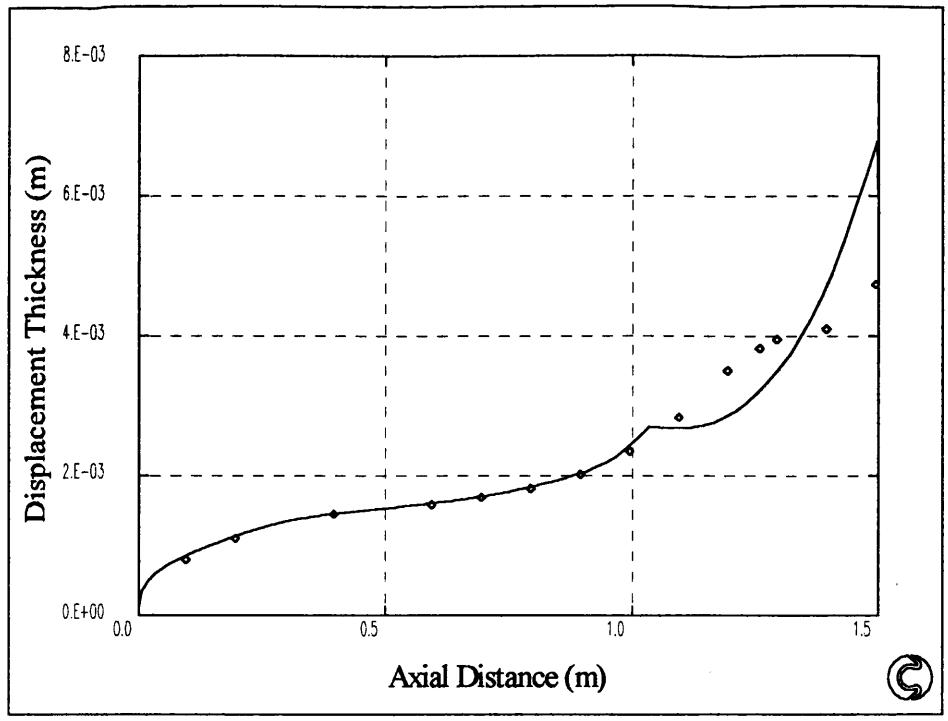

Figure 5.11: T3C3 Fraser/Dunham

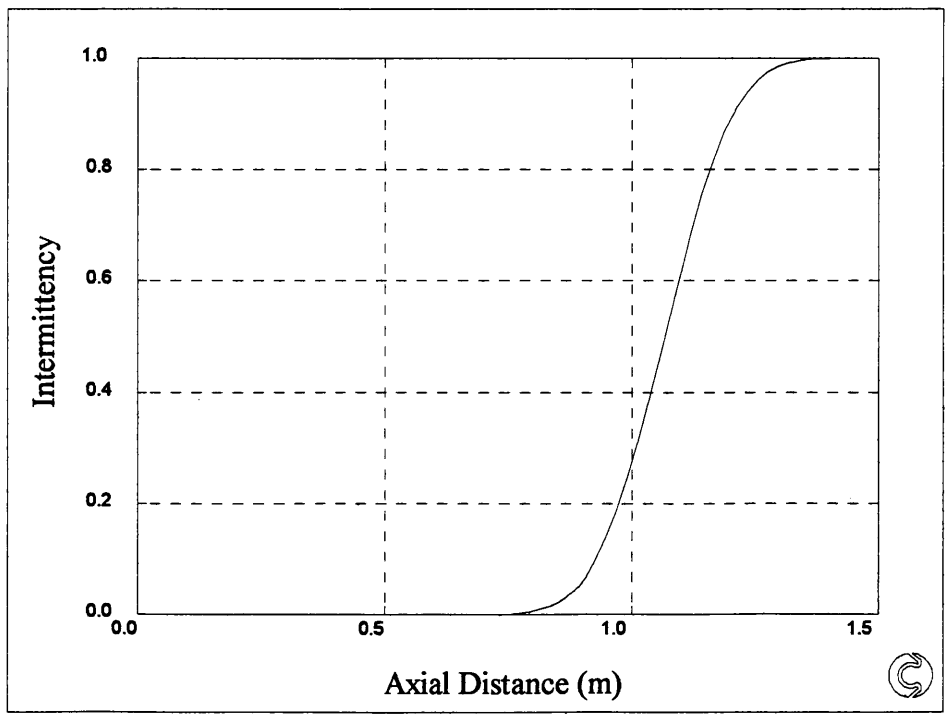

Figure 5.12: T3C3 Fraser/Dunham

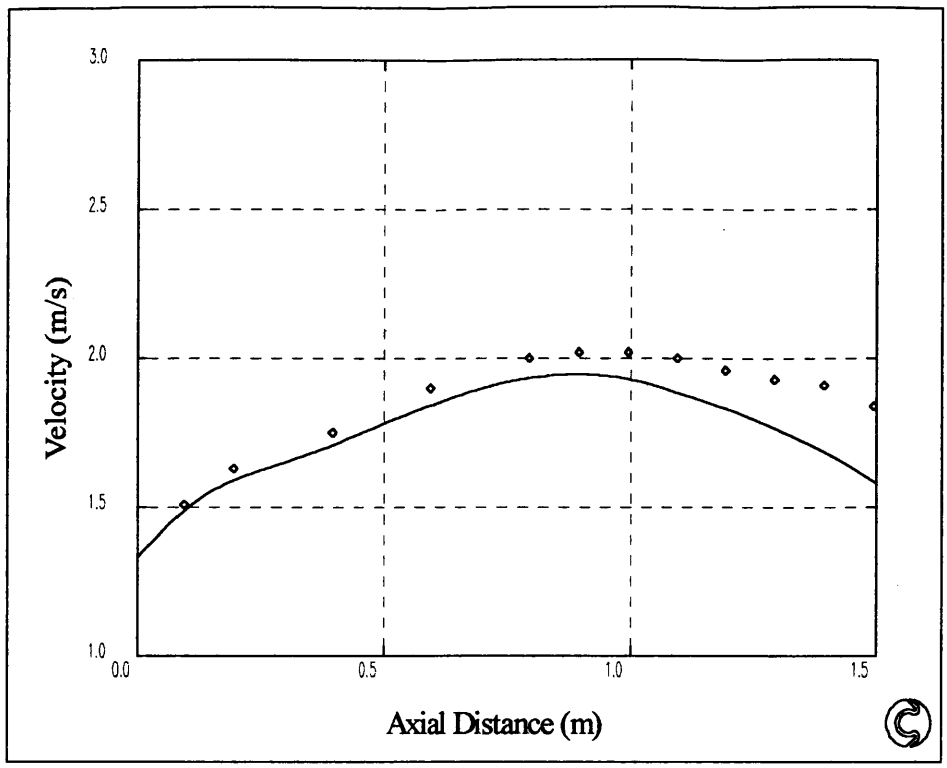

Figure 5.13: T3C4 Fraser/Dunham

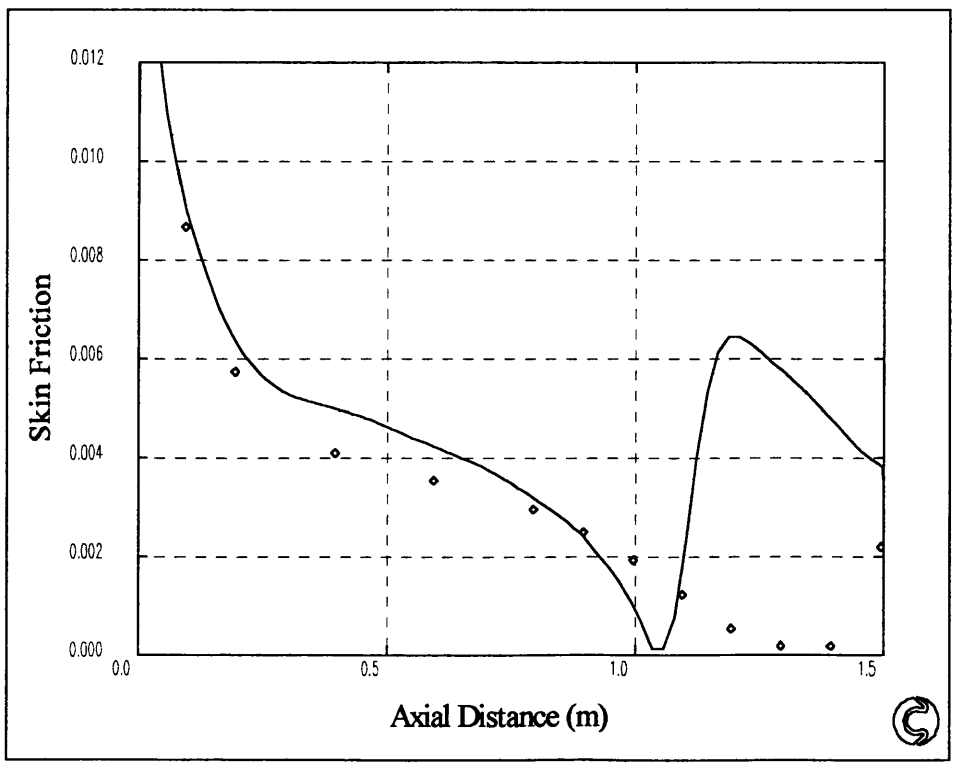

Figure 5.14: T3C4 Fraser/Dunham

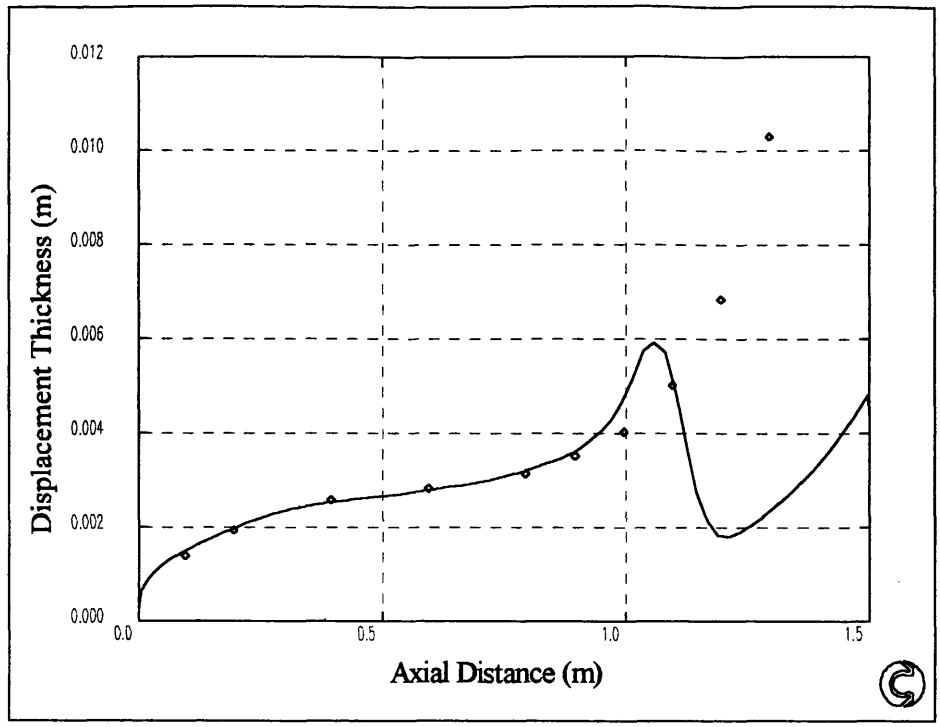

Figure 5.15: T3C4 Fraser/Dunham

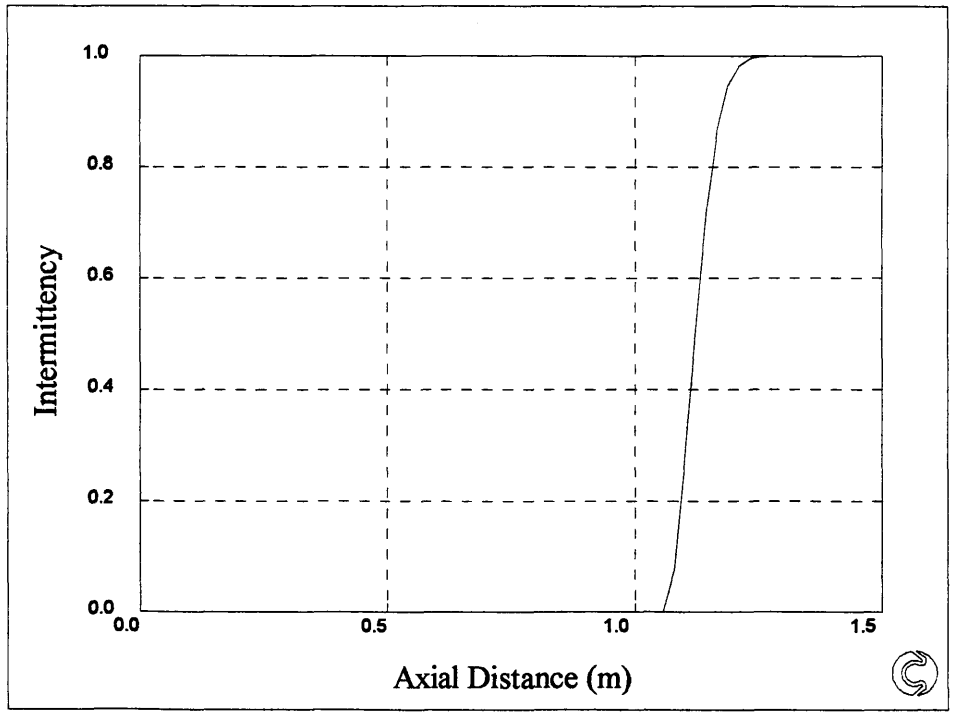

Figure 5.16: T3C4 Fraser/Dunham

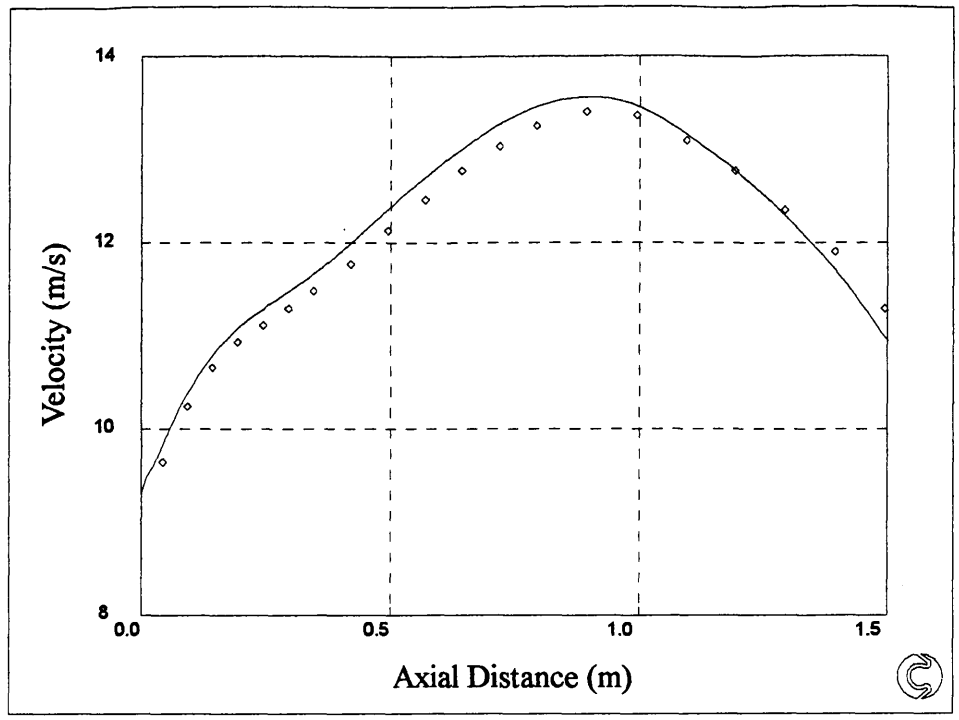

Figure 5.17: T3C5 Fraser/Dunham

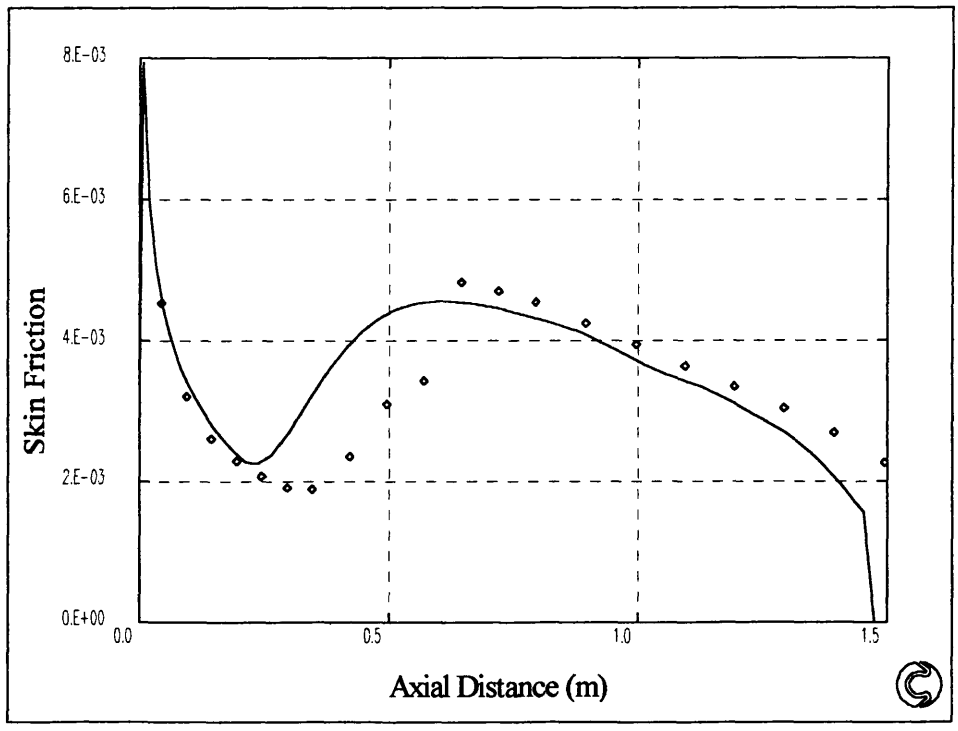

Figure 5.18: T3C5 Fraser/Dunham

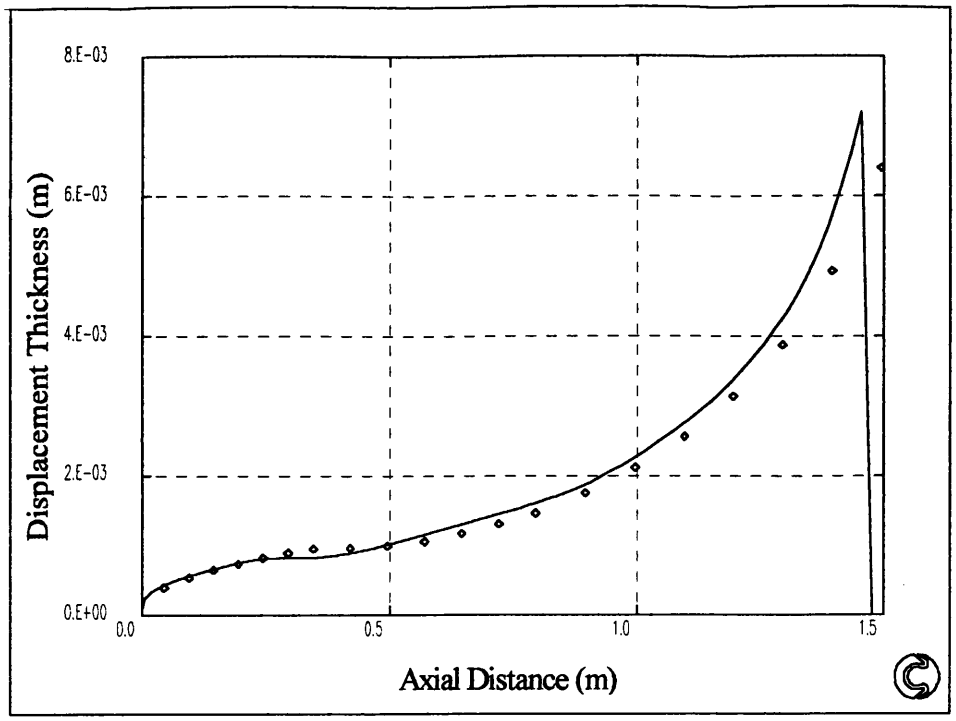

Figure 5.19: T3C5 Fraser/Dunham

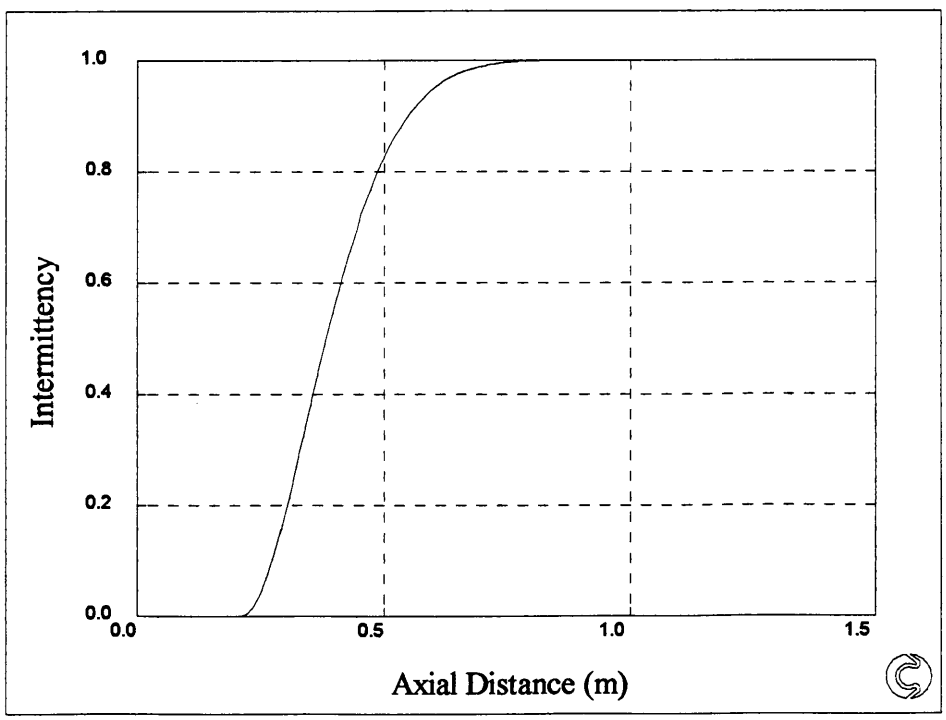

Figure 5.20: T3C5 Fraser/Dunham

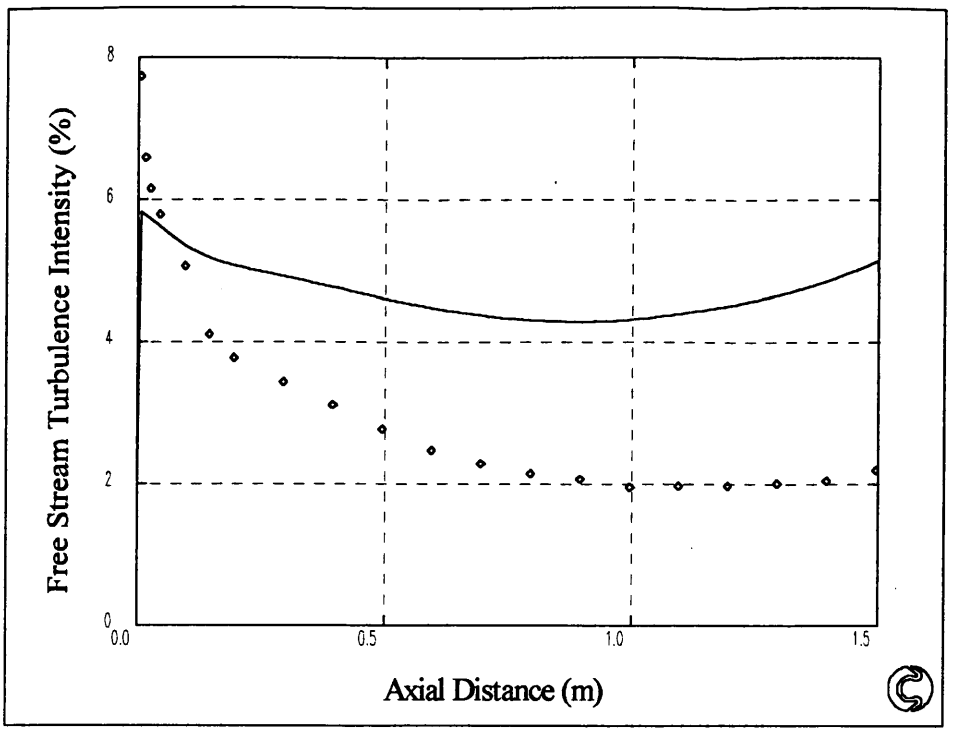

Figure 5.21: T3C1 Batchelor

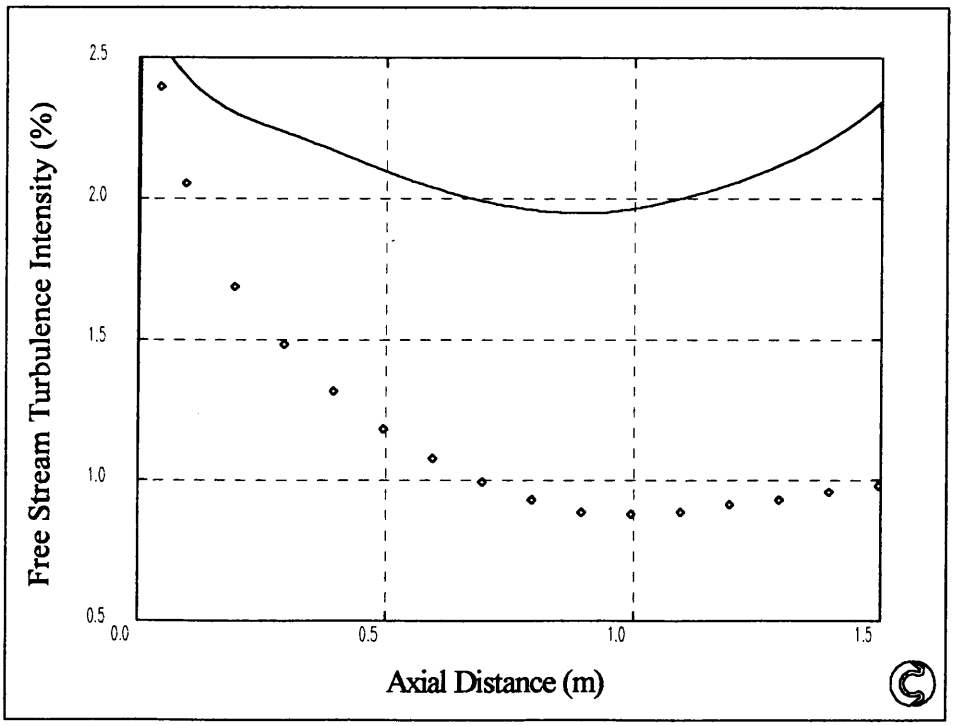

Figure 5.22: T3C2 Batchelor

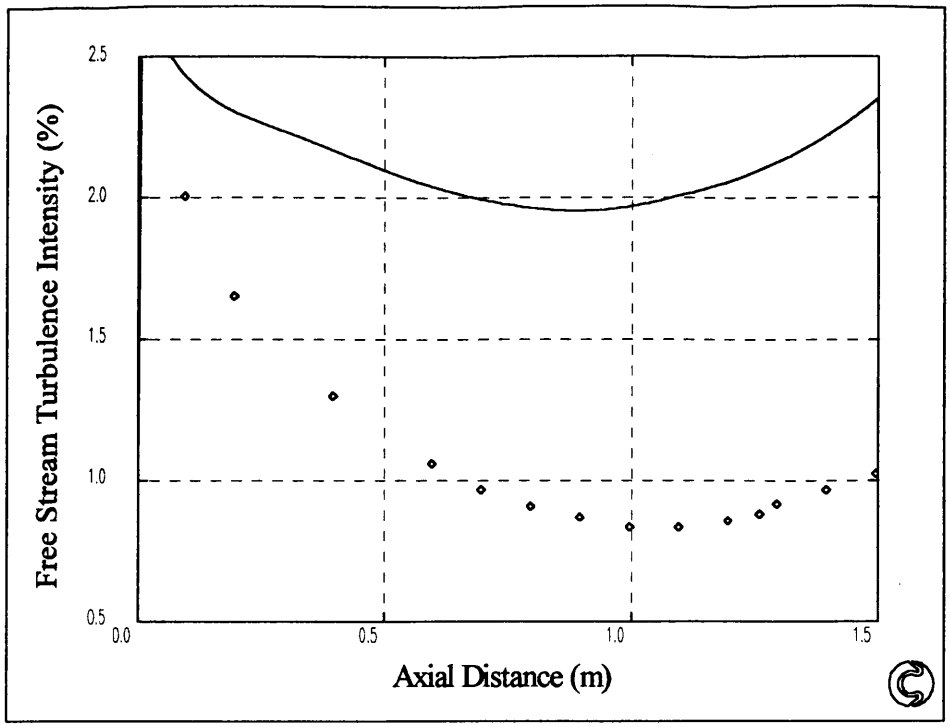

Figure 5.23: T3C3 Batchelor

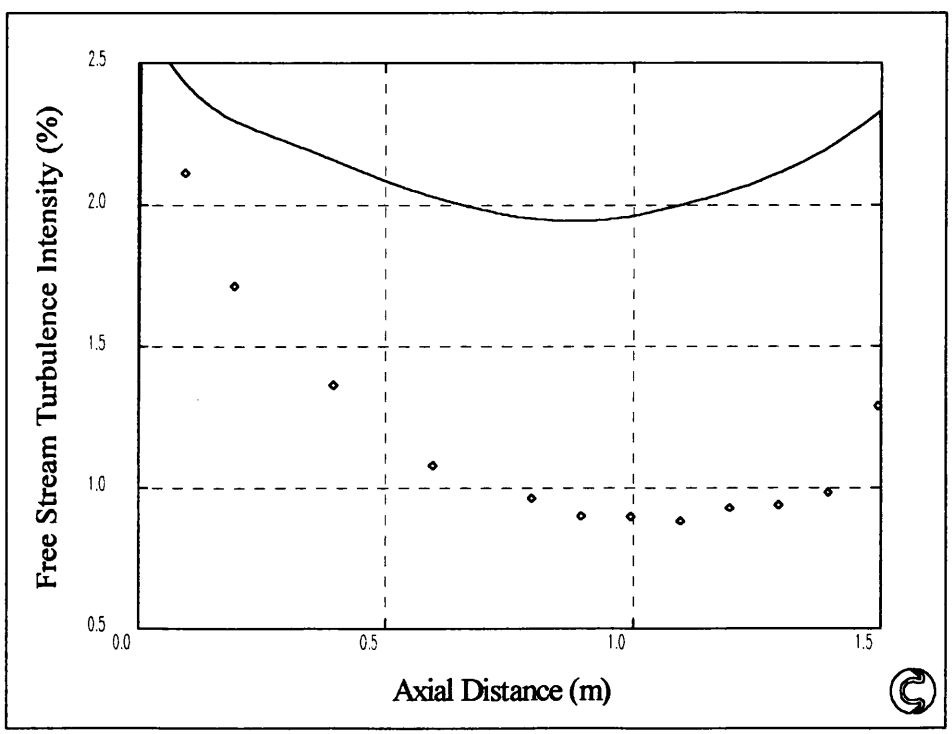

Figure 5.24: T3C4 Batchelor

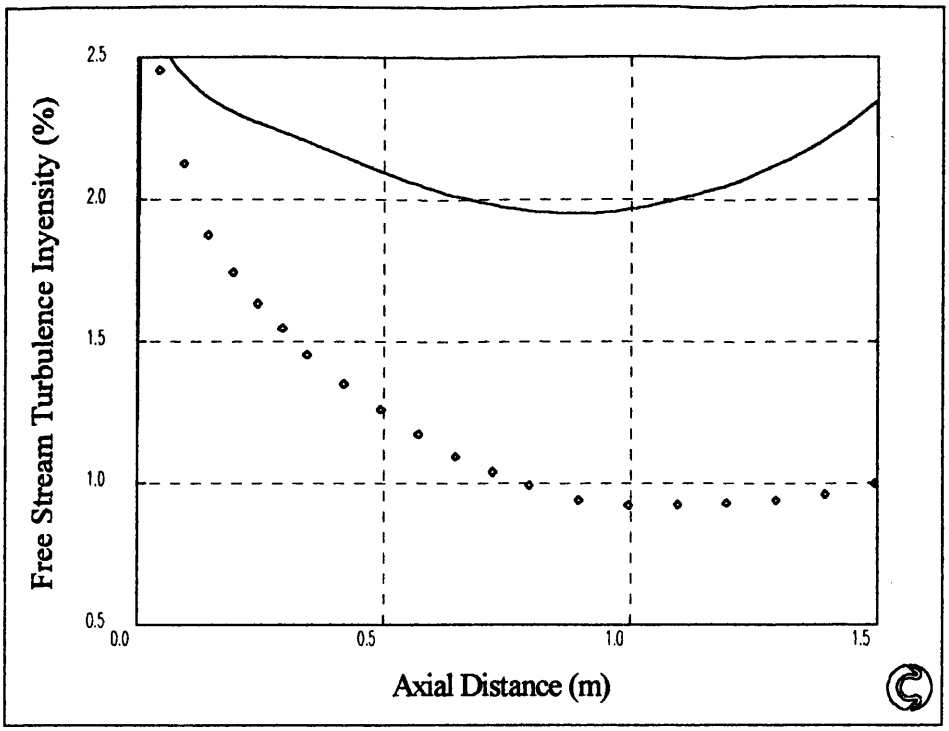

Figure 5.25: T3C5 Batchelor

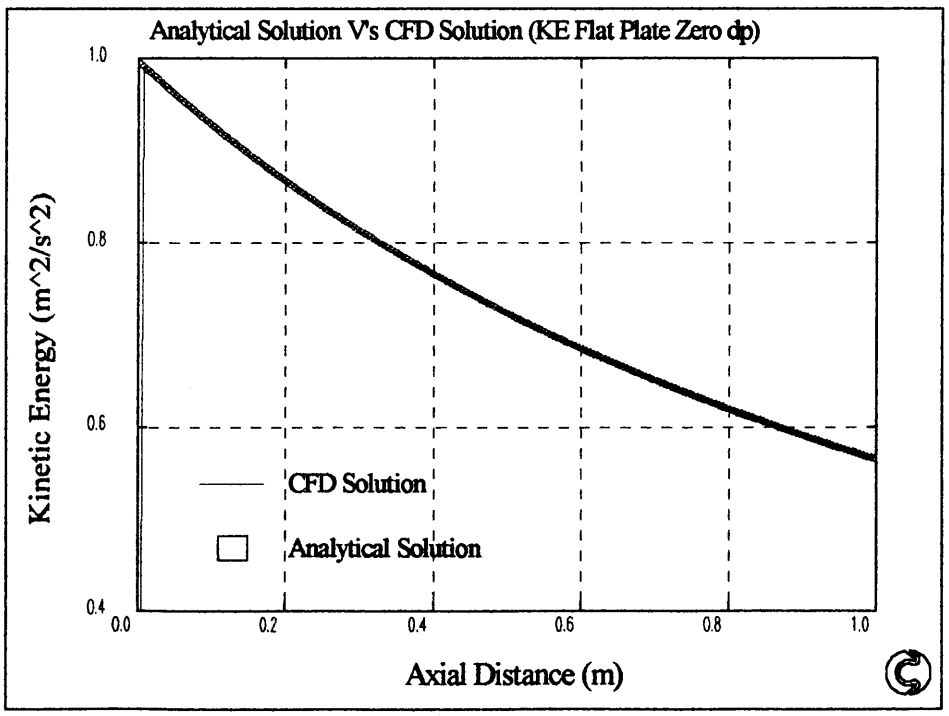

Figure 5.26: Malin's Turbulence Model

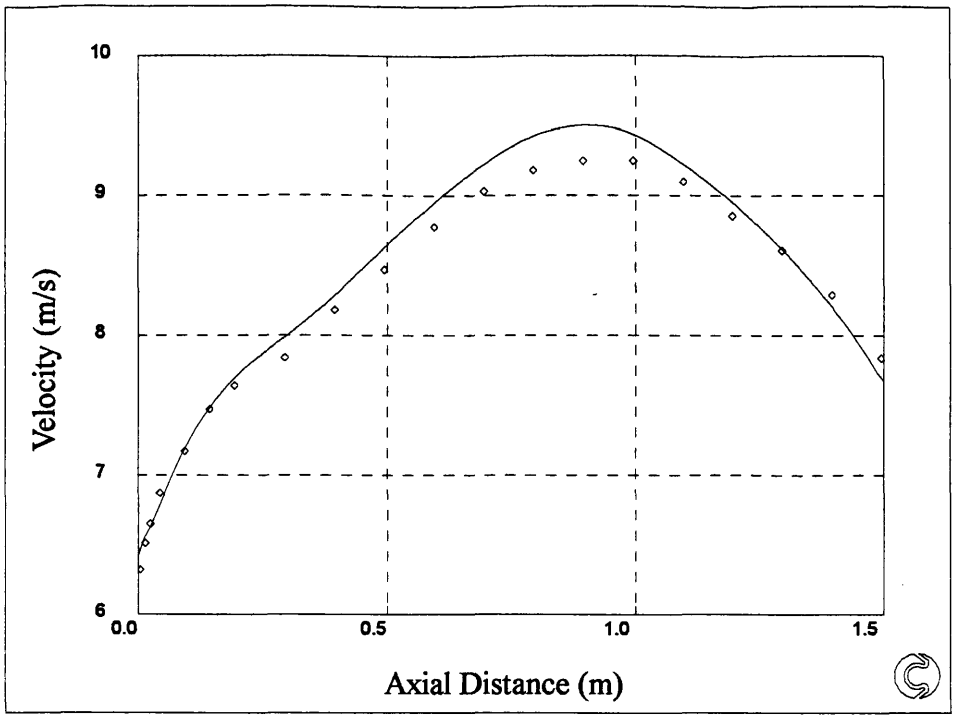

Figure 5.27: T3C1 Fraser/Malin/Dunham

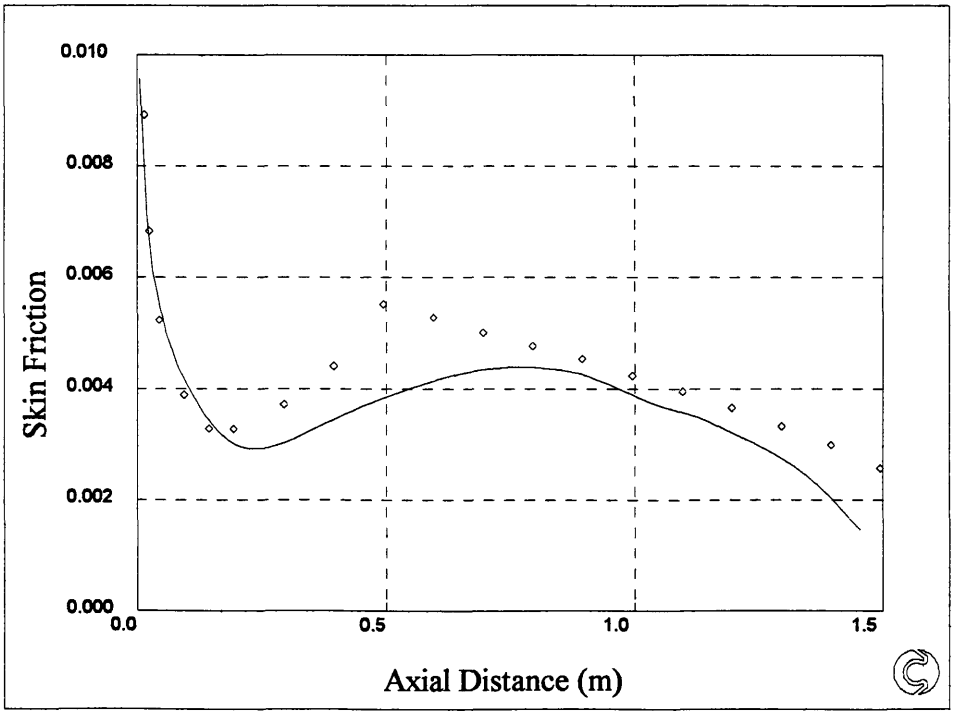

Figure 5.28: T3C1 Fraser/Malin/Dunham

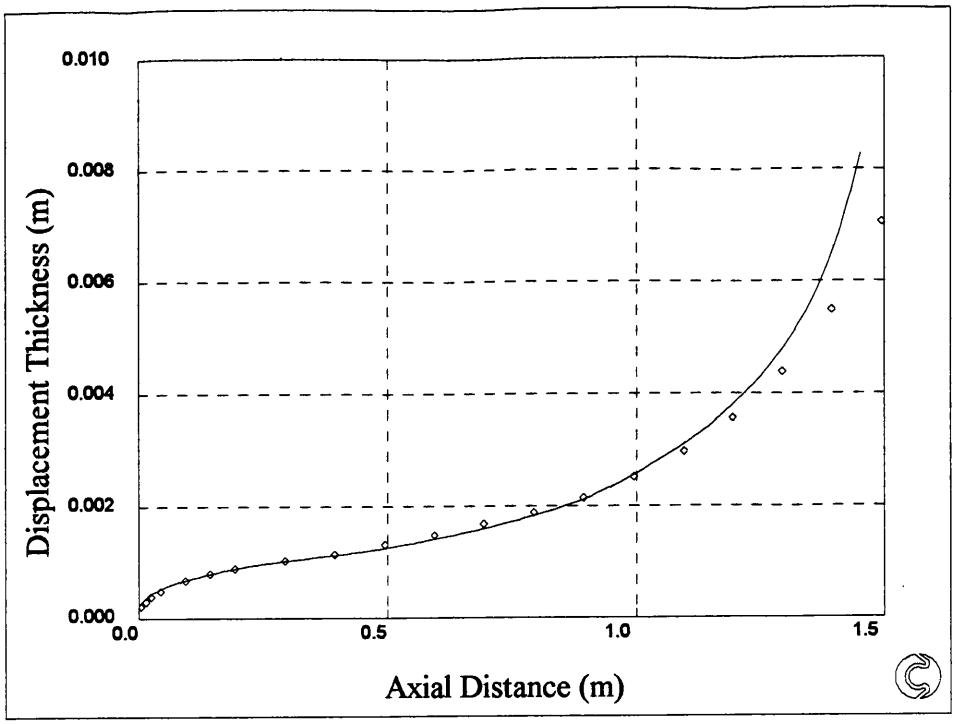

Figure 5.29: T3C1 Fraser/Dunham

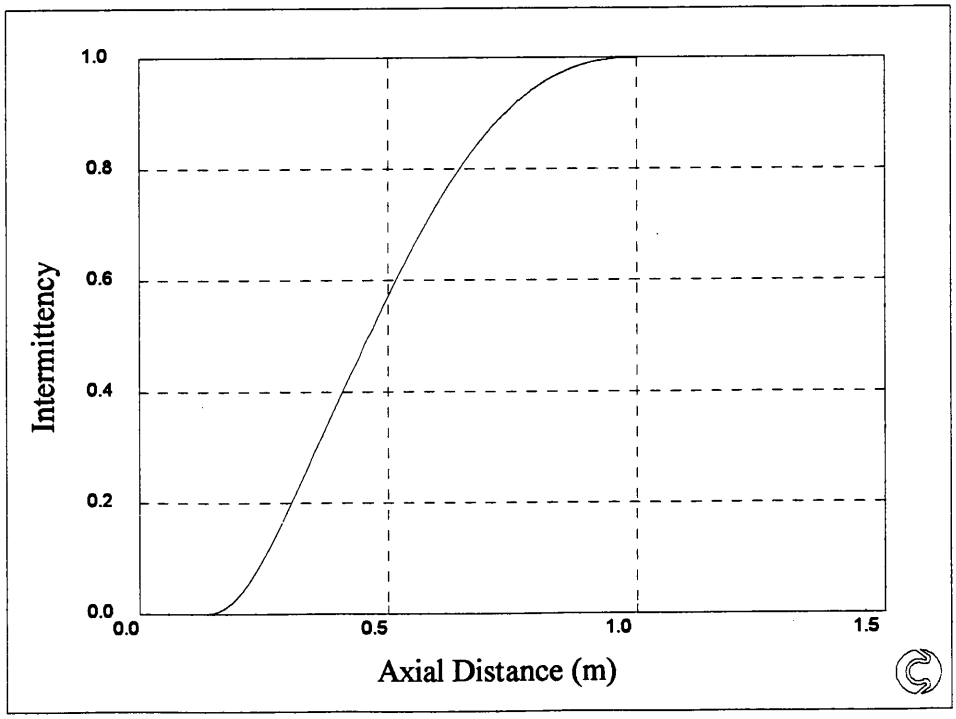

Figure 5.30: T3C1 Fraser/Dunham

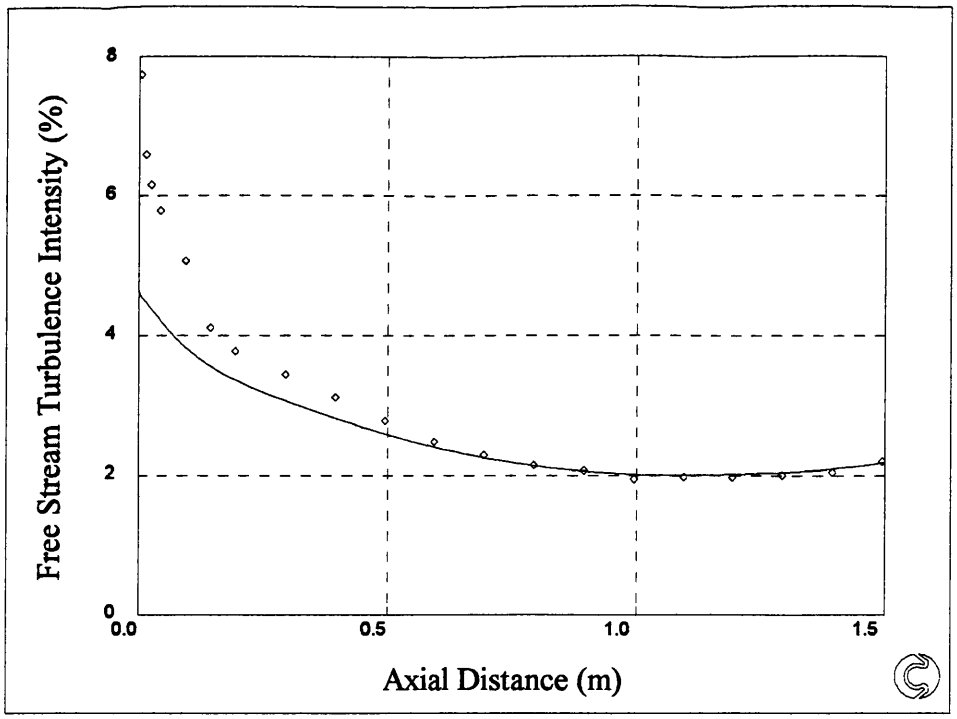

Figure 5.31: T3C1 Fraser/Malin/Dunham

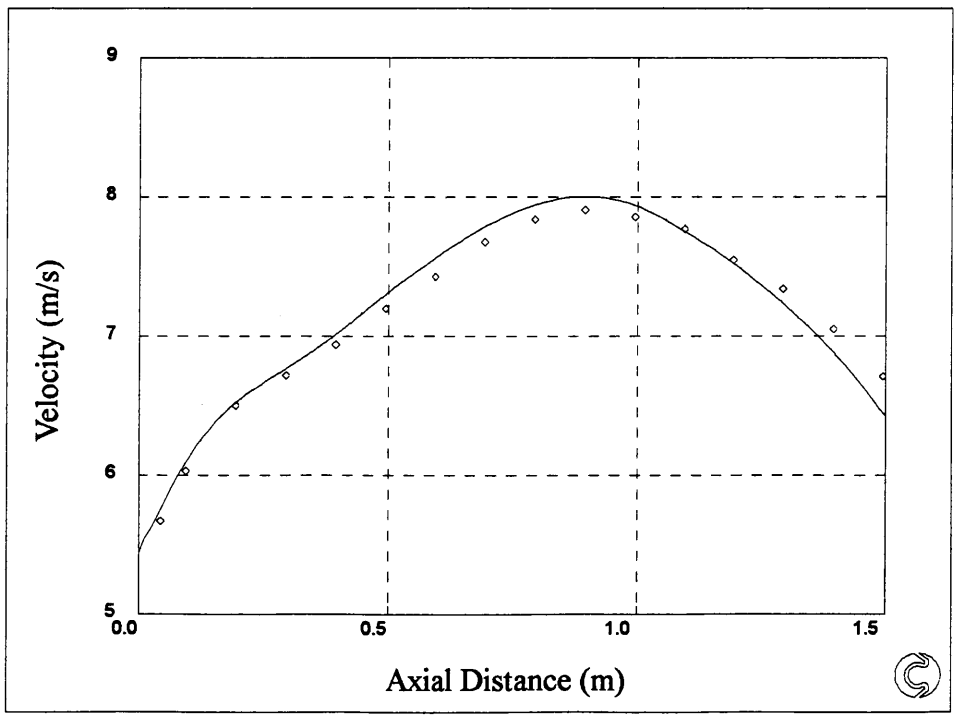

Figure 5.32: T3C2 Fraser/Malin/Dunham

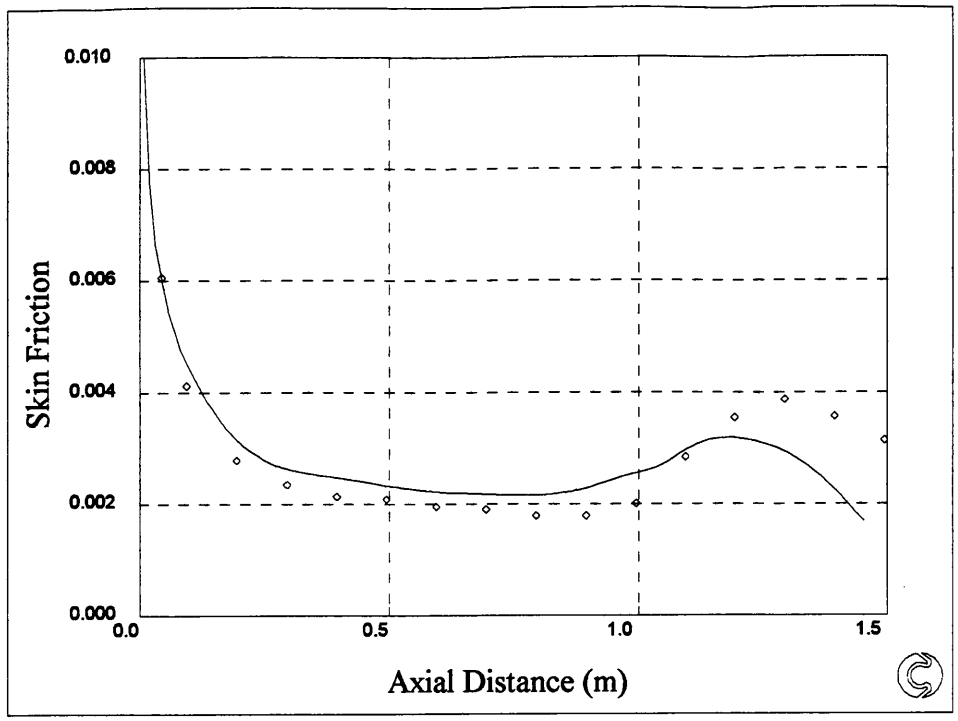

Figure 5.33: T3C2 Fraser/Malin/Dunham

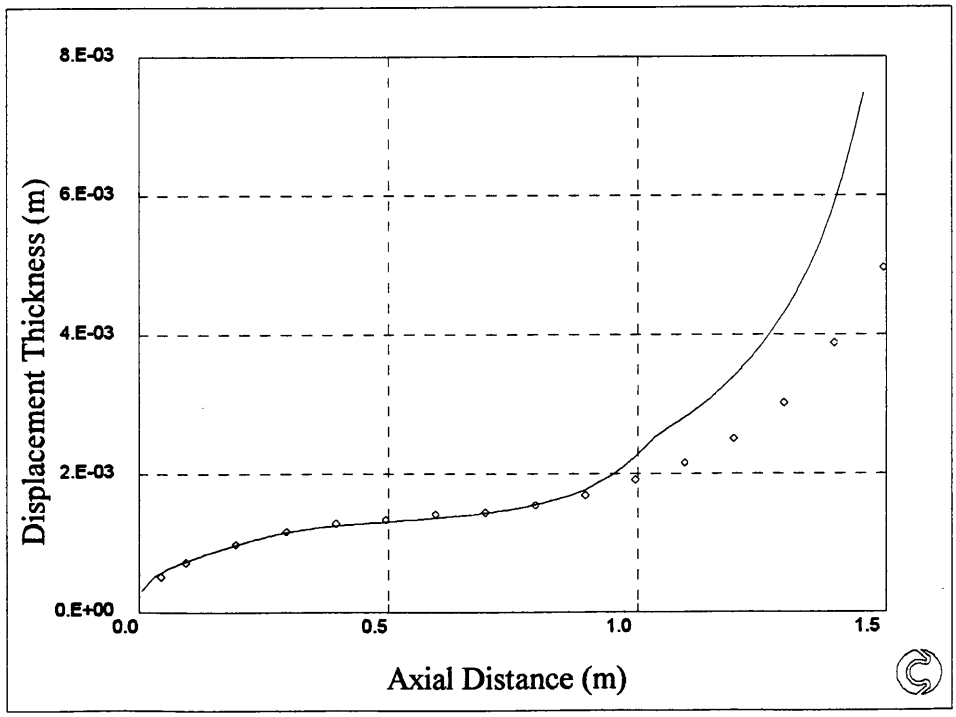

Figure 5.34: T3C2 Fraser/Malin/Dunham

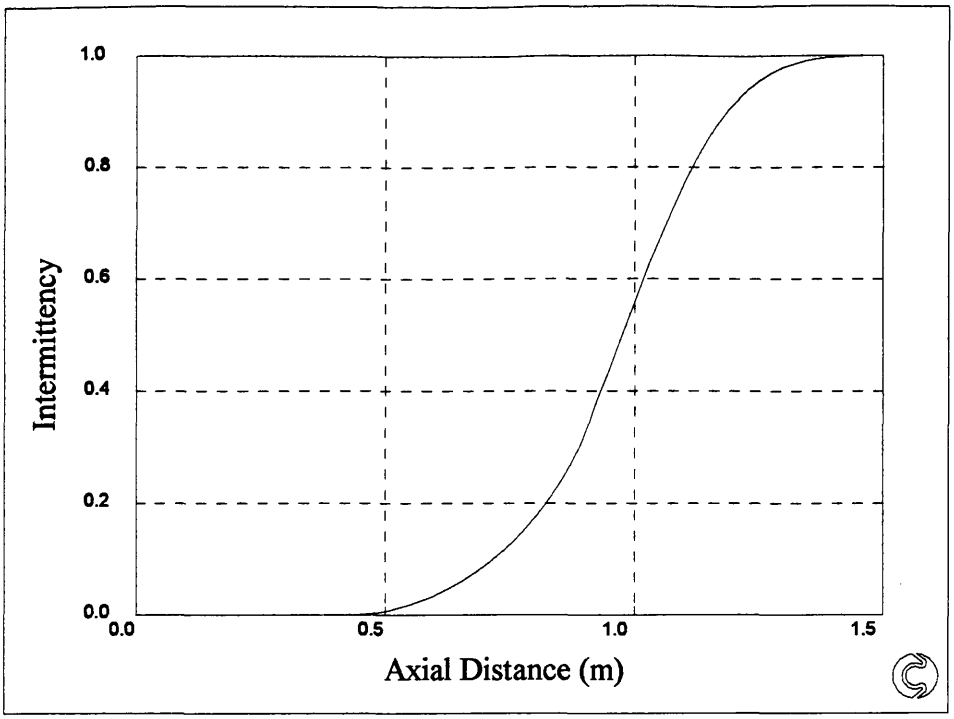

Figure 5.35: T3C2 Fraser/Malin/Dunham

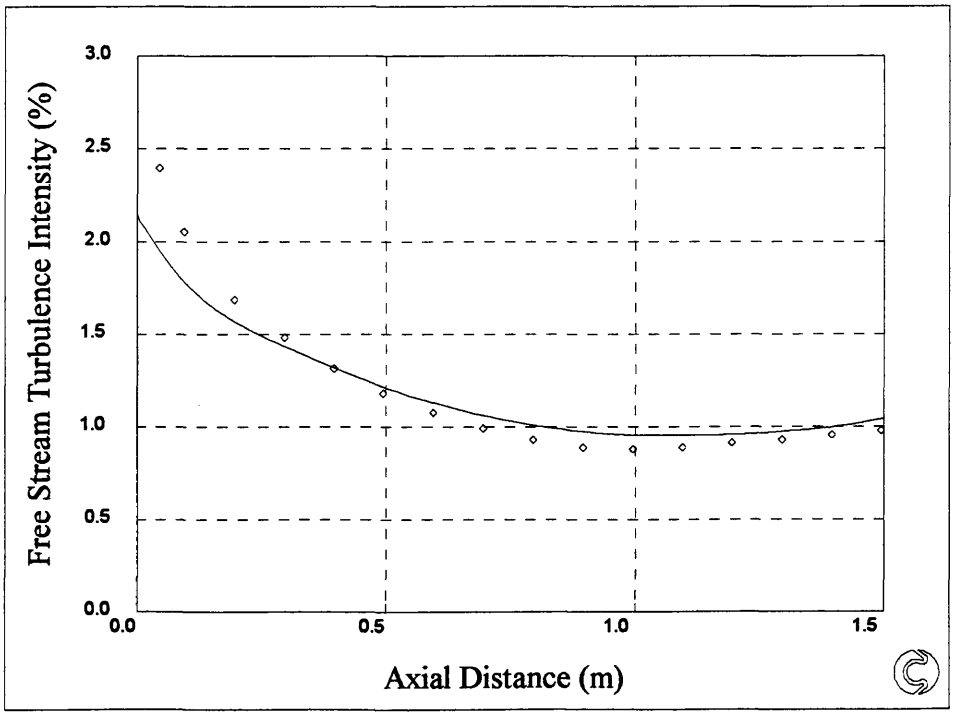

Figure 5.36: T3C2 Fraser/Malin/Dunham

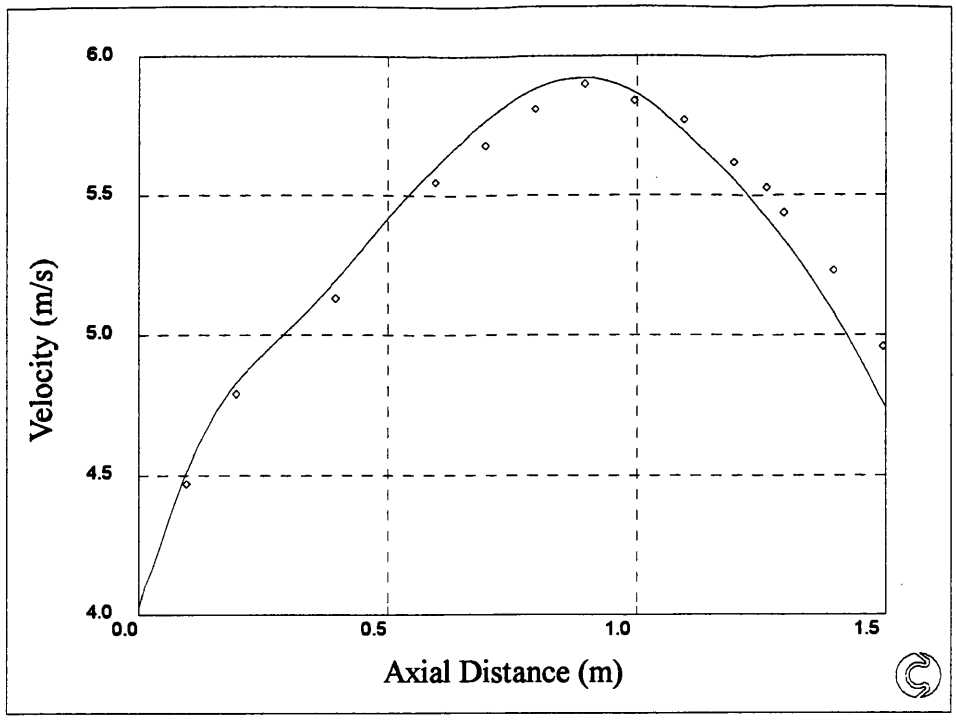

Figure 5.37: T3C3 Fraser/Malin/Dunham

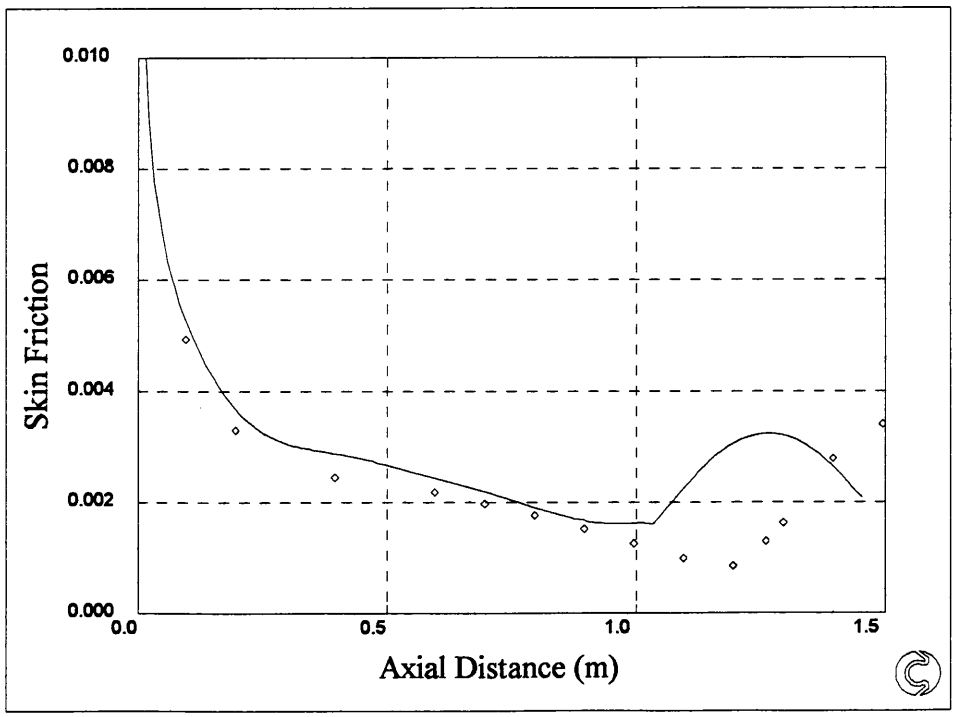

Figure 5.38: T3C3 Fraser/Malin/Dunham

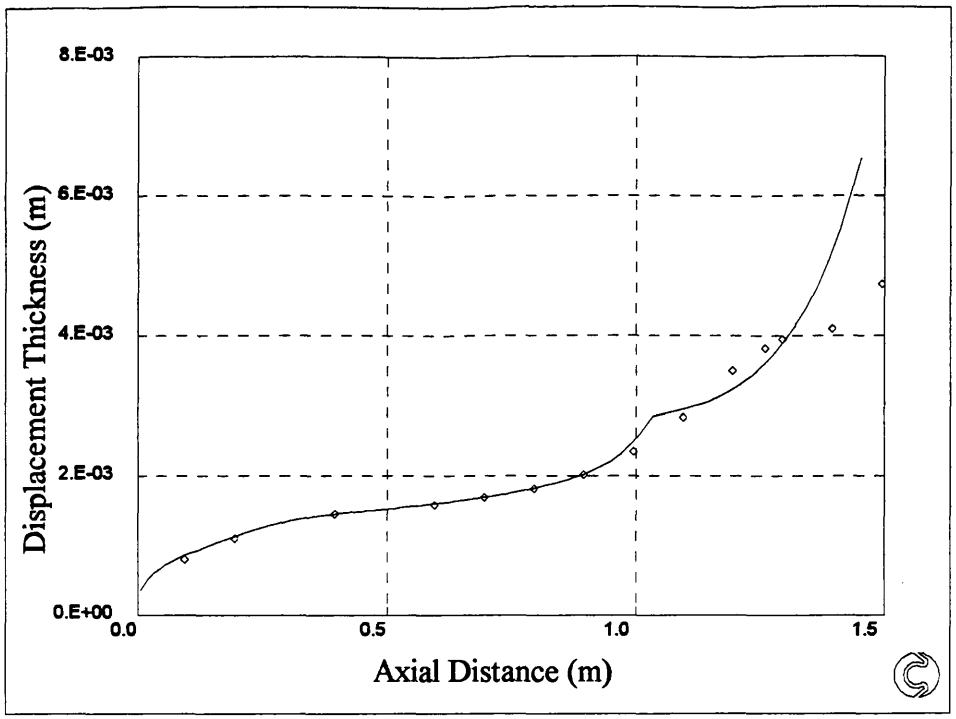

Figure 5.39: T3C3 Fraser/Malin/Dunham

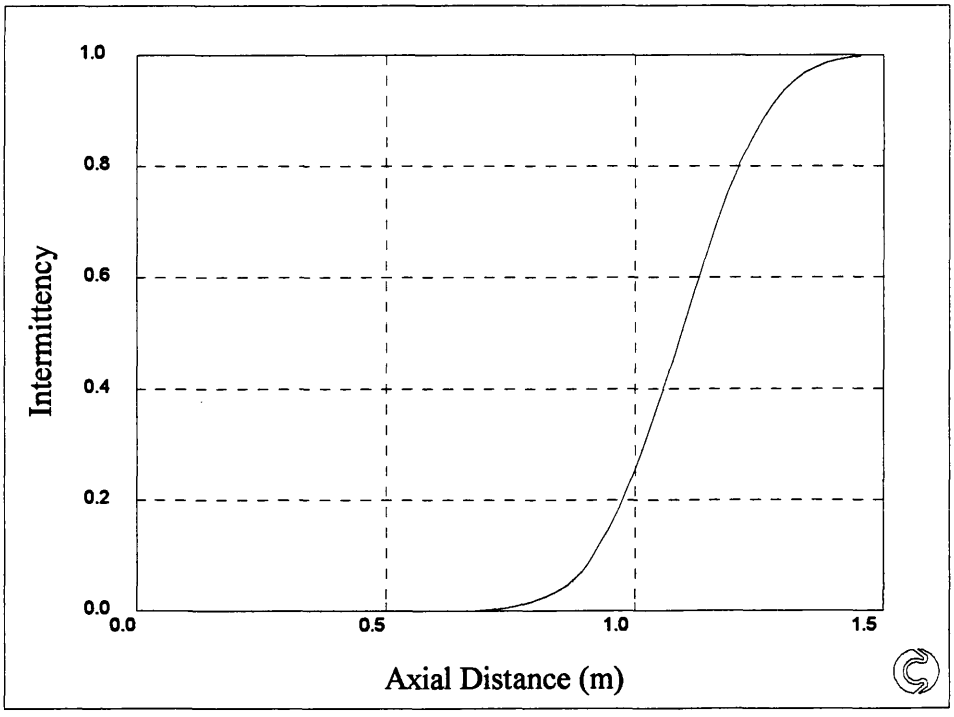

Figure 5.40: T3C3 Fraser/Malin/Dunham

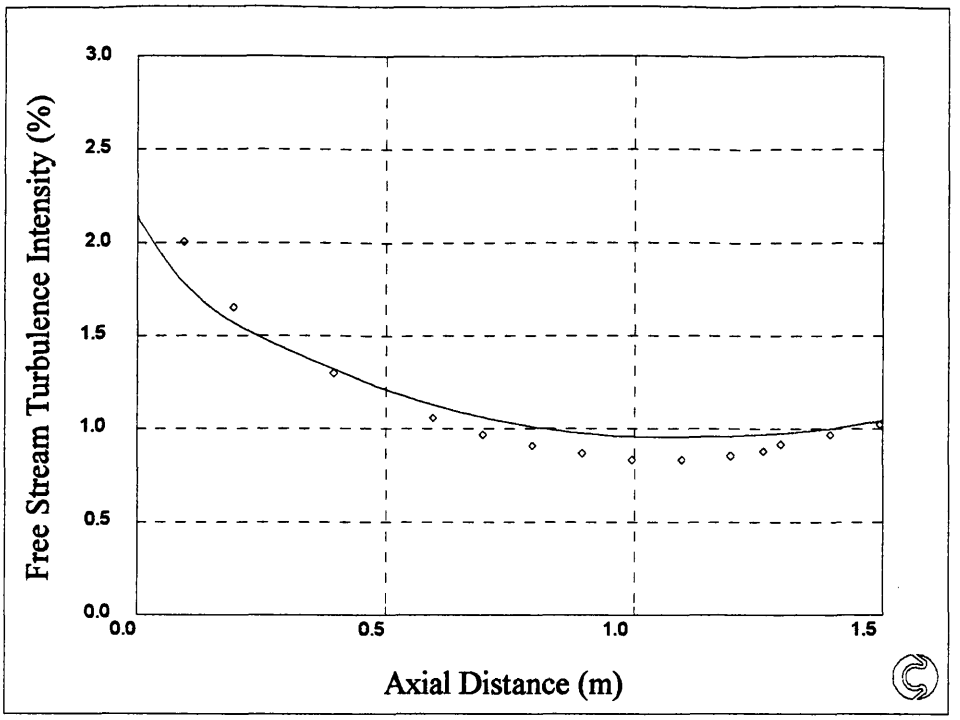

Figure 5.41: T3C3 Fraser/Malin/Dunham

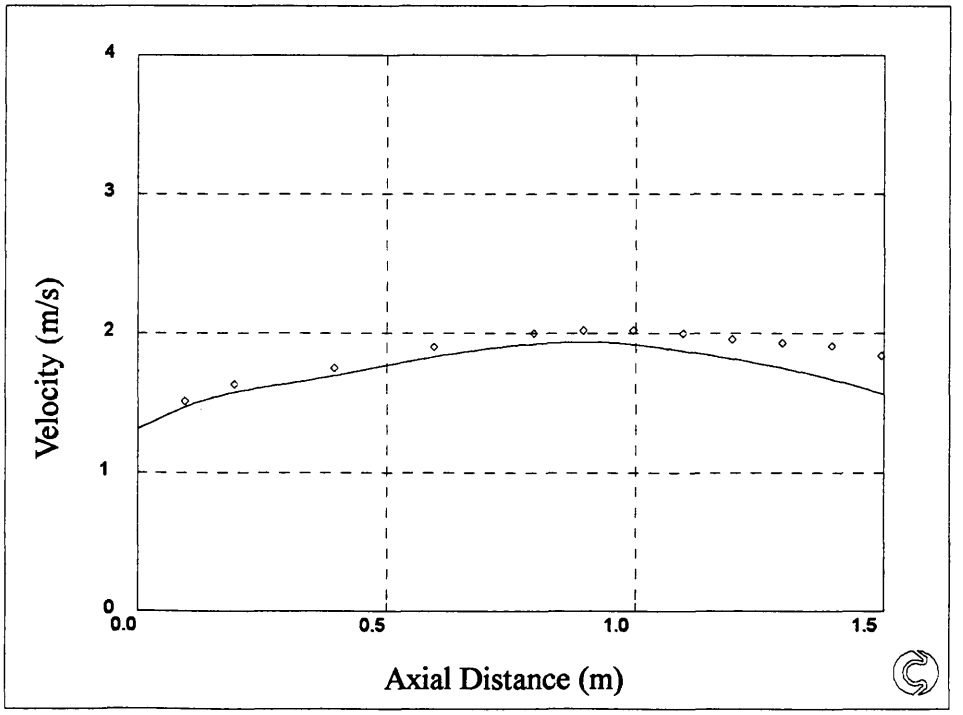

Figure 5.42: T3C4 Fraser/Malin/Dunham

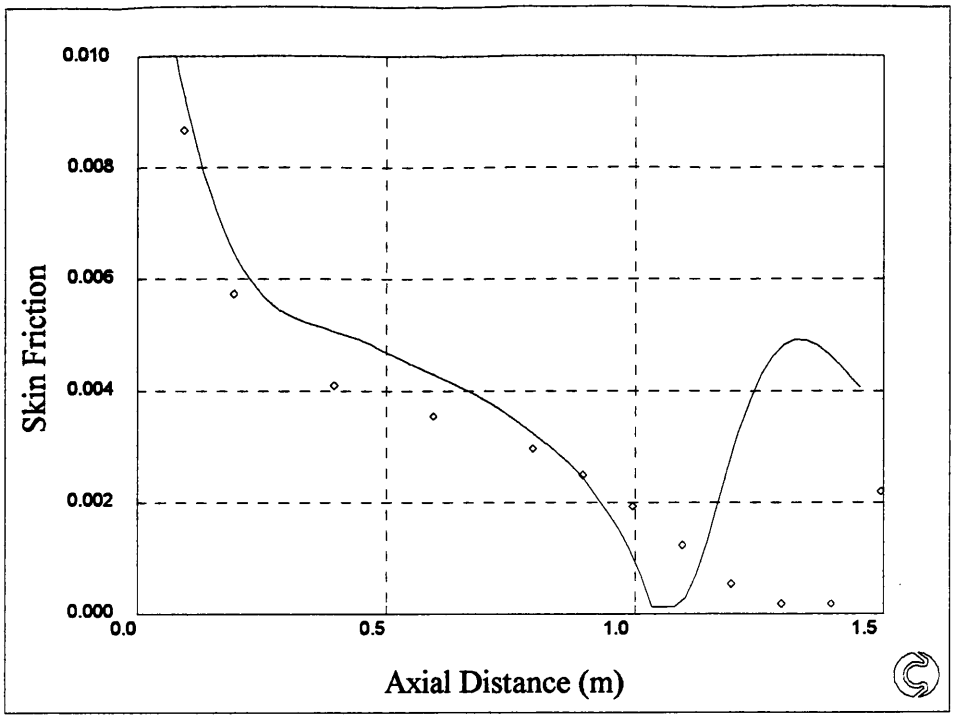

Figure 5.43: T3C4 Fraser/Malin/Dunham

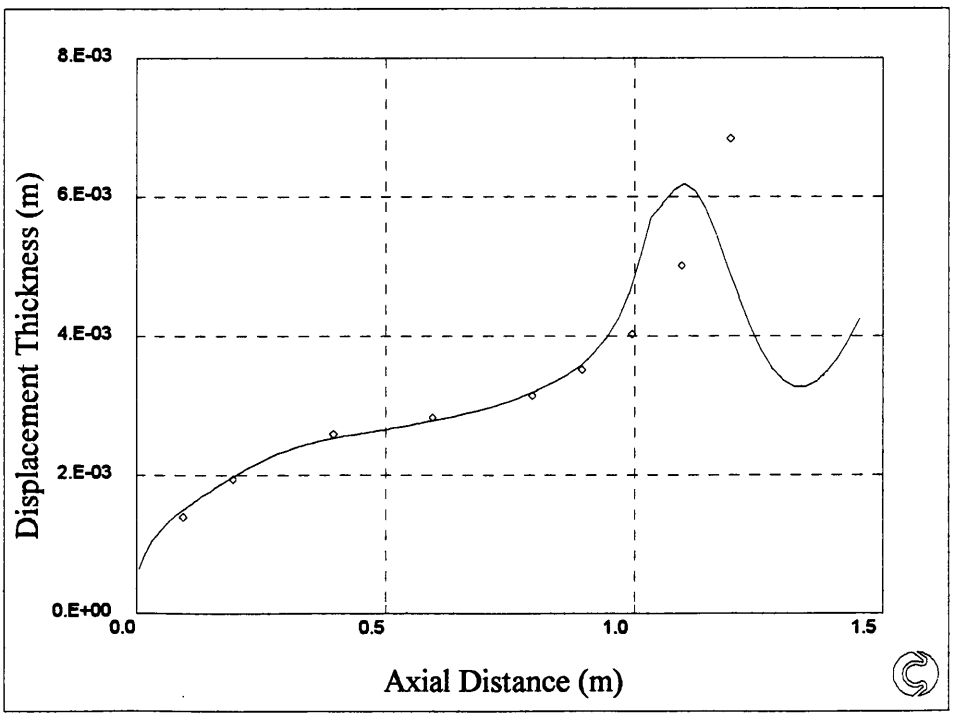

Figure 5.44: T3C4 Fraser/Malin/Dunham

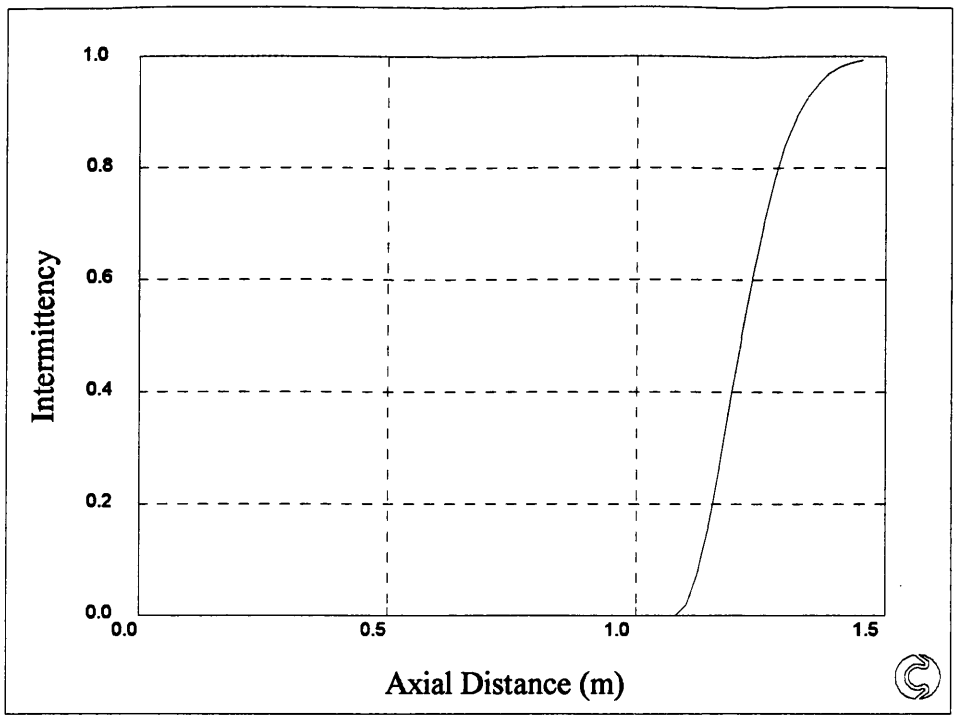

Figure 5.45: T3C4 Fraser/Malin/Dunham

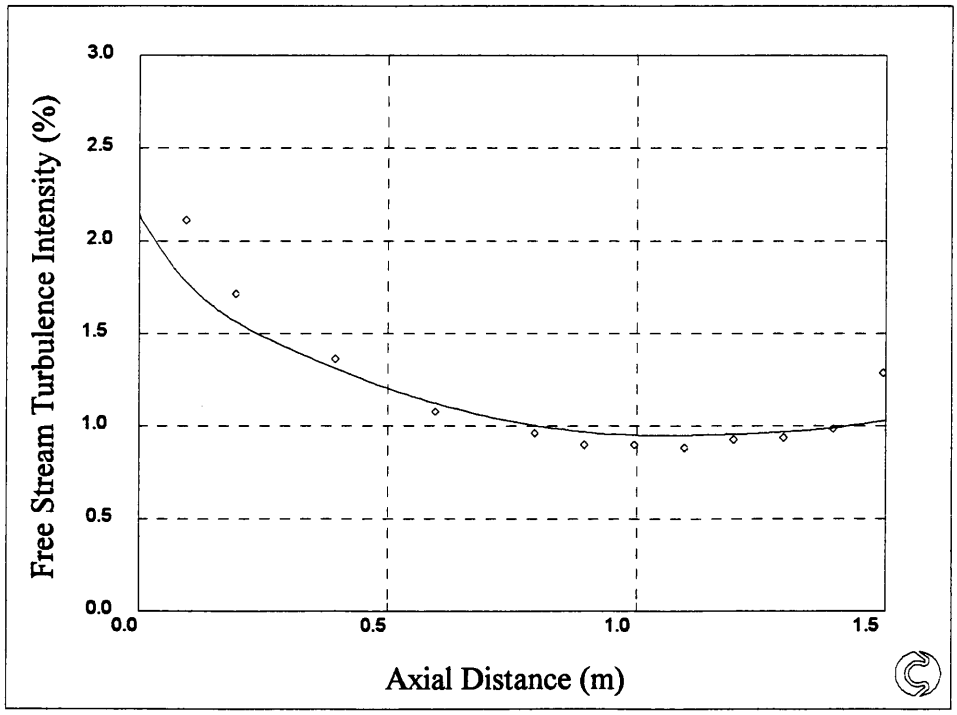

Figure 5.46: T3C4 Fraser/Malin/Dunham

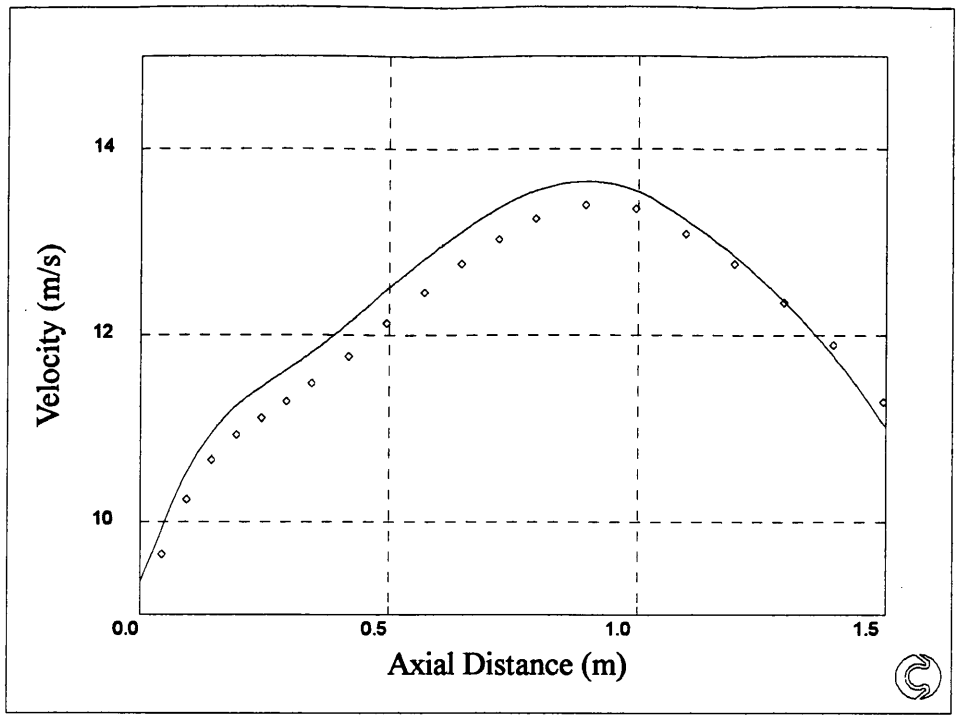

Figure 5.47: T3C5 Fraser/Malin/Dunham

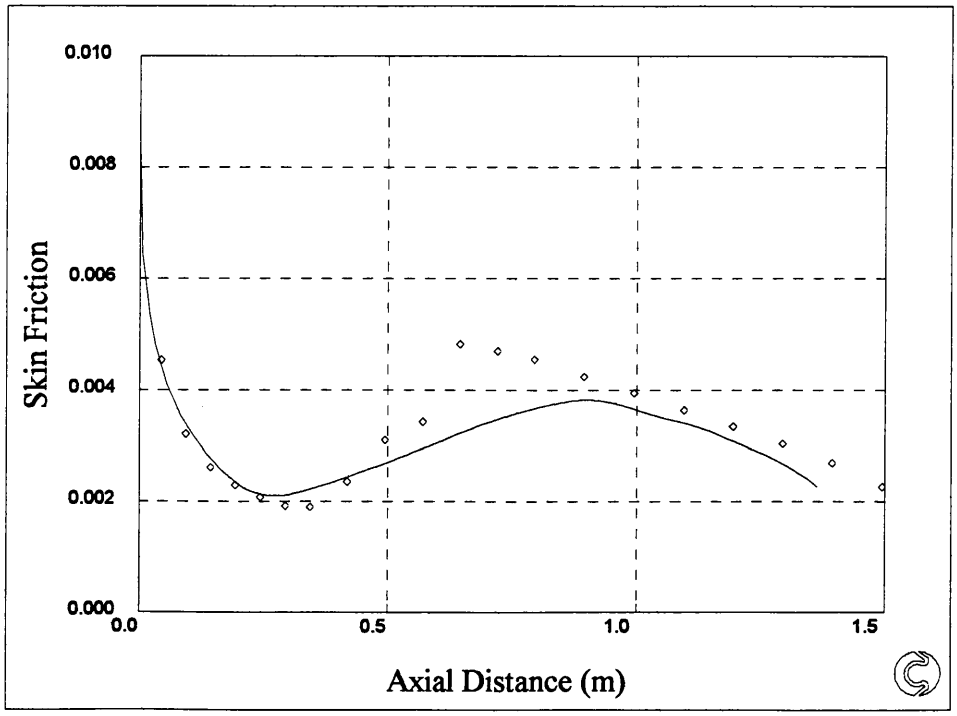

Figure 5.48: T3C5 Fraser/Malin/Dunham

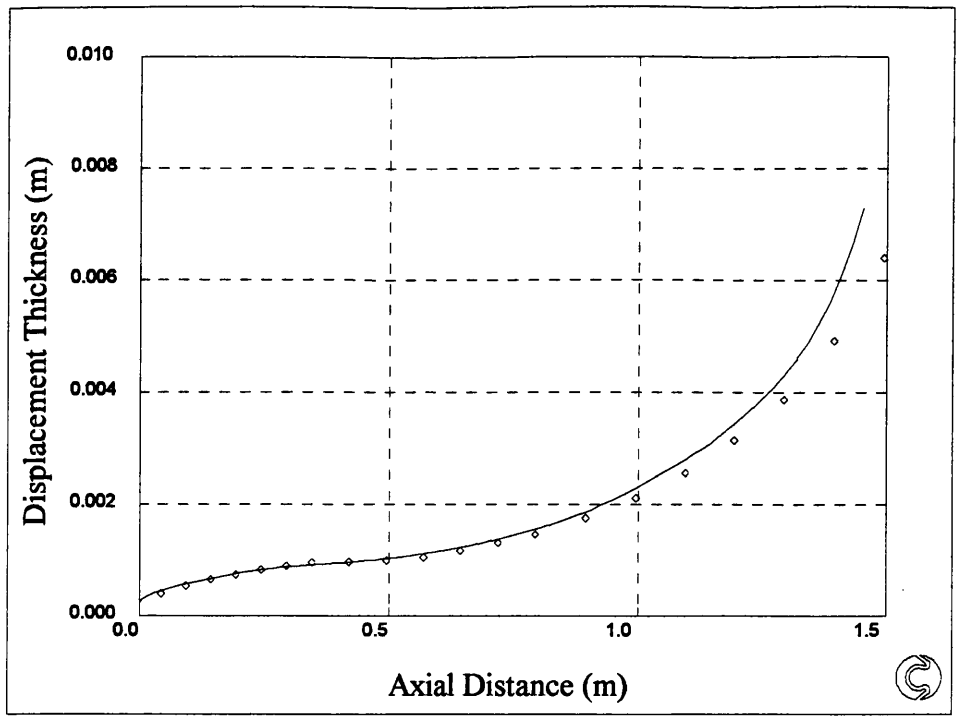

Figure 5.49: T3C5 Fraser/Malin/Dunham

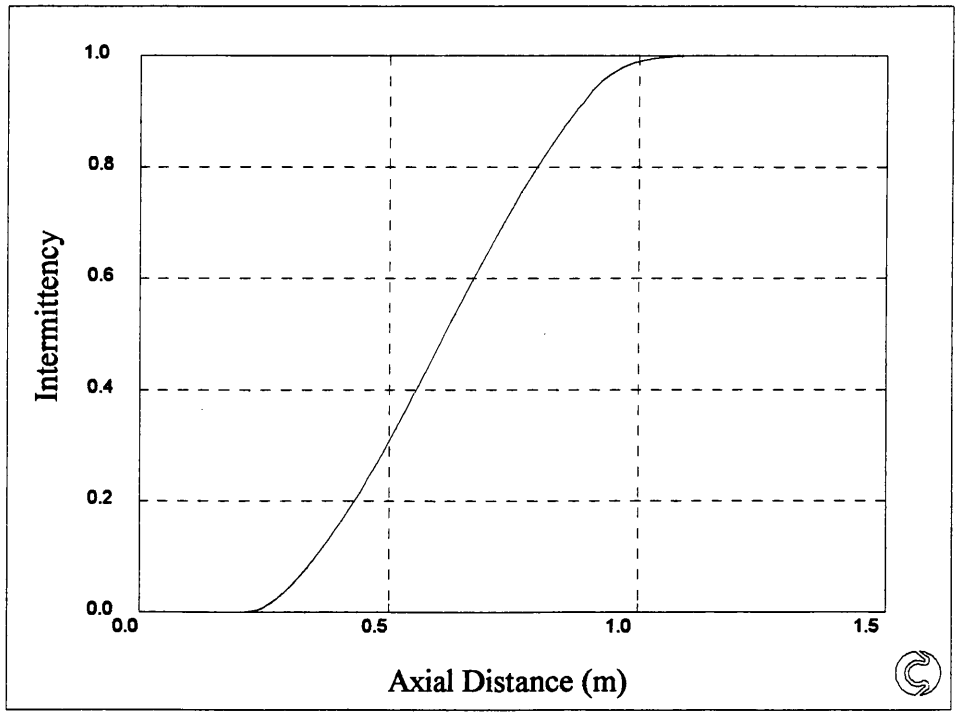

Figure 5.50: T3C5 Fraser/Malin/Dunham

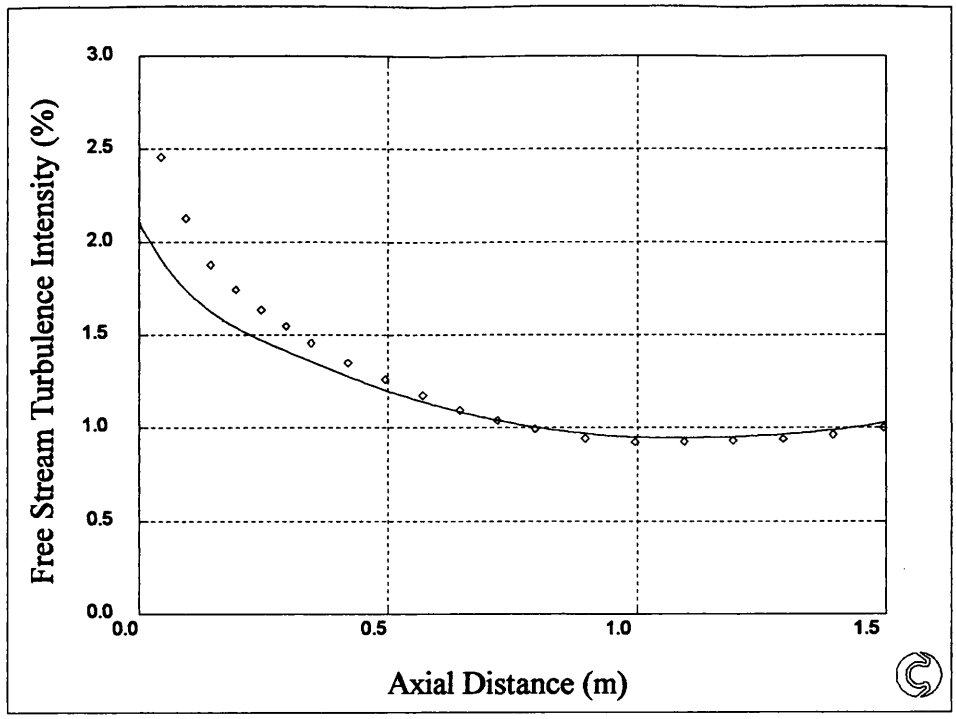

Figure 5.51: T3C5 Fraser/Malin/Dunham

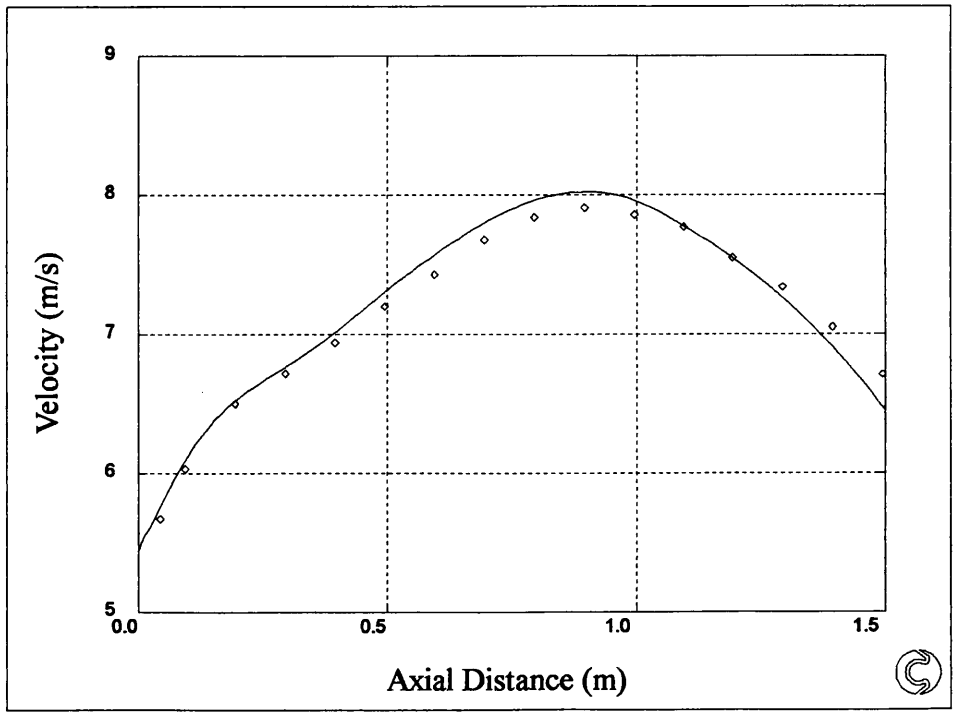

Figure 5.52: T3C2 Solomon/Malin/Dunham

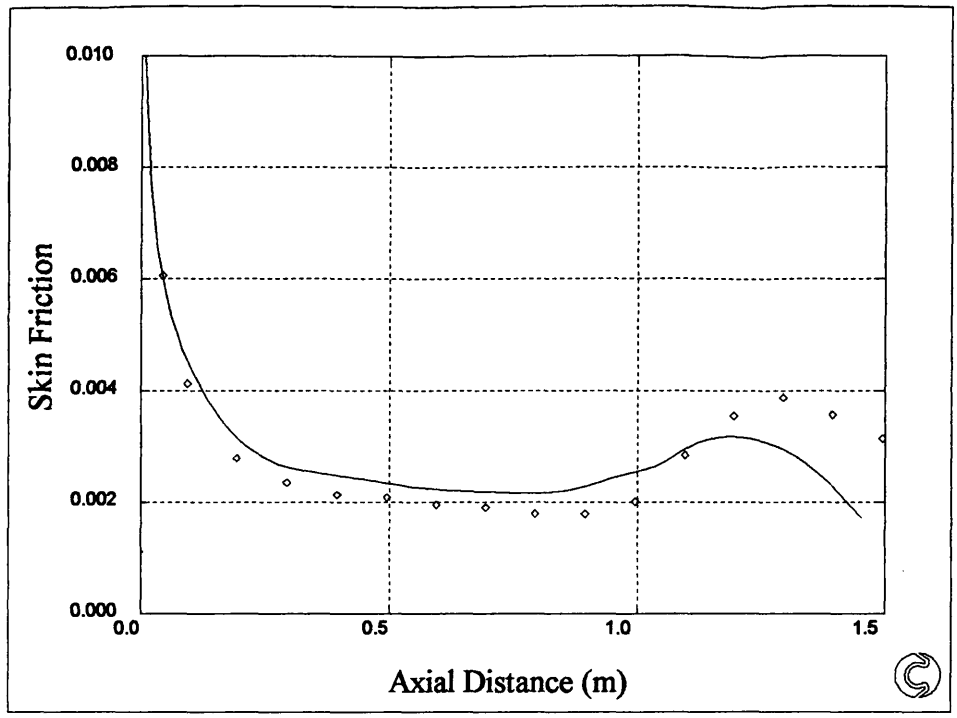

Figure 5.53: T3C2 Solomon/Malin/Dunham

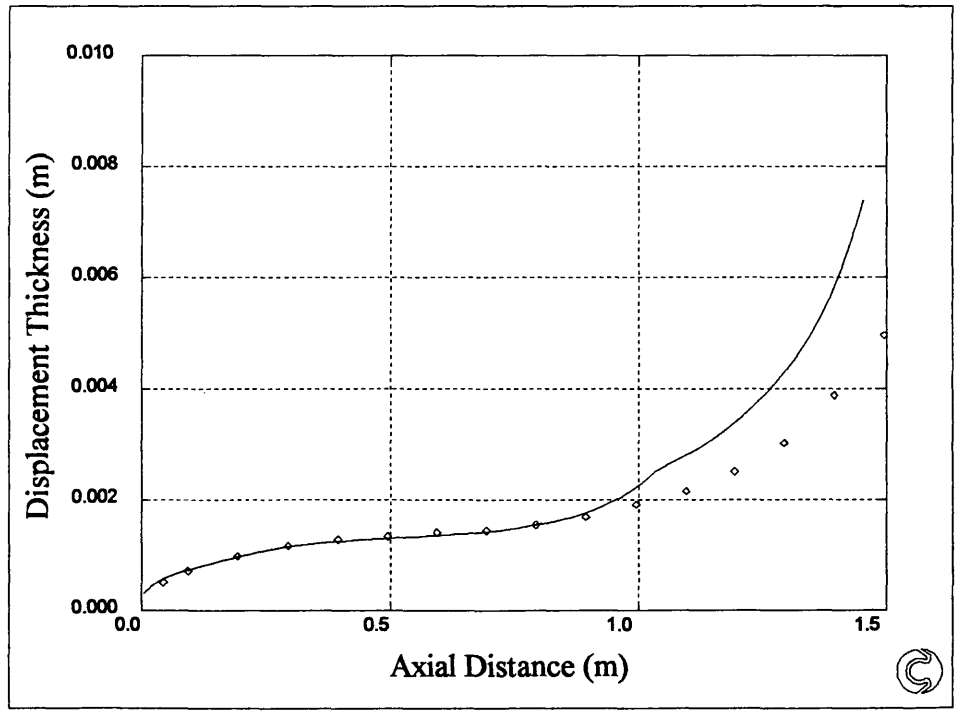

Figure 5.54: T3C2 Solomon/Malin/Dunham

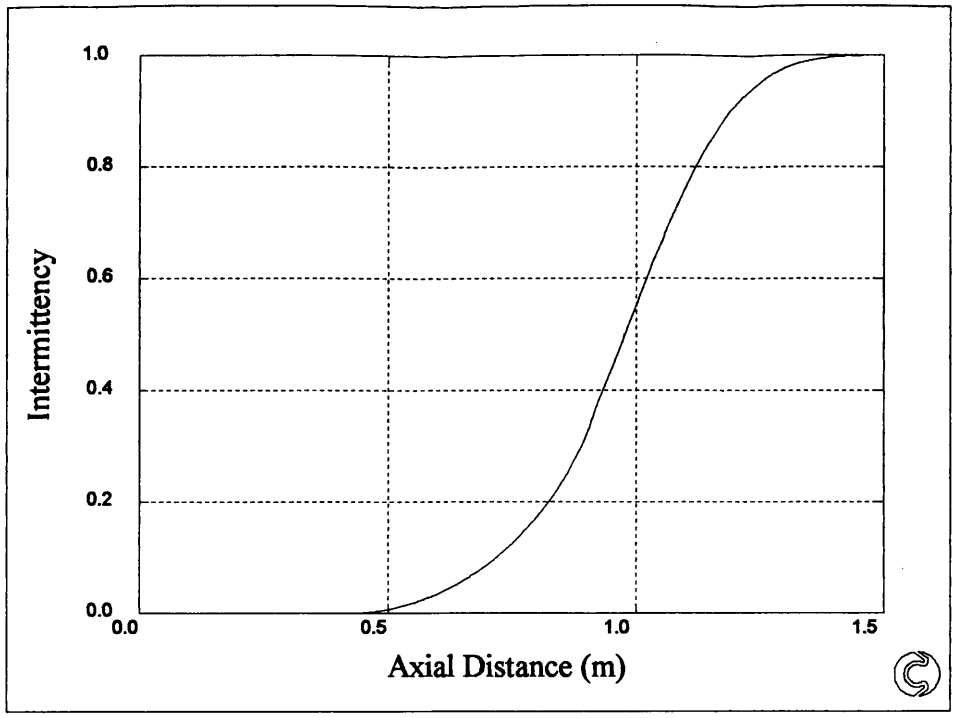

Figure 5.55: T3C2 Solomon/Malin/Dunham

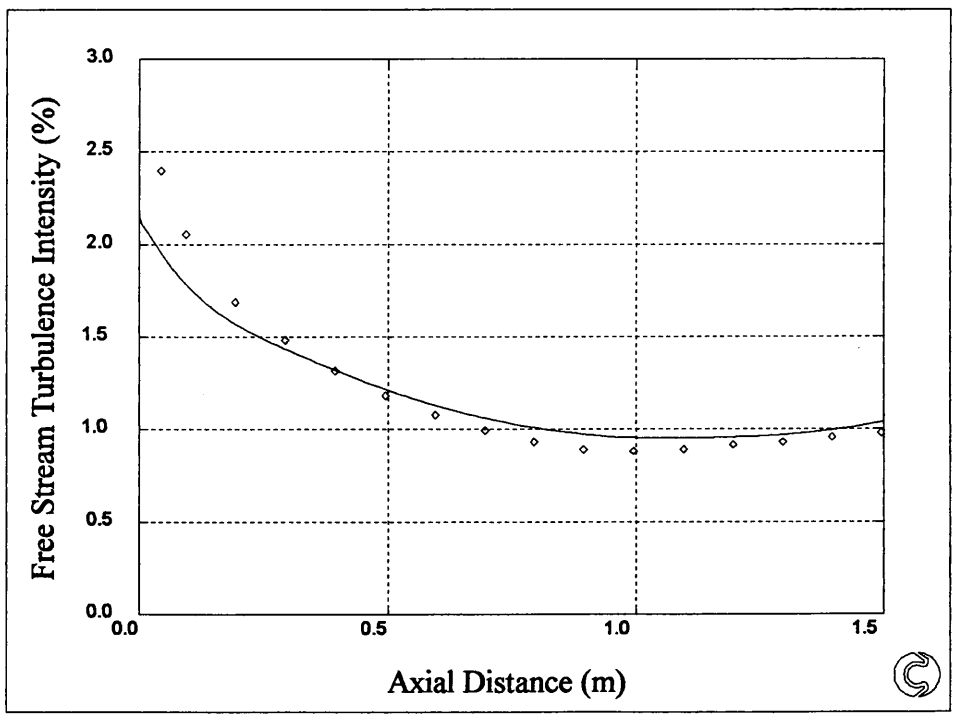

Figure 5.56: T3C2 Solomon/Malin/Dunham

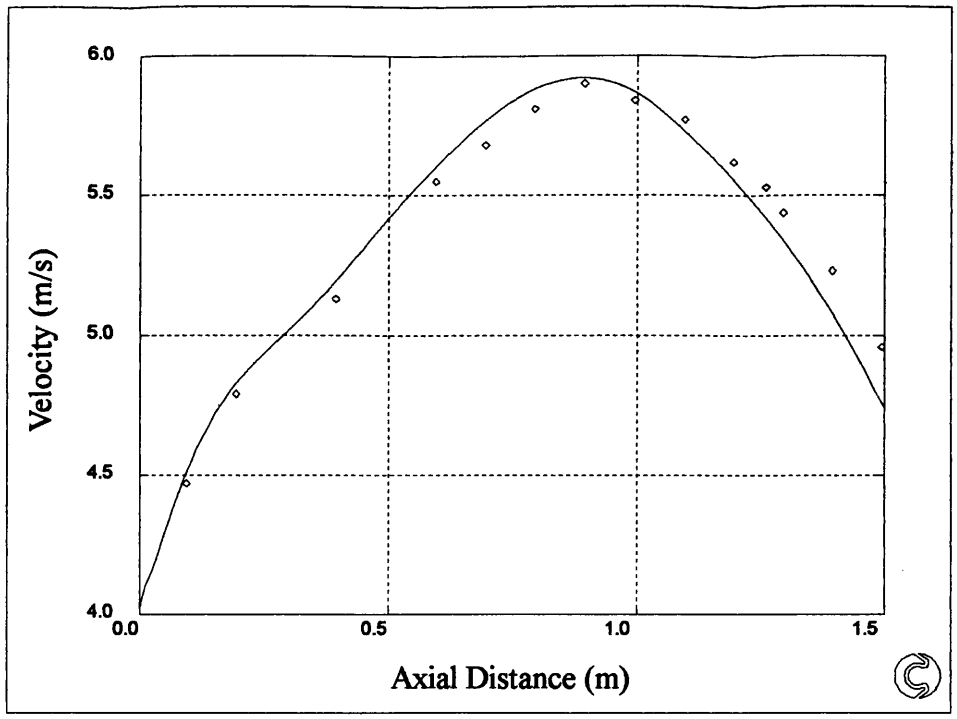

Figure 5.57: T3C3 Solomon/Malin/Dunham

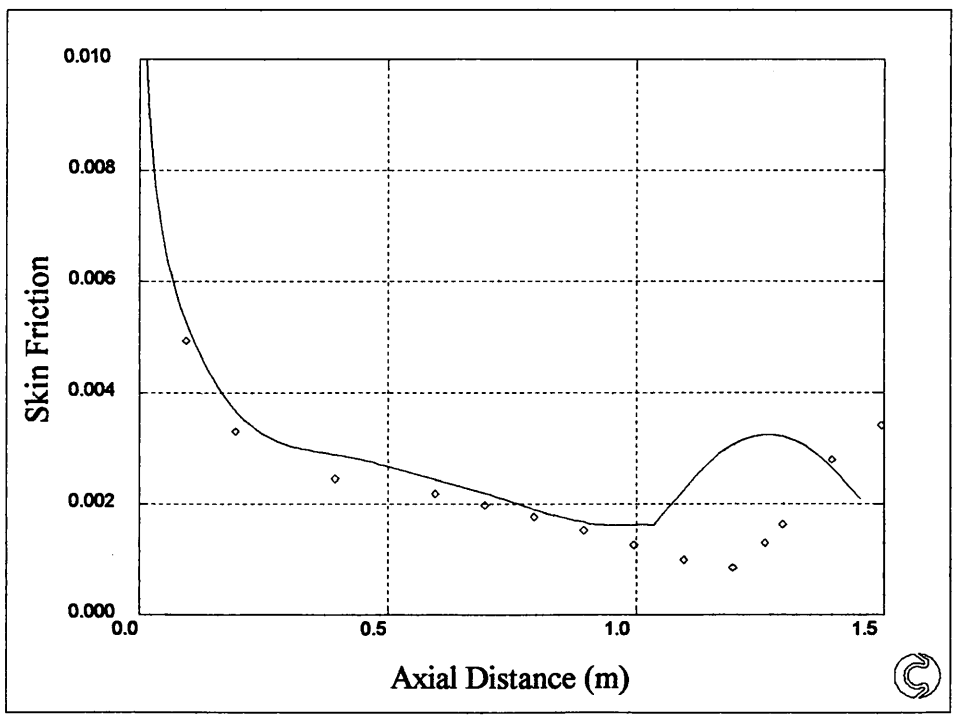

Figure 5.58: T3C3 Solomon/Malin/Dunham

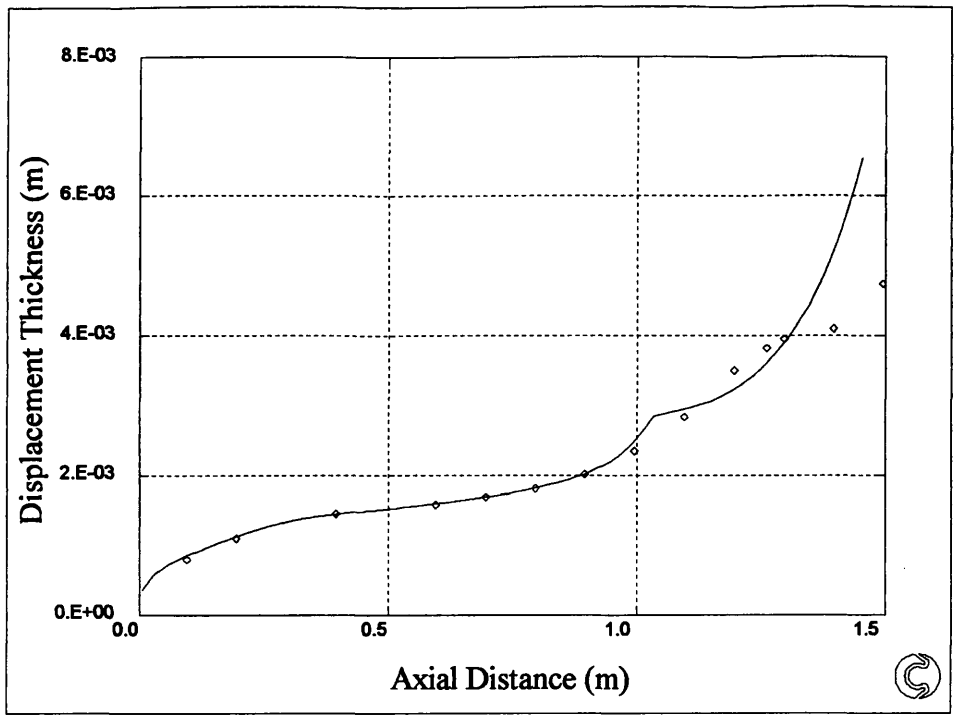

Figure 5.59:T3C3 Solomon/Malin/Dunham

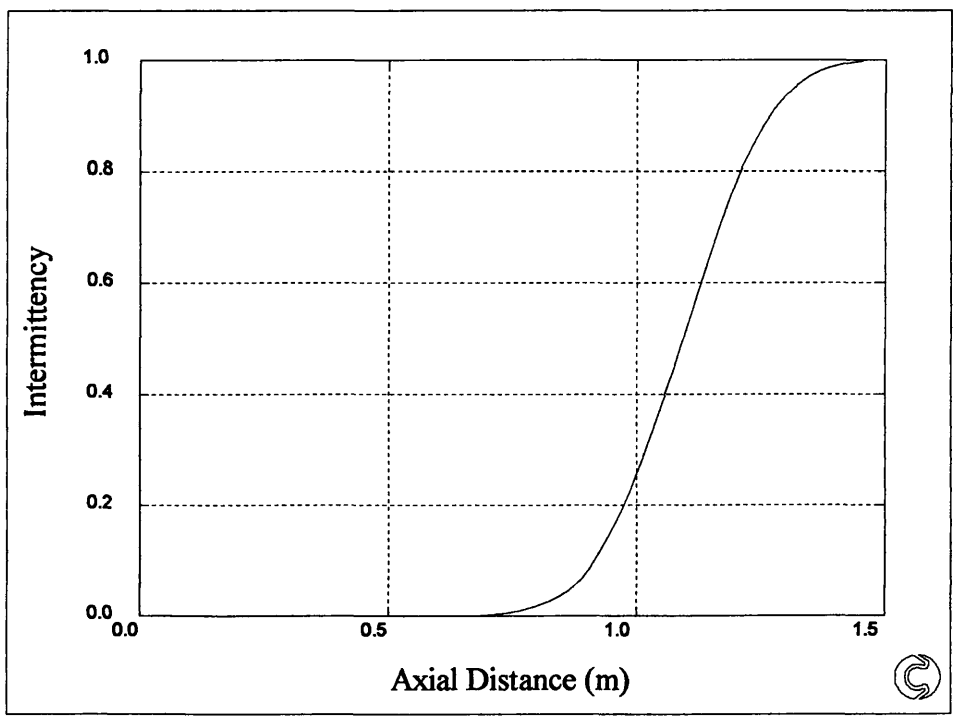

Figure 5.60: T3C3 Solomon/Malin/Dunham

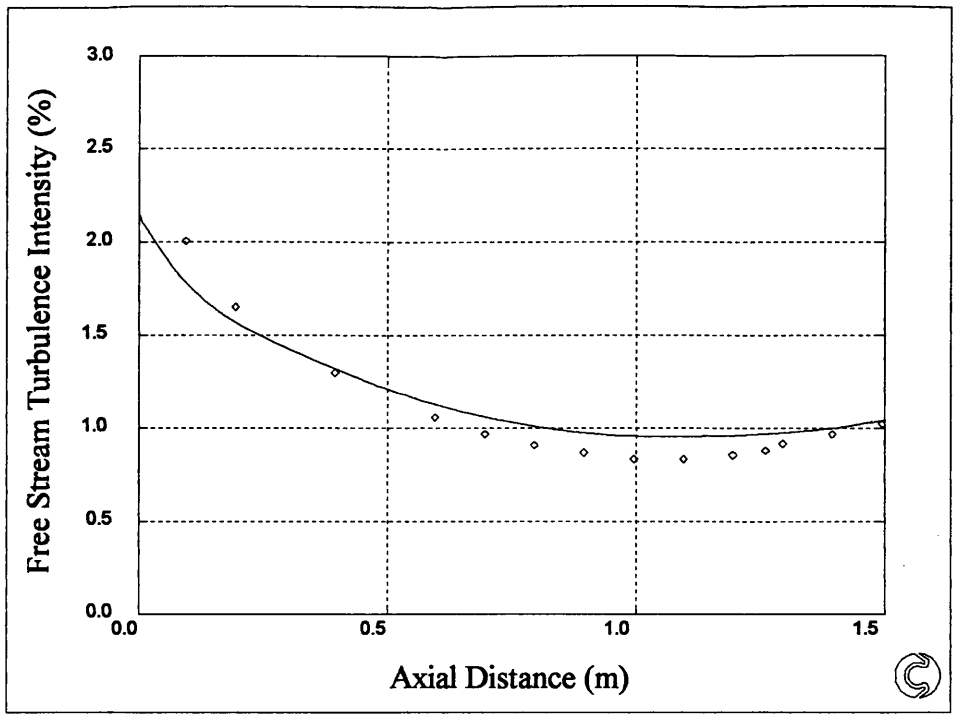

Figure 5.61: T3C3 Solomon/Malin/Dunham

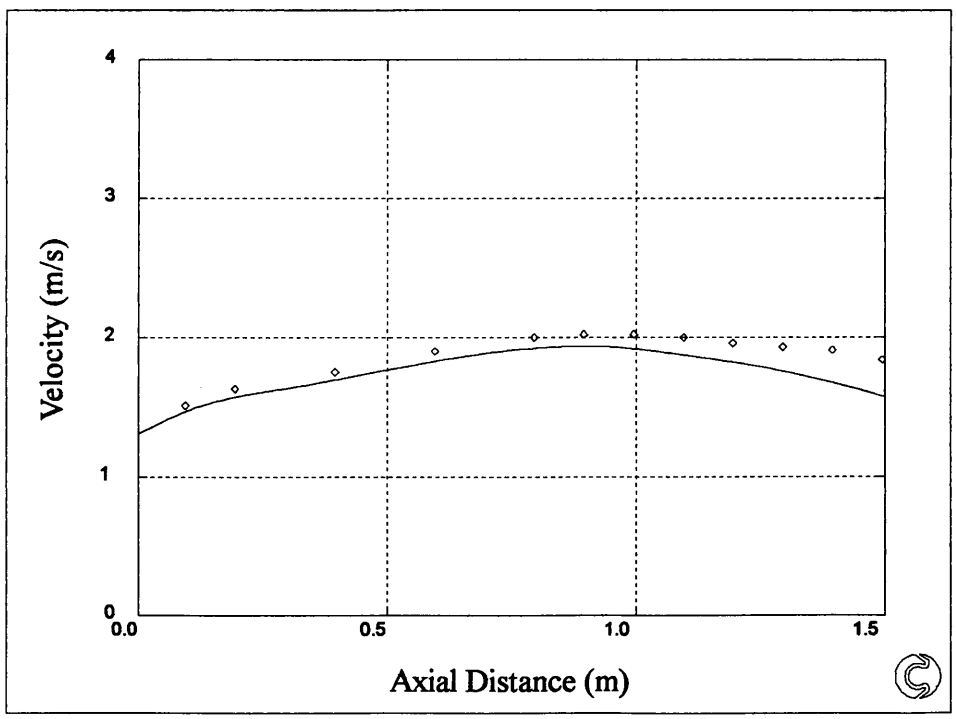

Figure 5.62: T3C4 Solomon/Malin/Dunham

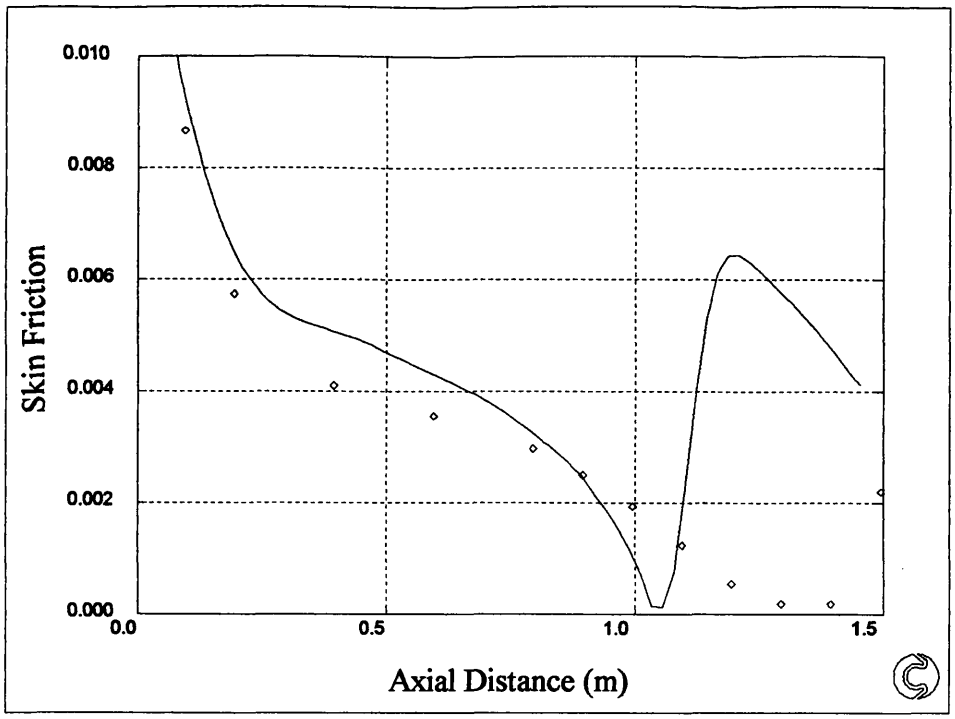

Figure 5.63: T3C4 Solomon/Malin/Dunham

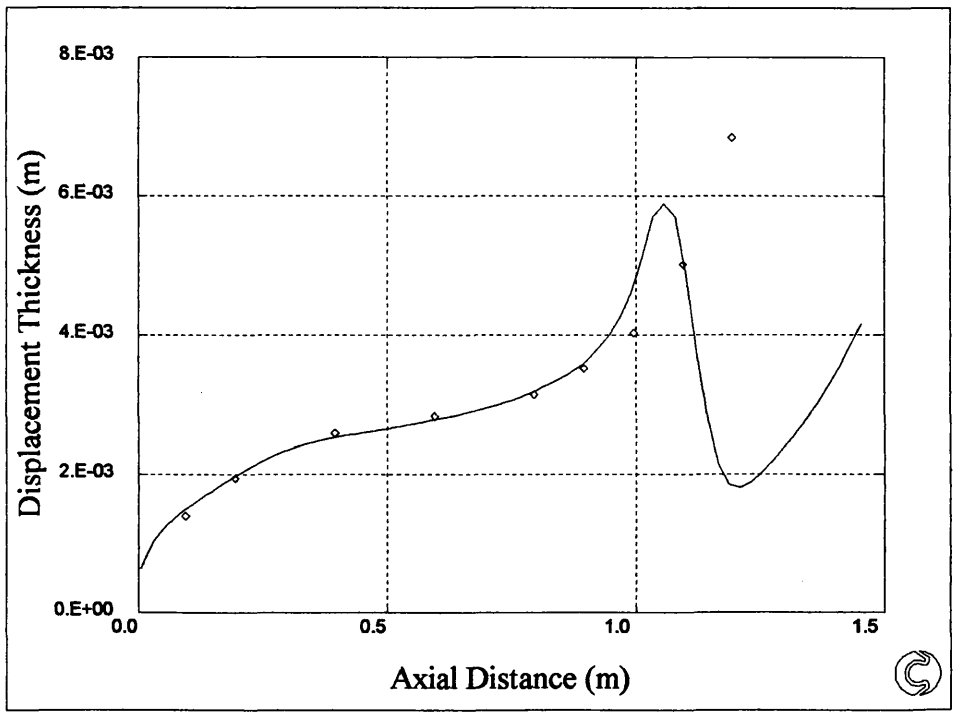

Figure 5.64: T3C4 Solomon/Malin/Dunham

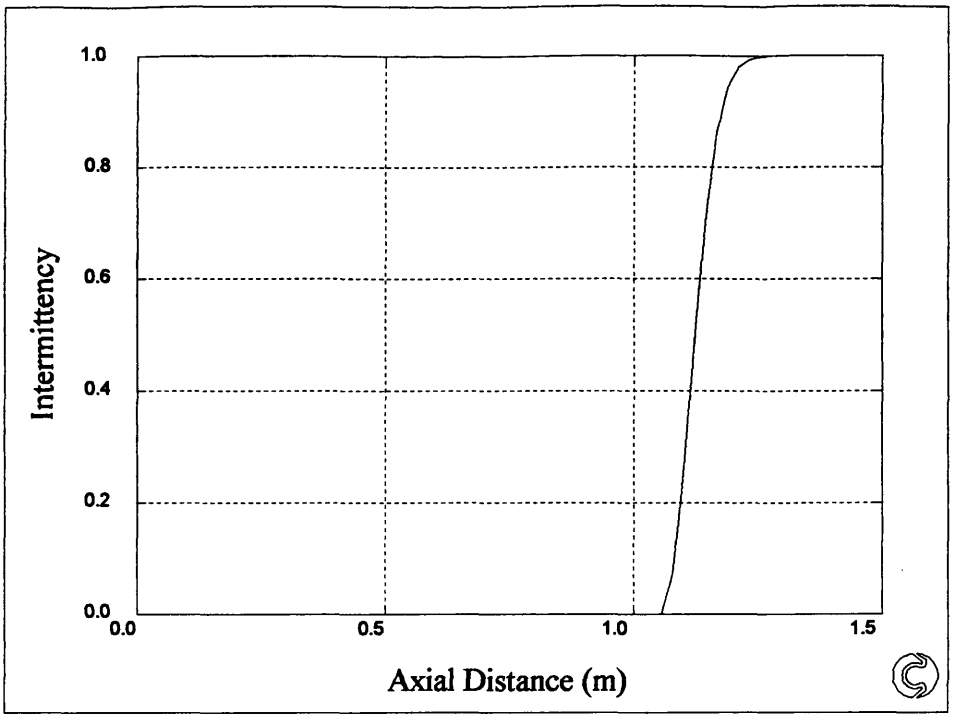

Figure 5.65: T3C4 Solomon/Malin/Dunham

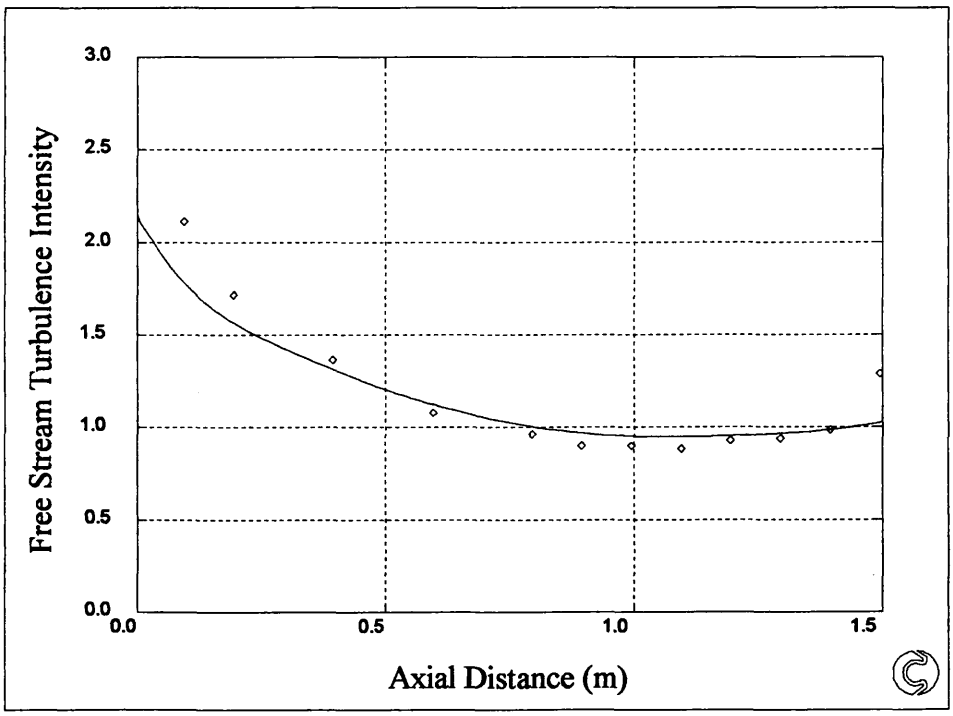

Figure 5.66: T3C4 Solomon/Malin/Dunham

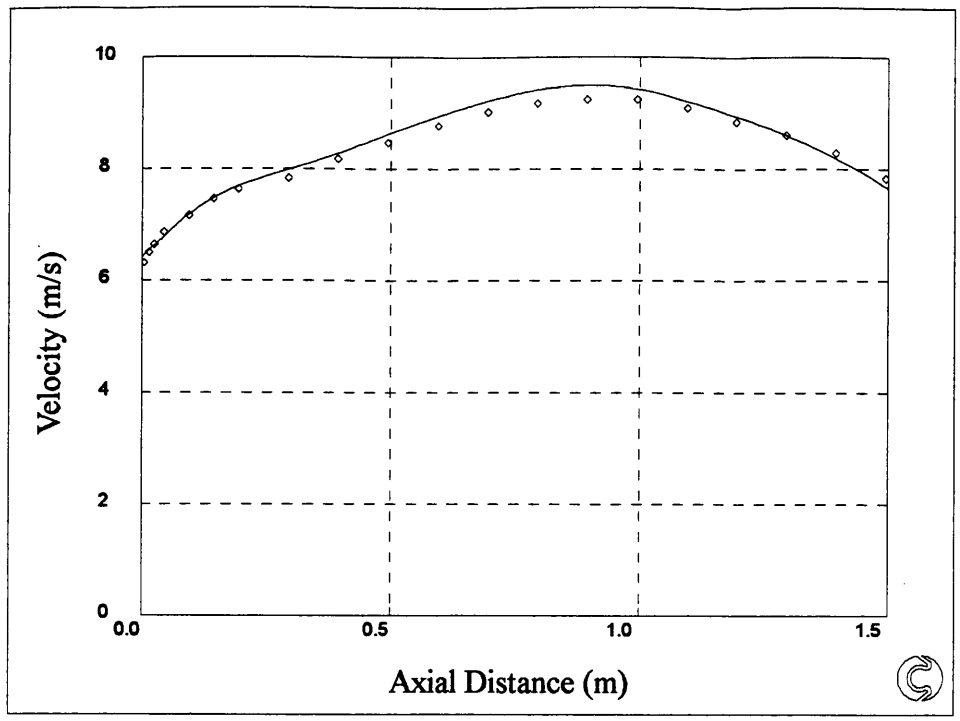

Figure 5.67: T3C1 Fraser/Malin/Integrated Average

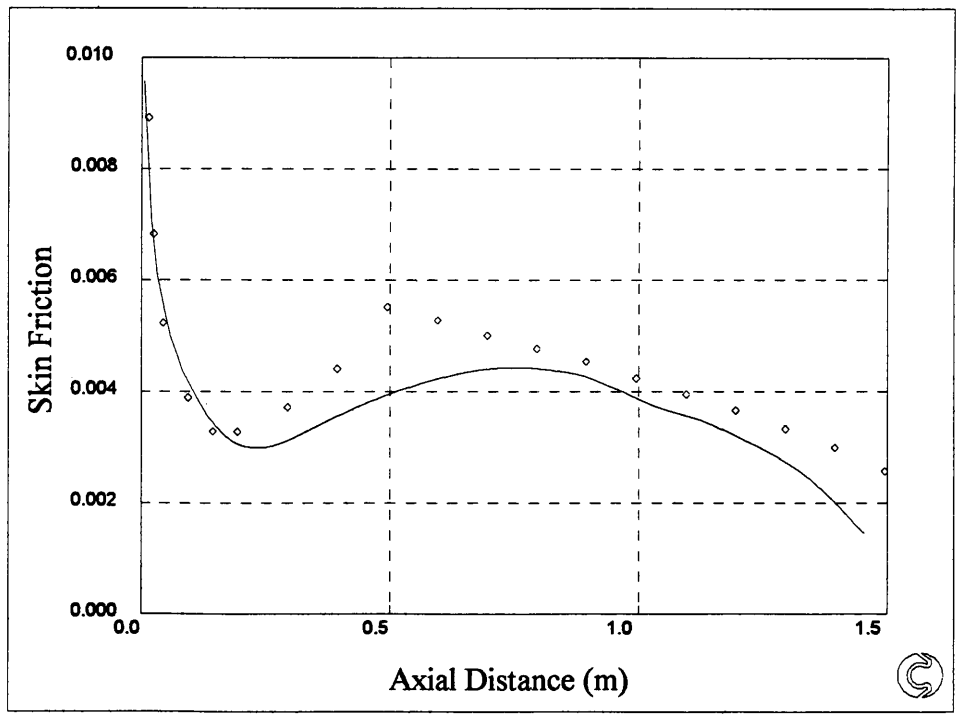

Figure 5.68: T3C1 Fraser/Malin/Integrated Average

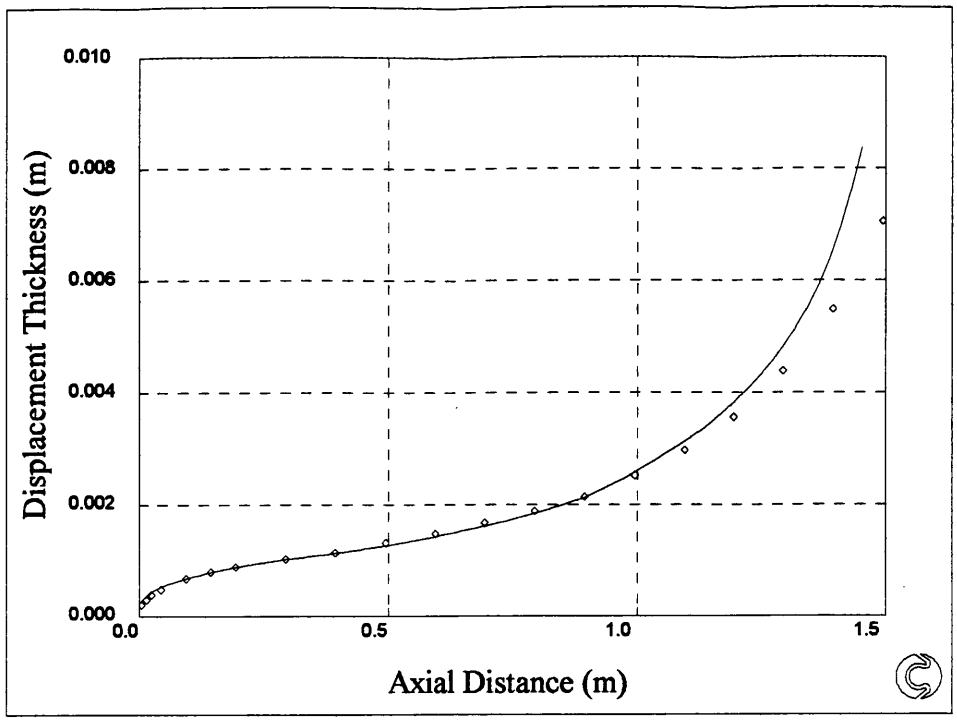

Figure 5.69: T3C1 Fraser/Malin/Integrated Average

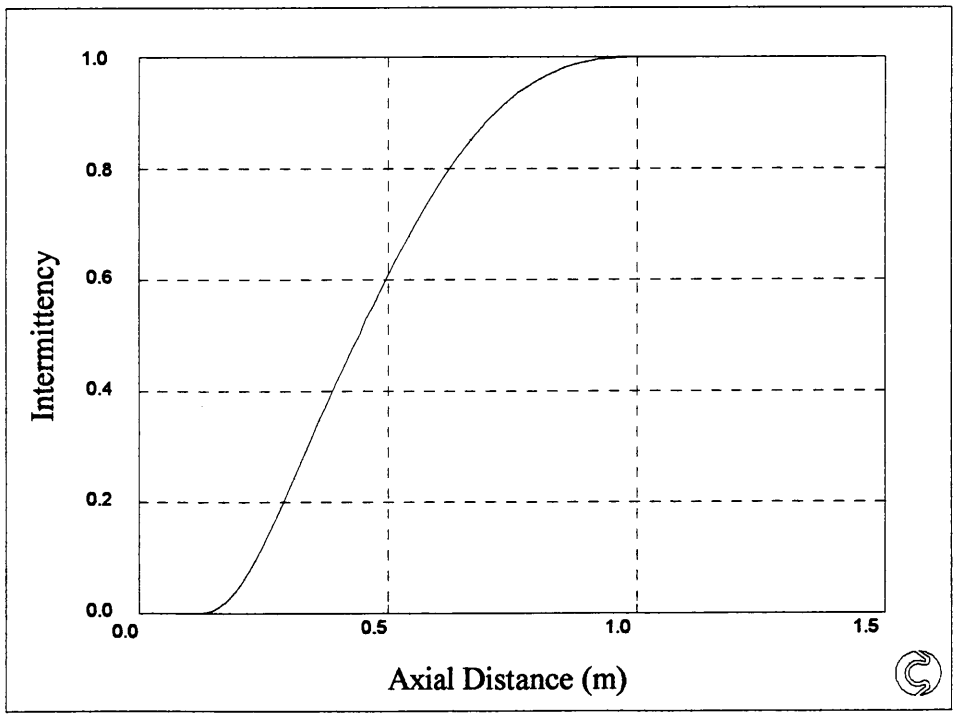

Figure 5.70: T3C1 Fraser/Malin/Integrated Average

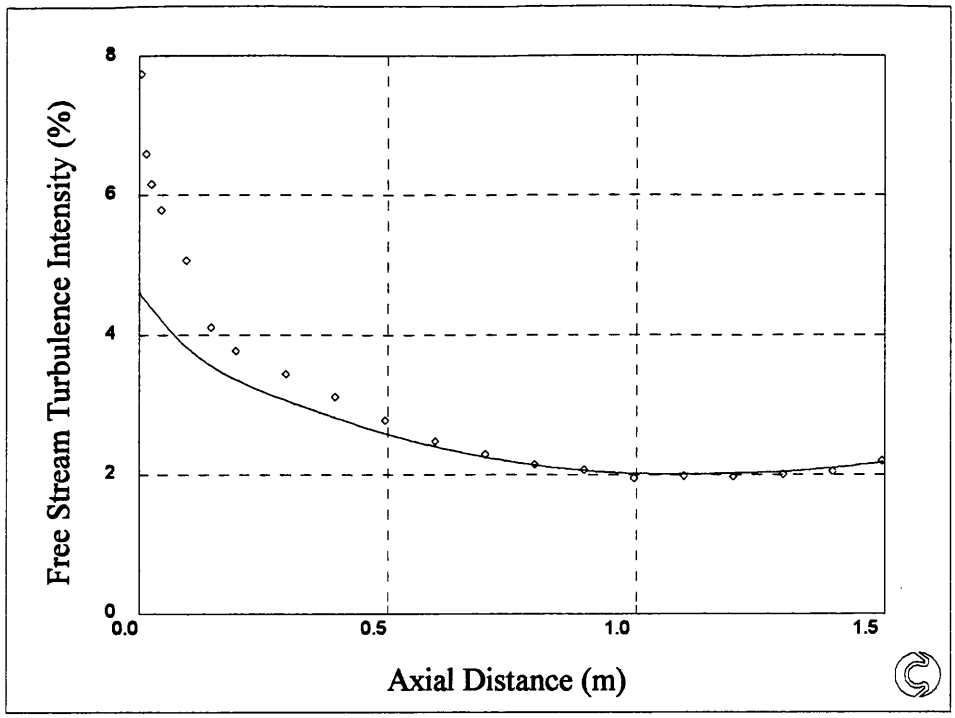

Figure 5.71: T3C1 Fraser/Malin/Intagrated Average

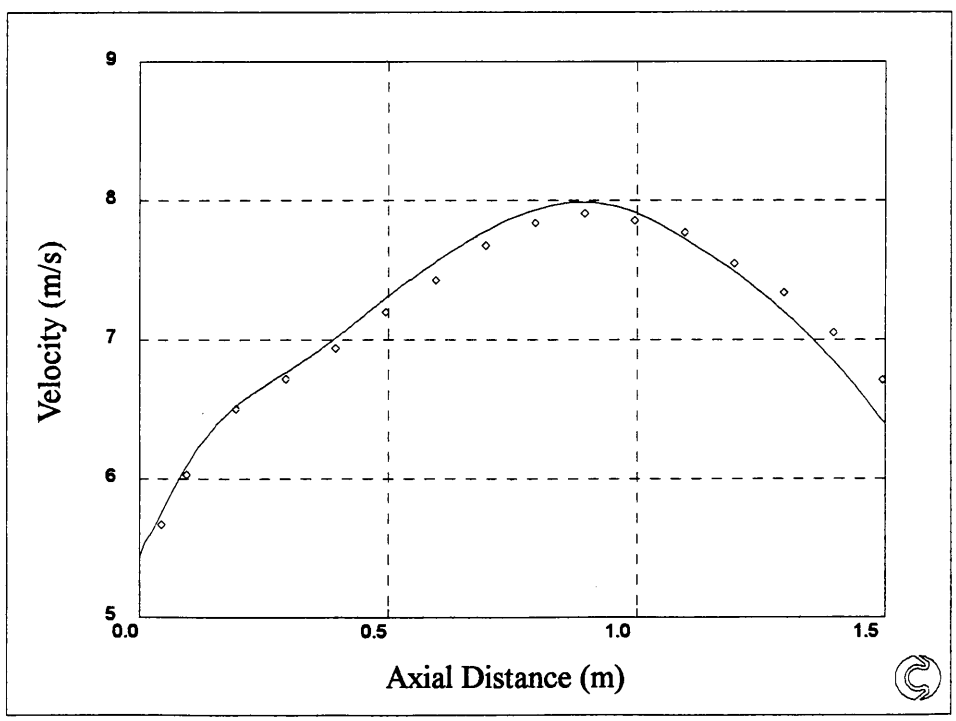

Figure 5.72: T3C2 Fraser/Malin/Integrated Average

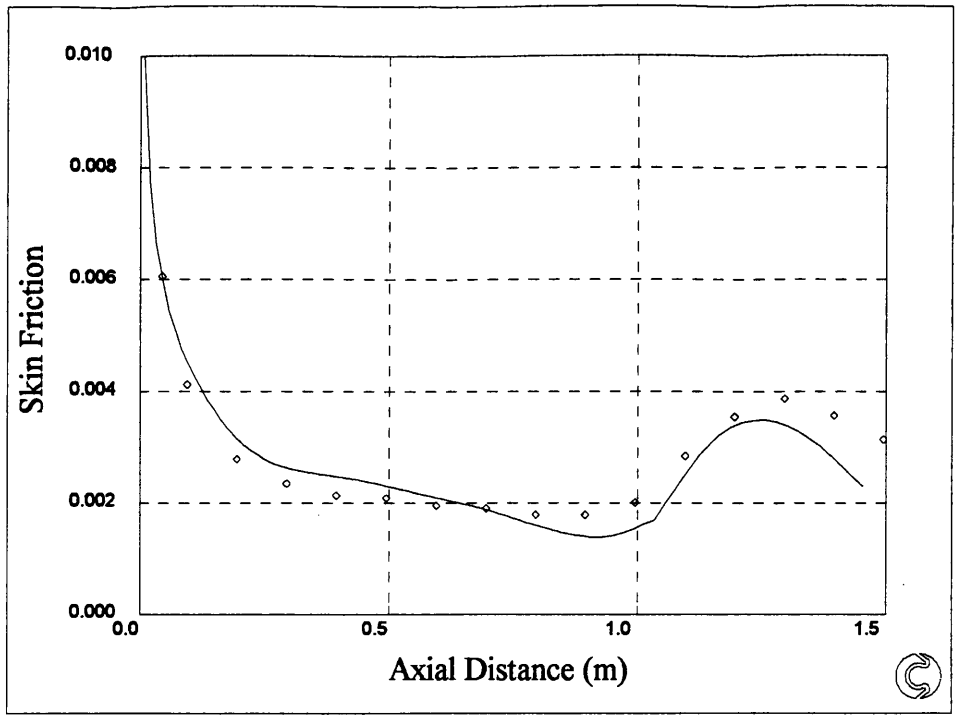

Figure 5.73: T3C2 Fraser/Malin/Integrated Average

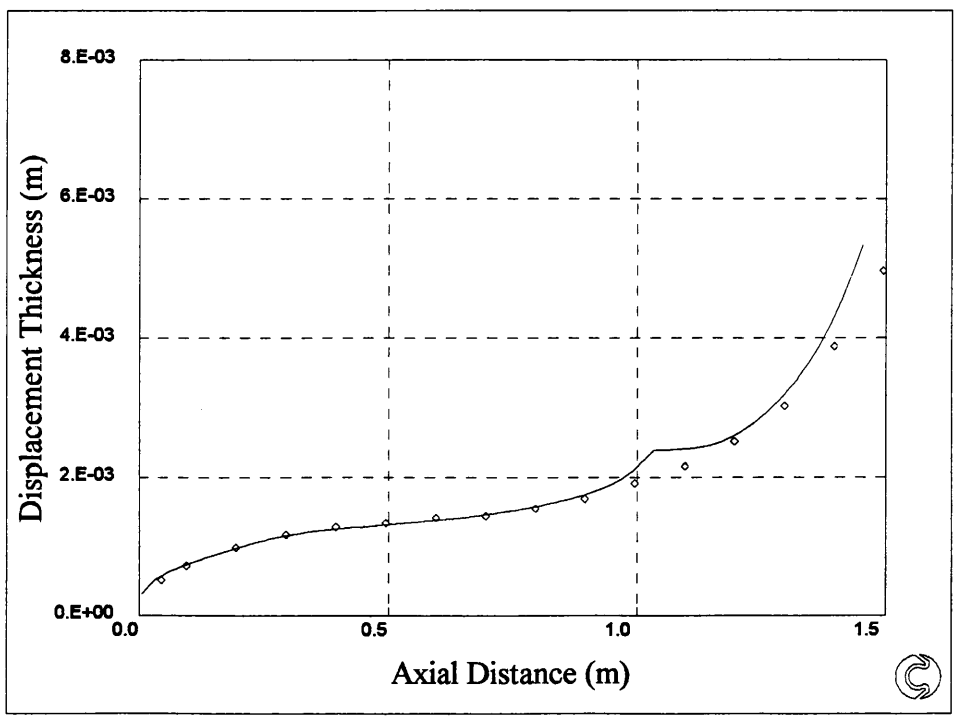

Figure 5.74: T3C2 Fraser/Malin/Integrated Average

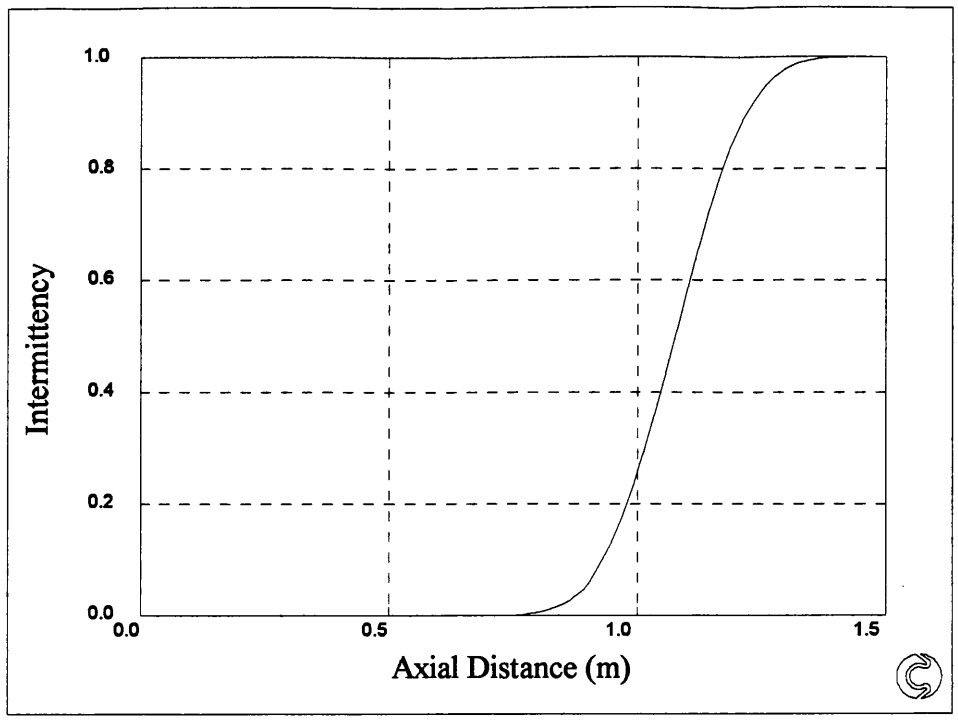

Figure 5.75: T3C2 Fraser/Malin/Integrated Average

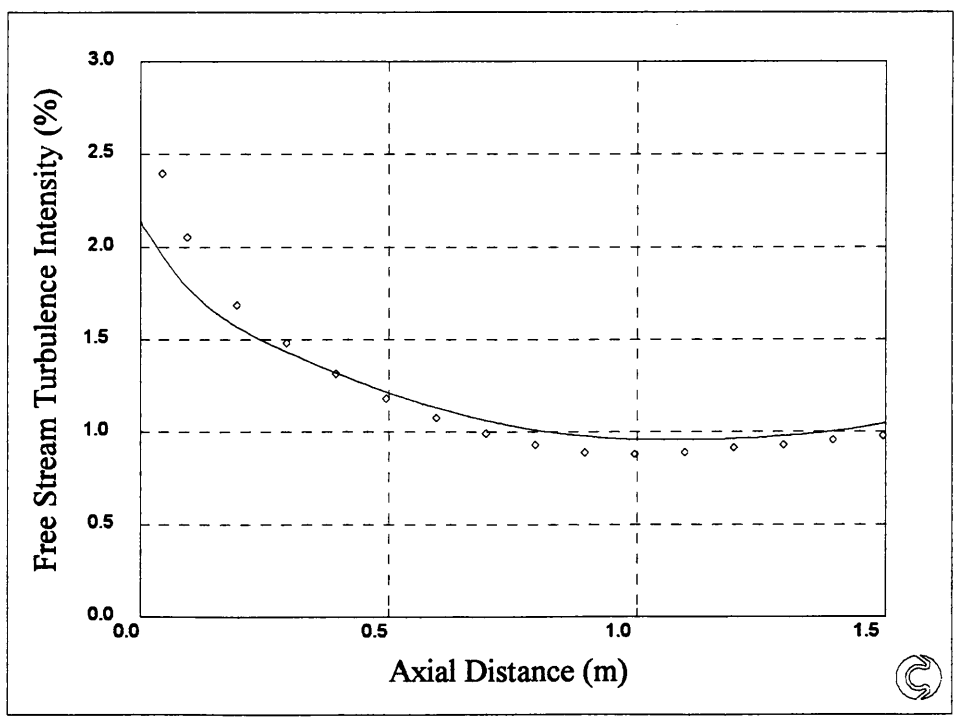

Figure 5.76: T3C2 Fraser/Malin/Integrated Average

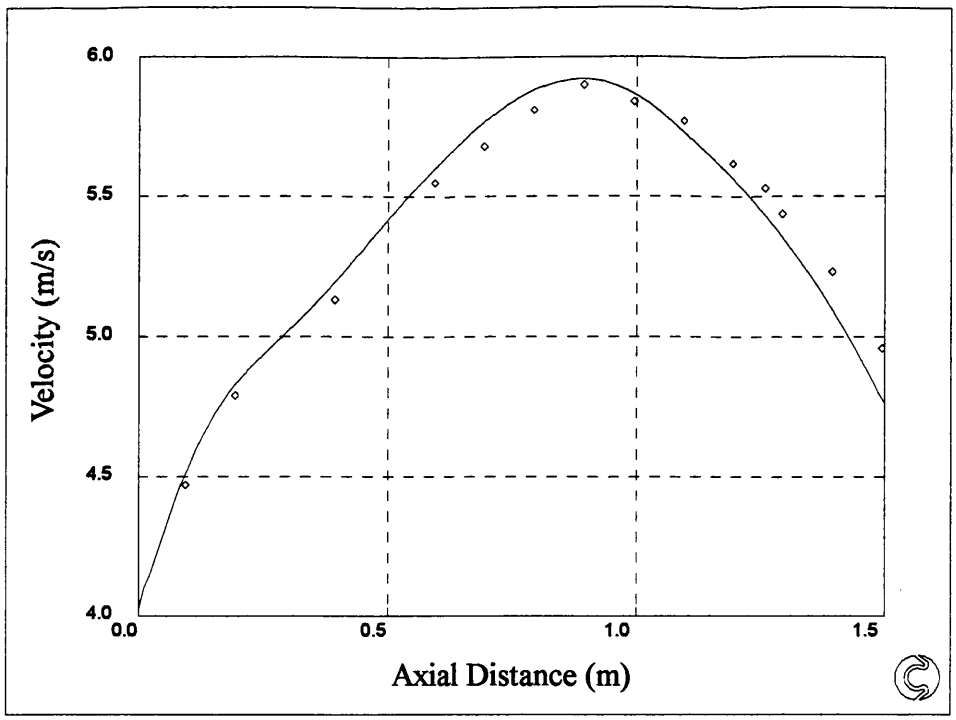

Figure 5.77: T3C3 Fraser/Malin/Integrated Average

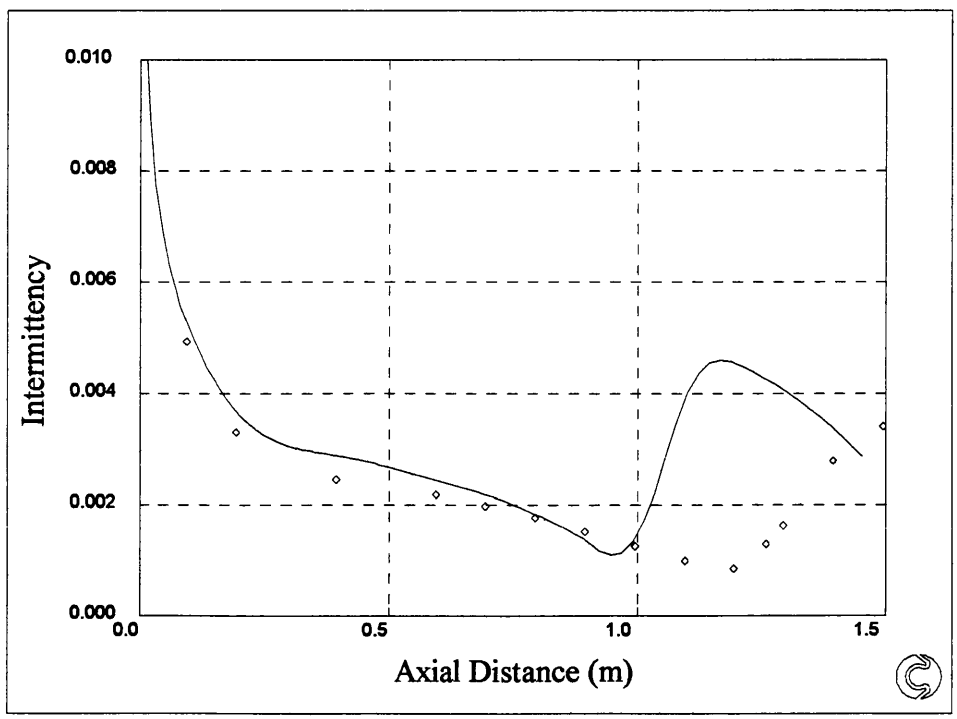

Figure 5.78: T3C3 Fraser/Malin/Integrated Average

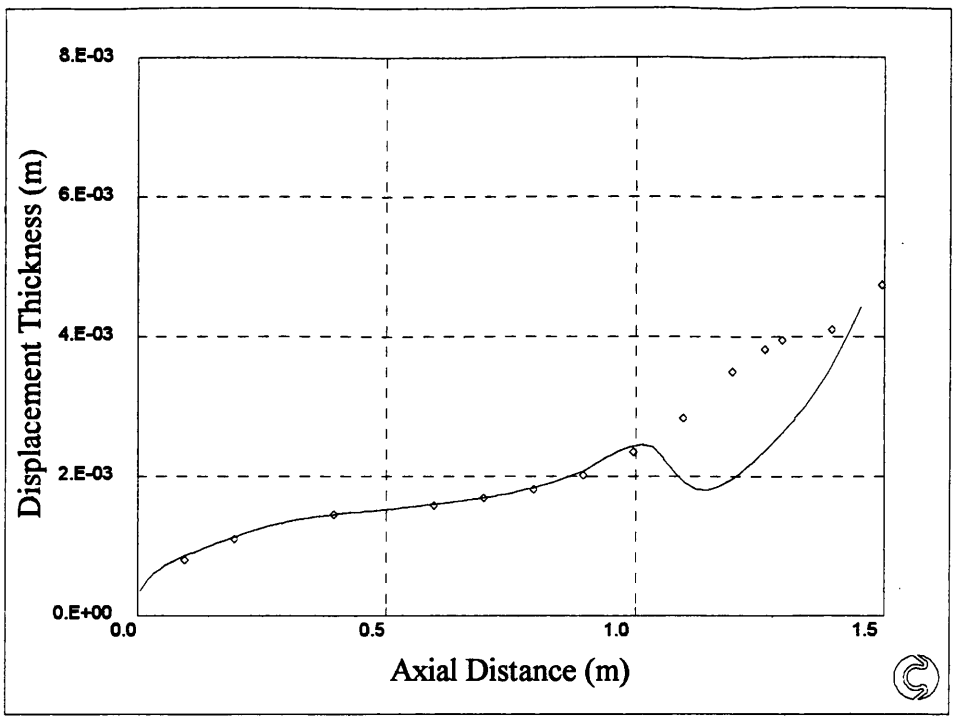

Figure 5.79: T3C3 Fraser/Malin/Integrated Average

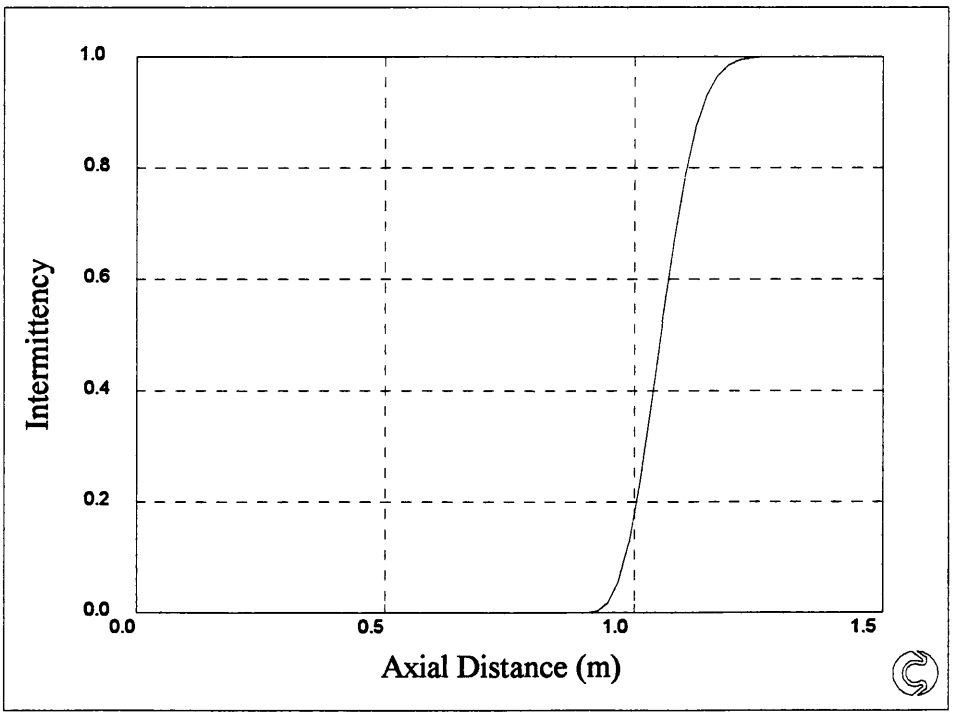

Figure 5.80: T3C3 Fraser/Malin/Integrated Average

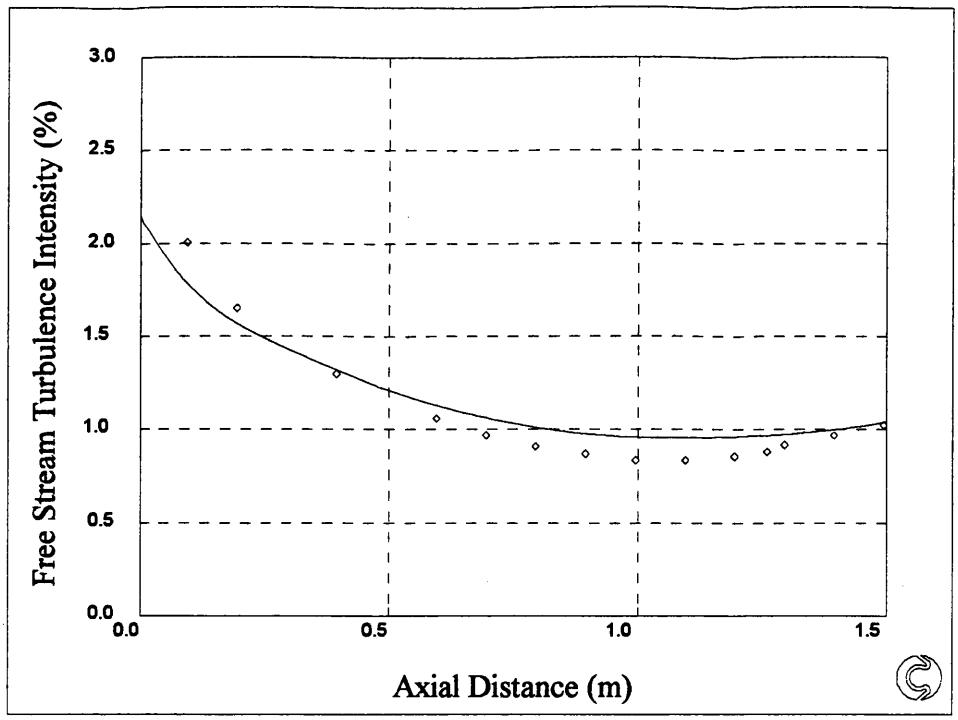

Figure 5.81: T3C3 Fraser/Malin/Integrated Average

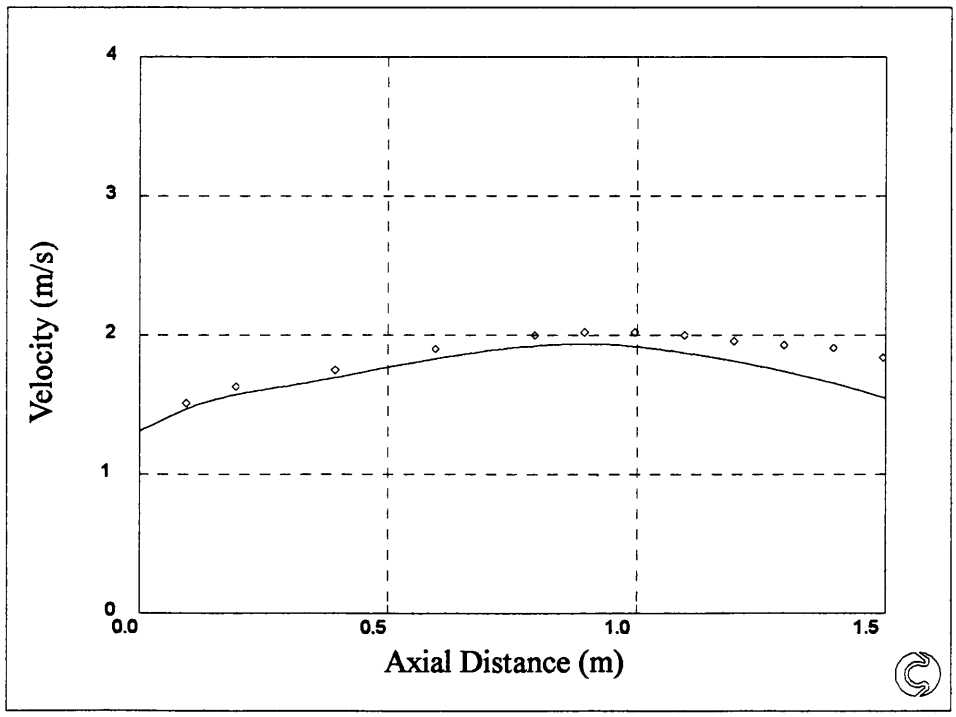

Figure 5.82: T3C4 Fraser/Malin/Integrated Average

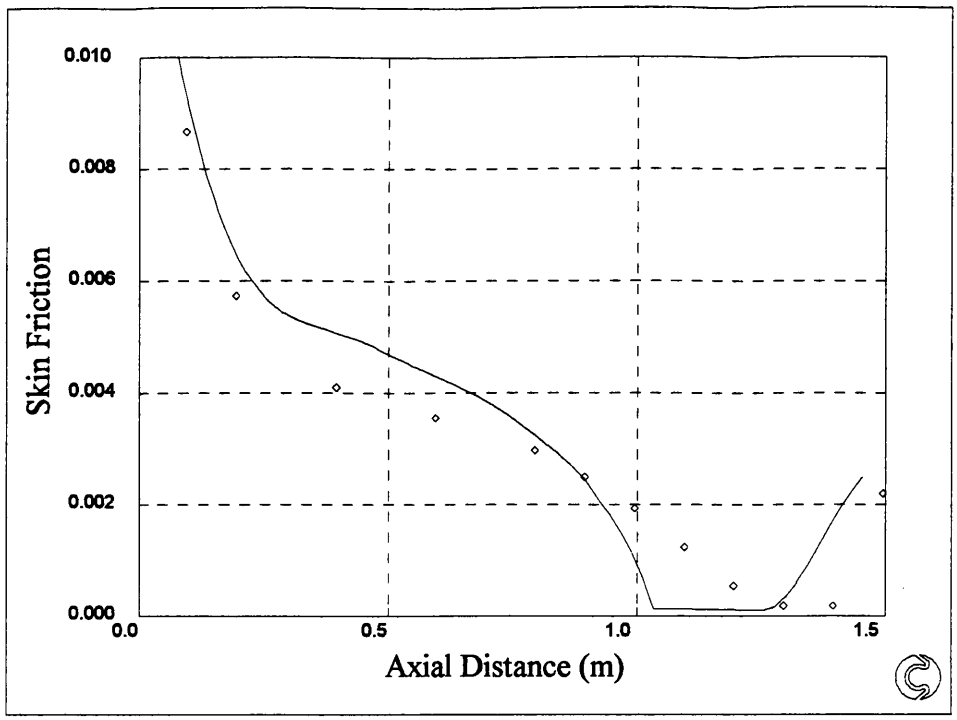

Figure 5.83: T3C4 Fraser/Malin/Integrated Average

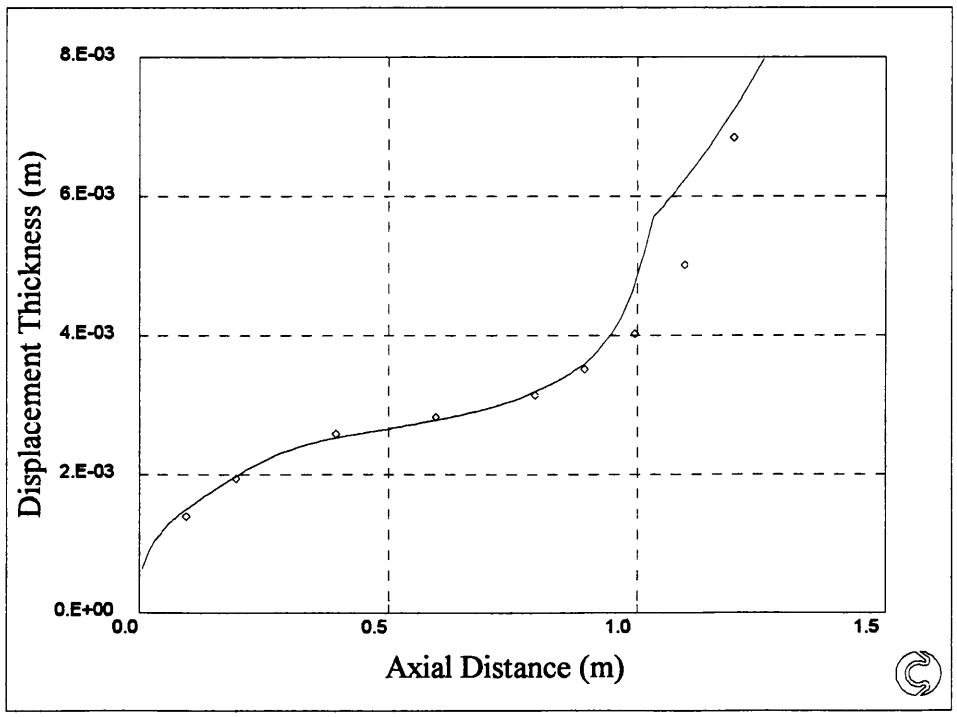

Figure 5.84: T3C4 Fraser/Malin/Integrated Average

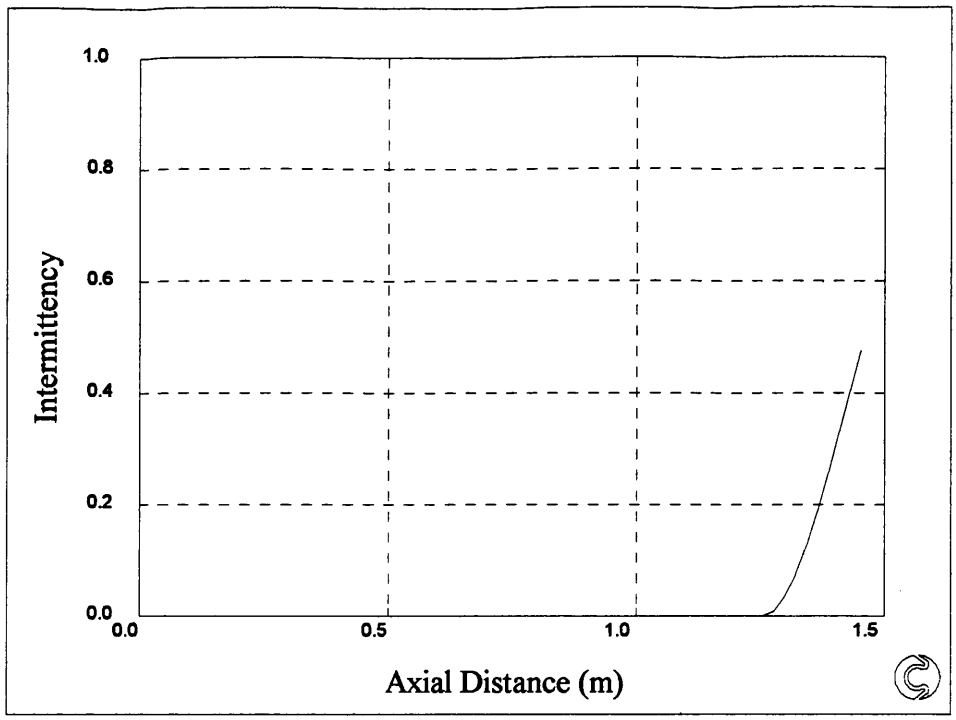

Figure 5.85: T3C4 Fraser/Malin/Integrated Average

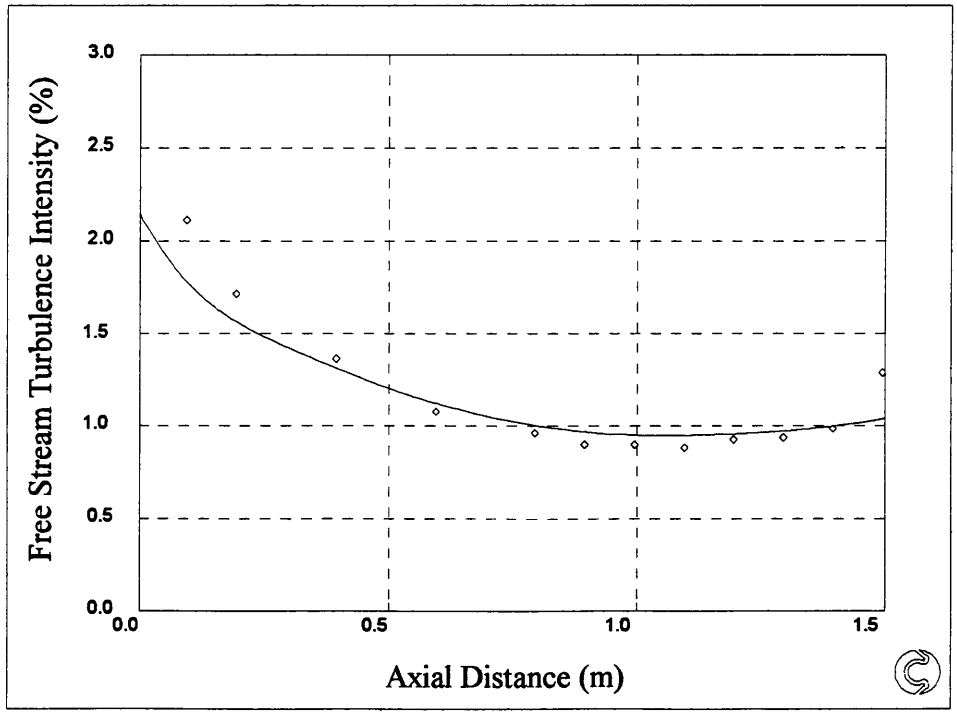

Figure 5.86: T3C4 Fraser/Malin/Integrated Average

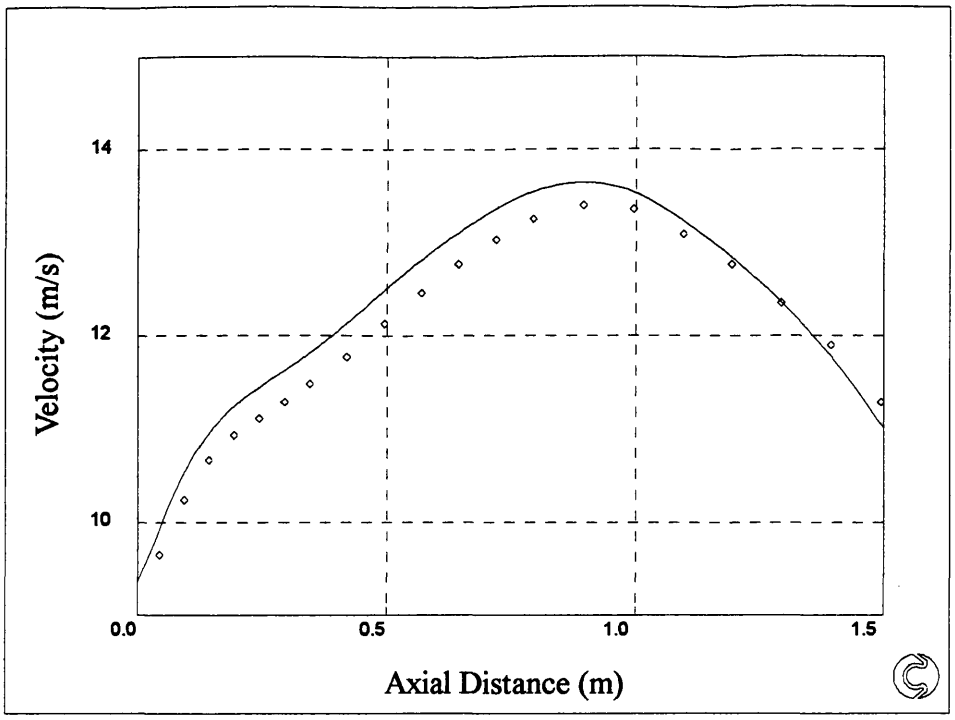

Figure 5.87: T3C5 Fraser/Malin/Integrated Average

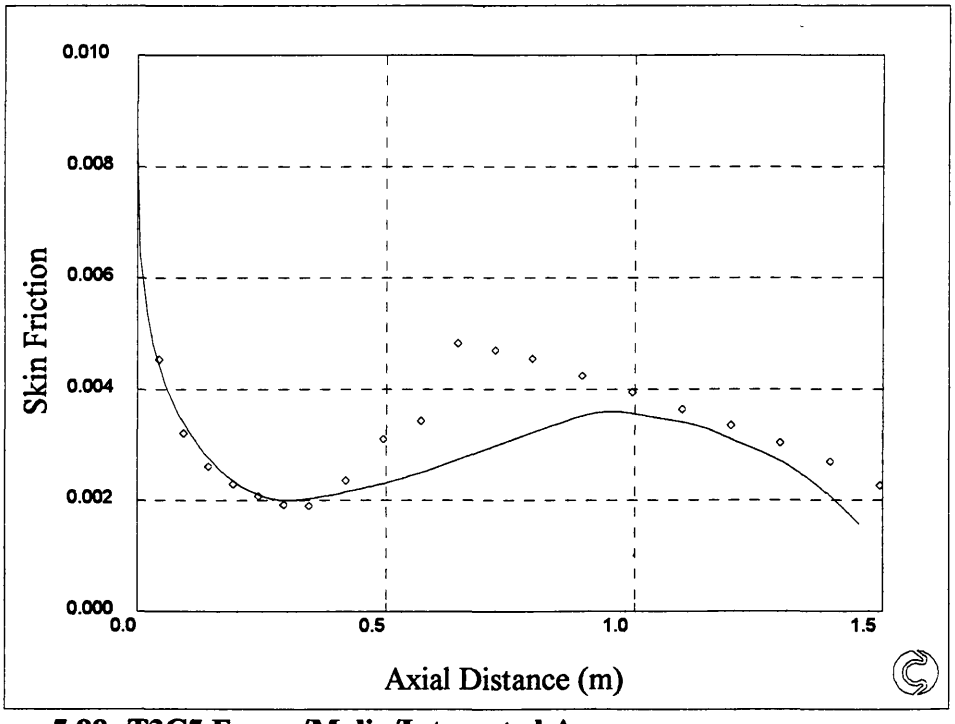

Figure 5.88: T3C5 Fraser/Malin/Integrated Average

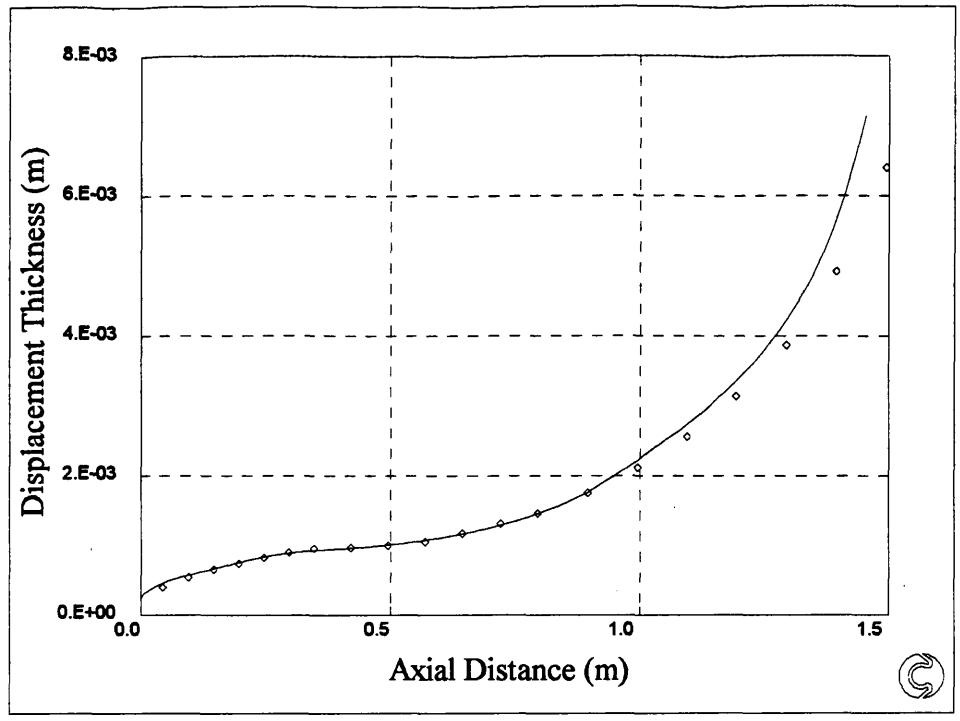

Figure 5.89: T3C5 Fraser/Malin/Integrated Average

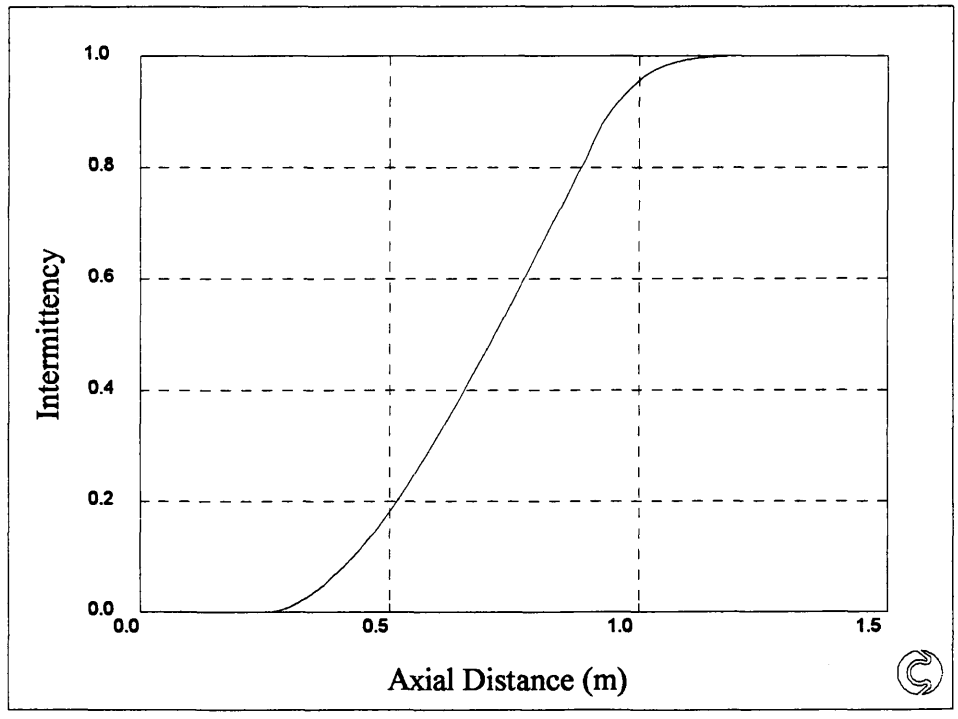

Figure 5.90: T3C5 Fraser/Malin/Integrated Average

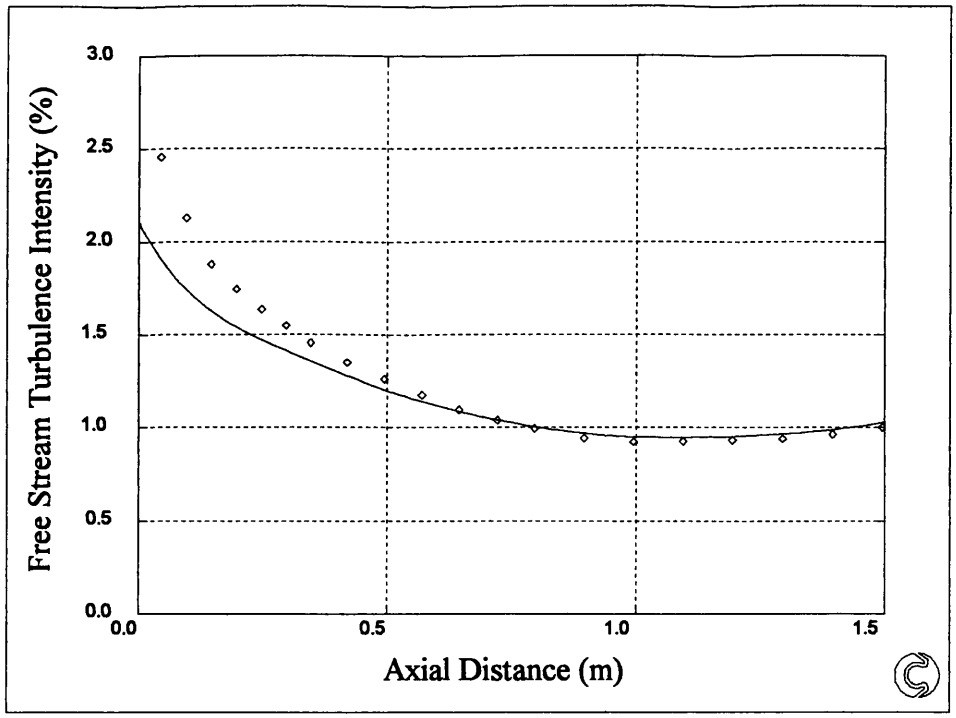

Figure 5.91: T3C5 Fraser/Malin/Integrated Average

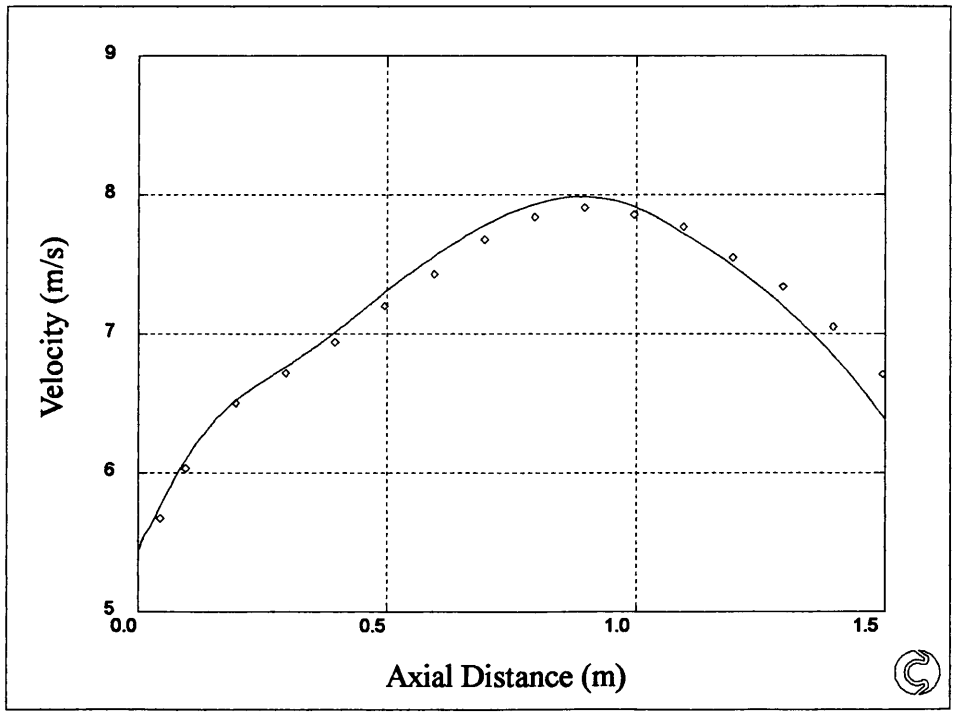

Figure 5.92: T3C2 Solomon/Malin/Integrated Average

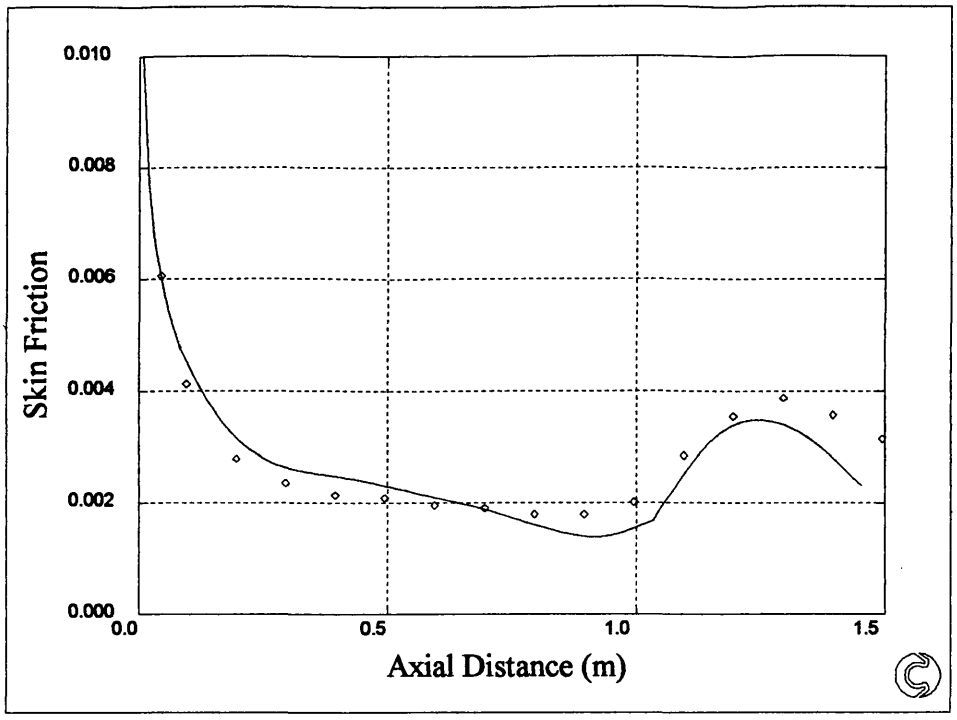

Figure 5.93: T3C2 Solomon/Malin/Integrated Average

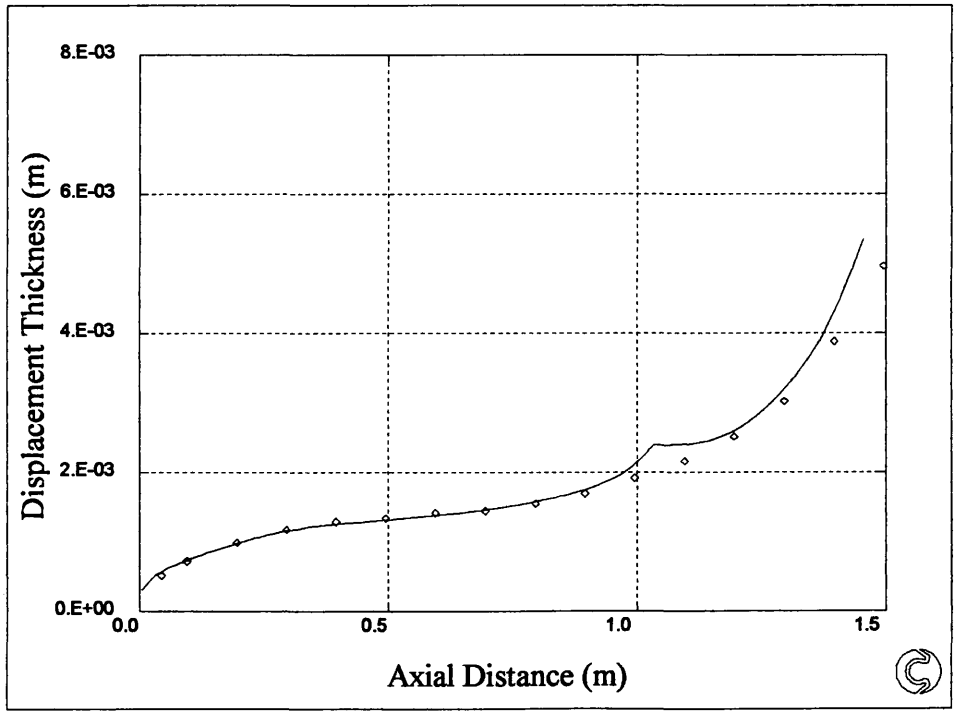

Figure 5.94: T3C2 Solomon/Malin/Integrated Average

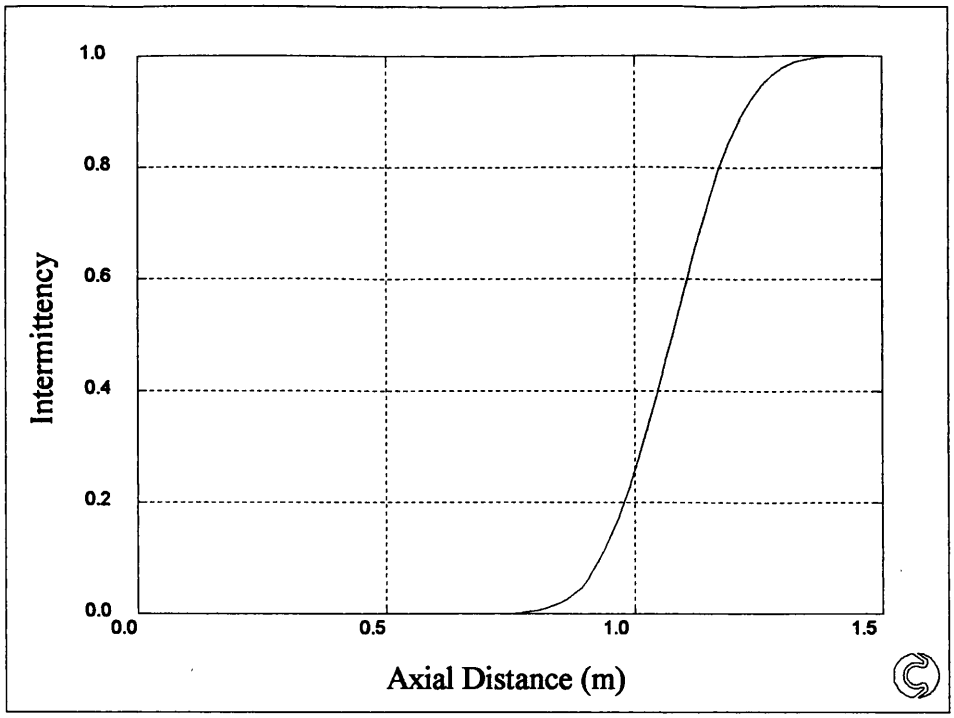

Figure 5.95: T3C2 Solomon/Malin/Integrated Average

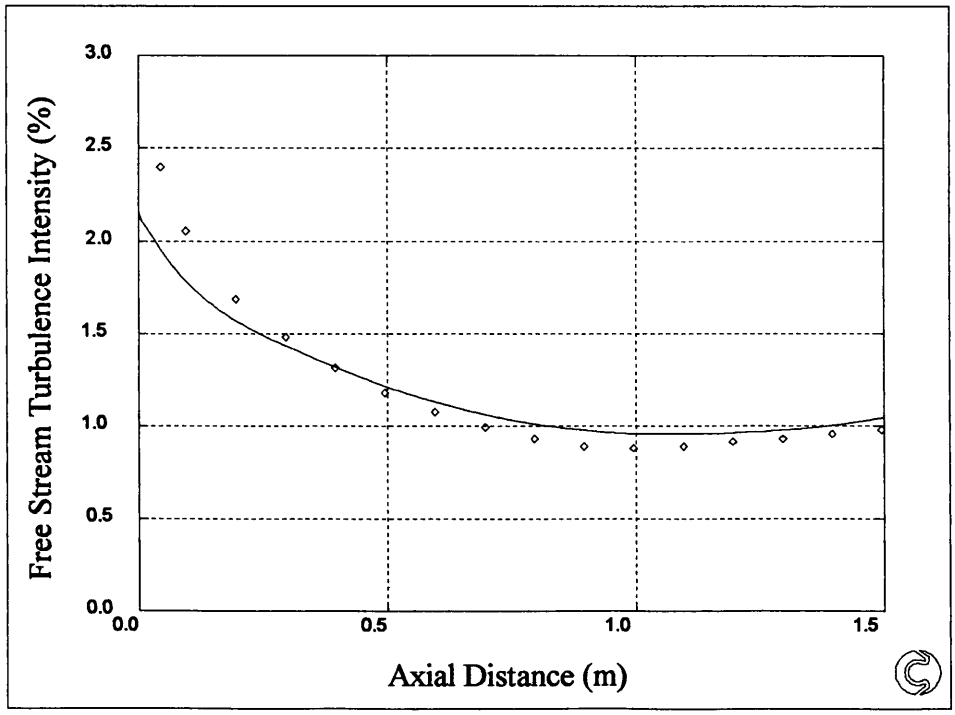

Figure 5.96: T3C2 Solomon/Malin/Integrated Average

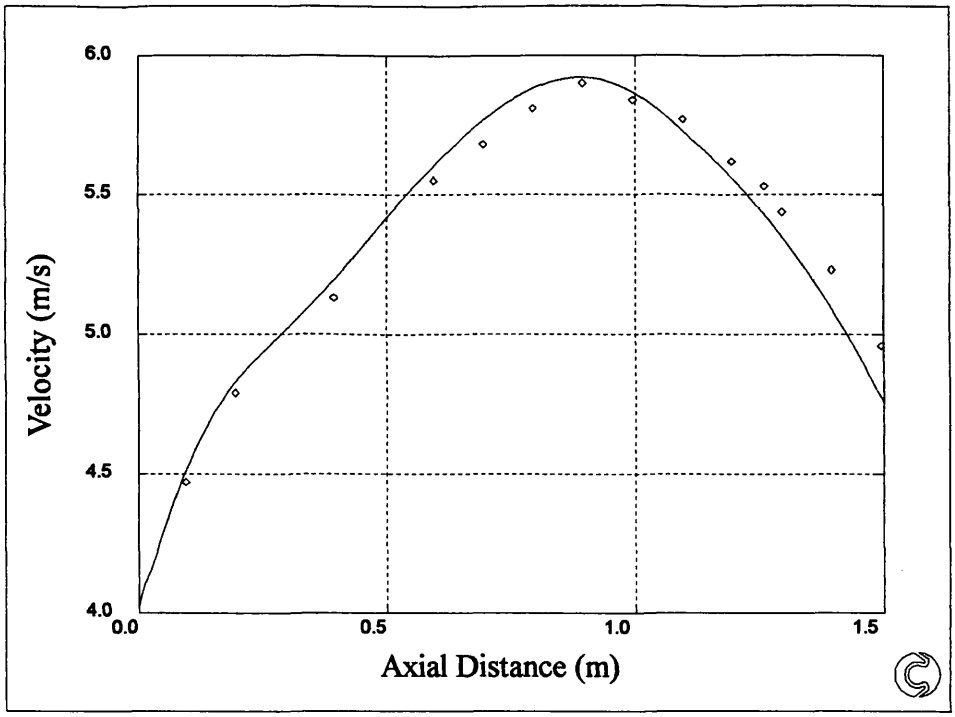

Figure 5.97: T3C3 Solomon/Malin/Integrated Average

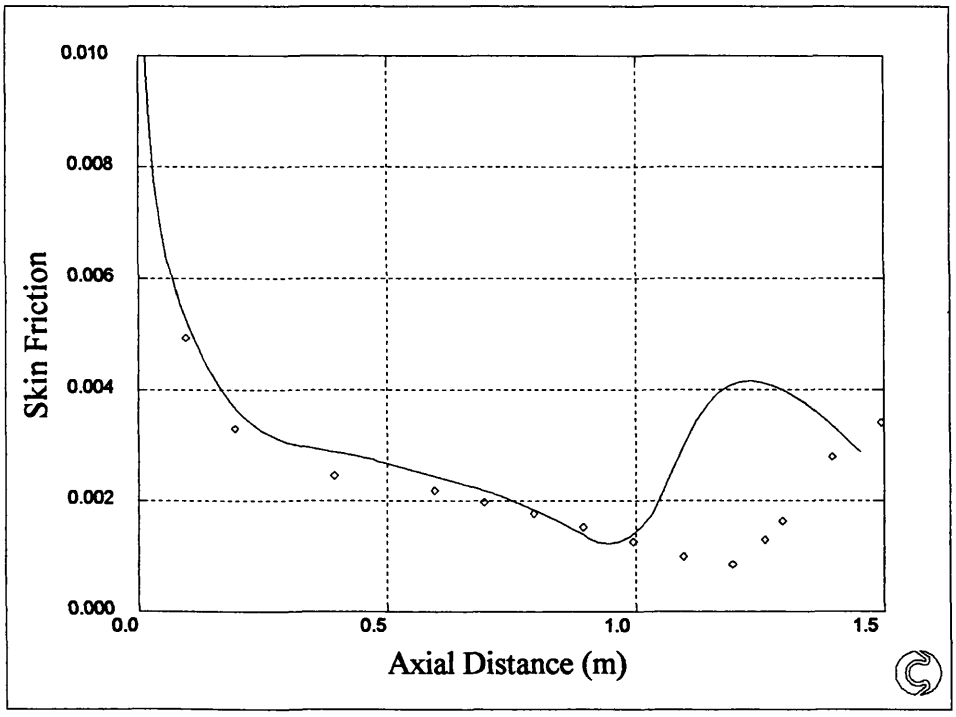

Figure 5.98: T3C3 Solomon/Malin/Integrated Average

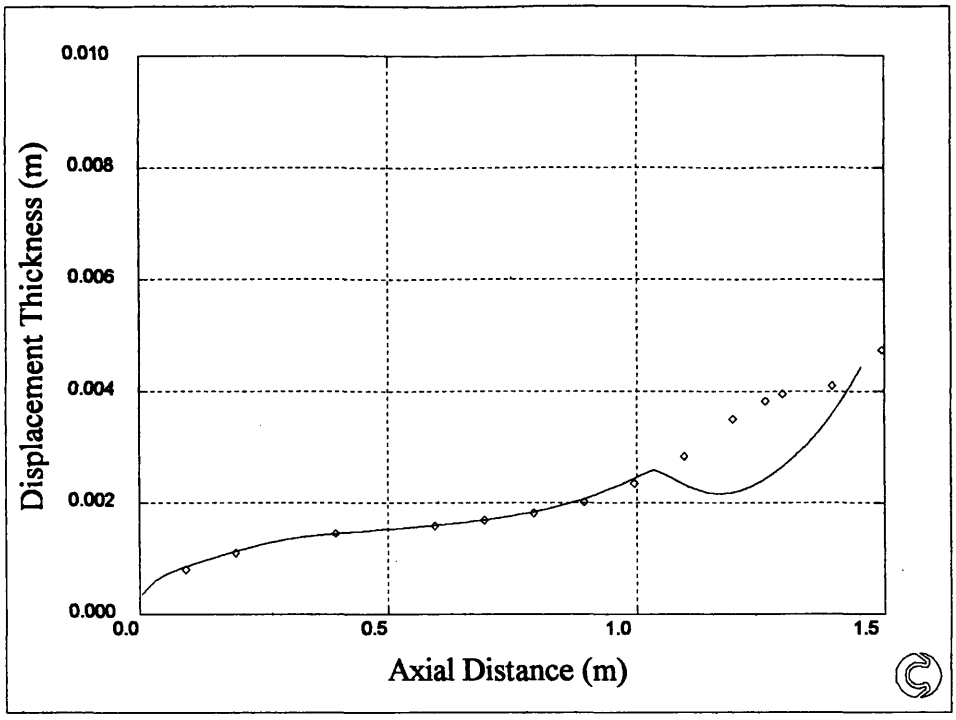

Figure 5.99: Solomon/Malin/Integrated Average

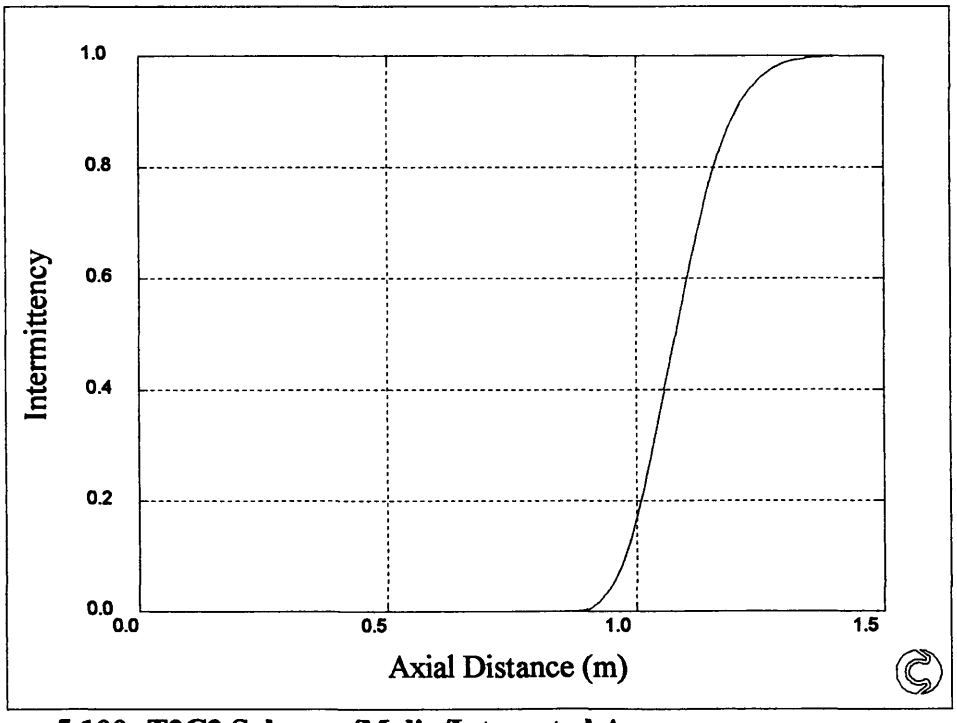

Figure 5.100: T3C3 Solomon/Malin/Integrated Average

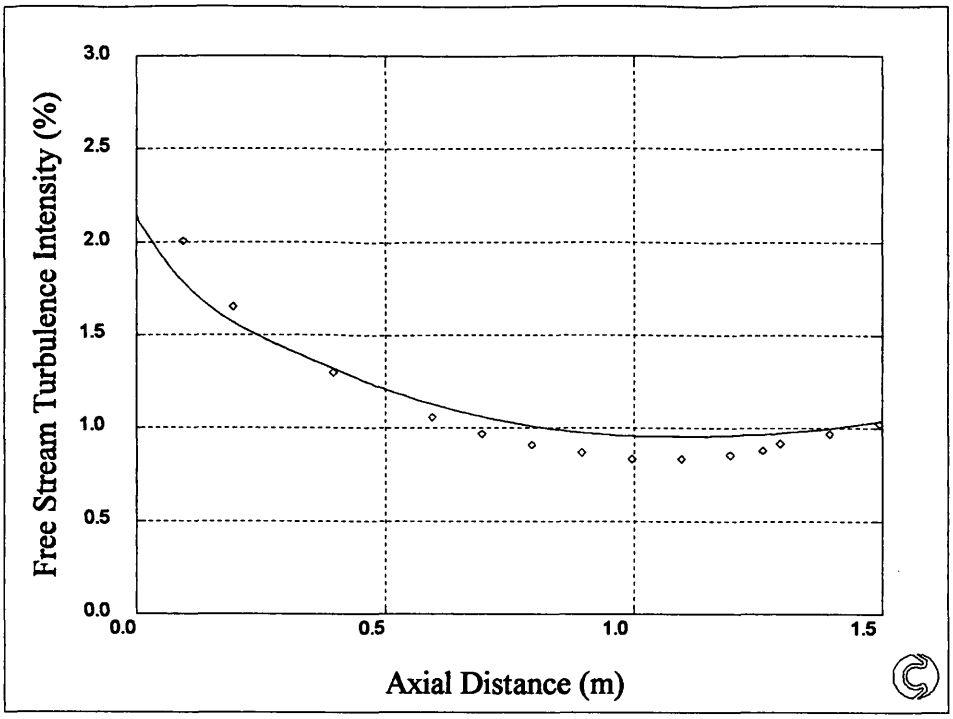

Figure 5.101: T3C3 Solomon/Malin/Integrated Average

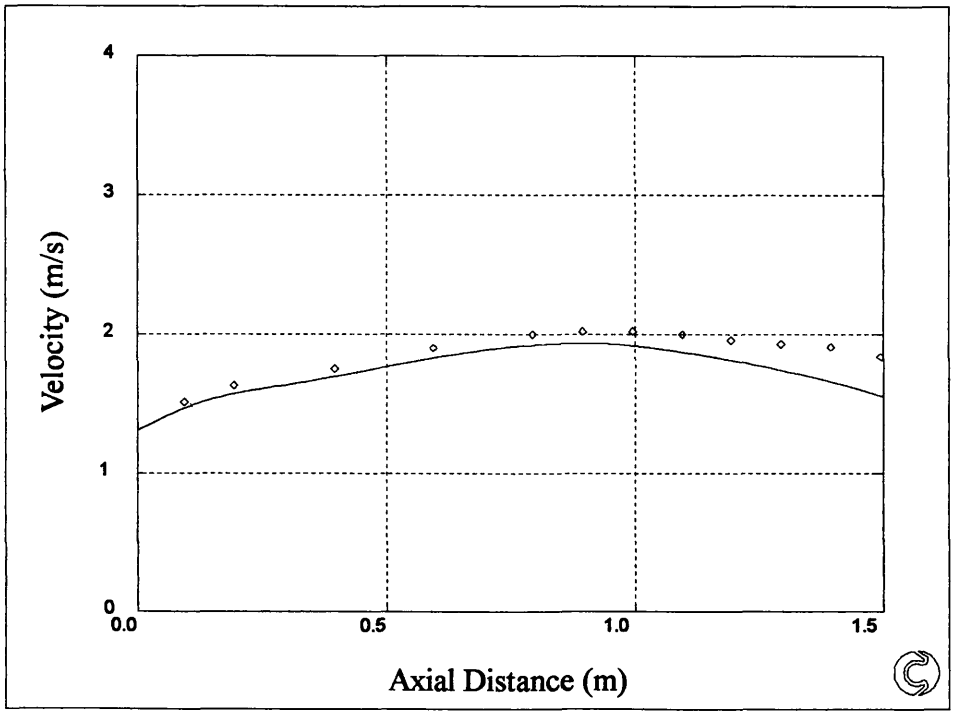

Figure 5.102: T3C4 Solomon/Malin/Integrated Average

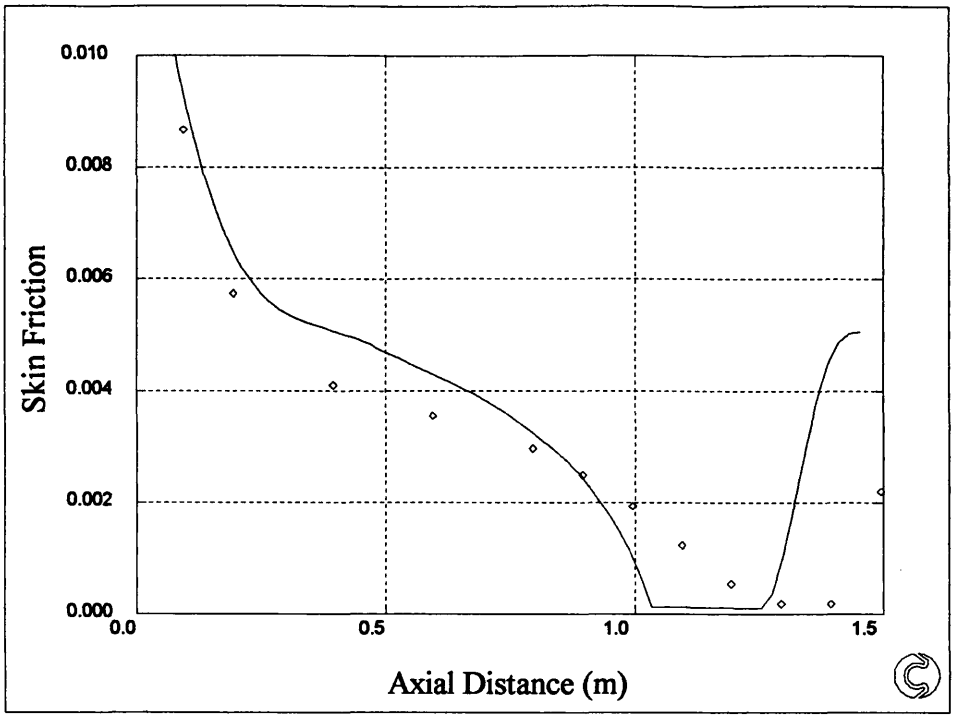

Figure 5.103: T3C4 Solomon/Malin/Integrated Average

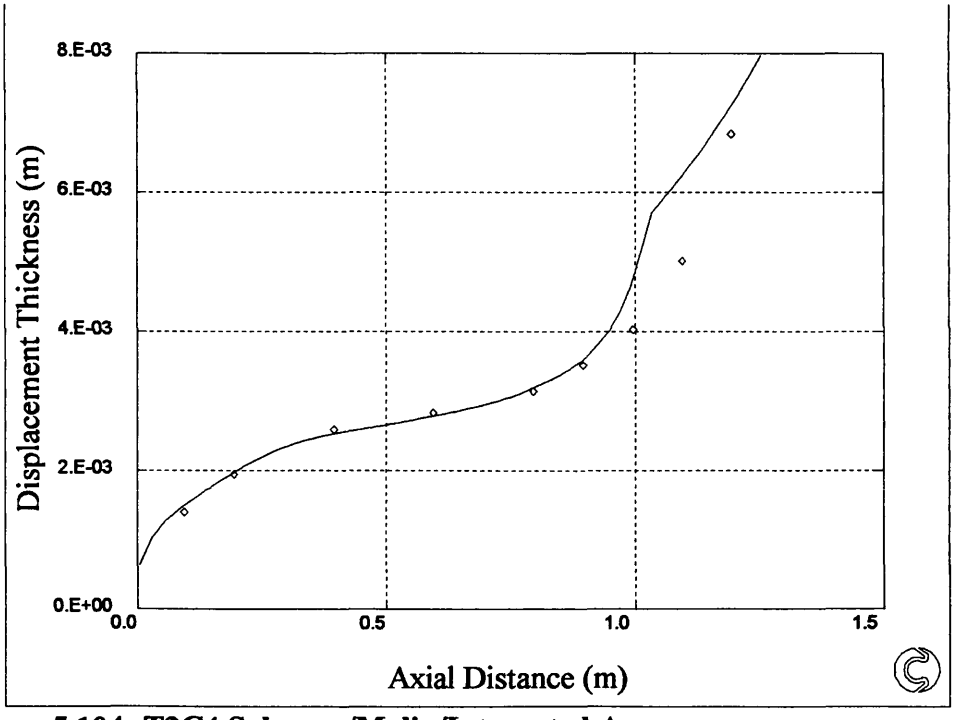

Figure 5.104: T3C4 Solomon/Malin/Integrated Average

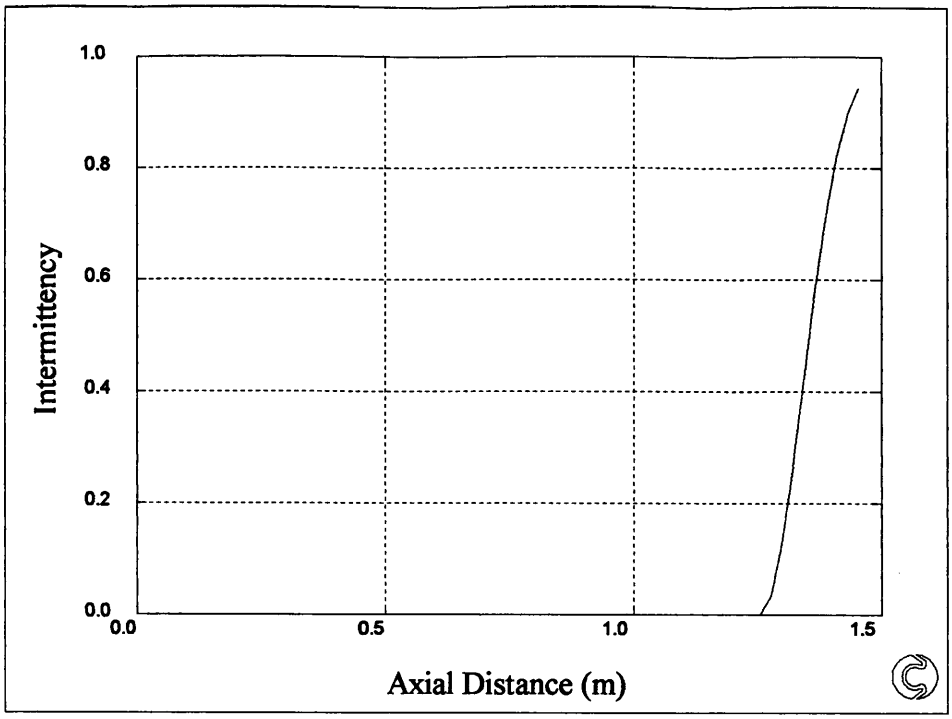

Figure 5.105: T3C4 Solomon/Malin/Integrated Average

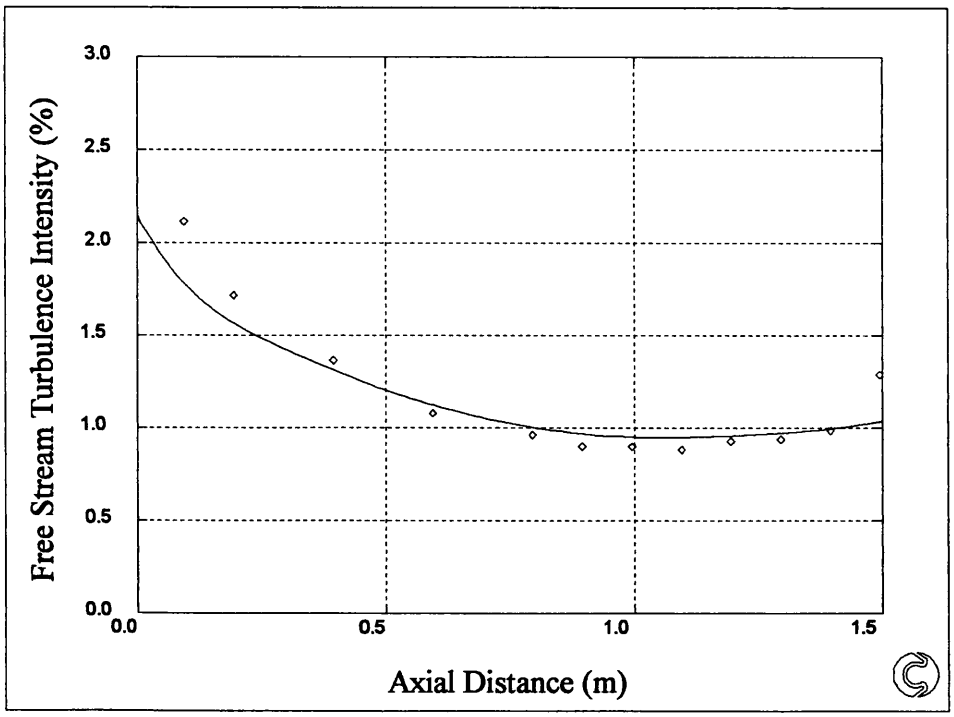

Figure 5.106: T3C4 Solomon/Malin/Integrated Average

6. Gas Turbine Rotor Blade Flows

6.1 Introduction

Axial flow turbines are by far the most common type of turbine for aircraft engines, industrial gas turbines and steam turbines. Hence they are very highly developed and achieve high levels of performance.

Until the early 1970's turbines were largely designed by empirical methods, based on the accumulated experience of the designers company. This has produced some very successful designs. However, significant improvements in efficiency and/or in stage loading have been achieved using results from the numerical methods of flow prediction and from the improved experimental measurements that have become available over the last two decades. The combination of numerical predictions and more detailed experimental measurements in real turbines has lead to a great improvement in physical understanding of the flow mechanisms.

The computation of viscous drag around/over a body is often critically dependent upon the modelling of the laminar - turbulent transition in the boundary layer. Prediction of the boundary layer in gas turbine engines is critical in order to predict the following losses:

(a) *Profile loss* - associated with boundary layer growth over the blade profile (including separation loss under adverse conditions of extreme angles of incidence or high inlet Mach number).

(b) *Annulus loss* - associated with boundary layer growth on the inner and outer walls of the annulus.

(c) *Secondary loss* - arising from secondary flows which are always present when a wall boundary layer is turned through an angle by an adjacent curved surface.

(d) *Tip clearance loss* - near the rotor blade tip the gas does not follow the intended path, fails to contribute its design quota of work output, and interacts with the outer wall boundary layer.

Initial turbine blade profile design calculations are considered as a two-dimensional flow at mid span.

The integral method boundary layer modelling technique proposed in this thesis was used to predict skin friction on the pressure and suction surfaces at mid-span on a rotor blade of a low pressure turbine, in an industrial gas turbine engine. Blade nomenclature used here is shown in Figure 6.1.

6.2 Validation of PHOENICS CFD Software

Before any boundary layer modelling/skin friction predictions could be made for this blade, it was essential to validate the PHOENICS software. An already existing accepted inviscid solution was available, courtesy of European Gas Turbines Limited (EGT) which was considered suitable for this purpose.

A structured body fitted co-ordinate grid was constructed comprising of 76 x 20 x 1 (z, x, y) computational cells, see Figure 6.2 was constructed. The inlet was a fixed mass flow boundary situated at the low z end of the grid and the outlet as constant pressure situated at high z. Cyclic (constant pressure) boundaries were attached to east and west faces of z slabs 1 to 10 and 67 to 76.

The blade surfaces were assumed to be adiabatic walls with no friction. The grid was solved assuming laminar compressible flow.

The flows were solved to within the default 1% error, which took about 2000 iterations (approximately 1 hour using a 486 DX4/133 MHz computer). To ensure that convergence had been achieved, the solution procedure was restarted and run for a further 100 iterations and compared with the field values obtained previously. There was no appreciable difference between these solutions.

Comparisons were made using the PHOENICS solved laminar flow case with the accepted solution on flow field Mach number, static pressure and blade surface pressure distribution, supplied by EGT (Figures 6.3 - 6.8). The comparison could be described as good in all cases. The PHOENICS code has therefore been validated for this case. To ensure the solution was grid independent, the number of cells in the axial (z direction) was increased from 76 to 195 and a laminar solution was performed. There was no appreciable difference in the solution, and therefore the original grid could be adopted for the frictional flow calculation.

6.3 Skin Friction Prediction

Two flow regimes were solved, these being laminar flow and turbulent flow. The turbulence model used in the turbulent analysis was the well known high Reynolds number k - ε. The turbulence intensity at inlet was quoted as 4%, and the dissipation length scale was taken to be 10% of the blade spacing width at mid-span at inlet. Transitional parameters were modelled using the method described by Fraser, Higazy and Milne (1994). The turbulence intensity used in their correlations was the inlet value. The boundary conditions were the same as

the non-friction analysis except that the blade surfaces now had a boundary layer model attached to them, which was considered as a momentum sink.

The same computational grid was used for the analysis and the frictional calculations were restarted from the converged non-frictional laminar or turbulent solution. The frictional analysis converged in about 700 iterations for the laminar case and in about 1000 for the turbulent case.

It can be seen when comparing the laminar and turbulent free stream velocity profiles adjacent to the blade surfaces (Figures 6.9 and 6.10) that they are almost identical.

Comparison of the laminar and turbulent velocity profile prediction of skin friction on the pressure and suction surfaces are shown in Figure 6.11. The profiles are almost identical. Unfortunately there was no data or accepted solution to compare the prediction with, but it agrees with the generally expected results: about 50% of the suction surface is essentially covered by transitional flow, i.e. the value of intermittency is greater than zero. The pressure surface is completely laminar. Figure 6.12 shows a plot of the intermittency distribution for the suction surface. Prediction of the start of transition using either a laminar or turbulent analysis is almost identical, Figure 6.13.

It should be noted that on the pressure surface a separation point was predicted. This is unlikely to have occurred in practice because of efficient blade design, and according to White (1991), Thwaites method could be as much as 15% in error close to separation. Bearing this in mind, it was decided to limit the pressure gradient parameter, m to -0.089, when separation was predicted, and continue the calculation, assuming the flow was still attached. This was thought to be a more

accurate representation than to believe that the flow had separated. In fact some trials were done where the flow was made turbulent at this separation point, and further downstream the momentum thickness Reynolds number fell well below its value for the start of transition indicted by the Abu-Ghannam and Shaw correlation. This would suggest that the flow had perhaps relaminarized, or at least did not undergo transition to turbulence.

The overall running time for a transitional analysis using a laminar free stream velocity distribution was comparable, in computational cost, to a laminar non-frictional analysis i.e. about 45 minutes (486 DX4 133). This represents an enormous saving in computer time (the k - ε non-frictional analysis, restarting from a solved laminar flow field, alone took approximately 90 minutes) and convergence problems associated with Lam-Bremhorst low Reynolds number turbulence analysis or a large eddy simulation due to the large number and relatively small size of the computational cells. Both these analysis techniques are readily available in PHOENICS.

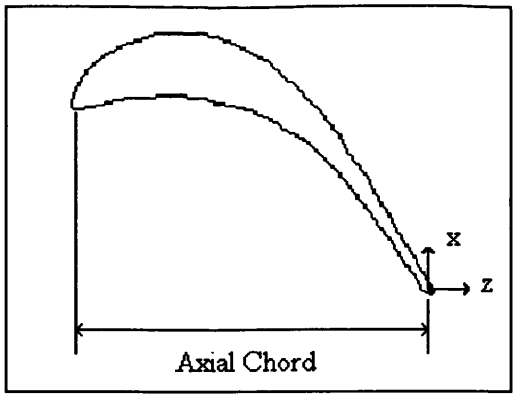

Figure 6.1: Blade Co-ordinate System

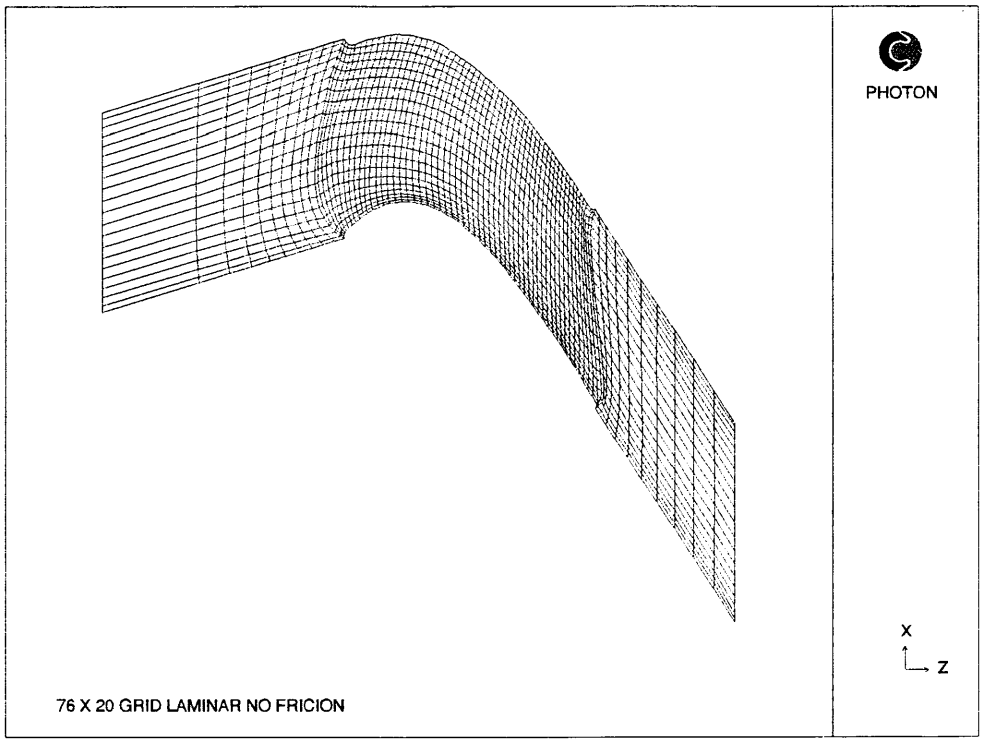

Figure 6.2: Computational Grid

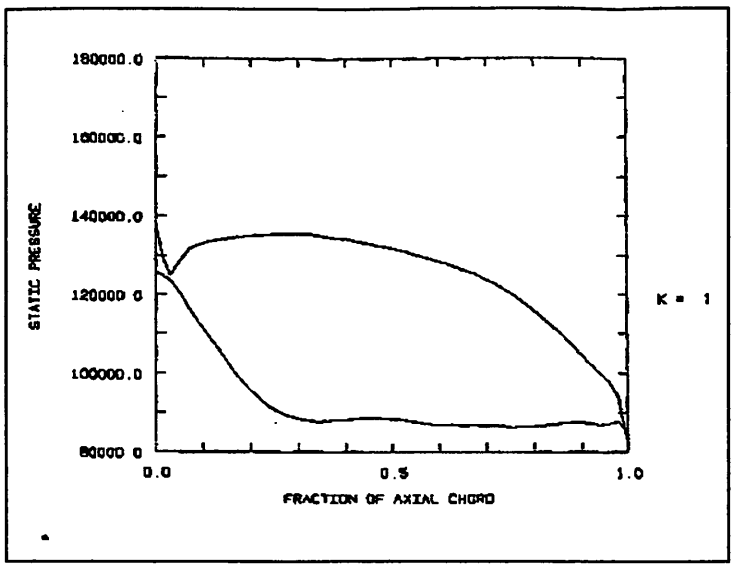

Figure 6.3: Surface Pressure Distribution (Courtesy European Gas Turbines Ltd)

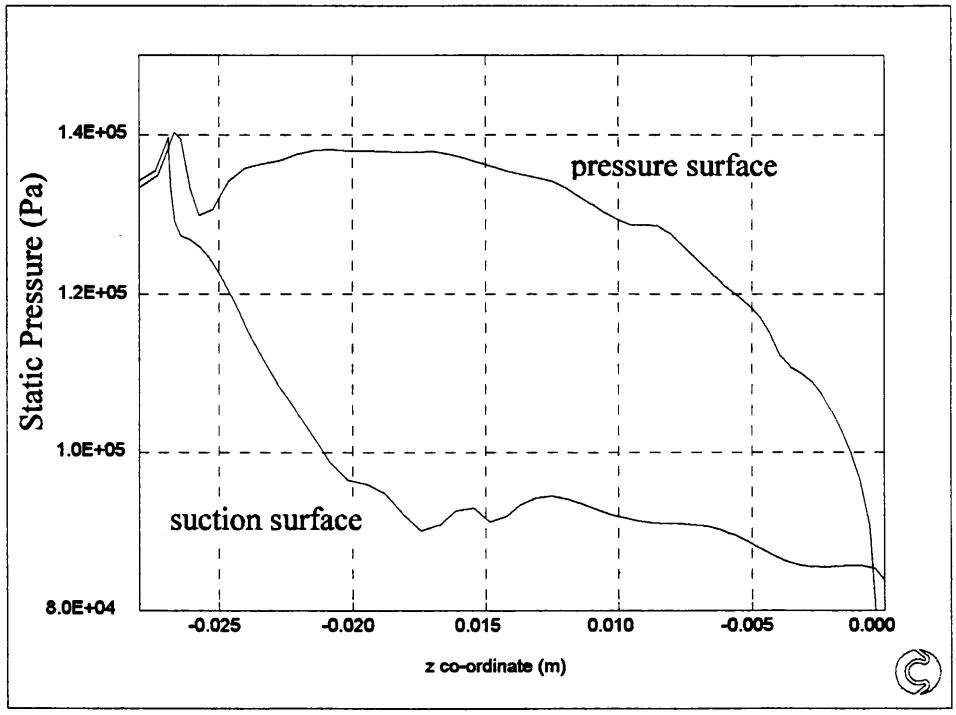

Figure 6.4: Surface Pressure Distribution (PHOENICS Solution)

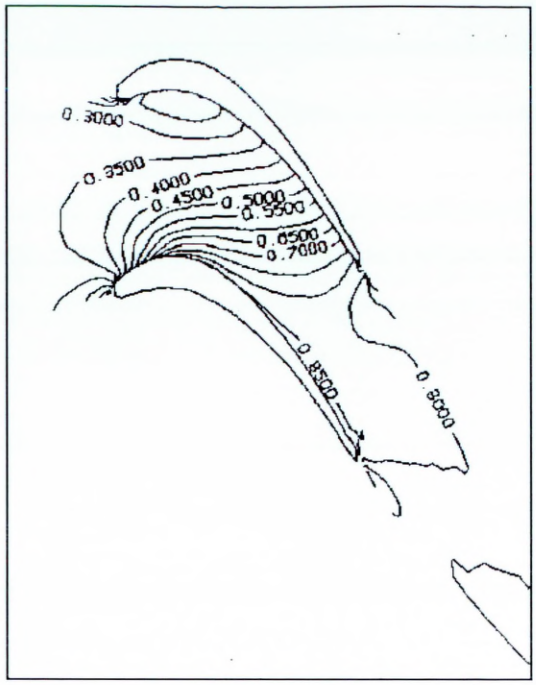

Figure 6.5: Mach Number Distribution (Courtesy European Gas Turbines Ltd)

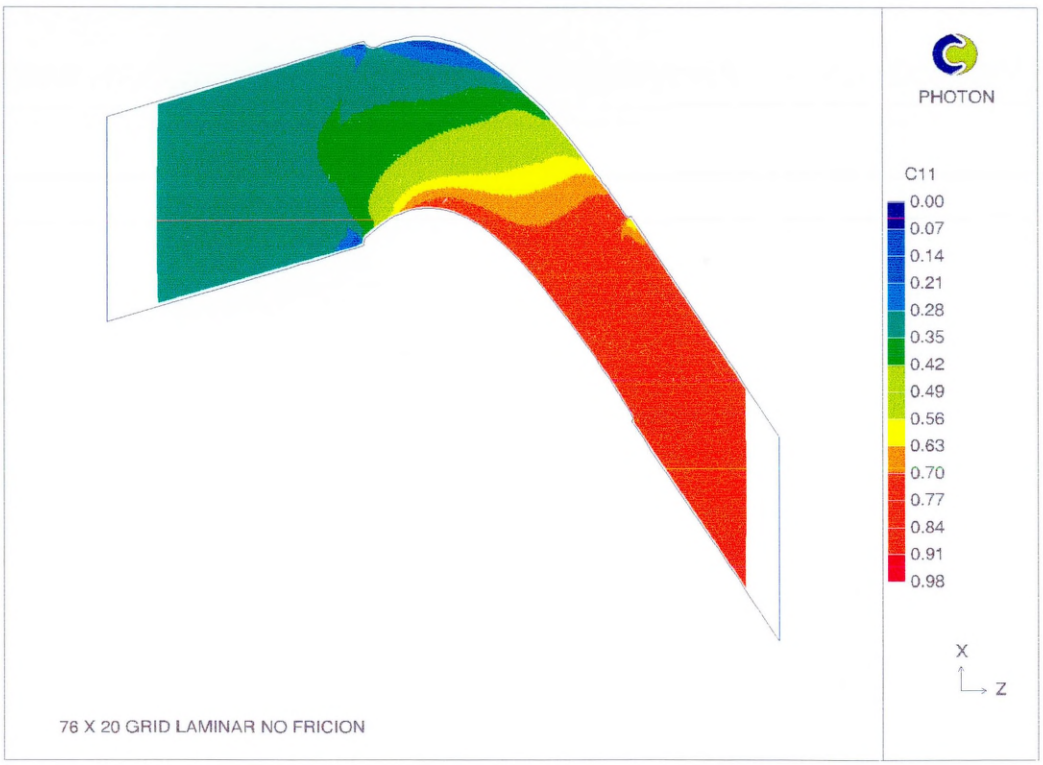

Figure 6.6: Mach Number Distribution (PHOENICS Solution)

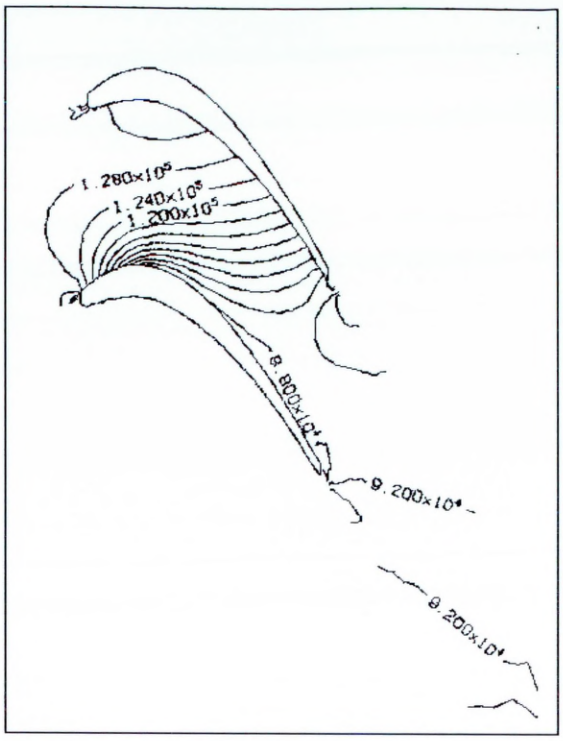

Figure 6.7: Static Pressure Distribution **(Courtesy European Gas Turbines Ltd)**

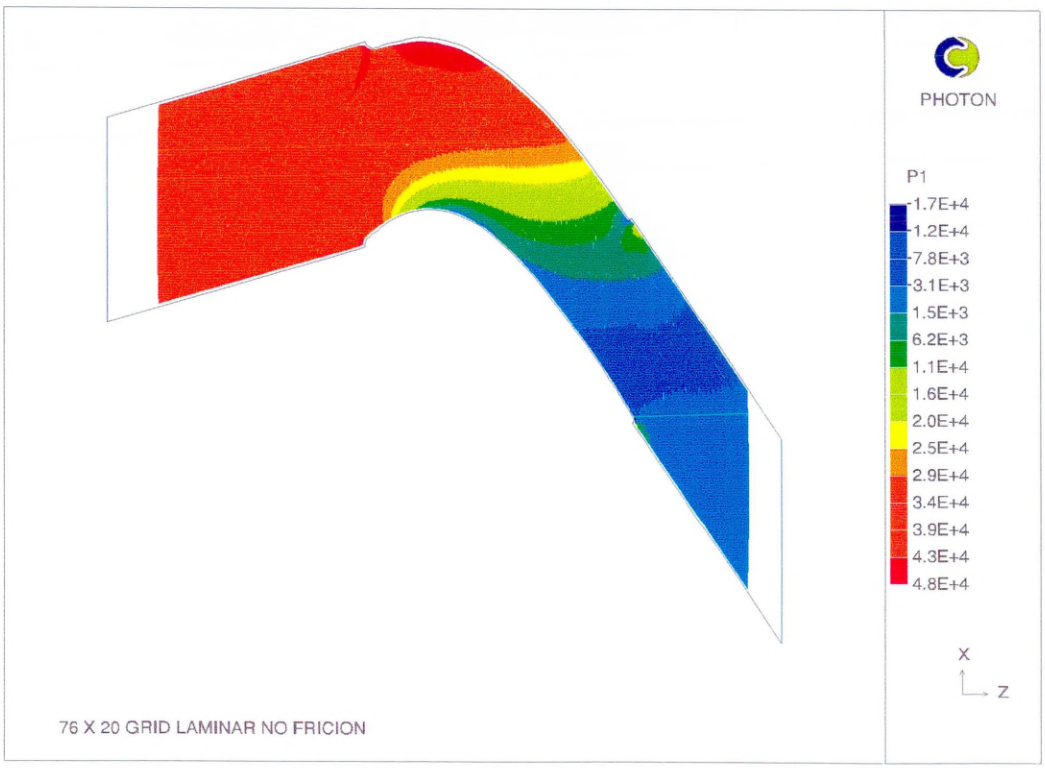

Figure 6.8: Static Pressure Plot (Relative to 92176 Pa) **(PHOENICS Solution)**

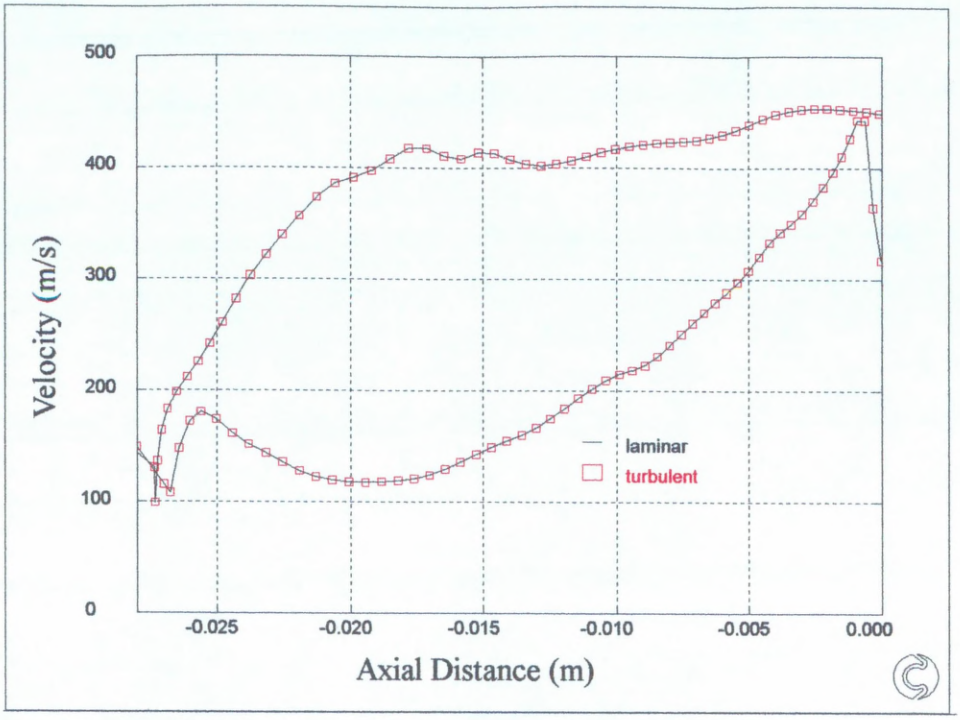

Figure 6.9: Blade Non-Friction Free Stream Velocity Profile

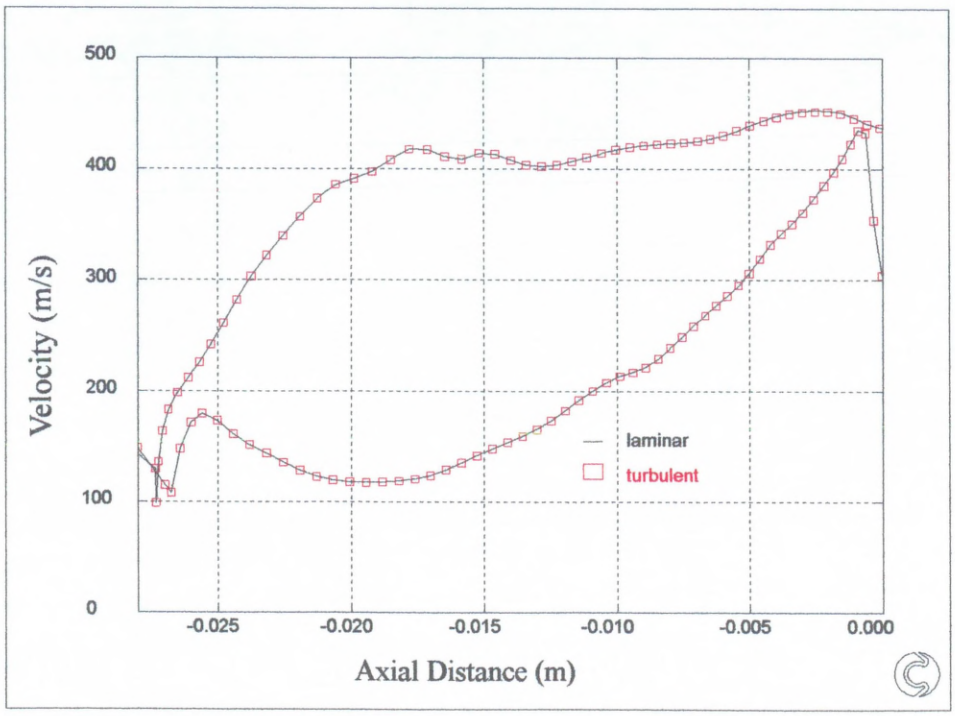

Figure 6.10: Blade Friction Free Stream Velocity Profile

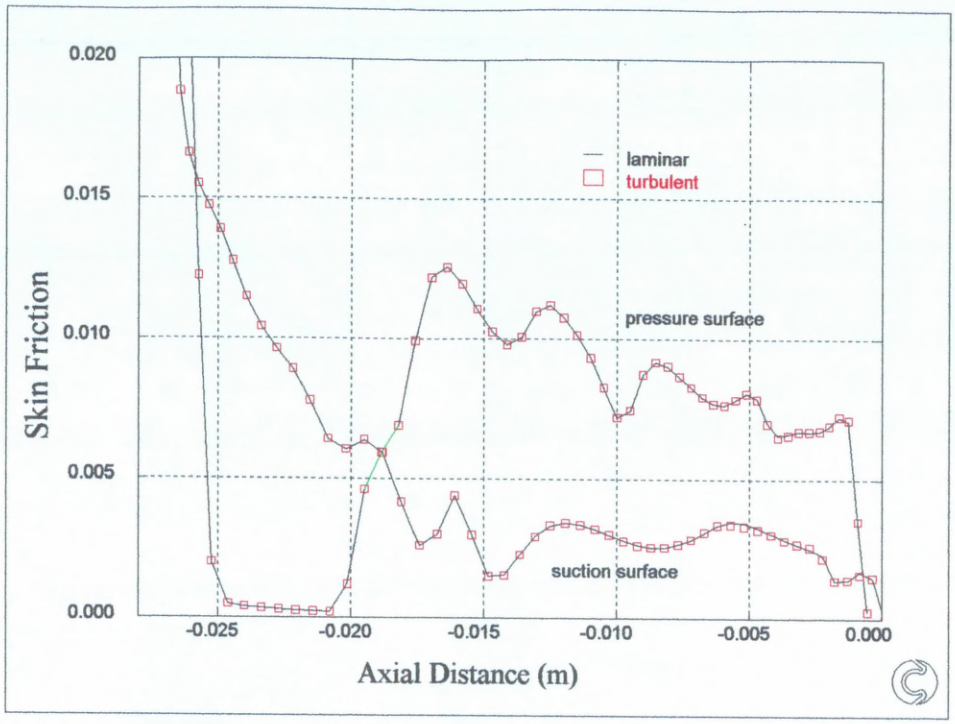

Figure 6.11: Skin Friction Prediction

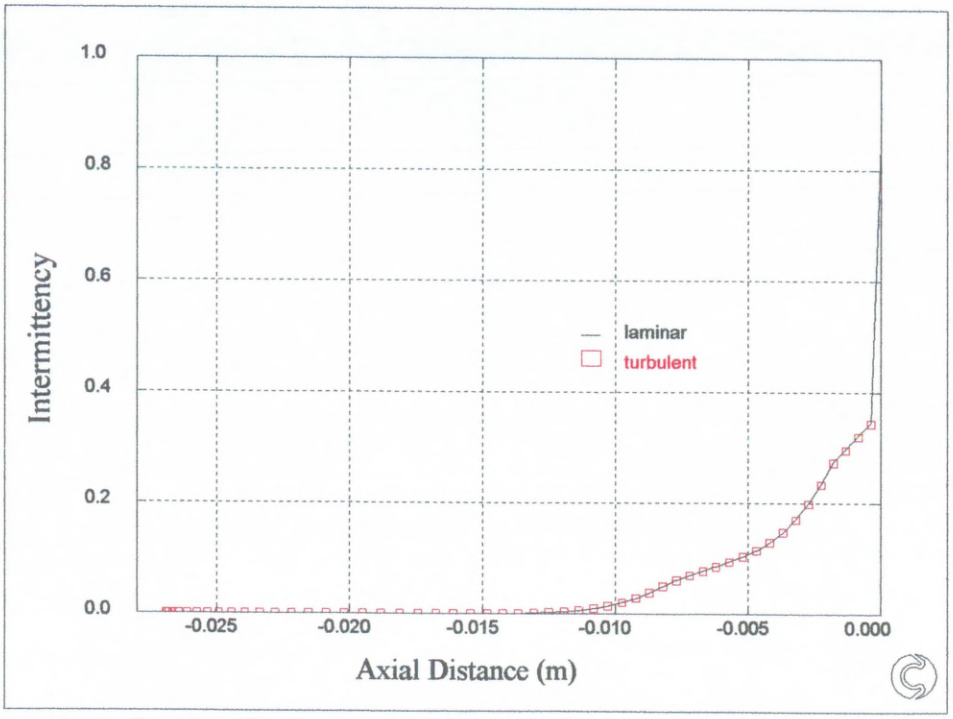

Figure 6.12: Suction Surface Intermittency Distribution

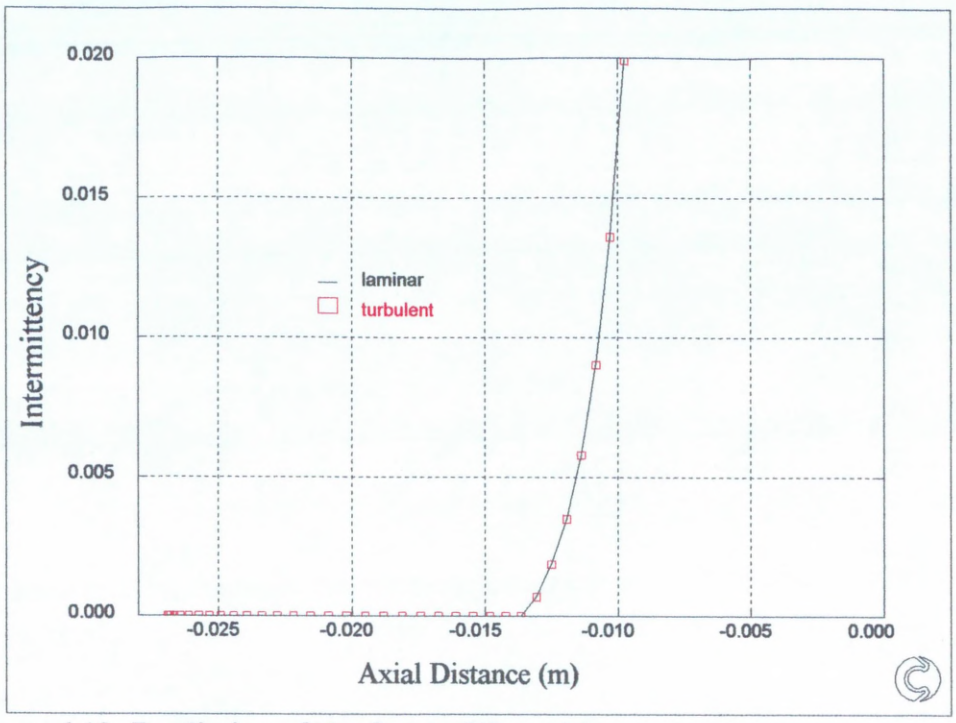

Figure 6.13: Prediction of the Start of Transition

7. Modes of Transition

7.1 Natural Transition

Schlichting (1979) describes natural transition as having several major stages. Upstream of the start of transition there is a critical momentum thickness Reynolds number where the laminar boundary layer becomes receptive to small disturbances which develop into an instability which forms two dimensional Tollmien-Schlichting waves. The infinitesimal disturbances are amplified to a point where three dimensional instabilities grow and develop into loop vortices with large fluctuations. These fluctuating fragments of the flow finally develop into turbulent spots, which will stretch then grow and convect downstream within the laminar boundary layer to combine into a fully turbulent boundary layer. The critical point can be found by solving the stability equations, Orr (1907), Sommerfeld (1908), but this can lead to complex time consuming calculations. Arnal (1984) reports that for practical applications where the momentum thickness Reynolds number (R_θ) is calculated, it is possible to compare it to a local "fictitious" momentum thickness Reynolds number ($R_{\theta f}$), such that if $R_\theta < R_{\theta f}$ then the flow is locally stable. If $R_\theta > R_{\theta f}$ then the flow is locally unstable. Arnal (1984) reports that the critical momentum thickness Reynolds number depends only on local shape factor. An approximate representation of the stability calculations is the following:-

$$R_{\theta f} = \exp\left[\frac{32}{H} - 14.8\right] \tag{7.1}$$

7.2 By-pass Transition

Arnal (1984) describes an alternative model of transition in accelerating flows where the laminar boundary layer remains well below the stability limit i.e. the momentum thickness Reynolds number never reaches the fictitious critical Reynolds number, but transition still occurs. The linear stability mechanism must therefore be completely "by-passed" for these high turbulence level flows. This is also confirmed by Blair (1990) who found that no Tollmien-Schlichting waves were produced in his measured favourable pressure gradient flows. Mayle (1991) also reports that for high free stream turbulence levels, the first and possibly second stages of the natural transition process are bypassed. This would suggest therefore that turbulent spots can be produced within the laminar boundary layer directly from the influence of the free stream disturbances.

8. New Method

It has been shown previously, that the use of correlations for the start of transition and transition length, give rapid solutions to transitional type flows, but the appropriate definition of turbulence intensity and pressure gradient parameter, m, are somewhat ambiguous. Most researchers quote the turbulence intensity in their correlations, but they do not state where the intensity was measured. As turbulence intensity will generally decay as the flow moves downstream, this was proven to be a limiting factor as the start of transition can be moved around to any arbitrary starting position depending on the value chosen for the free stream turbulence intensity.

A new method has been developed and programmed into PHOENICS in a similar manner to the integral methods in Chapter 3 i.e. the boundary layer was represented as a sink of momentum. The correlations used for transition length were attributed to Fraser, Higazy and Milne (1994). The method predicted the start of transition, using no ambiguous boundary conditions and has been shown to predict the start of transition well with Rolls-Royce flows T3A, T3A-, T3B, T3C1, T3C2 and T3C5. The method was shown to be quite sensitive to step size (cell density) in the axial direction and to the accuracy of the solution of equations (8.4) and (8.5) which follow.

8.1 Derivation of the Reduced Form of the Turbulent Energy Equations

The turbulent energy equations for kinetic energy and its dissipation rate can be formulated by multiplying the Navier-Stokes equations by the appropriate

fluctuating velocities for each cartesian direction. The derivation is quite tedious and is not generally given in any of the major textbooks. After some manipulation however the equations reduce, for two-dimensional flows, to the frequently quoted forms:-

$$\rho\overline{w}\frac{\partial k}{\partial z}+\rho\overline{u}\frac{\partial k}{\partial x}=\frac{\partial}{\partial x}\left[\left(\mu+\frac{\mu_t}{\sigma_k}\right)\frac{\partial k}{\partial x}\right]+\mu_t\left(\frac{\partial\overline{w}}{\partial x}\right)^2-\rho\varepsilon \tag{8.1}$$

$$\rho\overline{w}\frac{\partial \varepsilon}{\partial z}+\rho\overline{u}\frac{\partial \varepsilon}{\partial x}=\frac{\partial}{\partial x}\left[\left(\mu+\frac{\mu_t}{\sigma_\varepsilon}\right)\frac{\partial \varepsilon}{\partial x}\right]+C_1\mu_t\left(\frac{\partial\overline{w}}{\partial x}\right)^2\frac{\varepsilon}{k}-C_2\rho\frac{\varepsilon^2}{k} \tag{8.2}$$

Where k is the turbulent kinetic energy, ε the energy dissipation rate and μ_t is the turbulent viscosity i.e.

$$\mu_t=\rho C_\mu C_D\frac{k^2}{\varepsilon} \tag{8.3}$$

By estimating suitable integrated average values across the boundary layer it is possible to further reduce equations (8.1) and (8.2) to:-

$$\frac{d\hat{k}}{dz}=\hat{k}\left[\frac{a\tau_0}{W_\infty\mu}-\frac{1}{W_\infty}\frac{dW_\infty}{dz}-\frac{1}{\delta}\frac{d\delta}{dz}\right]-2.86\frac{\bar{\varepsilon}}{W_\infty} \tag{8.4}$$

$$\frac{d\bar{\varepsilon}}{dz}=\bar{\varepsilon}\left[\frac{1.04a\tau_0}{W_\infty\mu}-\frac{1}{W_\infty}\frac{dW_\infty}{dz}-\frac{1}{\delta}\frac{d\delta}{dz}\right]-\frac{5.486\,\bar{\varepsilon}^2}{W_\infty\,\hat{k}} \tag{8.5}$$

A more detailed description is given in Appendix C. By choosing a suitable starting value for turbulence intensity, equations (8.4) and (8.5) would predict the maximum kinetic energy and its dissipation rate in the boundary layer as the flow moves downstream.

8.2 Boundary Conditions

Initially it was thought that the above equations would not be valid from the leading edge of the surface because there would be a region where the laminar flow would be stable. The equations would only apply to the flow in the boundary layer in a region downstream of where the momentum thickness Reynolds number was greater than its critical value. The boundary conditions required for this method were:-

(1) the maximum value of turbulence intensity at the critical momentum thickness Reynolds number (w'/W)

(2) the integral length scale at the critical momentum thickness Reynolds number

(3) the maximum value of turbulence intensity at the start of transition

(4) a function for 'a' in the above equations, Bradshaw, et al (1967)

Examination of the data from Fraser (1978) shows that the maximum turbulence intensity in the boundary layer at the start of transition is approximately 5%. This agrees with Arnal (1984) who reports that a high turbulence intensity (5% - 6%) of external velocity has been encountered in laminar boundary layers at the start of transition.

Arnal (1984) reports that unstable wavelengths lie between 6 and 18 times the boundary layer thickness. This is confirmed by White (1991) who reports that the smallest unstable Tollmien-Schlichting wavelength is approximately equal to 6 times the boundary layer thickness. The smallest wavelength was chosen to be the integral length scale.

In equations 8.1, 8.2, 8.3, 8.4 and 8.5 there appear the constants C_1, C_2, $C_\mu C_D$ and

'a'. Various workers have proposed values for these constants based on well established experiments including the decay of turbulence intensity behind a grid and from measurement in fully developed turbulent boundary layer flows. The following values are often quoted:

$$C_1 = 1.45 \qquad C_2, = 1.92 \qquad C_\mu C_D = 0.09 \qquad a = 0.3$$

The parameter 'a', is defined as the ratio of the major Reynolds stress, $-u'w'$, to the turbulent kinetic energy, k, i.e.

$$a = \frac{-u'w'}{k} \tag{8.6}$$

The particular value of a = 0.3 strictly applies to the log-law region of a fully developed turbulent boundary layer. Closer to the extremities of the boundary layer the value of 'a' decreases. It would be expected, therefore that in a laminar boundary layer subject to fluctuations induced by free stream turbulence level, that the value of 'a' would be considerably less than 0.3. To evaluate the range of representative magnitudes for 'a', the behaviour of transition in zero pressure gradient flows was studied. Transition in a zero pressure gradient flow is adequately correlated by the function proposed by van Driest and Blumer (1963)

$$Re_{x,tr}^{½} = \frac{-1 + \sqrt{1 + 132{,}500\left(\frac{q}{100}\right)^2}}{39.2\left(\frac{q}{100}\right)^2} \tag{8.7}$$

A value of turbulence intensity was chosen and the start of transition was determined using the above correlation. Using equations (8.4) and (8.5), a value was chosen for 'a' so that the start of transition coincided with the prediction using correlation (8.6). This procedure was repeated at different levels of

turbulence intensity, and the following quadratic was proposed as a curve fit for 'a' as a function of free stream turbulence intensity.

$$a = 0.021\left[1 - 0.3q + 1.43q^2\right] \tag{8.8}$$

The initial starting value of turbulence intensity in the boundary layer was taken to be the free stream value divided by 1000. This correlation for 'a' gave reasonable agreement using the criteria $\left(\frac{w'}{W_\infty}\right) = 5\%$ for the start of transition (Figure 8.1).

With three of the four required parameters known, it was thought that it would be possible to correlate the free stream turbulence intensity with boundary layer turbulence intensity at the critical momentum thickness Reynolds number.

This method was used to predict the start of transition using the Abu-Ghannam and Shaw (1980), zero, adverse and favourable pressure gradient flow skin friction data. The value of free stream turbulence intensity was divided by a constant and was used as the starting value of turbulence intensity at the critical momentum thickness Reynolds number. If the constant was given a value of 1320 then a good fit to the skin friction data for zero pressure gradient flows (Figure 8.2) was produced, 400 for adverse pressure gradient flows (Figure 8.3), and 400 for favourable pressure gradient flows (Figure 8.4). The variation in magnitude of the factor was considerable and at this point it was decided to try to predict the trends in the parameters; length scale, maximum turbulence intensity at the leading edge and maximum turbulence intensity at the start of transition.

A rapid and simple way to achieve this would be to use the Taguchi method. This method has a proven track record in computational fluid dynamics, Thomson and Fraser (1994), Thomson (1996).

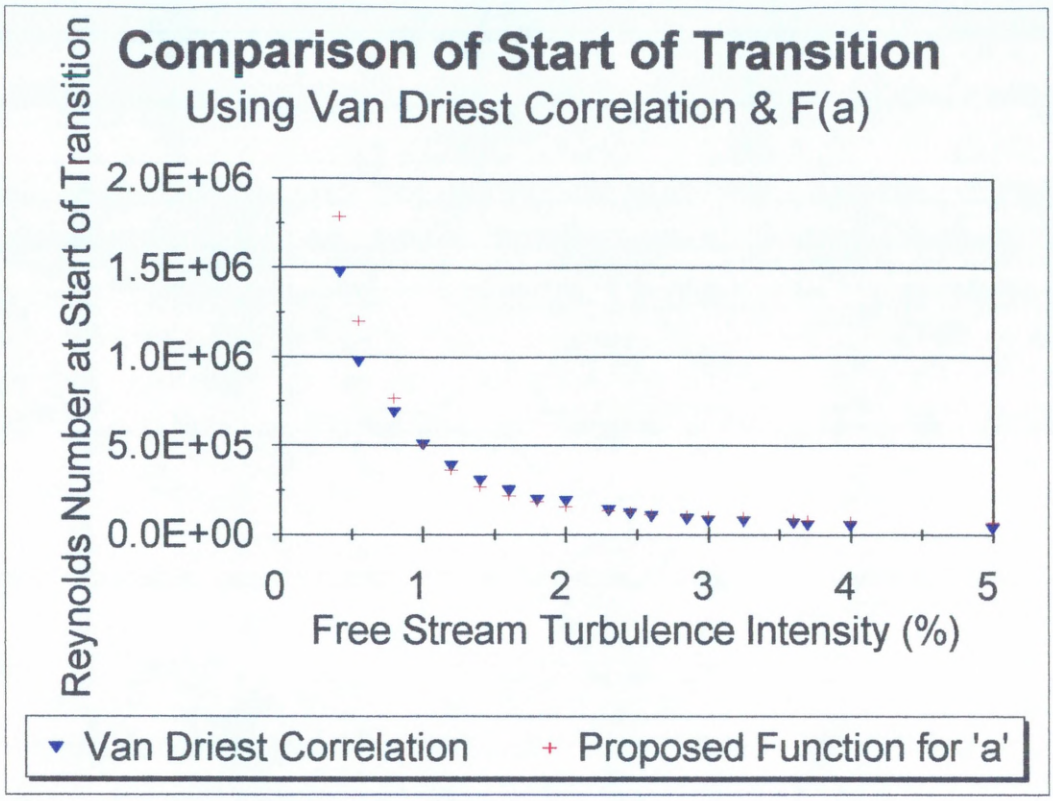

Figure 8.1: Proposed Function for 'a'

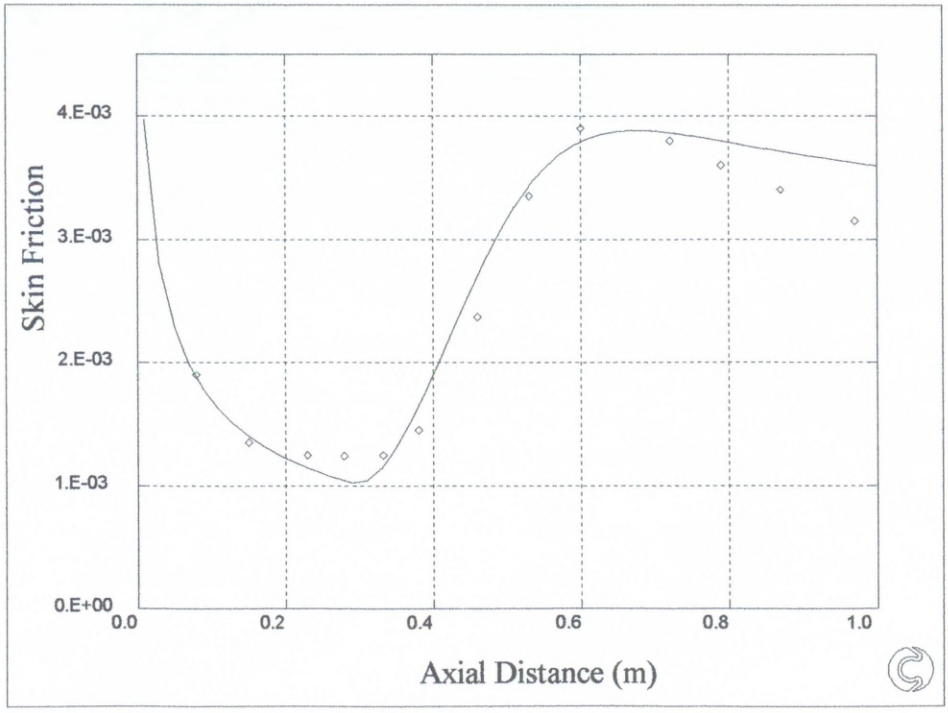

Figure 8.2: Abu-Ghannam & Shaw Zero Pressure Gradient

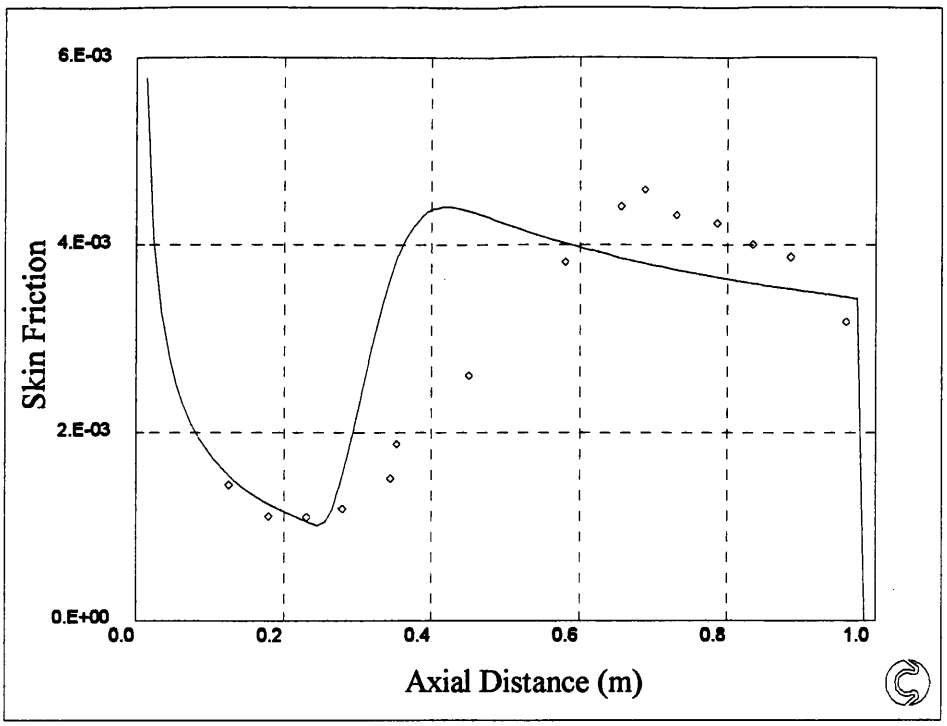

Figure 8.3: Abu-Ghannam & Shaw Adverse Pressure Gradient

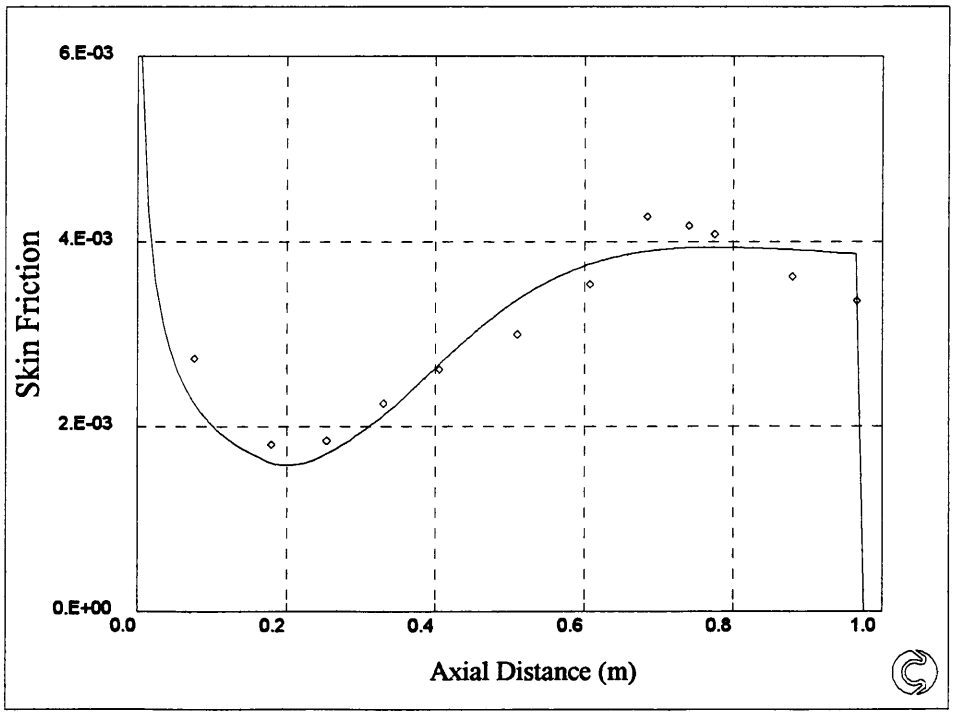

Figure 8.4: Abu-Ghannam & Shaw Favourable Pressure Gradient

9. Taguchi Analysis

9.1 Introduction

Dr. Genichi Taguchi was born in Japan in 1924 and graduated from Kiryu Technical College. He later received a Doctorate in Science from Kyushu University in 1962 and is presently honorary Professor at Nanjing Institute of Technology in the People's Republic of China.

His major contribution to science has involved the combination of engineering and statistical methods to achieve rapid improvements in costs and quality by optimizing product design and manufacturing processes. His methods were introduced into the United States in 1980-82 and later, 1986, into the United Kingdom.

9.2 Orthogonal Arrays

The use of orthogonal arrays, Taguchi and Konishi (1987) is the main tool of the Taguchi method. They express a particular combination of trials, from a full factorial experiment, that when carried out, will represent an investigation of the ***main*** effects of each factor. By adopting the use of orthogonal arrays a large number of factors can be investigated simultaneously. This is not possible using other techniques. However the major disadvantages with using orthogonal arrays is that the response variable being investigated must be measured fairly accurately, due to the fact that any inaccuracies will not be averaged out due to the small number of experiments being carried out.

The response variable was chosen to be the z (axial) distance from the critical momentum thickness Reynolds number. The four major factors that were thought

to effect the start of transition were: w/W at the critical momentum thickness Reynolds number, characteristic length at inlet, pressure gradient and w/W at the start of transition.

9.3 First Taguchi Analysis

Using a Taguchi analysis it would presumably be possible to predict the major effects of these factors assuming no interactive effects using an L_9 orthogonal array in 9 trials compared to 27 trials in the full factorial method (see Appendix D). Each factor would be assigned 3 levels, to ensure that any non-linear effects would also be captured. Turbulence intensity at the critical momentum thickness Reynolds number was taken to be the free stream value divided by a constant i.e. 500, 1000 or 1500. The conclusions from the results of the experiment were:

(1) when the divisor was increased from 500 to 1000 it had a major effect on moving the start of transition downstream, when the divisor was greater than 1000 the start of transition moved upstream but the effect is not as great

(2) as the characteristic length is increased from 1 mm to 10 mm the start of transition moves significantly upstream, greater than 10 mm, the start of transition is almost constant

(3) favourable pressure gradient produces the latest start of transition, zero pressure gradient the earliest

(4) increasing w/W_∞, from 3% to 5% moves the start of transition downstream, increasing w/W_∞, from 5% to 7% moves the start of

transition upstream

Clearly conclusion (3) is not consistent with established data, however there may be interactive effects between the factors, that were not taken into account in the experiment. It is possible to determine whether there were interactive effects present or not by plotting graphs of the factors suspected of interacting. The presence of interactions are indicated by the non-parallelism of line on the response graphs. In this case interaction was limited to two factors. According to the interactive plots, Figures D.5 - D.10, each factor interacts with at least one other factor and possibly more.

9.4 Second Taguchi Analysis

In order to try to reduce the effects of interactions, a second analysis was carried out, the geometry was kept the same as the previous analysis, but the free stream turbulence intensity and inlet velocity were kept constant. It was also thought that the range of levels of the factors, turbulence intensity at the critical momentum thickness Reynolds number and the characteristic length were unrealistic. The initial turbulence intensity was set to 1%, 2% and 2.9%, and the characteristic length was set to a function of boundary layer thickness, i.e. 6δ, 12δ and 18δ, according to Arnal (1984). Again an L_9 orthogonal array was used and the following conclusions were reached as a result of the trials:

(1) increasing the initial boundary layer turbulence intensity moved transition upstream

(2) increasing the integral characteristic length has little effect on the start of transition

(3) changing the pressure gradient from adverse to favourable to zero moved the start of transition downstream

(4) increasing the criteria for the start of transition, w'/W_∞, moved the start of transition downstream

All the conclusions reached above are based on plots of average values of the response variables and clearly conclusion (3) does not agree with accepted data. No account has been taken of any interactive effects. Examination of Figures D.15-D.20, show that interactive effects were prominent.

9.5 Third Taguchi Analysis

Considering the amount of interactions present using varying pressure gradients, it was thought that the expectation of the analysis may have been over optimistic. It was decided to choose the adverse pressure gradient mode, rejecting zero pressure gradient mode because no flow is exactly zero pressure gradient, and rejecting favourable pressure gradient mode as it may result in a strong by-pass transition mechanism, Arnal (1984). A non-interactive analysis was carried out using an L_9 orthogonal array. The analysis lead to the following conclusions:

(1) increasing the initial turbulence intensity at the critical momentum thickness Reynolds number moves the start of transition upstream

(2) increasing characteristic length from 6δ to 12δ moves start of transition slightly upstream, increasing further to 18δ moves the start of transition downstream

(3) increasing the severity of the adverse pressure gradient moves transition downstream

(4) increasing the values of the criteria for the start of transition moves the start of transition dramatically downstream

Again conclusion (3) disagrees with established data, and examination of the interactive plots, Figures D.25-D.30, show that there is a very strong interaction between pressure gradient and the criteria for the start of transition. Another explanation is that increasing the criteria for the start of transition (moves start of transition downstream) has such a large effect that it offsets the effect of increasing the adverse pressure gradient (moves start of transition upstream).

9.6 Fourth Taguchi Analysis

In the previous three analyses there have always been interactive effects present, but they have not been taken into account in the orthogonal array. In the previous analysis the pressure gradient interacted strongly with the other three factors, and therefore it was decided that this interaction was most significant. There were, of course other interactions, but in order to carry out a full interactive analysis an excess of 81 experiments would have to be carried out, and it was therefore deemed not to be practical. An interactive analysis was carried out using an L_{27} orthogonal array and the following conclusions were reached:

(1) increasing the initial turbulence intensity at the critical momentum thickness Reynolds number moves the start of transition upstream

(2) increasing characteristic length has little effect on start of transition

(3) pressure gradient has little effect on the start of transition (for the pressure gradients considered here)

(4) increasing the criteria for start of transition moves the start of transition

significantly downstream

Bearing in mind the results of the Taguchi analysis the following conditions were adopted for adverse pressure gradient flows:

(1) set the criteria (w'/W) for the start of transition to 5%

(2) set the characteristic length to 6δ

It was proposed at this juncture to try to develop a universal correlation for turbulence intensity at the critical momentum thickness Reynolds number based on free stream turbulence intensity and the pressure gradient parameter m.

10. Development of the Function for 'a'

Using the previous conditions (1) and (2), in Chapter 9 (page 9-6), for the Abu-Ghannam and Shaw (1980) zero pressure gradient flow it was found that a starting value of turbulence intensity of 0.4% at the critical momentum thickness Reynolds number gave a good fit to skin friction data. It was possible to modify this starting value by a function of pressure gradient parameter to give other starting values for other non-zero pressure gradient flows. The following correlation was developed:

$$q \text{ at } Re_{critical} = \frac{0.004}{\left(1 - 11.5\,|m|\right)^{8}} \qquad (10.1)$$

Using |m| allowed a good prediction of skin friction to the Abu-Ghannam and Shaw (1980) zero, adverse and favourable pressure gradient flows, Figures 10.1, 10.2 and 10.3 and the Rolls-Royce T3C2 flow, Figure 10.4. The start of transition was predicted late in T3C1 and T3C5 flows Figures 10.5 and 10.6.

Correlation (10.1) was used to predict the start of transition using adverse pressure gradient intermittency data from Gardiner (1987). It was found that the start of transition was not predicted well, in addition it was not consistently predicted early or late. Clearly something was wrong.

Probably the most accurate way to determine the start of transition is by looking at the intermittency data. This was not available for the Rolls-Royce T3A, T3A-, T3B or T3C flows. Gardiner (1987) had intermittency data for 23 flows comprising of 4 zero pressure gradient flows (1-4), 16 adverse pressure gradient flows (5-20) and 3 favourable pressure gradient flows (21-23). The flows had almost no decay of turbulence. It was decided to develop a correlation for the

turbulence intensity at the critical momentum thickness Reynolds number based on free stream turbulence intensity for the zero pressure gradient cases (flows 1-4). Again a value of turbulence intensity was chosen at the critical momentum thickness Reynolds number and modified until the start of transition coincided with the intermittency data.

The following correlation was proposed:-

$$q_{Recrit} = \frac{q_{freestream}^{6}}{164.4} \tag{10.2}$$

Using correlation (10.2), the start of transition was predicted well in zero pressure gradient flows 1 and 4, Figures 10.7 and 10.10, but early in flows 2 and 3, Figures 10.8 and 10.9. The correlation was used to predict the start of transition in other zero pressure gradient flows namely: Abu-Ghannam and Shaw (1980), and Rolls Royce flows T3A, T3A- and T3B. Since no intermittency data was available for these flows, comparison was made between predictions of skin friction and the experimental data. Good fits were obtained for the Abu-Ghannam and Shaw flow and the Rolls Royce T3A flow Figure 10.11 and 10.12. The start of transition was predicted early for T3A-, Figure 10.13, and late for T3B, Figure 10.14. It was concluded that the value of turbulence intensity at the critical momentum thickness Reynolds number had to be accurately prescribed. Using data from Gardiner (1987) it had been hoped to modify the zero pressure gradient correlation to predict the start of transition in adverse and favourable pressure gradient flows. However there was too much scatter of the turbulence intensity starting values and pressure gradient parameter (m) at critical momentum thickness Reynolds number to allow any meaningful correlation to be developed.

This information led to the dilemma: was the critical momentum thickness Reynolds number meaningful at this range of free stream turbulence intensities, and was there any position in the boundary layer where the flow was capable of damping out infinitesimal fluctuations. Wazzan (1979) published data on the critical displacement thickness Reynolds number versus shape factor, which can be simply curve fit by:

$$\mathrm{Log}\left(\mathrm{Re}_{\delta^*}\right) = -3.134\mathrm{H} + 11.19 \qquad (10.3)$$

According to Gardiner's data this displacement thickness Reynolds number in some pressure gradient flows was not reached until well after the start of transition.

It was therefore concluded that in the engineering type flows under consideration here, there was no region in the boundary layer that damped out turbulent fluctuations i.e. the fluctuations were present from the surface leading edge. Using data from Gardiner (1987) it was found that it was possible to fit the intermittency data in zero, adverse and favourable pressure gradient flows, by choosing a suitable value of maximum boundary layer turbulence intensity at the leading edge. This procedure was used to develop a correlation for the start of transition in zero pressure gradient flows. The following correlation was proposed:

$$q_{1e} = \frac{q_{\text{free stream}}^{5.2}}{2679} \qquad (10.4)$$

Correlation (10.4) gave a good prediction of the start of transition for Gardiner's flows 1 - 4, Figures 10.15 to 10.18 and Abu-Ghannam and Shaw (1980) flow, Figure 10.19. Prediction of the start of transition in the Rolls Royce zero pressure gradient flows T3A, T3A- and T3B however was not good, Figures 10.20, 10.21

and 10.22. No correlation could be developed for non-zero pressure gradient flows between free stream turbulence intensity and the leading edge boundary layer turbulence intensity as the boundary layer starting values required to fit the intermittency data were too randomly distributed.

It became evident at this stage that further information was required on the growth of turbulence intensity within the boundary layer.

This turbulence intensity data was in fact available for the Rolls-Royce T3A, T3A-, T3B and T3C flows. A plot of the maximum turbulence intensity at each axial station was compared with the prediction from equations (8.4) and (8.5) using the quadratic function for 'a'. The prediction of maximum turbulence intensity at axial stations downstream was not correct, and transition only occurred when the prediction locus intercepted the data from below. The function initially assumed for 'a' was patently therefore incorrect. Further investigation of the Rolls Royce turbulence intensity data, indeed showed that it was far from isotropic. In consequence therefore the predicted value of the growth of turbulence intensity within the boundary layer would be qualitative and not quantitative. As the measurements of the Rolls-Royce flows were so extensive, it was decided that a correlation for 'a' would be developed from that data.

The maximum turbulence intensity in the boundary layer at the leading edge was determined by extrapolation of the maximum boundary layer turbulence intensity data downstream. This showed that for all pressure gradient flows, within the boundary layer at the leading edge the maximum turbulence intensity was approximately the same as the turbulence intensity (based on the free stream velocity) at inlet, Figures 10.23 and 10.24.

The value of turbulence intensity for the start of transition was chosen to be the maximum value in the boundary layer at the location before the minimum value of skin friction. This value was found to be in the region of 11%-13%, based on the free stream velocity. This value is approximately twice that quoted by Fraser (1978) and Arnal (1984).

It was thought that since the maximum turbulence intensity at the boundary layer leading edge was similar to the turbulence intensity at inlet, it would be reasonable to assume that the length scales would be similar also.

Further analysis of the zero pressure gradient flows (T3A, T3A- and T3B), showed two distinct types of maximum turbulence intensity profiles. Cross referencing with the free stream velocity profiles, showed that the nominally zero pressure gradient flows, T3A and T3B were in fact slightly favourable pressure gradient flows, whilst T3A- was an adverse pressure gradient flow. This was also the case with the varying pressure gradient T3C flows, they showed two turbulence intensity profiles, one for the start of transition occurring in favourable pressure gradient and the other for the start of transition occurring in adverse pressure gradient, Figures 10.23 and 10.24.

10.1 Favourable Pressure Gradient

The shape of the turbulence intensity profiles suggested an inverse exponential rise from the leading edge. This is consistant with the e^n method (Chapter 3) and also agrees with Seiger et al (1995) who also model the effects of free stream turbulence intensity on a laminar boundary layer as an empirical exponential function. It was decided to develop a function for 'a' for the two different types of profile i.e. adverse and favourable. The parameter 'a' would take the form:-

$$a = \exp\left[f(q, l_e, m)\right] \tag{10.5}$$

Johnson (1994) proposes that a functional relationship exits in terms of free stream turbulence level and length scale between the streamwise pressure gradient and laminar boundary layer pressure fluctuations. This agrees with the above proposal.

Initial trials with the T3B flow showed that 'a' was not a constant as is found with the fully turbulent boundary layer. The parameter 'a' was required to decrease as the flow progressed downstream. For the T3B flow it was found that if 'a' was given the value:

$$a = \exp\left[\frac{-19}{q}\right] \tag{10.6}$$

Then a good approximation to skin friction data was achieved. Similarly in the T3A flow, if 'a' was given the value:

$$a = \exp\left[\frac{-8.9}{q}\right] \tag{10.7}$$

then a good fit to the skin friction data was produced. This process was repeated for flows T3C1 and T3C5. It was found that good prediction of skin friction could be achieved if the constant took the value of 13.75 and 7 respectively. A family of curves were produced which all appeared similar Figure 10.25.

The choice of the constants, 19 and 8.9 for the zero pressure gradient flows was quite critical, and can be seen to be in the ratio of approximately two. This value is almost the same ratio as the length scales at inlet i.e. T3A and T3B flows had the length scales 4 mm and 2 mm respectively. The T3A flow was given the length scale value of 1.873 mm (8.9/19 x 0.004) at inlet and was shown to still

provide a good approximation to the free stream turbulence intensity. A correlation was proposed for nominally zero (favourable) pressure gradient flows:

$$a = \exp\left[\frac{-19}{q}\frac{L_e}{0.004}\right] \tag{10.8}$$

It was possible to further modify the zero pressure gradient correlation for 'a' by a function of pressure gradient parameter, 'm' to account for favourable pressure gradient flows:-

$$a = \exp\left[\left(\frac{-19}{q}\right)\left(\frac{L_e}{0.004}\right)\left(1-5.3m^2\right)\right] \tag{10.9}$$

This above correlation gave good prediction of skin friction data for T3A, T3B, T3C1 and T3C5 (Figures 10.27, 10.31, 10.35, 10.39) flows without adversely affecting the prediction of free stream turbulence intensity, Figures 10.29.

10.2 Adverse Pressure Gradient

The same form of function for 'a' was proposed for adverse pressure gradient flows. Initially using the nominally zero pressure gradient T3A- flow, it was found that if correlation (10.8) was used, then transition was predicted far too early. By trial and error the function for 'a' that gave an excellent fit to the skin friction data was found to be:

$$a = \exp\left[\frac{-3.26}{q}\right] \tag{10.10}$$

However there was one imposed condition, in that 'a' was not allowed to fall below a limiting value of 0.008 as the flow moved downstream. The limiting value was found by trial and error. Properties for the T3A- flow are shown in Figures 10.42-10.45.

One of the drawbacks with the Rolls-Royce data was that for the flows in which the start of transition occurred in adverse pressure gradient, T3C3 and T3C4, separation was predicted by Thwaites (1949) method before the start of transition occurred. Thus the only adverse pressure gradient test case that was suitable was T3C2. The function for 'a' that was found to give a relatively good fit to the skin friction data was:

$$a = \exp\left[\frac{-6.85}{q}\right] \tag{10.11}$$

provided that 'a' was restricted to values greater than 0.009. Properties for the T3C2 flow are shown in Figures 10.46-10.49.

Grid independency tests showed that a computation cell distribution in the axial direction of 1000 cells per metre was adequate. Solution of equations (8.4) and (8.5) required the use of the 6th order Runge-Kutta method for consistently accurate results.

It was thought that it would be possible to use the correlation for 'a' in favourable pressure gradient flows and enforce a limiting value on 'a' to successfully predict the start of transition. Using different limiting values for 'a', it was found that the start of transition was always predicted early, i.e. the rise of the predicted maximum turbulence intensity in the boundary layer was too great.

Prediction of the start of transition in other flows was not attempted as no meaningful results would be achieved. There were too many parameters that were not measured e.g. free stream turbulence intensity distribution and hence the length scale, and the maximum turbulence intensity in the boundary layer at the start of transition.

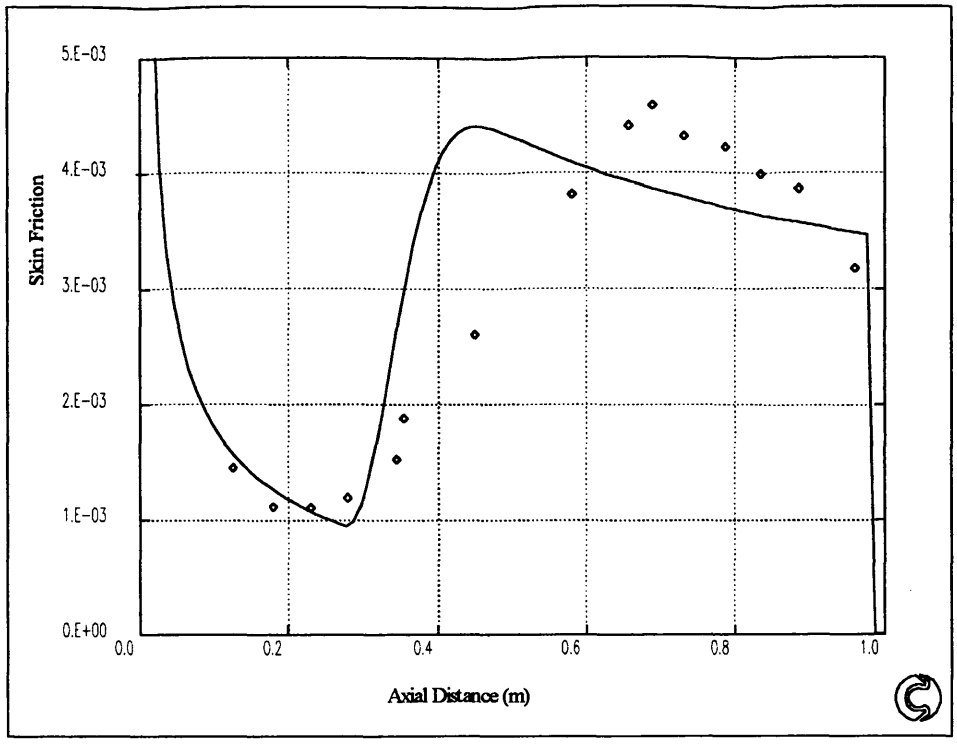

Figure 10.1: Abu-Ghannam & Shaw 1st Adverse

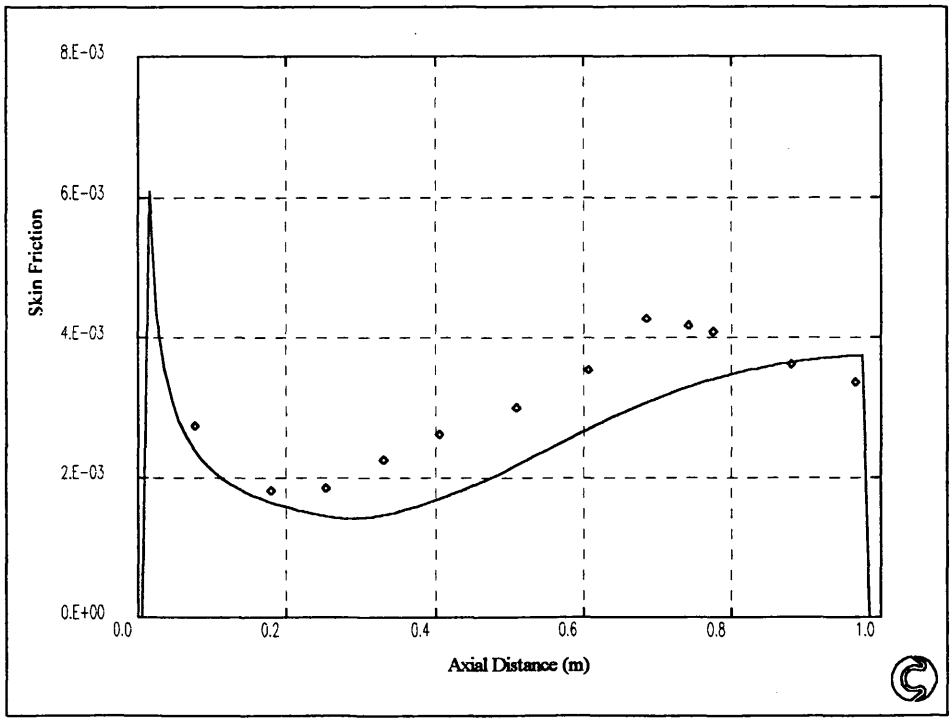

Figure 10.2: Abu-Ghannam & Shaw 1st Favourable

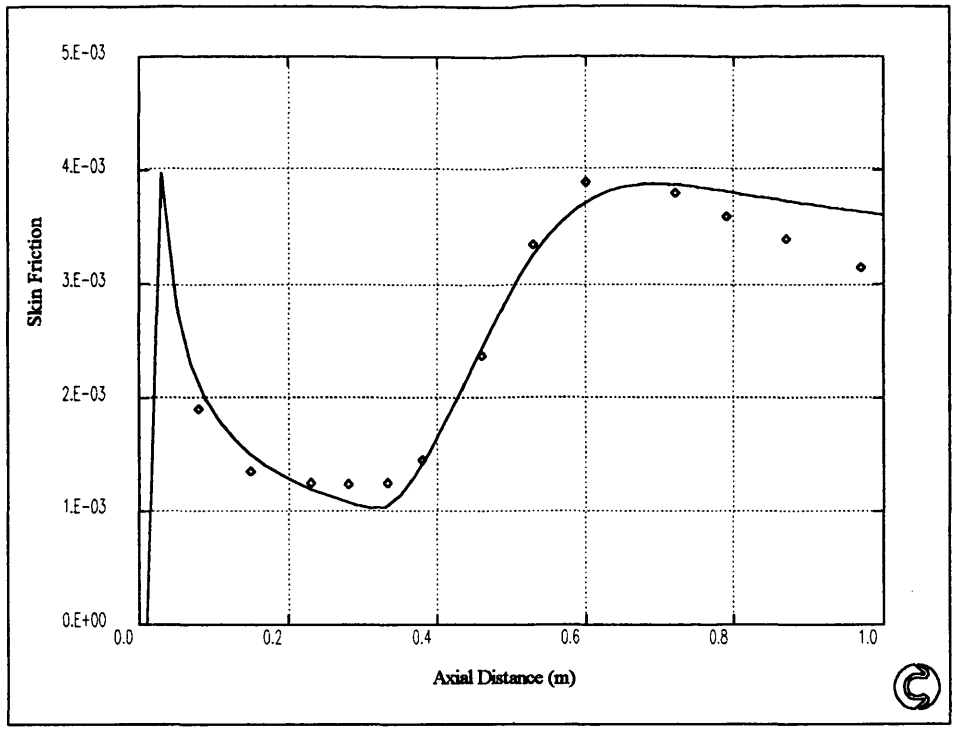

Figure 10.3: Abu-Ghannam & Shaw Zero Pressure Gradient Flow

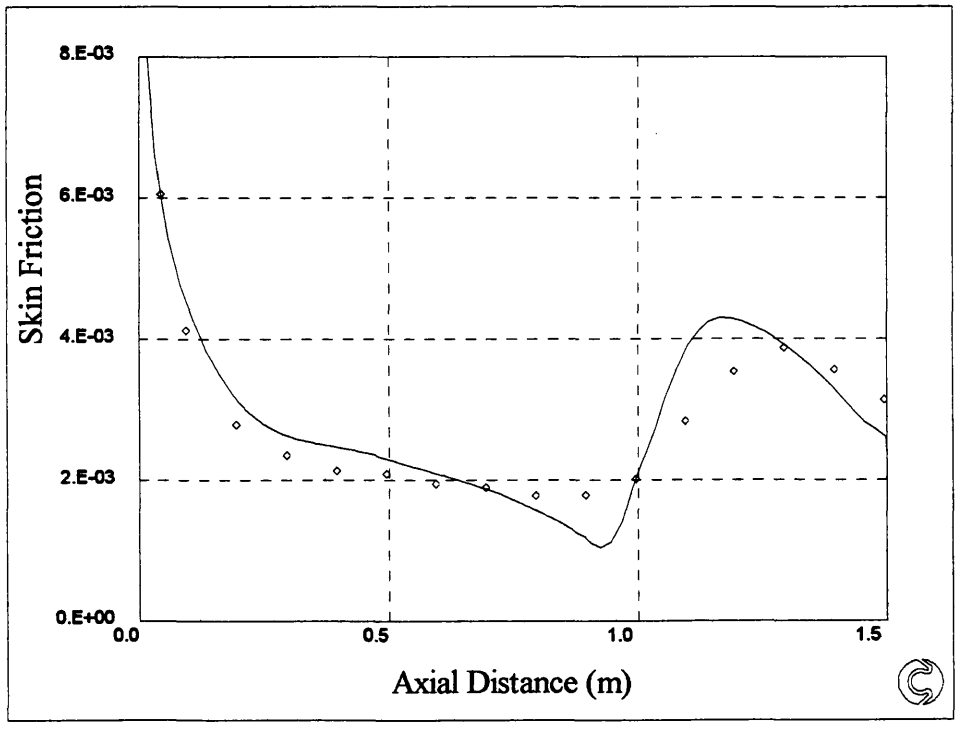

Figure 10.4: T3C2 Flow Skin Friction

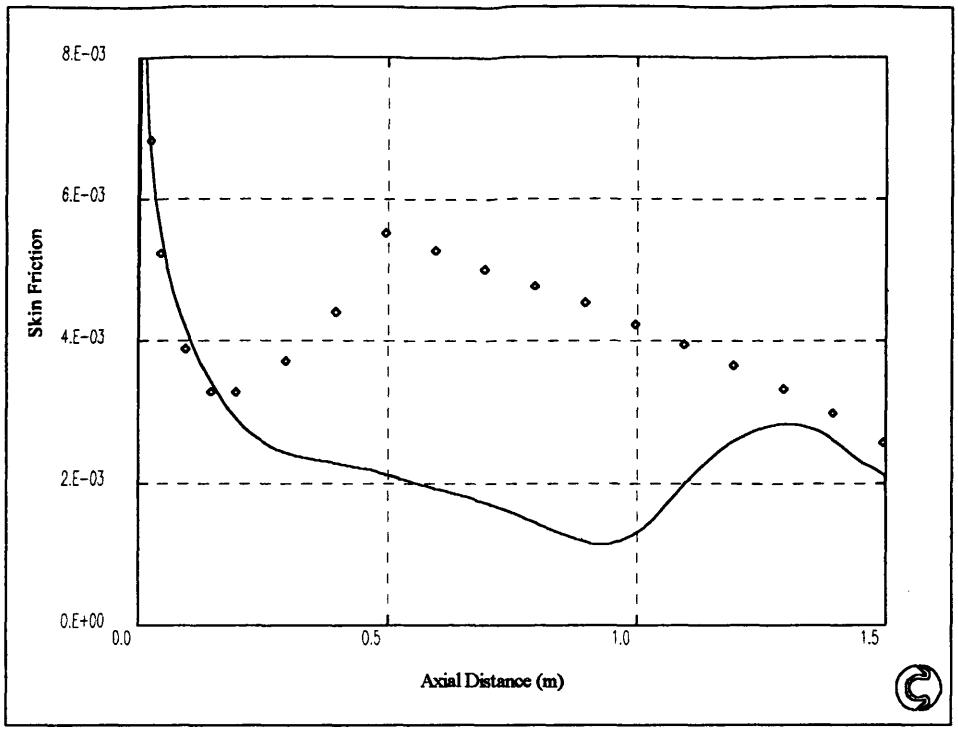

Figure 10.5: T3C1 Flow Skin Friction

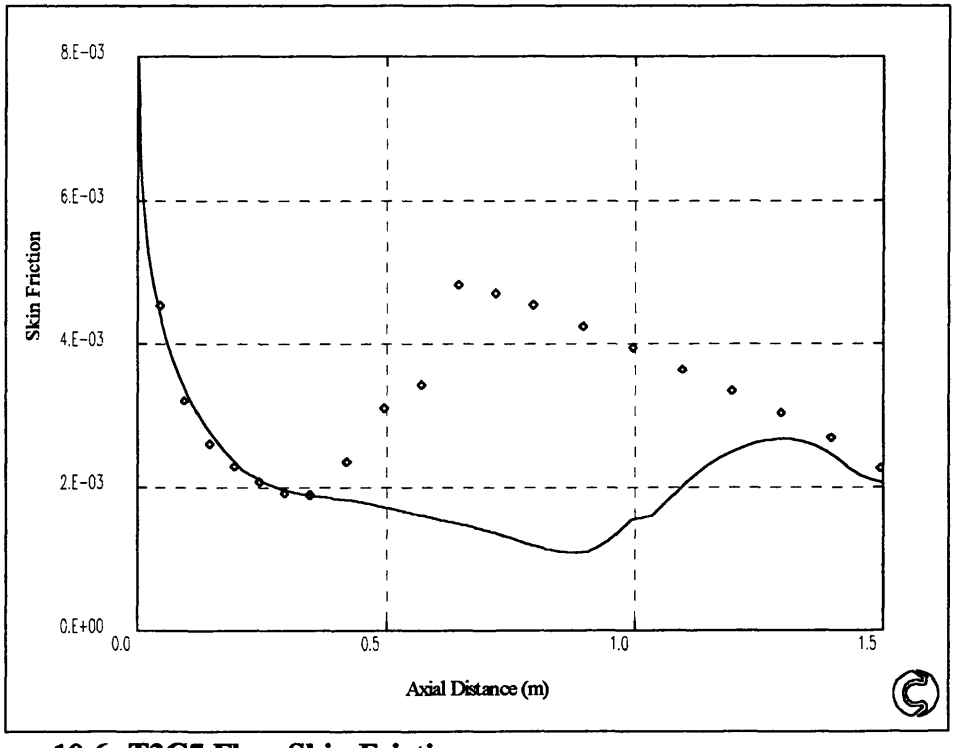

Figure 10.6: T3C5 Flow Skin Friction

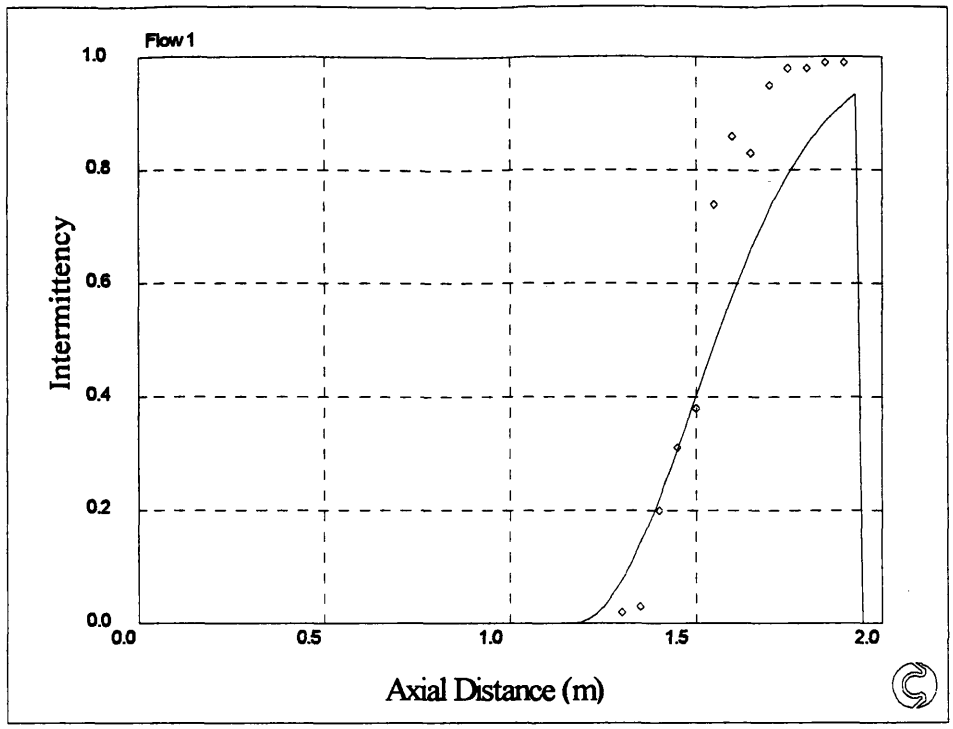

Figure 10.7: Intermittency Data From Gardiner

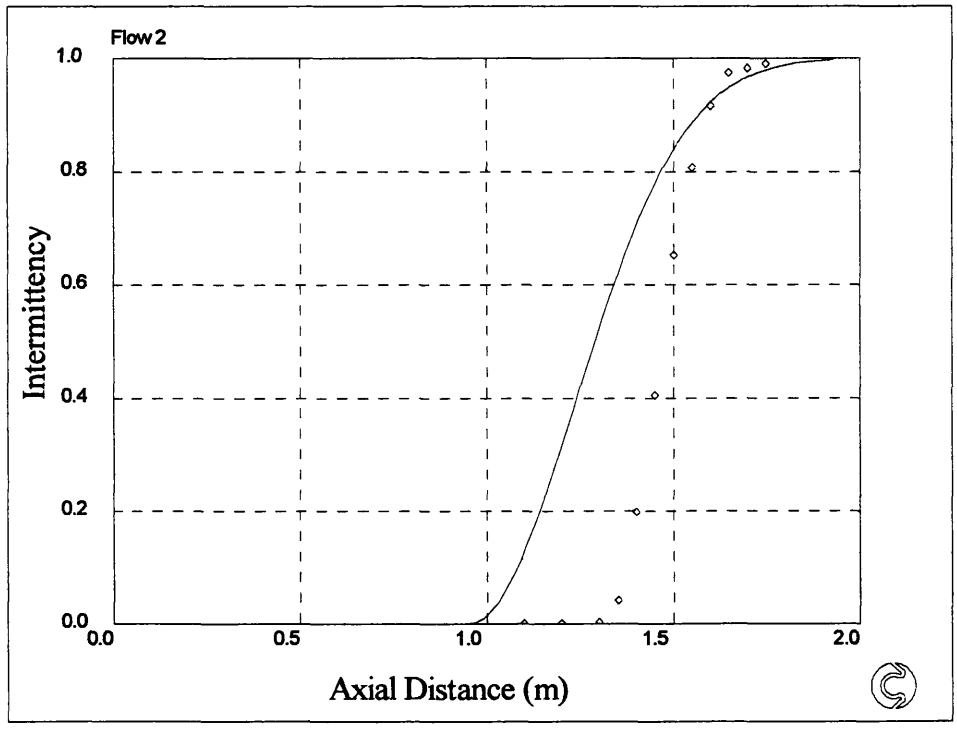

Figure 10.8: Intermittency Data From Gardiner

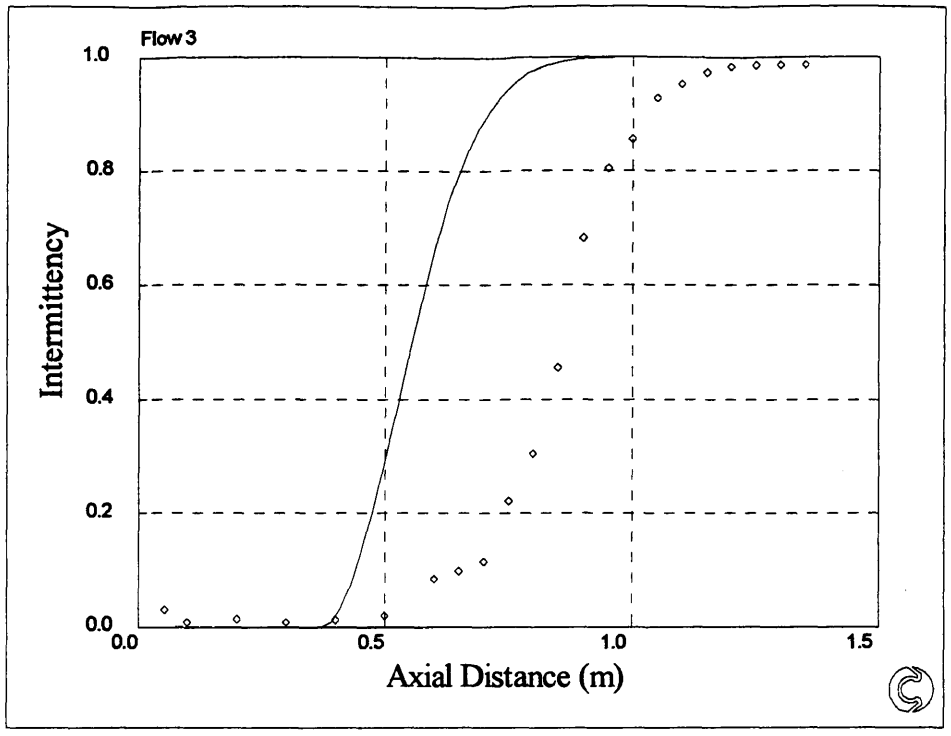

Figure 10.9: Intermittency Data From Gardiner

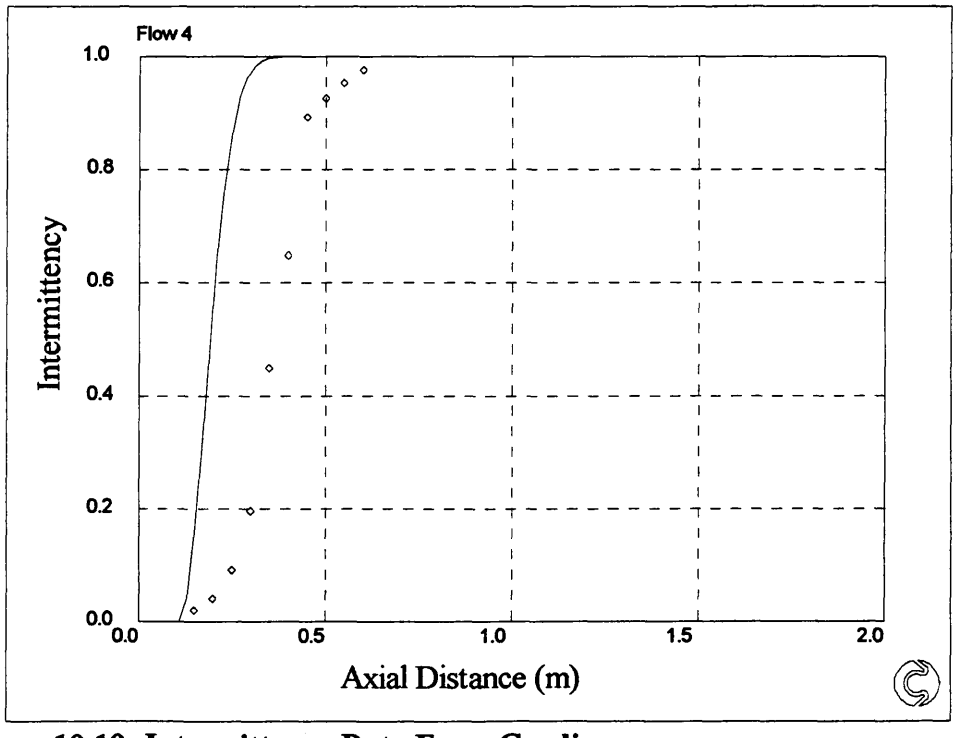

Figure 10.10: Intermittency Data From Gardiner

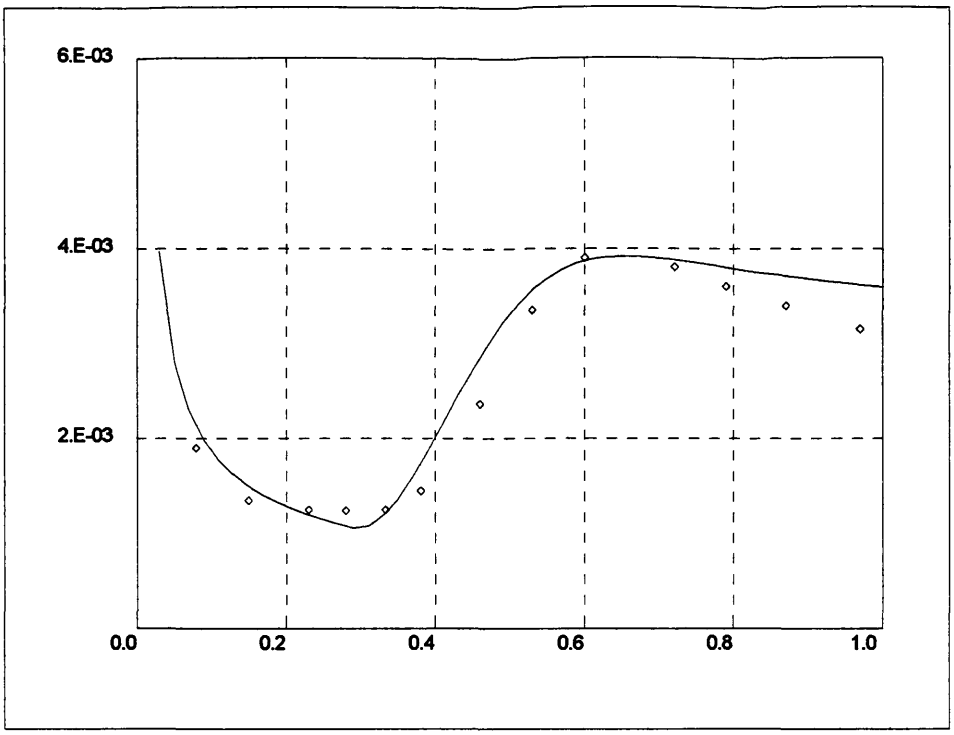

Figure 10.11: Abu-Ghannam & Shaw Zero Pressure Gradient

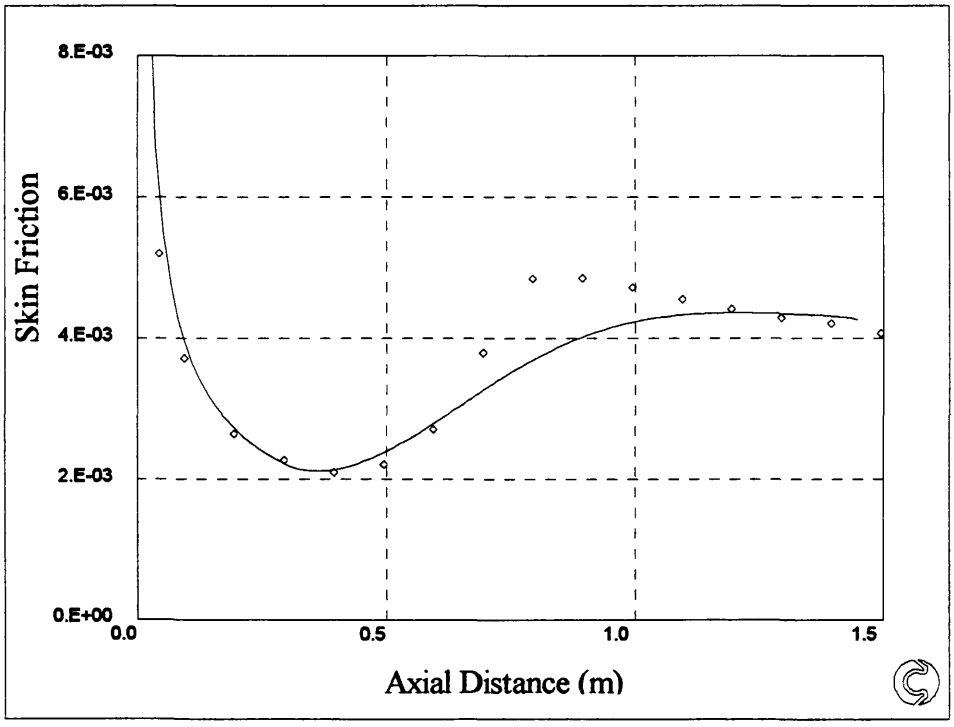

Figure 10.12: T3A Zero Pressure Gradient Flow

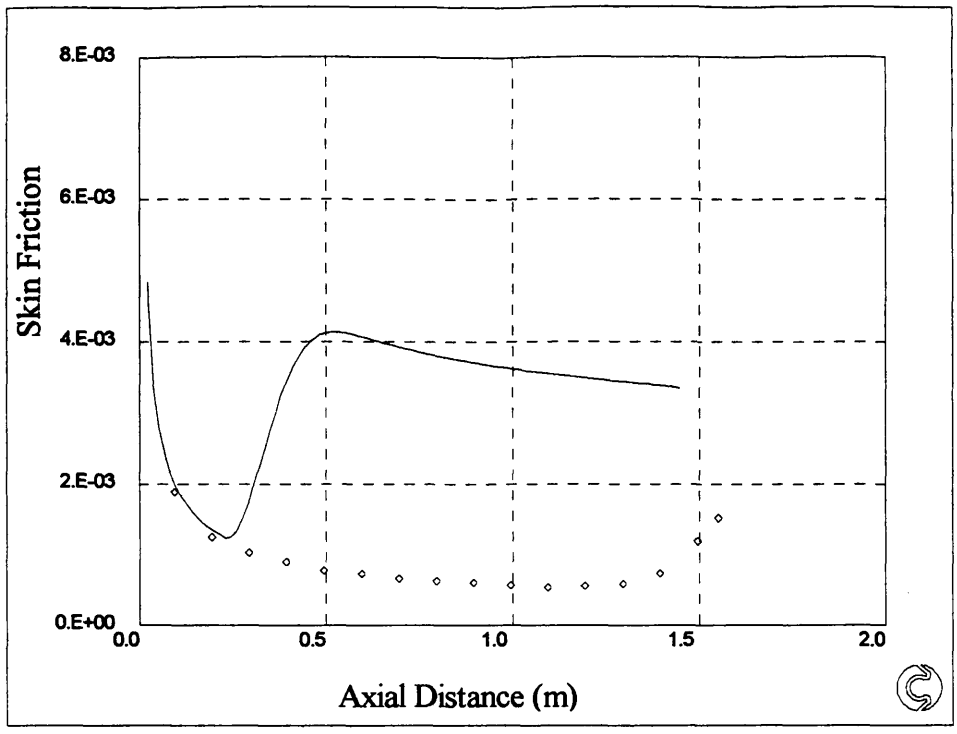

Figure 10.13: T3A- Zero Pressure Gradient Flow

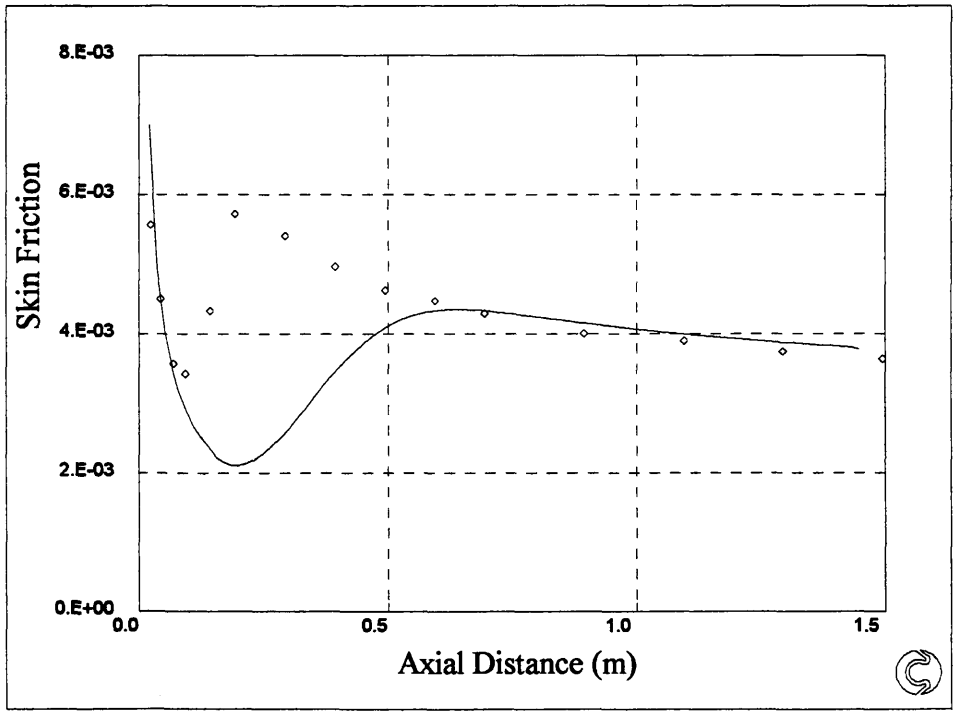

Figure 10.14: T3B Zero Pressure Gradient Flow

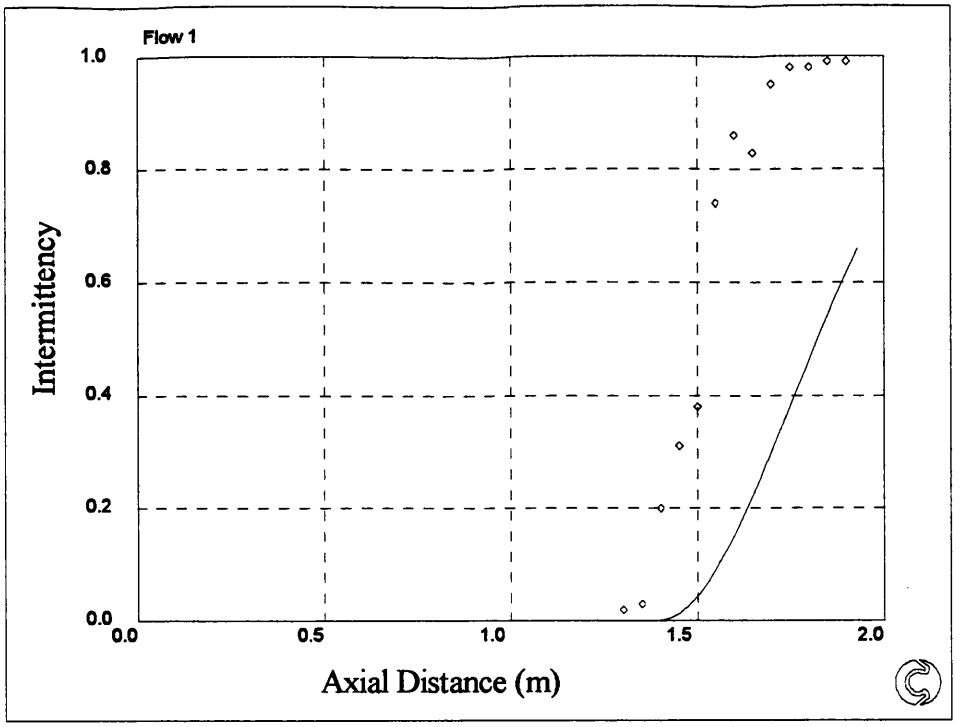

Figure 10.15: Intermittency Data From Gardiner

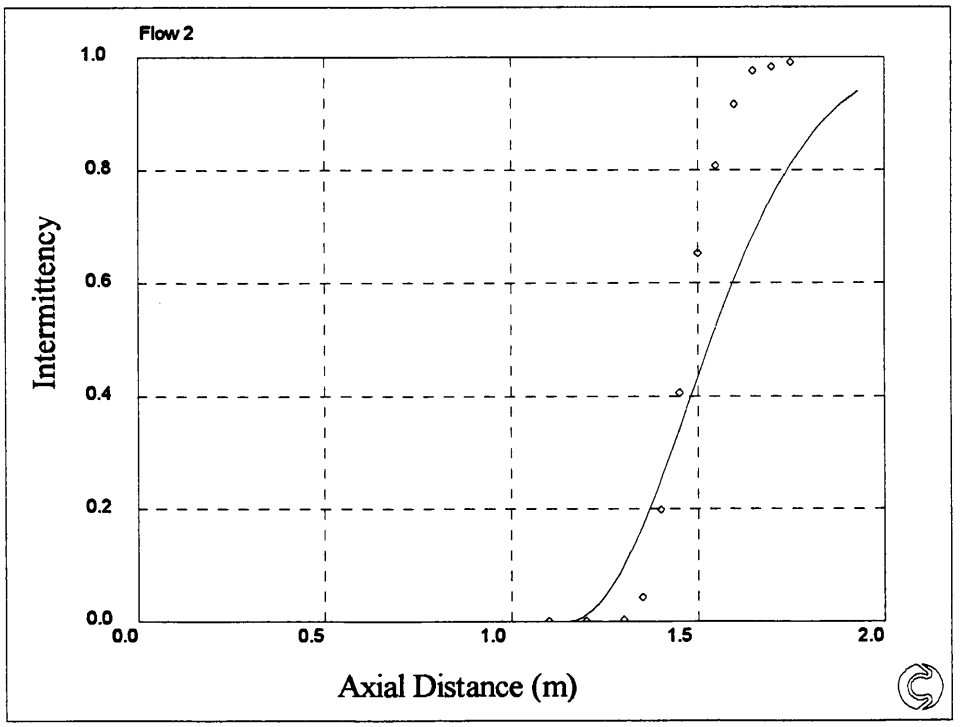

Figure 10.16: Intermittency Data From Gardiner

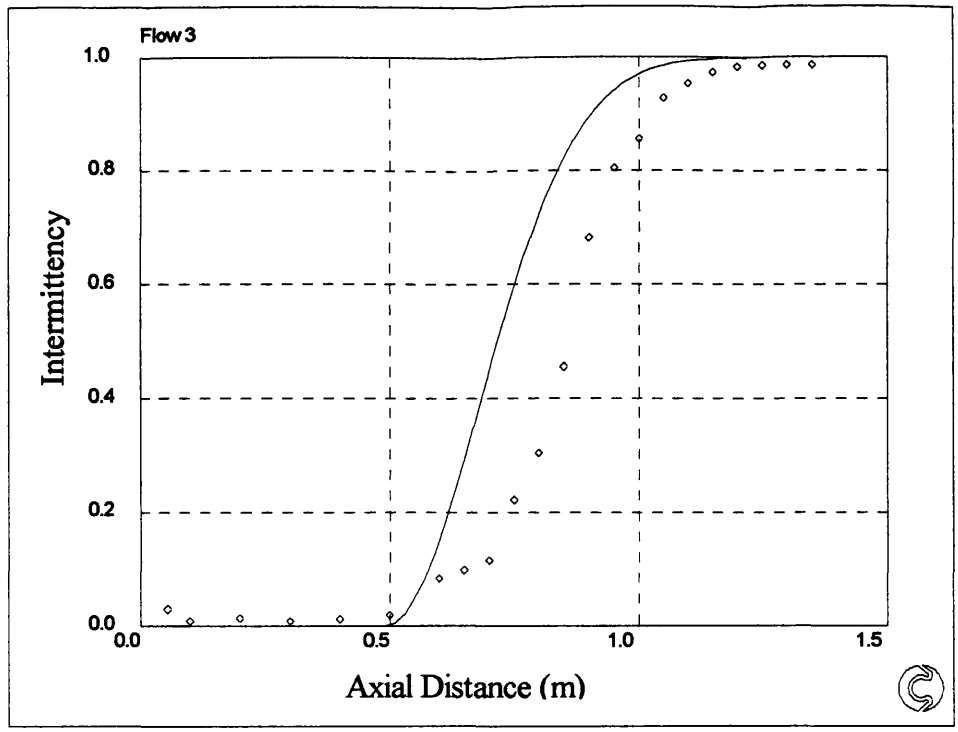

Figure 10.17: Intermittency Data From Gardiner

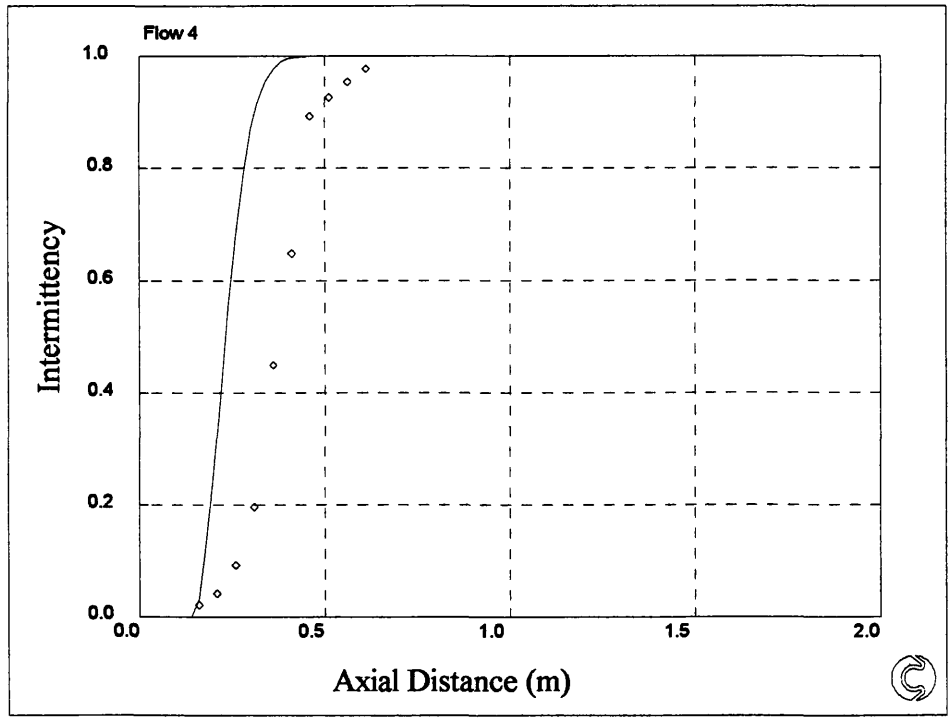

Figure 10.18: Intermittency Data From Gardiner

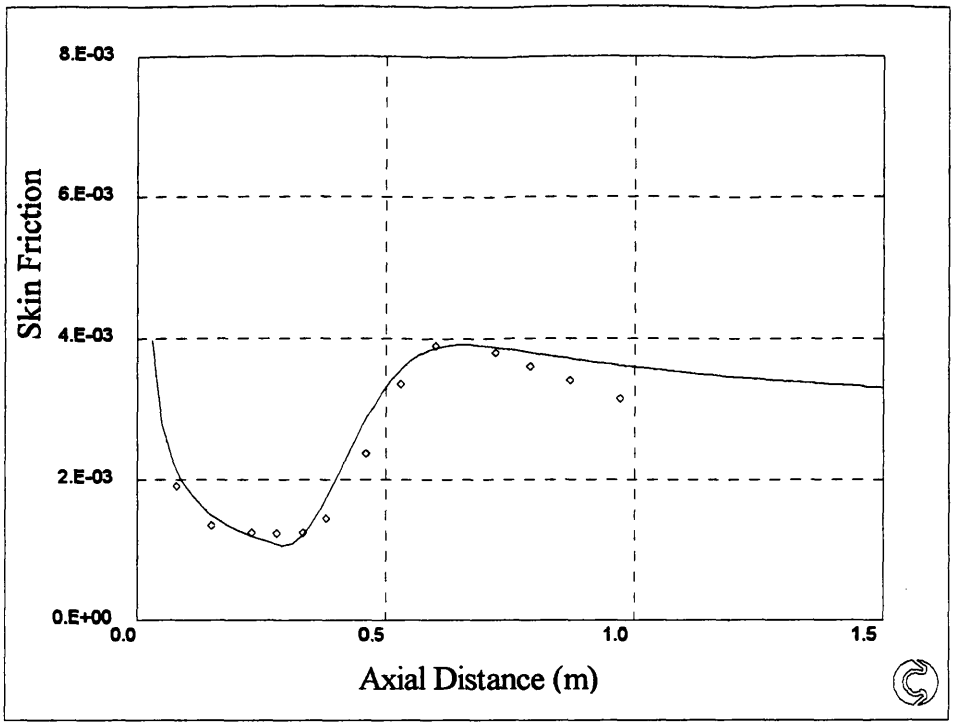

Figure 10.19: Abu-Ghannam & Shaw Zero Pressure Gradient Flow

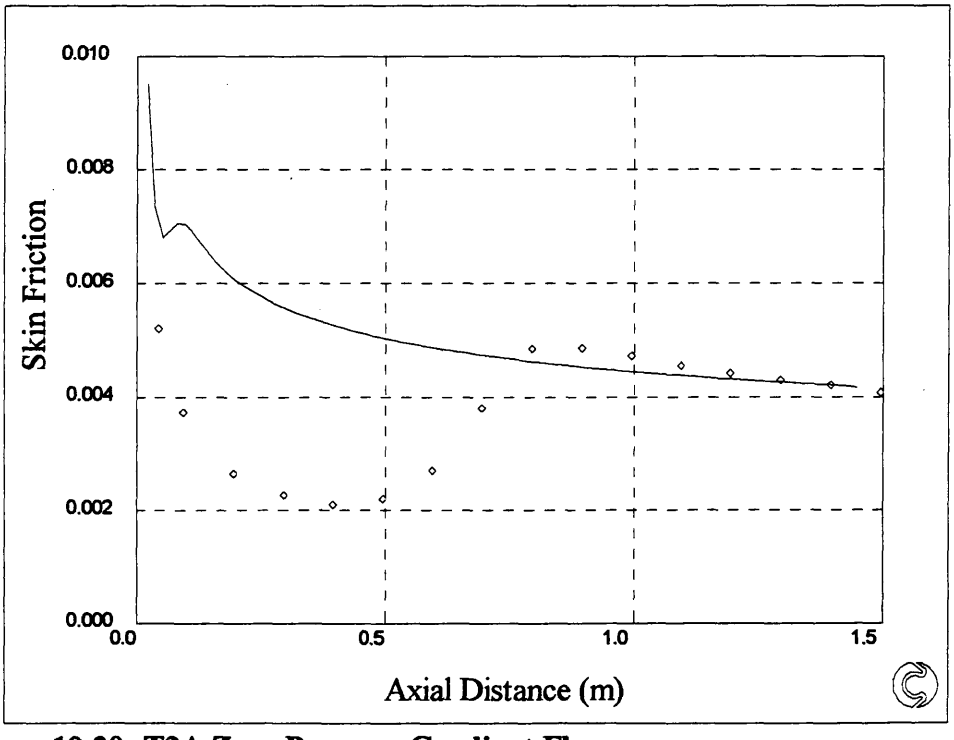

Figure 10.20: T3A Zero Pressure Gradient Flow

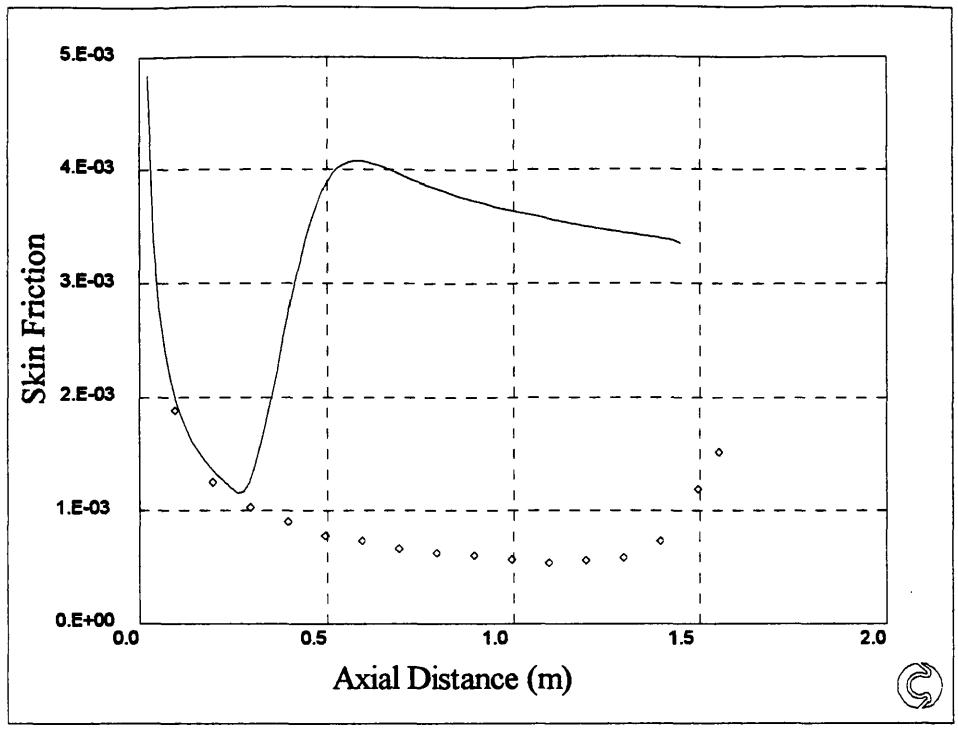

Figure 10.21: T3A- Zero Pressure Gradient Flow

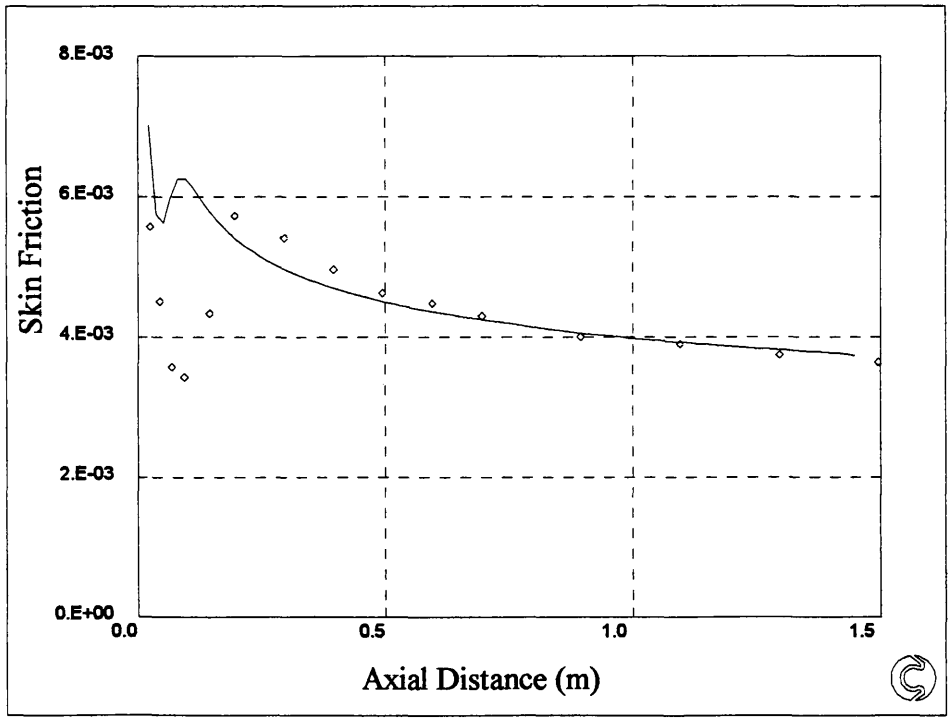

Figure 10.22: T3B Zero Pressure Gradient Flow

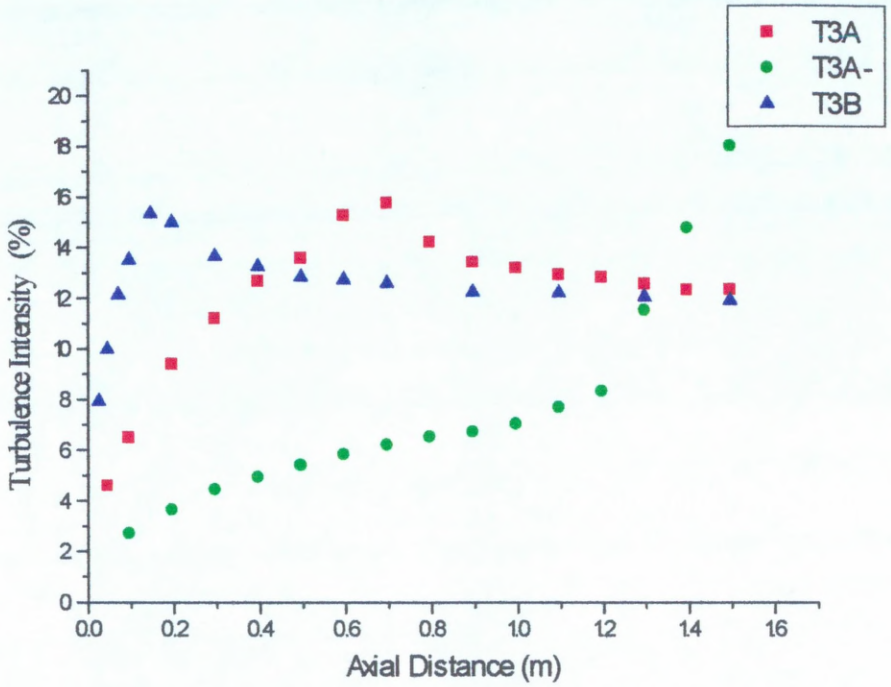

Figure 10.23: Plot of Maximum Turbulence Intensity in Boundary Layer

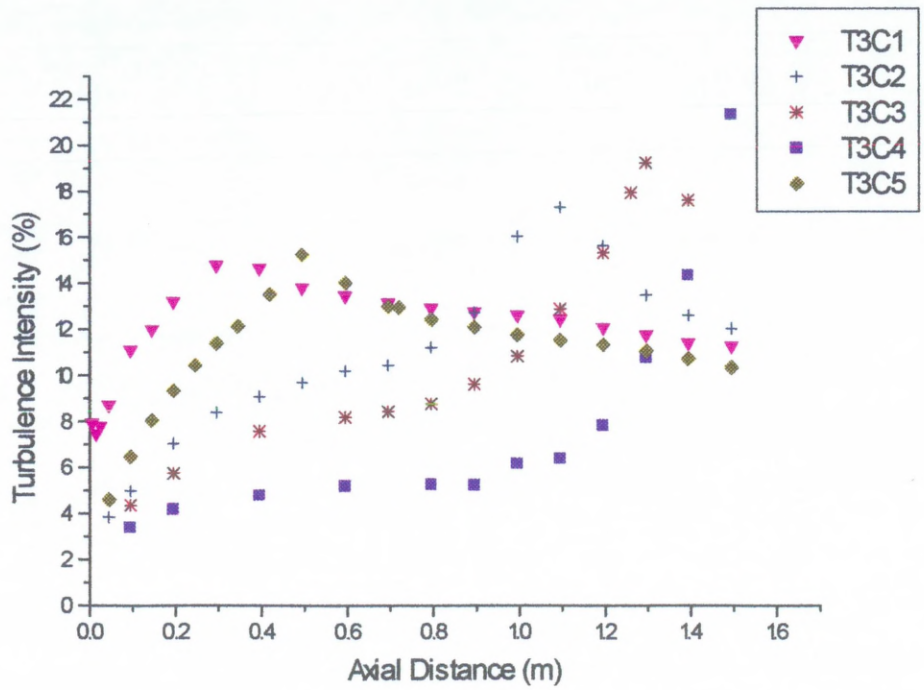

Figure 10.24: Plot of Maximum Turbulence Intensity in Boundary Layer

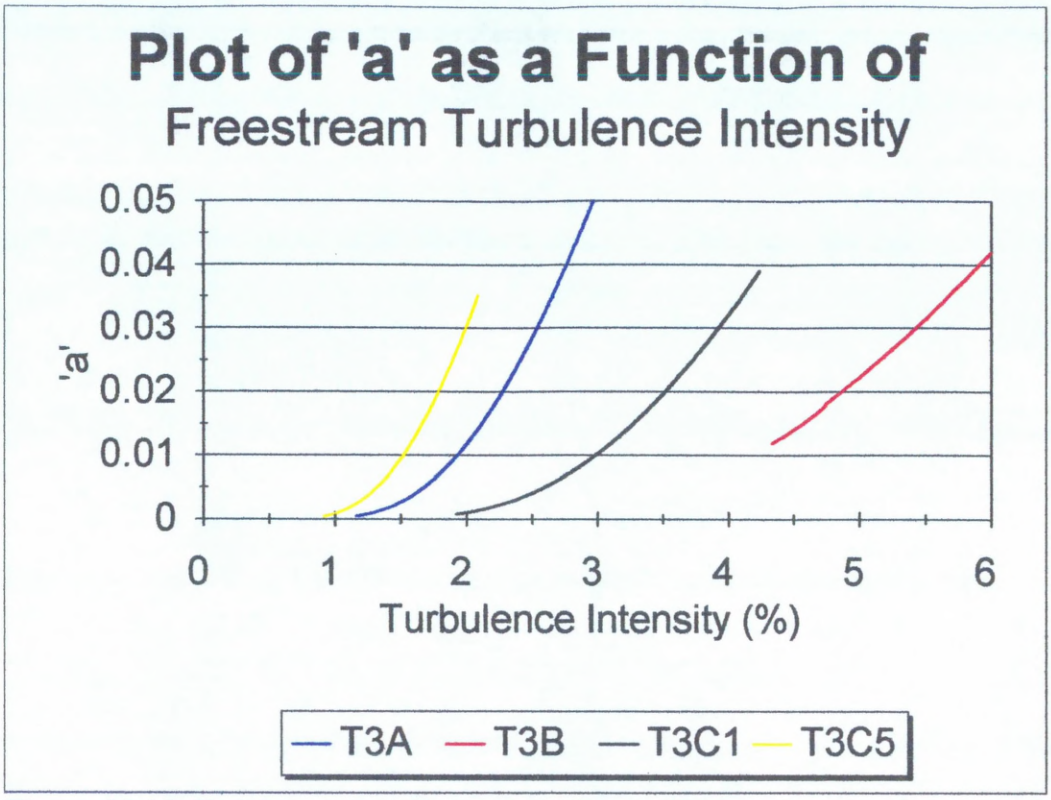

Figure 10.25: F(a) Developed Using Rolls Royce Data

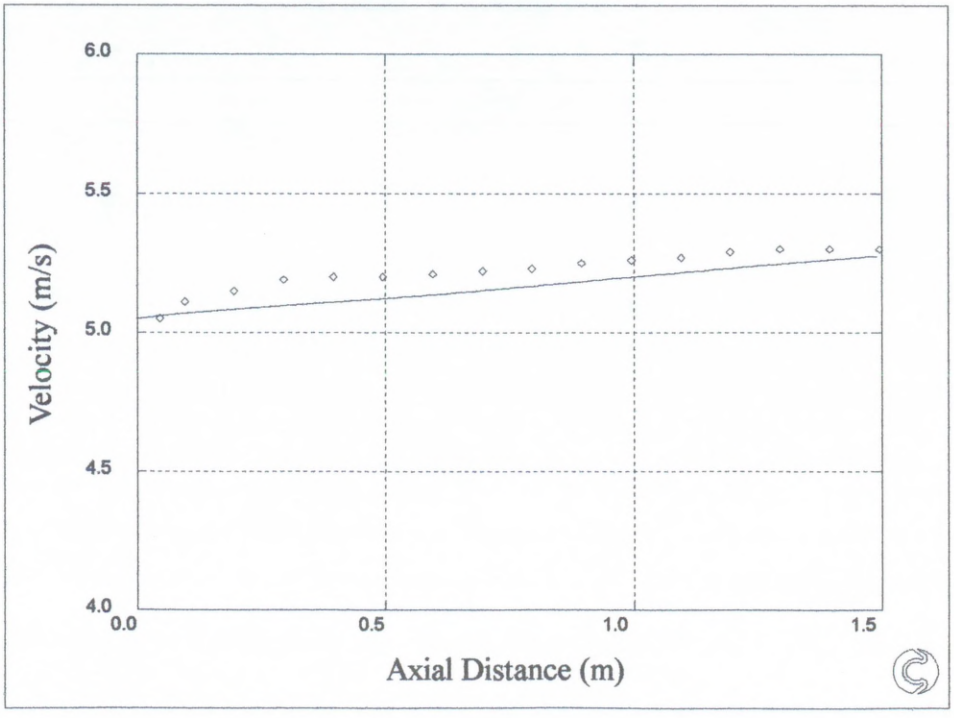

Figure 10.26: T3A Free Stream Velocity Profile

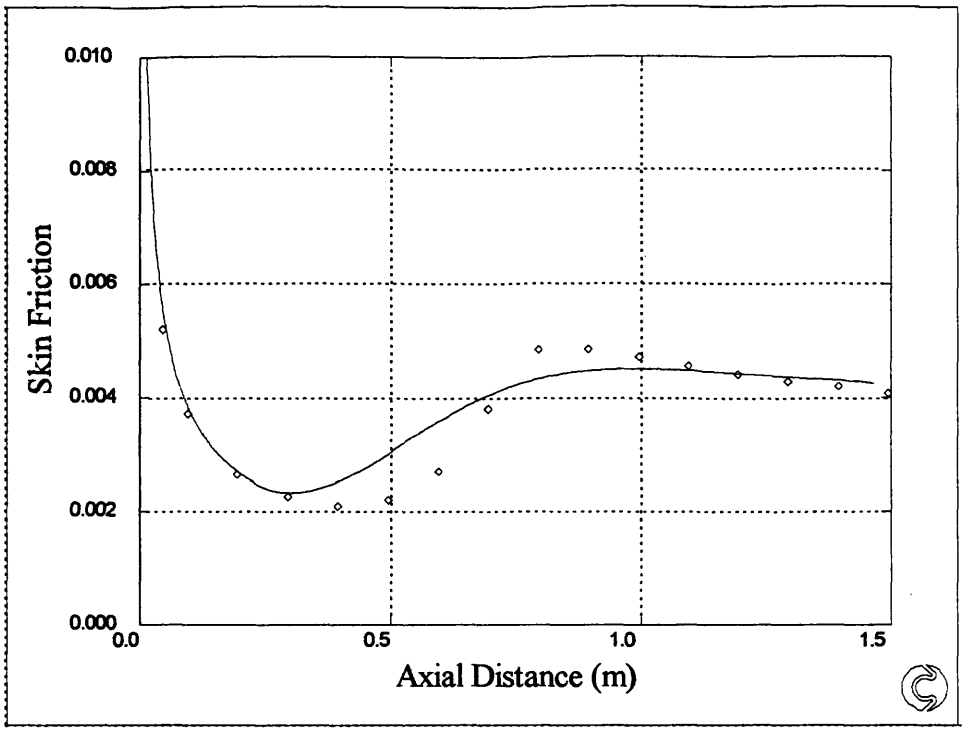

Figure 10.27: T3A Skin Friction

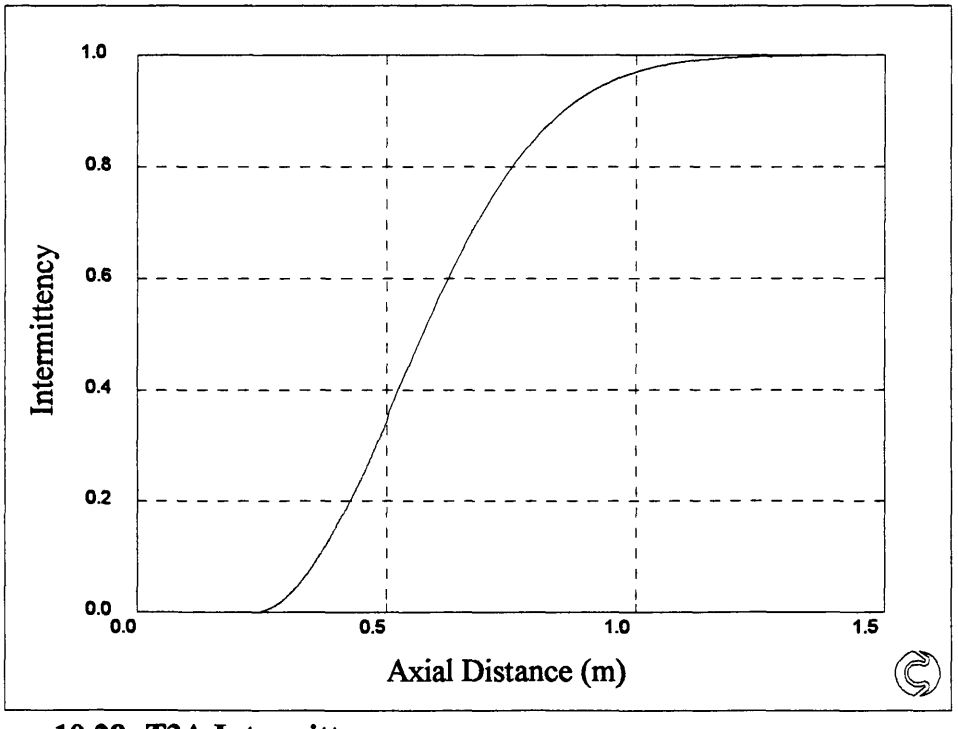

Figure 10.28: T3A Intermittency

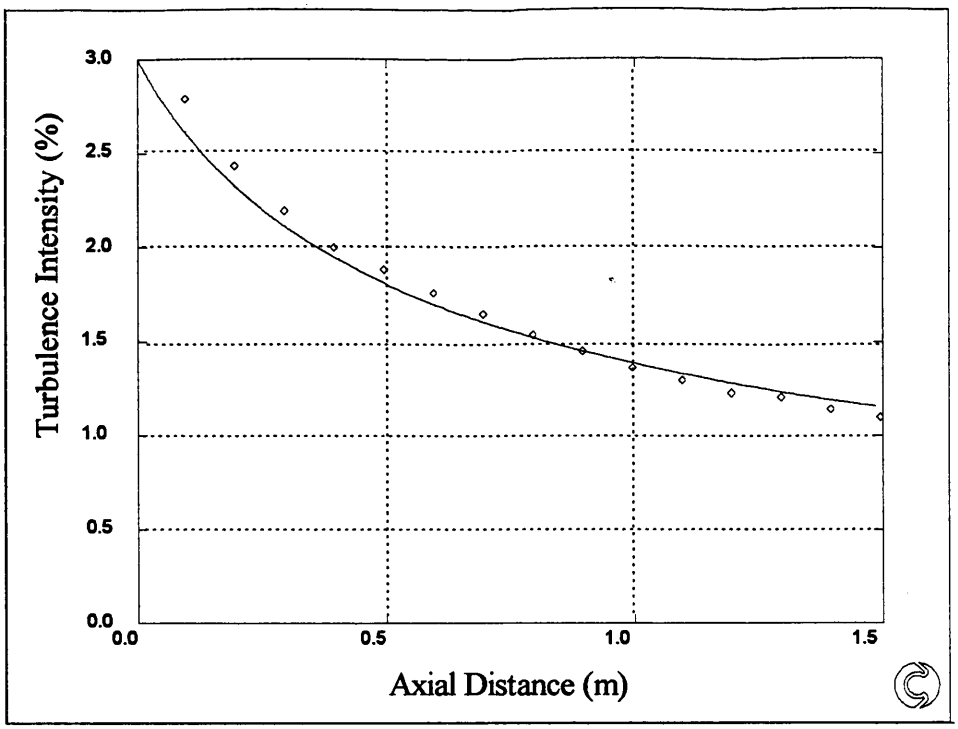

Figure 10.29: T3A Free Stream Turbulence Intensity

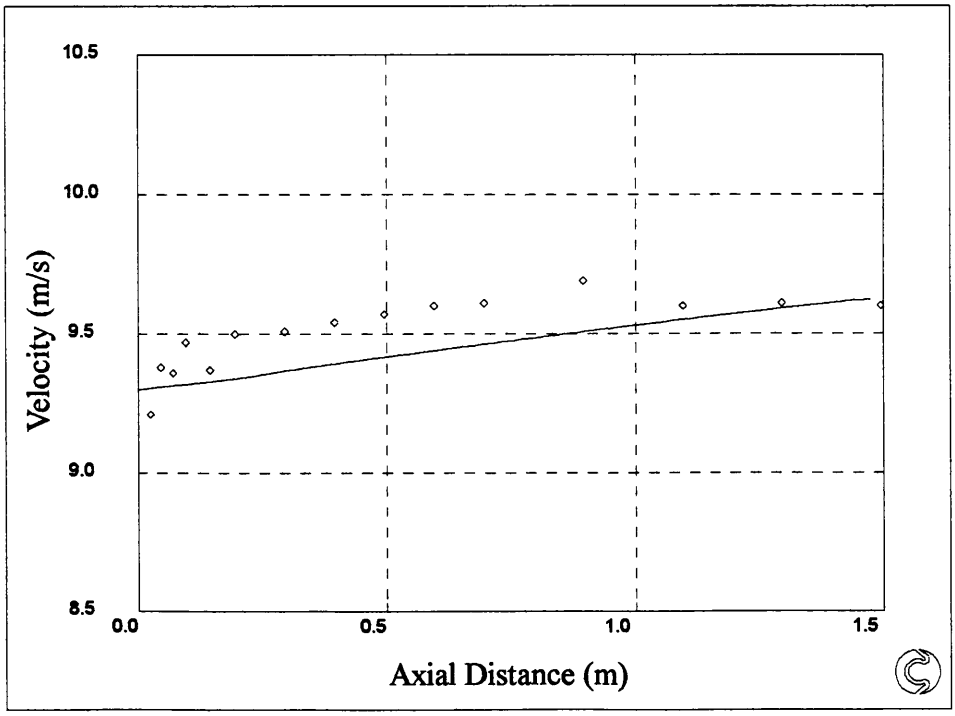

Figure 10.30: T3B Free Stream Velocity Profile

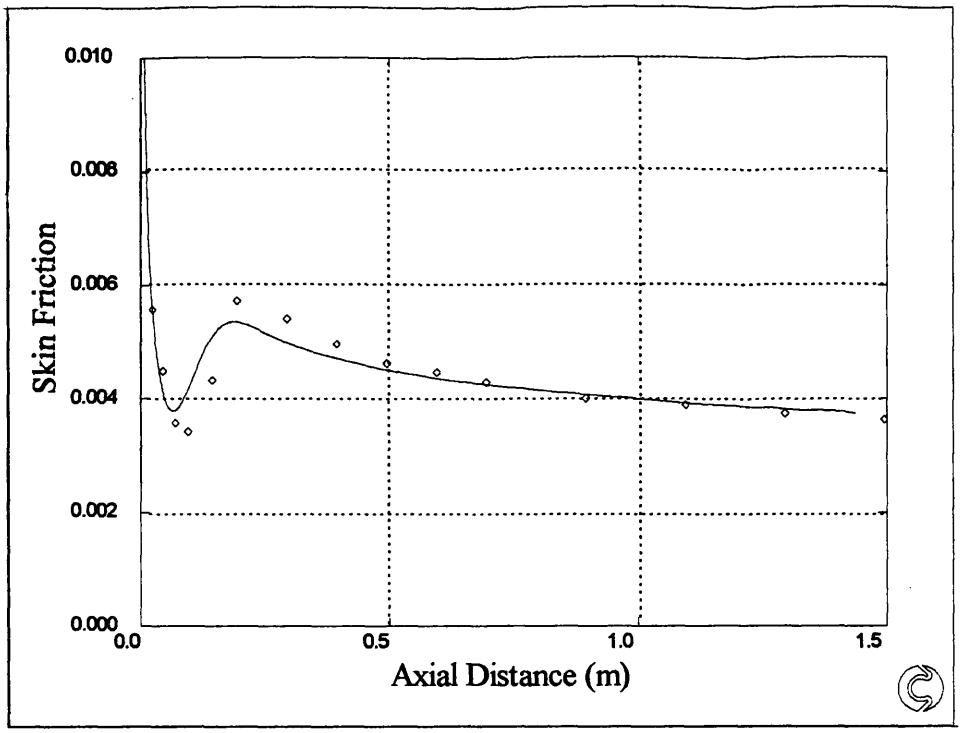

Figure 10.31: T3B Skin Friction

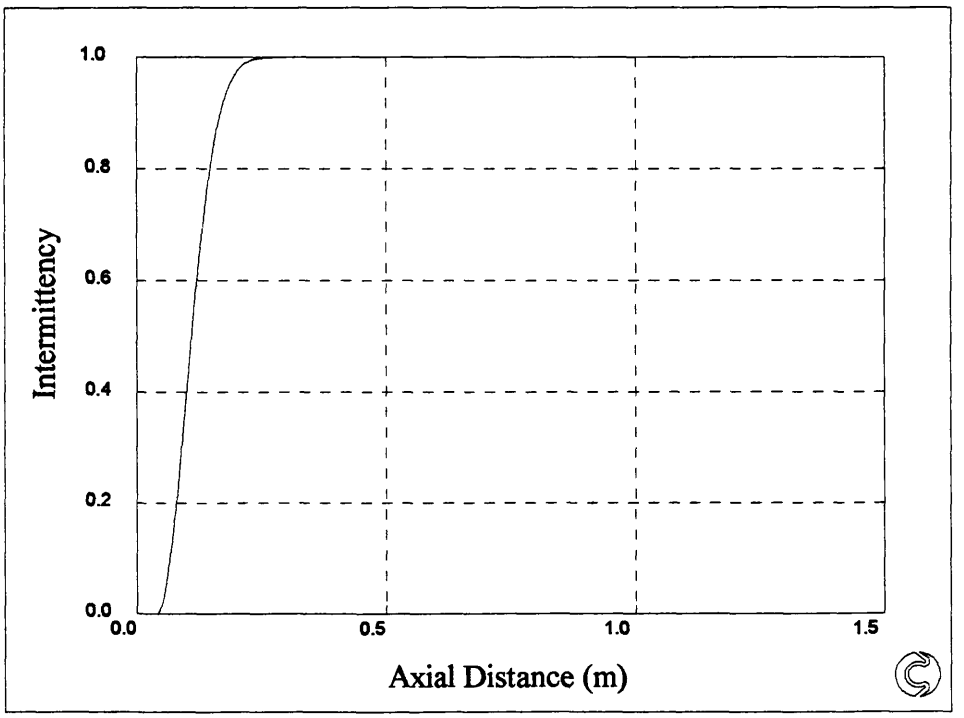

Figure 10.32: T3B Intermittency

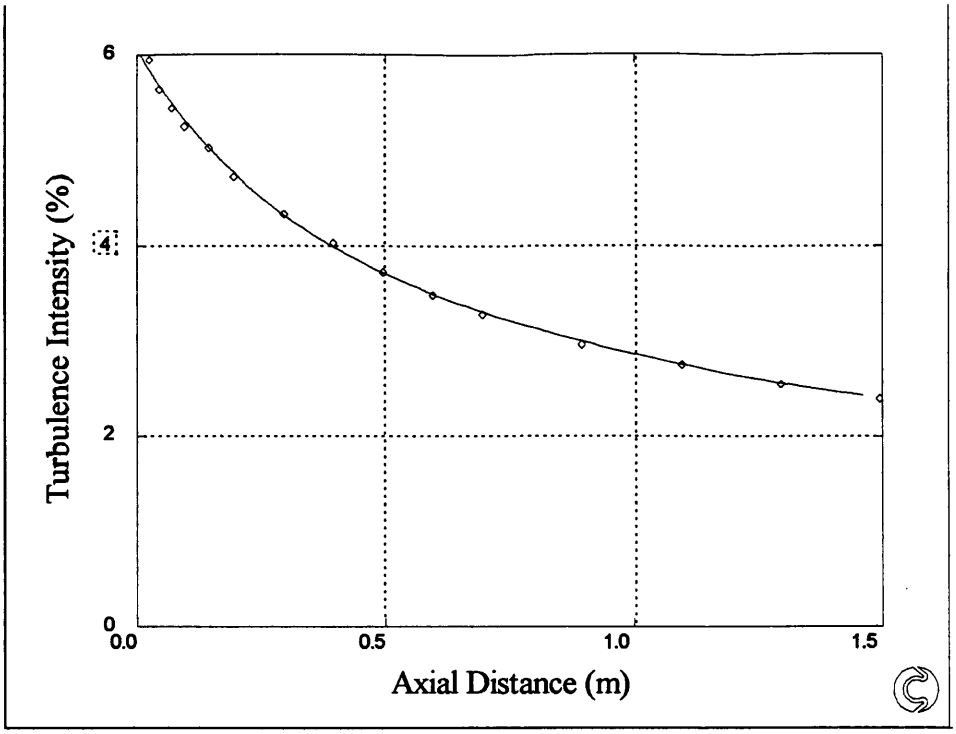

Figure 10.33: T3B Free Stream Turbulence Intensity

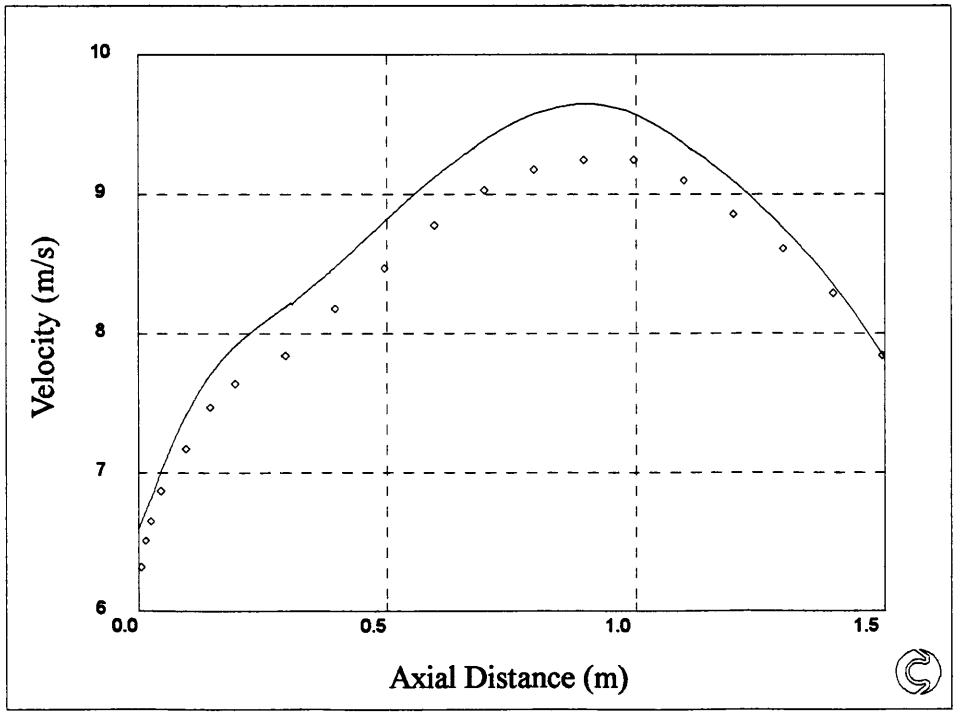

Figure 10.34: T3C1 Free Stream Velocity Profile

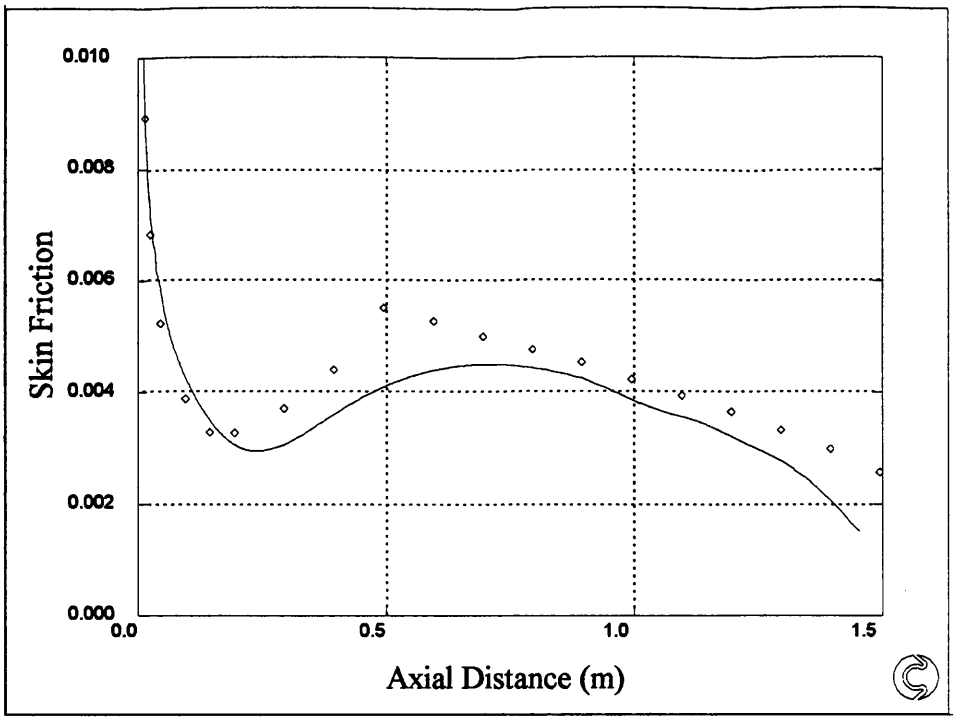

Figure 10.35: T3C1 Skin Friction

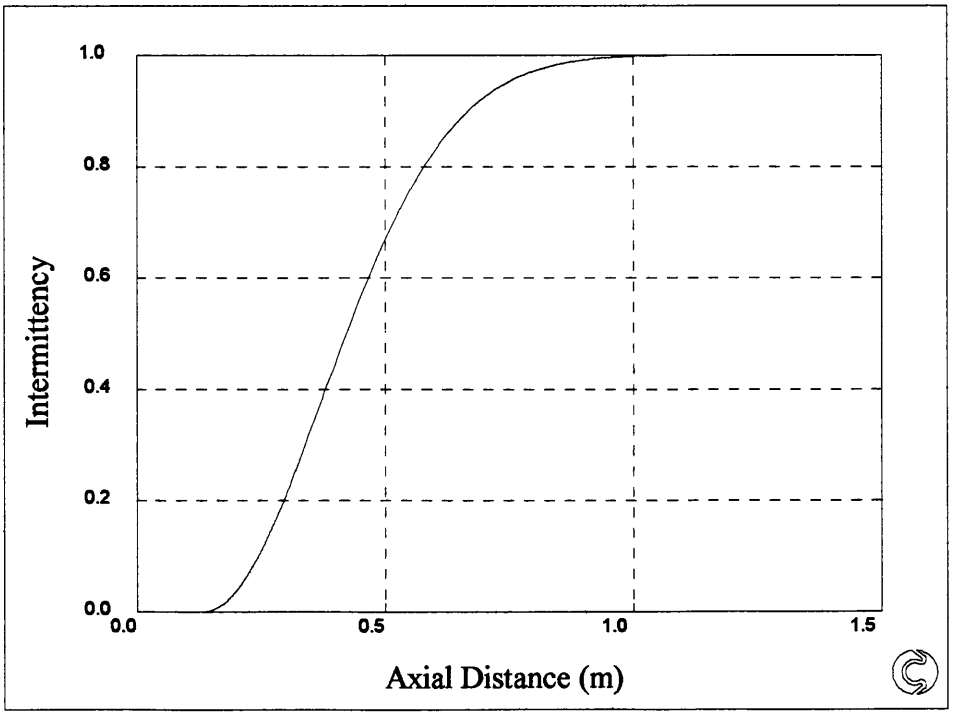

Figure 10.36: T3C1 Intermittency

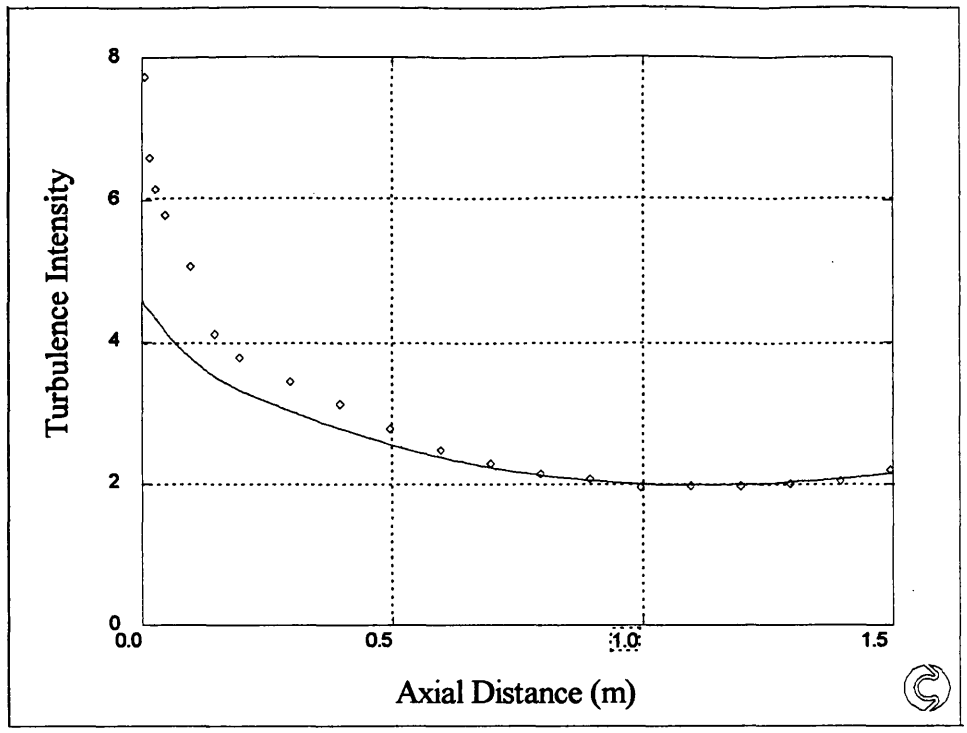

Figure 10.37: T3C1 Free Stream Turbulence Intensity

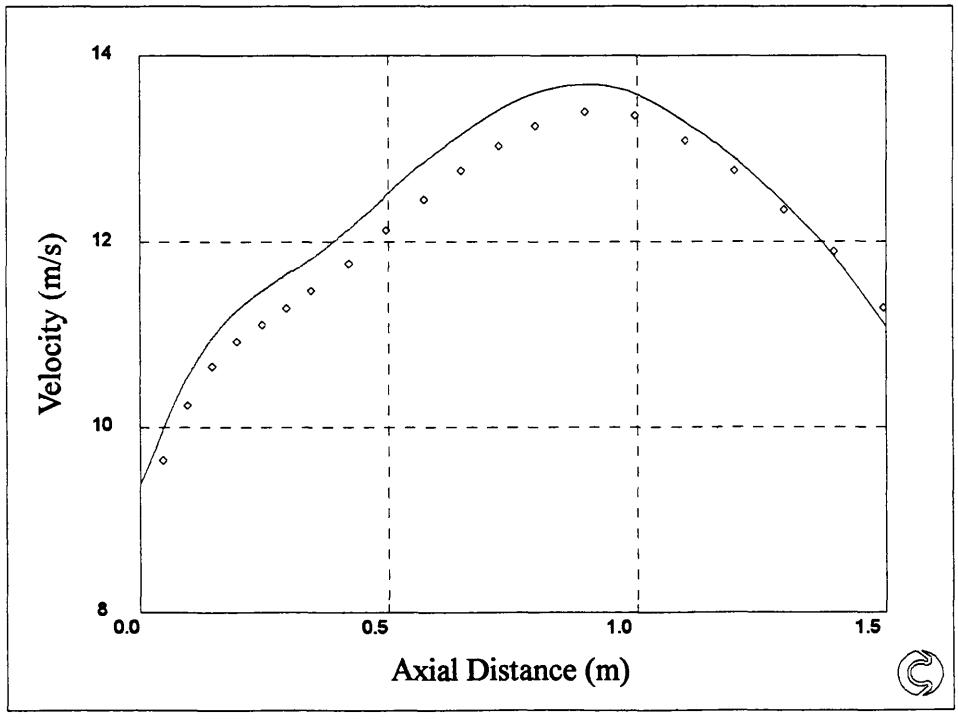

Figure 10.38: T3C5 Velocity Profile

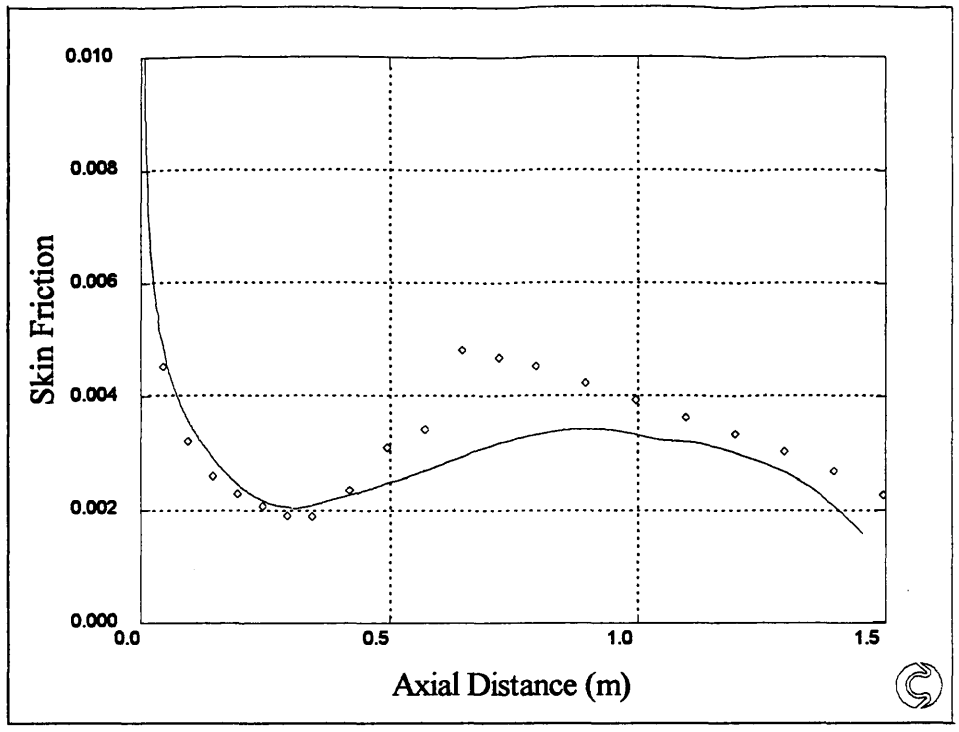

Figure 10.39: T3C5 Skin Friction

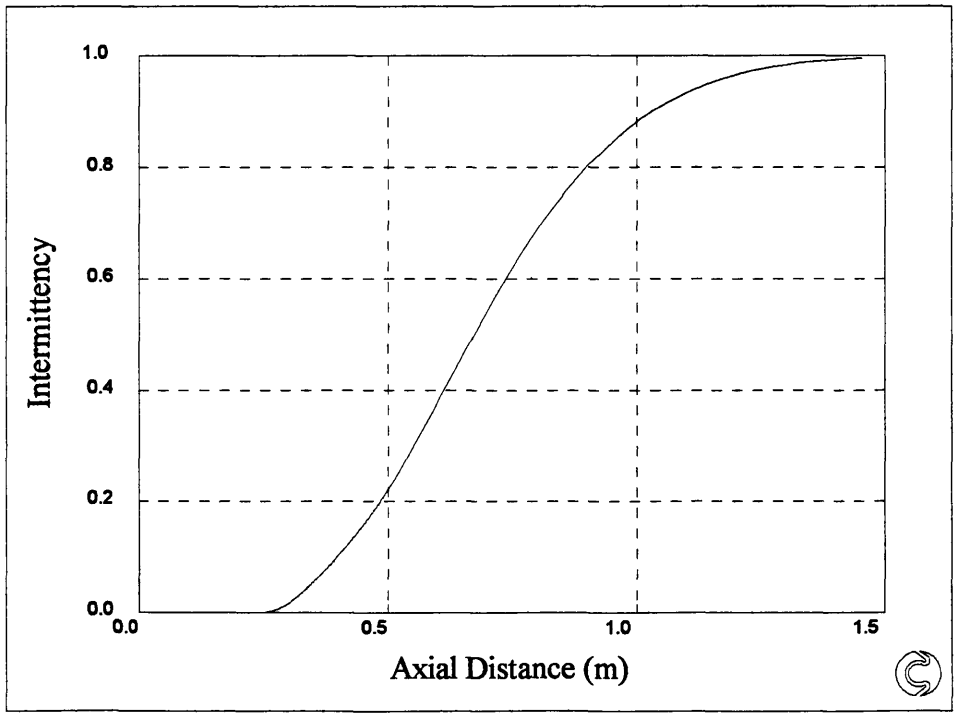

Figure 10.40: T3C5 Intermittency

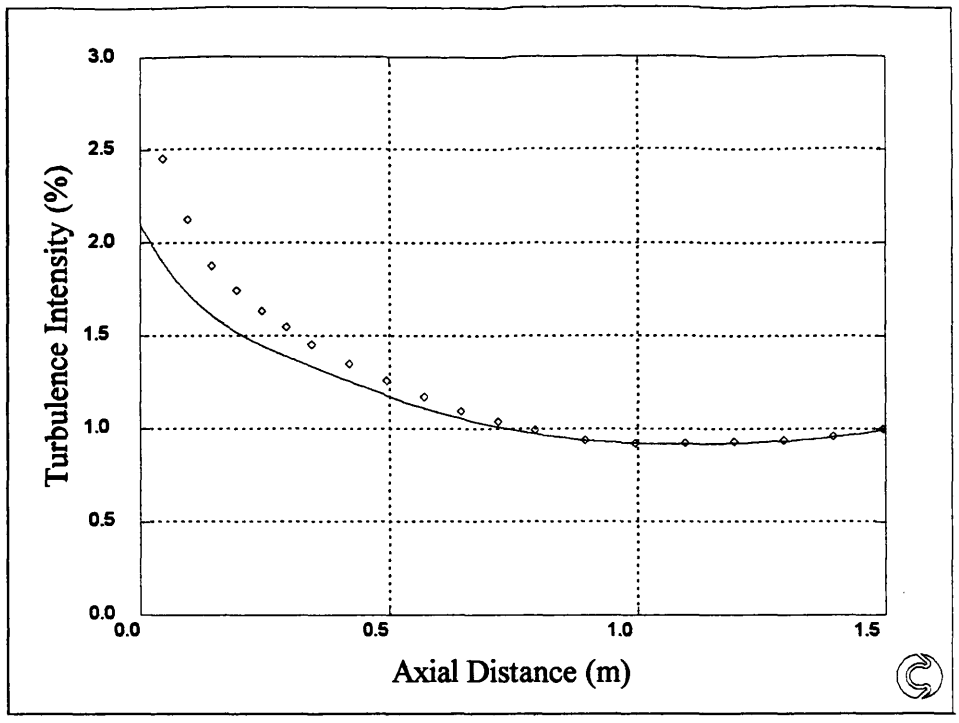

Figure 10.41: T3C5 Free Stream Turbulence Intensity

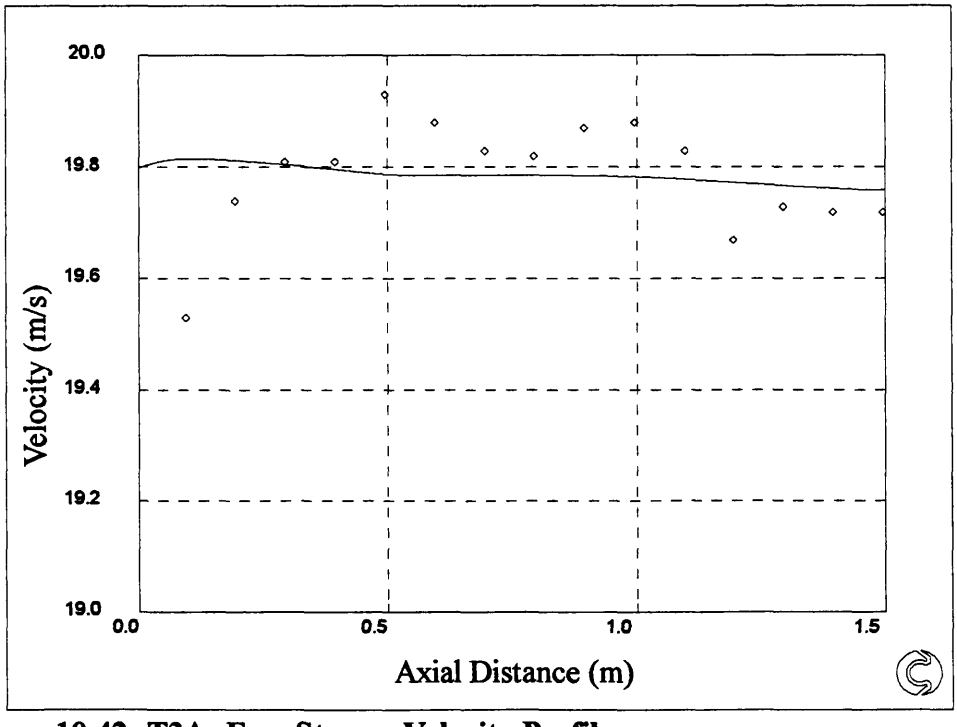

Figure 10.42: T3A- Free Stream Velocity Profile

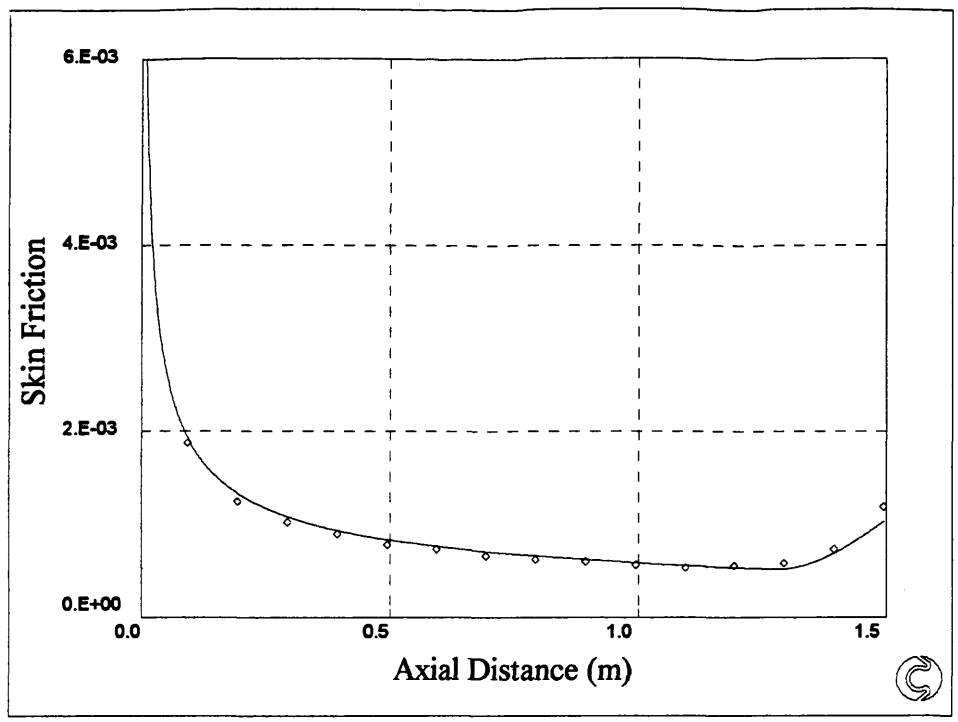

Figure 10.43: T3A- Skin Friction

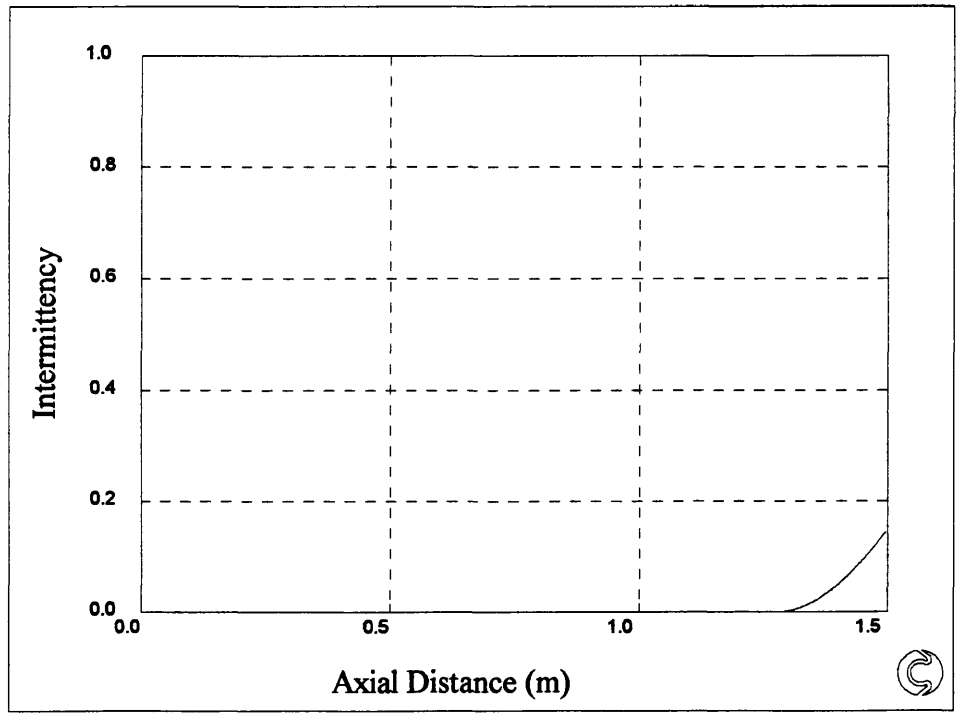

Figure 10.44: T3A- Intermittency

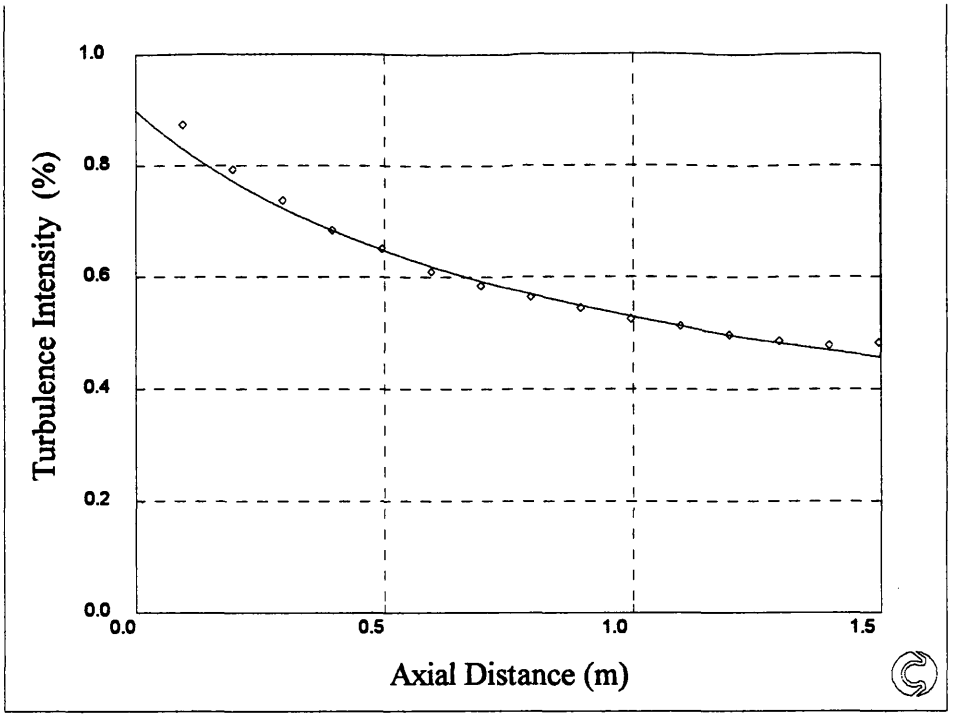

Figure 10.45: T3A- Free Stream Turbulence Intensity

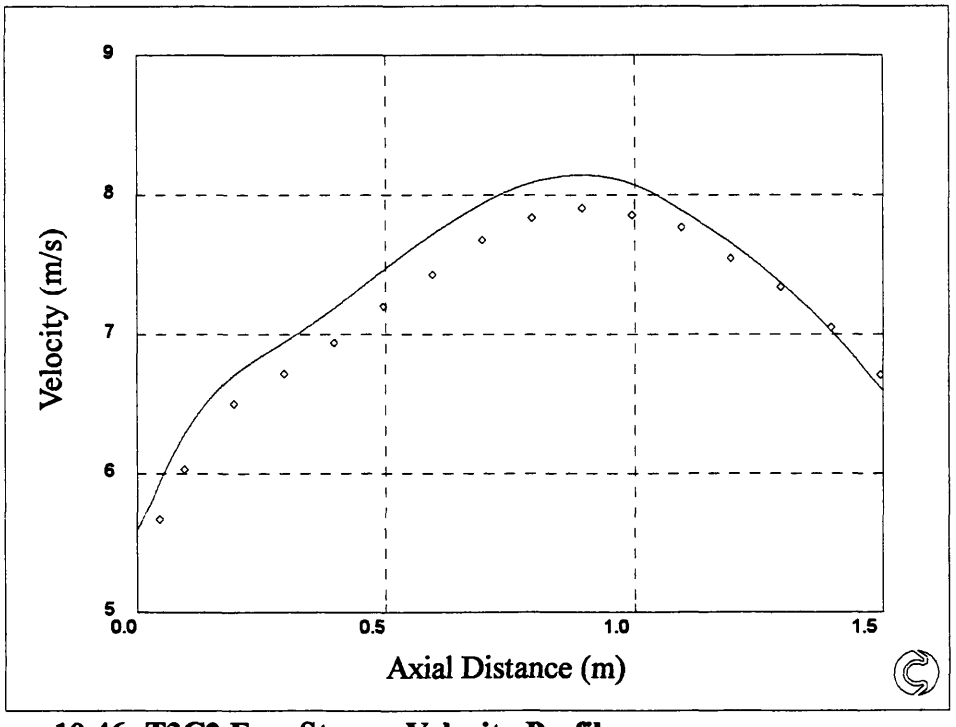

Figure 10.46: T3C2 Free Stream Velocity Profile

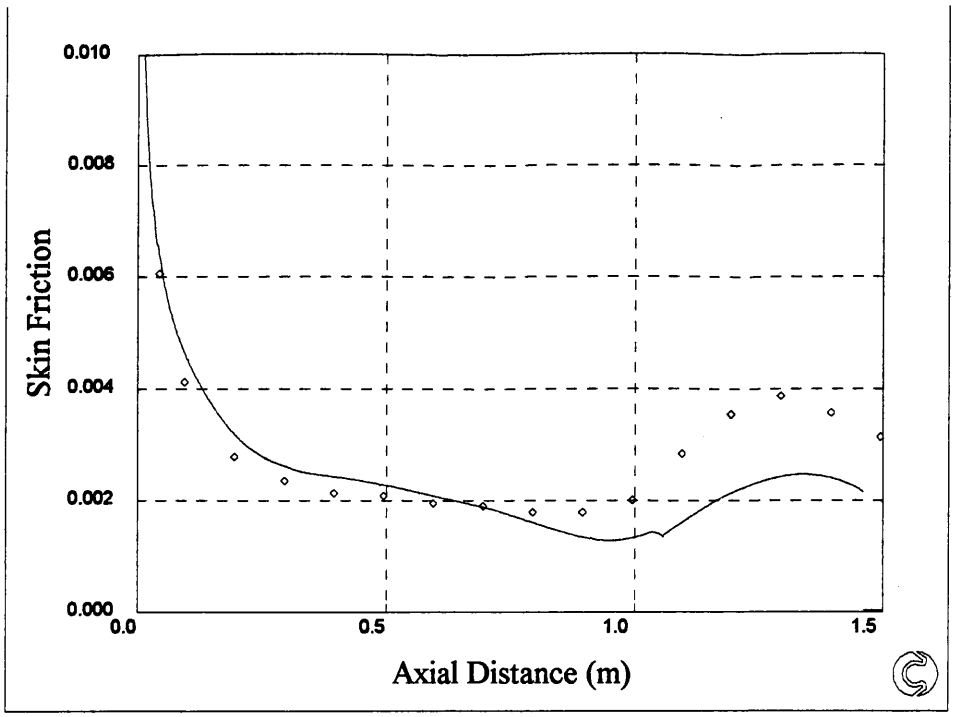

Figure 10.47: T3C2 Skin Friction

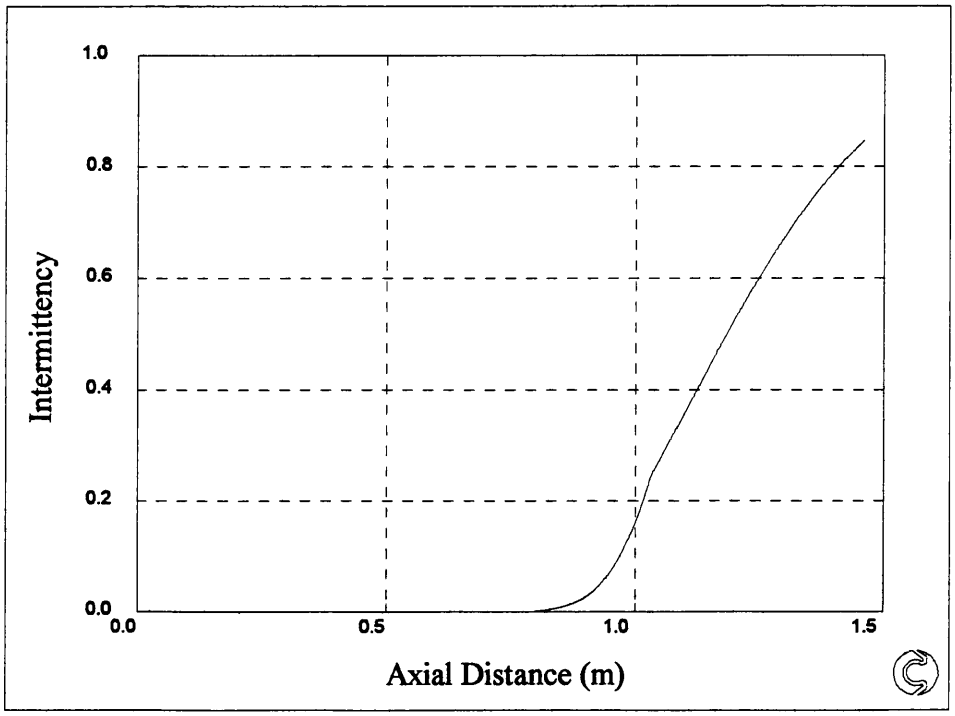

Figure 10.48: T3C2 Intermittency

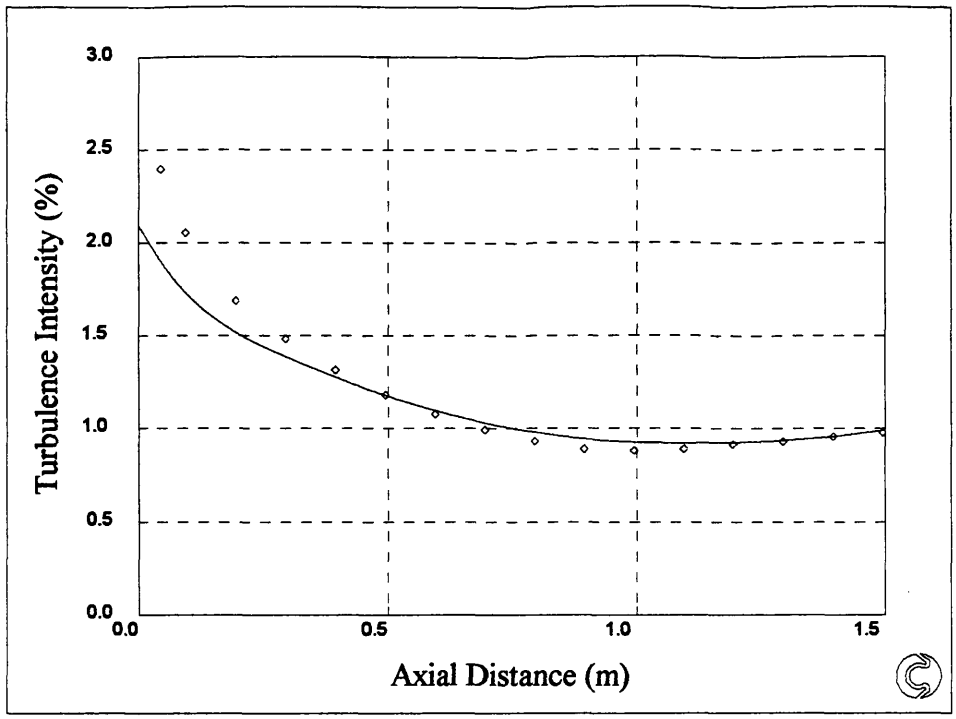

Figure 10.49: T3C2 Free Stream Turbulence Intensity

11. Results and Discussion

Two linear combination transition models, as described in Chapter 3 have been encoded into the PHOENICS computational fluid dynamics suite of software:

(a) the model described by Fraser, Higazy and Milne (1994) for favourable and adverse pressure gradients

(b) the model described by Solomon, Walker and Gostelow (1995) for adverse pressure gradient

Each model was programmed in two different ways:

(1) operating on a solved frictionless laminar flow field i.e. a post-processing model

(2) assuming the boundary layer to be a sink of momentum in a laminar flow field

It has been shown (Chapter 4, Figures 4.16 - 4.21) that for the Abu-Ghannam and Shaw (1980), simple constant pressure gradient flows, using model (a), there was practically no difference between predictions of skin friction and intermittency using methods (1) and (2).The predictions could be described as quite good. The momentum sink version of model (b) appeared to give better predictions for the adverse pressure gradient case tested, probably due to the start of transition being well predicted.

The above models (a) and (b) using method (2) were used to predict transitional boundary layer properties using Rolls-Royce T3C data. These flows had a considerable amount of decay of free stream turbulence, and the question arose through computational experiment as to what value of turbulence intensity should

be used in the Abu-Ghannam and Shaw (1980) correlation for the start of transition?. It has been shown in Chapter 4, Figures 4.24 to 4.63 that it was not the value quoted at the inlet or the start of transition. Further research into the original report revealed that the free stream turbulence intensity was measured at some upstream position between the inlet and the start of transition.

The averaging method suggested by Dunham (1972) was initially adopted using turbulence intensity data at the inlet and start of transition. The prediction of transitional properties, using model (a), by this method were significantly better (Chapter 5 Figures 5.1 to 5.20) than the predictions in Chapter 4 (Figures 4.24 to 4.63).

The method of the prediction of free stream turbulence intensity by Batchelor (1953) was also coded, but the predictions were in error by up to 125% in some cases, therefore this method was discarded.

A free stream turbulence model according to Malin (1995) was added and initially the averaging suggested by Dunham (1972). The predictions of boundary layer properties using the calculated average rather than the data are almost identical (Figures 5.1 to 5.20 and 5.27 to 5.51). It should be noted that the predictions by the two transition models (a) and (b) for adverse pressure gradient are almost identical (Figures 5.32 to 5.46 and 5.52 to 5.66). This is probably due to the fact that although the data suggests that the start of transition is in adverse pressure gradient, the averaging of turbulence intensity used in the Abu-Ghannam and Shaw (1980) correlation for the start of transition probably predicted that the start was in zero or favourable pressure gradient.

To obtain a better measure of free stream turbulence intensity which took into

account the flow history, it was decided to obtain an average by integrating the free stream turbulence intensity from the inlet. This method used in conjunction with the Abu-Ghannam and Shaw correlation (1980) gave a better approximation to the start of transition for the T3C flows (Figures 5.67 to 5.106). In flow T3C2, however the start of transition was still predicted in a favourable pressure gradient regime. Since model (b) requires properties to be evaluated at the start of transition, clearly there was a requirement for either better correlations or a new method to predict the start of transition.

Transition model (a), combined with the turbulence model due to Malin (1995) and using the integrated average of turbulence intensity in the Abu-Ghannam and Shaw (1980) correlation was applied to the flow over a subsonic gas turbine blade. A non-frictional PHOENICS laminar flow analysis was compared with an accepted non-frictional analysis, courtesy of European Gas Turbines Ltd and the comparison could be described as good, therefore validating the model. A turbulent analysis was also carried out in PHOENICS using the already coded k - ε turbulence model and it was found that the free stream velocity profiles, non-frictional and frictional, Figure 6.9, 6.10, over the blade surfaces were almost identical. The skin friction and intermittency predictions on the blade surfaces Figures 6.11 and 6.12 agree with what was expected; the pressure surface did not undergo transition to turbulence, while half of the suction surface was covered in transitional flow. Figure 6.13 shows that the start of transition, using either a laminar or turbulent flow field, is identical.

A new method was developed in order to predict the start of transition, using data from the Rolls Royce T3A, T3A-, T3B and T3C flows. The method predicted the

maximum kinetic energy and average dissipation at an axial station in the boundary layer using no ambiguous boundary conditions. The boundary layer model was coupled to the free stream turbulence intensity by the function 'a' as shown on page 8-4. The predictions at the previous step being the starting conditions for the predictions at the current step. The result of this method was an increased cell density in the axial direction over the previous correlation method. The method was based on two flow types: adverse, and favourable pressure gradient. Each flow type had a distinctive maximum boundary layer turbulence intensity profile shown in Figures 10.23 and 10.24.

The method was coded into PHOENICS as a sink of momentum in a similar manner to the correlation method described above. It was based on the turbulent energy equations, and estimated the start of transition by calculating the isotropic growth of kinetic energy, using integrated averages of properties across the boundary layer, from the leading edge. The method required the following boundary conditions: (1) the maximum turbulence intensity at the leading edge, (2) an average dissipation length scale at the leading edge, (3) a turbulence intensity criteria for the start of transition, (4) a function, 'a' to simulate the effect of turbulence on the laminar boundary layer.

Initially the turbulence intensity criterion for the start of transition was taken to be 5% and the function for 'a' was determined to be a quadratic, equation (8.7), based on the correlation of van Driest and Blumer (1963). A suitable starting value based on free stream turbulence intensity was chosen to allow the prediction of skin friction to fit the data of Abu Ghannam and Shaw (1980). There was quite considerable variation in the value of this factor and it was decided to carry out a

Taguchi analysis to predict then trends in the factors (1) to (3) above.

The Taguchi analysis showed that this method may not be suitable for favourable pressure gradient flows and it was therefore decided to concentrate effort towards adverse pressure gradient flows. Zero pressure gradient flows were rejected as no flow is exactly zero pressure gradient. The Taguchi analysis quickly showed that for adverse pressure gradients:

(a) increasing the turbulence intensity at the critical momentum thickness Reynolds number moves the start of transition upstream

(b) for the range of chactaristic lengths used in this analysis, they had little effect on the start of transition,

(c) for the adverse pressure gradients considered within the analysis the pressure gradient did not effect the start of transition greatly

(d) increasing the criteria for the start of transition moved the start of transition significantly downstream

Based on the results of the Taguchi analysis it was proposed to try to develop a universal correlation for adverse pressure gradient based on the turbulence intensity at the critical momentum thickness Reynolds number. A correlation, based on dissipation length scale and pressure gradient parameter, equation (10.1) was developed to predict skin friction using the Abu-Ghannam and Shaw (1980) adverse, favourable and zero pressure gradient and the Rolls Royce T3C2 data. The predictions can be described as quite good. These predictions were extended to favourable pressure gradient, Rolls Royce T3C1 and T3C5, flows but the start of transition was predicted very late (Figures 10.1 to 10.6).

A further correlation, equation (10.2) based on free stream turbulence intensity at

the critical momentum thickness Reynolds number was developed based on zero pressure gradient intermittency data from Gardiner (1987), but this correlation could not consistently predict the start of transition in other zero pressure gradient flows successfully.

Originally it was thought that the boundary layer would be laminar from the leading edge up to a critical momentum thickness Reynolds number and any instabilities in this portion of the flow in the boundary layer would be damped out and the flow would remain laminar. A simple correlation 'suitable for engineering type flows', Arnal (1984), equation (7.1), had been used to predict this critical momentum thickness Reynolds number.

Wazzan (1979) published data which was simply curve fit by equation (10.3), but it was found that when compared with data from Gardiner (1987), sometimes the start of transition was reached before this critical displacement thickness Reynolds number. The two correlations also gave widely differing predictions of the axial distance from the leading edge where the point of instability occurred. Therefore, it was concluded that at the values of turbulence intensity considered here, the transition process was in the by-pass mode and therefore the turbulent fluctuations would be present from the leading edge.

Correlation (10.4) was developed from intermittency data from Gardiner (1987) for zero pressure gradient flows. It gave good predictions for the start of transition for Gardiner flows 1 - 4 and the zero pressure gradient Abu-Ghannam and Shaw flow. Prediction of the start of transition in flows T3A, T3A- and T3B was poor, it was always predicted very early. An attempt was made to extend correlation (10.4) to Gardiner's non zero pressure gradient flows, but the

relationship between the free stream turbulence intensity and the maximum boundary layer turbulence intensity was too randomly distributed.

After inspection of the Rolls Royce T3A, T3A-, T3B, T3C boundary layer maximum turbulence intensity data, it was found that the proposed function for 'a' could not be correct. Transition was predicted only when the calculated value intercepted the maximum turbulence intensity data from below. It did not follow the data. Further inspection of the data revealed that the maximum turbulence intensity in the boundary layer at the leading edge was almost the same as the average free stream turbulence intensity at inlet. The inlet value would therefore be assumed to be the starting value in the boundary layer calculations. It was proposed that the average dissipation length scale at the leading edge of the boundary layer was also the same as that at inlet. The criterion for the start of transition was taken directly from the maximum turbulence intensity data and was found to be approximately 12%. This was almost twice the value quoted by Fraser (1978) and Arnal (1984).

An inverse exponential function was proposed based on the free stream turbulence intensity, dissipation length scale and pressure gradient. The proposed function would not attempt to predict the maximum turbulence intensity in the boundary layer as the data was found to be far from isotropic. The predicted profile, would, however be qualitatively correct. This was shown to be the case in Figures 10.23 and 10.24, where the isotropic prediction of the maximum boundary layer turbulence intensity has been plotted for each flow type scenario.

Correlation (10.8), was a function of free stream turbulence intensity and length scale only, and was proposed for the nominally zero, but slightly favourable

pressure gradient flows T3A and T3B. Prediction of skin friction can be described as good (Figures 10.27 and 10.31). Correlation (10.8) was extended, by including a function of the pressure gradient parameter, m, (correlation 10.9) to take into account the start of transition in favourable pressure gradients, T3C1 and T3C5. Again the prediction of skin friction can be described as good. The start of transition was perhaps predicted slightly late.

Unfortunately, there was only one nominally zero, adverse pressure gradient flow, T3A-, and Thwaites method, which was used to predict laminar boundary layer properties, predicted separation before transition on flows T3C3 and T3C4, therefore excluding these two flows from any further analysis. Thus there was only one variable pressure gradient flow, T3C2 where the start of transition occurred in adverse pressure gradient that could be utilised. No attempt was made to develop a function for 'a' in adverse pressure gradient flows due to the limited data available. However an attempt was made to predict skin friction using this new method. The method was shown to give excellent prediction of skin friction in flow T3A- Figure 10.43, but not quite as good for flow T3C2. Figure 10.47. Again the parameter 'a' was made a function of free stream turbulence intensity, but in the case of adverse pressure gradient, 'a' was limited to a constant value, after initially being a function of free stream turbulence intensity.

12. Conclusion

12.1 Integral Method

One of the objectives in this thesis was to program into an existing commercially available computational fluid dynamics suite of software (PHOENICS), existing integral methods that were available for the prediction of transitional boundary layer parameters. The integral methods programmed were Thwaites (1949) method for the laminar boundary layer, a relatively new, simple method attributable to White (1991) for the turbulent layer, the start of transition used the well known Abu-Ghannam and Shaw (1980) correlation, transitional parameters were calculated using the method described by Fraser, Higazy and Milne (1994) for favourable and adverse pressure gradient flows and also the method described by Soloman, Walker and Gostelow (1995) for adverse pressure gradient.
These methods were tested against a variety of flows, including zero and constant adverse and favourable pressure gradient, and the varying pressure gradient Rolls Royce T3C flows. The following conclusions were reached after using this method:

(1) integral methods coded into PHOENICS as a momentum sink are an extremely fast and quite accurate way of predicting boundary layer parameters, the solution time is similar to a laminar analysis

(2) turbulent boundary layer parameters can be successfully predicted from a laminar free stream velocity profile

(3) the method requires only two computational cells across the boundary layer in the transverse direction

(4) it was not possible to predict the start of transition in a variable pressure gradient flow, using the Abu-Ghannam and Shaw correlation with a single value of turbulence intensity measured at the inlet or start of transition, or even an average of the two as suggested by Dunham (1972)

(5) the method found by the author to give the best prediction of the start of transition in the T3C flows using the Abu-Ghannam and Shaw correlation was an integrated average of turbulence intensity, using the turbulence model due to Malin (1995), from the inlet to the start of transition.

(6) the transition method described by Fraser, Higazy and Milne (1994) gives good prediction of skin friction and transition length in zero and favourable pressure gradient flows, but the transition length is always under predicted in adverse pressure gradient flows

(7) the transition method described by Solomon, Walker and Gostelow (1995) will probably give an improved prediction of intermittency distribution and transition length for adverse pressure gradient flows, but its results are highly dependent on the properties of the flow at the start of transition

12.2 New Method

A new method which used the turbulent energy equations was developed to predict the start of transition. The method used integrated averages of properties across the boundary layer starting at the leading edge and marched downstream. The boundary layer model is coupled to the free stream via a correlation which was found to be a function of free stream turbulence intensity, dissipation length scale and pressure gradient parameter. This method was also programmed into

PHOENICS as a sink of momentum. It was developed and validated using the Rolls Royce T3A, T3A-, T3B and T3C flows. The following conclusions were reached:

(1) the method is slower that the previous correlation method, it requires a computational cell density of about 1000 per metre in the axial direction

(2) only two computational cells across the boundary layer in the transverse direction are required

(3) starting and boundary conditions are not ambiguous

(4) the start of transition and skin friction in favourable pressure gradient flows were well predicted

(5) it was possible to predict the start of transition in adverse pressure gradient flows, but there was not enough data available to develop a more representative correlation

13. Suggestions for Further Work

The following suggestions are made for work which would be useful for the continued endeavour to improve the prediction of transitional boundary layer flows.

(1) The functions developed for the parameter 'a' are somewhat controversial. In the present work these were intuitively based and were fine tuned on the basis of the overall performance of the predictions obtained for the start of transition. An experimental programme of work to study the growth of the disturbance spectra in the laminar boundary layer under the conditions of zero, favourable and adverse pressure gradients is advisable together with moderate to high freestream turbulence levels. This would generate a range of by-pass transition routes where the disturbance growth rates appear to be only marginally related to the classic stability mechanisms. This effort would provide the basic data from which a universal correlation for 'a' might at least be founded on sounder physically arguments.

(2) It would be desirable to have some reliable measurements of the dissipation length scales at entry to the flow control volume. Presently these length scales are intuitively guessed and it is not at all clear what significant influence, if any, they have on the start of transition. This is equally the case for the flow in the laminar boundary layer where the dissipation length scales are not generally available for a critical judgement to be made.

(3) In the present work no meaningful appraisal could be made of the start of transition prediction method under adverse pressure gradient conditions. The Rolls Royce data included only one single case where good data could be evaluated for transitional flow in adverse pressure gradient conditions. It is recommended that a particular study of the disturbance growth rates in adverse pressure gradient flows should be undertaken.

(4) The pressure gradient parameter, $m = \frac{\theta^2}{\nu}\frac{dW}{dz}$ does not provide a particularly useful measure of the strength, or effect of the prevailing pressure gradient on the transitional flow properties. The influence of the momentum thickness, θ, means that 'm' is also Reynolds number dependant and it is thought that the true effect of the pressure gradient on transitional behaviour is hidden, or swamped by what might be more dominant Reynolds number effects. The normal pressure gradient parameter is still useful as a guide to the imminence of separation. It is less convincing as a general measure of the freestream influence on the behaviour and growth of disturbances in the laminar boundary layer undergoing a by-pass transition. Consideration should therefore be given to alternative, or preferable completely new parameters which ideally would uncouple the effects of pressure gradient from other influencing parameters.

14. Bibliography

1. Abu-Ghannam, B. J. and Shaw, R. 1980. Natural transition of boundary layers - the effects of turbulence, pressure gradient and flow history. *Jour. Mech. Eng. Sci*: 22 892.
2. Amos, I. G. 1994. Advanced Engineering and Future Products, European Gas Turbines Ltd., P.O. Box 1, Thorngate House Lincoln. Personal Communication.
3. Arnal, D 1984. Description and Prediction of Transition in Two-Dimensional Incompressible Flow. AGARD Special Course on Stability and Transition of Laminar Flow, AGARD-R-709
4. Batchelor, G.K. 1953. The theory of homogeneous turbulence. *Cambridge University Press*, p 68.
5. Batchelor, G.K. and Proudman, I. 1954. The effect of rapid distortion of a fluid in turbulent motion. *Quarterly Jour. of Mech. and App. Math.*, Vol. 7 p83
6. Birch, N. T. 1987. Navier-Stokes prediction of transition, loss and heat transfer in a turbine cascade. *ASME 87-GT-22.*
7. Blair, M. F. 1983. Influence of free-stream turbulence on turbulent boundary layer heat transfer and mean profile development, part1-experimental data. *Trans. ASME J. Heat Trans.*: vol.105 33 - 40.
8. Blair, M. F. 1982. Influence of free-stream turbulence on turbulent boundary layer transition in favourable pressure gradients. *Trans. ASME J. Eng. for Power*: vol.104 743 - 750.
9. Blair, M.F. 1990. Boundary Layer Transition in Accelerating Flows with Intense Freestream Turbulence. submitted for pubilcation in J. Fluid Mech.
10. Blair, M. F. and Werle, M. J. 1981.Combined influence of free-stream turbulence and favourable pressure gradients on boundary layer transition and heat transfer. *United Tech. Research Centre*: Report R81-914388-17.
11. Bradshaw, P., Ferriss, D.H. and Atwell, N.P. 1967. Calculation of BoundaryLayer Development Using the Turbulent Energy Equation. *J. Fluid Mech.* vol. 28, p 593.
12. Chen, K. K. and Tyson, N. A. 1971. Extension to Emmons' Spot Theory to Flows on Blunt Bodies. *AIAA Jour.* vol 9, No. 5 pp. 821 825.
13. Chen, Y.S. and Kim, S.W. 1987. Computation of turbulent flows using an extended k - ε turbulence closure model, *NASA CR-179204.*
14. Clauser, F. H. 1954. Turbulent boundary layers in adverse pressure gradients. *J.Aero. Sci.*: vol. 21 91 - 108
15. Coles, D. E. and Hirst, E. A. 1968. Computation of turbulent boundary layers -1968 AFOSRIFP Stanford Conference, *Proc 1968 Conf. vol. 2 Stanford Univ., Stanford, Calif.*
16. Concentration, Heat and Momentum. 1995. *PHOENICS Training Course Notes.* CHAM TR/300
17. Coupland, J. 1995. Aerothermal Methods, Rolls Royce plc, PO Box 31, DERBY DE24 8BJ. Personal communication.
18. Das, D. K. 1987. A numerical study of turbulent separated flows. *ASME Forum on Turbulent Flows*, FED vol. 51, 85 - 88

19. Davidson, L. 1990. Calculation of the turbulent buoyancy-driven flow in a rectangular cavity using an efficient solver and two different low Reynolds number k - ε turbulence models, *Num. Heat Transfer*, Part A, Vol.18, p129.
20. Dey, J. and Narisimha, R. 1989. An extension of the Thwaites method for calculation of incompressible laminar boundary layers. *Jour. Indian Inst. Sci.* 1990, 70, 1 - 11.
21. Dhawan, S and Narisimha, R. 1958. Some properties of boundary layer flow during transition from laminar to turbulent flow. *Jour. of Fluid Mech.*, 3.
22. Dring, R. P. Joslyn, H. D. Hardin, L. W. and Wagner J.H. 1982. Turbine Rotor - Stator Interaction. *ASME* paper no. 82-GT-3
23. Dunham, J. 1972. Predictions of boundary layer transition on turbomachinery blades. *AGARD Meeting on Boundary Layers on Turbomachines.*
24. Emmons, H. W. 1951. The laminar - turbulent transition in a boundary layer - Part 1. *Jour. of Aero. Sci.* Vol. 18: 490 - 498
25. Fraser, C.J. 1978. *Boundary Layer Development From Transition Provoking Devices.* (PhD Thesis. University of Abertay Dundee)
26. Fraser, C. J. 1987. A local skin friction relation for turbulent boundary layers. *Int. Jour. of Mech. Eng. Ed.* Vol. 16: No.3: 197 - 206
27. Fraser, C. J., Higazy, M. G. and Milne, J. S. 1994. End-stage boundary layer transition models for engineering calculations. *Proc. Instn. Mech. Engrs. Vol 208, Part C: Jour. of Mech. Eng. Sci.*: 47-58.
28. Gardiner, I. D. 1987. *Transition in Boundary Layer Flows.* (PhD Thesis. University of Abertay Dundee)
29. Gosman, A. D. and Issa, R. I.1992. Post Experience Course in Computational Fluid Dynamics. Imperial College of Science Technology and Medicine, London. 16th - 18th November 1992
30. Gostelow, J.P, Blunden and Walker 1994 Effects of free-stream turbulence and adverse pressure gradients on boundary layer transition. *ASME Jour. of Turbo.* vol. 116, pp 392-404
31. Gostelow, J. P.. Hong, G., Walker, G. J. and Dey, J. 1994. Modelling of Boundary Layer Transition in Turbulent Flows by Linear Combination Integral Method. *ASME 94-GT-358.*
32. Gostelow, J. P.. Melwani, N. and Walker, G. J. 1995. Effects of Self-Similar Adverse Pressure Distribution on Turbulent Spot Development. *AIAA 26th Fluid Dynamics Conference*, San Diego.
33. Harlow, F.H. and Nakayama, P.I. 1968. Transport of turbulence energy decay rate, LA-3854, *Los Alamos Science Lab.*, U. California, USA.
34. Head, M.R. 1958. Entrainment in the Turbulent Boundary Layer, *Aero. Res. Council London.* R & M 3152
35. Herrero, J. et al. 1991. A near-wall k - ε formulation for high Prandtl number heat transfer, *Int.J.Heat Transfer*, Vol.34, No.3, p711.
36. Hernández, J. and Crespo, A. 1991. Parabolic and elliptic models of wind-turbine wakes. Application to the interaction between different wakes and turbines. *PHOENICS Jour. 1991/14.*

37. Hinze, J.O. 1975. *Turbulence: 2nd Edition.* New York: McGraw-Hill. p. 647
38. Holstein, H. and Bohlen, T 1940. Ein einfaches Verfahren zur Berechnung laminarer Reibungsschichten, die dem Näherungsverfahren von K. Pohlhausen genügen. *Lilenthal Ges. Luftfahrtforsch.* S-10 5 - 16
39. Hourmouziadis, J. 1989, Aerodynamic Design of Low Pressure Turbines, *AGARD Lecture Series* No. 167
40. Johnson, M. W. 1994. A Bypass Transition Model for Boundary Layers.Trans. *ASME, J of Turbo.*, vol 116 pp759-764
41. Kármán, T. von 1911. Über den Mechanismus des Widerstandes, den ein bewegter Körper in einer Flüssigkeit erzeugt. *Nachr. Ges. Wiss. Göttingen Math.-Phys.* Kl. II, p. 509 - 517, p. 547 - 556.
42. Lam, C.K.G. and Bremhorst, K. 1981. A modified form of the k-e model for predicting wall turbulence, *ASME J. Fluids Eng.*, Vol.103, p456.
43. Launder, B.E. and Spalding, D.B. 1972. *Lectures in mathematical models of turbulence.* Academic Press.
44. Launder, B.E and Spalding, D.B. 1974. The numerical computation of turbulent flow. *Comp. Meth. in App. Mech. and Eng.* Vol. 3 p269.
45. Madhav, M. 1996. Concentration, Heat and Momentum, Bakery House, 40 High Street, Wimbledon Village, London SW19 5AU Personal communication
46. Malin, M.R. 1995. Concentration, Heat and Momentum, Bakery House, 40 High Street, Wimbledon Village, London. SW19 5AU. Personal communication.
47. Markatos, N.C. 1984. The computation of thick axisymmetric boundary layers and wakes around bodies of revolution. *Proc. Instn. Mech. Engrs.* Vol 198C No.4: 51 - 62.
48. Mayle, R. E. 1991. The Role of Laminar - Turbulent Transition in Gas Turbine Engines. *Trans. ASME Jour. of Turbo.*, Vol. 113: 509-537
49. Morkovin, M. V. and Baltimore, M. D. 1958. Transition From Laminar to Turbulent Shear Flow - A Review of Some Recent Advances in Its Understanding. *Trans. ASME* 1958: 1121 - 1128.
50. Narasimha, R. 1957. On the Distribution of Intermittency in the Transition Region of the Boundary Layer. *J. Aero. Sc.* vol. 24, pp. 711-712
51. Narisimha, R. 1985. The laminar - turbulent transition zone in the boundary layer. *Prog. Aerospace Sci.* 22.
52. Olovsson, S. Löfdahl, L, and Olsson, E. 1985. Flow calculations in a turbine cascade using PHOENICS-BFC. *PHOENICS Journal 1985/47.*
53. Orr,W.M'F 1907. The stability or Instability of the Steady Motions of a Perfect Liquid and of a Viscous Liquid. *Proc. Roy. Irish Acad. Sect. A*, vol 27, pp 9-68, 69-138
54. Prandtl, L. 1925. Bericht über Untersuchungen zur ausgebildeten Turbulenz. *ZAAM* 5, 136
55. Rodi, W. 1980. Turbulence models and Their Application in Hydraulics - A Sate of the Art Review. IAHR, Delft, The Netherlands.
56. Roy, R. R. K. 1990. *A Primer on the Taguchi Method.* Van Nostrand Reinhold.

57. Savill, A. M. 1992.Predicting By-pass Transition with Turbulence Models, *11th Australasian Fluid Mechanics Conf.*, Hobart, pp. 949-952
58. Savill, A. M. 1993 Further Progress in the Turbulence Modelling of By-pass Transition, Engineering Turbulence Modelling and Experiments 2, W. Rodi and F. Martelli (Eds.) Elsevier, pp.583-592.
59. Seiger, K., Schiele, R., Kaufmann, F., Wittig, S. and Rodi, W. 1995. A Two-Layer Turbulence Model for the Calculation of Transitional Boundary Layers, *ERCOFTAC Bulltin* pp. 21-25 March 1995
60. Sharma, O. P. Wells, R. A. Schlinker, R. H. and Bailey D. A. 1982. Boundary Layer Development on Turbine Airfoil Suction Surfaces. *Trans. ASME* Vol. 104: 698 - 702
61. Schlichting, H., 1979. *Boundary-Layer Theory*, McGraw-Hill, New York
62. Singer, B. A. 1993. Modeling the Transition Region. *NASA Contractor Report 4492,* Contract NASI - 18240 Feb. 1993
63. Singer, B. A., Dinavahi, S. P. G. and Iyer, V. 1991. Testing of Transition Region Models: Test Cases and Data. *NASA Contractor Report 4371*, Contracts NASI 18240, NASI - 18599, and NASI - 18585 May 1991.
64. Smith, A. M. O. and Gamberoni, N. 1956. Transition, Pressure Gradient and Stability Theory. *Douglas Aircraft Company, Long Beach, Calif.* Rep. ES 26388.
65. Soloman, W. J., Walker, G. J., and Gostelow, J.P. 1995. Transition Length Prediction for Flows with Rapidly Changing Pressure Gradients. *International Gas Turbine Congress*, Houston, 1995.
66. Sommerfeld, A. 1908. Ein Beitrag zur hydrodynamischen Erklaerung der turbulenten Fluessigkeitsbewegungen. *Proc. Fourth Inter. Cong. Math.*, Rome, vol. III,pp 116-124
67. Spalding, D.B. 1969. The prediction of two-dimensional steady turbulent flows. *Imperial College Heat Transfer Section*, Rep EF/TN/A/16.
68. Taguchi, G. and Konishi, S. 1987. *Orthogonal Arrays and Linear Graphs.* American Supplier Institute, Inc., Dearborn Michigan.
69. Thomson, A. and Fraser, C.J. 1994. Taguchi Method in CFD. *Proc. PHOENICS European User Conference. 16th-18th Nov.1994.* Flowsolve Limited.
70. Thomson, A. 1996. Optimised Mixing of Air and Gas in a Slot. Ninth *Scottish Fluid Mechanics Meeting. University of Paisley*, 21st June 1996.
71. Thwaites, B. 1949. Approximate calculation of the laminar boundary layer. *Aero. Quart.* vol. 1: 245 - 280.
72. Van Dreist, E.R. and Blumer, C.B. 1963.Boundary Layer Transition, Free stream Turbulence and Pressure Gradiant Effects. *AIAA J.*, vol. 1 pp. 1303-1306
73. Van Ingen, J. L 1956. A Suggested Semi-Empirical Method for the calculation of the boundary layer transition region. *Univ. of Delft, Dept. of Aerosp. Eng., Delft, The Netherland*, Rep. VTH-74 1956..
74. Versteeg, H.K. and Malalasekera, W. 1995. *An introduction to computational fluid dynamics: the finite volume method*, Ch. 3. p41.
75. Wazzan, A. R., Gazley, Jr., and A. M. O. Smith 1979. Tollmien-Schlichting Waves and Transition, *Prog. Aerosp. Sci.* vol. 18, no. 2 pp 351-392

76. White, F. M. 1991. *Viscous Fluid Flow:*2nd Ed., New York: McGraw-Hill. p. 450 - 452, p. 268 - 270, p. 351.
77. White, F. M. 1974. *Viscous Fluid Flow:*1st Ed., New York: McGraw-Hill. p. 467.

Appendix A

```
' ******************************
' ** PROGRAM TRANSIT7.BAS **
' ******************************

COMMON SHARED relamdat, lamdat, m, n, no, rethetalts, aa, cfl, cf120, utot, bb
DECLARE SUB laminar (z, dz, l, uo, u, u2, nu, mu, delta1l, thetal)
DECLARE SUB turbulent (q, z, zt, dz, l, uo, u, u2, nu, mu, thetalts, delta1t,
thetat, cf120)

DEF FNderiv# (cf, h, thetat, dudz, u)
STATIC dtheta#
dthetat# = cf / 2 - (2 + h) * thetat * dudz / u
FNderiv# = dthetat#
END DEF

dl = 0: lamdaave = 0
gamma = 0: w = 0
b = TIMER
r = 0: aa = 1
't is freestream turbulence level
t = 1.2
nu = .0000151
mu = .0000151
REM STEP SIZE IN z ALONG PLATE
z = .01
dz = .01
REM FREESTREAM VELOCITY AT INLET
q = 0
REM LENGTH OF PLATE IN VELOCITY CALCULATION
l = 1.2
rethetas = 5

DEF fnvprof# (z, zt)
STATIC u#
u# = 18 * (1.146 - .146 * z / l): REM t=1.2:l=1.2
REM u# = 24.4 * (.775 + .225 * z / l): REM t=1.55 :l=1.2
REM u# = 22: REM t=1.25
REM u# = 36.17 - 3.116 * z
fnvprof# = u#
END DEF

FOR p = 1 TO 1000 * l

IF gamma > .999 GOTO 2
aa = 1
CALL laminar(z, dz, l, uo, u, u2, nu, mu, delta1l, thetal)
```

```
rethetal = fnvprof#(z, 0) * thetal / nu
m = thetal ^ 2 * (fnvprof#(z + dz, 0) - fnvprof#(z, 0)) / dz / nu

IF m > 0 THEN
g = 6.91 + 2.48 * m - 12.27 * m ^ 2
ELSE
g = 6.91 + 12.75 * m + 63.64 * m ^ 2
END IF

rethetas = .85 * (163 + EXP(g * (1 - t / 6.91)))

IF rethetal > rethetas THEN
' integrating lamda between x(G=0) to x(G=0.25)

IF gamma < .25 THEN
IF w = 0 THEN
rethetast = rethetas
END IF

aa = 0
dl = dl + dz
no = .04723 / (10 - EXP(1.7 - t / 2)) ^ 2

IF m = 0 THEN
n = no
ELSEIF m < 0 THEN
n = no * EXP(m * (1 - 55 * m ^ 2) * (2.6 * t + 3.6 * t ^ .5 - 86))
ELSE
n = no * EXP(-10 * m ^ .5) + 300 * m ^ 4: REM EQN 28
END IF

relamdati = (.411 * rethetast ^ 3 / n) ^ .5
lamdati = nu * relamdati / fnvprof#(z, 0)
z2 = z + dz
bb = 1
CALL laminar(z2, dz, l, uo, u, u2, nu, mu, delta112, thetal2)
bb = 0
rethetal2 = fnvprof#(z + dz, 0) * thetal2 / nu
m2 = thetal2 ^ 2 * (fnvprof#(z + 2 * dz, 0) - fnvprof#(z + dz, 0)) / dz / nu

IF m2 > 0 THEN
g = 6.91 + 2.48 * m2 - 12.27 * m2 ^ 2
ELSE
g = 6.91 + 12.75 * m2 + 63.64 * m2 ^ 2
END IF
```

```
no2 = .04723 / (10 - EXP(1.7 - t / 2)) ^ 2

IF m2 = 0 THEN
n2 = no2
ELSEIF m2 < 0 THEN
n2 = no2 * EXP(m2 * (1 - 55 * m2 ^ 2) * (2.6 * t + 3.6 * t ^ .5 - 86))
ELSE
n2 = no2 * EXP(-10 * m2 ^ .5) + 300 * m2 ^ 4
END IF

relamdat2 = (.411 * rethetast ^ 3 / n2) ^ .5
lamdat2 = nu * relamdat2 / fnvprof#(z + dz, 0)
lamdaave = lamdaave + (lamdati + lamdat2) / 2 * dz

lamdat = lamdaave / dl

IF w = 0 THEN
thetalts = thetal
relamdatst = (.411 * rethetast ^ 3 / n) ^ .5: REM EQN 18
lamdatst = nu * relamdatst / fnvprof#(z, 0)
w = 1
END IF

ELSE
' uncomment the next line if no averaging of lamda is wanted
'lamdat = lamdatst
END IF

END IF

IF w = 0 THEN
GOTO 1
END IF

2
CALL turbulent(q, z, zt, dz, l, uo, u, u2, nu, mu, thetalts, delta1t, thetat, cf120)

IF q = 1 THEN zs = z
gamma = 1 - EXP(-.411 * (z - zs) ^ 2 / lamdat ^ 2): REM EQN 10

IF gamma > 0 AND gamma < .999 THEN
delta1tr = (1 - gamma) * delta1l + gamma * delta1t: REM EQN 11
END IF

OPEN "c:\qb45\transitn\transit.txt" FOR APPEND AS #4
```

```
PRINT #4, USING "##.###^^^^_ "; z; gamma; cfl; cf120; (1 - gamma) * cfl +
gamma * cf120
CLOSE #4

1
z = z + dz
NEXT
CLOSE #1: CLOSE #2: CLOSE #3

END

SUB laminar (z, dz, l, uo, u, u2, nu, mu, delta1l, thetal)
i = ((fnvprof#(z, 0)) ^ 5 + (fnvprof#(z - dz, 0) ^ 5)) / 2 * dz

IF bb = 0 THEN
utot = utot + i
thetal = (.45 * nu * utot / fnvprof#(z, 0) ^ 6) ^ .5
ELSEIF bb = 1 THEN
utot2 = utot + i
thetal = (.45 * nu * utot2 / fnvprof#(z, 0) ^ 6) ^ .5
END IF

lamda = thetal ^ 2 * (fnvprof#(z + dz, 0) - fnvprof#(z, 0)) / dz / nu

IF lamda < -.09 THEN
PRINT : PRINT "flow has seperated"
lamda=-.089
END IF

shear = (lamda + .09) ^ .62
tau = mu * fnvprof#(z, 0) * shear / thetal
cfl = 2 * tau * nu / (mu * fnvprof#(z, 0) ^ 2)
zz = (.25 - lamda)
shape = 2! + 4.14 * zz - 83.5 * zz ^ 2 + 854 * zz ^ 3 - 3337 * zz ^ 4 + 4576
* zz ^ 5
delta1l = thetal * shape

IF aa = 1 THEN
OPEN "c:\qb45\transitn\laminar.txt" FOR APPEND AS #1
PRINT #1, USING "##.###^^^^_ "; z; lamda; shear; shape; thetal; delta1l; cfl
PRINT USING "##.###^^^^_ "; z; lamda; shear; shape; thetal; delta1l; cfl
CLOSE #1
aa = 1
END IF

END SUB
```

```
SUB turbulent (q, z, zt, dz, l, uo, u, u2, nu, mu, thetalts, deltalt, thetat, cf120)

q = q + 1
h = 5
kappa = .41

IF q = 1 THEN
zt = 0
'AB&S ZDP FLOWS PUT
'theta=.000001:cf=.1
'D&N ZDP FLOWS PUT
'theta=.00001:cf=.01

thetat = .000001
cf = .1
dudz = (fnvprof#(zt + dz, 0) - fnvprof#(zt, 0)) / dz
rethetat = fnvprof#(zt, 0) * thetat / nu
FOR J = 1 TO 20
f = cf * (LOG(rethetat) / LOG(10)) ^ (1.74 + .31 * h) - .3 * EXP(-1.33 * h)
df = cf * (LOG(rethetat) / LOG(10)) ^ (1.74 + .31 * h) * .31 * LOG(1.74 + .31 *
h) + (.3 * 1.33) * EXP(-1.33 * h)
h = h - f / df
NEXT
k1 = dz * FNderiv#(cf, h, thetat, dudz, fnvprof#(zt, 0))
k2 = dz * FNderiv#(cf, h, thetat + .5 * k1, dudz, fnvprof#(zt, 0))
k3 = dz * FNderiv#(cf, h, thetat + .5 * k2, dudz, fnvprof#(zt, 0))
k4 = dz * FNderiv#(cf, h, thetat + k3, dudz, fnvprof#(zt, 0))
thetat = thetat + 1 / 6 * (k1 + 2 * (k2 + k3) + k4)

OPEN "c:\qb45\transitn\turb.txt" FOR APPEND AS #2
PRINT #2, "ORIGIN OF TURBULENT B - L = "; z; "cf = "; cf; "thetat = "; thetat
PRINT #2, USING "##.###^^^^_ "; z; zt; thetat; h2 * thetat; cf120
CLOSE #2

DO
zt = zt + dz

IF dudz < 0 THEN
h2 = 5: REM for unfavourable dp
ELSE
h2 = 1: REM for favourable or zero dp
END IF

DO
```

```
cf120 = .3 * EXP(-1.33 * h2) / (LOG(fnvprof#(zt, 0) * thetat / nu) / LOG(10)) ^
(1.74 + .31 * h2)
beta = -2 * h2 * thetat * dudz / cf120 / fnvprof#(zt, 0)
'beta is a quadratic eqn in pi, with coefficients a, b & c.
a = 1: b = .76 / .42: c = -(.4 + beta) / .42
'the limit for beta is -0.7438 or it goes complex
'usually means bad first choice of h2
pi = (-b + (b ^ 2 - 4 * a * c) ^ .5) / 2
fpi = (2 + 3.179 * pi + 1.5 * pi ^ 2) / (kappa * (1 + pi))
lamda = (2 / cf120) ^ .5
h119 = lamda / (lamda - fpi)

IF dudz < 0 THEN

IF h2 > h119 THEN
h2 = h2 - .001
ELSE
a = 5
END IF

ELSE

IF h2 < h119 THEN
h2 = h2 + .001
ELSE
a = 5
END IF

END IF
LOOP UNTIL a = 5


OPEN "c:\qb45\transitn\turb.txt" FOR APPEND AS #2
PRINT #2, USING "##.###^^^^_ "; z; zt; thetat; h2 * thetat; cf120
CLOSE #2

k1 = dz * FNderiv#(cf120, h2, thetat, dudz, fnvprof#(zt, 0))
k2 = dz * FNderiv#(cf120, h2, thetat + .5 * k1, dudz, fnvprof#(zt, 0))
k3 = dz * FNderiv#(cf120, h2, thetat + .5 * k2, dudz, fnvprof#(zt, 0))
k4 = dz * FNderiv#(cf120, h2, thetat + k3, dudz, fnvprof#(zt, 0))
thetat = thetat + 1 / 6 * (k1 + 2 * (k2 + k3) + k4)
delta1t = thetat * h2
LOOP UNTIL thetat > thetalts / 4

z0 = zt
ELSE
```

```
zt = zt + dz
dudz = (fnvprof#(z + dz, 0) - fnvprof#(z, 0)) / dz
rethetat = fnvprof#(z, 0) * thetat / nu

IF dudz < 0 THEN
h2 = 5: REM for unfavourable dp
ELSE
h2 = 1: REM for favourable or zero dp
END IF

DO
cf120 = .3 * EXP(-1.33 * h2) / (LOG(fnvprof#(z, 0) * thetat / nu) / LOG(10)) ^
(1.74 + .31 * h2)
beta = -2 * h2 * thetat * dudz / cf120 / fnvprof#(z, 0)
'beta is a quadratic eqn in pi, with coefficients a, b & c.
a = 1: b = .76 / .42: c = -(.4 + beta) / .42
'the limit for beta is -0.7438 or it goes complex
'usually means bad first choice of h2
pi = (-b + (b ^ 2 - 4 * a * c) ^ .5) / 2
fpi = (2 + 3.179 * pi + 1.5 * pi ^ 2) / (kappa * (1 + pi))
lamda = (2 / cf120) ^ .5
h119 = lamda / (lamda - fpi)

IF dudz < 0 THEN

IF h2 > h119 THEN
h2 = h2 - .001
ELSE
a = 5
END IF

ELSE

IF h2 < h119 THEN
h2 = h2 + .001
ELSE
a = 5
END IF

END IF

LOOP UNTIL a = 5

IF h2 > 3 THEN
PRINT #1, "flow has separated"
CLOSE #1
```

```
END

END IF

h2 = (h2 + h119) / 2
delta1t = thetat * h2

OPEN "c:\qb45\transitn\turb.txt" FOR APPEND AS #2
PRINT #2, USING "##.###^^^^_ "; z; zt; thetat; h2 * thetat; cf120
CLOSE #2

k1 = dz * FNderiv#(cf120, h2, thetat, dudz, fnvprof#(zt, 0))
k2 = dz * FNderiv#(cf120, h2, thetat + .5 * k1, dudz, fnvprof#(zt, 0))
k3 = dz * FNderiv#(cf120, h2, thetat + .5 * k2, dudz, fnvprof#(zt, 0))
k4 = dz * FNderiv#(cf120, h2, thetat + k3, dudz, fnvprof#(zt, 0))
thetat = thetat + 1 / 6 * (k1 + 2 * (k2 + k3) + k4)

END IF

END SUB
```

```
' ******************************
' ** PROGRAM TRANSIT8.BAS **
' ******************************

' there is no integrating of lamda in this program
' incorporates new way of calculating turbulent boundary layer by bisection.

' SOLOMAN'S METHOD FOR ADVERSE DP

COMMON SHARED relamdat, lamdat, M, n, no, rethetalts, aa, cfl, cfT, utot, bb,
nu
COMMON SHARED kappa

DECLARE SUB laminar (z, dz, l, uo, u, u2, nu, mu, delta1l, thetal)
DECLARE SUB turbulent (h2l, u, dudz, thetat, h119l, cf120)

DEF FNderiv (cf, h, thetat, dudz, u)
   STATIC dtheta
   dthetat = cf / 2 - (2 + h) * thetat * dudz / u
   FNderiv = dthetat
END DEF

pi = 3.141593
INTEG1 = 0!: INTEG2 = 0!
kappa = .41
dl = 0: lamdaave = 0
gamma = 0: W = 0
bb = 0
r = 0: aa = 1
't is freestream turbulence level
t = 1.2
nu = .00001505#
mu = .00001816#
REM STEP SIZE IN z ALONG PLATE
z = 0!
dz = .01
REM FREESTREAM VELOCITY AT INLET
Q = 0
REM LENGTH OF PLATE IN VELOCITY CALCULATION
l = 1.2
rethetas = 5

DEF FNVPROF (z, zt)
STATIC u

' VELOCITY PROFILES IN HERE
```

```
    u = 18 * (1.146 - .146 * z / l): REM t=1.2:l=1.2
    REM u  = 24.4 * (.775 + .225 * z / l): REM t=1.55 :l=1.2
    REM u  = 22: REM t=1.25
    REM u  = 36.17 - 3.116 * z
    REM blair & werle, singer data flow 2 case 1
    REM zx = z * 1000 / 25.4
    REM u  = 14800 * (200 - zx) ^ -1.066
    REM blair & werle, singer data flow 2 case 2
    REM u  = 3780 * (83.3 - zx) ^ -1.075
    REM u  = u  * 12 * .0254
    FNVPROF = u
END DEF

FOR p = 1 TO 100 * l
z = z + dz

IF gamma > .999 GOTO 2
aa = 1
u = FNVPROF(z, 0)
CALL laminar(z, dz, l, uo, u, u2, nu, mu, delta1l, thetal)
M = thetal ^ 2 * (FNVPROF(z + dz, 0) - FNVPROF(z, 0)) / dz / nu
IF M > 0 THEN
g = 6.91 + 2.48 * M - 12.27 * M ^ 2
ELSE
g = 6.91 + 12.75 * M + 63.64 * M ^ 2
END IF

rethetal = FNVPROF(z, 0) * thetal / nu
rethetas = .85 * (163 + EXP(g * (1 - t / 6.91)))

IF W = 0 THEN
rethetast = rethetas
thetast = thetal
thetat = thetal / 4!
zs = z
mst = M
SIGMAST = .03 + (.1 / (.115 + EXP(42.9 * mst))): REM eqn 10
END IF

IF rethetal > rethetast THEN
IF W = 0 THEN
W = 1
GOTO 1
END IF
```

```
aa = 0
no = .04723 / (10 - EXP(1.7 - t / 2)) ^ 2: REM EQN 23

IF M = 0 THEN
n = no
ELSEIF M < 0 THEN
n = .00086 * EXP(2.134 * mst * LOG(t) - 59.23 * mst - .564 * LOG(t))
alpha = 4 + (22.14 / (.79 + 2.72 * EXP(47.63 * M))): REM eqn 9
SIGMA = .03 + (.1 / (.115 + EXP(42.9 * M))): REM eqn 10
smalln = n * nu / (SIGMAST * thetast ^ 3): REM eqn 3
ELSE
n = no * EXP(-10 * mst ^ .5) + 300 * mst ^ 4: REM EQN 28
relamdat = (.411 * rethetast ^ 3 / n) ^ .5
lamdat = nu * relamdat / FNVPROF(zs, 0)
END IF

IF z > zs AND M < 0 THEN
z2 = z - dz
bb = 1
CALL laminar(z2, dz, l, uo, u, u2, nu, mu, delta112, THETAL2)
bb = 0
M1 = THETAL2 ^ 2 * (FNVPROF(z, 0) - FNVPROF(z - dz, 0)) / dz / nu
alpha1 = 4 + (22.14 / (.79 + 2.72 * EXP(47.63 * M1)))
sigma1 = .03 + (.1 / (.115 + EXP(42.9 * M1)))
END IF

END IF

IF z > zs THEN

IF M < 0 THEN
alpha = alpha * pi / 180
alpha1 = alpha1 * pi / 180
save = (SIGMA + sigma1) / 2
aave = (TAN(alpha) + TAN(alpha1)) / 2
vave = (FNVPROF(z, 0) + FNVPROF(z - dz, 0)) / 2
INTEG1 = INTEG1 + dz * save / (aave * vave)
INTEG2 = INTEG2 + dz * aave
gamma = 1 - EXP(-smalln * INTEG1 * INTEG2)
ELSE
gamma = 1 - EXP(-.411 * (z - zs) ^ 2 / lamdat ^ 2)
END IF

END IF

2
```

```
h2l = 1
h2u = 3.5
' e IS THE ACCEPTABLE ERROR
e = .0001
iter = 1 + (LOG((ABS(h2l - h2u)) / e) / LOG(2))

FOR tt = 1 TO iter
dudz = (FNVPROF(z + dz, 0) - FNVPROF(z, 0)) / dz
CALL turbulent(h2l, FNVPROF(z, 0), dudz, thetat, h119l, cf120)
CALL turbulent(h2u, FNVPROF(z, 0), dudz, thetat, h119u, cf120)
h2m = (h2l + h2u) / 2
CALL turbulent(h2m, FNVPROF(z, 0), dudz, thetat, h119m, cf120)

IF h119l - h2l > 0 AND h119m - h2m < 0 THEN
h2u = h2m
ELSE
h2l = h2m
END IF

NEXT

OPEN "c:\qb45\transitn\turb.txt" FOR APPEND AS #2
PRINT #2, USING "##.###^^^^_ "; z; h2m; thetat; h2m * thetat; cf120
CLOSE #2

thetat = thetat + dz * (cf120 / 2 - (2 + h2m) * thetat * dudz / FNVPROF(z,
0))

IF gamma > 0 AND gamma < .999 THEN
delta1tr = (1 - gamma) * delta1l + gamma * delta1t
END IF

OPEN "c:\qb45\transitn\trans.txt" FOR APPEND AS #4
PRINT #4, USING "##.###^^^^_ "; z; gamma
CLOSE #4

1
NEXT
CLOSE #1: CLOSE #2: CLOSE #3
END


SUB laminar (z, dz, l, uo, u, u2, nu, mu, delta1l, thetal)
i = ((FNVPROF(z, 0)) ^ 5 + (FNVPROF(z - dz, 0) ^ 5)) / 2 * dz
```

```
IF bb = 0 THEN
utot = utot + i
thetal = (.45 * nu * utot / FNVPROF(z, 0) ^ 6) ^ .5
ELSEIF bb = 1 THEN
utot2 = utot - i
thetal = (.45 * nu * utot2 / FNVPROF(0, 0) ^ 6) ^ .5
END IF

lamda = thetal ^ 2 * (FNVPROF(z + dz, 0) - FNVPROF(z, 0)) / dz / nu

IF lamda < -.09 THEN
PRINT : PRINT "flow has seperated"
lamda=-.089
END IF

shear = (lamda + .09) ^ .62
tau = mu * FNVPROF(z, 0) * shear / thetal
cfl = 2 * tau * nu / (mu * FNVPROF(z, 0) ^ 2)

IF lamda < .25 THEN
zz = (.25 - lamda)
shape = 2! + 4.14 * zz - 83.5 * zz ^ 2 + 854 * zz ^ 3 - 3337 * zz ^ 4 + 4576
* zz ^ 5
ELSE
shape = 1.431 * lamda ^ -.2155
END IF

delta11 = thetal * shape

IF aa = 1 THEN
OPEN "c:\qb45\transitn\laminar.txt" FOR APPEND AS #1
PRINT #1, USING "##.###^^^^_ "; z; lamda; shear; shape; thetal; delta11; cfl
PRINT USING "##.###^^^^_ "; z; lamda; shear; shape; thetal; delta11; cfl
CLOSE #1
aa = 1
END IF

END SUB


SUB turbulent (h2, u, dudz, thetat, h119new, cf120)
cf120 = .3 * EXP(-1.33 * h2) / (LOG(u * thetat / nu) / LOG(10)) ^ (1.74 + .31
* h2)
beta = -2 * h2 * thetat * dudz / cf120 / u
a = 1: b = .76 / .42: c = -(.4 + beta) / .42
pi = (-b + (b ^ 2 - 4 * a * c) ^ .5) / 2
```

```
fpi = (2 + 3.179 * pi + 1.5 * pi ^ 2) / (kappa * (1 + pi))
lamda = (2 / cf120) ^ .5
h119new = lamda / (lamda - fpi)
END SUB
```

Appendix B

```
C FILE NAME GROUND.FTN--------------------------------011093
C     LAST MODIFIED 25/6/95
C
C     ********************************
C     ** POST PROCESSING MODEL **
C     ********************************
C
C
++++++++++++++++++++++++++++++++++++++++++++++++++++++++++++++
+++
C     ++ FOR BFC'S ONLY, Z-X PLANE, Z - MAJOR FLOW DIRECTION ++
C     ++ FRASER'S METHOD FOR B-L TRANSITIONAL PARAMETERS     ++
C
++++++++++++++++++++++++++++++++++++++++++++++++++++++++++++++
+++
C
C     IG(1) IS THE START START Z SLAB + 1
C     IG(2) IS THE END Z SLAB + 1
C     IG(3) IS THE NORTH IX CELL WHERE THE FREESTREAM VELOCITY IS REQUIRED
C     RG(1) IS KINEMATIC VISCOSITY
C     RG(2) IS TURBULENCE INTENSITY (%)
C     RG(3) IS A DIVISOR OF THETAL AT THE ORIGIN OF THE TURBULENT
C          BOUNDARY LAYER, I.E. THETAT=THETAL/RG(3)
C     SCALERS C1, C2, C3, C4 ARE NOT USED
C     SCALER C5   LAMINAR MOMENTUM THICKNESS
C     SCALER C6   LAMINAR DISPLACEMENT THICKNESS
C     SCALER C7   LAMINAR SKIN FRICTION
C     SCALER C8   INTERMITTENCY
C     SCALER C9   TURBULENT DISPLACEMENT THICKNESS
C     SCALER C10  TURBULENT SKIN FRICTION
C     SCALER C11  TRANSITIONAL DISPLACEMENT THICKNESS
C     SCALER C12  TRANSITIONAL SKIN FRICTION

      SUBROUTINE GROUND
      INCLUDE '\d_phoe20\d_includ\satear'
      INCLUDE '\d_phoe20\d_includ\grdloc'
      INCLUDE '\d_phoe20\d_includ\grdear'
      INCLUDE '\d_phoe20\d_includ\grdbfc'
CXXXXXXXXXXXXXXXXXXXXXXXXXXXXXXXXXXXXXXXX USER SECTION STARTS:
C
C 1   Set dimensions of data-for-GROUND arrays here. WARNING: the
C     corresponding arrays in the MAIN program of the satellite
C     and EARTH must have the same dimensions.
      PARAMETER (NLG=100, NIG=200, NRG=200, NCG=100)
C
      COMMON/LGRND/LG(NLG)/IGRND/IG(NIG)/RGRND/RG(NRG)/CGRND/CG(NCG)
```

```
      LOGICAL LG
      CHARACTER*4 CG
      REAL NU,M,M2,N,NO,NO2,N2,LAMDAT1,LAMDAT2,LAMDAT,LAMDAAVE
      INTEGER GNX,GITER
      COMMON /PARAM1/NU,IBB,IW
      COMMON /PARAM2/IGQ,GNX,THETAT,TDIV
      SAVE
C
C 2   User dimensions own arrays here, for example:
C     DIMENSION GUH(10,10),GUC(10,10),GUX(10,10),GUZ(10)
      DIMENSION GBFCX(300,300),GBFCZ(300,300)
C
C 3   User places his data statements here, for example:
C     DATA NXDIM,NYDIM/10,10/
      DATA WTOT,WTOT2,TDIST,SURFDIST/0.0,0.0,0.0,0.0/
      DATA THETAT/0.0/
C
C 4   Insert own coding below as desired, guided by GREX examples.
C     Note that the satellite-to-GREX special data in the labelled
C     COMMONs /RSG/, /ISG/, /LSG/ and /CSG/ can be included and
C     used below but the user must check GREX for any conflicting
C     uses. The same comment applies to the EARTH-spare working
C     arrays EASP1, EASP2,....EASP20. In addition to the EASPs,
C     there are 10 GRound-earth SPare arrays, GRSP1,...,GRSP10,
C     supplied solely for the user, which are not used by GREX. If
C     the call to GREX has been deactivated then all of the arrays
C     may be used without reservation.
C
c*************************************************************************
c
      IXL=IABS(IXL)
      IF(IGR.EQ.13) GO TO 13
      IF(IGR.EQ.19) GO TO 19
      GO TO (1,2,3,4,5,6,25,8,9,10,11,12,13,14,25,25,25,25,19,20,25,
     125,23,24),IGR
   25 CONTINUE
      RETURN
C*************************************************************************
C
C---  GROUP 1. Run title and other preliminaries
C
    1 GO TO (1001,1002),ISC
 1001 CONTINUE
      WTOT=0.
      IGQ=0
      NU=RG(1)
```

```
      GTURIN=RG(2)
      TDIV=RG(3)
      WRITE(14,*)'GROUP 1'
      CALL MAKE(XG2D)
      CALL MAKE(ZGNZ)
      call make(DXG2D)
      CALL MAKE(DZGNZ)

C
C     User may here change message transmitted to the VDU screen
      IF(IGR.EQ.1.AND.ISC.EQ.1.AND..NOT.NULLPR)
     1  CALL WRYT40('GROUND file is GROUND.F    of:     020395 ')

      RETURN
 1002 CONTINUE
      RETURN

C*********************************************************************
C* Make changes to data for GROUPS 15, 16, 17, 18  GROUP 19.
C*********************************************************************
C
C--- GROUP 19. Special calls to GROUND from EARTH
C
   19 GO TO (191,192,193,194,195,196,197,198,199,1910),ISC
  191 CONTINUE
C   * -------------------- SECTION 1 ---- Start of time step.
      RETURN
  192 CONTINUE
C   * -------------------- SECTION 2 ---- Start of sweep.

      RETURN
  193 CONTINUE
C   * -------------------- SECTION 3 ---- Start of iz slab.
      RETURN
  194 CONTINUE
C   * -------------------- SECTION 4 ---- Start of iterations over
slab.
      RETURN
  199 CONTINUE
C   * -------------------- SECTION 9 ---- Start of solution sequence
for
C                                            a variable
      RETURN
 1910 CONTINUE
C   * -------------------- SECTION 10---- Finish of solution sequence
for
```

```
C                                                       a variable
      RETURN
  195 CONTINUE
C   * -------------------- SECTION 5 ---- Finish of iterations over
slab.
      RETURN
  196 CONTINUE
C   * -------------------- SECTION 6 ---- Finish of iz slab.

      LOU1=LOF(U1)
      LOX=LOF(XG2D)
      LOW1=LOF(W1)
      LOWL=LOF(LOW(W1))
      LOWH=LOF(HIGH(W1))
      LOWH2=LOF(ANYZ(W1,(IZ+2)))
      LOD1=LOF(DEN1)

C     STORES LAMINAR MOMENTUM THICKNESS,DISP THICKNESS, CFL
      LOC5=LOF(C5)
      LOC6=LOF(C6)
      LOC7=LOF(C7)

C     STORES TURBULENT DISP THICKNESS, SKIN FRICTION
      LOC9=LOF(C9)
      LOC10=LOF(C10)

c     STORES TRANSITIONAL DISP THICKNESS, CF,gamma
      LOC11=LOF(C11)
      LOC12=LOF(C12)
      LOC8=LOF(C8)
      IF(ISWEEP.EQ.(LSWEEP-1)) THEN

C     GETS CARTESIAN COMPONENTS OF VELOCITY

      CALL GETCAR

      LOUCRTL=LOF(LOW(LBNAME('UCRT')))
      LOUCRT=LOF(LBNAME('UCRT'))
      LOUCRTH=LOF(HIGH(LBNAME('UCRT')))
      LOUCRTH2=LOF(ANYZ(LBNAME('UCRT'),(IZ+2)))
      LOWCRTL=LOF(LOW(LBNAME('WCRT')))
      LOWCRT=LOF(LBNAME('WCRT'))
      LOWCRTH=LOF(HIGH(LBNAME('WCRT')))
      LOWCRTH2=LOF(ANYZ(LBNAME('WCRT'),(IZ+2)))

C     IG(1) IS THE START START SLAB + 1:IG(2) IS THE END SLAB + 1
```

```
      IF(IZ.GT.IG(1).AND.IZ.LT.IG(2)) THEN

      DO IY=1,NY
      DO IX =1,NX
      GNX=NX

C     IG(3) IS THE NORTH IX CELL WHERE THE FREESTREAM VELOCITY IS REQUIRED

      if (iX.eq.IG(3)) then
C
C     CALCULATE ABSOLUTE VELOCITY MAGNITUDE USING CARTESIAN COMPONENTS
C     UCRT AND WCRT.
C
      W=SQRT(F(LOUCRT+IX)**2+F(LOWCRT+IX)**2)
      WLOW=SQRT(F(LOUCRTL+IX)**2+F(LOWCRTL+IX)**2)
      WHIGH=SQRT(F(LOUCRTH+IX)**2+F(LOWCRTH+IX)**2)
      WHIGH2=SQRT(F(LOUCRTH2+IX)**2+F(LOWCRTH2+IX)**2)

C     X AND Z CO-ORDINATES OF CURRENT IZ SLAB
      CALL GTIZYX(XP,IZ,GBFCX,300,300)
      CALL GTIZYX(ZP,IZ,GBFCZ,300,300)
      GX=GBFCX(IY,IX)
      GZ=GBFCZ(IY,IX)

C     X AND Z CO-ORDINATES OF IZ+1 SLAB
      CALL GTIZYX(XP,IZ+1,GBFCX,300,300)
      CALL GTIZYX(ZP,IZ+1,GBFCZ,300,300)
      GXN=GBFCX(IY,IX)
      GZH=GBFCZ(IY,IX)

C     X AND Z CO-ORDINATES OF IZ+2 SLAB
      CALL GTIZYX(XP,IZ+2,GBFCX,300,300)
      CALL GTIZYX(ZP,IZ+2,GBFCZ,300,300)
      GXN2=GBFCX(IY,IX)
      GZH2=GBFCZ(IY,IX)

C     THIS IS A PSEUDO DZ IT IS THE SURFACE DISTANCE ALONG THE PLATE
      DZ=SQRT((GXN-GX)**2+(GZH-GZ)**2)
      DZ2=SQRT((GXN2-GXN)**2+(GZH2-GZH)**2)

      GRHO=F(LOD1+IX)

c     correction for surface distance

      IF(IZ.EQ.IG(1)+1) THEN
```

```
      DZI=DZ

      IF(IX.EQ.IG(3))THEN
      SURFDIST=-DZI
      ENDIF

      ENDIF

c     set variables to zero

      IF(IZ.EQ.IG(1)+1) THEN
      IW=0
      IGQ=0
      RETHETAST=0.0
      GAMMA=0.0
      DELTA1T=0.0
      DELTA1L=0.0
      DL=0.0
      ENDIF

      IF(GAMMA.GT.0.999) THEN
      h2l = 1.
      h2u = 3.5

C      e IS THE ACCEPTABLE ERROR
      e = .0001
      GIter = 1 + (ALOG10((h2U - h2L) / e) / ALOG10(2.))
      DO KZ=1,Giter
      CALL TURBULENT(h2l, GRHO,WLOW,W,WHIGH,DZ,CF120,H119L)
      CALL TURBULENT(h2u, GRHO,WLOW,W,WHIGH,DZ,CF120,H119U)
      h2m = (h2l + h2u) / 2.
      CALL TURBULENT(h2m, GRHO,WLOW,W,WHIGH,DZ,CF120,H119M)

      IF( (h119l - h2l).GT.0.0.AND. (h119m - h2m).LT.0.0) THEN
      h2u = h2m
      ELSE
      h2l = h2m
      END IF

      END DO

      DWZ=(WHIGH-W)/DZ
      DELTA1T=H119M*THETAT
      thetat = thetat + dz * (cf120/2. - (2. + h119m) * thetat * dWz /W)

C     TURBULENT ONLY ANALYSIS
```

```
      F(LOC9+IX)=DELTA1T
      F(LOC10+IX)=CF120

C     TRANSITIONAL ANALYSIS
      F(LOC11+IX)=DELTA1T
      F(LOC12+IX)=CF120
      F(LOC8+IX)=1.

C     END OF TURBULENT ONLY B - L

      ELSE

C     LAMINAR & TRANSITIONAL B - L

      IBB=0

      call laminar (GRHO,WLOW,W,WHIGH,DZ, delta1l, thetal,cfl)

C     SCALERS TO STORE LAMINAR PROPERTIES
      F(LOC5+IX)=THETAL
      F(LOC6+IX)=DELTA1L
      F(LOC7+IX)=CFL

      rethetal = W * thetal / nu
      m = thetal ** 2 * (WHIGH - W) / DZ / nu

      IF( m.gt.0.0 ) THEN
      g = 6.91 + 2.48 * m - 12.27 * m ** 2
      ELSE
      g = 6.91 + 12.75 * m + 63.64 * m ** 2
      END IF

      rethetas = .85 * (163. + EXP(g * (1 - RG(2) / 6.91)))
      SURFDIST=SURFDIST+DZ

      IF(rethetal.gt.rethetas) THEN
c     integrating lamda between x(G=0) to x(G=0.25)

      IF( gamma.lt.0.25 )THEN

      IF( iw .EQ.0 )THEN
      THETAT=THETAL/TDIV
      RETHETAST=RETHETAS
      TRSTART=SURFDIST
      DL=0.
      LAMDAAVE=0.
```

```
      IW=1
      END IF

      aa = 0
      dl = dl + DZ
      no = .04723 / (10. - EXP(1.7 - RG(2)/ 2.)) ** 2

      IF( m.eq.0.0 ) THEN
      n = no
      ELSE IF( m.lt.0.0) THEN
      n = no * EXP(m * (1. - 55. * m ** 2) * (2.6 * RG(2) + 3.6 * RG(2)
     + ** .5 - 86.))
      ELSE
      n = no * EXP(-10. * m ** .5) + 300. * m ** 4
      END IF

      relamdati = (.411 * rethetast ** 3 / n) ** .5
      lamdati = nu * relamdati / W
      ibb = 1
      call laminar (GRHO,W,WHIGH,WHIGH2,DZ2, delta112, thetal2,cf12)
      ibb = 0
      rethetal2 = WHIGH2 * thetal2 / nu
      m2 = thetal2 ** 2 * (WHIGH2 - WHIGH) / DZ2 / nu
      no2 = .04723 / (10. - EXP(1.7 - RG(2)/ 2.)) ** 2

      IF( m2.eq.0.0 )THEN
      n2 = no2
      ELSE IF( m2.lt.0.0 )THEN
      n2 = no2 * EXP(m2 * (1. - 55. * m2 ** 2) * (2.6 * RG(2) + 3.6 *
     + RG(2) ** .5 - 86.))
      ELSE
      n2 = no2 * EXP(-10. * m2 ** .5) + 300. * m2 ** 4
      END IF

      relamdat2 = (.411 * rethetast ** 3 / n2) ** .5
      lamdat2 = nu * relamdat2 / WHIGH
      lamdaave = lamdaave + (lamdati + lamdat2) / 2. * DZ
      lamdat = lamdaave / dl
      iw = 1
      ELSE
C     END OF GAMMA .LT. 0.25 LOOP
      END IF

      h2l = 1.
      h2u = 3.5
C     e IS THE ACCEPTABLE ERROR
```

```
      e = .0001
      GIter = 1 + (ALOG10((h2U - h2L) / e) / ALOG10(2.))
      DO KZ=1,GIter
      CALL TURBULENT(h2l, GRHO,WLOW,W,WHIGH,DZ,CF120,H119L)
      CALL TURBULENT(h2u, GRHO,WLOW,W,WHIGH,DZ,CF120,H119U)
      h2m = (h2l + h2u) / 2
      CALL TURBULENT(h2m, GRHO,WLOW,W,WHIGH,DZ,CF120,H119M)

      IF( (h119l - h2l).GT.0.0.AND. (h119m - h2m).LT.0.0) THEN
      h2u = h2m
      ELSE
      h2l = h2m
      END IF
      END DO

      DWZ=(WHIGH-W)/DZ
      DELTA1T=H119M*THETAT
      F(LOC9+IX)=DELTA1T
      thetat = thetat + dz * (cf120/2. - (2. + h119m) * thetat * dWz /W)
      F(LOC10+IX)=CF120
      gamma = 1. - EXP(-.411*(SURFDIST-TRSTART)**2/lamdat ** 2)

C     END OF rethetal.gt.rethetas LOOP
      END IF

C     STORE TRANSITIONAL DELTA1 AND CF IN SCALERS C11 AND C12
C     AND GAMMA IN C8

      F(LOC11+IX) = (1 - gamma) * F(LOC6+IX) + gamma * F(LOC9+IX)
      F(LOC12+IX) = (1 - gamma) * F(LOC7+IX) + gamma * F(LOC10+IX)
      F(LOC8+IX) = GAMMA

      WLOW=0.
      W=0.
      WHIGH=0.

C     END OF GAMMA.GT.0.99 LOOP
      ENDIF

C     END OF IG(3) LOOP

      end if
c     end of ix loop
      END DO
c     end of iy loop
      END DO
```

```
C     end of iz loop
      ENDIF
C     end of lsweep loop
      ENDIF


      RETURN
  197 CONTINUE
C   * -------------------- SECTION 7 ---- Finish of sweep.
      RETURN
  198 CONTINUE
C   * -------------------- SECTION 8 ---- Finish of time step.
C
      RETURN
C*****************************************************************
```

```
C     PLACED AFTER END OF SUBROUTINE GROUND

      SUBROUTINE laminar(GRHO,WLOW,W,WHIGH,DZ,delta11,thetal,cfl)

      COMMON /PARAM1/NU,IBB,IW

      INTEGER AA
      REAL lamda,NU
      SAVE WTOT,WTOT2
      DATA WTOT,WTOT2/2*0.0/

C     integrating W**5

      R = (W ** 5 + WLOW ** 5) / 2. * DZ

      IF( ibb.eq.0 ) THEN
      WTOT = WTOT + R
      thetal = (.45 * NU* WTOT / W ** 6) ** .5
      ELSE IF( ibb.EQ.1) THEN
      WTOT2 = WTOT + R
      thetal = (.45 * NU * WTOT2 / WHIGH ** 6) ** .5
      END IF

      lamda = thetal ** 2 * (WHIGH - W) / DZ / NU

      IF( lamda.lt.-0.09 ) THEN
```

```
      write(14,*) 'flow has sepArated'
      LAMDA=-0.089
      END IF

      shear = (lamda + .09) ** .62
C     shear stress
      tau = NU*GRH0 * W * shear / thetal
      cfl = 2. * tau  / (GRH0* W ** 2)
      zz = (.25 - lamda)
      shape = 2.0 + 4.14 * zz - 83.5 * zz ** 2 + 854 * zz ** 3 - 3337 *
     +zz ** 4 + 4576 * zz ** 5
      delta1l = thetal * shape
    6 CONTINUE
      RETURN
      END



      SUBROUTINE turbulent (H2,GRH0,WLOW,W,WHIGH,DZ,cf120,H119N)

      COMMON /PARAM1/ NU,WTOT,WTOT2
      COMMON /PARAM2/IGQ,GNX,THETAT,TDIV

      integer aa,GNX
      REAL kappa,lamda,nu
      DATA KAPPA/0.41/
      DWZ=(WHIGH-W)/DZ


c     CALCULATE SKIN FRICTION FROM EQUATION 6-120

      cf120 = .3 * EXP(-1.33 * h2) / ALOG10(w * thetat / nu)
     + ** (1.74 + .31 * h2)

c     USED GUESSED h2 AND CALCULATED cf120 TO CALCULATE PI VIA EQN 6-122
c     in favourable dp beta will be -ve
      beta = -2 * h2 * thetat * dwz / cf120 / w

c     beta is a quadratic eqn in pi, with coefficients a, b & c.
      a = 1
      b = .76 / .42
      c = -(.4 + beta) / .42

C     FIND pi EQN 6-121
      pi = (-b + (b ** 2 - 4. * a * c) ** .5) / 2.
```

```
c     FUNCTION OF PI REQUIRED IN 6-119 (a)

      fpi = (2 + 3.179 * pi + 1.5 * pi ** 2) / (kappa * (1 + pi))

c     USE EQUATION 6-119(a) WITH CALCULATED pi TO CALCULATE NEW h2 (h119)

      lamda = (2 / cf120) ** .5
      h119n = lamda / (lamda - fpi)
      RETURN
      END
```

```
C FILE NAME GROUND.FTN--------------------------------011093
C     LAST MODIFIED 03/02/96
C     ****************************************************************
C     ** MOMENTUM SINK CORRELATION BOUNDARY LAYER MODEL **
C     ****************************************************************
C
C     FRASER'S METHOD FOR adverse & FAVOURABLE DP
C
C     SOLOMAN'S METHOD HAS BEEN CODED, BUT COMMENTED OUT
C
C     START OF TRANSITION VARIABLES ARE STORED IN ARRAYS.
C
C     TURBULENCE MODEL INCLUDED IN GROUP 19
C     TURBULENT INTENSITY DECAY BEHIND A GRID, according to M. Malin, CHAM
C     PUT TU FOR START OF TRANSITION = 1/z*integral tu dz
C     TU FOR TRANSITION LENGTH = TUINLET

C     RG(2) IS TURBULENCE INTENSITY AT INLET (%)
C     RG(3) IS A DIVISOR OF THETAL AT THE ORIGIN OF THE TURBULENTBOUNDARY
C           LAYER, I.E. THETAT=THETAL/RG(3)
C     RG(5) IS THE VELOCITY (W1) AT INLET

C     SCALER C1 - TURBULENCE INTENSITY
C     SCALER C2 - INTEGRATING W1
C     SCALER C3 - KINETIC ENERGY
C     SCALER C4 - SUM OF (TU*CELL LENGTH)
C     SCALER C5 - CHANGED TO DISTANCE FROM INLET TO CURRENT HIGH OF
CELL
C                 HENCE AVERAGE TU = C4/C5
C     SCALER C6 - FLOW HEIGHT / DELTA
C     SCALER C7 - WTOT
C     SCALER C8 - GAMMA
C     SCALER C9 - TURBULENT MOMENTUM THICKNESS
C     SCALER C10 - SURFACE DISTANCE FROM LEADING EDGE
C     SCALER C11 - MACH NUMBER
C     SCALER C12 - SKIN FRICTION

      SUBROUTINE GROUND
      INCLUDE '\d_phoe21\d_includ\satear'
      INCLUDE '\d_phoe21\d_includ\grdloc'
      INCLUDE '\d_phoe21\d_includ\grdear'
      INCLUDE '\d_phoe21\d_includ\grdbfc'

CXXXXXXXXXXXXXXXXXXXXXXXXXXXXXXXXXXXXXXXX USER SECTION STARTS:
C
C 1   Set dimensions of data-for-GROUND arrays here. WARNING: the
```

```
C     corresponding arrays in the MAIN program of the satellite
C     and EARTH must have the same dimensions.
      PARAMETER (NLG=100, NIG=200, NRG=200, NCG=100)
      PARAMETER (MX = 500)
C
      COMMON/LGRND/LG(NLG)/IGRND/IG(NIG)/RGRND/RG(NRG)/CGRND/CG(NCG)
      LOGICAL LG
      CHARACTER*4 CG
      INTEGER GWW,GW

      REAL MH,MOLD,N,NO,NOH,NH,LAMDATI,LAMDATH,LAMDATW(MX),LAMDAAVE(MX)
      real mw
      REAL INTEG1W,INTEG2W,ML,MSTW(MX),MST,MOLDW,INTEG1,INTEG2

      INTEGER GNX,GITER

      COMMON /TURC/TDIV
C     WEST WALL

      COMMON /LAM/IBBW,WW,THETALW,THETAL2W,THETALLW
      COMMON /TUR/DSW

C     EAST WALL

      COMMON /LAM2/IBB,W
      COMMON /TUR2/DWZ

C     EAST WALL

      SAVE RETHETAST,LAMDAAVE,lamdat,TRSTART,IW,H119M
      SAVE MST,SIGMAST,THETAST,INTEG1,INTEG2,dl
      save m

C     WEST WALL

      SAVE RETHETASTW,LAMDAAVEW,LAMDATW,TRSTARTW,IWW,mw
      SAVE MSTW,SIGMASTW,THETASTW,INTEG1W,INTEG2W,dlw

      SAVE GKIN,GEPIN,SUMW,SD
C
C 2   User dimensions own arrays here, for example:
C     DIMENSION GUH(10,10),GUC(10,10),GUX(10,10),GUZ(10)

      DIMENSION GHEIGHT(100,100),TRST(MX),IWW(MX),RETHETASTW(MX)
      DIMENSION DLW(MX),IA(MX)
C
```

```
C 3   User places his data statements here, for example:
C     DATA NXDIM,NYDIM/10,10/
      DATA PI,M/3.14159,0.0/
      DATA GAMMA /0./
      DATA (TRST(I),I=1,MX) /MX*0./
      DATA (IWW(I),I=1,MX) / MX*0/
      DATA (RETHETASTW(I),I=1,MX) /MX*0./
      DATA (MSTW(I),I=1,MX) /MX*0./
      DATA (LAMDAAVE(I),I=1,MX) /MX*0./
      DATA (LAMDATW(I),I=1,MX) /MX*0./
      DATA (DLW(I),I=1,MX) /MX*0./
      DATA (IA(I),I=1,MX) /MX*0/
      DATA KK,SD,SUMW/0,0.0,0.0/
C
C 4   Insert own coding below as desired, guided by GREX examples.
C     Note that the satellite-to-GREX special data in the labelled
C     COMMONs /RSG/, /ISG/, /LSG/ and /CSG/ can be included and
C     used below but the user must check GREX for any conflicting
C     uses. The same comment applies to the EARTH-spare working
C     arrays EASP1, EASP2,....EASP20. In addition to the EASPs,
C     there are 10 GRound-earth SPare arrays, GRSP1,...,GRSP10,
C     supplied solely for the user, which are not used by GREX. If
C     the call to GREX has been deactivated then all of the arrays
C     may be used without reservation.

c**************************************************************************
c
      IXL=IABS(IXL)
      IF(IGR.EQ.13) GO TO 13
      IF(IGR.EQ.19) GO TO 19
      GO TO (1,2,3,4,5,6,25,8,9,10,11,12,13,14,25,25,25,25,19,20,25,
     125,23,24),IGR
   25 CONTINUE
      RETURN
C**************************************************************************
C
C--- GROUP 1. Run title and other preliminaries
C
    1 GO TO (1001,1002),ISC
 1001 CONTINUE
C
      CALL MAKE(APROJH)
      TDIV=RG(3)
C     User may here change message transmitted to the VDU screen
      IF(IGR.EQ.1.AND.ISC.EQ.1.AND..NOT.NULLPR)
     1  CALL WRYT40('GROUND file is GROUND.F    of:     011093 ')
```

```
C
      RETURN
 1002 CONTINUE
      RETURN



C*****************************************************************
C
C--- GROUP 13. Boundary conditions and special sources
C                                      Index for Coefficient - CO
C                                      Index for Value       - VAL
   13 CONTINUE
      GO TO (130,131,132,133,134,135,136,137,138,139,1310,
     11311,1312,1313,1314,1315,1316,1317,1318,1319,1320,1321),ISC
  130 CONTINUE
C-------------------- SECTION  1 ------------- coefficient =
GRND



C     ZERO LOCATION OF SCALERS FOR TURBULENCE MODEL

c     turbulence intensity
      LOC1=LOF(C1)

c     integral w dz
      LOC2=LOF(C2)

c     kinetic energy
      LOC3=LOF(C3)

c     tu * dz
      LOC4=LOF(C4)

c     surface distance from leading edge
      LOC5L=LOF(LOW(C5))
      LOC5=LOF(C5)

C     height/delta
      LOC6=LOF(C6)

C     laminar WTOT
      LOC7=LOF(C7)
      LOC7L=LOF(LOW(C7))
```

```
C     intermittency
      LOC8=LOF(C8)
      LOC8L=LOF(LOW(C8))

c     turbulent momentum thickness
      LOC9=LOF(C9)
      LOC9L=LOF(LOW(C9))

c     surface distance from inlet
      LOC10L=LOF(LOW(C10))
      LOC10=LOF(C10)


C      LOC11=LOF(C11)
      LOC12=LOF(C12)


C     ZERO LOCATION OF DENSITY
      LODL=LOF(LOW(DEN1))
      LOD=LOF(DEN1)
      LODH=LOF(HIGH(DEN1))
      LODH2=LOF(ANYZ(DEN1,IZ+2))

C     ZERO LOCATION OF VELOCITIES
      LOW1L=LOF(LOW(W1))
      LOW1=LOF(W1)
      LOW1H=LOF(HIGH(W1))
      LOW1H2=LOF(ANYZ(W1,IZ+2))

C     ZERO LOCATION OF COEFFICIENT CO
      LOCOF=LOF(CO)

      IF(IA(IXF).NE.1) THEN
      H119M=0.
      F(LOC10L+IXF)=0.
      F(LOC10+IXF)=0.0
      F(LOC7+IXF)=0.0
      F(LOC7L+IXF)=0.0
      F(LOC9+IXF)=0.0
      F(LOC9L+IXF)=0.0
      IWW(IXF)=0
      RETHETASTW(IXF)=0.
      LAMDAAVE(IXF) =0.
      TRST(IXF)=0.
      DLW(IXF)=0.
```

```
      LAMDATW(IXF)=0.
      IA(IXF)=1
      END IF

      CALL GTIZYX(APROJH,IZ,GHEIGHT,100,100)

      IF(((NPATCH(5:5).EQ.'E').OR.(NPATCH(5:5).EQ.'W')).AND.
     + (INDVAR.EQ.W1)) THEN

C     START OF NPATCH

       DO IX=IXF,IXL
       DO IY=IYF,IYL

      IF(NPATCH(5:5).EQ.'W') THEN
      IROW=IX+1
      ELSE
      IROW=IX-1
      ENDIF

      HEIGHT=GHEIGHT(IY,IX)

C     LENGTH OF (IZ) CELL
      DXL=XC(IROW,IY,IZ+1)-XC(IROW,IY,IZ)
      DZL=ZC(IROW,IY,IZ+1)-ZC(IROW,IY,IZ)
      DSL=SQRT(DXL**2+DZL**2)

C     LENGTH OF (IZ+1) HIGH CELL
      DX=XC(IROW,IY,IZ+2)-XC(IROW,IY,IZ+1)
      DZ=ZC(IROW,IY,IZ+2)-ZC(IROW,IY,IZ+1)
      DS=SQRT(DX**2+DZ**2)

C     LENGTH OF (IZ + 2) HIGH2 CELL
      DXH=XC(IROW,IY,IZ+3)-XC(IROW,IY,IZ+2)
      DZH=ZC(IROW,IY,IZ+3)-ZC(IROW,IY,IZ+2)
      DSH=SQRT(DXH**2+DZH**2)

      F(LOC10+IROW)=F(LOC10L+IROW)+DSL
      SURFDISTZ=F(LOC10+IROW)

C     GET W1 VELOCITIES
      W=F(LOW1+IROW)
      WLOW=F(LOW1L+IROW)
      WHIGH=F(LOW1H+IROW)
      WHIGH2=F(LOW1H2+IROW)
```

```
C     START OF BOUNDARY LAYER CALCS

      IF(F(LOC8L+IX).GT.0.9999) THEN
C     START OF TURBULENT ONLY BOUNDARY LAYER CALCS ONLY

      IF(H119M.GT.3.5) THEN
      CF120=1.E-6
      DELTA1T=0.0
      F(LOC8+IX)=1.
      GOTO 62
      ENDIF
      DWZ=(WHIGH-W)/DS
      h2l = 1.
      h2u = 3.5
C     e IS THE ACCEPTABLE ERROR
      e = .0001
      GIter = 1 + (ALOG10((h2U - h2L) / e) / ALOG10(2.))
      THETATW=F(LOC9L+IX)
      DO KZ=1,Giter
      CALL TURBULENT2(F(LOC9L+IX),ENUL,h2l,W,CF120,H119L)
      CALL TURBULENT2(F(LOC9L+IX),ENUL,h2u,W,CF120,H119U)
      h2m = (h2l + h2u) / 2.
      CALL TURBULENT2(F(LOC9L+IX),ENUL,h2m,W,CF120,H119M)

      IF( (h119l - h2l).GT.0.0.AND. (h119m - h2m).LT.0.0) THEN
      h2u = h2m
      ELSE
      h2l = h2m
      END IF
      END DO

      IF(H119M.GT.3.5) THEN
      CF120=1.E-6
      F(LOC8+IX)=1.
      GOTO 62
      ENDIF

      if(H119M.LE.1.6) then
      Gh1=3.3+0.8234/(H119M-1.1)**1.287
      else
      Gh1=3.3+1.5501/(H119M-0.6778)**3.064
      endif
      deltat=(Gh1+h119m)*F(LOC9L+IX)
      f(l0c6+ix)=height/DELTAT
      F(LOC9+IX)=F(LOC9L+IX)+DS*(cf120/2.-(2.+h119m)*F(LOC9L+IX)*DWZ/W)
```

```
      THETATZ=F(LOC9+IX)
   62 CONTINUE

C     INCLUDING TRANSITIONAL ANALYSIS
      F(LOC12+IX)=CF120
      F(LOC8+IX)=1.
C     END OF TURBULENT ONLY B - L

c     coefficient=density * w1 * cf120/2
      F(LOCOF+IX)=F(LOD+IX)*F(LOW1+IX)*CF120/2.

      ELSE

C     START OF TRANSITIONAL BOUNDARY LAYER

      CF120=1.E-10
      delta1t=1.e-10
      DWZ=(WHIGH-W)/DS
      R=(W**5+WLOW**5)/2.*DSL
      F(LOC7+IX)=F(LOC7L+IX)+R
      WTOTZ=F(LOC7+IX)
      THETAL=(.45*ENUL*F(LOC7+IX)/W**6)**.5
      CALL LAMINAR2(ENUL,F(LOD+IROW),W,WHIGH,DWZ,THETAL,SHAPE,cfl)
      rethetal = W * thetal / ENUL
      MOLDW=Mw
      mw = thetal ** 2 * DWZ / ENUL

C     IF(MW.LT.0.0) THEN UNCOMMENT THIS TO USE SOLOMAN'S METHOD

      IF(Mw.GT.0.08) THEN
C     FIXES G,n AND HENCE RETHETAS AND RELAMDAT.
      Mw=.08
      ELSEIF(Mw.LT.-0.08) THEN
      Mw=-0.08
      ENDIF

      IF( mw.gt.0.0 ) THEN
      g = 6.91 + 2.48 * mw - 12.27 * mw ** 2
      hdl=7.85+2.8*(1.-exp(-750.*mw**3))
      ELSE
      g = 6.91 + 12.75 * mw + 63.64 * mw ** 2
      hdl=7.85+10.5*mw+232.14*m**2
      END IF
      deltal=thetal*hdl
      f(l0c6+ix)=height/deltal
      GTUAVW=F(LOC4+IROW)/F(LOC5+IROW)
```

```
      rethetas= .85 * (163. + EXP(g * (1.-GTUAVW/6.91)))

C     START OF RETHETAL.GT.RETHETAS

      if(IWW(IX).eq.0) then
      rethetastW(IX)=rethetas
      MSTW(IX)=MOLDW
      thetastW = thetaL
      F(LOC9L+IX)=THETAL/TDIV
      TRST(IX)=F(LOC10+IROW)
      DL=0.
      LAMDAAVE(IX)=0.
      endif

      IF(rethetal.gt.rethetastW(IX)) THEN

      IF(IWW(IX).EQ.0) THEN
      IWW(IX)=1
      ENDIF
c     integrating lamda between Z(G=0) to Z(G=0.25)
C     START OF GAMMA.LT.0.25
C     FIND LAMDA AT HIGH END OF IZ SLAB

      IF( F(LOC8L+IX).lt.0.25 )THEN
      no = .04723 / (10.- EXP(1.7 - RG(2)/2.)) ** 2

      IF( mw.eq.0.0 ) THEN
      n = no
      ELSEIF(Mw.LT.0.) THEN
      N=NO*EXP(Mw*(1.-55.*Mw**2)*(2.6*RG(2)+3.6*SQRT(RG(2))-86.))
      ELSE
      n = no*(EXP(-10.* mw ** .5) + 300.*mw**4)
      END IF

      relamdati = (.411 * rethetastW(IX)** 3/ n) ** .5
      lamdati = ENUL * relamdati / W

C     FIND LAMDA AT HIGH END OF IZ + 1 SLAB +++++++++++++++

      DWZH=(WHIGH2-WHIGH)/DSH
      R=(WHIGH**5+W**5)/2.*DS
      WTOT2W=0.0
      WTOT2W=F(LOC7+IX)+R
      THETALH=(.45*ENUL*WTOT2W/WHIGH**6)**.5
      MH = thetalH ** 2 * DWZH / ENUL
```

```
      IF(MH.GT.0.08) THEN
      MH=0.08
      ELSEIF(MH.LT.-0.08)THEN
      MH=-0.08
      ENDIF
      noH = .04723 / (10. - EXP(1.7 - RG(2)/ 2.))**2

      IF( mH.eq.0.0 )THEN
      nH = noH
      ELSEIF(MH.LT.0.) THEN
      NH=NOH*EXP(MH*(1.-55.*MH**2)*(2.6*RG(2)+3.6*SQRT(RG(2))-86.))
      ELSE
      nH = noH*(EXP(-10.*mH**.5)+300.*mH**4)
      END IF

      relamdatH = (.411 * rethetastW(IX) ** 3/ nH) ** .5
      lamdatH = ENUL * relamdatH / WHIGH

C     CALCULATE AVERAGE LAMDA
      lamdaave(IX)=lamdaave(IX)+(lamdati + lamdatH) / 2.*DS
      dlW(IX) = dlW(IX) + DS
      lamdatW(IX) = lamdaave(IX) / dlW(IX)

C     END OF (GAMMA) F(LOC8L+IX) .LT. 0.25 LOOP
      END IF

C     UNCOMMENT THE FOLLOWING LINES TO USE SOLOMAN'S METHOD
c      ELSE

C      ADVERSE DPXX I.E. M < 0.0

C       CONSTANTS AT START OF TRANSITION \\\\\\\\\\\\\\\\\
c        nW = .00086 * EXP(2.134 *MSTW*ALOG(RG(2))-59.23*MSTW-.564*
c     + ALOG(RG(2)))

c       SIGMASTW = .03 + (.1 / (.115 + EXP(42.9 * MSTW)))
c        smallnW = nW* ENUL / (SIGMASTW * thetastW ** 3)

C     \\\\\\\\\\\\\\\\\\\\\\\\\\\\\\\\\\\\\\\\\\\\\\\\\\\\\\\\

C       HIGH END OF CELL ++++++++++++++++++++
c        alpha = 4.+ (22.14 / (.79 + 2.72 * EXP(47.63 * m)))
c        sigma = .03 + (.1 / (.115 + EXP(42.9 * m)))
C     ++++++++++++++++++++++++++++++++++++++++
C       LOW END OF CELL ----------------------
C     ****************************
```

```
c      DWZL=(W-WLOW)/DSL
c      R=(W**5+WLOW**5)/2.*DSL
c      WTOT3W=0.
c      WTOT3W=WTOTW-R
c      THETALL=(0.45*ENUL*WTOT3W/WLOW**6)**.5
C     ****************************
c      ML=thetalL ** 2 * DWZL/ ENUL
c      ALPHAL = 4. + (22.14 / (.79 + 2.72 * EXP(47.63 * ML)))
c      SIGMAL = .03 + (.1 / (.115 + EXP(42.9 * ML)))
C       ---------------------------------------
C           convert degrees to radians
c      alpha = alpha * pi / 180.
c      ALPHAL = ALPHAL * pi / 180.
C       calculate averages of sigma, alpha & velocity
c      slave = (sigma + SIGMAL) / 2.
c      aave = (TAN(alpha) + TAN(ALPHAL)) / 2.
c      vave = (WLOW+W) / 2.
c      integ1W = integ1W + DSL * slave / (aave * vave)
c      integ2W = integ2W + DSL * aave
C     END OF MW.GE.0.0
c      ENDIF

       IF(H119M.GT.3.5) THEN
       CF120=1.E-6
       DELTA1T=0.0
       F(LOC8+IX)=1.
       GOTO 17
       ENDIF

       h2l = 1.
       h2u = 3.5
C       e IS THE ACCEPTABLE ERROR
       e = .0001
       GIter = 1 + (ALOG10((h2U - h2L) / e) / ALOG10(2.))
       THETATW=F(LOC9L+IX)
       DO KZ=1,GIter
       CALL TURBULENT2(F(LOC9L+IX),ENUL,h2l,W,CF120,H119L)
       CALL TURBULENT2(F(LOC9L+IX),ENUL,h2u,W,CF120,H119U)
       h2m = (h2l + h2u) / 2.
       CALL TURBULENT2(F(LOC9L+IX),ENUL,h2m,W,CF120,H119M)

       IF( (h119l - h2l).GT.0.0.AND. (h119m - h2m).LT.0.0) THEN
       h2u = h2m
       ELSE
       h2l = h2m
       END IF
```

```
      END DO

      IF(H119M.GT.3.5) THEN
      CF120=1.E-6
      DELTA1T=0.0
      F(L0C8+IX)=1.
      GOTO 17
      ENDIF

      if(h119m.le.1.6) then
      Gh1=3.3+0.8234/(h119m-1.1)**1.287
      else
      Gh1=3.3+1.5501/(h119m-0.6778)**3.064
      endif
      deltat=(Gh1+h119m)*F(L0C9L+IX)
      if(deltat.gt.deltal) then
      f(l0c6+ix)=height/deltat
      else
      f(l0c6+ix)=height/deltal
      endif

      F(L0C9+IX)=F(L0C9L+IX)+DS*(cf120/2.-(2.+h119m)*F(L0C9L+IX)*DWZ/W)
      THETATZ=F(L0C9+IX)

C     IF USING SOLOMAN'S METHOD COMMENT OUT NEXT 3 LINES
      gamma=1.-EXP(-.411*(F(L0C10+IROW)-TRST(IX))**2/LAMDATW(IX)
     +**2)



C     UNCOMMENT FOR SOLOMAN'S METHOD

c      IF(MW.GE.0.0) THEN
c      ELSE
C      integrate to find gamma
c      F(L0C8+IX) = 1. - EXP(-smallnW * integ1W * integ2W)
c      ENDIF

C     END OF rethetal.gt.rethetas LOOP

      f(l0c8+ix)=gamma
      END IF
   17 CONTINUE
      F(L0C12+IX) = (1. - F(L0C8+IX)) * cfl + F(L0C8+IX) * cf120

C     CALCULATION OF TRANSITIONAL SKIN FRICTION
```

```
      IF(F(LOC8+IX).LT.0.0001) THEN
      CFTR=CFL
      ELSE
      CFTR=(1.-F(LOC8+IX))*CFL+F(LOC8+IX)*CF120
      ENDIF

c     coefficient=density * w1 * CFTR/2
      F(LOCOF+IX)=F(LOD+IX)*F(LOW1+IX)*CFTR/2.

C     END OF GAMMA.GT.0.999

      ENDIF

      END DO
      END DO
C     END OF NPATCH AND INDVAR
      END IF
      RETURN

  131 CONTINUE
C-------------------- SECTION  2 ------------- coefficient =
GRND1
      RETURN
  132 CONTINUE
C-------------------- SECTION  3 ------------- coefficient =
GRND2
      RETURN
  133 CONTINUE
C-------------------- SECTION  4 ------------- coefficient =
GRND3
      RETURN
  134 CONTINUE
C-------------------- SECTION  5 ------------- coefficient =
GRND4
      RETURN
  135 CONTINUE
C-------------------- SECTION  6 ------------- coefficient =
GRND5
      RETURN
  136 CONTINUE
C-------------------- SECTION  7 ------------- coefficient =
GRND6
      RETURN
  137 CONTINUE
C-------------------- SECTION  8 ------------- coefficient =
GRND7
```

```
      RETURN
  138 CONTINUE
C------------------- SECTION  9 ------------- coefficient =
GRND8
      RETURN
  139 CONTINUE
C------------------- SECTION 10 ------------- coefficient =
GRND9
      RETURN
 1310 CONTINUE
C------------------- SECTION 11 ------------- coefficient =
GRND10
      RETURN
 1311 CONTINUE
C------------------- SECTION 12 -------------------- value =
GRND
      RETURN
 1312 CONTINUE
C------------------- SECTION 13 -------------------- value =
GRND1
      RETURN
 1313 CONTINUE
C------------------- SECTION 14 -------------------- value =
GRND2
      RETURN
 1314 CONTINUE
C------------------- SECTION 15 -------------------- value =
GRND3
      RETURN
 1315 CONTINUE
C------------------- SECTION 16 -------------------- value =
GRND4
      RETURN
 1316 CONTINUE
C------------------- SECTION 17 -------------------- value =
GRND5
      RETURN
 1317 CONTINUE
C------------------- SECTION 18 -------------------- value =
GRND6
      RETURN
 1318 CONTINUE
C------------------- SECTION 19 -------------------- value =
GRND7
      RETURN
 1319 CONTINUE
```

```
C------------------- SECTION 20 ------------------- value =
GRND8
      RETURN
 1320 CONTINUE
C------------------- SECTION 21 ------------------- value =
GRND9
      RETURN
 1321 CONTINUE
C------------------- SECTION 22 ------------------- value =
GRND10
      RETURN
C*****************************************************************



C*****************************************************************
C* Make changes to data for GROUPS 15, 16, 17, 18  GROUP 19.
C*****************************************************************
C
C--- GROUP 19. Special calls to GROUND from EARTH
C
   19 GO TO (191,192,193,194,195,196,197,198,199,1910),ISC
  191 CONTINUE
C   * ------------------- SECTION 1 ---- Start of time step.
      RETURN
  192 CONTINUE
C   * ------------------- SECTION 2 ---- Start of sweep.
      RETURN
  193 CONTINUE
C   * ------------------- SECTION 3 ---- Start of iz slab.

      RETURN
  194 CONTINUE
C   * ------------------- SECTION 4 ---- Start of iterations over
slab.
      RETURN
  199 CONTINUE
C   * ------------------- SECTION 9 ---- Start of solution sequence
for
C                                          a variable
      RETURN
 1910 CONTINUE
C   * ------------------- SECTION 10---- Finish of solution sequence
for
C                                          a variable
      RETURN
```

```
  195 CONTINUE
C   * -------------------- SECTION 5 ---- Finish of iterations over
slab.
      RETURN
  196 CONTINUE
C   * -------------------- SECTION 6 ---- Finish of iz slab.
C     ZERO LOCATION OF DENSITY
      LODL=LOF(LOW(DEN1))
      LOD=LOF(DEN1)
      l0p1=l0f(p1)
      LODH=LOF(HIGH(DEN1))
      LODH2=LOF(ANYZ(DEN1,IZ+2))

C     ZERO LOCATION OF VELOCITIES
      LOW1L=LOF(LOW(W1))
      LOW1=LOF(W1)
      LOW1H=LOF(HIGH(W1))
      LOW1H2=LOF(ANYZ(W1,IZ+2))

C     ZERO LOCATION OF SCALERS
      LOC1=LOF(C1)
      LOC2=LOF(C2)
      LOC3=LOF(C3)
      LOC4=LOF(C4)
      LOC5=LOF(C5)
      l0c11=l0f(c11)
      LOC2L=LOF(LOW(C2))
      LOC3L=LOF(LOW(C3))
      LOC4L=LOF(LOW(C4))
      LOC5L=LOF(LOW(C5))

      GCMUCD=.09
      GC2E=1.92


      DO IX=1,NX
C     CALCULATION OF MACH NUMBER
      ac=sqrt(1.333*(PRESS0+f(l0p1+ix))/f(l0d+ix))
      f(l0c11+ix)=f(l0w1+ix)/ac

C     LENGTH OF (IZ) CELL
      GDXL=XC(IX,IY,IZ+1)-XC(IX,IY,IZ)
      GDZL=ZC(IX,IY,IZ+1)-ZC(IX,IY,IZ)
      GDSL=SQRT(GDXL**2+GDZL**2)

C     MALIN'S TURBULENCE MODEL
```

```
      IF(IZ.EQ.1) THEN
      GKIN=1.5*(RG(2)/100.*RG(5))**2
      GEPIN=GCMUCD**0.75*GKIN**1.5/RG(4)
      F(LOC2+IX)=(1./RG(5)+1./F(LOW1+IX))/2.*GDSL
      F(LOC4+IX)=RG(2)*GDSL
      F(LOC5+IX)=GDSL
      F(LOC1+IX)=RG(2)
      ENDIF

      IF(IZ.GT.1.AND.IZ.LT.NZ) THEN
C     SUM OF INTEGRAL HELD IN SCALER C2
      F(LOC2+IX)=F(LOC2L+IX)+(1./F(LOW1+IX)+1./F(LOW1L+IX))/2.*GDSL
      F(LOC3+IX)=(GKIN**(1.-GC2E)+(GC2E-1.)*GEPIN/GKIN**GC2E*
     +F(LOC2+IX))**(1./(1.-GC2E))
      F(LOC1+IX)=100.*SQRT(.667*F(LOC3+IX))/F(LOW1+IX)
      ATU=F(LOC1+IX)
C     TOTAL LENGTH FROM INLET
      F(LOC5+IX)=F(LOC5L+IX)+GDSL
      F(LOC4+IX)=F(LOC4L+IX)+F(LOC1+IX)*GDSL
      ENDIF
      END DO

      RETURN
  197 CONTINUE
C   * -------------------- SECTION 7 ---- Finish of sweep.

      SUMW=0.0
      SD=0.0
      KK=0
      DO IX=1,NX
      IA(IX)=0
      IWW(IX)=0
      LAMDAAVE(IX)=0.
      LAMDATW(IX)=0.
      END DO
      IWW(IXF)=0
      RETHETASTW(IX)=0.
      LAMDAAVE(IXF) =0.
      THETATW=0.
      TRSTARTW=0.

      H119MW=0.
      INTEG1W=0.
      INTEG2W=0.
      WTOT3W=0.
      RETURN
```

```
  198 CONTINUE
C   * -------------------- SECTION 8 ---- Finish of time step.
C
      RETURN
C*****************************************************************


C     ADDED AT THE END OF GROUND SUBROUTINE

      SUBROUTINE laminar2(ENUL,GRHO,W,WHIGH,WGRAD,THETAL,SHAPE,cfl)


      COMMON /LAM2/IBB
      REAL lamda

      lamda = thetal ** 2 * WGRAD/ ENUL

      IF( lamda.lt.-0.09 ) THEN
      lamda=-0.089
      END IF

      shear = (lamda + .09) ** .62
      tau = ENUL*GRHO * W * shear / thetal
      cfl = 2. * tau  / (GRHO* W ** 2)
      zz = (.25 - lamda)
      shape = 2.0 + 4.14 * zz - 83.5 * zz ** 2+ 854. * zz ** 3- 3337.*
     +zz ** 4 + 4576. * zz ** 5
      RETURN
      END


      SUBROUTINE turbulent2(THETATS,ENUL,H2,W,cf120,H119N)

      COMMON /TUR2/DWZ

      REAL kappa,lamda

      DATA KAPPA/0.41/
c     CALCULATE SKIN FRICTION FROM EQUATION 6-120

c     error trap here to stop alog being < 0
      crit=w*thetats/enul
      if(crit.lt.1.) then
      crit=1.1
      endif
```

```
      cf120 = .3 * EXP(-1.33 * h2) / ALOG10(crit)** (1.74 + .31 * h2)

c     USED GUESSED h2 AND CALCULATED cf120 TO CALCULATE PI VIA EQN 6-122
c      in favourable dp beta will be -ve

      beta = -2. * h2 * thetatS * dwz / cf120 / w
c     beta is a quadratic eqn in pi, with coefficients a, b & c.

      a = 1.
      b = .76 / .42
      c = -(.4 + beta) / .42

c      this is the limit for beta (-.7438) or it goes complex
c      usualy means bad first choice of h2 or cf

C     FIND pi EQN 6-121

      pi = (-b + (b ** 2 - 4. * a * c) ** .5) / 2.

c     FUNCTION OF PI REQUIRED IN 6-119 (a)

      fpi = (2.+ 3.179 * pi + 1.5 * pi ** 2) / (kappa * (1.+ pi))

c      USE EQN 6-119(a) WITH CALCULATED pi TO CALCULATE NEW h2 (h119)

      lamda = (2. / cf120) ** .5
      h119n = lamda / (lamda - fpi)

      RETURN
      END
```

```
C FILE NAME GROUND.FTN-------------------------------011093

C     LAST MODIFIED 6/05/96

C     ****************************
C     ** TURBULENT ENERGY METHOD **
C     ****************************

C     FRASER'S METHOD FOR ADVERSE & FAVOURABLE DP

C     PUT TU FOR START OF TRANSITION = 1/z*integral tu dz
C     TU FOR LENGTH = TUINLET
C     RUNGE KUTTA 6TH ORDER INTEGRATION METHOD REQUIRED
C     TO INTEGRATE TURBULENT ENERGY EQUATIONS
C     RG(2) IS TURBULENCE INTENSITY AT INLET (%)
C     RG(3) IS A DIVISOR OF THETAL AT THE ORIGIN OF THE TURBULENT
BOUNDARY
C          LAYER, I.E. THETAT=THETAL/RG(3)
C     RG(5) IS THE VELOCITY (W1) AT INLET
C     RG(8) IS LENGTH SCALE AT LEADING EDGE
C     RG(9) IS CRITERIA FOR START OF TRANSITION
C     SCALER C1 - TURBULENCE INTENSITY
C     SCALER C2 - INTEGRATING W1
C     SCALER C3 - KINETIC ENERGY
C     SCALER C4 - SUM OF (TU*CELL LENGTH)
C     SCALER C5 - CHANGED TO DISTANCE FROM INLET TO CURRENT HIGH OF
CELL
C               HENCE AVERAGE TU = C4/C5
C     SCALER C6 - FLOW HEIGHT / DELTA
C     SCALER C7 - WTOT
C     SCALER C8 - INTERMITTENCY
C     SCALER C9 - TURBULENT MOMENTUM THICKNESS
C     SCALER C10 - SURFACE DISTANCE FROM LEADING EDGE
C     SCALER C11 - DISSIPATION
C     SCALER C12 - SKIN FRICTION


      SUBROUTINE GROUND
      INCLUDE '\d_phoe21\d_includ\satear'
      INCLUDE '\d_phoe21\d_includ\grdloc'
      INCLUDE '\d_phoe21\d_includ\grdear'
      INCLUDE '\d_phoe21\d_includ\grdbfc'

CXXXXXXXXXXXXXXXXXXXXXXXXXXXXXXXXXXXXXX USER SECTION STARTS:
C
C 1   Set dimensions of data-for-GROUND arrays here. WARNING: the
```

```
C     corresponding arrays in the MAIN program of the satellite
C     and EARTH must have the same dimensions.
      PARAMETER (NLG=100, NIG=200, NRG=200, NCG=100)
      PARAMETER (MX = 500)
C
      COMMON/LGRND/LG(NLG)/IGRND/IG(NIG)/RGRND/RG(NRG)/CGRND/CG(NCG)
      LOGICAL LG
      CHARACTER*4 CG
      INTEGER GWW,GW

      REAL MH,MOLD,N,NO,NOH,NH,LAMDATI,LAMDATH,LAMDATW(MX),LAMDAAVE(MX)
      real mw
      REAL INTEG1W,INTEG2W,ML,MSTW(MX),MST,MOLDW,INTEG1,INTEG2
      REAL KV1,KV2,KV3,KV4,KV5,KV6,KV7,KV8
      REAL KD1,KD2,KD3,KD4,KD5,KD6,KD7,KD8
      REAL KS1,KS2,KS3,KS4,KS5,KS6,KS7,KS8
      INTEGER GNX,GITER

      COMMON /TURC/TDIV
C     WEST WALL

      COMMON /LAM/IBBW,WW,THETALW,THETAL2W,THETALLW
      COMMON /TUR/DSW

C     EAST WALL

      COMMON /LAM2/Ibb
      COMMON /TUR2/DWZ

      SAVE GKIN,GEPIN,SUMW,SD

C 2   User dimensions own arrays here, for example:
C     DIMENSION GUH(10,10),GUC(10,10),GUX(10,10),GUZ(10)

      DIMENSION GHEIGHT(100,100),TRST(MX),IWW(MX),RETHETASTW(MX)
      DIMENSION DLW(MX),IA(MX),IAA(MX),RECRIT(MX),TRANSIT(MX)


C
C 3   User places his data statements here, for example:
C     DATA NXDIM,NYDIM/10,10/
      DATA PI,M/3.14159,0.0/


      DATA GAMMA,lamdac/0.,0/
      DATA (TRST(I),I=1,MX) /MX*0./
```

```
      DATA (IWW(I),I=1,MX) / MX*0/
      DATA (RETHETASTW(I),I=1,MX) /MX*0./
      DATA (MSTW(I),I=1,MX) /MX*0./
      DATA (LAMDAAVE(I),I=1,MX) /MX*0./
      DATA (LAMDATW(I),I=1,MX) /MX*0./
      DATA (DLW(I),I=1,MX) /MX*0./
      DATA (IA(I),I=1,MX) /MX*0/
      DATA (IAA(I),I=1,MX) /MX*0/
      DATA (RECRIT(I),I=1,MX) /MX*0/
      DATA (TRANSIT(I),I=1,MX) /MX*1.E-10/
      DATA KK,SD,SUMW/0,0.0,0.0/
C
C 4   Insert own coding below as desired, guided by GREX examples.
C     Note that the satellite-to-GREX special data in the labelled
C     COMMONs /RSG/, /ISG/, /LSG/ and /CSG/ can be included and
C     used below but the user must check GREX for any conflicting
C     uses. The same comment applies to the EARTH-spare working
C     arrays EASP1, EASP2,....EASP20. In addition to the EASPs,
C     there are 10 GRound-earth SPare arrays, GRSP1,...,GRSP10,
C     supplied solely for the user, which are not used by GREX. If
C     the call to GREX has been deactivated then all of the arrays
C     may be used without reservation.

c**********************************************************************
c
      IXL=IABS(IXL)
      IF(IGR.EQ.13) GO TO 13
      IF(IGR.EQ.19) GO TO 19
      GO TO (1,2,3,4,5,6,25,8,9,10,11,12,13,14,25,25,25,25,19,20,25,
     125,23,24),IGR
   25 CONTINUE
      RETURN
C**********************************************************************
C
C--- GROUP 1. Run title and other preliminaries
C
    1 GO TO (1001,1002),ISC
 1001 CONTINUE
C
      CALL MAKE(APROJH)
      TDIV=RG(3)
C     User may here change message transmitted to the VDU screen
      IF(IGR.EQ.1.AND.ISC.EQ.1.AND..NOT.NULLPR)
     1  CALL WRYT40('GROUND file is GROUND.F    of:    011093 ')
C
      RETURN
```

```
 1002 CONTINUE
      RETURN
C*********************************************************************
C*********************************************************************
C
C--- GROUP 13. Boundary conditions and special sources
C                                      Index for Coefficient - CO
C                                      Index for Value       - VAL
   13 CONTINUE
      GO TO (130,131,132,133,134,135,136,137,138,139,1310,
     11311,1312,1313,1314,1315,1316,1317,1318,1319,1320,1321),ISC
  130 CONTINUE
C-------------------- SECTION  1 ------------- coefficient =
GRND



C     ZERO LOCATION OF SCALERS FOR TURBULENCE MODEL

c     turbulence intensity
      LOC1L=LOF(LOW(C1))
      LOC1=LOF(C1)

c     integral w dz
      LOC2=LOF(C2)

c     kinetic energy
      LOC3L=LOF(LOW(C3))
      LOC3=LOF(C3)
      LOC3h=LOF(high(C3))

c     tu * dz
      LOC4=LOF(C4)

c     surface distance from leading edge
      LOC5L=LOF(LOW(C5))
      LOC5=LOF(C5)

C     height/delta
      LOC6L=LOF(LOW(C6))
```

```
      LOC6=LOF(C6)

C     laminar WTOT
      LOC7L=LOF(LOW(C7))
      LOC7=LOF(C7)


C     intermittency
      LOC8L=LOF(LOW(C8))
      LOC8=LOF(C8)


c     turbulent momentum thickness
      LOC9L=LOF(LOW(C9))
      LOC9=LOF(C9)


c     surface distance from inlet
      LOC10L=LOF(LOW(C10))
      LOC10=LOF(C10)

C     epsilon
      LOC11L=LOF(LOW(C11))
      LOC11=LOF(C11)


C     skin friction
      LOC12L=LOF(LOW(C12))
      LOC12=LOF(C12)


C     ZERO LOCATION OF DENSITY
      LODL=LOF(LOW(DEN1))
      LOD=LOF(DEN1)
      LODH=LOF(HIGH(DEN1))
      LODH2=LOF(ANYZ(DEN1,IZ+2))

C     ZERO LOCATION OF VELOCITIES
      LOW1L=LOF(LOW(W1))
      LOW1=LOF(W1)
      LOW1H=LOF(HIGH(W1))
      LOW1H2=LOF(ANYZ(W1,IZ+2))

C     ZERO LOCATION OF COEFFICIENT CO
      LOCOF=LOF(CO)
```

```
C     sets wtot = 0.0 at start of sweep

      IF(IA(IXF).NE.1) THEN
      H119M=0.
      F(LOC10L+IXF)=0.
      F(LOC10+IXF)=0.0
      F(LOC7+IXF)=0.0
      F(LOC7L+IXF)=0.0
      F(LOC9+IXF)=0.0
      F(LOC9L+IXF)=0.0
      F(LOC3+IXF)=1.E-10
      IWW(IXF)=0
      RETHETASTW(IXF)=0.
      LAMDAAVE(IXF) =0.
      TRST(IXF)=0.
      DLW(IXF)=0.
      LAMDATW(IXF)=0.
      IA(IXF)=1
      IAA(IXF)=0
      END IF

      CALL GTIZYX(APROJH,IZ,GHEIGHT,100,100)

      IF(((NPATCH(5:5).EQ.'E').OR.(NPATCH(5:5).EQ.'W')).AND.
     + (INDVAR.EQ.W1)) THEN

C     START OF NPATCH

       DO IX=IXF,IXL
       DO IY=IYF,IYL

      IF(NPATCH(5:5).EQ.'W') THEN
      IROW=IX+1
      ELSE
      IROW=IX-1
      ENDIF

      HEIGHT=GHEIGHT(IY,IX)
C     LENGTH OF (IZ) CELL
      DXL=XC(IROW,IY,IZ+1)-XC(IROW,IY,IZ)
      DZL=ZC(IROW,IY,IZ+1)-ZC(IROW,IY,IZ)
      DSL=SQRT(DXL**2+DZL**2)
C     LENGTH OF (IZ+1) HIGH CELL
      DX=XC(IROW,IY,IZ+2)-XC(IROW,IY,IZ+1)
      DZ=ZC(IROW,IY,IZ+2)-ZC(IROW,IY,IZ+1)
      DS=SQRT(DX**2+DZ**2)
```

```
C     LENGTH OF (IZ + 2) HIGH2 CELL
      DXH=XC(IROW,IY,IZ+3)-XC(IROW,IY,IZ+2)
      DZH=ZC(IROW,IY,IZ+3)-ZC(IROW,IY,IZ+2)
      DSH=SQRT(DXH**2+DZH**2)

      F(LOC10+IROW)=F(LOC10L+IROW)+DSL
      SURFDISTZ=F(LOC10+IROW)

C     GET W1 VELOCITIES

      W=F(LOW1+IROW)
      WLOW=F(LOW1L+IROW)
      WHIGH=F(LOW1H+IROW)
      WHIGH2=F(LOW1H2+IROW)

C     START OF BOUNDARY LAYER CALCS

      IF(F(LOC8L+IX).GT.0.9999) THEN
C     START OF TURBULENT ONLY BOUNDARY LAYER CALCS ONLY

      IF(H119M.GT.3.5) THEN
      CF120=1.E-6
      DELTA1T=0.0
      F(LOC8+IX)=1.
      GOTO 62
      ENDIF
      DWZ=(WHIGH-W)/DS
      h2l = 1.
      h2u = 3.5
C     e IS THE ACCEPTABLE ERROR
      e = .0001
      GIter = 1 + (ALOG10((h2U - h2L) / e) / ALOG10(2.))
      THETATW=F(LOC9L+IX)
      DO KZ=1,Giter
      CALL TURBULENT2(F(LOC9L+IX),ENUL,h2l,W,CF120,H119L)
      CALL TURBULENT2(F(LOC9L+IX),ENUL,h2u,W,CF120,H119U)
      h2m = (h2l + h2u) / 2.
      CALL TURBULENT2(F(LOC9L+IX),ENUL,h2m,W,CF120,H119M)

      IF( (h119l - h2l).GT.0.0.AND. (h119m - h2m).LT.0.0) THEN
      h2u = h2m
      ELSE
      h2l = h2m
      END IF
      END DO
```

```
      IF(H119M.GT.3.5) THEN
      CF120=1.E-6
      F(LOC8+IX)=1.
      GOTO 62
      ENDIF

      if(H119M.LE.1.6) then
      Gh1=3.3+0.8234/(H119M-1.1)**1.287
      else
      Gh1=3.3+1.5501/(H119M-0.6778)**3.064
      endif

      deltat=(Gh1+h119m)*F(LOC9L+IX)


      F(LOC9+IX)=F(LOC9L+IX)+DS*(cf120/2.-(2.+h119m)*F(LOC9L+IX)*DWZ/W)
      THETATZ=F(LOC9+IX)
   62 CONTINUE

C     INCLUDING TRANSITIONAL CALCULATIONS
      F(LOC12+IX)=CF120
      F(LOC8+IX)=1.
C     END OF TURBULENT ONLY B - L

c     coefficient=density * w1 * cf120/2
      F(LOCOF+IX)=F(LOD+IX)*F(LOW1+IX)*CF120/2.

      ELSE

C     START OF TRANSITIONAL BOUNDARY LAYER
      CF120=1.E-10
      delta1t=1.e-10
      DWZ=(WHIGH-W)/DS
      R=(W**5+WLOW**5)/2.*DSL
      F(LOC7+IX)=F(LOC7L+IX)+R
      THETAL=(.45*ENUL*F(LOC7+IX)/W**6)**.5
      CALL LAMINAR2(ENUL,F(LOD+IROW),W,WHIGH,DWZ,THETAL,SHAPE,cfl)
      rethetal = W * thetal / ENUL
      MOLDW=Mw
      mw = thetal ** 2 * DWZ / ENUL

      IF(Mw.GT.0.08) THEN
C     FIXES G,n AND HENCE RETHETAS AND RELAMDAT
      Mw=.08
      ELSEIF(Mw.LT.-0.08) THEN
      Mw=-0.08
```

```
      ENDIF

      IF( mw.gt.0.0 ) THEN
      g = 6.91 + 2.48 * mw - 12.27 * mw ** 2
      hdl=7.85+2.8*(1.-exp(-750.*mw**3))
      ELSE
      g = 6.91 + 12.75 * mw + 63.64 * mw ** 2
      hdl=7.85+10.5*mw+232.14*mw**2
      END IF
      deltal=thetal*hdl
      f(l0c6+ix)=deltal

      IF(RETHETAL.GT.0.0.AND.IAA(IX).EQ.0) THEN
      GCMUCD=0.09
      GC2E=1.92

C     rg(8) is length scale at z = 0
      F(L0C3+IX)=1.5*(start*W)**2
c     changed to epsilon average
      F(l0c11+IX)=GCMUCD**0.75*F(L0C3+IX)**1.5/RG(8)/2.
      IAA(IX)=1
      ELSEIF(RETHETAL.GT.0.0.AND.IAA(IX).EQ.1) THEN

c     ********************* kinetic energy equation ***************
c     integrate k/w dw
      gh=ABS(w-wlow)
      KV1=gH*VEL(W,f(l0c3l+ix))
      KV2=gH*VEL(W+gH/9.,f(l0c3l+ix)+KV1/9.)
      KV3=gH*VEL(W+gH/6.,f(l0c3l+ix)+(KV1+3.*KV2)/24.)
      KV4=gH*VEL(W+gH/3.,f(l0c3l+ix)+(KV1-3.*KV2+4.*KV3)/6.)
      KV5=gH*VEL(W+gH/2.,f(l0c3l+ix)+(-5.*KV1+27.*KV2-24.*KV3+6.*KV4)
     + /8.)
      KV6=gH*VEL(W+gH*2./3.,f(l0c3l+ix)+(221.*KV1-981.*KV2+867.*KV3-102.
     + *KV4+KV5)/9.)
      KV7=gH*VEL(W+gH*5./6.,f(l0c3l+ix)+(-183.*KV1+678.*KV2-472.*KV3-66.
     + *KV4+80.*KV5+3.*KV6)/48.)
      KV8=gH*VEL(W+gH,f(l0c3l+ix)+(716.*KV1-2079.*KV2+1002.*KV3+834.*KV4
     + -454.*KV5-9.*KV6+72.*KV7)/82.)

      DVEL=(41.*KV1+216.*(KV3+KV7)+27.*(KV4+KV6)+272.*KV5+41.*KV8)/840.


C     DELTA COMPONENT STEP H IN DELTA
c     integrate k/delta d(delta)
c     l0c6 is delta, l0c3 is kinetic energy
```

```
      gH=f(l0c6+ix)-f(l0c6l+ix)
      KD1=gH*VEL(f(l0c6l+ix),f(l0c3l+ix))
      KD2=gH*VEL(f(l0c6l+ix)+gH/9.,f(l0c3l+ix)+KD1/9.)
      KD3=gH*VEL(f(l0c6l+ix)+gH/6.,f(l0c3l+ix)+(KD1+3.*KD2)/24.)
      KD4=gH*VEL(f(l0c6l+ix)+gH/3.,f(l0c3l+ix)+(KD1-3.*KD2+4.*KD3)/6.)
      KD5=gH*VEL(f(l0c6l+ix)+gH/2.,f(l0c3l+ix)+(-5.*KD1+27.*KD2-24.
     + *KD3+6.*KD4)/8.)
      KD6=gH*VEL(f(l0c6l+ix)+gH*2./3.,f(l0c3l+ix)+(221.*KD1-981.*KD2+
     + 867.*KD3-102.*KD4+KD5)/9.)
      KD7=gH*VEL(f(l0c6l+ix)+gH*5./6.,f(l0c3l+ix)+(-183.*KD1+678.*KD2
     + -472.*KD3-66.*KD4+80.*KD5+3.*KD6)/48.)
      KD8=gH*VEL(f(l0c6l+ix)+gH,f(l0c3l+ix)+(716.*KD1-2079.*KD2+1002.
     + *KD3+834.*KD4-454.*KD5-9.*KD6+72.*KD7)/82.)


      DDEL=(41.*KD1+216.*(KD3+KD7)+27.*(KD4+KD6)+272.*KD5+41.*KD8)/840.

C     SHEAR STRESS COMPONENT STEP H IN Z
c     integrate (k a tau/w mu - 2.85 ep/w) dz
c     l0c10 is surface distance in in IROW
c     l0c12 is skin friction, l0dl is density, l0c11 is epsilon, l0c3 is ke

c     correlation for favourable pressure gradients

      ga=exp(-19.*(rg(8)/0.004)/f(l0c1+irow)*(1-5.3*m**2))

      gH=f(l0c10+irow)-f(l0c10l+irow)

      KS1=gH*SHEAR(f(l0c12l+ix),w,ENUL,GA,f(l0dl+ix),f(l0c11l+ix),
     + f(l0c3l+ix))
      KS2=gH*SHEAR(f(l0c12l+ix),w,ENUL,GA,f(l0dl+ix),f(l0c11l+ix),
     + f(l0c3l+ix)+KS1/9.)
      KS3=gH*SHEAR(f(l0c12l+ix),w,ENUL,GA,f(l0dl+ix),f(l0c11l+ix),
     + f(l0c3l+ix)+(KS1+3.*KS2)/24.)
      KS4=gH*SHEAR(f(l0c12l+ix),w,ENUL,GA,f(l0dl+ix),f(l0c11l+ix),
     + f(l0c3l+ix)+(KS1-3.*KS2+4.*KS3)/6.)
      KS5=gH*SHEAR(f(l0c12l+ix),w,ENUL,GA,f(l0dl+ix),f(l0c11l+ix),
     + f(l0c3l+ix)+(-5.*KS1+27.*KS2-24.*KS3+6.*KS4)/8.)
      KS6=gH*SHEAR(f(l0c12l+ix),w,ENUL,GA,f(l0dl+ix),f(l0c11l+ix),
     + f(l0c3l+ix)+(221.*KS1-981.*KS2+867.*KS3-102.*KS4+KS5)/9.)
      KS7=gH*SHEAR(f(l0c12l+ix),w,ENUL,GA,f(l0dl+ix),f(l0c11l+ix),f(l0c3
     +l+ix)+(-183.*KS1+678.*KS2-472.*KS3-66.*KS4+80.*KS5+3.*KS6)/48.)
      KS8=gH*SHEAR(f(l0c12l+ix),w,ENUL,GA,f(l0dl+ix),f(l0c11l+ix),f(l0c3
     + l+ix)+(716.*KS1-2079.*KS2+1002.*KS3+834.*KS4-454.*KS5-9.*KS6+72.
     +*KS7)/82. )
```

```
      DSHEAR=(41.*KS1+216.*(KS3+KS7)+27.*(KS4+KS6)+272.*KS5+41.*KS8)
     + /840.
      f(l0c3+ix)=f(l0c3l+ix)+DSHEAR-DDEL-DVEL

c     ********** epsilon equation **********

      gb=1.0357*ga

C     VELOCITY COMPONENT, STEP H IN W
      gH=abs(W-WLOW)

      KV1=gH*VEL(w,f(l0c11l+ix))
      KV2=gH*VEL(w+gH/9.,f(l0c11l+ix)+KV1/9.)
      KV3=gH*VEL(w+gH/6.,f(l0c11l+ix)+(KV1+3.*KV2)/24.)
      KV4=gH*VEL(w+gH/3.,f(l0c11l+ix)+(KV1-3.*KV2+4.*KV3)/6.)
      KV5=gH*VEL(w+gH/2.,f(l0c11l+ix)+(-5.*KV1+27.*KV2-24.*KV3+6.*KV4)
     + /8.)
      KV6=gH*VEL(w+gH*2./3.,f(l0c11l+ix)+(221.*KV1-981.*KV2+867.*KV3-
     + 102.*KV4+KV5)/9.)
      KV7=gH*VEL(w+gH*5./6.,f(l0c11l+ix)+(-183.*KV1+678.*KV2-472.*KV3
     + -66.*KV4+80.*KV5+3.*KV6)/48.)
      KV8=gH*VEL(w+gH,f(l0c11l+ix)+(716.*KV1-2079.*KV2+1002.*KV3+834.
     + *KV4-454.*KV5-9.*KV6+72.*KV7)/82.)

      DVEL=(41.*KV1+216.*(KV3+KV7)+27.*(KV4+KV6)+272.*KV5+41.*KV8)/840.

C     DELTA COMPONENT STEP H IN DELTA
      gh=f(l0c6+ix)-f(l0c6l+ix)

      KD1=gh*VEL(f(l0c6l+ix),f(l0c11l+ix))
      KD2=gh*VEL(f(l0c6l+ix)+gh/9.,f(l0c11l+ix)+KD1/9.)
      KD3=gh*VEL(f(l0c6l+ix)+gh/6.,f(l0c11l+ix)+(KD1+3.*KD2)/24.)
      KD4=gh*VEL(f(l0c6l+ix)+gh/3.,f(l0c11l+ix)+(KD1-3.*KD2+4.*KD3)/6.)
      KD5=gh*VEL(f(l0c6l+ix)+gh/2.,f(l0c11l+ix)+(-5.*KD1+27.*KD2-24.*
     + KD3+6.*KD4)/8.)
      KD6=gh*VEL(f(l0c6l+ix)+gh*2./3.,f(l0c11l+ix)+(221.*KD1-981.*KD2+
     + 867.*KD3-102.*KD4+KD5)/9.)
      KD7=gh*VEL(f(l0c6l+ix)+gh*5./6.,f(l0c11l+ix)+(-183.*KD1+678.*KD2-
     + 472.*KD3-66.*KD4+80.*KD5+3.*KD6)/48.)
      KD8=gh*VEL(f(l0c6l+ix)+gh,f(l0c11l+ix)+(716.*KD1-2079.*KD2+1002.
     + *KD3+834.*KD4-454.*KD5-9.*KD6+72.*KD7)/82.)


      DDEL=(41.*KD1+216.*(KD3+KD7)+27.*(KD4+KD6)+272.*KD5+41.*KD8)/840.
```

```
C     SHEAR STRESS COMPONENT STEP H IN Z
      gh=f(l0c10+irow)-f(l0c10l+irow)

      KS1=gh*SHEAREP(f(l0c12l+ix),w,ENUL,gA,f(l0dl+ix),f(l0c3l+ix),
     + f(l0c11l+ix))
      KS2=gh*SHEAREP(f(l0c12l+ix),w,ENUL,gA,f(l0dl+ix),f(l0c3l+ix),
     + f(l0c11l+ix)+KS1/9.)
      KS3=gH*SHEAREP(f(l0c12l+ix),w,ENUL,gA,f(l0dl+ix),f(l0c3l+ix),
     + f(l0c11l+ix)+(KS1+3.*KS2)/24.)
      KS4=gH*SHEAREP(f(l0c12l+ix),w,ENUL,gA,f(l0dl+ix),f(l0c3l+ix),
     + f(l0c11l+ix)+(KS1-3.*KS2+4.*KS3)/6.)
      KS5=gH*SHEAREP(f(l0c12l+ix),w,ENUL,gA,f(l0dl+ix),f(l0c3l+ix),
     + f(l0c11l+ix)+(-5.*KS1+27.*KS2-24.*KS3+6.*KS4)/8.)
      KS6=gH*SHEAREP(f(l0c12l+ix),w,ENUL,gA,f(l0dl+ix),f(l0c3l+ix),
     + f(l0c11l+ix)+(221.*KS1-981.*KS2+867.*KS3-102.*KS4+KS5)/9.)
      KS7=gH*SHEAREP(f(l0c12l+ix),w,ENUL,gA,f(l0dl+ix),f(l0c3l+ix),
     + f(l0c11l+ix)+(-183.*KS1+678.*KS2-472.*KS3-66.*KS4+80.*KS5+3.
     +*KS6)/48.)
      KS8=gH*SHEAREP(f(l0c12l+ix),w,ENUL,gA,f(l0dl+ix),f(l0c3l+ix),
     + f(l0c11l+ix)+(716.*KS1-2079.*KS2+1002.*KS3+834.*KS4-454.*KS5
     + -9.*KS6+72.*KS7)/82. )


      DSHEAR=(41.*KS1+216.*(KS3+KS7)+27.*(KS4+KS6)+272.*KS5+41.*KS8)
     + /840.
      f(l0c11+ix)=f(l0c11l+ix)+DSHEAR-DDEL-DVEL
      ENDIF
      ENDIF
C
C     START OF RETHETAL.GT.RETHETAS

      if(IWW(IX).eq.0) then
      rethetastW(IX)=rethetaL
      MSTW(IX)=MOLDW
      thetastW = thetaL
      F(L0C9L+IX)=THETAL/TDIV
      TRST(IX)=F(L0C10+IROW)
      DL=0.
      LAMDAAVE(IX)=0.
      endif

      IF(RETHETAL.GT.0.0.AND.TRANSIT(IX).GT.rg(9)) THEN

      IF(IWW(IX).EQ.0) THEN
      IWW(IX)=1
```

```
      ENDIF

c      UNCOMMENT NEXT LINE FOR SOLOMAN'S METHOD
c      IF(MW(IX).GE.0.)THEN
c     integrating lamda between Z(G=0) to Z(G=0.25)
C     START OF GAMMA.LT.0.25
C     FIND LAMDA AT HIGH END OF IZ SLAB ————————

      IF( F(LOC8L+IX).lt.0.25 )THEN
      no = .04723 / (10.- EXP(1.7 - RG(2)/2.)) ** 2

      IF( mw.eq.0.0 ) THEN
      n = no
      ELSEIF(Mw.LT.0.) THEN
      N=NO*EXP(Mw*(1.-55.*Mw**2)*(2.6*RG(2)+3.6*SQRT(RG(2))-86.))
      ELSE
      n = no*(EXP(-10.* mw ** .5) + 300.*mw**4)
      END IF

      relamdati = (.411 * rethetastW(IX)** 3/ n) ** .5
      lamdati = ENUL * relamdati / W

C     FIND LAMDA AT HIGH END OF IZ + 1 SLAB
      DWZH=(WHIGH2-WHIGH)/DSH
      R=(WHIGH**5+W**5)/2.*DS
      WTOT2W=0.0
      WTOT2W=F(LOC7+IX)+R
      THETALH=(.45*ENUL*WTOT2W/WHIGH**6)**.5
      MH = thetalH ** 2 * DWZH / ENUL

      IF(MH.GT.0.08) THEN
      MH=0.08
      ELSEIF(MH.LT.-0.08)THEN
      MH=-0.08
      ENDIF
      noH = .04723 / (10. - EXP(1.7 - RG(2)/ 2.))**2

      IF( mH.eq.0.0 )THEN
      nH = noH
      ELSEIF(MH.LT.0.) THEN
      NH=NOH*EXP(MH*(1.-55.*MH**2)*(2.6*RG(2)+3.6*SQRT(RG(2))-86.))
      ELSE
      nH = noH*(EXP(-10.*mH**.5)+300.*mH**4)
      END IF

      relamdatH = (.411 * rethetastW(IX) ** 3/ nH) ** .5
```

```
      lamdatH = ENUL * relamdatH / WHIGH
C     CALCULATE AVERAGE LAMDA
      lamdaave(IX)=lamdaave(IX)+(lamdati + lamdatH) / 2.*DS
      dlW(IX) = dlW(IX) + DS
      lamdatW(IX) = lamdaave(IX) / dlW(IX)

C     END OF (GAMMA) F(LOC8L+IX) .LT. 0.25 LOOP
      END IF

C     UNCOMMENT NEXT LINE FOR SOLOMAN'S METHOD
c      ELSE

C      ADVERSE DPXX I.E. M < 0.0

c       SOLOMAN'S CORRELATION
C       CONSTANTS AT START OF TRANSITION \\\\\\\\\\\\\\\\\
c        nW = .00086 * EXP(2.134 *MSTW*ALOG(RG(2))-59.23*MSTW-.564*
c     + ALOG(RG(2)))
c       SIGMASTW = .03 + (.1 / (.115 + EXP(42.9 * MSTW)))
c        smallnW = nW* ENUL / (SIGMASTW * thetastW ** 3)

C     \\\\\\\\\\\\\\\\\\\\\\\\\\\\\\\\\\\\\\\\\\\\\\\\\\\\\\\\

C       HIGH END OF CELL ++++++++++++++++++++
c        alpha = 4.+ (22.14 / (.79 + 2.72 * EXP(47.63 * m)))
c        sigma = .03 + (.1 / (.115 + EXP(42.9 * m)))
C     ++++++++++++++++++++++++++++++++++++++++

C       LOW END OF CELL ----------------------
c      DWZL=(W-WLOW)/DSL
c      R=(W**5+WLOW**5)/2.*DSL
c      WTOT3W=0.
c      WTOT3W=WTOTW-R
c      THETALL=(0.45*ENUL*WTOT3W/WLOW**6)**.5
C     ****************************
c      ML=thetalL ** 2 * DWZL/ ENUL
c      ALPHAL = 4. + (22.14 / (.79 + 2.72 * EXP(47.63 * ML)))
c      SIGMAL = .03 + (.1 / (.115 + EXP(42.9 * ML)))
C       ----------------------------------------

C           convert degrees to radians
c      alpha = alpha * pi / 180.
c      ALPHAL = ALPHAL * pi / 180.
C       calculate averages of sigma, alpha & velocity
c      slave = (sigma + SIGMAL) / 2.
c      aave = (TAN(alpha) + TAN(ALPHAL)) / 2.
```

```
c       vave = (WLOW+W) / 2.
c       integ1W = integ1W + DSL * slave / (aave * vave)
c       integ2W = integ2W + DSL * aave

C      END OF M.GE.0.0
c       ENDIF

       IF(TRANSIT(IX).LT.rg(9)) GOTO 39
       IF(H119M.GT.3.5) THEN
       CF120=1.E-6
       DELTA1T=0.0
       F(LOC8+IX)=1.
       GOTO 17
       ENDIF

       h2l = 1.
       h2u = 3.5


C       e IS THE ACCEPTABLE ERROR
       e = .0001
       GIter = 1 + (ALOG10((h2U - h2L) / e) / ALOG10(2.))
       THETATW=F(LOC9L+IX)
       DO KZ=1,GIter
       CALL TURBULENT2(F(LOC9L+IX),ENUL,h2l,W,CF120,H119L)
       CALL TURBULENT2(F(LOC9L+IX),ENUL,h2u,W,CF120,H119U)
       h2m = (h2l + h2u) / 2.
       CALL TURBULENT2(F(LOC9L+IX),ENUL,h2m,W,CF120,H119M)

       IF( (h119l - h2l).GT.0.0.AND. (h119m - h2m).LT.0.0) THEN
       h2u = h2m
       ELSE
       h2l = h2m
       END IF
       END DO

       IF(H119M.GT.3.5) THEN
       CF120=1.E-6
       DELTA1T=0.0
       F(LOC8+IX)=1.
       GOTO 17
       ENDIF

       if(h119m.le.1.6) then
       Gh1=3.3+0.8234/(h119m-1.1)**1.287
       else
```

```
      Gh1=3.3+1.5501/(h119m-0.6778)**3.064
      endif
      deltat=(Gh1+h119m)*F(L0C9L+IX)

      F(L0C9+IX)=F(L0C9L+IX)+DS*(cf120/2.-(2.+h119m)*F(L0C9L+IX)*DWZ/W)
      THETATZ=F(L0C9+IX)

      GAMMA = 1.-EXP(-.411*(F(L0C10+IR0W)-TRST(IX))**2/LAMDATW(IX)**2)

      39 CONTINUE

C     UNCOMMENT THIS LOOP FOR SOLOMAN'S METHOD
c      IF(MSTW.LE.0.0) THEN
C                integrate to find gamma
c      gamma = 1. - EXP(-smallnW * integ1W * integ2W)

c      ENDIF

       F(L0C8+IX) = GAMMA

C           END OF rethetal.gt.rethetas LOOP

     END IF
   17 CONTINUE

      F(L0C12+IX) = (1. - gamma) * cfl + gamma * cf120

      IF(GAMMA.LT.0.0001) THEN
      CFTR=CFL
      ELSE
      CFTR=(1.-GAMMA)*CFL+GAMMA*CF120
      ENDIF

c     coefficient=density * w1 * cfTR/2
      F(L0C0F+IX)=F(L0D+IX)*F(L0W1+IX)*CFTR/2.

C     END OF GAMMA.GT.0.999

      ENDIF
ccccccccccccccccccccccccccccccc
      mw=0.0
ccccccccccccccccccccccccccccccc
      END DO
      END DO
C     END OF NPATCH AND INDVAR
      END IF
```

```
      RETURN

  131 CONTINUE
C-------------------- SECTION  2 ------------- coefficient =
GRND1
      RETURN
  132 CONTINUE
C-------------------- SECTION  3 ------------- coefficient =
GRND2
      RETURN
  133 CONTINUE
C-------------------- SECTION  4 ------------- coefficient =
GRND3
      RETURN
  134 CONTINUE
C-------------------- SECTION  5 ------------- coefficient =
GRND4
      RETURN
  135 CONTINUE
C-------------------- SECTION  6 ------------- coefficient =
GRND5
      RETURN
  136 CONTINUE
C-------------------- SECTION  7 ------------- coefficient =
GRND6
      RETURN
  137 CONTINUE
C-------------------- SECTION  8 ------------- coefficient =
GRND7
      RETURN
  138 CONTINUE
C-------------------- SECTION  9 ------------- coefficient =
GRND8
      RETURN
  139 CONTINUE
C-------------------- SECTION 10 ------------- coefficient =
GRND9
      RETURN
 1310 CONTINUE
C-------------------- SECTION 11 ------------- coefficient =
GRND10
      RETURN
 1311 CONTINUE
C-------------------- SECTION 12 -------------------- value =
GRND
      RETURN
```

```
 1312 CONTINUE
C------------------- SECTION 13 ------------------- value =
GRND1
      RETURN
 1313 CONTINUE
C------------------- SECTION 14 ------------------- value =
GRND2
      RETURN
 1314 CONTINUE
C------------------- SECTION 15 ------------------- value =
GRND3
      RETURN
 1315 CONTINUE
C------------------- SECTION 16 ------------------- value =
GRND4
      RETURN
 1316 CONTINUE
C------------------- SECTION 17 ------------------- value =
GRND5
      RETURN
 1317 CONTINUE
C------------------- SECTION 18 ------------------- value =
GRND6
      RETURN
 1318 CONTINUE
C------------------- SECTION 19 ------------------- value =
GRND7
      RETURN
 1319 CONTINUE
C------------------- SECTION 20 ------------------- value =
GRND8
      RETURN
 1320 CONTINUE
C------------------- SECTION 21 ------------------- value =
GRND9
      RETURN
 1321 CONTINUE
C------------------- SECTION 22 ------------------- value =
GRND10
      RETURN
C*****************************************************************


C*****************************************************************
C* Make changes to data for GROUPS 15, 16, 17, 18  GROUP 19.
```

```
C*****************************************************************
C
C--- GROUP 19. Special calls to GROUND from EARTH
C
   19 GO TO (191,192,193,194,195,196,197,198,199,1910),ISC
  191 CONTINUE
C   * -------------------- SECTION 1 ---- Start of time step.
      RETURN
  192 CONTINUE
C   * -------------------- SECTION 2 ---- Start of sweep.
      RETURN
  193 CONTINUE
C   * -------------------- SECTION 3 ---- Start of iz slab.

      RETURN
  194 CONTINUE
C   * -------------------- SECTION 4 ---- Start of iterations over
slab.
      RETURN
  199 CONTINUE
C   * -------------------- SECTION 9 ---- Start of solution sequence
for
C                                          a variable
      RETURN
 1910 CONTINUE
C   * -------------------- SECTION 10---- Finish of solution sequence
for
C                                          a variable
      RETURN
  195 CONTINUE
C   * -------------------- SECTION 5 ---- Finish of iterations over
slab.
      RETURN
  196 CONTINUE
C   * -------------------- SECTION 6 ---- Finish of iz slab.
C     ZERO LOCATION OF DENSITY
      LODL=LOF(LOW(DEN1))
      LOD=LOF(DEN1)
      LODH=LOF(HIGH(DEN1))
      LODH2=LOF(ANYZ(DEN1,IZ+2))

C     ZERO LOCATION OF VELOCITIES
      LOW1L=LOF(LOW(W1))
      LOW1=LOF(W1)
      LOW1H=LOF(HIGH(W1))
      LOW1H2=LOF(ANYZ(W1,IZ+2))
```

```
C     ZERO LOCATION OF SCALERS
      LOC1=LOF(C1)
      LOC2=LOF(C2)
      LOC3=LOF(C3)
      LOC4=LOF(C4)
      LOC5=LOF(C5)

      LOC2L=LOF(LOW(C2))
      LOC3L=LOF(LOW(C3))
      LOC4L=LOF(LOW(C4))
      LOC5L=LOF(LOW(C5))

      GCMUCD=.09
      GC2E=1.92

C     ASSUMES THAT WALLS ARE AT IX = 1 AND IX = NX
      DO IX=2,NX-1

C     LENGTH OF (IZ) CELL
      GDXL=XC(IX,IY,IZ+1)-XC(IX,IY,IZ)
      GDZL=ZC(IX,IY,IZ+1)-ZC(IX,IY,IZ)
      GDSL=SQRT(GDXL**2+GDZL**2)

C     ON FIRST Z SLAB
      IF(IZ.EQ.1) THEN
      GKIN=1.5*(RG(2)/100.*RG(5))**2
      GEPIN=GCMUCD**0.75*GKIN**1.5/RG(8)
      F(LOC2+IX)=(1./RG(5)+1./F(LOW1+IX))/2.*GDSL
      F(LOC4+IX)=RG(2)*GDSL
      F(LOC5+IX)=GDSL
      F(LOC1+IX)=RG(2)
      ENDIF

      IF(IZ.GT.1.AND.IZ.LT.NZ) THEN
C     SUM OF INTEGRAL HELD IN SCALER C2
      F(LOC2+IX)=F(LOC2L+IX)+(1./F(LOW1+IX)+1./F(LOW1L+IX))/2.*GDSL
      F(LOC3+IX)=(GKIN**(1.-GC2E)+(GC2E-1.)*GEPIN/GKIN**GC2E*
     +F(LOC2+IX))**(1./(1.-GC2E))
      F(LOC1+IX)=100.*SQRT(.667*F(LOC3+IX))/F(LOW1+IX)
C     TOTAL LENGTH FROM INLET
      F(LOC5+IX)=F(LOC5L+IX)+GDSL
      F(LOC4+IX)=F(LOC4L+IX)+F(LOC1+IX)*GDSL
      ENDIF
      END DO
```

```
      RETURN
  197 CONTINUE
C   * -------------------- SECTION 7 ---- Finish of sweep.

      SUMW=0.0
      SD=0.0
      KK=0

      DO IX=1,NX
      IA(IX)=0
      IWW(IX)=0
      LAMDAAVE(IX)=0.
      LAMDATW(IX)=0.
      TRANSIT(IX)=0.
      TRST(IX)=0.
      IAA(IX)=0
      END DO

      RETHETASTW(IX)=0.
      LAMDAAVE(IXF) =0.
      THETATW=0.
      lamdac=0
      TRSTARTW=0.
      GAMMA=0.
      H119MW=0.
      INTEG1W=0.
      INTEG2W=0.
      WTOT3W=0.

      RETURN
  198 CONTINUE
C   * -------------------- SECTION 8 ---- Finish of time step.
C
      RETURN
C*********************************************************************


      SUBROUTINE laminar2(ENUL,GRHO,W,WHIGH,WGRAD,THETAL,SHAPE,cfl)

      COMMON /LAM2/Ibb
      REAL lamda

      lamda = thetal ** 2 * WGRAD/ ENUL

      IF( lamda.lt.-0.09 ) THEN
      lamda=-0.089
```

```
      END IF

      shear = (lamda + .09) ** .62
      tau = ENUL*GRHO * W * shear / thetal
      cfl = 2. * tau  / (GRHO* W ** 2)
      zz = (.25 - lamda)
      shape = 2.0 + 4.14 * zz - 83.5 * zz ** 2+ 854. * zz ** 3- 3337.*
     +zz ** 4 + 4576. * zz ** 5
      RETURN
      END


      SUBROUTINE turbulent2(THETATS,ENUL,H2,W,cf120,H119N)

      COMMON /TUR2/DWZ
      REAL kappa,lamda
      DATA KAPPA/0.41/

c     CALCULATE SKIN FRICTION FROM EQUATION 6-120

      cf120 = .3 * EXP(-1.33 * h2) / ALOG10(w * thetatS / ENUL)
     + ** (1.74 + .31 * h2)


c     USED GUESSED h2 AND CALCULATED cf120 TO CALCULATE PI VIA EQN 6-122
c      in favourable dp beta will be -ve

      beta = -2. * h2 * thetatS * dwz / cf120 / w

c     beta is a quadratic eqn in pi, with coefficients a, b & c.

      a = 1.
      b = .76 / .42
      c = -(.4 + beta) / .42

c      this is the limit for beta (-.7438) or it goes complex
c      usualy means bad first choice of h2 or cf
C      FIND pi EQN 6-121

      pi = (-b + (b ** 2 - 4. * a * c) ** .5) / 2.

c     FUNCTION OF PI REQUIRED IN 6-119 (a)

      fpi = (2.+ 3.179 * pi + 1.5 * pi ** 2) / (kappa * (1.+ pi))

c      USE EQN 6-119(a) WITH CALCULATED pi TO CALCULATE NEW h2 (h119)
```

```
      lamda = (2. / cf120) ** .5
      h119n = lamda / (lamda - fpi)

   75 CONTINUE
      RETURN
      END

C

      FUNCTION vel(WW,KK)
      real kk
      vel=kk/ww
      return
      end


      FUNCTION SHEAR(CF,WW,gENUL,A,gRHO,EP,KK)

      REAL KK
      TAU=CF/2*gRHO*WW**2
      TERM1=KK*A*TAU/(gENUL*gRHO*WW)
      TERM2=-2.86*EP/WW
      SHEAR=TERM1+TERM2
      RETURN
      END

      FUNCTION SHEAREP(CF,WW,gENUL,A,gRHO,KK,EP)

      REAL KK
      TAU=CF/2*gRHO*WW**2
      TERM1=EP*1.036*A*TAU/(gENUL*gRHO*WW)
      TERM2=-5.486*EP**2/WW/KK
      SHEAREP=TERM1+TERM2
      RETURN
      END
```

Appendix C

Integral Turbulent Energy Equation

The equations for kinetic energy and dissipation can be written as:-

$$\rho\overline{w}\frac{\partial k}{\partial z}+\rho\overline{u}\frac{\partial k}{\partial x}=\frac{\partial}{\partial x}\left[\left(\mu+\frac{\mu_t}{\sigma_k}\right)\frac{\partial k}{\partial x}\right]+\mu_t\left(\frac{\partial\overline{w}}{\partial x}\right)^2-\rho\varepsilon \qquad (1)$$

$$\rho\overline{w}\frac{\partial \varepsilon}{\partial z}+\rho\overline{u}\frac{\partial \varepsilon}{\partial x}=\frac{\partial}{\partial x}\left[\left(\mu+\frac{\mu_t}{\sigma_\varepsilon}\right)\frac{\partial \varepsilon}{\partial x}\right]+C_1\mu_t\left(\frac{\partial\overline{w}}{\partial x}\right)^2\frac{\varepsilon}{k}-C_2\rho\frac{\varepsilon^2}{k} \qquad (2)$$

Kinetic Energy Equation

Consider equation (1), integrating from x = 0 to x = δ gives:-

$$\int_0^\infty \rho\overline{w}\frac{\partial k}{\partial z}\,dx+\int_0^\infty \rho\overline{u}\frac{\partial k}{\partial x}\,dx= \qquad (1a)$$

$$-\int_0^\infty \frac{\partial}{\partial x}\left[\left(\mu+\frac{\mu_t}{\sigma_k}\right)\frac{\partial k}{\partial x}\right]dx+\int_0^\infty \mu_t\left(\frac{\partial\overline{w}}{\partial x}\right)^2 dx-\int_0^\infty \rho\varepsilon\,dx$$

Since $\overline{u}=0$ at both limits, then $\int_0^\infty \rho\overline{u}\frac{\partial k}{\partial x}\,dx=0$

The diffusion term is similarly zero.

$$\therefore \int_0^\infty \rho\overline{w}\frac{\partial k}{\partial z}\,dx=\int_0^\infty \mu_t\left(\frac{\partial\overline{w}}{\partial x}\right)^2 dx-\int_0^\infty \rho\varepsilon\,dx$$

$$\text{or } \int_0^\infty \rho\overline{w}\frac{\partial k}{\partial z}\,dx=\int_0^\infty \tau_t\left(\frac{\partial\overline{w}}{\partial x}\right)dx-\int_0^\infty \rho\varepsilon\,dx \qquad \text{c.f. White (1974)}$$

$$\therefore \frac{d}{dz}\left(\int_0^\infty \rho\overline{w}\,k\,dx\right)=\int_0^\infty \tau_t\left(\frac{\partial\overline{w}}{\partial x}\right)dx-\int_0^\infty \rho\varepsilon\,dx$$

For incompressible flow, density is constant, therefore:

$$\frac{d}{dz}\left(\int_0^\infty \overline{w}\,k\,dx\right)=\int_0^\infty \frac{\tau_t}{\rho}\left(\frac{\partial\overline{w}}{\partial x}\right)dx-\int_0^\infty \varepsilon\,dx$$

For fully turbulent flow Bradshaw, Ferriss and Atwell (1967) show that

$\frac{\tau_t}{\rho k}$ = constant, a, which takes the value 0.3

The kinetic energy equation becomes:-

$$\frac{d}{dz}\left(\int_0^\infty \overline{w}\, k\, dx\right) = \int_0^\infty ak\left(\frac{\partial \overline{w}}{\partial x}\right) dx - \int_0^\infty \varepsilon\, dx \qquad (1b)$$

Data from Fraser (1978) shows that the variation of streamwise turbulence intensity, i.e. u', in the laminar boundary layer for transitional flows takes the form:-

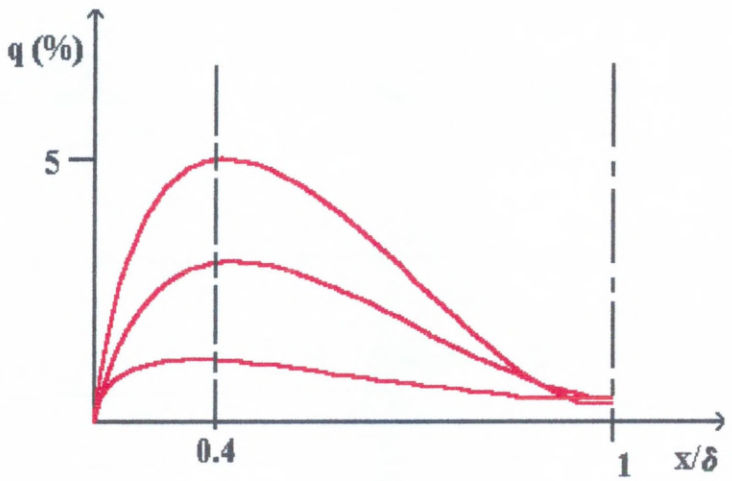

Figure C.1: Turbulence Intensity Profiles

It can be seen from Figure C.1 above, that the maximum value in the laminar boundary layer of turbulence intensity is approximately 5%, and occurs when $(x/\delta) \approx 0.4$. This is the point when the turbulence intermittency starts to become significant i.e. the occurence of turbulent spots.

The variation of kinetic energy across the laminar boundary layer is expected to be similar in form to that of the turbulence intensity and exhibiting a maximum value at $(x/\delta) \approx 0.4$ and decreasing to zero at the wall and some finite value in the free stream.

Consider the left hand side of equation (1b)

i.e. $\frac{d}{dz}\left(\int_0^{\infty} \overline{w}\, k\, dx\right)$

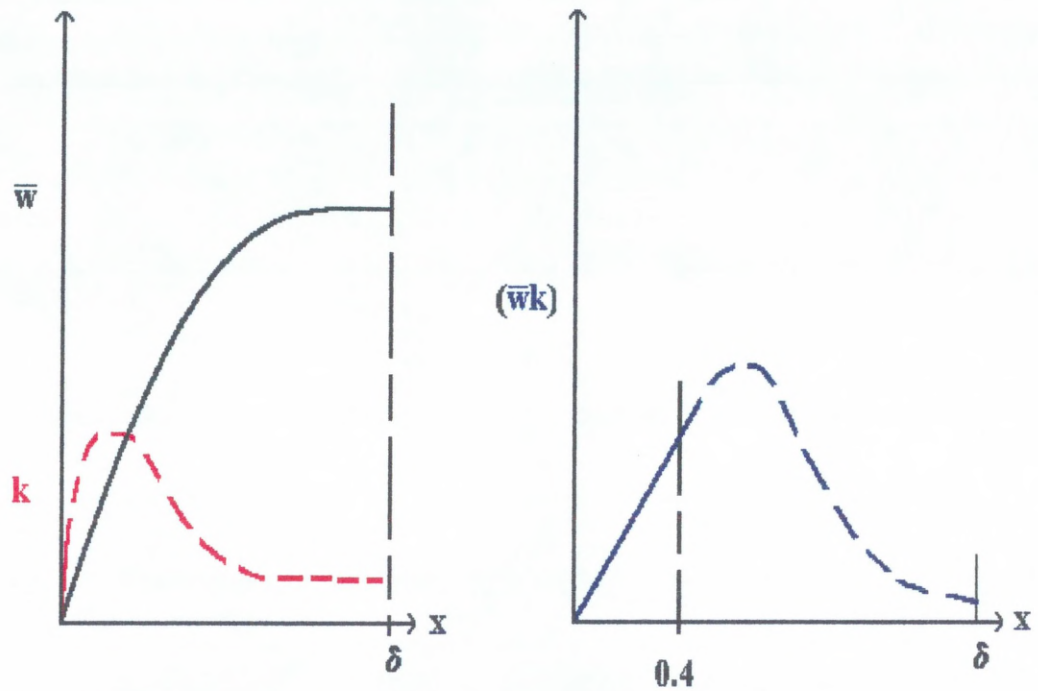

Figure C.2: Velocity and Kinetic Energy Profiles

The expected variation of $(\overline{w}k)$ with x is shown in Figure C.2. i.e. $(\overline{w}k)$ varies from x = 0 to a maximum and then decreases to almost zero at x = δ. Note that the maximum value of $(\overline{w}k)$ at (x/δ) > 0.4. Measurements from Fraser (1978) indicate that the mean velocity profile is essentially linear up to (x/δ) ≈ 0.5 i.e.

$$\frac{\overline{w}}{W_{\infty}} \approx 1.89\left(\frac{x}{\delta}\right)$$

It was assumed that the average velocity profile for all flows would be similar, therefore using the Blasius (1908) data the average mean velocity in the boundary layer was given by:-

$$\overline{w}_{ave} = \frac{1}{\delta}\int_0^{\delta} \overline{w}\, dx$$

This gives an average mean velocity in the boundary layer equal to approximately 70% of the free stream value. Inserting the vaules into equation (1b) gives:-

$$\begin{aligned}\int_0^{\delta}(\overline{w}\,k)\,dx &= \overline{w}_{av}\,k_{av}\,\delta \\ &= 0.7W_{\infty}\frac{1}{2\delta}\delta\hat{k}\delta \\ &= 0.35W_{\infty}\hat{k}\delta\end{aligned}$$

where $\hat{k}$ represents the maximum value of kinetic energy

$$\begin{aligned}\therefore \frac{d}{dz}\left(\int_0^{\delta}\overline{w}\,k\,dx\right) &= \frac{d}{dz}\left(0.35W_{\infty}\hat{k}\delta\right) \\ &= 0.35\frac{d}{dz}\left(W_{\infty}\hat{k}\delta\right)\end{aligned} \qquad (1c)$$

Consider the right hand side of equation (1b)

i.e. $$a\int_0^{\infty}k\left(\frac{\partial\overline{w}}{\partial x}\right)dx - \int_0^{\infty}\varepsilon\,dx$$

The kinetic energy and velocity gradient in the x direction can be represented by the following profiles:

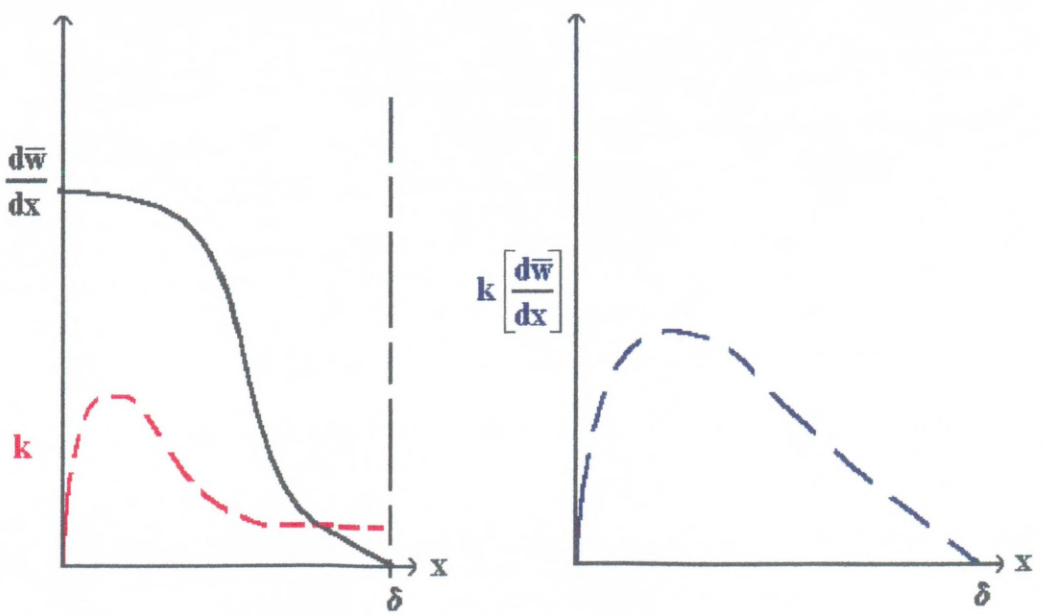

Figure C.3: Velocity Gradient and Kinetic Energy Profiles

To a first degree approximation:-

$$a\int_0^{\delta} k\left(\frac{\partial \overline{w}}{\partial x}\right) dx = a\,k_{ave}\left(\frac{\partial \overline{w}}{\partial x}\right)_{ave} \delta$$

$$= a\left(\frac{1}{\delta}\frac{1}{2}\delta\,\hat{k}\right)\left(\frac{1}{\delta}\frac{1}{2}\delta\left(\frac{\partial \overline{w}}{\partial x}\right)_{max}\right)\delta$$

$$= \frac{a\delta}{4}\hat{k}\left(\frac{\partial \overline{w}}{\partial x}\right)_{max}$$

The maximum value of $\left(\frac{\partial \overline{w}}{\partial x}\right)$ occurs at the wall

$$\text{i.e.} \quad \left(\frac{\partial \overline{w}}{\partial x}\right)_{max} = \left(\frac{\partial \overline{w}}{\partial x}\right)_{x=0} \quad \text{and } \tau_0 = \mu\left(\frac{\partial \overline{w}}{\partial x}\right)_{x=0}$$

$$\therefore \quad \left(\frac{\partial \overline{w}}{\partial x}\right)_{x=0} = \frac{\tau_0}{\mu}$$

Where τ_0 is the shear stress due to molecular viscosity, i.e. the laminar shear stress.

$$a\int_0^{\delta} k\left(\frac{\partial \overline{w}}{\partial x}\right) dx \approx \frac{a\delta}{4}\hat{k}\frac{\tau_0}{\mu} \tag{1d}$$

Hinze (1975) showed that for a fully turbulent boundary layer, the variation in dissipation length scale is approximately hyperbolic in x.

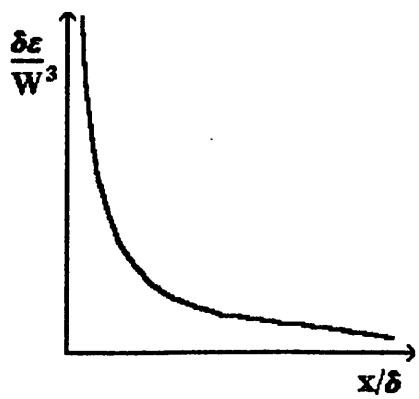

Figure C.4: Dissipation Profile, Turbulent Boundary Layer

Consider the second term on the rhs of equation (1b):-

i.e. $\int_0^\delta \varepsilon \, dx$ can be expressed as $\delta \int_0^1 \varepsilon \, d(x/\delta)$

$$\therefore \quad \int_0^\delta \varepsilon \, dx = \delta \int_0^1 \frac{W_\infty^3}{\delta}\left(\frac{1}{x/\delta}\right) d(x/\delta)$$

$$= W_\infty^3 \left[\ln(x/\delta)\right]_0^1$$

This cannot be integrated to produce a meaningful result, therefore it is assumed that:

$$\int_0^\delta \varepsilon \, dx = \varepsilon_{ave}\,\delta = \bar{\varepsilon}\delta \tag{1e}$$

Where ε_{ave} is some representative average value of ε across the boundary layer.

Substitution of the approximations (1c), (1d) and (1e) into equation (1b) gives:-

$$0.35\frac{d}{dz}\left(W_\infty \hat{k}\delta\right) = \frac{a\delta}{4}\hat{k}\frac{\tau_0}{\mu} - \bar{\varepsilon}\delta$$

re-arranging gives:-

$$\frac{d\hat{k}}{dz} = \hat{k}\left[0.714\frac{a}{W_\infty}\frac{\tau_0}{\mu} - \frac{1}{W_\infty}\frac{dW_\infty}{dz} - \frac{1}{\delta}\frac{d\delta}{dz}\right] - 2.86\frac{\bar{\varepsilon}}{W_\infty} \tag{1f}$$

Equation (1f) is the approximated form of the kinetic energy equation. The groups of terms on the l.h.s. are described below:

$\frac{\hat{k}a\tau_o}{W_\infty\mu}$ production term, i.e. the turbulent kinetic energy produced by skin friction

$\frac{\hat{k}}{W_\infty}\frac{dW_\infty}{dz}$ pressure gradient term i.e. favourable pressure gradient reduces turbulent kinetic energy, adverse increases turbulent kinetic energy

$\frac{\hat{k}}{\delta}\frac{d\delta}{dz}$ the rate of change of δ. Slow speed means a thick boundary layer and hence it can absorb more turbulence than a thin one.

$\frac{\bar{\varepsilon}}{W_\infty}$ viscous dissipation due to viscosity

Dissipation Equation

Equation (2) is repeated here for convenience

$$\rho\overline{w}\frac{\partial\varepsilon}{\partial z}+\rho\overline{u}\frac{\partial\varepsilon}{\partial x}=\frac{\partial}{\partial x}\left[\left(\mu+\frac{\mu_t}{\sigma_\varepsilon}\right)\frac{\partial\varepsilon}{\partial x}\right]+C_1\mu_t\left(\frac{\partial\overline{w}}{\partial x}\right)^2\frac{\varepsilon}{k}-C_2\rho\frac{\varepsilon^2}{k} \qquad (2)$$

Integrating equation (2) from $x = 0$ to $x = \infty$ gives:-

$$\int_0^\infty \rho\overline{w}\frac{\partial\varepsilon}{\partial z}\,dx+\int_0^\infty \rho\overline{u}\frac{\partial\varepsilon}{\partial x}\,dx= \qquad (2a)$$

$$\int_0^\infty \frac{\partial}{\partial x}\left[\left(\mu+\frac{\mu_t}{\sigma_k}\right)\frac{\partial\varepsilon}{\partial x}\right]dx+\int_0^\infty C_1\mu_t\left(\frac{\partial\overline{w}}{\partial x}\right)^2\frac{\varepsilon}{k}dx-\int_0^\infty C_2\rho\frac{\varepsilon^2}{k}dx$$

Integration across the boundary layer renders the diffusion term equal to zero c.f. equation 1. The term $\int_0^\delta \rho\overline{u}\frac{\partial\varepsilon}{\partial x}dx$ will be small since $\overline{u} = 0$ at $x = 0$ and

$\frac{\partial\varepsilon}{\partial x} = 0$ at $x = \infty$

Equation (2) reduces to:-

$$\frac{d}{dz}\left(\int_0^\infty \rho\overline{w}\varepsilon\,dx\right)=C_1\int_0^\infty \tau_t\left(\frac{\partial\overline{w}}{\partial x}\right)\frac{\varepsilon}{k}dx-C_2\int_0^\infty \rho\frac{\varepsilon^2}{k}dx$$

For incompressible flows, the density is constant:-

$$\frac{d}{dz}\left(\int_0^\infty \overline{w}\varepsilon\,dx\right)=C_1\int_0^\infty \frac{\tau_t}{\rho}\left(\frac{\partial\overline{w}}{\partial x}\right)\frac{\varepsilon}{k}dx-C_2\int_0^\infty \frac{\varepsilon^2}{k}dx$$

Similarly $\tau/\rho = a\,k$ and $\left(\frac{\partial\overline{w}}{\partial x}\right)_{x=0}=\frac{\tau_0}{\mu}$

$$\frac{d}{dz}\left(\int_0^\infty \overline{w}\varepsilon\, dx\right) = C_1\int_0^\infty a\varepsilon\left(\frac{\partial \overline{w}}{\partial x}\right)\frac{\varepsilon}{k}dx - C_2\int_0^\infty \frac{\varepsilon^2}{k}\,dx \qquad (2b)$$

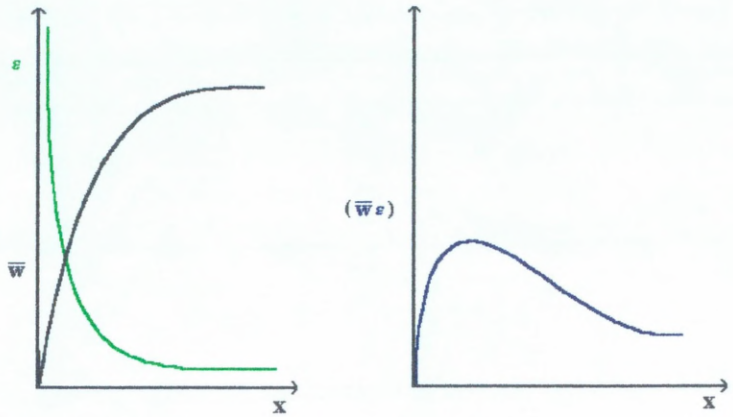

Figure C.5: Dissipation and Velocity Profiles

Consider the left hand side:-

$$\text{Assumming } \int_0^\infty (\overline{w}\varepsilon)dx = \overline{w}_{ave}\varepsilon_{ave}\delta \qquad (2c)$$
$$= 0.7W_\infty\overline{\varepsilon}\delta$$

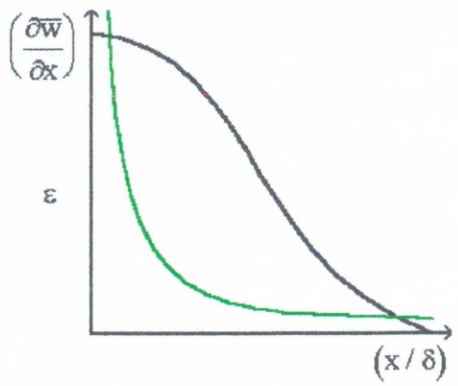

Figure C.6: Velocity Gradient and Dissipation Profile

Consider the right hand side:

i.e. $$C_1\int_0^\infty a\varepsilon\left(\frac{\partial \overline{w}}{\partial x}\right)dx = aC_1\int_0^\infty \varepsilon\left(\frac{\partial \overline{w}}{\partial x}\right)dx$$

$$\approx aC_1\varepsilon_{ave}\left(\frac{\partial \overline{w}}{\partial x}\right)_{ave}\delta$$

$$\approx aC_1\bar{\varepsilon}\frac{1}{\delta}\frac{1}{2}\delta\left(\frac{\partial\overline{w}}{\partial x}\right)_{max}\delta$$

$$\approx \frac{aC_1}{2}\bar{\varepsilon}\left(\frac{\partial\overline{w}}{\partial x}\right)_{max}\delta$$

but $\left(\frac{\partial\overline{w}}{\partial x}\right)_{max} = \left(\frac{\partial\overline{w}}{\partial x}\right)_{x=0} = \frac{\tau_0}{\mu}$

$$\therefore\ C_1\int_0^{\infty} a\varepsilon\left(\frac{\partial\overline{w}}{\partial x}\right)dx = \left(\frac{aC_1}{2}\right)\bar{\varepsilon}\frac{\tau_0}{\mu}\delta \qquad (2d)$$

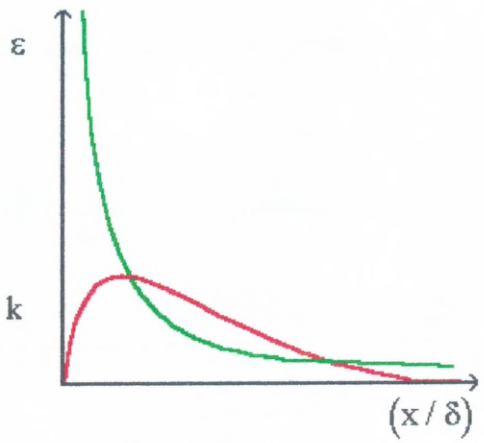

Figure C.7: Dissipation and Kinetic Energy Profiles

and $$C_2\int_0^{\infty}\frac{\varepsilon^2}{k}dx = C_2\varepsilon_{ave}^2\frac{\delta}{k_{ave}}$$

$$\approx C_2\bar{\varepsilon}^2\frac{2\delta}{\delta\hat{k}}\delta$$

$$\approx 2C_2\frac{\bar{\varepsilon}^2}{\hat{k}}\delta \qquad (2e)$$

The reduced equation becomes:

$$\frac{d}{dz}(0.7W_\infty \bar{\varepsilon}\delta) = \left(\frac{aC_1}{2}\right)\bar{\varepsilon}\frac{\tau_0}{\mu}\delta - 2C_2\frac{\bar{\varepsilon}^2}{\hat{k}}\delta$$

expanding and re - arranging gives:-

$$W_\infty \frac{d\bar{\varepsilon}}{dz} = \bar{\varepsilon}\left[\left(\frac{aC_1}{1.4}\right)\frac{\tau_0}{\mu} - \frac{1}{W_\infty}\frac{dW_\infty}{dz} - \frac{1}{\delta}\frac{d\delta}{dz}\right] - \left(\frac{2C_2}{0.7}\right)\frac{\bar{\varepsilon}^2}{\hat{k}}$$

Using the values, $C_1 = 1.45$ and $C_2 = 1.92$ gives:-

$$W_\infty \frac{d\bar{\varepsilon}}{dz} = \bar{\varepsilon}\left[1.036a\frac{\tau_0}{\mu} - \frac{1}{W_\infty}\frac{dW_\infty}{dz} - \frac{1}{\delta}\frac{d\delta}{dz}\right] - 5.486\frac{\bar{\varepsilon}^2}{\hat{k}} \qquad (2f)$$

Equation (2f) is the approximated form of the dissipation equation, which is coupled to the kinetic energy equation, hence the groups on the l.h.s are similar to that of equation (1f).

Appendix D

Taguchi Analysis Run 1

Factor	Meaning	Level 1	Level 2	Level 3
A	q at Re_{crit}	0.01	0.02	0.029
B	char. len. (m)	0.001	0.01	0.1
C	press. grad.	adverse	zero	favourable
D	criteria (%)	3	5	7

Table D.1: Factors and Levels

Trial No.	Results (z distance, m)
1	0.151
2	0.251
3	0.510
4	0.144
5	0.210
6	0.713
7	0.201
8	0.223
9	0.246

Table D.2: Results

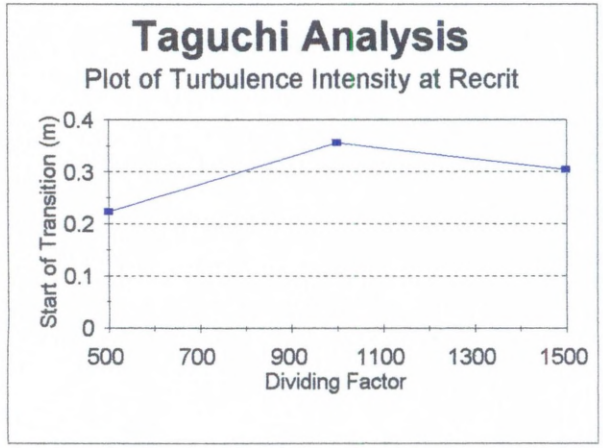

Figure D.1: Taguchi Analysis Run 1

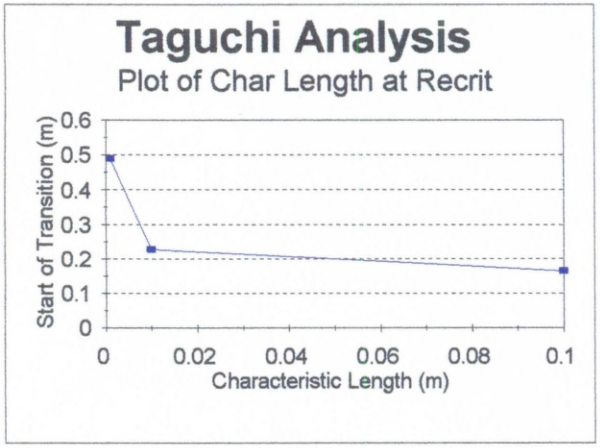

Figure D.2: Taguchi Analysis Run 1

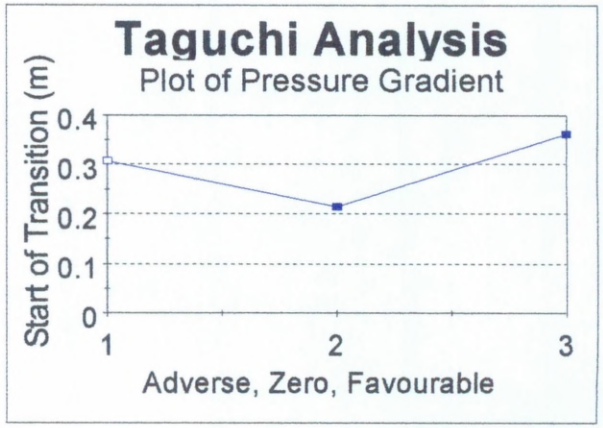

Figure D.3: Taguchi Analysis Run 1

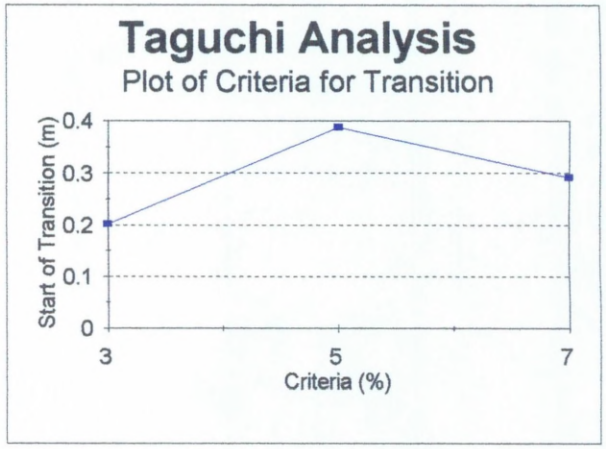

Figure D.4: Taguchi Analysis Run 1

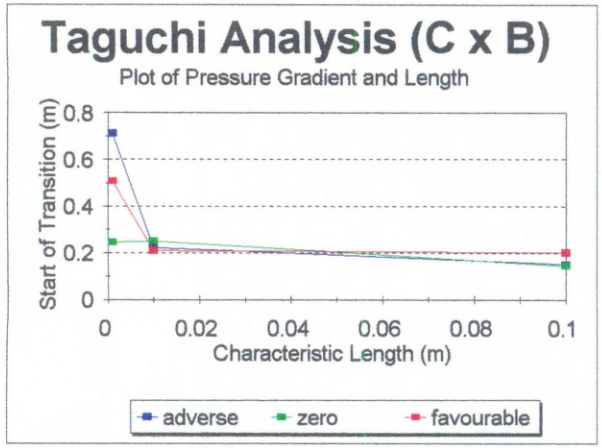

Figure D.5: Taguchi Analysis Run 1

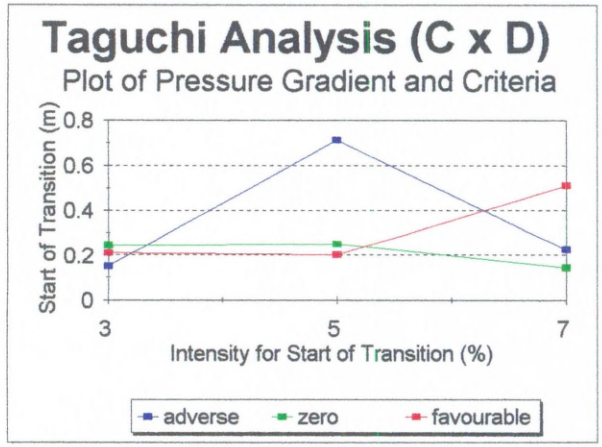

Figure D.6: Taguchi Analysis Run 1

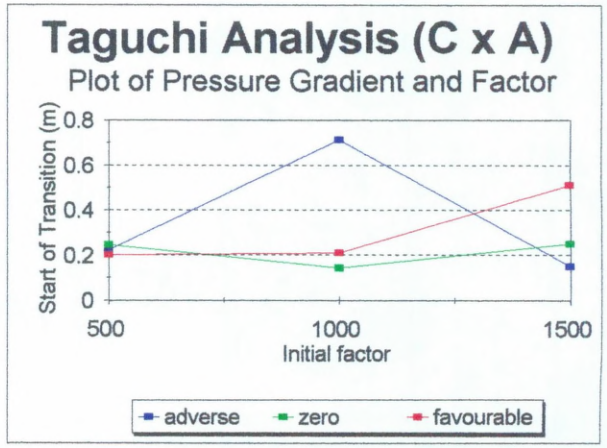

Figure D.7: Taguchi Analysis Run 1

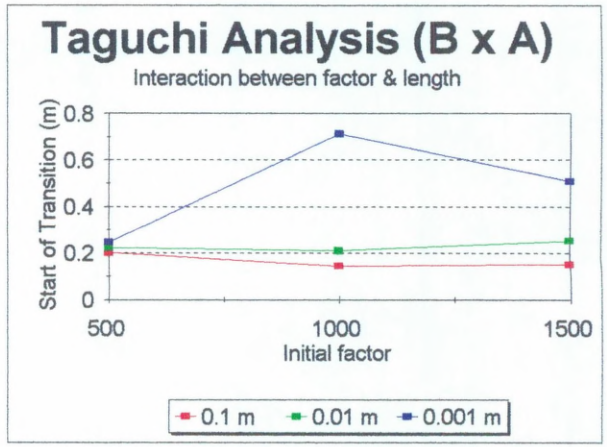

Figure D.8: Taguchi Analysis Run 1

Figure D.9: Taguchi Analysis Run 1

Figure D.10: Taguchi Analysis Run 1

Taguchi Analysis Run 2

Factor	Meaning	Level 1	Level 2	Level 3
A	q at Re_{crit}	0.01	0.02	0.029
B	char. length	6δ	12δ	18δ
C	press. grad.	adverse	zero	favourable
D	criteria (%)	3	5	7

Table D.3: Factors and Levels

Trial No.	Results (z distance, m)
1	0.154
2	0.215
3	0.292
4	0.189
5	0.165
6	0.133
7	0.174
8	0.133
9	0.102

Table D.4: Results

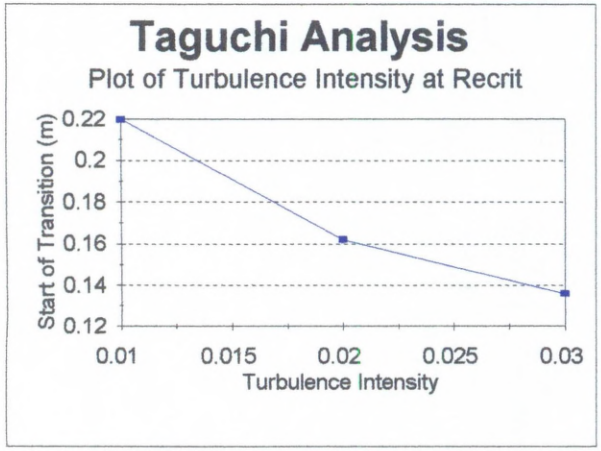

Figure D.11: Taguchi Analysis Run 2

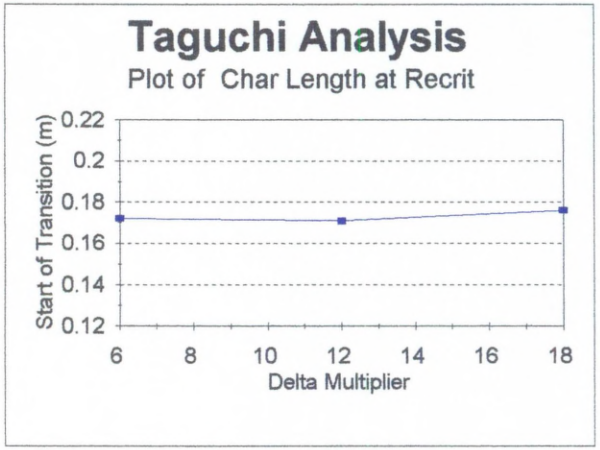

Figure D.12: Taguchi Analysis Run 2

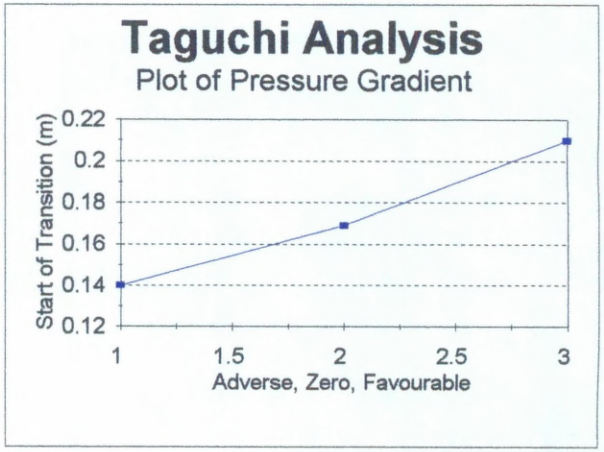

Figure D.13: Taguchi Analysis Run 2

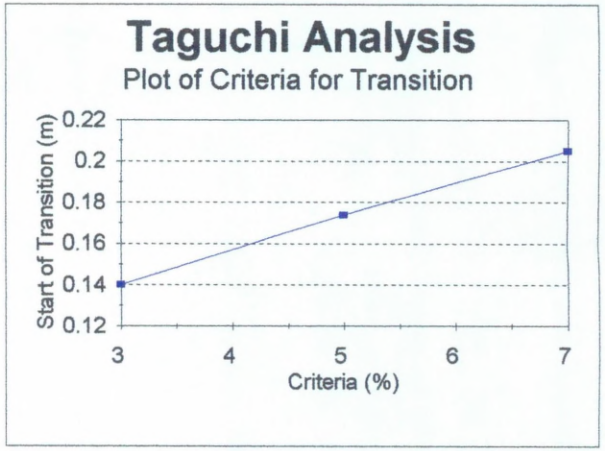

Figure D.14: Taguchi Analysis Run 2

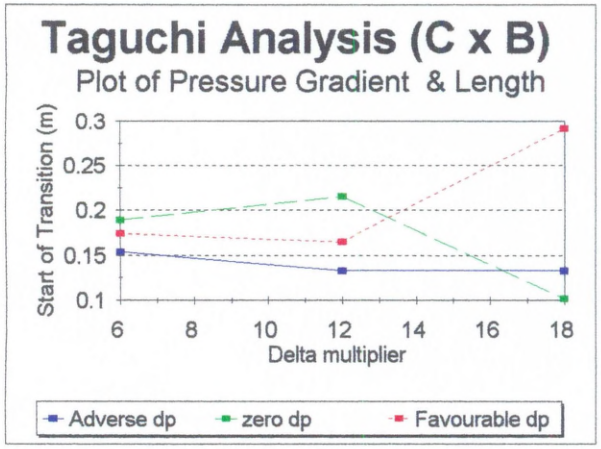

Figure D.15: Taguchi Analysis Run 2

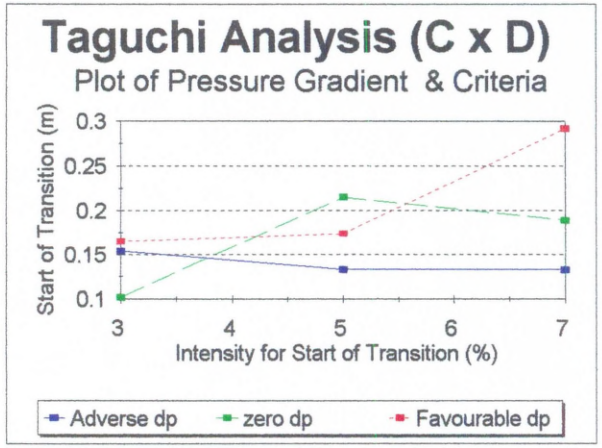

Figure D.16: Taguchi Analysis Run 2

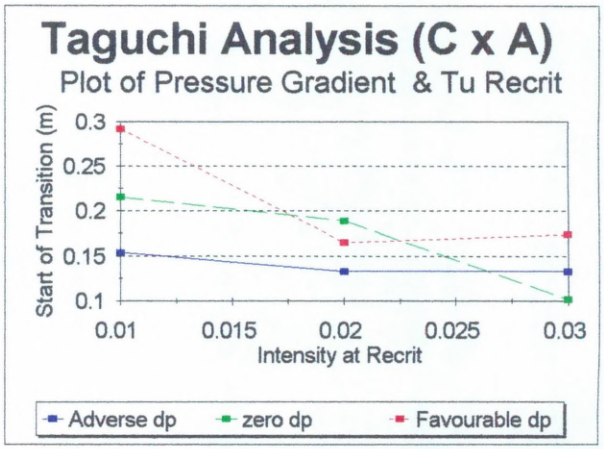

Figure D.17: Taguchi Analysis Run 2

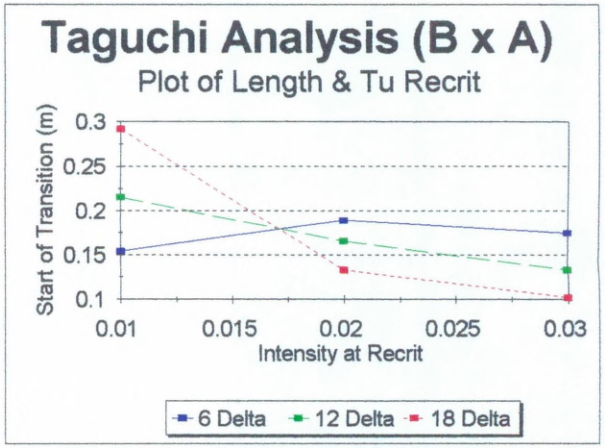

Figure D.18: Taguchi Analysis Run 2

Figure D.19: Taguchi Analysis Run 2

Figure D.20: Taguchi Analysis Run 2

Taguchi Analysis Run 3

Factor	Meaning	Level 1	Level 2	Level 3
A	q at Re_{crit}	0.01	0.02	0.029
B	char. length	6δ	12δ	18δ
C	x co-ord (m)	0.10005	0.1159	0.14
D	criteria (%)	3	5	7

Table D.5: Factors and Levels

Trial No.	Results (z distance, m)
1	0.165
2	0.205
3	0.315
4	0.190
5	0.095
6	0.145
7	0.105
8	0.145
9	0.075

Table D.6: Results

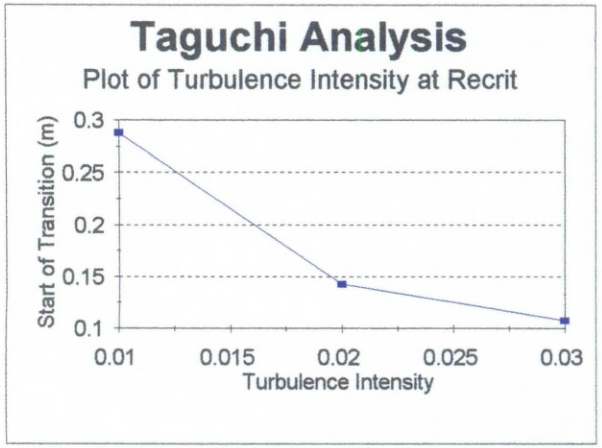

Figure D.21: Taguchi Analysis Run 3

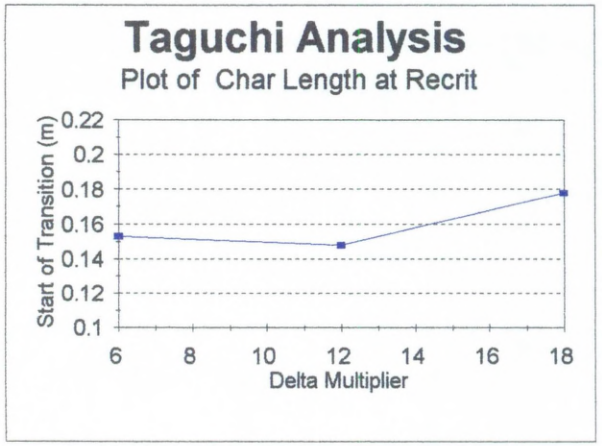

Figure D.22: Taguchi Analysis Run 3

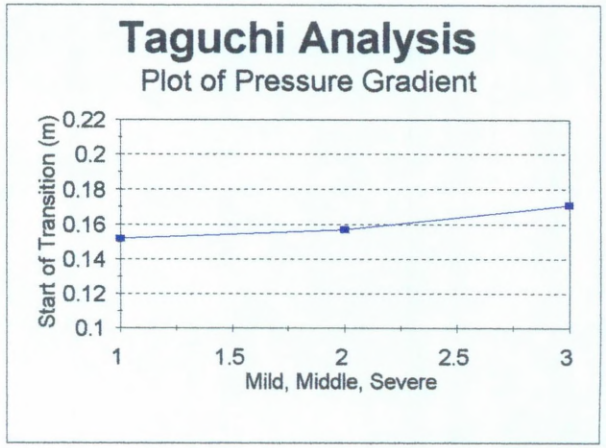

Figure D.23: Taguchi Analysis Run 3

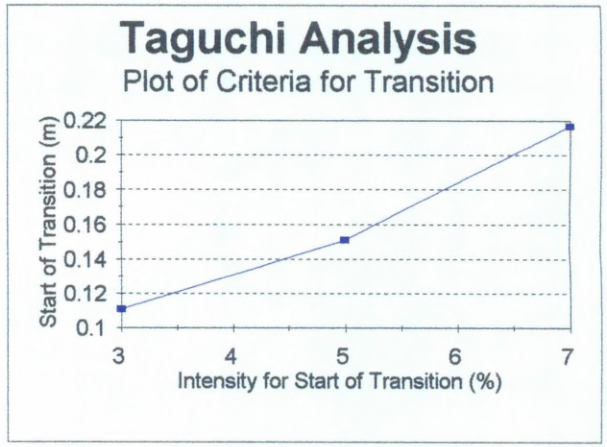

Figure D.24: Taguchi Analysis Run 3

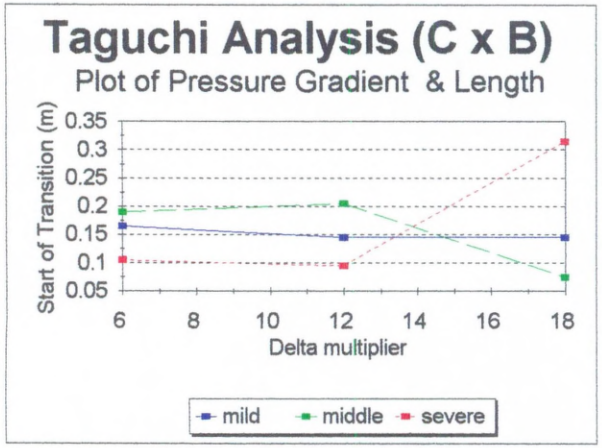

Figure D.25:Taguchi Analysis Run 3

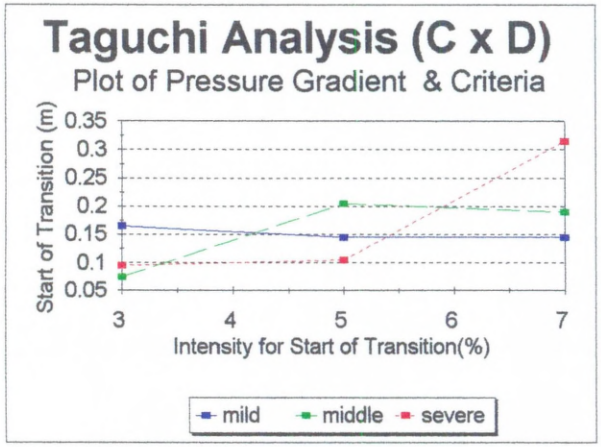

Figure D.26: Taguchi Analysis Run 3

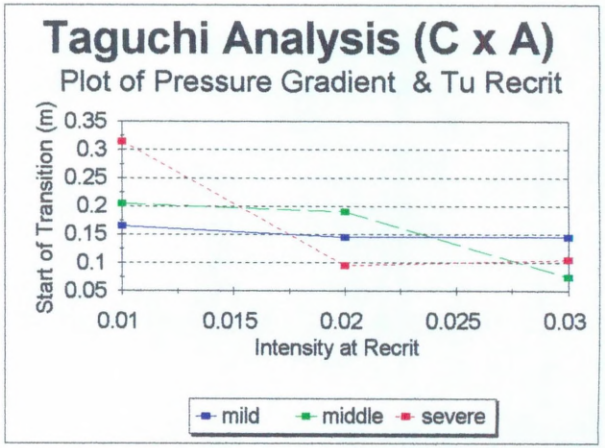

Figure D.27: Taguchi Analysis Run 3

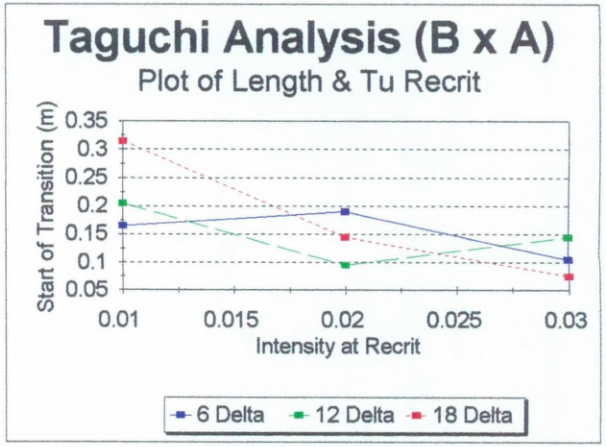

Figure D.28: Taguchi Analysis Run 3

Figure D.29: Taguchi Analysis Run 3

Figure D.30: Taguchi Analysis Run 3

Taguchi Analysis Run 4

Factor	Meaning	Level 1	Level 2	Level 3
A	q at Re_{crit}	0.01	0.02	0.029
B	char. length	6δ	12δ	18δ
C	x co-ord (m)	0.10005	0.1159	0.14
D	criteria (%)	3	5	7

Table D.7: Factors and Levels

Trial No.	Results (z distance m)
1	0.165
2	0.205
3	0.245
4	0.105
5	0.145
6	0.185
7	0.095
8	0.115
9	0.145
10	0.155
11	0.205
12	0.245
13	0.095
14	0.135
15	0.175
16	0.075
17	0.115
18	0.135
19	0.155
20	0.225
21	0.295
22	0.085
23	0.135
24	0.185
25	0.065
26	0.105
27	0.105

Table D.8: Results

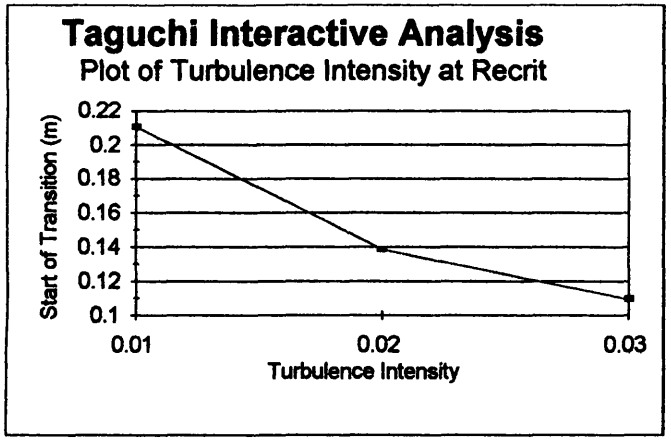

Figure D.31: Taguchi Analysis Run 4

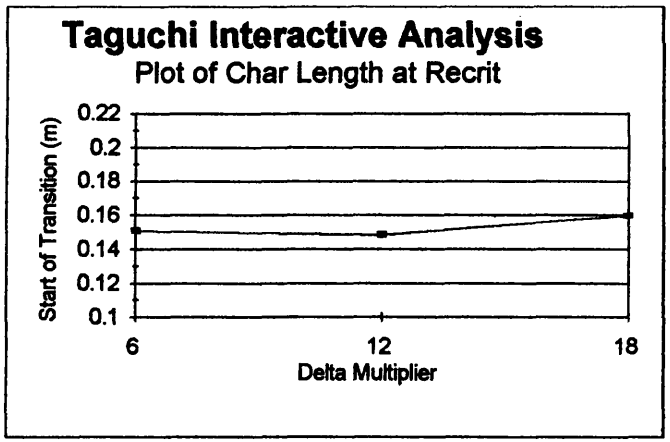

Figure D.32: Taguchi Analysis Run 4

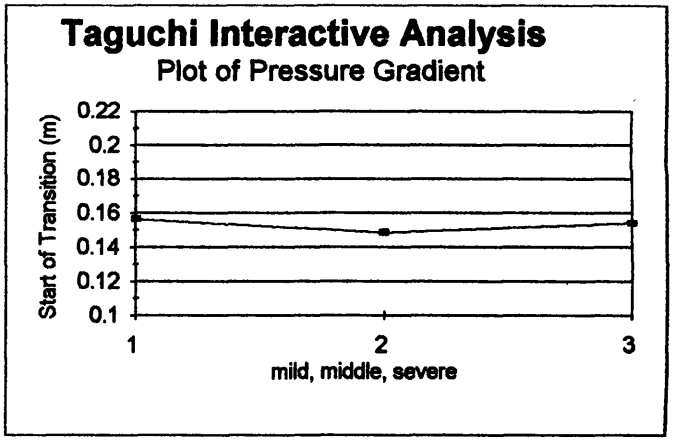

Figure D.33: Taguchi Analysis Run 4

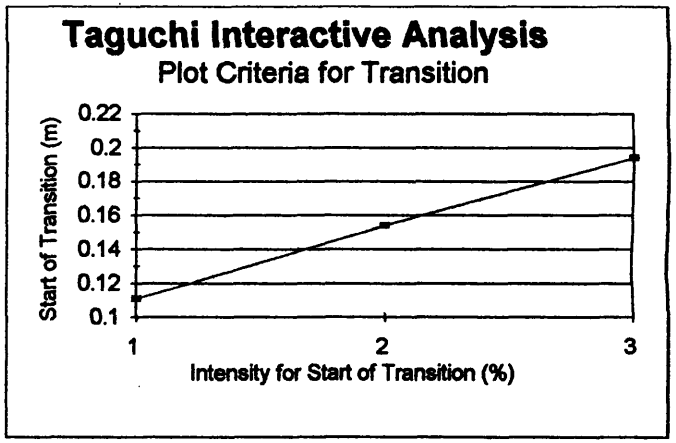

Figure D.34: Taguchi Analysis Run 4

Appendix E

Taguchi Methods in CFD

by

A. Thomson & C. J. Fraser
University of Abertay Dundee
Bell Street, Dundee, Scotland. DD1 1HG

Machine Type:	Western Systems 486 DX2 50
Operating System:	Microsoft DOS V6.0
Phoenics Version:	EasyFlow V2.0 January 1991

Abstract

EasyFlow, in conjunction with EasyMesh 2 - D and FLOWVIS was used in a Taguchi analysis in order to evaluate whether it was possible to produce flow separation on a flat plate in a wind tunnel with adverse pressure gradient, by varying free stream turbulence, inlet velocity and roof divergence angle.

The analysis successfully predicted the optimum combination of variables to give the best possibility of a separation point although given the present construction of the wind tunnel, it was highly unlikely that a separation point would actually be achieved.

1. Introduction

For some years CFD has been known to predict flow fields qualitatively although not always quantitatively. This is usually not too much of a problem unless a detailed analysis of a final design is ultimately required.

Usually time and cost are constraints where product design is concerned and it is not possible, or even practical, to try out every combination of factors, at every level which are thought to affect the design. Any method which allows a reduction in the number of experiments required to predict the optimum combination, and level would be worthwhile. The Taguchi method is one such method of analysis.

If the afore mentioned experiments could be carried out numerically on a computer and give consistent results, then large savings in time and hence cost would be achieved.

It was proposed to use the Taguchi method together with the CFD package EasyFlow to predict trends in factors in order to generate a flow separation on a flat plate in a wind tunnel.

2. Definition of the Problem

The wind tunnel was a suction type with adjustable roof (Fig. 1) constructed to simulate suction surface gas turbine blade flows, Sharma et al.[1], which are characterised by an initially large acceleration over about the first 10% of chord length. A relaxation zone occurs from about 10% - 40% of the chord and the remaining flow is subject to varying degrees of decelation depending upon design. In the deceleration region, flow separation is quite possible, and is ultimately manifested in the form of stall. The test surface was a flat plate made of 6 mm polished aluminium sheet, 2.4 m long and mounted at 3^{o} positive incidence to the flow.

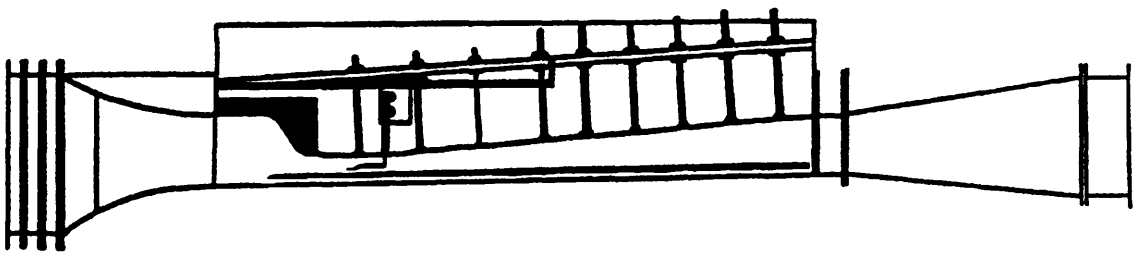

Figure 1 Wind Tunnel

3. Taguchi Method

The Taguchi method involves designing an experiment, using orthogonal arrays, which test all of the factors at all of the levels without having to test every level of each factor with all levels of every other factor.

It was thought that the major factors, most easily modified, affecting separation would be free stream turbulence, inlet velocity and roof divergence angle in the decelation zone. These factors were allowed to vary at three levels (Table 1). The full factorial experimental method required 27 experiments. The Taguchi method required 9 experiments.

The quality factor chosen was that the velocity parallel and adjacent to the flat plate should be minimised at a point 1 metre from its leading edge.

Factor	Level 1	Level 2	Level 3
Turbulence (%)	0.5	1.5	3.0
Inlet Velocity (m/s)	1.0	4.0	8.0
Roof Angle (deg)	5	10	15

Table 1: Factors and Levels

4. Mathematical Formulation

The flow domain was modelled as a two dimensional body fitted co-ordinate grid comprising of 69 x 20 cells (Fig. 2). The x direction being chosen as the major flow. The flat plate was modelled as a blocked region with friction. The flow was assumed incompressible, and the turbulence model used was the default k - ε. The mass flow was fixed at the upstream boundary as was the pressure at the downstream boundary. The Q1 file for the optimum case is given in Appendix 1.

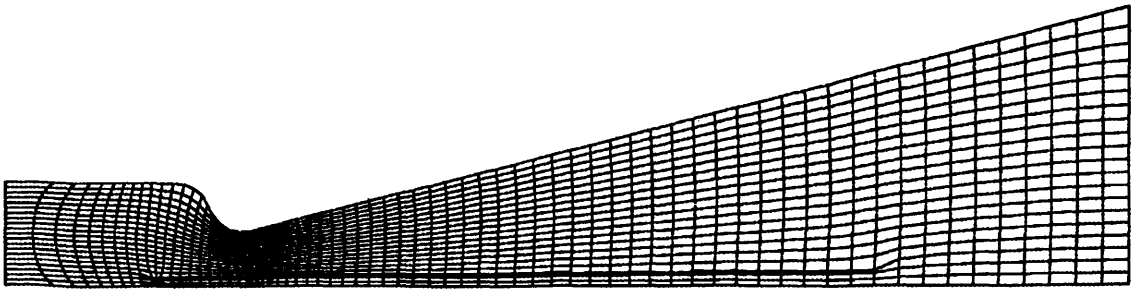

Figure 2 Computational Mesh

5. Validation of the Model

EasyFlow V2.0 was used for the analysis but was limited in the number of cells that could be defined. In order to ascertain that the results obtained had the desired accuracy., a model of the wind tunnel used by Sharma [1] was constructed and solved. The results obtained by EasyFlow showed some similarity to those in the text in that the computed pressure coefficient over the plate surface were alike.

6. Results

The nine CFD experiments that were carried out and each case solved to within 1% error. The experimental results are given in Appendix 2.

It was found that the lowest value of velocity at 1 metre from the leading edge was found when:

free stream turbulence level	0.5 %
inlet velocity	1 m/s
roof divergence angle	15^{o}

Although this combination was not carried out experimentally it was possible to predict the value, from the Taguchi method, of the velocity at this point. It was found to be -0.77 m/s.

When the optimum combination of the above factors was run to check the prediction the velocity at 1 metre downstream was found to be 1.09 m/s. This gave the lowest value of velocity for all of the experiments carried out.

The Taguchi method successfully predicted the optimum combination of factors.

7. Discussion

It can be seen that the CFD solutions used in conjunction with the Taguchi method of analysis, have successfully predicted the optimum combination of factors to give a minimum velocity on the flat plate at 1 metre from the leading edge.

However the Taguchi prediction of the velocity for the optimum combination was somewhat different from that predicted from the CFD analysis. This is due to a lack of cells in the computational domain.

8. Conclusion

The Taguchi method coupled with CFD represent a powerful tool which can be used to rapidly predict trends in factors, or assess whether a case is viable or not.

The time taken to construct, solve and complete the Taguchi analysis in conjunction with EasyFlow involved about 4 man - days. To complete the same analysis in the laboratory was conservatively estimated to take around 3 man - months. The savings in time have been shown in this case are over 20 fold.

In point of fact however, the maximum angle of divergence of the tunnel roof could only be increased to about 8^{o} without major modification.

It was thus confirmed that it would not be possible to create a separation on the flat plate in the wind tunnel without major modification to the tunnel layout

9. References

[1] Sharma, O.P. Wells, R.A., Schlinker, R.H. and Bailey D.A. 1982. Boundary Layer Development on Turbine Airfoil Surfaces. Trans ASME, Vol. 104: 698 - 706

[2] MacLeod, R.D. Fife College of Technology, Kirkcaldy, Scotland. Private conversation.

[3] EasyFlow V2.01 User Manual, CHAM Publication TR/223, January 1991.

[4] FLOWVIS V1.2 User Guide, FLOWSOLVE Publication, 1992/93.

[5] EasyMesh 2 - D User Guide, FLOWSOLVE Publication.

Appendix 1

```
TALK=F;RUN(1,1);VDU=0
  ************************************************************
  *
  * GROUP 1. Run title and other preliminaries.
  *
TEXT(OPTIMUM COMBINATION TU=.5%,U=1M/S,A=15 )
  *
  ************************************************************
  *
  * GROUP 2. Transience; time-step specification.
  *
  *
  ************************************************************
  *
  * GROUP 3. X-direction grid specification.
  *
  * Body Fitted Coordinates Grid Selected
  * Extent of the Domain in the X-Direction:  1.000E+00
  * Number of Cells in the X-Direction
NX=69
INTEGER(NXF01,NXL01); NXF01=1; NXL01=9
INTEGER(NXF02,NXL02); NXF02=10; NXL02=59
INTEGER(NXF03,NXL03); NXF03=60; NXL03=69
  *
  ************************************************************
  *
  * GROUP 4. Y-direction grid specification.
  *
  * Extent of the Domain in the Y-Direction:  1.000E+00
  * Number of Cells in the Y-Direction
NY=20
INTEGER(NYF01,NYL01); NYF01=1; NYL01=2
INTEGER(NYF02,NYL02); NYF02=3; NYL02=3
INTEGER(NYF03,NYL03); NYF03=4; NYL03=20
  *
  ************************************************************
  *
  * GROUP 5. Z-direction grid specification.
  *
  *
  ************************************************************
  *
  * GROUP 6. Body-fitted coordinates or grid distortion.
  *
BFC=T; NONORT=T; READCO(GRID)
  *
  ************************************************************
  *
  * GROUP 7. Variables stored, solved & named.
  *
  * Solve for the PRESSURE
  * (Slab-by-Slab Method)  * (Arithmetic Averaging)
SOLVE(P1)
  * Solve for the X-DIRECTION VELOCITY COMPONENT
  * (Slab-by-Slab Method)  * (Arithmetic Averaging)
SOLVE(U1)
```

```
  * Solve for the Y-DIRECTION VELOCITY COMPONENT
  * (Slab-by-Slab Method)  *  (Arithmetic Averaging)
SOLVE(V1)
  *
  ***************************************************************
  *
  * GROUP 8. Terms (in differential equations) & devices.
  *
  *
  ***************************************************************
  *
  * GROUP 9. Properties of the medium (or media).
  *
  * Set First-Phase Density Value
RHO1= 1.161E+00
  * Set Laminar Kinematic Viscosity Value
ENUL= 1.589E-05
  * Select K-E Turbulence Model
  * ENUT = CMU * (Mixing-Length) * K**0.5
  * EL1 = (CD * K**1.5)/E
TURMOD(KEMODL)
  *
  ***************************************************************
  *
  * GROUP 10. Inter-phase-transfer processes and properties.
  *
  *
  ***************************************************************
  *
  * GROUP 11. Initialization of variable or porosity fields.
  *
  * Initialize the TURBULENT KINETIC ENERGY
FIINIT(KE)= 5.000E-03
  * Initialize the KINETIC-ENERGY DISSIPATION RATE
FIINIT(EP)= 5.809E-04
  * Partially-Blocked (Porous) Region, Named OBS01
CONPOR(OBS01, 0.000E+00,CELL,NXF02,NXL02,NYF02,NYL02,1,1)
  *
  ***************************************************************
  *
  * GROUP 12. Convection and diffusion adjustments.
  *
  *
  ***************************************************************
  *
  * GROUP 13. Boundary conditions and special sources.
  *
  * INLET Boundary Condition, Named INLET01
PATCH(INLET01,WEST,NXF01,NXF01,NYF01,NYL03,1,1,1,1)
COVAL(INLET01,P1,FIXFLU,RHO1* 1.000E+00)
COVAL(INLET01,U1,ONLYMS, 1.000E+00)
COVAL(INLET01,V1,ONLYMS, 0.000E+00)
COVAL(INLET01,KE,ONLYMS,(1.000E+00**2)* 5.000E-03)
COVAL(INLET01,EP,ONLYMS,(0.1643*(5.000E-03)**1.5)/(0.1*YVLAST))
  * OUTLET Boundary Condition, Named OUTLET01
PATCH(OUTLET01,EAST,NXL03,NXL03,NYF01,NYL03,1,1,1,1)
COVAL(OUTLET01,P1,FIXP, 0.000E+00)
COVAL(OUTLET01,KE,ONLYMS,SAME)
COVAL(OUTLET01,EP,ONLYMS,SAME)
  * WALL Boundary Condition, Named WALL01
```

```
PATCH(WALL01,NWALL,NXF01,NXL03,NYL03,NYL03,1,1,1,1)
COVAL(WALL01,U1,GRND2, 0.000E+00)
COVAL(WALL01,KE,GRND2,GRND2)
COVAL(WALL01,EP,GRND2,GRND2)
  * WALL Boundary Condition, Named WALL02
PATCH(WALL02,SWALL,NXF01,NXL03,NYF01,NYF01,1,1,1,1)
COVAL(WALL02,U1,GRND2, 0.000E+00)
COVAL(WALL02,KE,GRND2,GRND2)
COVAL(WALL02,EP,GRND2,GRND2)
  *
  ************************************************************
  *
  * GROUP 14. Downstream pressure for PARAB=.TRUE..
  *
  *
  ************************************************************
  *
  * GROUP 15. Termination of sweeps.
  *
  * Number of Iterative Sweeps (Outer Iterations)
LSWEEP=500
  * Automatic Reference Residual for the PRESSURE
RESREF(P1)=-GRND1
  * Automatic Reference Residual for the X-DIRECTION VELOCITY COMPONENT
RESREF(U1)=-GRND1
  * Automatic Reference Residual for the Y-DIRECTION VELOCITY COMPONENT
RESREF(V1)=-GRND1
  * Automatic Reference Residual for the TURBULENT KINETIC ENERGY
RESREF(KE)=-GRND1
  * Automatic Reference Residual for the KINETIC-ENERGY DISSIPATION RATE
RESREF(EP)=-GRND1
  *
  ************************************************************
  *
  * GROUP 16. Termination of iterations.
  *
  *
  ************************************************************
  *
  * GROUP 17. Under-relaxation devices.
  *
  * Linear Relaxation Applied to P1
RELAX(P1,LINRLX, 2.000E-01)
  * False-Time-Step Relaxation Applied to U1
RELAX(U1,FALSDT, 1.000E+00)
  * False-Time-Step Relaxation Applied to V1
RELAX(V1,FALSDT, 1.000E+00)
  * Linear Relaxation Applied to KE
RELAX(KE,LINRLX, 8.000E-01)
  * Linear Relaxation Applied to EP
RELAX(EP,LINRLX, 8.000E-01)
  *
  ************************************************************
  *
  * GROUP 18. Limits on variables or increments to them.
  *
  *
  ************************************************************
  *
  * GROUP 19. Data communicated by satellite to GROUND.
```

```
  *
  *
  ************************************************************
  *
  * GROUP 20. Preliminary print-out.
  *
  * Activate Printout of Satellite Data.
ECHO=T
  *
  ************************************************************
  *
  * GROUP 21. Print-out of variables.
  *
  * Printout for the PRESSURE
OUTPUT(P1,Y,N,N,Y,Y,Y)
  * Printout for the X-DIRECTION VELOCITY COMPONENT
OUTPUT(U1,Y,N,N,Y,Y,Y)
  * Printout for the Y-DIRECTION VELOCITY COMPONENT
OUTPUT(V1,Y,N,N,Y,Y,Y)
  * Printout for the TURBULENT KINETIC ENERGY
OUTPUT(KE,Y,N,N,Y,Y,Y)
  * Printout for the KINETIC-ENERGY DISSIPATION RATE
OUTPUT(EP,Y,N,N,Y,Y,Y)
  *
  ************************************************************
  *
  * GROUP 22. Spot-value print-out.
  *
  * X-Direction Index of Spot-Value
IXMON=8
  * Y-Direction Index of Spot-Value
IYMON=3
  *
  ************************************************************
  *
  * GROUP 23. Field print-out and plot control.
  *
  * Frequency of tabulation/plots of Spot/Residuals Values
  * (DO NOT Reset)
NPLT=1
  * Print TABLES AND PLOTS of Spot-Values and Residuals
ITABL=3
  *
  ************************************************************
  *
  * GROUP 24. Preparations for continuation runs.
  *
  * Save the Final Flow Field in a RE-START File
SAVE=T; NSAVE=CHAM
  * Initialize ALL Variables From a Previously-Existing File
RESTRT(P1,U1,V1,KE,EP)
  *
  ************************************************************
STOP
```

EasyFlow 2 - D Mesh Generator File

```
imax 70
jmax 21
line 1 10 21 21 -300 205 -2 205 .5
spline 10 21 21 21
nd 18
data
-2 205
38 204
48 204
58 203.5
69 201.5
78 197.5
88 191
98 183.5
108 168.5
118 146.5
128 128.5
138 116.5
148 107.5
158 101.5
168 98.5
178 98.5
188 98.5
198 99
line 21 70 21 21 198 99 2000.92 582.09 1.5
line 1 10 4 4 -300 -2 1 -2 .5
line 10 12 4 4 1 -2 16.61 .14
line 12 21 4 4 16.61 .14 198 1.72
line 21 70 4 4 198 2.63 2000.92 17.45 1.5
line 1 10 3 3 -300 -4 1 -4 .5
line 10 12 3 3 1 -4 16.61 -5.86
line 12 21 3 3 16.61 -5.86 198 -4.28
line 21 70 3 3 198 -3.364 2000.98 11.45 1.5
line 1 10 1 1 -300 -20 -4 -20 .5
line 10 21 1 1 -4 -20 198 -20
line 21 70 1 1 198 -20 2000 -20 1.5
gr 1 70 4 21
gr 1 70 3 4
```

```
gr 1 70 1 3
fxy 10 60 3 3
fxy 10 60 4 4
fr west
fx west
fr east
fx east
il 10 1 21 3 1
```

Appendix 2

Experiment No.	Factor A Turbulence (%)	Factor B Velocity (m/s)	Factor C Roof angle (deg)	Velocity at 1 m from l.e. (m/s)
1	0.5	1.0	5	1.34
2	1.5	1.0	10	1.15
3	3.0	1.0	15	1.15
4	0.5	4.0	10	4.70
5	1.5	4.0	15	4.60
6	3.0	4.0	5	5.38
7	0.5	8.0	15	5.80
8	1.5	8.0	5	10.80
9	3.0	8.0	10	9.50

Table A1: Experiment no., factors, levels and velocities at 1 m from plate leading edge

Level	Factor A (Turbulence) ave velocity	Factor B (Velocity) ave velocity	Factor C (Roof Angle) ave velocity
1	3.95	1.22	5.83
2	5.52	4.84	4.96
3	5.34	8.58	3.83

Table A2: Average velocities for each factor at each level at 1 m from leading edge

It is clear that the optimum combination would be when:

turbulence = 0.5%,
velocity = 1 m/s
roof divergence angle = 15^{o}

The velocity can be predicted for this combination from:

predicted value = Σfactor averages - (no. of factors - 1) * overall experiment average

i.e. predicted value = 3.95 + 1.22 + 3.83 - (3 - 1) * 4.90

- 0.77 m/s

The published paper cited below has been removed from the e-thesis due to copyright restrictions:

Thomson, A. and Fraser, C.J. (1996) Modelling Boundary Layer Transition Using PHOENICS CFD Software. In: *PHOENICS Journal of Computational Fluid Dynamics & its applications*, 9(1), pp.169-180.

FIRST ANNOUNCEMENT AND CALL FOR PAPERS

SEVENTH INTERNATIONAL PHOENICS USER CONFERENCE

May 12 - 16, 1997

at the Hotel Principe de Asturias, Seville, Spain

Organised by CHAM

The Seventh International PHOENICS Conference is open to all those interested in learning more about Computational Fluid Dynamics, as well as to current PHOENICS users. It will provide an opportunity for CFD users from academic, research, commercial and governmental organisations to exchange ideas in the field of CFD.

Papers on all applications of PHOENICS are welcome, especially those explaining how a specific problem was solved using the code.

There will be lectures by experts in specific CFD fields, sessions for general papers, workshops to which participants can bring problems of particular interest, and poster sessions where participants can display and discuss their work. Information will be provided on the latest features of PHOENICS and on those planned for the future.

Location

The Conference will be held at the Hotel Principe de Asturias located on the outskirts of Seville, Spain. Seville is one of Spain's most historical cities and has a vibrant atmosphere with a thriving nightlife.

Paper submission and selection

Authors should submit three (3) copies of abstracts of about 250 words, to the Conference Organiser (Mrs Sylvie Stevens). The abstracts will be used for preliminary screening. All accepted papers will be published in the PHOENICS Journal of Computational Fluid Dynamics which will be available after the Conference. The official language of the Conference is English.

Deadlines

September 30, 1996:	Final date for receipt of abstract (3 copies)
November 30, 1996:	Notification of abstract acceptance
February 28, 1997:	Final date for receipt of paper

Conference Organiser

Mrs Sylvie Stevens
Concentration, Heat & Momentum Ltd
40 High Street
Wimbledon Village, SW19 5AU
London, UK

Telephone: (44) 181 947 7651
Telefax: (44) 181 879 3497
Email: sks@cham.demon.co.uk

Further details on the Conference and on the local arrangements will be given in the second announcement to be sent out in June 1996 Enquiries should be addressed to the Conference Organiser

Prediction of Optimised Mixing in a Slot

A Thomson, School of Engineering,
University of Abertay Dundee,

The computational fluid dynamics software STAR-CD was used in a Taguchi analysis to optimise the mixing of gas and air in a slot, by varying the following factors at three levels: gas injection hole size, step height and depth to width ratio.

Using the Taguchi technique the analysis was carried out in nine experiments rather than twenty seven for the full factorial method. The quality characteristic was chosen to be the minimisation of the maximum concentration of the gas in a computational cell on a plane 26 mm from the centre of the gas injection hole.

The optimum mix was found to be: injection hole size - 3 mm, step height - 0 mm and depth to width ratio - 1.75. Although this combination of factors was not carried out in the experiment, the prediction of the quality characteristic was found to be 0.12492.

A conformation run was carried out using the factors at the optimum levels. The quality characteristic on the plane at 26 mm was found to be 0.126367 (within 2% of the predicted value).

The Taguchi method successfully predicted the optimum levels of the factors under consideration and also the optimum concentration.

A New Approach to Calculating the Start of Transition for Engineering Type Flows

A. Thomson[1] and C. J. Fraser[2]

[1] Waste Water Technology Centre, University of Abertay Dundee, Bell Street, Dundee DD1 1HG.
[2] School of Engineering, University of Abertay Dundee, Bell Street, Dundee DD1 1HG.

Abstract

It can be shown that the use of correlations for the start of transition and transition length, give rapid solutions to transitional type flows, but the appropriate definition of turbulence intensity and pressure gradient parameter are somewhat ambiguous. Most researchers quote the turbulence intensity in their correlations, but they do not state where the intensity was measured. As freestream turbulence intensity will generally decay as the flow moves downstream, this was proven to be a limiting factor as the start of transition can be moved around to any arbitrary starting position depending on the value chosen for the free stream turbulence intensity.

A new method, based on a reduced form of the turbulent energy equation has been developed and programmed into PHOENICS. The boundary layer was represented as a sink of momentum. The method predicted the start of transition using no ambiguous boundary conditions, and has been shown to predict the start of transition well with Rolls-Royce ERCOFTAC flows T3A, T3A-, T3B, T3C1, T3C2 and T3C5. The method was shown to be quite sensitive to step size (cell density) in the axial direction and to the accuracy of the solution of the equations for kinetic energy and dissipation.

Nomenclature

a	$-u'w'/k$
C_{1E}, C_{2E}, C_{3E}	constants in k - ε model 1.44, 1.92, 1.0
C_f	local skin friction coefficient = $2\tau_w/\rho W^2$
$C_\mu C_D$	constant in k - ε turbulence model (= 0.09)
k	kinetic energy (m^2/s^2)
$\hat{k}$	maximum kinetic energy in the boundary layer at that z location (m^2/s^2)
l_ε	dissipation length scale (m)
ℓ_m	turbulent length scale (m)
m	pressure gradient parameter = $(\theta^2/\nu)(dW/dz)$
Pr	Prandtl number
q	turbulence intensity (%)
R_θ	momentum thickness Reynolds number = $W\theta/\nu$
$R_{\theta f}$	fictitious momentum thickness Reynolds number upstream of which infinitesimal disturbances are damped out.
u', v', w'	root mean square values of the fluctuating velocity components
$\bar{u}, \bar{v}, \bar{w}$	boundary layer average velocities (m/s)

W	flow velocity in streamwise direction (m/s)
x	transverse co-ordinate (m)
z	streamwise co-ordinate (m)

Greek Symbols

δ	boundary layer thickness (m)
ε	dissipation term in turbulence model (m^2/s^3)
$\bar{\varepsilon}$	average dissipation in the boundary layer at that z location (m^2/s^3)
μ	dynamic viscosity (Ns/m^2)
μ_t	turbulent viscosity (Ns/m^2)
ν	kinematic viscosity (m^2/s)
θ	momentum thickness (m)
ρ	fluid density (kg/m^3)
σ_ε	empirical constant in ε equation (= 1.314)
σ_k	empirical constant in kinetic energy equation (= 1.0)
τ_o	shear stress at the wall (N/m^2)

1. Introduction

Thomson and Fraser (1995), showed that it was possible to successfully predict skin friction in boundary layer transitional flows by using a laminar flow field and integral methods programmed in PHOENICS.

Most researchers only quote one value of turbulence intensity in their data, and therefore this was the value used in the Abu-Ghannam and Shaw (1980) correlation to predict the start of transition. This implies that there was no decay in turbulence intensity as the flow moves downstream. However the Rolls-Royce ERCOFTAC flows show that the free stream turbulence intensity decreases with distance in the downstream direction. This poses the problem of what value of turbulence intensity should be used in the Abu-Ghannam and Shaw correlation. It was found by using this data that the start of transition could be moved to almost any arbitrary position depending on the value of free stream turbulence intensity chosen.

A k - ε turbulence model, described by Malin (1995) was programmed in PHOENICS and by choosing a suitable length scale (10% of the distance between the turbulence grid spacing) it was possible to predict the decay of freestream turbulence intensity quite well. Various values of freestream turbulence intensity were chosen for the Abu-Ghannam and Shaw correlation and it was found that the value to give the best (most consistent) prediction of the start of transition was a freestream integrated average from the inlet.

To try to alleviate this short comming a new method to predict the start of transition was developed based on the turbulent energy equation.

2. New Method

The new method was programmed into PHOENICS in a similar manner to the integral methods mentioned above i.e. the boundary layer was represented as a sink of momentum. The correlations used for transition length were attributed to Fraser, Higazy and Milne (1994). The method predicted the start of transition, using no ambiguous boundary conditions and has been shown to predict the start of transition well with Rolls-Royce flows T3A, T3A-, T3B, T3C1, T3C2 and T3C5. The method was shown to be quite sensitive to step size (cell density) in the axial direction and to the accuracy of the solution of equations (2.4) and (2.5) which follow.

2.1 Derivation of the Reduced Form of the Turbulent Energy Equations

The turbulent energy equations for kinetic energy and its dissipation rate can be formulated by multiplying the Navier-Stokes equations by the appropriate fluctuating velocities for each cartesian direction. After some manipulation the equations reduce, for two-dimensional flows, to the frequently quoted forms:-

$$\rho\overline{w}\frac{\partial k}{\partial z}+\rho\overline{u}\frac{\partial k}{\partial x}=\frac{\partial}{\partial x}\left[\left(\mu+\frac{\mu_t}{\sigma_k}\right)\frac{\partial k}{\partial x}\right]+\mu_t\left(\frac{\partial\overline{w}}{\partial x}\right)^2-\rho\varepsilon \tag{2.1}$$

$$\rho\overline{w}\frac{\partial \varepsilon}{\partial z}+\rho\overline{u}\frac{\partial \varepsilon}{\partial x}=\frac{\partial}{\partial x}\left[\left(\mu+\frac{\mu_t}{\sigma_\varepsilon}\right)\frac{\partial \varepsilon}{\partial x}\right]+C_1\mu_t\left(\frac{\partial\overline{w}}{\partial x}\right)^2\frac{\varepsilon}{k}-C_2\rho\frac{\varepsilon^2}{k} \tag{2.2}$$

Where k is the turbulent kinetic energy, ε the energy dissipation rate and μ_t is the turbulent viscosity i.e.

$$\mu_t=\rho C_\mu\frac{k^2}{\varepsilon} \tag{2.3}$$

By estimating suitable integrated average values across the boundary layer it is possible to further reduce equations (2.1) and (2.2) to:-

$$\frac{d\hat{k}}{dz}=\hat{k}\left[\frac{a\tau_0}{W_\infty\mu}-\frac{1}{W_\infty}\frac{dW_\infty}{dz}-\frac{1}{\delta}\frac{d\delta}{dz}\right]-2.86\frac{\bar{\varepsilon}}{W_\infty} \tag{2.4}$$

$$\frac{d\bar{\varepsilon}}{dz}=\bar{\varepsilon}\left[\frac{1.04a\tau_0}{W_\infty\mu}-\frac{1}{W_\infty}\frac{dW_\infty}{dz}-\frac{1}{\delta}\frac{d\delta}{dz}\right]-\frac{5.486\,\bar{\varepsilon}^2}{W_\infty\,\hat{k}} \tag{2.5}$$

Where the parameter 'a' is the ratio of the turbulent shear stress to the turbulent kinetic energy i.e. $a=\dfrac{-u'w'}{k}$. By choosing a suitable starting value for turbulence intensity and length scale, equations (2.4) and (2.5) would predict the kinetic energy and its dissipation rate in the boundary layer as the flow moves downstream.

2.2 Boundary Conditions

Initially it was thought that the above equations would not be valid from the leading edge of the surface because there would be a region where the laminar flow would be stable. The equations would only apply to the flow in the boundary layer in a region downstream of where the momentum thickness Reynolds number was greater than its critical value. The boundary conditions required for this method were:-

(1) the maximum value of turbulence intensity at the critical momentum thickness Reynolds number (w/W)
(2) the integral length scale at the critical momentum thickness Reynolds number
(3) the maximum value of turbulence intensity at the start of transition in the boundary layer
(4) a function for the parameter 'a' in the above equations 2.4 and 2.5

In equations 2.1, 2.2, 2.3, 2.4 and 2.5 there appear the constants C_1, C_2, C_μ and 'a'. Various workers have proposed values for these constants based on well established experiments including the decay of turbulence intensity behind a grid and from measurement in fully developed turbulent boundary layer flows. The following values are often quoted:

$$C_1 = 1.45 \qquad C_2 = 1.92 \qquad C_\mu = 0.09 \qquad a = 0.3$$

The particular value of a = 0.3 strictly applies to the log-law region of a fully developed turbulent boundary layer. Closer to the extremities of the boundary layer the value of 'a' decreases. It would be expected, therefore that in a laminar boundary layer subject to fluctuations induced by free stream turbulence level, that the value of 'a' would be considerably less than 0.3.

3. Development of the Function for 'a'

Initially 'a' was assigned a value based upon free stream turbulence intensity at the critical momentum thickness Reynolds number and then at the leading edge of the flat plate, but research showed that this was clearly not the case. Comparison with data, Abu-Ghannam and Shaw (1980), Gardiner (1987) showed that in some flows the critical momentum thickness Reynolds number was in fact reached well after the start of transition had occurred. This mode of transition can occur Arnal (1984) and is termed by-pass transition.

It became evident at this stage that further information was required on the growth of turbulence intensity within the boundary layer.

This turbulence intensity data was in fact available for the Rolls-Royce T3A, T3A-, T3B and T3C flows.

Further investigation of this turbulence intensity data, indeed showed that it was far from isotropic. In consequence therefore the predicted value of the growth of turbulence intensity within the boundary layer should be qualitative and not

quantitative. As the measurements of the Rolls-Royce flows were so extensive, it was decided that a correlation for 'a' would be developed from that data.
The maximum turbulence intensity in the boundary layer at the leading edge was determined by extrapolation of the maximum boundary layer turbulence intensity data downstream. This showed that for all pressure gradient flows, within the boundary layer at the leading edge the maximum turbulence intensity was approximately the same as the turbulence intensity (based on the free stream velocity) at inlet, Figures 3.1 and 3.2.

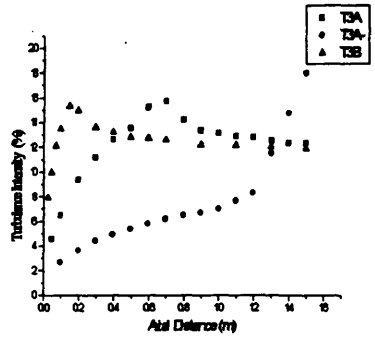

Figure 3.1: Plot of maximum turbulence intensity in boundary layer

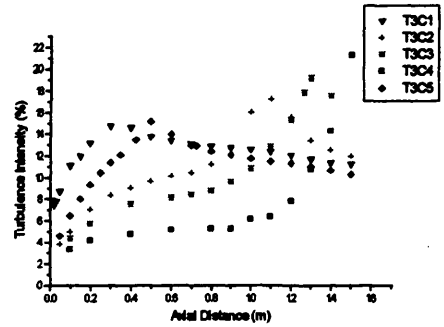

Figure 3.2: Plot of maximum turbulence intensity in boundary layer

The value of turbulence intensity for the start of transition was chosen to be the maximum value in the boundary layer at the location before the minimum value of skin friction. This value was found to be in the region of 11%-13%, based on the free stream velocity. This value is approximately twice that quoted by Fraser (1978) and Arnal (1984).

It was thought that since the maximum turbulence intensity at the boundary layer leading edge was similar to the turbulence intensity at inlet, it would be reasonable to assume that the length scales would be similar also.

Further analysis of the zero pressure gradient flows (T3A, T3A- and T3B), showed two distinct types of maximum turbulence intensity profiles. Cross referencing with the free stream velocity profiles, showed that the nominally zero pressure gradient flows, T3A and T3B were in fact slightly favourable pressure gradient flows, whilst T3A- was an adverse pressure gradient flow. This was also the case with the varying pressure gradient T3C flows, they showed two turbulence intensity profiles, one for the start of transition occurring in favourable pressure gradient and the other for the start of transition occurring in adverse pressure gradient, Figures 3.1 and 3.2.

3.1 Favourable Pressure Gradient

The shape of the turbulence intensity profiles suggested an inverse exponential rise from the leading edge. This agrees with Seiger et al (1995) who also model the effects of free stream turbulence intensity on a laminar boundary layer as an empirical exponential function. It was decided to develop a function for 'a' for the two different types of profile i.e. adverse and favourable. The parameter 'a' would take the form:-

$$a = \exp\left[f(q, l_e, m)\right] \tag{3.1}$$

Johnson (1994) proposes that a functional relationship exits in terms of free stream turbulence level and length scale between the streamwise pressure gradient and laminar boundary layer pressure fluctuations. This agrees with the above proposal.

Initial trials with the T3B flow showed that 'a' was not a constant as is found with the fully turbulent boundary layer. The parameter 'a' was required to decrease as the flow progressed downstream. For the T3B flow it was found that if 'a' was given the value:

$$a = \exp\left[\frac{-19}{q}\right] \tag{3.2}$$

Then a good approximation to skin friction data was achieved. Similarly in the T3A flow, if 'a' was given the value:

$$a = \exp\left[\frac{-8.9}{q}\right] \tag{3.3}$$

then a good fit to the skin friction data was produced. This process was repeated for flows T3C1 and T3C5. It was found that good prediction of skin friction could be achieved if the constant took the value of 13.75 and 7 respectively.

The choice of the constants, 19 and 8.9 for the zero pressure gradient flows was quite critical, and can be seen to be in the ratio of approximately two. This value is almost the same ratio as the length scales at inlet i.e. T3A and T3B flows had the length scales 4 mm and 2 mm respectively. The T3A flow was given the length scale value of 1.873 mm (8.9/19 x 0.004) at inlet and was shown to still provide a good approximation to the free stream turbulence intensity. A correlation was proposed for nominally zero (favourable) pressure gradient flows:

$$a = \exp\left[\frac{-19}{q}\frac{L_e}{0.004}\right] \tag{3.4}$$

It was possible to further modify the zero pressure gradient correlation for 'a' by a function of pressure gradient parameter, 'm' to account for favourable pressure gradient flows:-

$$a = \exp\left[\left(\frac{-19}{q}\right)\left(\frac{L_e}{0.004}\right)\left(1 - 5.3m^2\right)\right] \tag{3.5}$$

This above correlation gave good prediction of skin friction data for T3A, T3B, T3C1 and T3C5 (Figures 3.3, 3.4, 3.5, 3.6) flows without adversely affecting the prediction of free stream turbulence intensity.

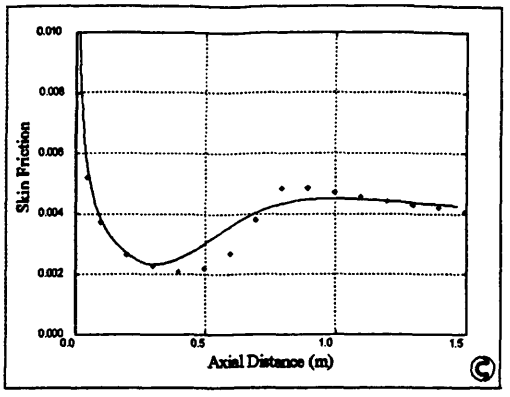

Figure 3.3: T3A Skin Friction

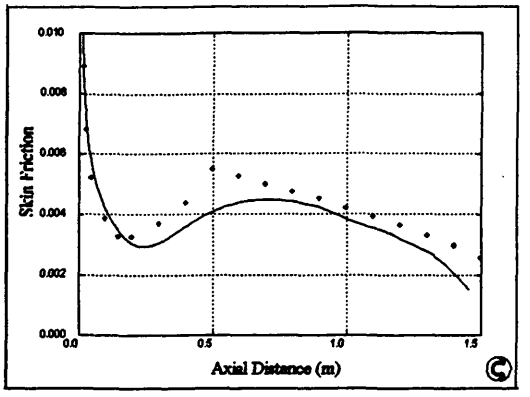

Figure 3.5: T3C1 Skin Friction

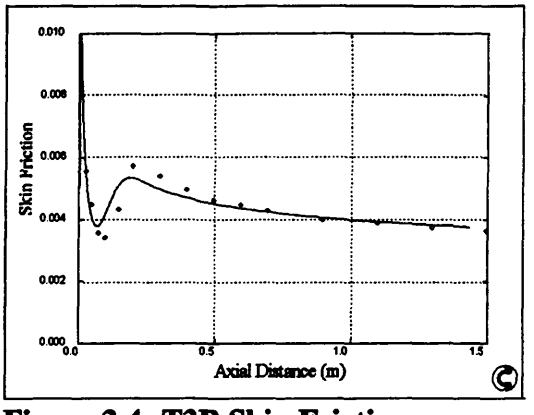

Figure 3.4: T3B Skin Friction

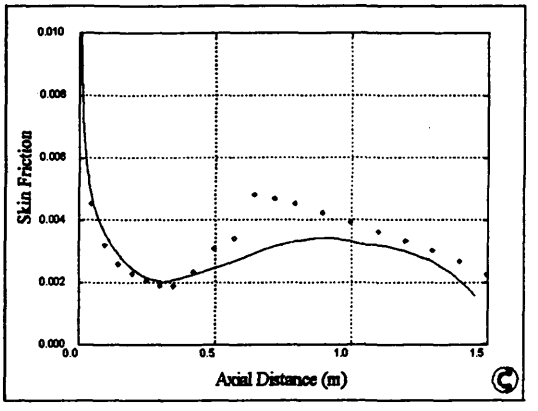

Figure 3.6: T3C5 Skin Friction

3.2 Adverse Pressure Gradient

The same form of function for 'a' was proposed for adverse pressure gradient flows. Initially using the nominally zero pressure gradient T3A- flow, it was found that if correlation (3.4) was used, then transition was predicted far too early. By trial and error the function for 'a' that gave an excellent fit to the skin friction data was found to be:

$$a = \exp\left[\frac{-3.26}{q}\right] \tag{3.6}$$

However there was one imposed condition, in that 'a' was not allowed to fall below a limiting value of 0.008 as the flow moved downstream. Properties for the T3A- flow are shown in Figure 3.7.

One of the drawbacks with the Rolls-Royce data was that for the flows in which the start of transition occurred in adverse pressure gradient, T3C3 and T3C4, separation was predicted by Thwaites (1949) method before the start of transition occurred. Thus the only adverse pressure gradient test case that was suitable was T3C2. The function for 'a' that was found to give a relatively good fit to the skin friction data was:

$$a = \exp\left[\frac{-6.85}{q}\right] \tag{3.7}$$

provided that 'a' was restricted to values greater than 0.009. Properties for the T3C2 flow are shown in Figure 3.8.

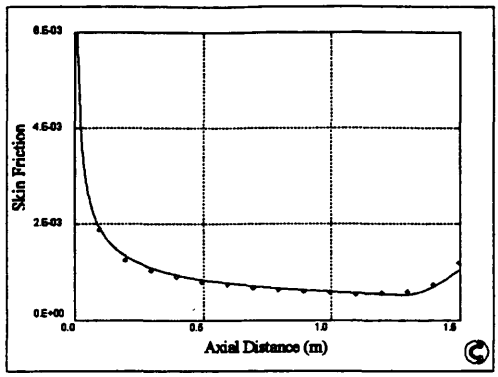

Figure 3.7: T3A- Skin Friction

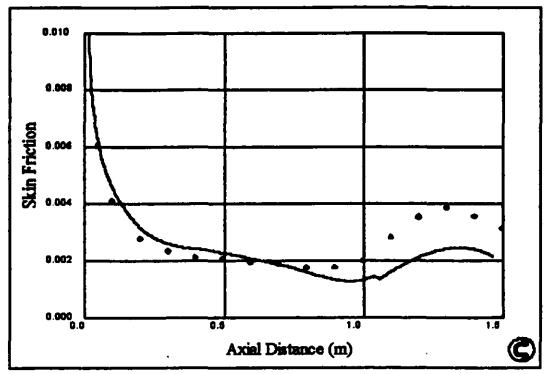

Figure 3.8: T3C2 Skin Friction

4. Results and Discussion

Grid independency tests showed that a computation cell distribution in the axial direction of 1000 cells per metre was adequate. Solution of equations (2.4) and (2.5) required the use of the 6th order Runge-Kutta method for consistently accurate results.

It was thought that it would be possible to use the correlation for 'a' in favourable pressure gradient flows and enforce a limiting value on 'a' to successfully predict the start of transition. Using different limiting values for 'a', it was found that the start of transition was always predicted early, i.e. the rise of the predicted maximum turbulence intensity in the boundary layer was too great.

Prediction of the start of transition in other flows was not attempted as no meaningful results would be achieved. There were too many parameters that were not measured e.g. free stream turbulence intensity distribution and hence the length scale, and the maximum turbulence intensity in the boundary layer at the start of transition.

A new method was developed in order to predict the start of transition, using data from the Rolls Royce T3A, T3A-, T3B and T3C flows. The method predicted the maximum kinetic energy and average dissipation at a axial station in the boundary layer using no ambiguous boundary conditions. The boundary layer model was coupled to the free stream turbulence intensity by the function 'a'. The predictions at the previous step being the starting conditions for the predictions at the current step. The result of this method was an increased cell density in the axial direction over the previous correlation method. The method was based on two flow types: adverse, and favourable pressure gradient. Each flow type had a distinctive maximum boundary layer turbulence intensity profile shown in Figures 3.1 and 3.2.

The method was coded into PHOENICS as a sink of momentum. It was based on the turbulent energy equations, and estimated the start of transition by calculating the

isotropic growth of kinetic energy, using integrated averages of properties across the boundary layer, from the leading edge. The method required the following boundary conditions: (1) the maximum turbulence intensity at the leading edge, (2) an average dissipation length scale at the leading edge, (3) a turbulence intensity criteria for the start of transition, (4) a function, 'a' to simulate the effect of turbulence on the laminar boundary layer.

Originally it was thought that the boundary layer would be laminar from the leading edge up to a critical momentum thickness Reynolds number and any instabilities in this portion of the flow in the boundary layer would be damped out and the flow would remain laminar. A simple correlation 'suitable for engineering type flows', Arnal (1984), had been used to predict this critical momentum thickness Reynolds number. However data suggests that for the flows considered here the mode of transition was by-pass.

After inspection of the Rolls Royce T3A, T3A-, T3B, T3C boundary layer maximum turbulence intensity data, it was found that the maximum turbulence intensity in the boundary layer at the leading edge was almost the same as the average free stream turbulence intensity at inlet. The inlet value would therefore be assumed to be the starting value in the boundary layer calculations. It was proposed that the average dissipation length scale at the leading edge of the boundary layer was also the same as that at inlet. The criteria for the start of transition was taken directly from the maximum turbulence intensity data and was found to be approximately 12%. This was almost twice the value quoted by Fraser (1978) and Arnal (1984).

An inverse exponential function was proposed based on the free stream turbulence intensity, dissipation length scale and pressure gradient. The proposed function would not attempt to predict the maximum turbulence intensity in the boundary layer as the data was found to be far from isotropic. The predicted profile, should, however be qualitatively correct.
Correlation (3.4), was a function of free stream turbulence intensity and length scale only, and was proposed for the nominally zero, but slightly favourable pressure gradient flows T3A and T3B. Prediction of skin friction can be described as good (Figures 3.3 and 3.4). Correlation (3.4) was extended, by including a function of the pressure gradient parameter, m, (correlation 3.5) to take into account the start of transition in favourable pressure gradients, T3C1 and T3C5 (Figs. 3.5 and 3.6). Again the prediction of skin friction can be described as good. The start of transition was perhaps predicted slightly late.

Unfortunately, there was only one nominally zero, adverse pressure gradient flow, T3A-, and Thwaites method, which was used to predict laminar boundary layer properties, predicted separation before transition on flows T3C3 and T3C4, therefore excluding these two flows from any further analysis. Thus there was only one variable pressure gradient flow, T3C2 where the start of transition occurred in adverse pressure gradient that could be utilised. No attempt was made to develop a function for 'a' in adverse pressure gradient flows due to the limited data available. However an attempt was made to predict skin friction using this new method. The method was shown to give excellent prediction of skin friction in flow T3A- Figure 3.7, but not quite as good for flow T3C2. Figure 3.8.

Again the parameter 'a' was made a function of free stream turbulence intensity, but in the case of adverse pressure gradient, 'a' was limited to a constant value, after initially being a function of free stream turbulence intensity.

5. Conclusion

A new method which used the turbulent energy equations was developed to predict the start of transition. The method used integrated averages of properties across the boundary layer starting at the leading edge and marched downstream. The boundary layer model is coupled to the free stream via a correlation which was found to be a function of free stream turbulence intensity, dissipation length scale and pressure gradient parameter. This method was programmed into PHOENICS as a sink of momentum. It was developed and validated using the Rolls Royce T3A, T3A-, T3B and T3C flows. The following conclusions were reached:

(1) the method is slower that the previous correlation method, it requires a computational cell density of about 1000 per metre in the axial direction
(2) only two computational cells across the boundary layer in the transverse direction are required
(3) starting and boundary conditions are not ambiguous
(4) the start of transition and skin friction in favourable pressure gradient flows were well predicted
(5) it was possible to predict the start of transition in adverse pressure gradient flows, but there was not enough data available to develop a more representative correlation

6. References

1. Abu-Ghannam, B. J. and Shaw, R. 1980. Natural transition of boundary layers - the effects of turbulence, pressure gradient and flow history. *Jour. Mech. Eng. Sci*: 22 892.
2. Arnal, D 1984. Description and Prediction of Transition in Two-Dimensional Incompressible Flow. AGARD Special Course on Stability and Transition of Laminar Flow, AGARD-R-709
3. Fraser, C. J., Higazy, M. G. and Milne, J. S. 1994. End-stage boundary layer transition models for engineering calculations. *Proc. Instn. Mech. Engrs. Vol 208, Part C: Jour. of Mech. Eng. Sci.*: 47-58.
4. Gardiner, I. D. 1987. *Transition in Boundary Layer Flows.* (PhD Thesis. University of Abertay Dundee)
5. Hinze, J.O. 1975. *Turbulence: 2nd Edition.* New York: McGraw-Hill. p. 647
6. Johnson, M. W. 1994. A Bypass Transition Model for Boundary Layers. ASME Jour. of Turbo. vol. 116 pp. 759-764
7. Malin, M.R. 1995. Concentration, Heat and Momentum, Bakery House, 40 High Street, Wimbledon Village, London. SW19 5AU. Personal communication.
8. Seiger, K., Schiele, R., Kaufmann, F., Wittig, S. and Rodi, W. 1995. A Two-Layer Turbulence Model for the Calculation of Transitional Boundary Layers,

ERCOFTAC Bullitin pp. 21-25 March 1995

9. Thomson, A. and Fraser, C.J. 1995. Modelling Boundary Layer Transition Using PHOENICS CFD Software. *Proc. PHOENICS European User Conf. 8th-10th Nov.1995*. Flowsolve Limited.
10. Thomson, A. and Fraser, C.J. 1994. Taguchi Method in CFD. *Proc. PHOENICS European User Conf. 16th-18th Nov.1994*. Flowsolve Ltd.
11. Thomson, A. 1996. Optimised Mixing of Air and Gas in a Slot. *Ninth Scot. Fluid Mech. Meeting. Univ. of Paisley*, 21st June 1996.
12. Thwaites, B. 1949. Approximate calculation of the laminar boundary layer. *Aero. Quart.* vol. 1: 245 - 280.